Characterisation of a Human DEAD-Box Protein (DDX3) and its Interaction with Hepatitis C Virus Core Protein

Martin James Scott

A Thesis Presented for the Degree Doctor of Philosophy

in

The Faculty of Science at the University of Glasgow

MRC Virology Unit
IBLS Division of Virology
Church Street
Glasgow G11 5JR

April 2002

Acknowledgements

Many thanks to:

Professor Duncan McGeoch for providing the opportunity to study at the MRC Virology Unit.

My supervisor, Dr Arvind Patel, for guidance on both theoretical and practical matters throughout these studies, for constructive criticism of this thesis, and for numerous invaluable reagents.

Dr Ania Owsianka, for the provision of similarly invaluable reagents and always offering helpful advice.

The inimitable Dr Wood, for the incessant lab banter, nights on the town, and expert guidance regarding experiments, and, more importantly, musical taste and fashion.

All other members of lab 300, past and present, for providing a pleasant working environment.

The Virology 5-a-side football crew for providing an outlet for sustained aggression and, occasionally, extreme violence, when things went wrong in the lab.

Last, but definitely not least, Eve, for constant support and generally being rather lovely.

Summary

Hepatitis C Virus (HCV) core protein is believed to form the viral nucleocapsid. However, numerous reports suggest it can also modulate diverse cellular processes. It is possible that at least some of these pleiotropic effects are exerted through the interaction of core protein with a range of host cellular factors, including a putative RNA helicase of the DEAD-box family termed DDX3.

The main aims of this study were to i) characterise DDX3, in terms of its basic properties and normal role in cellular metabolism, and ii) investigate the interaction of DDX3 with core protein and determine any influence of this association on HCV replication/pathogenesis. A number of anti-DDX3 immunological reagents were already available for study of the endogenous DDX3 protein, as well as various truncated or mutated forms of the protein that were subsequently cloned and expressed in a variety of systems. Core protein was produced using recombinant vaccinia virus (rVV) due to the lack of an efficient cell culture system for HCV. To allow comparisons with natural infection of permissive cells with this hepatotropic virus, studies were usually limited to human hepatocyte-derived cell lines, while core protein was generally expressed along with the HCV glycoproteins (E1-E2), as it would be *in vivo*, to ensure proper processing of core. Recombinant baculoviruses (rbacs) carrying the DDX3- and core-coding sequences were generated for further examination of these proteins.

Since little was generally known about DDX3, initial studies concentrated on its fundamental characteristics, including investigations into expression of its mRNA transcript and protein in human hepatocytes and other mammalian cell lines. The DDX3 mRNA transcript was also studied in a wide range of human tissues. These analyses strongly suggest that DDX3 is a ubiquitous and highly conserved cellular protein. Consistent with previous reports regarding the DDX3/core interaction, expression of core protein in hepatocytes led to a marked redistribution of endogenous or over-expressed DDX3. This redistribution of DDX3 in the presence of core also occurred in the recently described HCV sub-genomic replicon-expressing cell lines. These observations indicate that core protein aberrantly sequesters a ubiquitous, highly conserved cellular protein, likely disrupting its

potentially crucial function. Intriguingly, further studies suggested that core protein directly or indirectly modifies DDX3. An anti-DDX3 polyclonal antibody (PAb) specifically detected DDX3 in insect cell extracts previously infected with rbac expressing the protein, and detected the endogenous DDX3 in human hepatocytes; co-expression of rbacs expressing core (or core-E1-E2) and DDX3 in insect cells, or infection of human hepatocytes with rVV expressing core-E1-E2 led to the appearance of a higher molecular weight isoform of DDX3. This provides further evidence that the DDX3/core interaction is genuine, and possibly emphasises its significance in terms of HCV pathogenesis.

Several insights into DDX3 and its interaction with core protein were given by expression of DDX3 mutants from mammalian expression plasmids. Of particular interest was a mutant containing a single amino acid change within the DEAD-box, a motif that is highly conserved amongst members of the large family of known and putative RNA helicases to which DDX3 belongs. This mutant showed a very distinct subcellular distribution compared with the wild-type protein, although it retained its ability to interact with core. In collaboration with others, it was shown that this DDX3 mutant was enzymatically incapacitated, consistent with the involvement of the DEAD-box in ATP hydrolysis. These data suggest important features regarding DDX3 and its interaction with core: i) the functional capabilities of DDX3 are linked to its subcellular localisation; ii) the normal distribution of DDX3 is irrelevant for its association with core, possibly indicating that their interaction occurs prior to subcellular targeting of DDX3; iii) the enzymatic competence of DDX3 is not essential for its interaction with core. A putative nuclear export signal (NES) was also identified in DDX3 by comparison with its *Xenopus laevis* homologue. ΔNES-DDX3, lacking the N-terminal 21 amino acids of the protein, was cloned and expressed by plasmid in hepatocytes as before. However, although this protein appeared to be more concentrated in the nuclear periplasm, accumulation of the protein within the nucleus itself was not detected. This could suggest that the putative NES of DDX3 is not functional *in vivo*, or that more than one mechanism governs its nucleocytoplasmic transport. Consistent with the latter hypothesis, subcellular fractionation of hepatocyte cell extracts revealed a small quantity of DDX3 protein in the nucleus.

An insight into DDX3 itself was given by a detailed analyses of anti-DDX3 monoclonal antibody (MAb) reactivities to the full-length/truncated bacterially-expressed protein and the endogenous protein in hepatocyte cell extracts. Although the majority of MAbs bound bacterially-expressed DDX3 (and various deletion mutants used to map antibody epitopes), only two such antibodies were capable of detecting full-length DDX3 in hepatocytes. Analyses of the protein sequence of DDX3 indicated that a plausible reason for this anomaly could be extensive glycosylation and/or phosphorylation within an epitope bound by many of the anti-DDX3 MAbs. The biochemical properties of bacterially-expressed DDX3 were also examined. The protein was shown to dose-dependently hydrolyse dATP. This dATPase activity was stimulated by total RNA from hepatocytes, implying that a specific RNA activator exists within cells. RNA helicase activity was not detected for DDX3 expressed in this manner, in contrast to the HCV NS3 helicase cloned as a positive control. This could relate to the potentially inadequate post-translational processing of DDX3 as implied by the antibody binding data. Alternatively, it could suggest that a cellular co-factor is required for helicase activity of DDX3, as shown for many other such proteins.

In terms of the actual function of DDX3, a role in translation was studied in greatest detail due to a strong link of DDX3 homologues with this process. A novel assay based on the reported HCV 5'-noncoding region (NCR)-mediated translational block in insect cells was developed to test the possible role of DDX3 in translation of the HCV sequences. DDX3 did indeed remove the 5'NCR-mediated block in this system, suggesting it may have a role in HCV replication. However, DDX3 actually downregulated HCV 5'NCR-mediated translation in a plasmid-based reporter assay in human hepatocytes. This could be due to disruption of the normal balance of endogenous DDX3 and its cellular partners by plasmid-expressed DDX3. Interestingly, core protein was able by itself to modulate translational activity in the insect cell-based assay, while other proteins tested such as the HCV NS3 helicase had no effect. Core protein also markedly upregulated HCV 5'NCR-mediated translation in hepatocytes, suggesting the viral nucleocapsid protein can modulate production of itself and other HCV proteins.

In conclusion, the data presented suggest that core may subvert the normal role of DDX3, thus disrupting cellular processes, and/or that DDX3 is targeted by core to carry out some function required in HCV replication, such as unwinding the secondary structure in the viral genome allowing translation, replication and/or packaging of RNA into viral particles.

CONTENTS

LIST OF FIGURES AND TABLES

Figure	*Description*	*After Page*

CHAPTER FOUR - Results

Figure	*Description*	*After Page*

CHAPTER FIVE - Results

APPENDIX IV - Monoclonal and Polyclonal Antibodies

Table	*Description*	*Page*

ABBREVIATIONS

A	Adenine
aa	amino acid
ADP	Adenosine Diphosphate
AMP	Adenosine Monophosphate
ATP	Adenosine Triphosphate
ATPase	Adenosine Triphosphatase
bp	base pairs
C	Cytosine
C-	Carboxy-
CAT	Chloramphenicol Acetyl Transferase
cDNA	complimentary DNA
Ci	Curies
CTL	Cytotoxic T-lymphocyte
Da	Daltons
dADP	deoxy-ADP
dAMP	deoxy-AMP
dATP	deoxy-ATP
dH_2O	distilled H_2O
ds	double-stranded
DMSO	Dimethyl Sulphoxide
DNA	Deoxyribonucleic Acid
ECL	Enhanced Chemiluminescence
EDTA	Ethylenediaminetetra-acetic acid
eIF	eukaryotic Initiation Factor
ELISA	Enzyme-linked Immunosorbent Assay
EM	Electron Microscopy
ER	Endoplasmic Reticulum
FCS	Foetal Calf Serum
FSB	Final Sample Buffer
G	Guanine
HCC	Hepatocellular Carcinoma
HRP	Horse Radish Peroxidase
HVR	Hypervariable Region

IFN	Interferon
IRES	Internal Ribosome Entry Site
ISDR	Interferon Sensitivity-determining Region
L	Litre
LB	Luria-Bertani Broth
MAb	Monoclonal Antibody
mg	milligram
ml	millilitre
mm	millimetre
NANBH	Non-A, Non-B Hepatitis
NCS	New-born Calf Serum
NES	Nuclear Export Signal
NMR	Nuclear Magnetic Resonance
NS	Nonstructural
nt	nucleotide
NTP	Nucleoside Triphosphate
NTPase	Nucleoside Triphosphatase
OD	Optical Density
ORF	Open Reading Frame
PAb	Polyclonal Antibody (antiserum)
PBS	Phosphate-buffered Saline
PEG	Polyethylene Glycol
RdRp	RNA-dependent RNA polymerase
RNA	Ribonucleic Acid
rpm	revolutions per minute
RT	Room Temperature
SDS	Sodium Dodecyl-Sulphate
SDS-PAGE	SDS-Polyacrylamide Gel Electrophoresis
ss	single-stranded
T	Thymidine
TBE	Tris-Boric acid-EDTA
TLC	Thin-Layer Chromatography
U	Uracil
μg	microgram
μl	microlitre

THE GENETIC CODE

Amino Acid	*Three letter code*	*One letter code*	*Side-chain (R-group)*	*Codons*
Alanine	Ala	A	Neutral-Nonpolar	GCA GCC GCG GCU
Arginine	Arg	R	Basic	CGA CGC CGG CGU
				AGA AGG
Asparagine	Asn	N	Neutral-Polar	AAC AAU
Aspartic Acid	Asp	D	Acidic	GAC GAU
Cysteine	Cys	C	Neutral-Polar	UGC UGU
Glutamine	Gln	Q	Neutral-Polar	CAA CAG
Glutamic Acid	Glu	E	Acidic	GAA GAG
Glycine	Gly	G	Neutral-Nonpolar	GGA GGC GGG GGU
Histidine	His	H	Basic	CAC CAU
Isoleucine	Ile	I	Neutral-Nonpolar	AUA AUC AUU
Leucine	Leu	L	Neutral-Nonpolar	UUA CUC UUG CUU
				CUA CUG
Lysine	Lys	K	Basic	AAA AAG
Methionine	Met	M	Neutral-Nonpolar	AUG
Phenylalanine	Phe	F	Neutral-Nonpolar	UUC UUU
Proline	Pro	P	Neutral-Nonpolar	CCA CCC CCG CCU
Serine	Ser	S	Neutral-Polar	UCA UCC UCG UCU
				AGC AGU
Threonine	Thr	T	Neutral-Polar	ACA ACC ACG ACU
Tryptophan	Trp	W	Neutral-Polar	UGG
Tyrosine	Tyr	Y	Neutral-Polar	UAC UAU
Valine	Val	V	Neutral-Nonpolar	GUA GUC GUG GUU

CHAPTER ONE:

Introduction

1. 1 Clinical Features of HCV Infection

1.1. 1 Brief History of Non-A, Non-B Hepatitis and Discovery of Hepatitis C Virus

The hypothesis that hepatitis was not a single disease, and that very distinct viruses could be responsible for quite similar disease processes, was not proven unequivocally until almost halfway through the twentieth century. Moreover, it did not become clear until the 1970s, when specific diagnostic tests were developed for identifying infection with hepatitis A virus (HAV) and hepatitis B virus (HBV), that most cases of hepatitis following transfusion of blood or blood products were not aetiologically linked with these viruses (Bradley, 1999). The main agent responsible for this so-called post-transfusion non-A, non-B hepatitis (NANBH), a form of hepatitis that was separate from the disease caused by viruses already identified (Alter *et al*, 1975; Prince *et al.*, 1974), was also virus-like in nature (Bradley, 1999). However, unlike HAV and HBV, the agent responsible for NANBH proved to be elusive and remained undetectable by even the most sensitive serologic tests available at the time.

Following years of struggle to isolate the agent, modern techniques of molecular cloning and phage display aided the discovery in 1989 of a novel RNA virus, termed hepatitis C virus (HCV), which was associated with NANBH (Choo *et al.*, 1989). Currently, HCV is the major cause of chronic hepatitis, with an estimated prevalence of 170 million chronic carriers world-wide (Lavanchy *et al.*, 1999). Most importantly, the virus, unlike other known RNA viruses, causes a persistent infection in the majority of infected individuals that can lead to cirrhosis of the liver and hepatocellular carcinoma (HCC) (Houghton, 1996; Saito *et al.*, 1990; Shimotohno, 2000). This fact, coupled with its world-wide prevalence, highlights HCV as a major human pathogen.

1.1. 2 Classification

Comparative analyses of the genomes of several HCV strains have indicated the virus is a member of the *Flaviviridae* (Choo *et al.*, 1989, 1991; Kato *et al.*, 1990; Takamizawa *et al.*, 1991), which comprises the *flaviviruses* and the *pestiviruses*

(Rice, 1996). Although there is no significant overall sequence homology of HCV to other members of this family, alignment of the genomes of representative members of each genus revealed regions of sequence similarity and a comparable genomic organisation (Miller and Purcell, 1990). Members of the *Flaviviridae* possess a positive-sense single-stranded (ss) RNA genome containing a single open reading frame (ORF), which produces a long polyprotein incorporating viral structural proteins at the N-terminus, followed by the nonstructural proteins which are presumed to function in viral replication (Fig. 1; Reed and Rice, 1999). Specifically, the HCV ORF encodes a polyprotein of around 3010 amino acid residues (Choo *et al.*, 1991), a comparable size to that of flaviviruses, such as yellow fever virus (YFV; ~3460 aa), and pestiviruses, such as bovine viral diarrhoea virus (BVDV; ~3960 aa), in agreement with its designation as a member of the *Flaviviridae* (Rice, 1996). Based on additional similarity in the RNA sequence (Bukh *et al.*, 1992; Han *et al.*, 1991), and regarding secondary structures in the 5′-non-coding region (NCR) (Brown *et al.*, 1992), HCV appears to be more closely related to the pestiviruses than the flaviviruses. Furthermore, while flavivirus 5′NCRs are thought to bind ribosomes via 5′-cap structures, analogous to that of most eukaryotic mRNAs (see section 1.3.3), to initiate translation (Rice, 1996), both HCV and pestivirus 5′NCRs appear to act as internal ribosome entry sites (IRESs; see section 1.3.1) which direct the cap-independent translation of the HCV ORF (Fig. 1; Poole *et al.*, 1995; Tsukiyama-Kohara *et al.*, 1992). However, although there are similarities with both flavi- and pestivirus genera, significant differences between members of both genera and HCV recently led to proposal of a third genus, *hepacivirus*, for HCV (Robertson *et al.*, 1998). In fact, HCV appears to be more closely related to a group of recently cloned unclassified viruses, termed the GB agents (Leary *et al.*, 1996; Linnen *et al.*, 1996; Muerhoff *et al.*, 1995; Simons *et al.*, 1995a, 1995b).

An important feature of HCV replication is the rapid generation of virus variants (Gómez *et al.*, 1999), an attribute that is presumably responsible for the wide variability of HCV sequences isolated from infected individuals. Indeed, based on the variation of a small region of the genome, HCV has been classified into six major genotypes which differ by up to 30% (Simmonds *et al.*, 1995), and 5 smaller

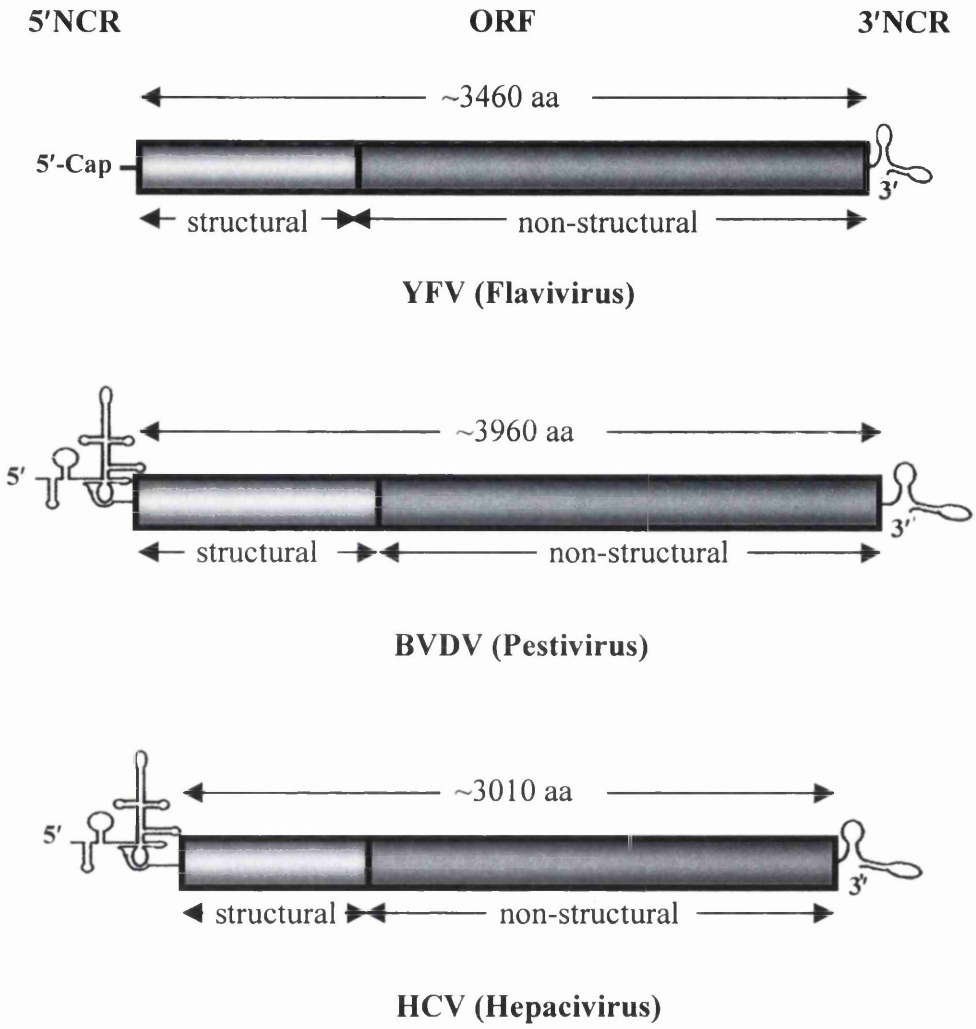

Figure 1: Comparison of representative members from each genus of the *Flaviviridae*. Although each virus genome possesses a similar organisation of their ORFs, and the resulting polyprotein is of comparable length, HCV is more closely related to the pestiviruses than the flaviviruses due in part to the structure and mechanism of translation from the 5'NCR. Sizes and structures of the non-coding genomic termini are very rough approximations (adapted from Bartenschlager, 1999).

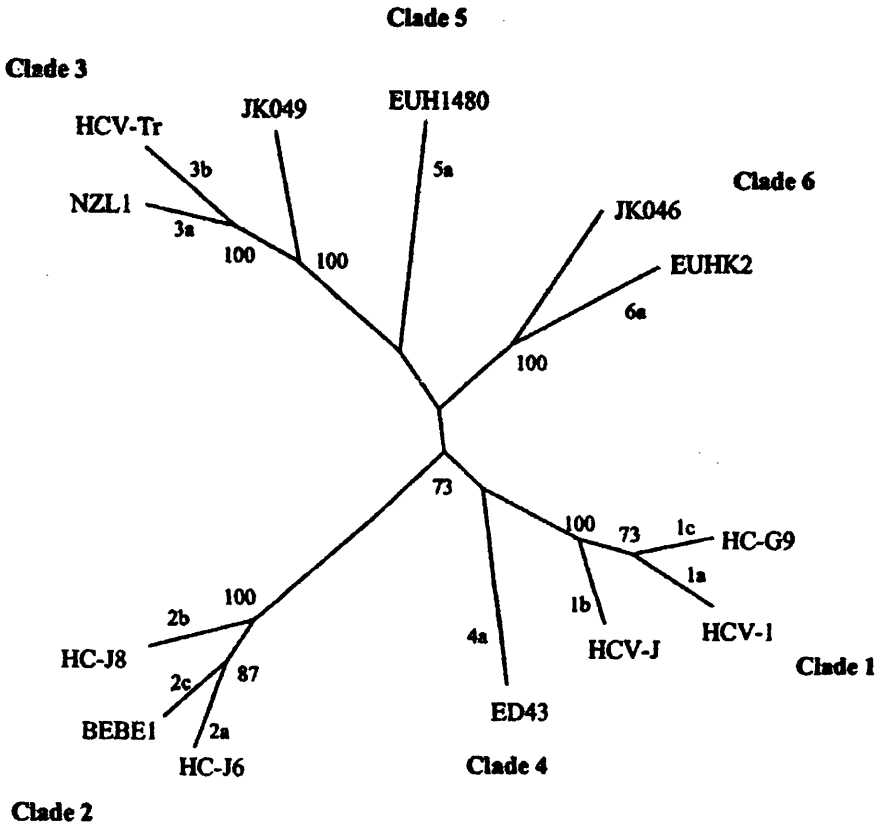

Figure 2: Classification of HCV genotypes. Whole representative genomes were subjected to phylogenetic analysis, allowing delineation of six separate clades for HCV (taken from Robertson *et al.*, 1998)

although many people are already infected with transfused blood contaminated with the agent prior to such screening procedures. Although HCV RNA has been found in seminal fluid, sexual transmission is not common (Thomas, 1999). In contrast, mother-to-baby transmission has been well-documented - however, while some studies suggest that infection takes place during birth or within a few weeks of birth (Ohto *et al.*, 1994), others have indicated transplacental infection occurs during pregnancy (Weiner *et al.*, 1993).

1.1. 4 Clinical Manifestations and Natural History of HCV Infection

Acute infection with HCV is generally not associated with clinical disease, with only ~25% of patients exhibiting clinical symptoms such as jaundice (Houghton, 1996). While rapid, fulminant liver failure has been associated with acute HCV infection in Japan (Yoshiba *et al.*, 1994), it is not common elsewhere. HCV infection becomes chronic in about 75% of patients, as demonstrated by persistence of viral RNA in serum (Shimotohno, 2000). Chronically infected individuals exhibit a slow course of disease development, with most patients exhibiting normal liver histology and no apparent signs of illness ten years post-infection (Lavanchy *et al.*, 1999). Cirrhosis of the liver occurs in less than 20% of chronically infected HCV patients, usually in the second or third decade following infection (Yano *et al.*, 1996). This pathological feature is due to a response of the liver to injury or death of some of its cells by production of intertwining strands of fibrous tissue between which are pockets of regenerating cells. Complications include portal hypertension, ascites (accumulation of fluid in the peritoneal cavity causing abdominal swelling), hepatic encephalopathy, and hepatocellular carcinoma (HCC). In fact, a direct link between HCV and HCC is not as clear as for HBV, and many cases of HCV-associated HCC may be related to cirrhosis (Idilman *et al.*, 1998). Crucially, however, development of HCC occurs in as many as 10% of infected individuals - since there are an estimated 170 million infected individuals world-wide, around 17 million infected individuals are at risk for HCV-associated HCC. Indeed, globally, there are 0.5-1.2 million new cases of HCC confirmed each year (Idilman *et al.*, 1998). The magnitude of this current and potential cancer burden presents an impetus to understand the mechanisms of HCV pathogenesis, including

immunological responses to the virus (see section 1.1.6), and development of therapeutic and/or antiviral strategies (see section 1.1.7). Further complications of HCV pathogenesis include host immune-mediated disorders (see section 1.1.6) and, occasionally, encephalomyelitis and other syndromes associated with the central nervous system (CNS) (see below; Radkowski *et al.*, 2002).

1.1. 5 Sites of Viral Replication and Viral Dynamics

HCV nonstructural proteins and RNA have been detected in the livers of both infected patients and experimentally infected chimpanzees (Blight and Gowans, 1995), confirming the hepatotropic nature of the virus. In addition to liver cells, there is strong evidence that HCV can infect peripheral blood mononuclear cells (PBMCs) (Bartenschlager and Lohmann, 2000). This is thought to be responsible for detection of viral replication in the CNS and reports of HCV-associated pathologies in these tissues (see above; Radkowski *et al.*, 2002). Analyses of viral dynamics during treatment of infected patients with IFN-α suggest a virion half-life of 3-5 hours, and clearance/production rate of 10^{12} particles per day (Neumann *et al.*, 1998; Ramratnam *et al.*, 1999; Zeuzem *et al.*, 1998). Assuming around 10% of hepatocytes in the liver are infected, and there are approximately 2×10^{11} such cells, this corresponds to a virion production rate of ~50 particles per day per cell (Neumann *et al.*, 1998).

1.1. 6 Immune Response

One of the key features of HCV is its propensity to cause chronic infections despite the presence of specific cellular and humoral immunity targeted against the virus (Battegay *et al.*, 1995; Chien *et al.*, 1993; Koziel *et al.*, 1993; Lai and Ware, 1999). Indeed, although immunisation with envelope glycoproteins has been linked with partial protection against homologous challenge in chimpanzees (Choo *et al.*, 1994), HCV infection itself does not appear to elicit protective immunity against re-infection with homologous or heterologous strains of the virus (Okamoto *et al.*, 1994). Interestingly, comparison of the protein sequence of many HCV isolates has revealed two highly variable regions, the first of which is located in the N-terminus

of the E2 envelope glycoprotein and designated hypervariable region 1 (HVR-1) (see section 1.2.4.2; Dubuisson, 1999). A second HVR is found within one of the nonstructural proteins, and may determine response to antiviral therapy with interferon (see sections 1.1.7 and 1.2.5.5). Although it is possible that variation within the HVR-1 of E2 allows differential cell/tissue tropism of HCV (Smith, 1999), it is proposed that E2 variants, likely arising by random mutation and subsequent selection against the pressure of the antibody response, may be a critical mechanism of viral persistence (Farci *et al.*, 1994, 1996; Houghton, 1996; Kato *et al.*, 1993; Shimizu *et al.*, 1996; Weiner *et al.*, 1992). In fact, while antibody responses directed against the capsid protein and a nonstructural protein have been detected in the acute phase of infection (Chang *et al.*, 1999; Hosein *et al.*, 1991), the HVR-1 domain is currently one of only a small number of defined targets for neutralising antibodies (Hijikata *et al.*, 1991a; Kato *et al.*, 1993; Sherlock, 1999; Weiner *et al.*, 1991, 1992). Supporting the notion that that HCV pathogenesis is at least partially immunologically-mediated, an HCV-specific cytotoxic T-lymphocyte (CTL) response has been detected in hepatic infiltrates and the circulatory system of patients chronically infected with HCV (Kita *et al.*, 1993). Hepatocyte death via this mechanism is consistent with studies of immunosuppressed HCV-infected individuals who exhibited high HCV viral loads, yet no liver damage (Chazouilleres and Wright, 1995).

While the main site of viral replication is thought to be hepatocytes, there is strong evidence that HCV can infect PBMCs both *in vivo* and in experimentally infected B- and T-cell lines (section 1.1.5; Bartenschlager and Lohmann, 2000). This may account for the numerous immunological disorders associated with chronic HCV infection, in particular type I and II cryoglobulinaemia which is observed in over 50% of HCV patients (Esteban *et al.*, 1993). Evidence has also been accumulating to suggest that the HCV capsid protein can alter immune responses to the virus by interaction with key mediators of these responses (see section 1.9.6; Lai and Ware, 1999), and can modulate antigen presentation of viral products (Large *et al.*, 1999). However, a recent report suggests neither this core protein, nor the envelope glycoproteins, are able to suppress intrahepatic immune responses in transgenic

mice (Sun *et al.*, 2001). A broad account of host immune system modulation by core protein is presented in section 1.8.2.

1.1. 7 Therapy of Hepatitis C

Therapeutic strategies for chronic HCV infection are rapidly evolving. The present treatments for HCV infection are α-interferon (IFN-α) in combination with the nucleoside analogue ribavarin, or, more recently, a modified (pegylated) form of IFN-α (Glue *et al.*, 2000; Hu *et al.*, 2001; Reddy *et al.*, 2001). However, response rates with these treatment regimens are at best reasonable - 60-80% of patients either do not respond or relapse after cessation of treatment (Theodore and Fried, 1999). In some cases though, the efficacy of treatment for a particular patient may be predicted by analysis of the viral genomic RNA sequence (see section 1.2.5.5; Neumann *et al.*, 1998). Further development of anti-HCV therapeutics has been hampered by the lack of a valid small animal model, as described in the following section.

1.1. 8 Animal Models

It was demonstrated in the 1970s that HCV, at that time known as the NANBH agent, could be transmitted to chimpanzees after intravenous administration of human inocula (Bradley, 1999). In fact, this species represents the only validated and reproducible animal model for the disease caused by HCV. However, due to the endangered status of chimpanzees and the variable course that infection with HCV takes in this animal model, the development of a more practicable small animal model is essential for the study of this virus. It has been suggested that since a recently discovered virus, GBV-B, is highly related to HCV and can infect tamarins, GBV-B infection of tamarins could be used as a surrogate animal model for HCV infection of humans (Bukh *et al.*, 1999). However, there have been few studies comparing individual polyprotein cleavage products from each virus. A recent advance that may alleviate the need for chimpanzees as an animal model and negate the need for a surrogate animal model is the production of transgenic mice with humanised livers (Mercer *et al.*, 2001). Following inoculation with serum from

HCV-infected individuals, mice with these chimeric human livers showed initial increases in viral loads of almost 2000-fold (Mercer *et al.*, 2001). This system could potentially allow development of HCV vaccines and/or further anti-HCV therapeutics.

1. 2 Molecular Properties of HCV

1.2. 1 Virus Morphology

Due to the inability to isolate sufficient quantities of virus from infected individuals and the lack of an efficient cell culture system, classical virological methods have been somewhat redundant in the study of the molecular properties of HCV. Nevertheless, preliminary filtration analysis suggested the diameter of the NANBH agent was between 30 and 60 nm (He *et al.*, 1987). Furthermore, the presence of a lipid envelope was inferred from abrogated infectivity of chloroform-treated inocula (Feinstone *et al.*, 1983). These initial data suggested the agent was a small, enveloped virus. In agreement with these data, electron microscopic (EM) studies on plasma samples containing particularly high HCV RNA titres with specific monoclonal and polyclonal antibodies (MAbs and PAbs, respectively) directed against the putative viral envelope proteins, allowed visualisation of spheroidal particles of diameter 60 to 70 nm (Fig. 3a; Kaito *et al.*, 1994; Prince *et al.*, 1996). Prominent (6-8 nm) spikes were observed on the surface of the virus particles, which probably represent viral attachment/cell fusion proteins embedded in the host-derived virion lipid membrane (Grakoui *et al.*, 1993a). The recent description of HCV virus-like particles (VLPs) expressed via recombinant baculovirus in insect cells (Baumert *et al.*, 1998) represents a valuable approach in the study of many aspects of the HCV structural proteins, owing to the difficulties described above. Such VLPs have morphological, biophysical and antigenic properties analogous to those putative virions isolated from HCV-infected individuals (Fig. 3b; Baumert *et al.*, 1998; Owsianka *et al.*, 2001; Wellnitz *et al.*, 2002). Since HCV structural proteins are presumed to be presented in a native, virion-like conformation, these VLPs also provide a potential vaccine candidate (Baumert *et al.*, 1999). However,

A

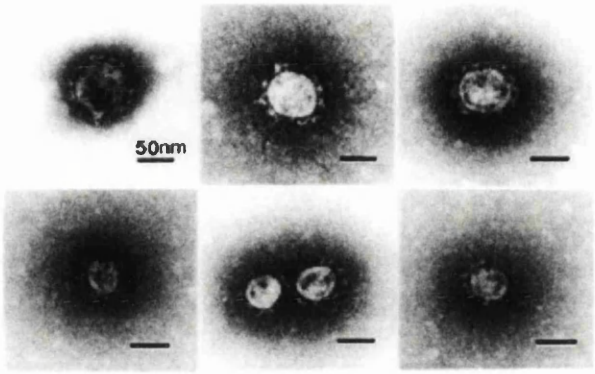

B

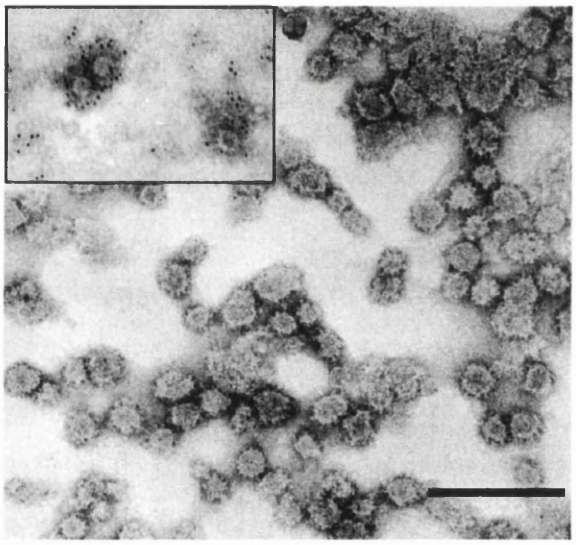

Figure 3: Morphology of HCV virions and virus-like particles (VLPs) as viewed by EM. (A) Virions and putative defective interfering particles isolated from HCV-infected individuals. Top panel: 60-70 nm virions. Lower panel: 30-40 nm putative defective interfering particles (taken from Prince *et al.*, 1996). (B) HCV VLPs isolated from insect cells infected with recombinant baculovirus carrying the HCV structural coding region. Inset: VLPs stained with an MAb directed against the E2 envelope glycoprotein and anti-mouse IgG conjugated to 5 nm gold particles. Bar represents 200 nm (taken from Owsianka *et al.*, 2001)

the system is not without its flaws, and virions are found in intracellular vesicles late in infection and are not secreted (Bartenschlager and Lohmann, 2000).

1.2. 2 Putative HCV Receptors

The first step in any virus replication cycle is the attachment of the viral particle to the host cell, for which a specific cell surface receptor is required. Two cell surface molecules have been suggested as potential HCV receptors: i) CD81, a member of the tetraspanin family that has been shown to interact with the E2 glycoprotein, an HCV-encoded protein that would be expected to play at least some role in cellular entry of HCV (see sections 1.2.4.2 and 1.5.1), as well as virus particles *in vitro* (Pileri *et al.*, 1998); ii) the low density lipoprotein receptor (LDLR), which is thought to be a target of as yet undefined components of the viral envelope that may have incorporated LDLs or very low density lipoproteins (VLDLs) following budding from host cellular membranes (Agnello *et al.*, 1999; Monazahian *et al.*, 1999).

The significance of the interaction of HCV with CD81 has been studied in detail. Binding of HCV E2 to CD81 is mediated by the large extracellular loop of the cell surface molecule (Higginbottom *et al.*, 2000; Flint *et al.*, 1999; Chan-Fook *et al.*, 2000; Patel *et al.*, 2000; Petracca *et al.*, 2000), and a crystal structure for this region has been resolved (Kitadokoro *et al.*, 2001). Binding of E2 to CD81 appears to have a co-stimulatory effect on T-cell activation (Wack *et al.*, 2001). However, expression of CD81 is not restricted to cells susceptible to infection with HCV, and it is not sufficient *in vitro* to permit virus infection (Meola *et al.*, 2000), suggesting the importance of other factors.

The role of the LDLR has attracted less attention and as a result has not been as well-characterised as CD81 at the molecular level. The rational basis for this route of entry was the observation that HCV particles are associated with β-lipoproteins, believed to be recognised and endocytosed via the LDLR (Thomssen *et al.*, 1992). Using *in situ* hybridisation to determine HCV RNA-positive cells, a direct correlation between the cell surface expression of LDLR and the number of infected

cells was seen (Agnello *et al.*, 1999). Furthermore, HCV does not bind COS-7 cells unless they have been transfected with plasmid containing the LDLR-coding sequence (Monazahian *et al.*, 1999) and anti-LDLR antibodies appear to significantly block HCV entry (Agnello *et al.*, 1999). Nevertheless, whether interaction of HCV with CD81 or LDLR leads to a productive infection remains to be determined.

1.2. 3 General Features of the HCV Genome

Since study of HCV is currently hampered by difficulties in establishing *in vitro* and *in vivo* models of viral replication, knowledge of the events following liberation of HCV genomic RNA into the cell has been restricted. However, significant progress in understanding the molecular biology of the virus has been made by expression of cloned viral cDNAs in a variety of systems. HCV possesses a positive-sense ssRNA genome of approximately 9.6 kb, encoding a long polyprotein (section 1.1.2). Following infection of target cells, the HCV ORF is translated into a single polyprotein of 3010-3033 aa, depending on the strain (Choo *et al.*, 1991; Kato *et al.*, 1990; Okamoto *et al.*, 1991; Takamizawa *et al.*, 1991), and subsequently processed by both viral and cellular proteases (Major and Feinstone, 1997). The genomic termini are not translated. Translation of the HCV ORF occurs via an IRES in the 5'NCR (Fukushi *et al.*, 1997; Reynolds *et al.*, 1995), and both NCRs may play important roles in replication and packaging of HCV RNA (Reed and Rice, 1999; Friebe *et al.*, 2001).

The major HCV structural proteins are core protein and two envelope glycoproteins, termed E1 and E2, and are located at the N-terminus of the polyprotein (Fig. 4; Bartenschlager, 1999; Clarke, 1997; Houghton, 1996). A further protein, designated p7, is generated by cleavage at the junction of E2 and the nonstructural proteins, although its function is currently unclear (Lin *et al.*, 1994a; Mizushima *et al.*, 1994; Selby *et al.*, 1994). The remaining polyprotein is cleaved by HCV-encoded proteases to produce four major nonstructural proteins termed NS2, NS3, NS4 and NS5 - two of these proteins (NS4 and NS5) undergo further processing to produce smaller polypeptides called NS4A, NS4B, NS5A and NS5B (Fig. 4; Bartenschlager,

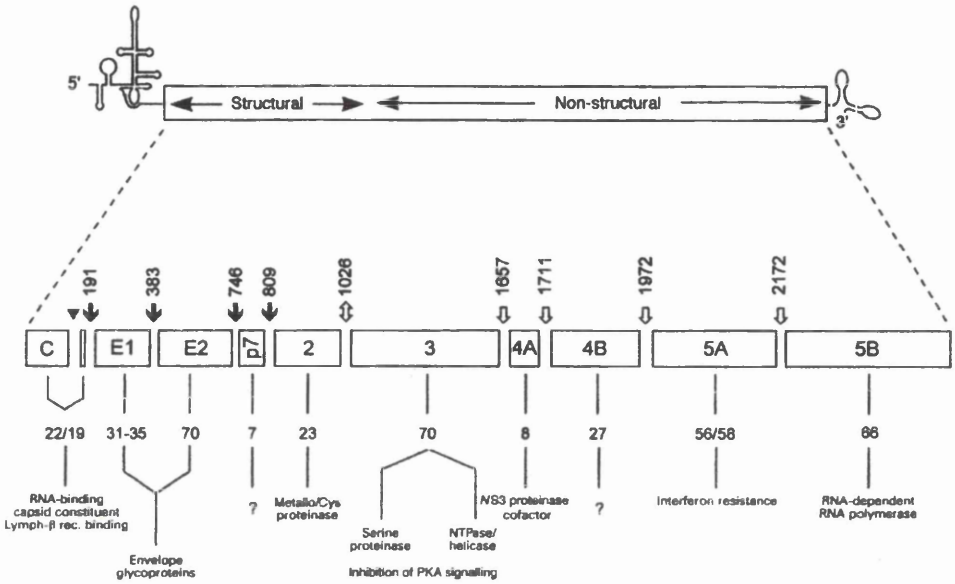

Figure 4: General features of the HCV genome, polyprotein processing and properties of individual cleavage products. 5′ and 3′NCRs flank the HCV ORF, which generates a single polyprotein with structural proteins (capsid protein C or core, envelope glycoproteins E1 and E2, and p7) grouped at the N-terminus followed by the nonstructural proteins (NS2-5B). Cleavage sites for host cell signalase (↓), the NS2-3 proteinase (⇕), the NS3/4A proteinase (⇓), and an unknown cellular proteinase (▼) are highlighted. Approximate molecular weights (in kDa) and properties of each protein are indicated (taken from Bartenschlager, 1999).

1999; Clarke, 1997; Houghton; 1996). A homologue of NS1, a protein of unknown function present in flavivirus and pestivirus genomes, is not present in HCV (Rice, 1996). Most of the HCV nonstructural proteins have enzymatic activity that are critical for viral replication or are co-factors for such enzymes, although NS4B and NS5A have no well-defined functions as yet (Rosenberg, 2001). The HCV polyprotein cleavage products are individually described in the following sections.

1.2. 4 HCV Structural Proteins

1.2.4. 1 Core

The general properties, putative pathogenic roles, and interactions of core protein are discussed in detail in sections 1.7 to 1.9.

1.2.4. 2 E1 and E2

E1 and E2 are released from the viral polyprotein by host cell signal peptidases and are heavily glycosylated (Miyamura and Matsuura, 1993). The addition of these carbohydrate moieties slows the migration of E1 and E2 in polyacrylamide gels so that they appear to have larger molecular weights than those predicted based on protein sequence alone (~30-35 and 70 kDa, respectively) (Reed and Rice, 1999). Both E1 and E2 contain C-terminal hydrophobic domains that appear to be inserted in the ER, while the remainder is translocated into the ER lumen (Reed and Rice, 1999). E1 has been shown to associate via its C-terminus with core protein (see section 1.9.3; Lo *et al.* 1996), while E2 associates with NS2 (Matsuura *et al.*, 1994; Selby *et al.*, 1994). Although these interactions may play important roles during HCV infection, the interaction between E1 and E2 themselves has been given most attention since this interaction is likely to be critical in viral morphogenesis. Native E1-E2 complexes appear to be held together by non-covalent interactions (Deleersnyder *et al.*, 1997; Dubuisson *et al.*, 1994; Matsuura *et al.*, 1994; Ralston *et al.*, 1993), although heterogenous disulphide-linked aggregates have also been observed (Dubuisson *et al.*, 1994; Grakoui *et al.*, 1993a). E2 is apparently required for proper folding of E1 (Michelak *et al.*, 1997), and contains a C-terminal transmembrane domain that is thought to be an ER-retention signal (Cocquerel *et*

al., 1998). This domain is presumably masked during assembly of viral particles allowing egress through the secretory pathway (Reed and Rice, 1999). The N-terminal region of E2 exhibits a high degree of variability, representing the most variable region of the HCV genome (section 1.1.6). E2 has also been shown to inhibit the activity of double-stranded RNA-activated protein kinase R (PKR), possibly due to the presence of a sequence in E2 that is similar to that of an autophosphorylation site in PKR (Taylor *et al.,* 1999), though a detailed mechanism is currently unclear (Taylor *et al.,* 2001). This may nevertheless be important as a further strategy to evade the host antiviral response. Possible receptors for virion-associated E2, cell-surface molecules CD81 and the low density lipoprotein receptor (LDLR), have been implicated in cell attachment and/or entry of HCV (section 1.2.2; Agnello *et al.*, 1999; Monazahian *et al.*, 1999; Pileri *et al.* 1998). However, the role of E1 should not be ignored - indeed, both HCV glycoproteins appear to be required in an HCV cell-fusion assay (Matsuura *et al.*, 2001; Takikawa *et al.,* 2000). Further discussion of the role of the HCV glycoproteins in virus attachment/entry is presented in section 1.5.1 as part of an overview of the viral replication cycle.

1.2.4. 3 p7

Although the cleavage events at the core/E1 and E1/E2 junctions occur rapidly during or immediately after translation, processing is delayed at the E2-p7-NS2 junctions, while it is incomplete at the E2-p7 junction, resulting in the generation of fully processed E2 and uncleaved E2-p7 (Lin *et al.*, 1994a; Mizushima *et al.*, 1994; Selby *et al.*, 1994). The significance of fully cleaved p7 and E2-p7 regarding HCV virion morphogenesis or other functions pertinent to the viral replicative cycle are as yet undetermined. Interestingly, a comparable inefficient cleavage is seen at a similar position in pestiviruses BVDV and classical swine fever virus (CSFV), although analyses of these virions suggest neither p7 nor E2-p7 are critical structural components (Elbers *et al.*, 1996). Nevertheless, it has yet to be confirmed that HCV p7 and E2-p7 follow this trend.

1.2. 5 HCV Nonstructural Proteins

1.2.5. 1 NS2

NS2 is a hydrophobic protein with an apparent molecular weight of 23 kDa (Reed and Rice, 1999). Although NS2 is dispensable in HCV sub-genomic replicon-expressing cell lines (see section 1.6.2; Lohmann *et al.*, 1999a), it is apparently required *in vivo* (Kolykhalov *et al.*, 2000). Some studies suggest NS2 is a transmembrane protein with its C-terminus protruding into the lumen of the ER and its N-terminus in the cytosol (Santolini *et al.* 1995) - however, these data do not correlate with the presence of a putative signal sequence at the p7/NS2 junction (Grakoui *et al.,* 1993c; Mizushima *et al.,* 1994). The exact function of NS2 in the viral replication cycle is unclear, although unexpected proteinase activity, in conjunction with the N-terminus of NS3, has been attributed to the C-terminus of the protein, mediating cleavage at the NS2/NS3 junction (Grakoui *et al.,* 1993c; Hijikata *et al.*, 1993). Cleavage at this site is stimulated by zinc and inhibited by metal chelators such as EDTA, suggesting NS2 is a metalloprotease (Grakoui *et al.,* 1993c; Hijikata *et al.,* 1993). However, the conserved motifs and structure of active centre are more consistent with that of a cysteine protease (Gorbalenya and Snijder, 1996; Reed and Rice, 1999). NS2 does not appear to influence downstream cleavage events, since mutations which abolish activity of the NS2-3 protease have little or no effect on further processing of the HCV polyprotein (Grakoui *et al.*, 1993c; Hijikata *et al.*, 1993).

1.2.5. 2 NS3

NS3 is a moderately hydrophilic protein of around 70 kDa (Reed and Rice, 1999). It has been shown to be essential, both in HCV sub-genomic replicon-expressing cell lines (Lohmann *et al.*, 1999a), and *in vivo* (Kolykhalov *et al.*, 2000). Consistent with these data, NS3 shows high sequence conservation (> 80%) amongst HCV strains (Kwong *et al.*, 1999). The protein is a multi-functional enzyme that consists of a serine proteinase domain in the N-terminal 181 aa (Bartenschlager, 1999; Grakoui *et al.*, 1993c), and a nucleic acid-stimulated nucleotide triphosphatase (NTPase)/RNA helicase domain in the C-terminal 450 aa (D'Souza *et al.* 1995; Gwack *et al.* 1996;

Kwong *et al.*, 1999). Although one group has suggested internal processing of the NS3 protein occurs in insect and mammalian cells (Shoji *et al.*, 1998), there is little evidence to suggest that the serine proteinase and helicase domains are separated by further processing (DeFranscesco and Steinkühler, 1999). Nevertheless, it is unclear whether the two distinct enzymes residing in the HCV NS3 protein are linked because of a functional interdependence between the two domains, or have evolved fortuitously (Kwong *et al.*, 1999). The structure of the full-length NS3 protein in complex with one of its reputed co-factors, NS4A (see section 1.2.5.3), has been solved. These data suggest a tight association of the enzyme with the co-factor (Yao *et al.*, 1999). The HCV NS3 helicase is one of the most studied viral RNA helicases. When compared with all others characterised so far, observations suggest that this enzyme is unique, acting in a 3′ → 5′ direction (Tai *et al.*, 1996) and it is able to unwind RNA-RNA as well as DNA-DNA duplexes and RNA/DNA heteroduplexes *in vitro* (Gwack *et al.*, 1996, 1997; Tai *et al.*,1996; Wardell *et al.*, 1999). Related viruses, including pestiviruses such as BVDV, and flaviviruses such as YFV and West Nile virus (WNV), encode a similar RNA helicase in their homologous NS3 proteins (Warrener and Collett, 1995; Warrener *et al.*, 1993; Wengler and Wengler, 1991), suggesting that the NS3 helicase plays an important role in the viral replication cycle (Kadaré and Haenni, 1997; Miller and Purcell, 1990). However, the actual role of the NS3 helicase in the viral replication cycle or pathogenesis is currently unknown. It is possible that the NS3 helicase acts to unwind complimentary negative-stranded replication intermediates and positive-stranded genomic RNA prior to packaging (Kwong *et al.*, 1999). There is also a possibility that the NS3 protein is involved in unwinding highly stable secondary structures in the HCV genome, such as the IRES within the 5′NCR, the 3′X region (see section 1.4.1), or clusters of unusually conserved RNA sequence which may represent conserved stem-loops in the ORF (see section 1.7.4; Han and Houghton, 1992; Walewski *et al.*, 2001). This function presumably would allow more efficient access of the viral replicase complex to HCV genomic RNA. The interaction of the NS3 protein with the 3′NCR (see section 1.4.3; Banerjee and Dasgupta, 2001) could be viewed as adding credibility to either hypothesis, if this interaction merely serves to orientate the helicase prior to processive unwinding of complimentary strands, or

scanning of the genome for stable secondary structures. The recently elucidated crystal structure of the HCV helicase suggests it consists of three distinct structural domains separated by clefts in the protein, forming a Y-shaped structure (Fig. 5; Cho *et al.*, 1998; Yao *et al.*, 1997).

The NS3 protein is also implicated in modulation of cellular processes. Expression of NS3 in NIH3T3 cells led to cellular transformation and, when inoculated into nude mice, the NS3-transfected cells caused tumourigenesis (Sakamuro *et al.*, 1995). These results correlate with a specific interaction and inhibition of the catalytic subunit of cAMP-dependent protein kinase A (PKA C-subunit) (Aoubala *et al.*, 2001; Borowski *et al.*, 1996, 1997), a molecule closely linked with cellular signal transduction (Francis and Corbin, 1994).

1.2.5. 3 NS4A

NS4A is a hydrophobic protein of ~8 kDa (Reed and Rice, 1999) which acts in conjunction with NS3 as a co-factor in its proteinase activity (section 1.2.5.2). NS4A is required for efficient processing at the NS3/4A, 4A/4B, and 4B/5A sites, while stimulating cleavage at the NS5A/5B site (Bartenschlager *et al.*, 1994; Failla *et al.*, 1994; Lin *et al.*, 1994b; Tanji *et al.*, 1994). NS4A may also anchor NS3, and perhaps other members of the replication complex, to cellular membranes via its N-terminal hydrophobic domain (Hijikata *et al.*, 1993; Kim *et al.*, 1996). The protein interacts directly with NS5A and regulates its phosphorylation by a cellular kinase (see section 1.2.5.5; Asabe *et al.*, 1997; Tanji *et al.*, 1995), although the relevance of this function is currently unclear (Bartenschlager and Lohmann, 2000).

1.2.5. 4 NS4B

NS4B is a hydrophobic protein of approximately 30 kDa (Reed and Rice, 1999). Kinetic studies of HCV polyprotein cleavage show that the last cleavage event releases NS4B from NS5A (Bartenschlager *et al.*, 1994). While it is known that NS4B is ER-associated and complexed with other HCV nonstructural proteins in

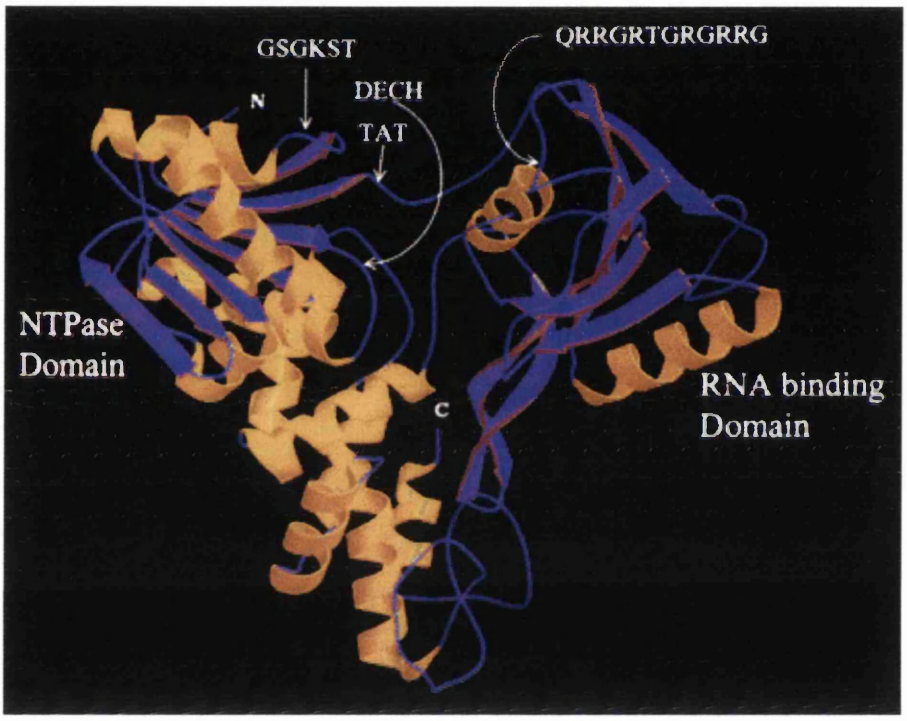

Figure 5: Three-dimensional structure of the HCV NS3 helicase. The protein consists of three distinct structural domains separated by a cleft, forming a Y-shaped structure. The cleft functions as the NTP binding site and is shaped by discontinuous epitopes on the protein sequence containing conserved motifs as shown (taken from Cho *et al.*, 1998)

transfected cells, its function in the HCV replication cycle is currently unknown (Hugle *et al.*, 2001; Lin *et al.*, 1997).

1.2.5. 5 NS5A

NS5 is proteolytically processed by the NS3/4A proteinase to produce the mature proteins NS5A (p56/p58 depending on phosphorylation) and NS5B (p65). Both are localised in nuclear periplasmic membranes suggesting they may be components of a membrane-bound replication complex (Hwang *et al.*, 1997). Phosphorylation of NS5A is mediated by an as yet undetermined cellular kinase (Ide *et al.*, 1997; Reed *et al.*, 1997; Tanji *et al.*, 1995). The function of NS5A is currently unclear, but may act as a regulator of replication by analogy with phosphoproteins from other RNA viruses (Bartenschlager and Lohmann, 2000, Kapoor *et al.*, 1995; Reed *et al.*, 1998). Nevertheless, a role for NS5A in disruption of antiviral resistance has been suggested by reports of NS5A-mediated inactivation of interferon (IFN)-induced protein kinase (PKR) (Gale *et al.*, 1997, 1998). This is potentially a major mechanism of immune avoidance by HCV since PKR is a critical factor in the host response to IFN through its phosphorylation of the α-subunit of eukaryotic initiation factor 2 (eIF2α) (Goodburn *et al.*, 2000). Interestingly, analyses of HCV RNA isolated from patients undergoing IFN therapy suggested the presence of a cluster of mutations in the C-terminal half of NS5A (Enomoto *et al.*, 1995), in addition to the HVR-1 (section 1.3.4.2). This was mapped further to aa 2209 to 2248 in this region, and designated the interferon sensitivity-determining region (ISDR; Enomoto *et al.*, 1995, 1996). Additional analyses by independent groups suggest ISDR sequences may affect the response to IFN treatment, but they do not seem to have a general predictive value in determining the outcome of IFN treatment (Pawlotsky *et al.*, 1998; Reed and Rice, 1999). NS5A has also recently been shown to associate with lipoproteins at the surface of storage sites for such proteins where HCV core protein is also found (Shi *et al.*, 2002).

1.2.5. 6 NS5B

NS5B was first recognised as the putative viral polymerase due to the presence of a conserved motifs characteristic of all known RdRps (Lohmann *et al.,* 1997; Reed and Rice, 1999). Accordingly, NS5B has been shown to copy full-length HCV genomic RNA (Oh *et al.,* 1999). Although there is no significant *in vitro* specificity (Behrens *et al.,* 1996; Lohmann *et al.,* 1997), it appears that the HCV 3′X and poly(U)/polypyrimidine regions of the 3′NCR, and high concentrations of GTP, can stimulate primer-dependent synthesis (Lohmann *et al.*, 1999b; Luo, 1999). It is presumed that transcription initiation via NS5B, in co-operation with other virally encoded and host proteins, occurs at both genomic termini using positive- and negative-stranded viral RNAs as templates (Rosenberg, 2001). Interestingly, however, NS5B appears to only bind stable stem-loops structures in its own coding region *in vitro*, together with a small portion of a poorly conserved variable region in the 3′NCR which may confer genotype specificity, and not the 5′NCR or the remainder of the 3′NCR (Cheng *et al.*, 1999). NS5B co-factors, in addition to the localisation of the replication complex in specific subcellular compartments, are presumed to confer added specificity for NS5B on HCV RNA (Rosenberg, 2001). In fact, several HCV nonstructural proteins can be co-immunoprecipitated with NS5B antibodies, implicating NS3, NS4A, and NS5A in the replication process (Ishido *et al.,* 1998).

1. 3 The 5′ Non-coding Region

1.3. 1 General Properties

The HCV genome is flanked by untranslated 5′ and 3′ termini (section 1.2.3). These NCRs are presumed to contain the signals necessary for initiation and termination of viral replication (Rosenberg, 2001). The 5′NCR has been shown to be capable of forming extensive secondary structures (Fig. 6; Brown *et al.*, 1992) - this highly ordered structure acts as an IRES, that initiates translation of the HCV ORF (Hellen and Pestova, 1999). This mechanism of translation initiation was previously documented for picornaviruses (Jackson *et al.*, 1990) and some eukaryotic mRNAs (Hellen and Pestova, 1999), though it is distinct from most eukaryotic mRNAs that

initiate translation via 5′-cap structures and ribosomal scanning (see section 1.3.3). The 5′NCR is the most conserved region of the entire genome, indicative of its importance in the HCV replication cycle.

1.3. 2 Structure/function Studies

The HCV 5′NCR is typically 341 nts in length, although an additional sequence of 8 nts has been reported by one group (Trowbridge and Gowans, 1998). The IRES is contained within an approximately 300 nt region immediately upstream of the initiation codon. The secondary structure in the 5′NCR is not only conserved amongst HCV genotypes, but also in GBV-B and pestiviruses (Reed and Rice, 1999). In fact, the HCV IRES can substitute for that of BVDV (Frolov *et al.*, 1998) as well as poliovirus (Lu and Wimmer, 1996). Similar features amongst some members of the *Flaviviridae* include a large stem loop (III), a pseudo-knot near the initiation codon, and, in HCV and GBV-B, a smaller stem-loop (IV) which contains the initiation codon (Fig. 6; Honda *et al.*, 1996a). Nuclear magnetic resonance (NMR) and EM methods have allowed partial visualisation of this organisation of the HCV IRES (Beales *et al.*, 2001; Lukavsky *et al.,* 2000). IRES activity seems to require the entire 5′NCR, with the possible exception of stem-loop I (Honda *et al.*, 1996b; Reynolds *et al.*, 1995; Rijnbrand *et al.*, 1995; Tsukiyama-Kohara *et al.*, 1992). While some studies suggest the requirement of a small portion of the core-coding sequence for full IRES activity (Honda *et al.*, 1996b; Lu and Wimmer, 1996; Reynolds *et al.*, 1995), others indicate the core-coding sequence can down-regulate translation (see section 1.3.5; Wang *et al.*, 2000). However, whether the core-coding sequence is a real component of the IRES, or whether it serves merely to prevent unfavourable base-pairings of the IRES with downstream sequences which disturb its secondary structure, is not clear. HCV IRES activity appears to be cell cycle dependent, since expression of a reporter gene under its translational control was found to be greatest in mitotic and lowest in quiescent (G_0) hepatocytes (Honda *et al.*, 2000). This has been confirmed in the recently described HCV sub-genomic replicon-expressing cell lines (see section 1.6.2; Lohmann *et al.*, 1999a; Pietschmann *et al.*, 2001). Further studies in such cell lines have shown that sequences upstream of the IRES in the 5′NCR are required for replication (Friebe *et*

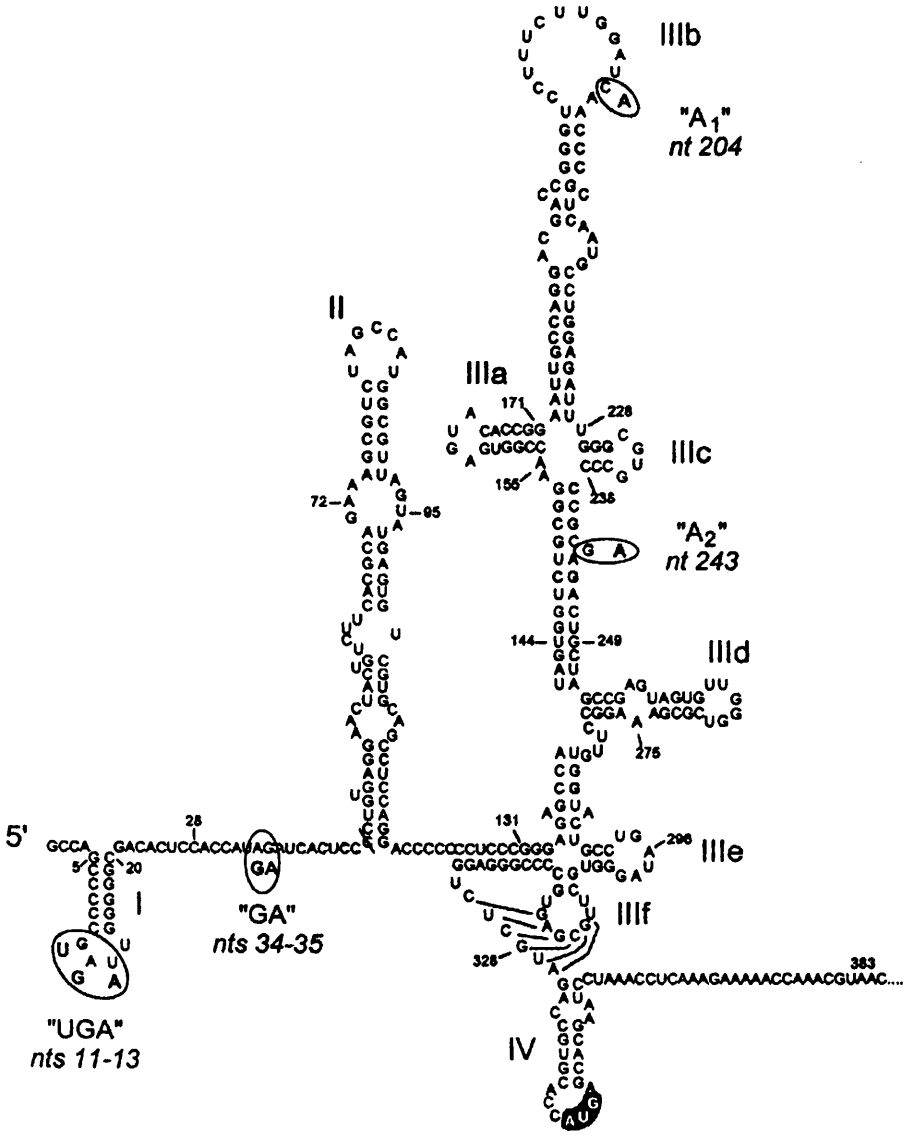

Figure 6: Proposed secondary and tertiary structure of the HCV 5′NCR, together with a small portion of the core-coding sequence, from a genotype 1b infectious clone (HCV-N). Major structural domains are labelled with Roman numerals and the initiator AUG codon within stem-loop IV is highlighted. Circled nucleotides represent differences with the genotype 1a HCV-H strain (taken from Honda *et al.*, 1999).

al., 2001), suggesting that the 5'NCR plays a role in the replication cycle of HCV other than that of translation of the viral polyprotein.

1.3. 3 Translation of Eukaryotic mRNAs

In contrast to IRES-mediated translation, initiation of translation of most eukaryotic mRNAs is dependent on the modified m^7G 5'-terminal 'cap'. A step-wise model for this process has been proposed (Fig. 7; Merrick, 1992), and is presented here for comparison with IRES-mediated translation and for future reference: i) a 43S complex forms by binding of eIF3 and an eIF2-GTP-Met-tRNA complex to the 40S ribosomal subunit; ii) eIF4F binds the capped 5'-end of the mRNA and, together with eIF4A and eIF4B unwinds inherent secondary structure in this region to create a binding site for the 43S complex; iii) the 43S complex scans downstream of the 5'-end and forms a stable 48S complex at the first AUG codon - at this point, eIF5 stimulates GTP hydrolysis, eIFs are released, and the initiator Met-tRNA is left in the P site of the 40S subunit; iv) the 60S ribosomal subunit then joins the 40S subunit to permit synthesis of the polypeptide.

1.3. 4 Interaction of eIFs and Other Cellular Factors with the HCV 5'NCR

Unlike most eukaryotic mRNAs (see above) and the IRESs of picornaviruses such as encephalomyocarditis virus (EMCV), the HCV IRES does not appear to interact with, or functionally require, many of the canonical eIFs (Pestova *et al.*, 1998). Nevertheless, translation is enhanced by a specific interaction of eIF3 with stem-loop III (Sizova *et al.*, 1998), and there is a functional requirement for two of the subunits of eIF2 (eIF2χ and eIF2Bχ) in a cellular context (Kruger *et al.*, 2000). A specific interaction of the IRES with the 40S ribosomal subunit has been reported, which is thought to drive formation of the ternary complex to initiate protein synthesis in a manner akin to that described above (Kieft *et al.*, 2001). The accumulating evidence suggests HCV translation initiation occurs via a unique mechanism that has many features in common with prokaryotic translation, with the IRES functionally analogous to the Shine-Delgarno sequence (Pestova *et al.*, 1998). This conserved stretch of six nucleotides base pairs with the 16S rRNA in the

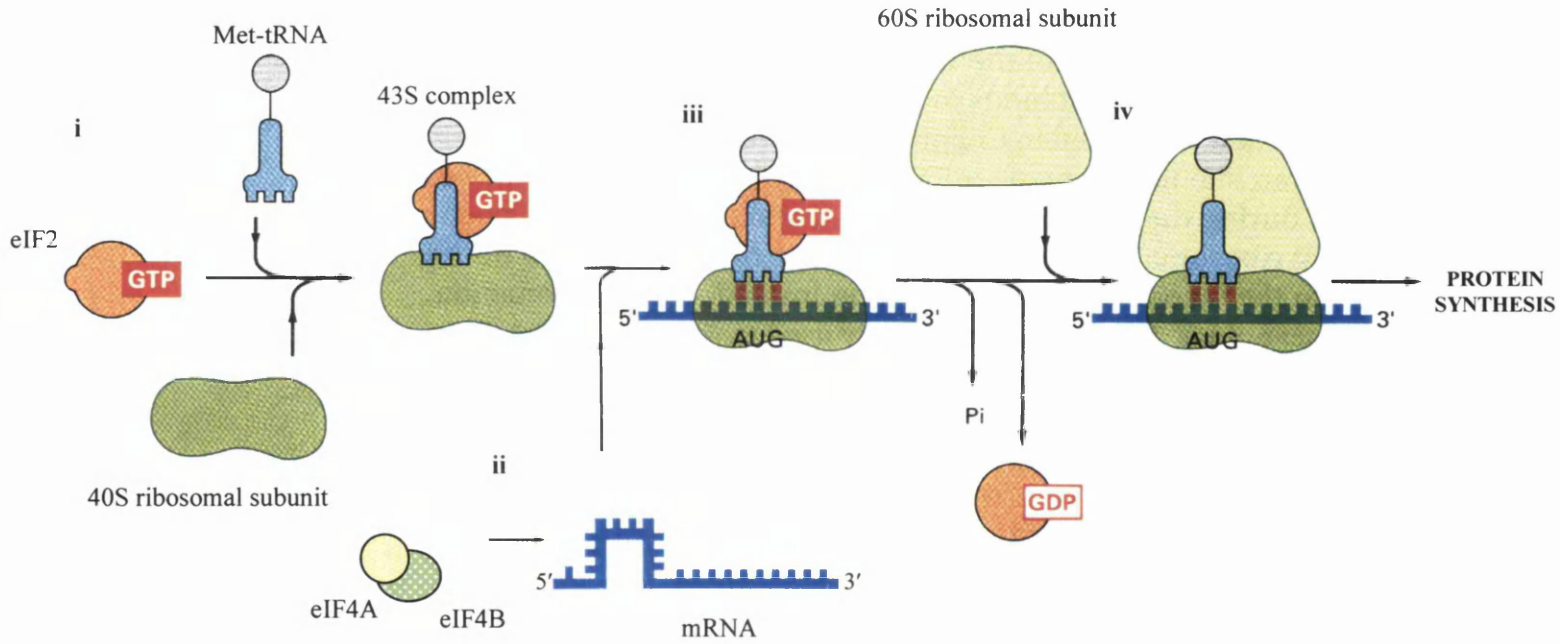

Figure 7: General scheme of eukaryotic translation initiation: i) an eIF2-GTP-Met-tRNA complex binds to the 40S ribosomal subunit to produce a 43S complex; ii) eIF4F binds the capped 5′-end of the mRNA (not shown) and, together with eIF4A and eIF4B, unwinds the secondary structure in this region (denoted by a kink in the mRNA) to create a binding site for the 43S complex; iii) the 43S complex scans downstream of the 5′-end and forms a stable 48S complex at the first AUG codon - at this point, eIF5 stimulates GTP hydrolysis, eIFs are released, and the initiator Met-tRNA is left in the P site of the 40S subunit; iv) the 60S ribosomal subunit then joins the 40S subunit to permit synthesis of the polypeptide (adapted from Alberts *et al.*, 1994).

bacterial small ribosomal subunit, thereby correctly positioning the initiator AUG in the ribosome (Alberts *et al.*, 1994). It is possible that the redundancy of several eIFs regarding HCV IRES translation reflects its complex structure, which may induce conformational changes in the 40S ribosomal subunit to align the P site with the initiation codon (Rosenberg, 2001). Interestingly, three-dimensional structures of the IRES in complex with the 43S particle suggest binding induces a significant conformational change in the secondary structure of the IRES itself (Kieft *et al.*, 1999; Spahn *et al.*, 2001).

Other cellular proteins that have been shown to specifically interact with the 5′NCR include polypyrimidine tract binding protein (PTB) (Ali and Siddiqui, 1995), heterogenous nuclear protein L (hnRNP L) (Hahm *et al.*, 1998), the La autoantigen (Ali and Siddiqui, 1997), and ribosomal protein S5 (Fukushi *et al.*, 2001). Interaction of these proteins with the 5′NCR is likely to occur in a complex, and may have effects on translation and/or replication of the HCV genome (Reed and Rice, 1999). The possible requirements of cellular factors for IRES activity may explain the dependence on the cell cycle (section 1.3.2; Honda *et al.*, 2000; Pietschmann *et al.*, 2001), since the abundance of these proteins may alter in different points in the cell cycle. Nevertheless, the extent to which these proteins alter translation and/or replication, if indeed at all, will require testing in a currently unavailable cell culture system for HCV. Interestingly, the HCV 5′NCR is not functional in insect cells (Wang *et al.*, 1997). This is not due to a block in transcription of recombinant baculoviruses containing the HCV IRES, possibly suggesting that specific cellular factors are lacking in insect cells that mediate translation initiation from the HCV IRES in mammalian cell systems (Wang *et al.*, 1997).

1.3. 5 Effect of Core Protein or its Coding-sequence on IRES Activity

A specific interaction of core protein with the 5′-end of the HCV genome has been reported (see section 1.9.1; Fan *et al.*, 1999; Shimoike *et al.*, 1999), which was further shown in one such study to suppress translation of HCV coding sequences (Shimoike *et al.*, 1999). This effect was dose-dependent and specific to the IRES of

HCV, since modulation of translation by core protein following substitution of the HCV IRES for the EMCV IRES in the reporter constructs used was not seen. These data could suggest that the specific interaction of core protein with the 5′NCR is the signal to switch from translation/replication to virion assembly, or it could indicate an involvement in the establishment and/or maintenance of viral persistence. However, other studies have suggested that it is the core-coding sequence that can modulate IRES activity (Rijnbrand *et al.*, 2001; Wang *et al.*, 2000). Thus, the actual role of core protein in HCV IRES-mediated translation is currently unclear. A PTB-binding site has also been discovered at the 3′-end of the core-coding sequence - this strongly inhibited HCV 5′NCR-mediated translation in a reporter assay, but the effect could be relieved by addition of the 3′X region to the 3′end of the reporter constructs (Ito and Lai, 1999).

1. 4 The 3′ Non-coding Region

1.4. 1 General Properties

Although the first full-length clone of the HCV genome contained a poly(A) tail at its 3′-terminus (Han *et al.*, 1991), this was probably an artifact attributable to the methods used in isolation of HCV RNA (Reed and Rice, 1999). It was only relatively recently that alternative techniques indicated the 3′ terminus of HCV is a tripartite structure composed of a poorly conserved ~40 nt sequence termed the variable region, a poly(U)/polypyrimidine tract of widely varying length, and a highly conserved 98 nt sequence known as the 3′X or X-tail, which has been shown to form a highly stable elaborate stem-loop structure (Fig. 8; Blight and Rice, 1997, Kolykhalov *et al.*, 1996; Tanaka *et al.*, 1995; Yamada *et al.*, 1996). The highly conserved nature of the 3′X suggests it may play a crucial role in the production of negative-sense RNA intermediates, as previously shown for many positive-strand viruses (Reed and Rice, 1999). This hypothesis is supported by the inability of HCV RNAs lacking the 3′X to replicate in chimpanzees (Forns *et al.*, 2000; Kolykhalov *et al.*, 2000; Yanagi *et al.*, 1999), although some low level replication has been observed with HCV RNAs that terminate with poly(A) or within the

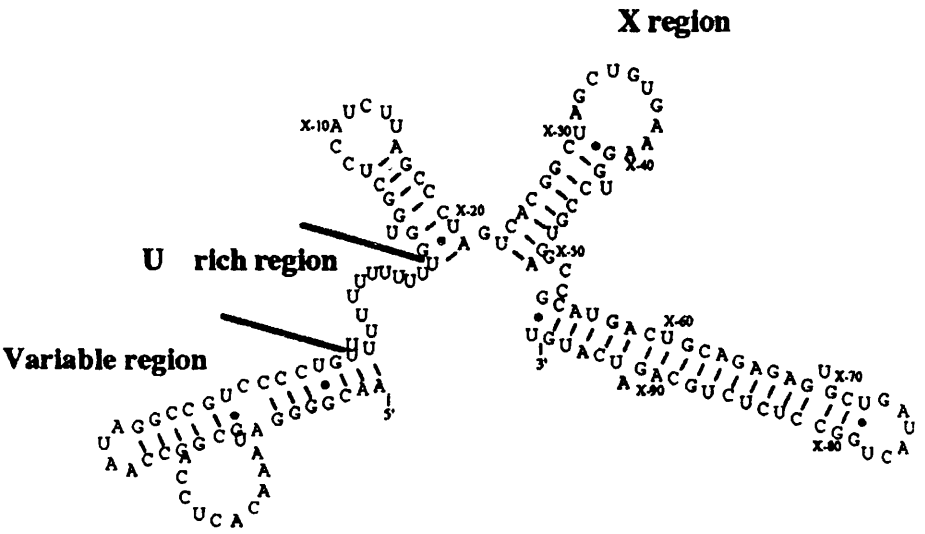

Figure 8: Predicted secondary structure of the HCV 3′NCR. Computer-assisted folding analysis suggests a tripartite structure, consisting of a poorly conserved sequence termed the variable region, a poly(U) tract of varying length (commonly interspersed with polypyrimidine stretches, although not shown above), and a highly conserved 98 nt sequence known as the 3′X tail (designated X region above) which forms three energetically stable stem-loop structures (taken from Ito and Lai, 1997)

poly(U)/pyrimidine tract in Huh-7 (Yoo *et al.*, 1995) and HepG2 human hepatocyte cell lines (Dash *et al.*, 1997).

1.4. 2 Cellular Factors Binding to 3'NCR

In addition to its interaction with the 5'NCR, a specific interaction of the 3'NCR with PTB has been reported, with possible effects on replication (Ito and Lai *et al.*, 1997; Tsuchihara *et al.*, 1997). Binding of PTB to the 3'NCR has also been implicated in low level stimulation of HCV or EMCV IRES activity, suggesting cross-talk between the genomic terminii (Ito *et al.*, 1998a). A ribosomal protein (L22) has been reported to specifically interact with the 3'X tail (Wood *et al.*, 2001). Evidence is accumulating for diverse extra-ribosomal roles for this group of proteins. However, like PTB, this protein appears to enhance translation from the 5'NCR (Wood *et al.*, 2001), further highlighting possible cross-talk between the two NCRs. Glyceraldehyde-3-phosphate dehydrogenase (GAPDH), La, hnRNP C, and other unidentified cellular proteins have also been shown to interact with the 3'NCR (Luo, 1999; Petrik *et al.*, 1999; Spangberg *et al.*, 1999). As for all RNA-protein and protein-protein interactions regarding HCV, the actual role of the interactions of the above proteins with the 3'NCR in the HCV replication cycle awaits development of an efficient cell culture system for the virus.

1.4. 3 Interaction of HCV NS3 Helicase with 3'NCR

Recently, a specific interaction of the HCV NS3 protein with the 3'-termini of both positive- and negative-stranded HCV RNA has been demonstrated (Banerjee and Dasgupta, 2001), suggesting a role for the HCV helicase in replication of both HCV genomic RNA and negative-stranded intermediates. Using UV cross-linking, an interaction of full-length NS3 or the helicase domain alone with radiolabelled negative-stranded HCV 3'NCR RNA that could be competitively inhibited by homologous, but not heterologous, unlabelled RNA probes was shown (Banerjee and Dasgupta, 2001). The region required for interaction with negative sense HCV RNA appeared to be a predicted stem-loop at the extreme 3'-end. NS3 seemed to have a less specific binding site on positive-sense HCV 3'NCR RNAs, requiring the

entire region for binding. Nevertheless, a lack of binding of HCV 5′NCR in the positive or negative orientation (Banerjee and Dasgupta, 2001) confirmed the specificity of the interaction of the NS3 helicase domain with the 3′NCR in both orientations. Since other regions of the HCV genome were not tested in this study, it is not clear whether sequences in the HCV ORF are also specifically recognised by NS3.

1. 5 HCV Replication Cycle

Due to the lack of a convenient and reproducible animal model (section 1.1.8) and difficulties in establishing an efficient cell culture system for HCV, the current model of the HCV replicative cycle is based primarily on analogies with related viruses, studies of the properties of HCV RNA in various systems, and characterisation of recombinant HCV proteins (Bartenschlager and Lohmann, 2000). Using this restricted information, for the most part described previously (sections 1.2 to 1.4), a concise account of the HCV replication cycle, shown schematically in Fig. 9, is as follows: i) attachment and entry of the virus, allowing liberation of the genomic RNA; ii) translation from the IRES at the 5′ end of this genomic RNA and polyprotein processing; iii) formation of a replicase complex associated with intracellular membranes and synthesis of minus-strand RNA intermediate, prior to production of new positive-strand genomic RNA for further use as a template or for packaging into virions; iv) virion release from the infected cell. Each step in the replication cycle of HCV is considered briefly in the following sections.

1.5. 1 Virus Attachment and Entry

Current theories regarding HCV receptors are presented in section 1.2.2. While the exact nature of the HCV receptor is yet to be determined, there is a general consensus that E2 mediates viral attachment to the host cell, since E2-specific antisera can block binding to cells (Farci *et al.*, 1996; Rosa *et al.*, 1996; Zibert *et al.*, 1995). The role of E1 in viral attachment/entry is less clear, although the presence of a putative E1 fusion peptide, a stretch of hydrophobic residues displaying

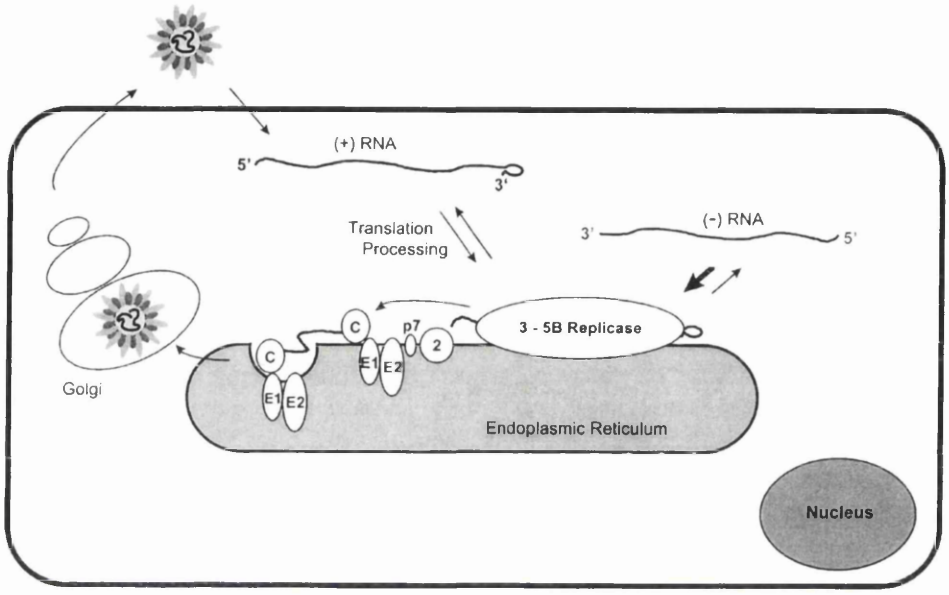

Figure 9: Putative model for the HCV replication cycle. Following attachment and entry to the cell, positive-sense (+) genomic ssRNA is liberated into the cytoplasm and translated. The resulting polyprotein is processed by host cell and viral proteinases. A membrane-bound replicase complex composed of NS3-5B generates negative-sense replication intermediates (-) which serve as the template for production of more genomic RNA. This is either used to generate more negative-sense RNA, or is encapsidated by core protein. Nucleocapsids are enveloped by budding into the ER lumen, prior to egress via the secretory pathway (taken from Bartenschlager and Lohmann, 2000)

similarities to paramyxovirus and flavivirus sequences, suggests E1 could be involved in membrane fusion (Flint *et al.*, 1999).

1.5. 2 Translation and Processing of the Viral Polyprotein

Following liberation of the viral genome into the cell, the RNA is translated directly via the IRES (section 1.3.1; Tsukiyama-Kohara *et al.*, 1992; Wang *et al.*, 1993). Since mutagenesis or insertion of AUG initiator codons upstream from the authentic HCV polyprotein start site have little effect on translation, ribosomes appear to bind in close proximity to this site with little or no scanning (Reynolds *et al.*, 1996; Rijnbrand *et al.*, 1996). The polyprotein is believed to be translated at the rough ER and cleaved co- and post-translationally by host cell and viral proteases (section 1.2.3; Major and Feinstone, 1997).

1.5. 3 Replication of HCV Genomic RNA

As determined using co-immunoprecipitation by several groups, most or all of the HCV nonstructural proteins form a replicase complex that is associated with intracellular membranes (section 1.2.5.6; Hijikata *et al.*, 1993; Ishido *et al.*, 1998; Lin *et al.*, 1997; Rice, 1996). It is likely that this complex also contains cellular proteins (sections 1.3.4 and 1.4.2). Formation of such replication complexes presumably allows production of viral proteins in a distinct compartment and tight coupling of their functions, and is a feature of many plus-stranded RNA viruses (Bolten *et al.*, 1998; Westaway *et al.*, 1997). HCV replicates through a negative-strand intermediate, as shown by strand-specific RT-PCR (Lanford *et al.*, 1994; Reed and Rice, 1999). The NS5B RdRp is clearly a key player in replication of HCV RNA, but its mechanism of action and specificity are not precisely understood (section 1.2.5.6). Although many reports have suggested that NS5B can utilise and bind virtually any RNA, or indeed DNA (Rosenberg, 2001), studies using gel mobility shift and competition assays indicate that there is preferential binding to nucleotides at the 3′-end of the NS5B-coding sequence (section 1.2.5.6; Cheng *et al.*, 1999). Recently, conserved complementary cyclisation sequences in the genomic termini of certain flaviviruses that are essential for RNA replication have

been discovered (Khromykh *et al.*, 2001). By analogy with these viruses, HCV may possess similar sequences that are required for replication. These sequences could be present at the extreme genomic terminii of the HCV genome - indeed, deletion of the sequences at the extreme 5′-end abolishes replication in the HCV sub-genomic replicon expressing cell lines (section 1.3.2; Friebe *et al.*, 2001), and the 3′X tail is required *in vivo* for HCV replication (section 1.4.1).

1.5. 4 Virion Assembly and Release

In the absence of systems allowing sufficient production of HCV virions, it is difficult to study viral morphogenesis. One potential approach to overcome this is the demonstration of virus-like particles (VLPs) that are produced in insect cells, as described in section 1.2.1. Other evidence suggests core protein initiates particle formation through a specific interaction at the 5′-end of the HCV genome and suppression of translation from the IRES (section 1.3.5; Shimoike *et al.*, 1999), although an independent report is not in agreement with these data (Wang *et al.*, 2000). If this is correct, it provides a model of selective packaging of positive-sense HCV RNA and suggests a mechanism by which the virus switches from translation/replication to assembly of viral particles (section 1.3.5; Shimoike *et al.*, 1999). The oligomerisation of core protein, a property anticipated for a protein forming the nucleocapsid, has been well-characterised although no consensus has been reached on the precise domains involved (see section 1.9.2; Matsumoto *et al.*, 1996a; Nolandt *et al.*, 1997; Yan *et al.*, 1998). In terms of virus egress, the demonstration of actual retention of E1 and E2 in the ER (Cocquerel *et al.*, 1999; Duvet *et al.*, 1998) indicates that viral nucleocapsids acquire their envelope by budding through ER membranes and are exported via the constitutive secretory pathway (Bartenschlager and Lohmann, 2000). Consistent with this hypothesis, complex N-linked glycans have been found on the surface of partially purified virus particles, suggesting virion release via the Golgi (Sato *et al.*, 1993).

1. 6 Important Advances in Molecular HCV Research

The investigation of HCV receptors (section 1.2.2) and studies with mouse models with chimeric human livers (section 1.1.8) are significant advances with a view to relieving the cancer burden represented by HCV. Two further important recent advances in the molecular biology of HCV are presented below.

1.6. 1 HCV Infectious Clones

One of the pitfalls of working with HCV-derived cDNAs in expression systems is that it is possible that they are derived from defective genomes. A large number of quasispecies exist within HCV-infected individuals (section 1.1.2; Gómez *et al.*, 1999), and it is likely that not all of these are able to elicit a persistent hepatitis. Recently, reports of the first clones of HCV which resulted in viral replication following direct intrahepatic injection of *in vitro* transcribed RNA, were published (Kolykhalov *et al.*, 1997; Yanagi *et al.*, 1997). This demonstrated use of the first infectious molecular clones of HCV. These clones represent genomes that contain all the information necessary for the assembly of functionally intact, infectious virus particles that can elicit a persistent hepatitis and lead to HCV-associated pathologies. Following these reports of infectious clones of HCV genotype 1a strains, HCV genotype 1b and 2a infectious clones were generated (Hong *et al.*, 1999; Yanagi *et al.*, 1998, 1999). Interestingly, a chimeric genotype 1a-2b clone, comprising the structural genes of a genotype 1a strain in a 2a background was not viable (Yanagi *et al.*, 1999), indicating there are complex relationships between the structural and nonstructural proteins encoded by the HCV ORF. Nevertheless, the demonstration of HCV infectious clones has not only increased confidence in the use of cDNAs from such clones in expression systems, but has also allowed mutational analyses of HCV genomic RNAs that can be tested *in vivo*. Inactivation of the key virally-encoded enzymes (section 1.2.5; NS2-3 and NS3-4A proteinases, NS3 NTPase/helicase, NS5B RdRp), and subsequent injection of the RNA into chimpanzees has confirmed their essential role in viral replication since these clones are non-viable while the parental strain causes disease (Kolykhalov *et al.*, 2000). Furthermore, detailed *in vivo* analysis of the 3′NCR using this approach suggests that the 3′X, the conserved 98 nt stretch at the extreme 3′ end of the genome, and

the upstream poly(U)/polypyrimidine tract are essential for infectivity, while the 5′ end of the variable region is not (Forns *et al.*, 2000; Kolykhalov *et al.*, 2000; Yanagi *et al.*, 1999).

1.6. 2 HCV Sub-genomic Replicon-expressing Cell Lines

While there have been reports of low level and intermittent replication of the entire HCV genome in human hepatocyte and T-cell lines (Dash *et al.*, 1997; Sugiyama *et al.*, 1997; Yoo *et al.*, 1995), the development of HCV sub-genomic replicon-expressing cell lines (Lohmann *et al.*, 1999a) paves the way for a robust cell culture system that allows stable, high level replication of HCV RNA. This approach permits introduction of a well-defined HCV RNA, and the opportunity to manipulate such RNAs with a view to performing a detailed molecular analysis of viral processes. This has previously been successful for several positive-sense RNA viruses (Boyer and Haenni, 1994). The first generation HCV sub-genomic replicons consisted of a bi-cistronic RNA containing the HCV 5′NCR fused to the neomycin phosphotransferase (*neo*) gene for G418 selection in the human hepatoma cell line Huh-7, followed by the EMCV IRES that drives expression of the nonstructural region (Fig. 10; Lohmann *et al.*, 1999a). Quantitation of replicon RNA following direct transfection into cells suggested 1000-5000 RNA molecules per cell, a figure that is several orders of magnitude over infection systems (Blight and Gowans, 1995). Interestingly, NS2 was not required for replication in this system (section 1.2.5.1), suggesting it plays a non-essential role in the viral replication cycle, although replication was discernibly inhibited in its absence. The HCV structural region was omitted since high level expression of HCV structural proteins could be cytotoxic (Moradpour *et al.*, 1998), and structural proteins are not required for replication of many positive-sense RNA viruses, including flavi- and pestiviruses (Behrens *et al.*, 1998; Khromykh and Westaway, 1997). Replication in the absence of structural genes indicates that the ability to couple replication to virus particle assembly is not essential for HCV (Rosenberg, 2001).

During propagation of Huh-7 cell lines stably expressing HCV sub-genomic replicons, a series of mutations were identified throughout the nonstructural region

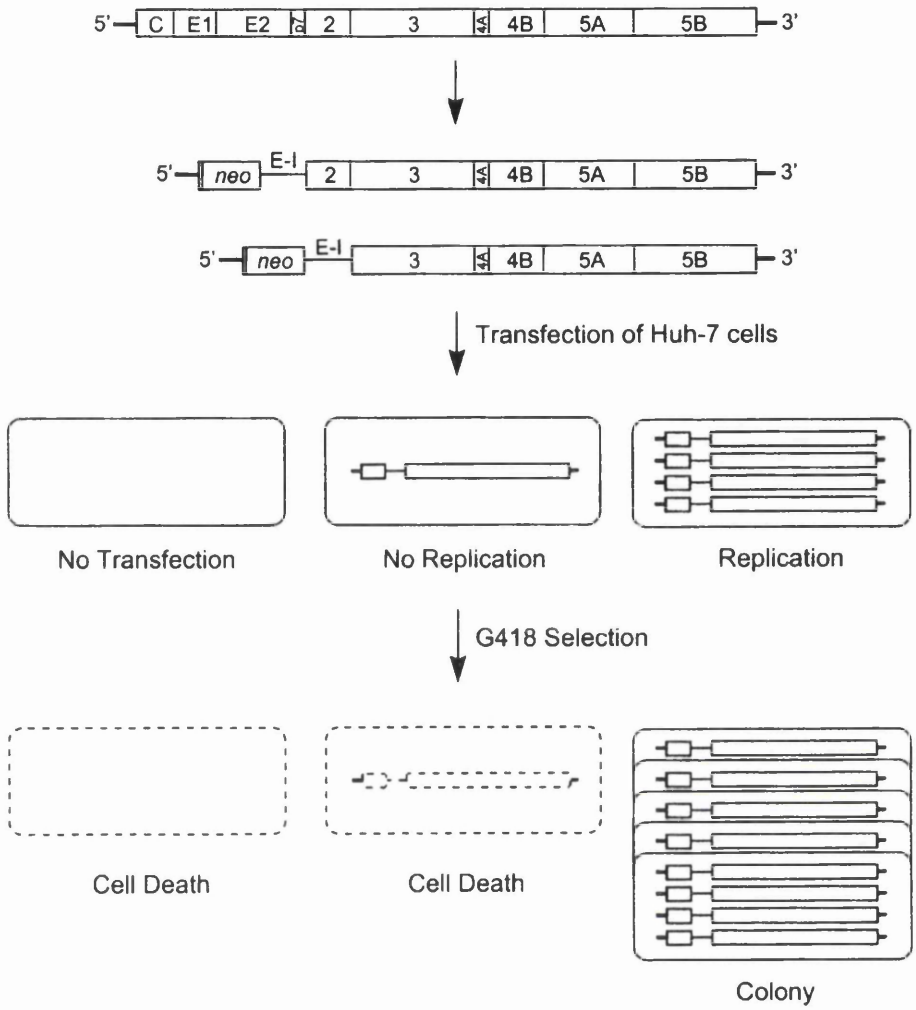

Figure 10: Establishment of HCV sub-genomic replicon-expressing cell lines. Constructs carrying the HCV sequences as shown (either NS2-5B or NS3-5B), together with the neomycin phosphotransferase gene (*neo*) and the EMCV IRES (E-I), were generated. A small portion of the core-coding sequence was included since there is some evidence that this region is part of the IRES. *In vitro* translated RNA was transfected into Huh-7 cells - those supporting replication of the *neo* gene within the sub-genomic replicon RNA developed resistance to G418. Only these cells formed colonies, while untransfected cells and those that did not support replication of the replicon RNA were eliminated (taken from Bartenschlager and Lohmann, 2000).

following extraction of RNA from Huh-7 cells and direct sequencing, some of which conferred greatly increased replication efficiency when transfected back into cells (Blight *et al.*, 2000; Lohmann *et al.*, 2001). Construction of one such adapted HCV sub-genomic replicon containing the luciferase gene instead of *neo* has facilitated transient transfection studies of replication (Krieger *et al.*, 2001). Interestingly, only sub-genomic replicons derived from a genotype 1b isolate of HCV that has not yet been shown to be infectious in chimpanzees were able to replicate, while those derived from the H77 strain, an infectious clone of HCV (section 1.7.1), were not able to establish G418-resistant colonies (Blight *et al.*, 2000). Furthermore, it appeared that Huh-7 is the only cell line that supports HCV RNA replication in this manner (Lohmann *et al.*, 1999a). These data make Huh-7 cells the cell line of choice for HCV research in general, as there appears to be factors present in these cells that allows replication of HCV RNAs. Consistent with previous studies suggesting the HCV IRES is cell-cycle regulated (Honda *et al.*, 2000), HCV sub-genomic replicon RNA levels correlated with the cell cycle (section 1.3.2; Pietschmann *et al.*, 2001). The localisation of nonstructural proteins produced in this system concur with the localisation of those expressed transiently in mammalian cells (Bartenschlager *et al.*, 1994; Grakoui *et al.*, 1993a; Selby *et al.*, 1993). These data suggest that the HCV sub-genomic replicon-expressing cell lines are a good system to study HCV, since at least some aspects of HCV replication are reproduced. Recently, full-length HCV genomic RNA replicons have been generated (Pietschmann *et al.*, 2002), which permit investigation of aspects of the structural proteins of HCV, including virion morphogenesis, and detailed analyses of individual structural region products, such as core protein. This HCV-encoded protein will be discussed in detail in the following sections.

1. 7 Properties of Core Protein and Its Coding Sequence

1.7. 1 Maturation of Core Protein

Core protein lies at the extreme N-terminus of the polyprotein encoded by the HCV ORF, and is generated via cleavage by host cell proteases (Grakoui *et al.*, 1993a; Hijikata *et al.*, 1991b; Selby *et al.*, 1993). Cleavage events are believed to take place

at two sites in the core protein of all HCV strains (Fig. 4, section 1.2.3; McLauchlan, 2000), except perhaps the HCV-1 strain (see below; Lo *et al.*, 1994, 1995). Since the N-terminal residue of E1 is HCV aa 192, one such cleavage event in the vast majority of HCV strains is believed to take place at aa 191 (Hijikata *et al.*, 1991b). Consistent with the requirements of signal peptidase cleavage sites (Martoglio and Dobberstein, 1998), mutation at aa 189 and 191 (-3 and -1 relative to aa 192) abolishes this cleavage event (Hussy *et al.*, 1996). Based on mass spectrometry measurements of core protein expressed in insect cells, the other cleavage event is believed to take place somewhere between aa 179 and 182 (Hussy *et al.*, 1996). However, others have placed this cleavage event at approximately aa 172-174 (Liu *et al.*, 1997; Lo *et al.*, 1995; Santolini *et al.*, 1994) on the basis of observed electrophoretic mobilities of mature core protein and various truncations. Cleavage at these two sites is not interdependent, since p21 can be generated under conditions where the cleavage event at aa 191/192 does not occur (Hussy *et al.*, 1996). There is some confusion surrounding the exact nomenclature for the resulting digestion products, which have been named according to their apparent molecular weights on polyacylamide gels. These digestion products have been designated p21 and p19, respectively (Hussy *et al.*, 1996; Lo *et al.*, 1994, 1995), but will be denoted p23 and p21 here and in following sections in accordance with recent publications (McLauchlan, 2000; Yasui *et al.*, 1998). Both p23 and p21 are generated by *in vitro* translation in the presence of microsomal membranes (Hussy *et al.*, 1996; Sanotolini *et al.*, 1994), suggesting membrane-associated proteases direct cleavage at these sites. The extreme C-terminus of p23 is highly hydrophobic and is known to act as a signal sequence which directs E1 to the ER lumen (see section 1.8.2; Santolini *et al.*, 1994). If processing of core is consistent with other ER-bound proteins, cleavage to generate p23 is mediated on the luminal side of the ER by the cellular signal peptidase complex (Martoglio and Dobberstein, 1998). Further cleavage to generate the mature p21 product would then be mediated by a cellular signal peptide peptidase. While p23 has been detected following expression in mammalian cells, truncated p21 core is the major product identified in such studies (Lo *et al.*, 1995; Santolini *et al.*, 1994). Although one study of detergent-stripped virions isolated from infected individuals detected a core protein of approximately 26 kDa

(Takahashi *et al.*, 1992), core protein of identical molecular weight to p21 has been isolated in sera from infected individuals (Yasui *et al.*, 1998) and HCV VLPs (section 1.2.1; Baumert *et al.*, 1998; Owsianka *et al.*, 2001; Wellnitz *et al.*, 2002), indicating this form is indeed the mature and stable form that acts as the viral nucleocapsid.

A cleavage event at around aa 151, so far only determined in the HCV-1 strain, the first molecular clone of HCV (Choo *et al.*, 1989), gives rise to a product termed p16 (Lo *et al.*, 1994, 1995). In contrast to p23 and p21, generation of p16 does not require the presence of membranes. However, while p16 is the predominant form produced by *in vitro* translation or transfection in mammalian cells of the core sequences alone, fusion of the HCV-1 E1 coding sequence downstream of the core-coding sequence, generated p23 and p21 (Lo *et al.*, 1994, 1995). Thus, it appears that p16 core is of no actual *in vivo* significance.

1.7. 2 Features of the Protein Sequence

Core protein is highly conserved in different strains among the six main HCV genotypes (Bukh *et al.*, 1994; Cha *et al.*, 1992). Indeed, the core-coding sequence is the most conserved region of the entire HCV ORF, suggesting the protein plays a critical role in the viral replication cycle. On the basis of hydrophobicity and aa content, core protein has been divided into three distinct regions (Hope and McLauchlan, 2000). The N-terminal aa 1-122 contains a large proportion of basic residues (23.8% in HCV strain H77c), mainly consisting of arginine with a few lysine residues. Such basic patches may be responsible for the reported interaction of core with nucleic acid (see section 1.9.1; Santolini *et al.*, 1994). This N-terminal region also contains a putative DNA binding motif (SPRG) at aa 99-102 (Bukh *et al.*, 1994) and putative nuclear localisation signals (NLSs) (Chang *et al.*, 1994). Two short but distinct hydrophobic regions reside in this region. A second domain (aa 123-174) is characterised by a much lower content of basic residues (5.9%), but is generally more hydrophobic than the N-terminal region. The third domain (aa 175-191) at the extreme C-terminus of the unprocessed protein is highly hydrophobic and is involved in ER-targeting of E1 (Santolini *et al.*, 1994). Analysis

of the protein sequence of core also suggests there are several potential recognition sites for protein kinases A and C (Kemp and Pearson, 1990), and it is possible that this protein exhibits different properties through the phosphorylation and dephosphorylation process (Hunter and Karin, 1992). Studies indicate the main core phosphorylation sites are Ser-53, -99 and -116 (Shih *et al.*, 1995). The main features of the core protein sequence, as described above, are summarised in Fig. 11.

1.7. 3 Subcellular Localisation

Unfortunately, studies of the localisation of core protein in biopsy samples from HCV-infected individuals have been hampered by the apparently low abundance of the protein in infected cells, and the low proportion of cells which appear to express the protein (McLauchlan, 2000). However, in biopsy samples with sufficient quantities of core for detection, the protein exhibited a predominantly cytoplasmic, granular localisation (Gonzalez-Peralta *et al.*, 1994; Yap *et al.*, 1994). A more defined localisation has been elucidated in cell lines transiently or stably transfected with constructs containing the core-coding sequence, or infected with recombinant viruses containing the same sequence. EM studies have suggested the granular structures to which core protein binds as lipid droplets (Moradpour *et al.*, 1996; Barba *et al.*, 1997). This association has been confirmed by indirect immunofluorescence (Hope and McLauchlan, 2000; Shi *et al.*, 2002). Studies have also suggested that core localises in much lower quantities to the cytoplasmic side of the ER (Harada *et al.*, 1991; Santolini *et al.*, 1994; Selby *et al.*, 1993; Suzuki *et al.*, 1995). In contrast, although the *in vivo* relevance of the p16 core species has not been confirmed (section 1.7.1), it appears to localise to the nucleus or at the nuclear membrane (Lo *et al.* 1994b), suggesting it plays a different biological role to p23 and p21. Interestingly, a nuclear form of the p21 core species has also been detected, albeit in low amounts. This nuclear species appears to be conformationally-distinct to the cytoplasmic form since specific monoclonal antibodies can discriminate between the two core species (Yasui *et al.*, 1998). Other groups have also detected core in low abundance in the nucleus (Chang *et al.*, 1994; Liu *et al.*, 1997; Ravaggi *et al.*, 1994; Shih *et al.*, 1993; Suzuki *et al.*, 1995).

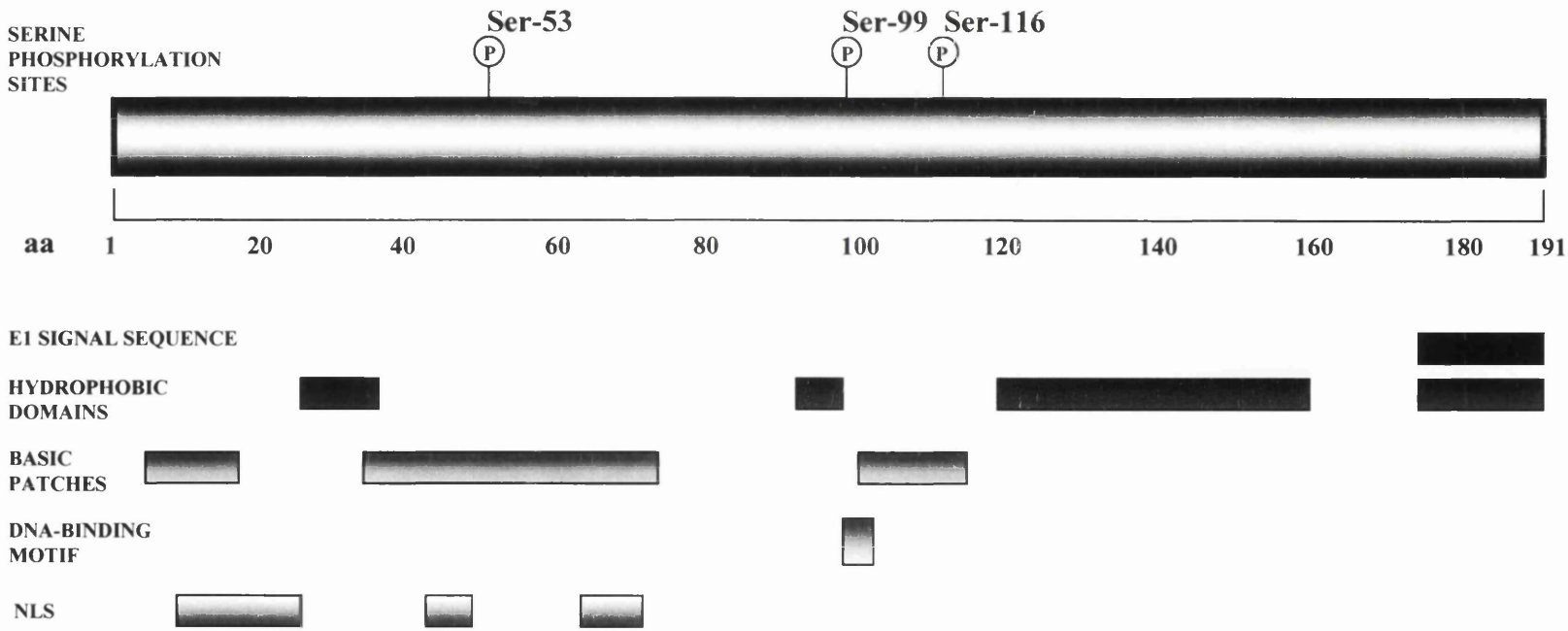

Figure 11: Features of the protein sequence of core. Serine phosphorylation sites (P), the E1 signal sequence, hydrophobic and basic regions, a putative DNA-binding motif, and putative nuclear localisation signals (NLSs) are highlighted.

1.7. 4 Ribosomal Frameshift in Core-coding Sequence

Recently, doubt has been cast over whether HCV does indeed possess a single ORF encoding one large polyprotein as detailed previously (section 1.2.3). Two groups have independently reported that an alternative reading frame, possibly generated by ribosomal frameshifting, is present in the core-coding sequence (Walewski *et al.*, 2001; Xu *et al.*, 2001). A rational basis for the presence of alternate reading frames using analysis of sites of marked suppression of synonymous variability in the HCV ORF was used in one study (Fig. 12; Walewski *et al.*, 2001), and unusual features of the identified region have previously been reported (Ina *et al.*, 1994; Smith and Simmonds, 1997). The newly discovered HCV-encoded protein was termed ARFP for 'alternate reading frame protein' (Walewski *et al.*, 2001), or F for 'frameshift' (Xu *et al.*, 2001); the term F protein is retained here for clarity. In both studies, specific antibodies to the F protein were demonstrated in the sera of a small but significant proportion of HCV infected individuals, but not uninfected individuals, ascribing possible *in vivo* relevance during HCV infection to the alternative reading frame (Walewski *et al.*, 2001; Xu *et al.*, 2001). The F protein is predicted to be between ~124 and 160 aa in length, depending on the genotype, and is highly basic. A similar overlapping ORF has been observed in the related GBV-B (Bukh *et al.*, 1999), suggesting that this protein has been conserved due to a crucial role in the HCV replication cycle (Xu *et al.*, 2001).

1.7. 5 The Structural Role of Core Protein

The highly basic nature of HCV core protein and its similarity to the core protein of other *Flaviviridae* members indicates that the protein is probably the nucleocapsid component of the HCV virion (Houghton, 1996). The demonstration of ribosome and RNA binding (Santolini *et al.*, 1994) is in agreement with the potential role of the core protein as the virion component involved in RNA packaging and viral assembly, even although explicit demonstration of the capsid-forming ability of core protein in mammalian cells has not been achieved. This is largely because, following expression of the HCV structural region or the full-length HCV ORF in such cells, no virus particles or too few to analyse are generated. In addition, detection of virus particles is a rare event in both human and chimpanzee livers

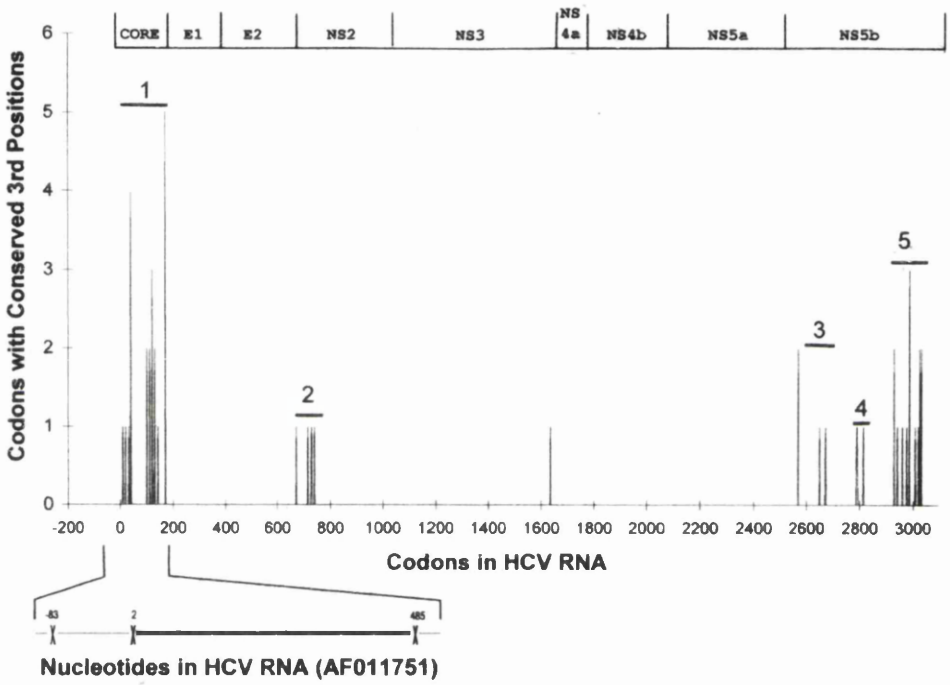

Figure 12: Marked suppression of synonymous variability in distinct clusters in the HCV ORF. Eight diverse HCV sequences were aligned and analysed - codons with conserved third positions were identified and mapped to the HCV ORF. A prominent cluster was detected in the core-coding sequence, providing a rational basis for an alternate reading frame in this region. The insert shows the presence of an alternative ORF in the +1 reading frame (denoted by a solid bar) of the H77c infectious clone of HCV (taken from Walewski *et al.*, 2001)

infected with HCV (section 1.2.1). Nevertheless, formation of nucleocapsids with core protein expressed in *E. coli* have been observed by EM (Kunkel *et al.*, 2001), and particles with the physicochemical, morphological and antigenic properties of naked core-derived nucleocapsids are apparently present in the serum of infected individuals (Maillard *et al.*, 2001).

The ability of core protein to multimerise, crucial in capsid assembly, has been extensively studied (Matsumoto *et al.*, 1996a; Nolandt *et al.*, 1997; Yan *et al.*, 1998). Core also interacts with the E1 glycoprotein (Lo *et al.*, 1996) which may facilitate maturation of the HCV virion. The reported interaction of core protein with intracellular membranes (Santolini *et al.*, 1994) may also play a role in facilitating assembly and/or budding of the virus, as previously shown for both flavivirus and pestivirus genera (Rice, 1996). The interactions of core presented above that are relevant to its role as the viral capsid protein are described in more detail in section 1.9.

1. 8 Possible Pathogenic Roles of Core Protein

While it is accepted that core protein forms the viral nucleocapsid (see above), several studies have also implicated the protein in many aspects of HCV pathogenesis. It therefore appears that HCV core is pleiotropic in nature, exerting varied effects on cellular metabolism. These effects broadly fall into the categories presented in the following sections: interference in cell signalling, immune avoidance, effects on cell transformation, interference in gene transcription, and effects on lipid metabolism.

1.8. 1 Interference in Cell Signalling

A number of studies suggest core protein can modulate apoptosis, as shown for gene products encoded by an array of other viruses (O'Brien, 1998). Apoptosis is often referred to as programmed cell death, and by definition is an orderly process by which a cell dies through a series of morphological changes that include cell shrinkage, blebbing of the plasma membrane, chromatin condensation and,

eventually, cell fragmentation into apoptotic bodies that are subsequently phagocytosed (Vaux and Strasser, 1996; White, 1996). In addition to its role in embryonic development and tissue homeostasis in adults, the process of apoptosis has protective responsibilities, eliminating cells that could prove harmful if they were to survive, for example those which have received a significant genetic insult via chemicals or irradiation, or virus-infected cells. Since HCV core protein is the first protein produced after infection of target cells, it may play a role in delaying apoptosis before the cell is able to mount a sufficient antiviral defence (Chen *et al.*, 1997). Accordingly, core protein has been proposed to alter normal cellular apoptosis via three members of the tumour necrosis factor receptor (TNFR) superfamily (Ware *et al.*, 1995); these are *Fas*, TNFR-1 and LT-βR, as shown schematically in Fig. 13. Initial studies into modulation of apoptosis by core protein suggested it could sensitise cells to the *Fas*-mediated arm (Ruggieri *et al.*, 1997), although a more recent study suggests core protein may have opposing effects in the same hepatocyte cell line to the first study (Marusawa *et al.*, 1999). A possible reason for the discrepancy between the two reports is the different techniques used to induce *Fas*-mediated apoptosis (anti-*Fas* antibody alone, or anti-*Fas* antibody plus cyclohexamide, a protein synthesis inhibitor that is required in some cell types to induce apoptosis), and the constitutive or transient expression of core in the cell lines. Sensitisation of cells by core to *Fas*-mediated apoptosis was proposed to be due to downstream effector modulation since altered levels of cell surface *Fas* antigen was not seen (Ruggieri *et al.*, 1997), although a direct interaction between *Fas* and core has recently been reported (see section 1.9.6.3; Hahn *et al.*, 2000).

As previously found with studies of the effect of core on *Fas*-mediated apoptosis, the effect of core on TNF-α-mediated apoptosis is somewhat confusing. Although initial studies suggested core protein, constitutively-expressed in Huh-7, HepG2 and HeLa cells, had no significant effect on cytotoxicity induced by TNF-α in the presence of cyclohexamide (Chen *et al.*, 1997), a subsequent report observed enhanced TNF-mediated apoptosis in a similar range of cell types in the presence of the RNA synthesis inhibitor actinomycin D (Zhu *et al.*, 1998). Two additional reports suggest core protein can inhibit TNF-α-mediated apoptosis in MCF-7 cells,

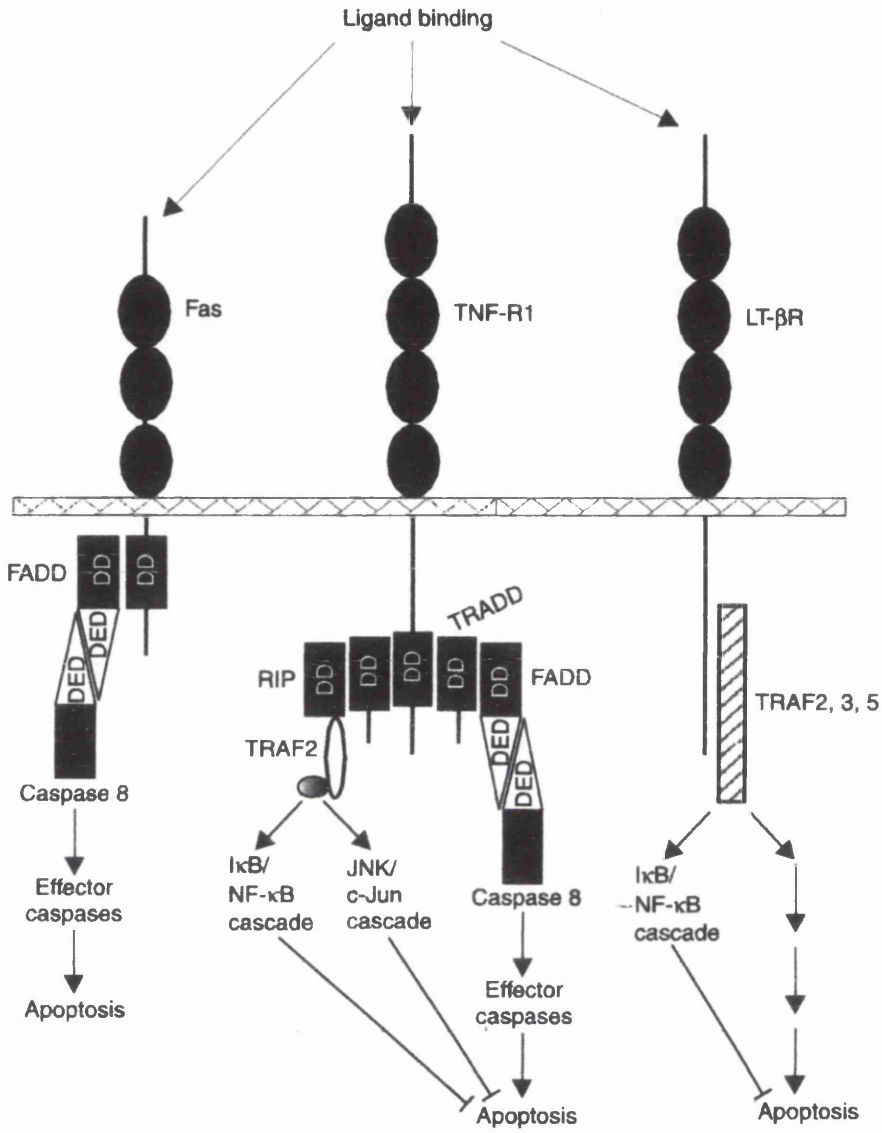

Figure 13: TNFR superfamily members and associated signaling proteins that are targeted by core protein. The signals from members of this superfamily are transduced by two major mechanisms: via a death domain (DD) (*Fas*, TNFR-1) or TNFR-associated factors (TRAFs) (LT-βR). Abbreviations: FADD/TRADD, *Fas*/TNFR-associated DD proteins; DED, death effector domain; RIP, receptor-interacting protein (taken from McLauchlan, 2000).

which are derived from a mammary carcinoma tissue (Beidler *et al.*, 1995; Marasawa *et al.*, 1999; Ray *et al.*, 1998). However, recent reports indicate MCF-7 cells lack caspase-3, an effector protease crucial in induction of apoptosis (Li *et al.*, 1997; Jänicke *et al.*, 1998), suggesting that these cells die via an alternative form of programmed cell death. Consistent with the effect of core protein on *Fas*-mediated apoptosis (see above), core did not alter levels of cell surface TNFR-1 (Zhu *et al.*, 1998). Less is known about the modulation of the LT-βR pathway. Core moderately increases LT-βR-mediated cell death in HeLa, but not Huh-7 or HepG2 cell lines (Chen *et al.*, 1997). However, the relationship of core protein with a modulation these particular apoptotic pathways gained credence from the demonstration of core protein binding to the cytoplasmic domains of both the tumour necrosis factor receptor 1 (TNFR-1) (Zhu *et al.*, 1998) and the lymphotoxin-β receptor (LT-βR) (Chen *et al.*, 1997; Matsumoto *et al.*, 1997), as discussed in sections 1.9.6.1 and 1.9.6.2.

1.8. 2 Immune Avoidance

Intriguingly, HCV persists despite the presence of virus-specific circulating antibody and CTLs (section 1.1.6). Indeed, T-cell responses in HCV infection are thought to play a role in pathology as well as clearance of virally infected cells. One possible reason for this immune avoidance could be that the T-cell response is insufficient to clear the virus. However, it is more likely that viral gene products modulate the immune system, as has been described for a wide variety of other viruses (Goodling, 1992). The interaction of core protein with members of the TNFR family (see above, and sections 1.9.6.1 and 1.9.6.2) could play a crucial role in this aspect of HCV pathogenesis. An association of core with LT-βR, which directs the development of peripheral lymphoid tissue and also functions in the formation of germinal centres during immune responses (Crowe *et al.*, 1994; Matsumoto *et al.*, 1996b), may be of particular relevance. Additional studies suggest expression of core protein by recombinant vaccinia virus in mice markedly decreases the CTL response, resulting in increased virulence of this virus compared to the wild type (Large *et al.*, 1999). Consistent with reports of an impaired allostimulation of peripheral blood cells recovered from HCV-infected patients

(Kanto *et al.*, 1999), infection of dentritic cells with a recombinant adenovirus expressing core, E1 and E2 reduced stimulation of allogenic T-cells and release of interleukin (IL)-12 (Hiasa *et al.*, 1998). Major histocompatability complex (MHC) II molecules at the cell surface are apparently not affected by either core alone in mice, or core in the context of E1 and E2 in dendritic cells (Hiasa *et al.*, 1998; Large *et al.*, 1999). Over-produced non-enveloped nucleocapsids formed by core in the serum of HCV-infected individuals could contribute to the immunopathological effects of HCV (section 1.7.5; Maillard *et al.*, 2001). In contrast to this possible immune avoidance of HCV mediated by core protein, a further study with transgenic mice expressing core together with the HCV envelope glycoproteins indicated no apparent modulation of the intrahepatic immune response to a hepatotropic adenovirus (Sun *et al.*, 2001).

1.8. 3 Effect on Cell Transformation

Although multiple factors probably contribute to HCV-associated HCCs, the most compelling viral candidate oncoprotein is core protein. Hepatocarcinogenesis involves alterations in the combined action of proto-oncogenes, growth factors, and tumour suppressor genes (Rogler and Chisari, 1992), and core protein has been shown to modulate all of these elements. Initial studies indicated it interacts with cellular proto-oncogenes at the transcriptional level (see section 1.8.4; Ray *et al.*, 1995). This may lead to promotion of cell proliferation, thereby disrupting normal hepatocyte growth. The pathogenesis of hepatocellular tissue damage mediated by HCV, therefore, may partly be due to deregulation of normal hepatocyte growth by core protein. Furthermore, since TNF-α has been specifically implicated in liver damage, actual damage to liver tissue may also be caused indirectly by the interaction of core protein with TNFR-1 (see section 1.9.6.2; Zhu *et al.*, 1998). Core protein can transform primary rat embryo fibroblasts in co-operation with the H-*ras* or c-*myc* oncogene (Ray *et al.*, 1996), implicating it as a co-factor in the development of HCC. An independent report failed to reproduce this effect of core/H-*ras* in the same cell line (Chang *et al.*, 1998), although it may have been due to differential localisation of the core species observed - a predominantly nuclear localisation of p16 core produced by HCV-1-derived sequences (section 1.7.3; Lo *et*

al., 1995) seen in the study by Ray *et al.* (1996), as opposed to a mainly cytoplasmic abundance of p21 core seen with HCV-K- and HCV-RH-derived sequences, as observed by Chang *et al.* (1998). A more recent report involving transfection of the core-coding sequence alone into primary hepatocytes resulted in an immortalised phenotype (Ray *et al.*, 2000). Core protein could potentially exert its effects on the regulation of cell growth through its suppressive effect on the promoter activity of p53 (Ray *et al.*, 1997), a pivotal factor in cellular transformation, although core has also been shown to activate p53 through direct physical interaction (see section 1.9.6.4; Lu *et al.*, 1999). The most compelling evidence that core protein can induce HCC comes from studies of transgenic mice expressing the protein (Moriya *et al.*, 1998). By 16-19 months, 25-30% of mice developed HCC that correlated with higher levels of core protein in tumourous than non-tumourous tissue. However, the same histopathological changes were not observed by several independent groups using a similar approach (Kawamura *et al.*, 1997; Pasquinelli *et al.*, 1997; Wakita *et al.*, 1998).

1.8. 4 Interference in Gene Transcription

The presence of conserved nuclear localisation signals and a DNA binding motif in HCV core protein (section 1.7.2), in addition to the visualisation of certain forms of the protein in the nucleus (section 1.7.3), suggests a further functional role as a gene regulatory protein. Actual evidence of this property was first indicated by the apparent inhibition of gene expression and replication of HBV in Huh-7 cells (Shih *et al.*, 1993). A dramatic reduction of ~14-fold in the amount of encapsidated HBV RNA was observed, suggesting that the documented ability of HCV to interfere with HBV replication *in vivo* (Bradley *et al.*, 1983; Fong *et al.*, 1991; Liaw *et al.*, 1991; Sheen *et al.*, 1992) is not primarily a general effect of competition between the two viruses, but rather is largely due to core protein. A separate study reported the ability of core to interfere in expression of co-infecting genomes of human immunodeficiency viruses (HIVs) through a downregulation of transcription of the HIV-1 long terminal repeat (LTR) (Srinvas *et al.*, 1996). The importance of this is not known, although interactions between these two viruses in super-infection may be important (Giovannini *et al.*, 1990). Using reporter gene assays, core protein has

been shown to increase expression from the simian virus 40 (SV40) early promoter and Rous sarcoma virus (RSV) LTR (Ray *et al.*, 1995). In terms of cellular gene expression, core suppresses the promoters c-*fos* and $p21^{WAF}$ (Ray *et al.*, 1995, 1998). On the other hand, it has been shown to activate c-*myc* (Ray *et al.*, 1995).

The effect of core on modulation of expression and function of the nuclear transcription factor NF-κB and related proteins has been studied in some detail. The involvement of these proteins in the expression of numerous cytokines and acute phase proteins supports a co-ordinating role in both apoptosis and the inflammatory response (Fig. 14; Ghosh *et al.*, 1998). NF-κB proteins are held in an inactive state by inhibitory IκB proteins in the cytosol. Following induction, for example by stimulation of certain TNFR superfamily members, these inhibitory proteins are targeted for degradation, revealing a nuclear localisation signal on NF-κB proteins that allows their translocation to the nucleus to modulate gene transcription of specific factors (Fig. 14). However, as before regarding the interference of core protein on cell signalling (section 1.8.1), the reports concerning disruption of this process by core protein are somewhat conflicting. This is further complicated by the ability of NF-κB proteins to enhance or suppress apoptosis, depending on cell type and the stimulus used (Lin *et al.*, 1999). The DNA-binding activity of NF-κB following induction can be both enhanced (Yoshida *et al.*, 2001; You *et al.*, 1999a) and reduced (Shrivastava *et al.*, 1998) by core protein. The nuclear expression of one NF-κB protein, RelA, is not affected by core protein in Huh-7, HepG2, or HeLa cells (You *et al.*, 1999a; Zhu *et al.*, 1998), although there is a slight reduction in BC10ME cells (Zhu *et al.*, 1998). Following induction with TNF-α or LT-α1β2, expression of RelA is elevated in Huh-7 cells expressing core protein (You *et al.*, 1999a), while it is unchanged in HepG2 and HeLa cells (You *et al.*, 1999a; Zhu *et al.*, 1998). There is also some evidence for a modulation of IκB degradation in the presence of core protein (Shrivastava *et al.*, 1998; Yoshida *et al.*, 2001; You *et al.*, 1999a).

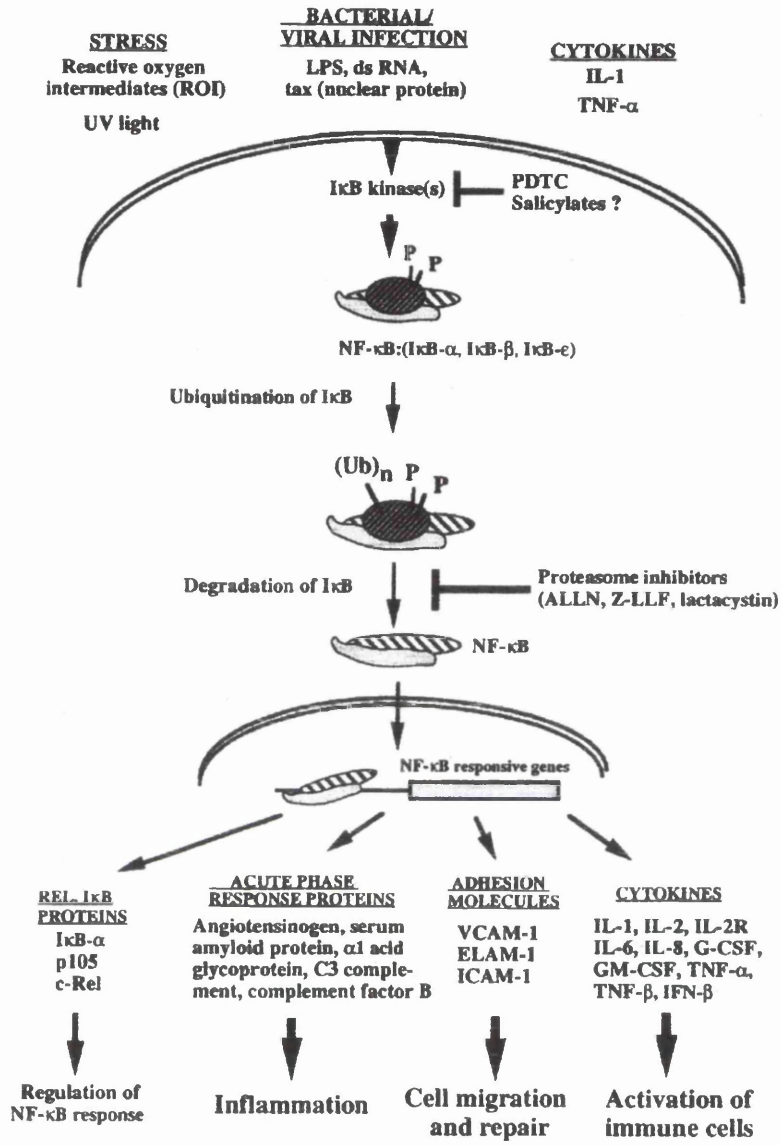

Figure 14: Proposed model for induction of NF-κB proteins. NF-κB proteins normally exist in cells in an inactive state bound by the inhibitory IκB proteins (IκBα, IκBβ, IκBε). Extracellular inducers that create stress, or markers of microbial infection, cause the activation of IκB kinase by a poorly defined mechanism, leading to phosphorylation and subsequent degradation of IκB proteins. This unmasks the NF-κB nuclear localisation signal. The protein translocates to the nucleus, where it directly upregulates expression from many genes involved in immune and inflammatory responses as shown (taken from Ghosh *et al.*, 1998).

1.8. 5 Effect on Lipid Metabolism

In addition to these potentially disruptive effects of core protein on cellular processes, there is evidence to suggest the characteristic lipid accumulation, or 'steatosis', commonly seen in patients with chronic HCV infection (Lefkowitch *et al.*, 1993; Scheuer *et al.*, 1992), is due to a direct or indirect effect of core protein on lipid metabolism. Core was shown to associate with the surface of lipid droplets in the cytoplasm of infected cells (Barba *et al.*, 1997). Indeed, it has been shown to interact directly with apolipoprotein AII (Sabile *et al.*, 1999), and displace a further lipid droplet-associated protein, adipophilin (Hope *et al.*, 2000). Moreover, an *in vivo* study has demonstrated that expression of core protein in transgenic mice resulted in hepatic steatosis after ~2 months (Moriya *et al.*, 1997), prior to development of HCC in some cases (section 1.8.3; Moriya *et al.*, 1998).

1. 9 Interactions of Core Protein with Host or Viral Factors

Although the exact role core protein plays in the molecular pathogenesis of HCV is still unclear, it appears that this protein is vitally important both as a viral structural protein involved in RNA packaging and virion assembly (section 1.7.5) and as a modulator of normal cellular function and host defence in infected cells (section 1.8). The exact mechanism for the functional versatility of core protein could be due to its ability to bind directly to nucleic acid and/or its ability to physically interact with cellular proteins, as described in detail in the following sections.

1.9. 1 Interaction of Core Protein with DNA and RNA

Analysis of the core protein sequence suggests the presence of a putative DNA binding motif (SPRG) at aa 99-102 and a large number of basic residues that may also be involved in binding nucleic acid (section 1.7.2). While actual DNA binding activity has been demonstrated for core protein (Santolini *et al.*, 1994), and this could influence gene transcription (section 1.8.4), a direct link of this property to HCV pathogenesis has not yet been made. The ability of core to bind RNA is not disputed - however, the specificity of RNA binding is a contentious issue. Initial studies using North-Western analyses revealed an interaction of core with HCV

genomic RNA, although core could also bind HBV RNA (Santolini *et al.*, 1994). However, the interaction of core protein with HBV RNA could be specific, since binding of this RNA by core is proposed to be a mechanism used by HCV to suppress replication of the HBV genome (section 1.8.4; Shih *et al.*, 1993). Further studies testing the interaction of core protein with the entire HCV genome suggested a specificity for viral sense RNA in a large portion of the genome at the 5′-end (Shimoike *et al.*, 1999). Interestingly, this interaction was coupled with a suppression of translation, suggesting that core protein may be involved in the switch between translation/replication and virion assembly (section 1.3.5). Studies with HCV VLPs produced in insect cells (section 1.2.1) also suggest a selective encapsidation of HCV genomic RNAs (Baumert *et al.*, 1998). A more recent study redefines this interaction to include highly structured RNAs, rather than a specific interaction with the 5′NCR alone (Kunkel *et al.*, 2001). However, these studies were performed with truncated bacterially-expressed core rather than HCV VLPs, and the results are in direct contrast to gel mobility shift assays detailing specific binding of recombinant core protein to *in vitro* transcribed HCV 5′NCR RNA but not other structured RNAs (Fan *et al.*, 1999).

1.9. 2 Interaction of Core Protein with Itself

In addition to binding HCV RNA, core protein would be anticipated to interact with itself, forming homo-oligomers, in its role as the viral capsid protein (section 1.7.5). Accordingly, three independent studies using the yeast two-hybrid system, originally described by Chien *et al.* (1991), confirmed this hypothesis (Matsumoto *et al.*, 1996a; Nolandt *et al.*, 1997; Yan *et al.*, 1998). However, there is apparently no consensus on the actual domains that are involved in self-interaction of core protein. The first study suggested a region within the hydrophilic N-terminus of core (aa 36-91) was responsible for homo-oligomerisation, although since interaction of this region with core aa 1-115 was relatively weak, other domains within the N-terminal region were believed to contribute to the homotypic interaction of core (Matsumoto *et al.*, 1996a). The interacting domains were comprehensively mapped by Nolandt *et al.* (1997). This study indicated a tryptophan-rich sequence (aa 82-102) was the main homotypic interaction domain, although residues in the hydrophobic C-

terminus were also partly implicated in the process. The most recent study indicates that a C-terminal series of leucine or hydrophobic residues arranged in heptad repeats are responsible for self-association of core (Yan *et al.*, 1998).

1.9. 3 Interaction with Other HCV-encoded Proteins

Several investigators have looked for the anticipated interaction of core with HCV envelope glycoproteins, due to the implication of this association for virion morphogenesis. However, co-immunoprecipitation of core with E1 and E2 has not been readily detected, possibly owing to the highly insoluble nature of the protein, and the fact that the protein is mainly membrane-bound when extracted from cells (Matsumoto *et al.*, 1996a; Moradpour *et al.*, 1996; Santolini *et al.*, 1994). Nevertheless, one group has shown that an anti-core antibody is able to co-precipitate E1 in the presence of core in mammalian cells (Lo *et al.*, 1996). E2 could not be co-precipitated with core, although core may interact indirectly with E2 through E1, since E1 associates with E2 (section 1.2.4.2; Dubuisson and Rice, 1996; Grakoui *et al.*, 1993b; Matsuura *et al.*, 1994; Ralston *et al.*, 1993). So far, direct interactions of core with other components of the virus have not been reported, though co-localisation of core with NS5A has recently been shown (section 1.2.5.5).

1.9. 4 Association with Ribosomes and ER Membranes

An unexpected sedimentation pattern of core protein expressed by *in vitro* translation suggested it may associate with the 60S ribosomal subunit (Santolini *et al.*, 1994). This property could facilitate uncoating of the HCV virion, as previously described for the core protein of alphavirus (Wengler *et al.*, 1992). However, the observed phenomenon is probably due to the interaction with RNA (section 1.9.1), since the association was abrogated by treatment with RNase, and the domain involved in RNA binding was important for the interaction with ribosomes (Santolini *et al.*, 1994). The *in vivo* relevance of these data is also somewhat doubtful, since ribosome binding was not seen when core protein was expressed via plasmid in cell lines (Santolini *et al.*, 1994).

A more convincing association of core protein with intracellular membranes has been elucidated. Core protein requires the presence of such membranes for proper maturation (section 1.7.1; Santolini *et al.*, 1994), and sedimentation patterns correlated with a close relationship of mature core with the ER. Chemical treatment of core translated in the presence of membranes suggested it was an integral membrane protein (Santolini *et al.*, 1994). This contrasts, however, with EM and indirect immunofluorescence studies that indicate core protein is mainly present on the surface of lipid droplets (section 1.7.3), as emphasised in the following section, in addition to a much lower quantity at the ER (section 1.7.3).

1.9. 5 Association with Lipid Droplets

EM and immunofluorescence studies have suggested an association of core with lipid droplets (see above, and section 1.7.3), which are cellular storage compartments for various forms of lipids used for membrane formation and as energy stores (Londos *et al.*, 1999; Murphy and Vance, 1999). Attachment of core to these structures may be indirectly mediated by an interaction with apolipoprotein AII (see section 1.9.6.8; Barba *et al.*, 1997; Sabile *et al.*, 1999), a component of high-density lipoproteins. Furthermore, it has been shown that core protein displaces a second lipid-droplet associated protein, termed adipophilin, in tissue culture cells (section 1.8.5; Hope *et al.*, 2000). The precise role of the attachment of core to lipid droplets is currently unclear, but it may upset normal lipid metabolism in the cell, aiding subversion of cell processes. Truncation of core abrogates binding to lipid droplets, typically leading to nuclear accumulation of these species (Liu *et al.*, 1997; Marusawa *et al.*, 1999; Moradpour *et al.*, 1996; Suzuki *et al.*, 1995). In fact, the precise domain required for association with lipid droplets resides in the second domain of core (section 1.7.2), a region that is unique when compared with related pesti- and flavivirus core protein sequences (Hope and McLauchlan, 2000).

1.9. 6 Interaction of Core Protein with Host Cellular Factors

A number of studies detailing interaction of core with a variety of cellular proteins have been reported. These interactions have largely been identified by yeast two-

hybrid screening of human (liver-derived) cDNA libraries (Chien *et al.*, 1991), and confirmed by co-localisation in mammalian cell lines and/or *in vitro* methods. Furthermore, an assortment of functional assays have often been employed to assess the significance of these interactions with core protein for HCV pathogenesis. However, it should be noted that due to the lack of an efficient cell culture system for HCV, these interactions, and indeed their *in vivo* significance, are as yet unconfirmed. For reference, the region of core protein that interacts with each of the host cell factors described below is shown schematically in Fig. 15.

1.9.6. 1 Lymphotoxin-β Receptor (LT-βR)

As outlined previously (sections 1.8.1 and 1.8.2), two independent reports suggest core protein interacts with the cytoplasmic tail of LT-βR (Chen *et al.*, 1997; Matsumoto *et al.*, 1997), with possible significance for modulation of cellular signalling and the immune response to HCV. The interacting domains of the two proteins were mapped to aa 36-91 (Matsumoto *et al.*, 1997) or, in contrast, aa 1-40 (Chen *et al.*, 1997) of core protein (Fig. 15), and aa 338-395 of LT-βR (Matsumoto *et al.*, 1997). Since this region on LT-βR is also the target of TRAF-3, a putative signalling molecule for a variety of receptors in the TNFR family (Fig. 13, section 1.8.1; Baker and Reddy, 1996), binding of core protein to this receptor may prevent binding by TRAF-3 and possibly other cellular factors. To test for an effect of core on LT-βR-mediated signalling, cell viability following challenge with LT-β in the presence and absence of core protein was monitored. The cytotoxic effect of LT-β was indeed potentiated in HeLa cells stably expressing core protein, although LT-β was not able to exert a cytotoxic effect, even at high concentrations, with or without core protein in human hepatoma cell lines Huh-7 or HepG2 (Chen *et al.*, 1997). Co-localisation of core and LT-βR in cell lines was not reported in either study, although core protein has been shown to associate with the cytoplasmic side of the ER (Santolini *et al.*, 1994) where the cytoplasmic tail of LT-βR may be exposed prior to translocation to the cell surface (Matsumoto *et al.*, 1997).

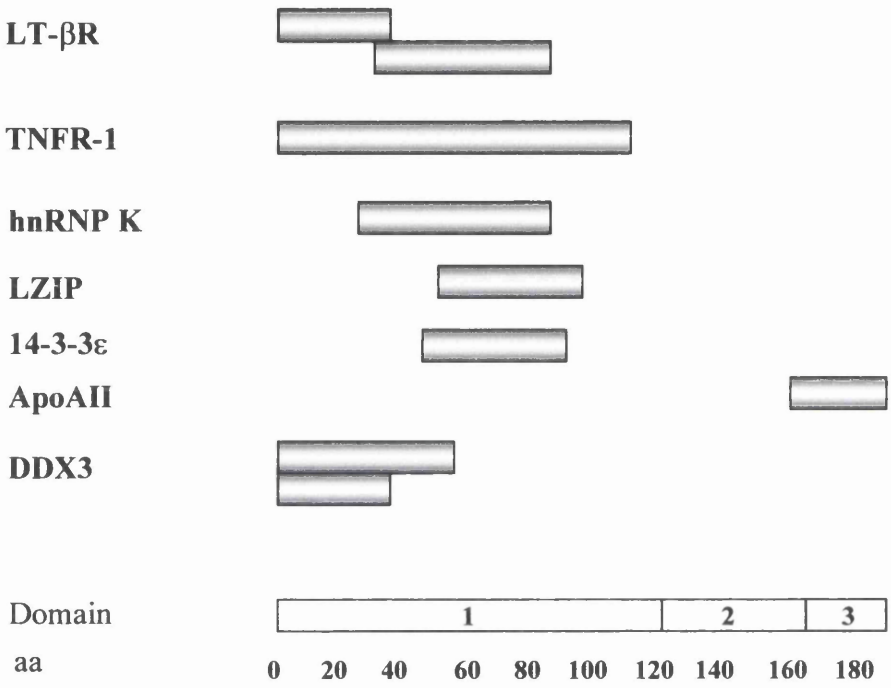

Figure 15: Regions of core protein involved in interaction with host cell factors. Boxes represent an approximate mapping of the binding site of each cellular factor as shown to the protein sequence of HCV core. A rough guide for aa numbers and the three domains of core described previously (section 1.7.2) are indicated (adapted from McLauchlan, 2000)

1.9.6. 2 Tumour Necrosis Factor Receptor-1 (TNFR-1)

Since core protein was shown to interact with the cytoplasmic tail of the LT-βR (see above), a possible association of core with TNFR-1, the prototype TNFR family member that is highly related to LT-βR (Beutler and van Huffel, 1994), was investigated. *In vitro* protein-protein binding assays suggested core and the cytoplasmic tail of TNFR-1 proteins do indeed interact (Zhu *et al.*, 1998), while the extracellular domain of TNFR-1 and the cytoplasmic tail of another member of the TNFR family (CD40; Baker and Reddy, 1996) were not able to bind core in the same assay. Interestingly, the interacting domain on TNFR-1 was mapped to aa 345-407 at the C-terminus of the 426 aa full-length protein (Zhu *et al.*, 1998) which corresponds to the death domain (Fig. 13, section 1.8.1) that is required for cell death signalling (Tartaglia *et al.*, 1993). It is well established that several cellular proteins which are components of the TNFR-1-mediated signalling complex bind directly or in close proximity to this domain. These proteins include RIP and TRAF-2 which are responsible for TNF-induced JNK or NF-κB activation (Fig. 13, section 1.8.1; Liu *et al.*, 1996), and FADD and TRADD which can induce apoptosis (Fig. 13, section 1.8.1; Chinnaiyan *et al.*, 1995). Therefore, the interaction between core and this domain on TNFR-1 may disrupt these interactions, resulting in altered TNFR-1 signalling. Furthermore, since TNF is one of the major mediators of cell death in chronic liver diseases (Gonzalez-Amaro *et al.*, 1994; Hussain *et al.*, 1994), this interaction could be significant for HCV-associated cirrhosis (section 1.8.3). Consistent with this hypothesis, core protein sensitised three separate cell lines to TNF-induced cell death (Zhu *et al.*, 1998), although these data are in direct contradiction to a previous report (Chen *et al.*, 1997). Furthermore, an indepednent group has specifically been unable to show an *in vitro* interaction of core and TNFR-1 (Hahn *et al.*, 2000).

1.9.6. 3 TNFR Family Member Fas

An interaction with the cytoplasmic region of *Fas* has been demonstrated by *in vitro* methods (Hahn *et al.*, 2000) following studies that suggested core could sensitise cells to *Fas*-mediated apoptosis (section 1.8.1; Ruggieri *et al.*, 1997; Hahn *et al.*,

2000). This study, when considered with those studies presented above detailing interactions of core protein with other members of the TNFR superfamily, strongly suggests that signalling via these receptors is a prime target for core protein and may be a major mechanism of HCV pathogenesis.

1.9.6. 4 Tumour Suppressor Protein p53

An interaction with this crucial factor in cellular transformation was discovered following studies that suggested core protein could suppress hepatocellular growth via alteration of p53 gene expression (Lu *et al.*, 1999; Ray *et al.*, 1997). The interaction was confirmed by *in vitro* protein-protein binding assays, as well as co-immunoprecipitation from transfected cell lines (Lu *et al.*, 1999). The peturbation of p53 by direct physical interaction may have important consequences for HCV pathogenesis and development of HCC. Subsequent studies have indicated core protein enhances the function of p53 by increasing its DNA-binding affinity and ability to regulate transcription (Otsuka *et al.*, 2000).

1.9.6. 5 Heterogenous Nuclear Ribonucleoprotein K (hnRNP K)

Core protein has been shown by Hsieh *et al.* (1998) to associate with hnRNP K and alter its cellular function. Since hnRNP K is known to bind both DNA and RNA (Takimoto *et al.*, 1993) and shuttles between the nucleus and the cytoplasm (Buchenau *et al.*, 1997; Michael, 1997), it is believed to participate in the processing and transport of pre-mRNAs (Dreyfuss *et al.*, 1993). The protein may also be a transcriptional regulator, since it stimulates the c-*myc* promoter *in vitro* (Takimoto *et al.*, 1993). The functional significance of its interaction with core was implied by partial reversal of the reported suppression by hnRNP K of the human thymidine kinase promoter (Alter *et al.*, 1992) in the presence of core protein (Hseih *et al.*, 1998). This suggests core protein may alter gene expression (section 1.8.4) through interaction with host cellular factors. The interacting domains on the two proteins were mapped to aa 25-91 of core (Fig. 15), a hydrophilic area near the N-terminus, and aa 250-392 of hnRNP K, which contains three proline-rich domains critical for the interaction of this protein with its cellular partners (Bomsztyk *et al.*, 1997).

These factors include transcriptional activators and repressors (Denisenko *et al.*, 1996; Michelotti *et al.*, 1996), and tyrosine kinases involved in signal transduction (Kai *et al.*, 1997; Taylor and Shalloway, 1994; Weng *et al.*, 1994).

1.9.6. 6 Leucine-zipper Protein (LZIP)

Consistent with the study described above, which suggests that the observed effects of core protein on gene expression are mediated by interaction with cellular factors (Hseih *et al.*, 1998), core has been shown to interact with a novel bZIP-like transcription factor (Jin *et al.*, 2000). This protein, designated LZIP, activates cyclic-AMP responsive element (CRE)-dependent transcription and appears to modulate cell proliferation (Jin *et al.*, 2000). The specificity of the core/LZIP interaction was verified in yeast, indicating core binds LZIP, but not related proteins such as CREB, ATF4, c-*Jun*, or c-*Fos* (Jin *et al.*, 2000). The significance of the interaction in terms of HCV pathogenesis was revealed by the apparent effects of core protein on LZIP localisation and function. Core aberrantly sequesters LZIP in the cytoplasm and apparently inactivates it, leading to effects on cellular transformation. While LZIP expressed via plasmid was detected in HeLa cells by specific MAbs in the nucleus, a substantial quantity of LZIP relocated to the cytoplasm in cells expressing core protein (Jin *et al.*, 2000). Core appeared to inhibit the putative cellular function of LZIP, since increasing the amount of core-expressing plasmid led to decreasing LZIP-mediated reporter gene activity in hepatocytes (Jin *et al.*, 2000). Interestingly, consistent with the ability of retroviral bZIP-like proteins such as v-*Jun* and v-*Fos* to transform cells (Maki *et al.*, 1987; Motohashi *et al.*, 1997; Nishizawa *et al.*, 1987), loss of LZIP function as a result of core protein expression correlated with cellular transformation (Jin *et al.*, 2000).

1.9.6. 7 Epsilon Isoform of 14-3-3 Protein (14-3-3ε)

Further insight into the oncogenic potential of core protein is suggested by its reported interaction with 14-3-3ε (Aoki *et al.*, 2000). This protein belongs to a family of cellular factors known to associate with components of several signal transduction pathways which may play an organisational role in mitogenic pathways

(Aitken, 1996; Morrison, 1994). The functional relevance of the interaction between 14-3-3ε and core protein to HCV pathogenesis was confirmed by the activation by 14-3-3ε of the Raf-1 kinase in the presence of core (Aoki *et al.*, 2000). Raf-1 kinase is believed to be a central component of the mitogen-activated (MAP) kinase pathway in mammalian cells (Howe *et al.*, 1992; Kyriakis *et al.*, 1992; Morrison and Cutler, 1997), and is associated with HCCs in humans (Ito *et al.*, 1998b). The interacting domains of the two proteins were further mapped in yeast to aa 49-97 of the full-length 191 aa core protein (Fig. 15), and aa 165-234 of the full-length 255 aa 14-3-3ε protein (Aoki *et al.*, 2000). Consistent with a previous report that 14-3-3 proteins bind cellular partners via phosphorylated serine residues (Yaffe *et al.*, 1997), mutation of a serine residue in core likely to be phosphorylated by PKA and/or PKC (Ser-53) (section 1.7.2; Shih *et al.*, 1995) within the interacting domain abolished its binding to 14-3-3 protein (Aoki *et al.*, 2000).

1.9.6. 8 Apolipoprotein AII (ApoAII)

As described previously (section 1.8.5), core protein may be directly responsible for the characteristic lipid degeneration, or 'steatosis', seen in patients with chronic HCV infection due to effects of this protein on lipid metabolism (Barba *et al.*, 1997; Moriya *et al.*, 1997). Further evidence for this is the strong co-localisation of core protein with apoAII (Barba *et al.*, 1997). Two independent HepG2 cell lines stably-expressing the HCV ORF from core to NS3 were used to show co-localisation of core with lipid droplets in the cytoplasm and endogenous apoAII at the surface of these droplets, in contrast to a lack of co-localisation of core with endogenous apoAI, a related lipid droplet-associated factor (Barba *et al.*, 1997). Consistent with these results, core was subsequently shown to directly interact with apoAII (Sabile *et al.*, 1999). Mapping of the region on core required for interaction with apoAII suggested a unique role, in terms of the association of core with cellular factors, for the extreme C-terminus of the protein (Fig. 15).

1.9.6. 9 Putative RNA Helicase (DDX3)

Finally, three independent reports have shown core protein interacts with a human cellular putative RNA helicase belonging to the DEAD-box family (Mamiya and Worman, 1999; Owsianka and Patel, 1999; You *et al.*, 1999b), a group of proteins so named due to the presence of a highly conserved motif (D-E-A-D) that is involved in ATP hydrolysis. Proteins of this family participate in many cellular processes, such as ribosome biogenesis and translation (see section 1.12; Anderson and Parker, 1996; Chuang *et al.*, 1997; Schmid and Linder, 1992). As such, an interaction of core protein with this putative RNA helicase could influence expression of the HCV polyprotein. In fact, functional studies have suggested a possible role of the protein in translation, although the assays have been carried out in artificial systems outwith mammalian cells (Mamiya and Worman, 1999), or with non-specific substrates distinct from HCV genomic sequences (You *et al.*, 1999b). Furthermore, there is disagreement as to whether core protein enhances or reduces the putative function of this cellular protein. The protein has been designated CAP-Rf for 'core-associated protein-RNA helicase full-length' (You *et al.*, 1999b), and DBX (Mamiya and Worman, 1999), which is in fact a previously reported cellular factor to which the protein is closely related (Lahn and Page, 1997), but the HUGO/GDB Nomenclature Committee approved name for this DEAD-box putative RNA helicase is DDX3 (Chung *et al.*, 1995; Owsianka and Patel, 1999), and will be referred to as such here and in following sections. Evidence suggests that this protein is highly conserved among eukaryotes, with homologues in mice (mDEAD3 and PL10; Gee and Conboy, 1994; Leroy *et al.* 1989), *Xenopus laevis* (An3; Gururajan *et al.*, 1991), and yeast (Ded1p; Jamieson *et al.*, 1991). In fact, mouse PL10 (95% identity with DDX3 at aa level) can interact with core in yeast, although Ded1p was sufficiently diverse (65% aa identity) to not interact (Mamiya and Worman, 1999). DDX3 also appears to be ubiquitous in human tissues (Chung *et al.*, 1995). This high degree of conservation and its ubiquitous cellular presence suggests that DDX3 has an essential role in some aspect of RNA metabolism.

The interacting domains of the two proteins were mapped to aa 1-59 (Owsianka and Patel, 1999) or 1-40 (You *et al.*, 1999b) of core protein (Fig. 15), and aa 553-622

(Owsianka and Patel, 1999) or 473-611 (You *et al.*, 1999b) of the full-length 662 aa DDX3. Interestingly, the interacting domain on DDX3 contains a short 'RS'-like domain which appear to be important in protein-protein interactions between splicing factors (Fu, 1995; Kohtz *et al.*, 1994; Wu and Maniatis, 1993). These basic domains, rich in arginine and serine residues, have been shown to be critical for protein-protein interactions between *Drosophila* splicing factors Sx1 (Bell *et al.*, 1991; Inoue *et al.*, 1990) and Tra (Li and Bingham, 1991), and between mammalian splicing factors ASF/SF2 (Ge *et al.*, 1991; Krainer *et al.*, 1991), SC-35 (Fu and Maniatis, 1992; Fu *et al.*, 1992) and their cellular co-factors. Most proteins containing RS domains are believed to participate in and regulate pre-mRNA splicing (You *et al.*, 1999b). However, the RS domain of DDX3 is considerably shorter (seven SR or RS dipeptides) (Owsianka and Patel, 1999) than RS domains of many other splicing factors (Fu, 1995).

While investigation of the subcellular localisation of DDX3 potentially represents an important insight into the function of this protein, reports regarding this aspect are inconsistent, if not wholly confusing. Indeed, the reported localisation of DDX3 ranges from a diffuse cytoplasmic staining of HeLa or COS-7 cells transfected with mammalian expression plasmid expressing c-*myc*-tagged DDX3 (Mamiya and Worman, 1999), and a similar punctate staining of the cytoplasm of over-expressed FLAG-tagged DDX3 in Huh-7 cells (You *et al.*, 1999b), to apparent staining of nuclear speckles with some cytoplasmic distribution in HeLa cells expressing endogenous DDX3 detected by a specific PAb (Owsianka and Patel, 1999). A nuclear localisation for over-expressed DDX3 was supported by subcellular fractionation of cell lines transiently expressing the protein from a plasmid followed by immunoblotting (You *et al.*, 1999b). However, only HeLa cells were tested and, more importantly, these results directly contradict with the author's immunofluorescence data (see above; You *et al.*, 1999b). Regardless of the original localisation of DDX3, the protein co-localised with core around what is presumably lipid droplets, given previous studies of the cellular distribution of core (section 1.7.3; Barba *et al.*, 1997; Hope and McLauchlan, 2000) in COS-7, HeLa, or Huh-7 cell lines (Mamiya and Worman, 1999; Owsianka and Patel, 1999; You *et al.*,

1999b). Using truncated core constructs lacking the hydrophobic domain, some co-localisation with DDX3 in the nucleus was seen (You *et al.*, 1999b), suggestive of core protein carrying DDX3 into the nucleus due to differential targeting of truncated core (section 1.7.3). Some slight co-localisation of DDX3 and core in the nucleus when transfected with a full-length core protein-expressing construct was seen (You *et al.*, 1999b), although others did not observe this effect (Owsianka and Patel, 1999).

As briefly described above, functional assays suggested DDX3 was involved in translation (Mamiya and Worman, 1999; You *et al.*, 1999b). Since *Saccharomyces cerevisiae* has a DDX3 homologue which is required for translation initiation (Chuang *et al.*, 1997) and is therefore essential for cell growth, the ability of DDX3, mouse PL10 or Ded1p supplied *in trans* to rescue a lethal Ded1p-deletion mutant was tested. Consistent with previous data for PL10 (Chuang *et al.*, 1997), all three proteins could rescue the functionally crippled yeast (Mamiya and Worman, 1999). In agreement with data presented above suggesting DDX3 and PL10 but not Ded1p could interact with core protein in yeast, co-expression of full-length core protein (aa 1-191) severely inhibited rescue of Ded1p-deletion mutant yeast by DDX3 or PL10, but not Ded1p itself. Core protein aa 1-123 did not significantly inhibit the growth of the DDX3 or PL10-complemented mutant yeast (Mamiya and Worman, 1999), presumably because this truncated form of core is targeted to the nucleus (section 1.7.3; Lo *et al.*, 1995). DDX3 was also shown to upregulate translation from a reporter plasmid in transfected Huh-7 cells (You *et al.*, 1999b). However, possible effects at the transcriptional level were not investigated. Nevertheless, core protein (aa 1-122) increased the level of reporter an astonishing 34-fold above that of DDX3 alone. Once again, however, since only truncated (nuclear-targeted) core constructs were used in transfections the actual *in vivo* significance of this effect is unclear. In terms of the enzymatic properties of DDX3, nucleoside triphosphate (NTP) hydrolysis by DDX3 expressed as a histidine-tagged fusion protein has been investigated biochemically (You *et al.*, 1999b). DDX3 expressed in this manner was able to hydrolyse all radiolabelled NTP or deoxy-NTPs (dNTPs), although it appeared to preferentially hydrolyse dATP. More insight into the DDX3-core

interaction was given by the apparent stimulation of ATP- or dATPase activity of DDX3 by, albeit, truncated forms of core protein produced in *E. coli* as GST-fusion proteins (You *et al.*, 1999b). While core protein aa 1-101 and aa 1-122 alone did not hydrolyse radiolabelled ATP or dATPs, these truncated forms were able to stimulate both ATPase and dATPase activity of DDX3. Interestingly, while many DDX3 homologues in other organisms have been shown to possess ATP-dependent RNA helicase activity (Chuang *et al.*, 1997; Gururajan and Weeks, 1997; Liang *et al.*, 1994), and the presence of conserved motifs associated with known RNA helicases (see section 1.10.6), an actual ability to unwind standard artificial RNA or DNA substrates was not observed (You *et al.*, 1999b). It is possible, therefore that DDX3 requires a specific RNA or cellular co-factor to stimulate enzymatic activity, as has been shown for *E. coli* DbpA or yeast Slt22, and eIF4A or *E. coli* RhlB, respectively (see section 1.10.7).

The preceding data makes it reasonable to suggest that the core-DDX3 interaction is responsible for some of the effects of core on host gene expression (section 1.8.4). DDX3 may also be aberrantly sequestered in a particular subcellular compartment to co-operate with core in some aspect of the viral replication cycle (section 1.5), such as packaging of the viral genome or translation of the HCV ORF. Due to seemingly ubiquitous nature of DDX3 (Chung *et al.*, 1995), and the altered localisation of this protein in the presence of core (Mamiya and Worman, 1999; Owsianka and Patel, 1999; You *et al.*, 1999b), it is likely that this interaction plays some part in subversion of the host cell following infection with HCV. However, while previous functional studies suggested that DDX3 had some role in translation (Mamiya and Worman, 1999; You *et al.*, 1999b), the exact role of DDX3 in cellular metabolism is presently unknown. It is crucial to establish this function for DDX3 to understand the significance of its interaction with core protein. Prior to characterising DDX3 and its interaction with core protein experimentally, an understanding of the normal role of RNA helicases in cellular metabolism is important. This group of proteins will be discussed in the following sections.

1. 10 Features of RNA Helicases

1.10. 1 General Characteristics

Helicases are proteins that mediate the NTP-dependent unwinding of nucleic acid duplexes, a necessary prerequisite for basic genetic processes such as gene expression and genome replication (Gorbalenya and Koonin, 1993). Specifically, RNA helicases catalyse the unwinding of base-paired regions in RNA-RNA, or RNA-DNA hybrids, although they may also unwind DNA-DNA duplexes. They are ubiquitous proteins, found in all cellular organisms and in many viral genomes (Linder and Daugeron, 2000), and have a pivotal role in all processes involving RNA such as transcription, splicing, translation, ribosomal biogenesis, RNA transport, and RNA turnover (Anderson and Parker, 1996; Chuang *et al.*, 1997; de la Cruz *et al.*, 1999; Schmid and Linder, 1992; Schroder *et al.*, 1990; Schwer, 2001). Some are also implicated in cellular processes such as spermatogenesis, embryogenesis, and cell growth and division, since they are expressed in a developmentally regulated way (Schmid and Linder, 1992). The wide range of processes described above is likely to require specific rearrangements of particular RNA structures or RNA-protein complexes by a range of proteins working on different substrates and in distinct subcellular locations. RNA helicases are part of a larger group of proteins, the RNA chaperones, which assure correct folding and maintain specific secondary and tertiary structures of RNAs in their informational, structural and even catalytic roles (Caprara and Nilsen, 2000; de la Cruz *et al.*, 1999). A diverse array of RNA helicases has evolved in all living organisms to meet the needs of the cell. Indeed, the sheer number of known and putative RNA helicases in mammalian genomes strongly implies that modulation and control of RNA secondary structure and RNA-protein interactions is one of the major preoccupations for a cell.

1.10. 2 Designation of Helicases into Three Superfamilies and Two Smaller Families.

Comparative analysis of the protein sequence of putative and known helicases has allowed accurate delineation of conserved motifs and patterns. Two of the helicase-

specific 'signatures', termed the ATPase or Walker A and B motifs, are shared by all helicases, and indeed a wide variety of other NTP-hydrolysing enzymes (Schulz, 1992; Walker *et al.*, 1982). Additional motifs are likely to play an essential role in helicase activity and associated processes, specifically those involved in catalysis and substrate/ligand binding (Gorbalenya and Koonin, 1993). Three vast superfamilies and two smaller families have been described on the basis of sequence similarity (Fig. 16; Gorbalenya and Koonin, 1993), and several clearly defined families exist within each superfamily. As yet, proteins that possess helicase activity but do not fall into one of these groups, as described below, have not been identified.

1.10. 3 SF1 and SF2

The majority of putative and known helicases belong to the superfamilies SF1 (Gorbalenya *et al.*, 1988a, 1988b; Hodgeman, 1988) and SF2 (Gorbalenya *et al.*, 1989; Lain *et al.*, 1989; Linder *et al.*, 1989), containing over 50 and 100 proteins, respectively (Hall and Matson, 1999). Proteins of both these superfamilies contain seven conserved aa motifs, whose sequences and structural arrangements are, by and large, very similar (Gorbalenya *et al.*, 1993). This similarity possibly suggests that proteins in SF1 and SF2 might have evolved from a common ancestor (Gorbalenya *et al.*, 1989). The conserved motifs are distributed in a domain of between approximately 200 and 700 residues.

1.10. 4 SF3

SF3 appears to consist entirely of putative and known helicases of small DNA and RNA viruses (Gorbalenya *et al.*, 1990). The exception to this rule is an RNA helicase encoded by human herpesvirus 6 (HHV-6), a large DNA virus, although the gene responsible is likely to have been acquired via recombination with a parvovirus (Thomson *et al.*, 1991). Proteins in this superfamily contain just three conserved motifs, including the ATPase A and B motifs necessary for ATP binding and hydrolysis, tightly organised in a short ~100 aa stretch.

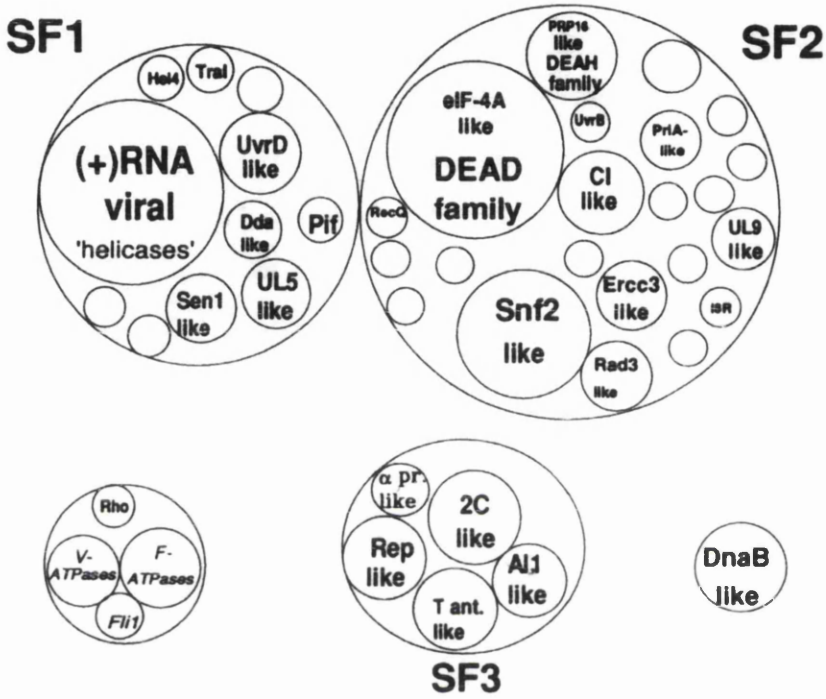

Figure 16: Designation of helicases into three superfamilies and two smaller families. Groups of helicases are expressed as circles, with their diameters roughly proportional to the number of proteins in each group (taken from Gorbalenya and Koonin, 1993)

1.10. 5 F4 and F5

The remaining helicases which do not fall into SF1/SF2 or SF3 may be grouped into two further unrelated families termed F4 and F5 (Gorbalenya and Koonin, 1993). F4 contains the bacterial DnaB helicase and a small number of related proteins which are all functionally and physically associated with DNA primases. These proteins contain five distinct conserved motifs, including ATPase A and B (Ilyina *et al.*, 1992). So far, only bacterial and bacteriophage members of this family have been reported (Gorbalenya and Koonin, 1993). F5 contains the bacterial transcription termination factor Rho, a DNA-RNA helicase (Brennan *et al.*, 1987), and groups of proton-translocating ATPases that are highly related to this protein (Gorbalenya and Koonin, 1993). This provides the first evidence of an evolutionary relationship between a helicase and non-helicase ATPases.

1.10. 6 Analysis of Specific Conserved Motifs.

Although found in all superfamilies, most RNA helicases are of the SF2 family and can be further classified on the basis of particular consensus sequences within the conserved motifs (Fig. 17). The first domain (motif I; AxxGxGKT using the aa one letter code, x represents any aa), the ATPase A domain, participates in ATP binding by direct association with the β- and γ-phosphates of the molecule (Kadaré and Haenni, 1997; Rozen *et al.*, 1990; Walker *et al.*, 1982). The fourth domain (motif II; DEAD), the DEAD-box or ATPase B domain, participates in ATP binding and/or ATP hydrolysis (Gorbalenya *et al.*, 1989; Linder *et al.*, 1989; Walker *et al.*, 1982; Wasserman and Steitz, 1991). As one of the most conserved motifs, this gives rise to the designation of many RNA helicases as members of the DEAD-box family (Gorbalenya *et al.*, 1989). Mutations in either the ATPase A or B sites dramatically affect the ATPase and helicase activities of eIF4A (Pause and Sonenberg, 1992) and vaccinia virus nucleoside triphosphate phosphodehydrolase (NPH-II) (Gross and Schuman, 1995). Variations in the DEAD-box and in other motifs give rise to distinct subsets of RNA helicases - the DExH-box proteins are highlighted in Fig. 17. The fifth domain (motif III; SAT), adjacent to the DEAD-box, is essential for RNA unwinding and is believed to couple ATP hydrolysis to RNA unwinding (Pause and Sonenberg, 1992). The eighth domain (motif VI; HRIGRxxR) forms part

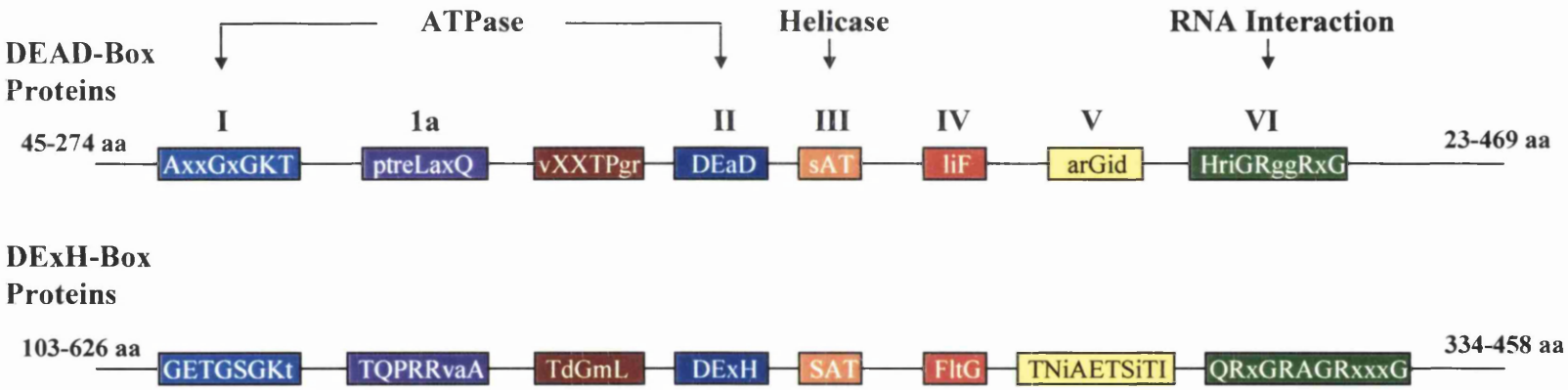

Figure 17: Conserved motifs of the DEAD-box family of RNA helicases, and the related but distinct DExH-box proteins. The conserved central core domain containing motifs I through IV is flanked by diverse N- and C-terminal extensions of varying size which are presumed to govern nucleic acid substrate specificity, interactions with cellular co-factors, and subcellular targeting of the individual proteins (adapted from de la Cruz *et al.*, 1999)

of a larger basic patch and is involved in RNA binding and ATP hydrolysis (Pause and Sonenberg, 1992). This motif, together with motifs I and II are the most conserved throughout SF1 and SF2 helicases (Kadaré and Haenni, 1997), pointing to their crucial role in the functional coherence of these proteins. Motifs Ia, IV and V await detailed analysis to delineate their functions. Interestingly, sequence comparisons of several DEAD-box proteins reveals that the central conserved region is flanked by diverse N- and C-terminal extensions (Fig. 17). It is proposed that these diverse extensions govern nucleic acid substrate specificity, interactions with cellular co-factors, and subcellular targeting of the individual proteins (Schmid and Linder, 1992; Wang and Guthrie, 1998).

1.10. 7 Experimental Analysis of RNA Helicase Activity.

Unwinding of RNA substrates is typically assayed by constructing duplex RNAs with single-stranded overhangs that allow binding of protein to the nucleic acid, and visualisation of the duplex and monomeric products by electrophoretic separation (Fig. 18; Venkatesan *et al.*, 1982; Matson *et al.*, 1983). The shorter of the two RNA species is usually radiolabelled, in order to increase electrophoretic separation between the displaced ssRNA and the unwound duplex. The polarity of the single-stranded overhangs allows helicases to be classified as those which translocate in a 5′ → 3′ or 3′ → 5′ direction (Lohman and Bjornson, 1996). Using the above approach, a rapidly growing number of putative RNA helicases from different organisms ranging from *E. coli* and viruses to humans have been identified.

Proteins containing the previously described conserved motifs (section 1.10.6) are commonly called RNA helicases on the basis of sequence similarity to known DNA and RNA helicases (Gorbalenya and Koonin, 1993), and because they take part in processes that are expected to involve unwinding of RNA (Schmid and Linder, 1992). However, although there are growing numbers of putative RNA helicases, *in vitro* activity has been shown for only a few cellular proteins, notably elFA (Pause and Sonenberg, 1992; Rozen *et al.*, 1990; Jaramillo *et al.*, 1991), p68 (Hirling *et al.*, 1989), *X. laevis* An3 (Gururajan and Weeks, 1997), and *Drosophila* Vasa (Liang *et al.*, 1994). Discussion regarding An3 and Vasa, which are DDX3 homologues, is

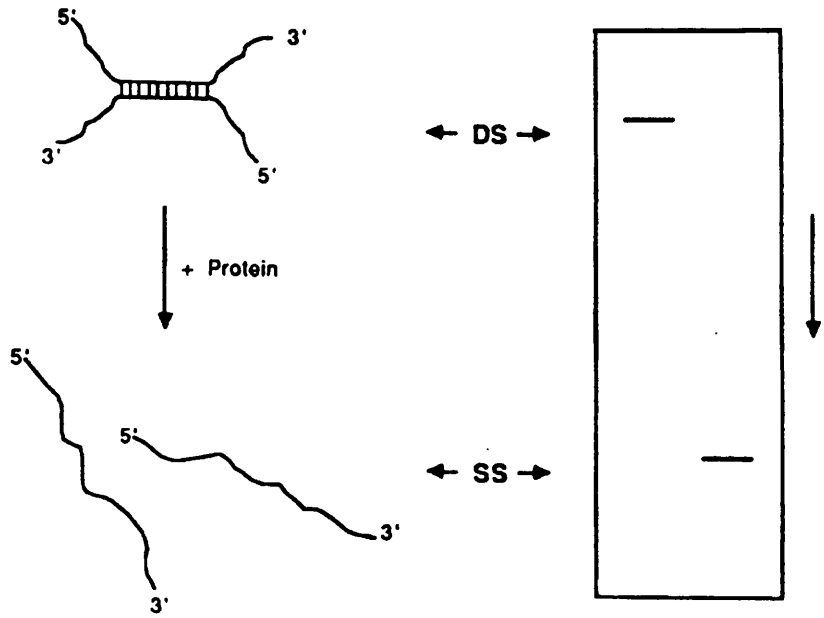

Figure 18: Schematic representation of an RNA helicase assay. Unwinding of RNA substrates by a protein under investigation is typically assayed by constructing radiolabelled duplex RNAs (DS) with single-stranded overhangs. Visualisation of the duplex RNA and any monomeric products (SS) unwound by the protein is achieved by electrophoretic separation (depicted by large rectangle) and detection of the radiolabelled RNAs (taken from Gururajan and Weeks, 1997).

presented in section 1.13. Viral helicases with confirmed NTP-dependent RNA helicase activity include simian virus 40 (SV40) large T antigen (Scheffner *et al.*, 1989) vaccinia virus NPH-II (Shuman, 1992), and the NS3 protein of HCV, BVDV and YFV (section 1.2.5.2; Jin and Peterson, 1995; Kim *et al.*, 1995; Warrener and Collet, 1995). A possible reason for the lack of demonstrable helicase activity for a large number of putative helicases is believed to be at least partly due to the requirement of such proteins for cellular (or viral) co-factors (Linder and Daugeron, 2000). Characterised examples of DNA and RNA helicases which require such accessory proteins include the requirement of eIF4A for eIF4B (Rozen *et al.*, 1990), the association of *E. coli* UvrA with UvrB necessary for UvrB-mediated helicase activity (Oh and Grossman, 1987), and the herpesvirus UL52/UL5 interaction that is necessary for helicase activity of UL5 (Dodson and Lehman, 1991). Furthermore, several RNA helicases have been shown to require a specific stimulatory RNA sequence for ATPase or helicase activity. Examples of this include the enzymatic stimulation of *E. coli* DbpA and yeast Slt22 proteins in the presence of the peptidyl transfer centre of 23S rRNA (Diges and Uhlenbeck, 2001; Fuller-Pace *et al.*, 1993), and U2/U6 small nuclear RNA (Xu *et al.*, 1996), respectively.

1. 11 Mechanism of Helicase Activity

Despite detailed kinetic and structural analysis of several helicase proteins for which actual helicase activity has been reported, a complete understanding of how ATP binding and hydrolysis are coupled to unwinding of a double-stranded nucleic acid substrate is not available at present (Lohman and Bjornson, 1996). Indeed, RNA helicases were originally presumed to be unlike DNA helicases in their action, and proposed to only unwind short duplexes of RNA (de la Cruz *et al.*, 1999), which gained credence from studies with eIF4A (Rogers *et al.*, 1999). However, viral helicases, which may have to unwind long stretches of genomic RNA with extensive secondary structure were postulated to have a different mechanism (Lorsch and Herschlag, 1998). Accordingly, evidence of a processive mode of action for an RNA helicase has been reported (Jankowsky *et al.*, 2000). Vaccinia virus NPH-II, a DExH-box RNA helicase of the SFII family that is essential to the replication cycle of this DNA virus, was demonstrated to be a highly processive 3′ → 5′ helicase. The

step size was found to be ~6 bp, comparable to that of the DNA helicase UvrD (Ali and Lohman, 1997). This suggests that RNA helicases may be more similar to DNA helicases than originally thought, with the differences between them residing in their cellular partners and their substrates (Linder and Daugeron, 2000).

1.11. 1 Visualisation of Unwinding Activity by a DEAD-box RNA Helicase.

While the biochemical demonstration of an RNA helicase migrating in a step-wise fashion along an RNA substrate without dissociating from it (Jankowsky *et al.*, 2000) was an important advance, the precise mode of action of RNA unwinding was still unclear. Actual visualisation of RNA duplex melting by *E. coli* DbpA (Henn *et al.*, 2001) has provided valuable insight into this aspect of helicase function. The enzymatic activity of this protein, a well-characterised RNA helicase and homologue of human cellular p68 (Gorbalenya and Koonin, 1988), has been shown to be significantly stimulated in the presence of 23S rRNA (Diges and Uhlenbeck, 2001; Fuller-Pace *et al.*, 1993). Furthermore, since this stimulation is abolished in the presence of intact ribosomal particles, it has been implicated in ribosomal biogenesis (Tsu and Uhlenbeck, 1998). Visualisation of this RNA helicase 'caught in the act' of unwinding a stretch of RNA has been made possible by atomic force microscopy (Henn *et al.*, 2001). In the absence of protein or ATP, the 480 bp non-specific dsRNA substrate was seen as worm-like structures (Fig. 19a). Although ATPase activity, and hence helicase activity, is stimulated by the peptidyl centre of 23S rRNA, DbpA is apparently non-specific in its ability to unwind RNA *in vitro* (Henn *et al.*, 2001). Upon incubation of the RNA with DbpA in the absence of ATP, the protein, detected as globular structures, was seen to bind specifically to one end of the duplex RNA (Fig. 19b). In the presence of ATP, the protein was seen to translocate along the dsRNA, yielding Y-shaped structures (Fig. 19c). Some DbpA was observed at the origin of unwinding, and it is possible this serves to prevent the ssRNA strands from reannealing (Henn *et al.*, 2001). These images provide further evidence of that RNA helicases are *bona fide* ATP-dependent proteins capable of processively unwinding long stretches of RNA.

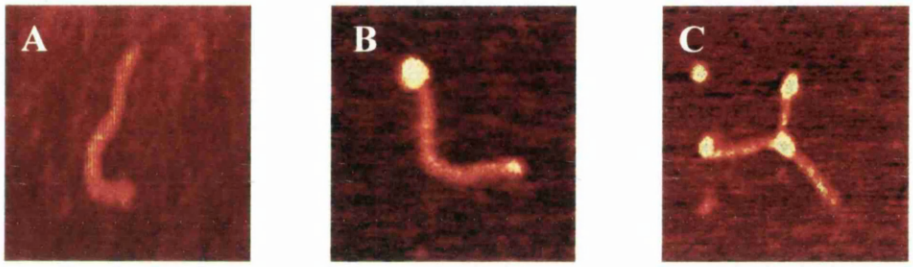

Duplex RNA | Duplex RNA **+DbpA** | Duplex RNA **+ DbpA +ATP**

Figure 19: Visualisation of a DEAD-box RNA helicase unwinding a large RNA duplex. Atomic force microscopic images of protein and RNA at the single molecular level are shown: (A) in the absence of protein or ATP, the dsRNA substrate was seen as worm-like structures; (B) upon incubation of this RNA with *E. coli* DbpA in the absence of ATP, the protein, detected as globular structures, was seen to bind specifically to one end of the duplex RNA; (C) in the presence of ATP, the protein was seen to translocate along the dsRNA, yielding Y-shaped structures (taken from Henn *et al.*, 2001).

1. 12 Functional Classification of RNA Helicases

Although experimental demonstration of helicase activity has not always been possible, recent functional analyses of various RNA helicases has given new insights into to these proteins, and indeed verified their significance in most cellular metabolic processes involving RNA. With the advent of the *S. cerevisiae* genome sequence, it has been possible to estimate, on the basis of sequence homology, the minimum number of putative RNA helicases encoded by a eukaryotic cell (de la Cruz *et al.*, 1999). Thus, *S. cerevisiae* contains 39 SFII known and putative RNA helicases comprising 26 DEAD-box and 13 DExH-box proteins. Two further proteins of the SFI family, Upf1p and Sen1p, are also implicated in RNA metabolism. Studies in *S. cerevisiae* suggest it contains several RNA helicases that have homologues in mammalian cells which, in some instances, are real orthologues (de la Cruz *et al.*, 1999). However, there are some cases of putative mammalian RNA helicases without clear homologues in *S. cerevisiae*, probably representing proteins that are involved in processes not required in this lower eukaryote (Lee *et al.*, 1998). Analyses of the *S. cerevisiae* genome and a reverse genetics approach to determine the role of putative RNA helicases in cellular metabolism have been enhanced by comprehensive studies of protein-protein interactions in this organism (Uetz *et al.*, 2000). This technique has allowed delineation of protein complexes involved in RNA metabolic and other processes (Schwikowski *et al.*, 2000; Uetz *et al.*, 2000).

Following the course of eukaryotic gene expression, processes believed to directly involve RNA helicases include transcription, pre-mRNA splicing, ribosomal biogenesis, RNA export, translation, and RNA decay (de la Cruz *et al.*, 1999). As yet, while there have been extensive studies of DNA helicases in transcription (Guzder *et al.*, 1994; Pazin and Kadonaga, 1997), there have been no clear reports of a yeast RNA helicase involved this process, although one such protein, Dhh1p, has been shown to interact with Pop2p (Hata *et al.*, 1998), a component of the multi-subunit transcriptional regulator complex CCR4. The involvement of RNA helicases in the remaining aspects of eukaryotic gene expression are presented below, and summarised schematically in Fig. 20.

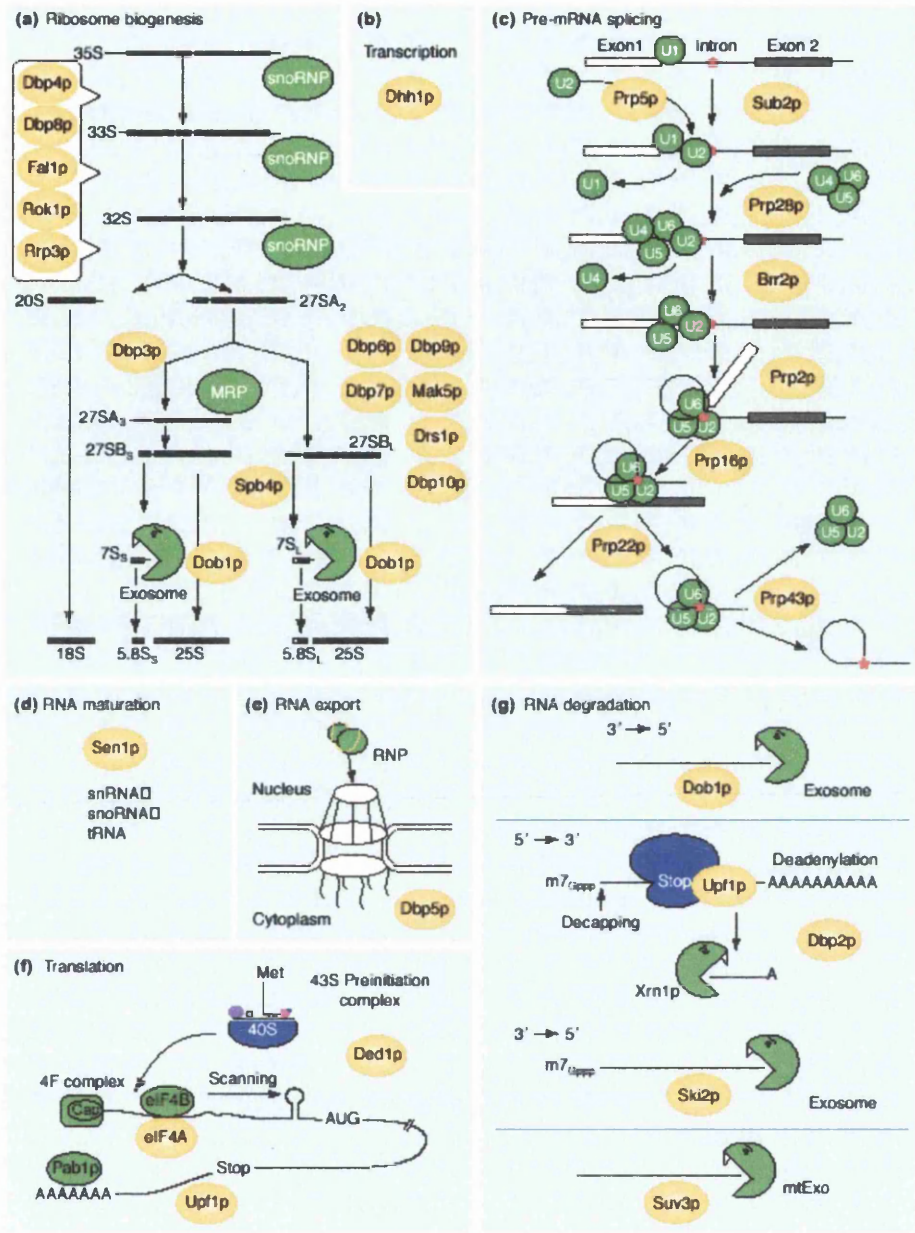

Figure 20: Functional classification of RNA helicases. The involvement of each RNA helicase (highlighted in yellow) from *S. cerevisiae* in the processes essential for eukaryotic gene expression (panels a to g) is shown schematically. Important non-helicase components of each process are indicated in green (taken from de la Cruz *et al.*, 1999)

1.12. 1 Pre-mRNA Splicing

Following transcription, pre-mRNA molecules are capped at the 5′-end, processed at the 3′end and undergo intron removal (Alberts *et al.*, 1994). Excision of introns is achieved by two separate trans-esterification reactions. The spliceosome, a large protein and small nuclear RNA (snRNA) complex, mediates these reactions, including the formation and stabilisation or dissociation of RNA-protein and RNA-RNA interactions (de la Cruz *et al.*, 1999). RNA helicases are likely the driving force behind the extensive structural rearrangements that are required, conferring speed and accuracy (Staley and Guthrie, 1998). Eight RNA helicases have been implicated in the process of pre-mRNA splicing in yeast (Staley and Guthrie, 1998). DEAD-box proteins Prp5p and Prp28, and DExH-box protein Brr2p, are thought to mediate assembly or release of the different components of the complex (Fig. 20; Chen *et al.*, 2001; Raghunathan and Guthrie, 1998; Staley and Guthrie, 1999). Two DEAH-box proteins, Prp2p and Prp16p, are involved in the first and second transesterification steps, respectively. Two further proteins of this family, Prp22p and Prp43p, are essential for release of the spliced mRNA and dissolution of the spliceosome complex, respectively (Wagner *et al.*, 1998). Based on sequence homology, three additional Prp22p-like DEAH-box proteins, a sub-set of helicases that have so far only been implicated in pre-mRNA splicing, are linked with this cellular process (de la Cruz *et al.*, 1999).

1.12. 2 Ribosome biogenesis

Synthesis of ribosomes in yeast involves the assembly of around 80 different proteins and four rRNAs (de la Cruz *et al.*, 1999). A single precursor (35S pre-mRNA) is used to generate three of these rRNAs (18S, 25S and 5.8S rRNAs) (Fig. 20). Maturation of the 35S pre-mRNA requires ordered processing involving many proteins and small nucleolar RNAs (snoRNAs) (Venema and Tollervey, 1995). The majority of these snoRNAs function as guides for the various required reactions via direct base-pairing to rRNA sequences. So far 14 putative RNA helicases have been implicated in ribosome synthesis, in three distinct aspects: i) establishment and/or dissociation of snoRNA-pre-rRNA base-pairing - specifically, Rok1p is linked with the snRNA snR10 and its partner Gar1p, a snoRNP protein, while Dbp4p is linked

with snoRNA U14 (Liang *et al.*, 1997; Venema *et al.*, 1997); ii) facilitation of the activities of the endo- and exo-nucleases required to process the pre-rRNA - for example, Dbp3p is believed to unwind a highly structured region of a particular pre-mRNA region (Weaver *et al.*, 1997); iii) recruitment, rearrangement, or dissociation of *trans*-acting factors and ribosomal proteins in formation of the ribosome - depletion of DEAD-box proteins Dbp6p and Dbp9p results in abortive assembly of ribosomes (Kressler *et al.*, 1998; Daugeron *et al.*, 2001), while accumulation of pre-ribosomal particles is seen following depletion of DEAD-box protein Spb4p (de la Cruz *et al.*, 1998).

1.12. 3 Processing of Other RNAs

Around one-fifth of pre-tRNAs in *S. cerevisiae* contain a single intron that must be removed. Although not part of the pre-tRNA splicing machinery, Sen1p, a putative DNA-RNA helicase of the SFI family, is implicated indirectly in this removal process since mutations in the gene coding for this protein lead to increased levels of pre-tRNAs (de la Cruz *et al.*, 1999).

1.12. 4 RNA Export

Following processing in the nucleus, mature mRNAs, in the form of RNPs, together with tRNAs and ribosomes, are exported to the cytoplasm via the nuclear pore complex (NPC). RNA helicases could be envisioned as being involved in proper packaging or structuring of RNPs for efficient transit through the NPC, and reassembly of these packaged structures into functional units when in the cytoplasm (Fig. 20; de la Cruz *et al.*, 1999). Two independent reports suggest the RNA helicase Dbp5p/Rat8p, which accumulates around the nuclear envelope on the cytoplasmic side, is involved in mRNA export since functional inactivation of the protein leads to the accumulation of poly(A)$^+$ RNA, and mutations can be lethal when combined with nucleoporin or RNA transport factor mutants (Snay-Hodge *et al.*, 1998; Tseng *et al.*, 1998).

1.12. 5 Translation

Eukaryotic translation is preceded by the recruitment of the 40S ribosomal subunit by eIFs to the 5′-end of mRNA (Fig. 7, section 1.3.3; Alberts *et al.*, 1994; Kozak, 1999; Pain, 1996). The 40S ribosomal subunit scans the mRNA for the initiator codon, where the 60S subunit joins prior to commencement of translation. The human cellular DEAD-box RNA helicase eIF4A is presumed to unwind the extensive secondary structure in the 5′NCR of mRNA, which would normally significantly decrease translational efficiency (Rozen *et al.*, 1990). The yeast homologue of eIF4A, Tif1/2p is required for translation *in vivo* and *in vitro* (Fig. 20; de la Cruz *et al.*, 1999; Schmid and Linder, 1991). Indeed, Tif1/2p is even required for translation of mRNAs in which ribosomal scanning probably does not occur (Blum *et al.*, 1992). A further protein, Ded1p, another DEAD-box RNA helicase, is also essential for translation (Chuang *et al.*, 1997; de la Cruz *et al.*, 1997). Although the functions of Tif1/2p and Ded1p overlap, they are not redundant (de la Cruz *et al.*, 1999). In contrast, Dbp1p, which shares 72% identity with Ded1p, is a multi-copy suppressor of the *DED1*-null mutant, suggesting the function of these two proteins is redundant (de la Cruz *et al.*, 1997; Jamieson and Beggs, 1991). Interestingly, Ded1p and Tif1/2p have been shown to interact directly with each other in the yeast two-hybrid system (Uetz *et al.*, 2000), although further analyses are required to confirm this association. DDX3, a human cellular protein that is the focus of this thesis, can functionally support otherwise lethal mutants in the *ded1* gene (section 1.9.6.9; Mamiya and Worman, 1999), suggesting DDX3 could be involved in translation initiation, possibly in concert with eIF4A. So far, RNA helicases have not been implicated in the translational elongation process in *S. cerevisiae*, since it is generally accepted that the translating ribosome can unwind secondary structures within the mRNA itself (de la Cruz *et al.*, 1999). In contrast, during termination of translation, the SFI helicase Upf1p may interact with translation release factors (eRFs), although it does not appear to be required directly for this process (Czaplinski *et al.*, 1998).

1.12. 6 RNA Decay

Regulated expression of genes and removal of defective RNA molecules requires complex turnover systems. In *S. cerevisiae*, mRNAs are rapidly degraded by 5′ → 3′ or 3′ → 5′ exonucleolytic processing following shortening of their poly(A) tails and decapping. RNA helicases have so far only been implicated in 3′ → 5′ exonuclease activity, a process that requires components of the exosome complex, Ski3p, Ski8p, and the putative RNA helicase Ski2p (Fig. 20; Anderson and Parker, 1998). An additional RNA turnover pathway, non-sense-mediated decay (NMD), promotes rapid degradation of mRNAs that contain a premature termination codon that could give rise to incomplete and potentially harmful proteins (Ruiz-Echevarria *et al.*, 1996). The Upf1p protein that is involved in translation termination is essential for this pathway as part of a complex that detects aberrant mRNAs (He *et al.*, 1997). A further RNA helicase Dbp2p is possibly associated with this process due to its interaction with Upf1p (He and Jacobson, 1995).

1. 13 Current Knowledge on DDX3 and its Cellular Homologues in Other Organisms

The motifs that characterise the DEAD-box family of RNA helicases (Fig. 17, section 1.10.6; Pause and Sonenberg, 1993) are perfectly conserved from human DDX3 to its homologue in yeast, Ded1p. Interestingly, DDX3 homologues DBX, DBY, PL10, An3, and Vasa are all germ cell-specific, or developmentally-regulated (You *et al.*, 1999b), suggesting they function in a tissue-specific or developmental manner. However, DDX3 is an apparently ubiquitous cellular protein and it is not known if it is developmentally regulated (Chung *et al.*, 1995). Nevertheless, the presence of DDX3 in different human tissues suggest it plays an essential role in cellular metabolism. Current understanding of DDX3 and its homologues is presented below. Much of the data on DDX3 itself has been presented in section 1.9.6.9. Similarly, many features of Ded1p have been noted previously (section 1.12.5).

1.13. 1 DDX3

The human DDX3 gene is encoded on the X chromosome between bands p11.3 and p11.23 (Fig. 21; Park *et al.*, 1998). A Y chromosomal counterpart (DDXY) was also mapped (Park *et al.*, 1998), and was found at the same locus as DBY (see below; Lahn and Page, 1997). It is possible the X and Y forms of DDX3 are functionally interchangeable (Lahn and Page, 1997; Watanabe *et al.*, 1993). Analysis of the organisation of the DDX3 gene suggests it consists of 17 exons that span approximately 16 kb (Kim *et al.*, 2001), and possess a similar organisation to that of human DBY.

Enzymatic characterisation of DDX3 suggests its NTP/dNTPase activity is markedly inhibited by all synthetic polynucleotides, particularly poly(G) RNA (You *et al.*, 1999b). This effect is distinct from most other RNA helicases, which are in fact stimulated by polynucleotides (Fuller and Pace, 1994; Lee and Hurwitz, 1992; Schmid and Linder, 1992). A notable exception is the DDX3 homologue, *X. laevis* An3 (see section 1.13.4), which is inhibited (~10-fold) by an apparently non-specific RNA that is a known substrate for helicase activity, possibly indicating the ssRNA generated can interfere with ATPase activity of the protein (Gururajan and Weeks, 1997). Reported knowledge on DDX3 and its interaction with core protein (section 1.9.6.9) suggests that DDX3 is involved in cellular translation, but can be inhibited or enhanced in this cellular function by core protein, depending on the experimental conditions (Mamiya and Worman, 1999; You *et al.*, 1999b).

1.13. 2 DBX and DBY

DBX and its Y-chromosome counterpart DBY are ubiquitous proteins, suggesting essential 'house-keeping' roles in cellular metabolism (Lahn and Page, 1997). It is proposed that DBX and DBY, and other such proteins with homologues on the X and Y chromosome are functionally interchangeable (section 1.13.1), despite significant divergence of their genes' nucleotide sequences (Lahn and Page, 1997; Watanabe *et al.*, 1993). There is little published data on DBX, while there is some interest in DBY due to a possible role in spermatogenesis. DBY is frequently deleted in male infertile patients leading to severe spermatogenic damage that

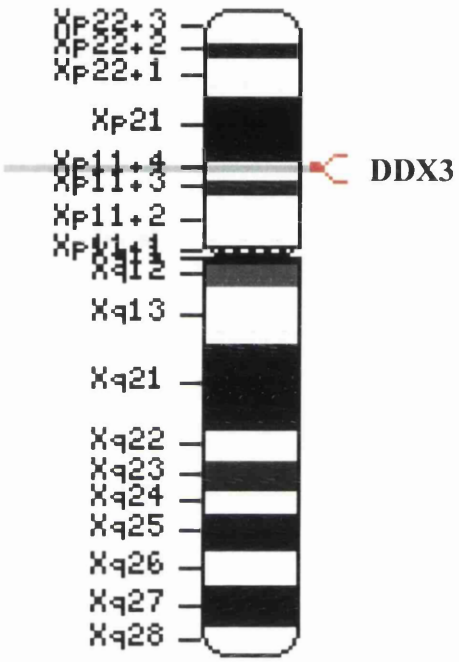

Figure 21: Location of DDX3 gene on the human X chromosome. The NCBI LocusLink resource was used to specifically locate DDX3 in the human genome. The DDX3 gene maps to the p moiety of the X chromosome at position 11.3-11.23 (Xp11.3-p11.23) (LocusLink is at http://www.ncbi.nlm.nih.gov/LocusLink)

significantly reduces or abolishes production of germ cells (Foresta *et al.*, 2000). Interestingly, full-length DBY transcripts are ubiquitously expressed, while a truncated form is apparently only produced in the testis (Foresta *et al.*, 2000).

1.13. 3 Mouse PL10 and mDEAD3

PL10 is encoded by a transcript that is male germ cell-specific, and shows homology to the murine form of eIF4A (Leroy *et al.*, 1989). Expression of the PL10 transcript is developmentally regulated during the meitoic and haploid stages of spermatogenesis (Leroy *et al.*, 1989). The cellular and temporal specificity of expression in germ cells suggests a specific regulatory role for PL10 during spermatogenesis.

The gene encoding mDEAD3 was identified using PCR techniques during a search for DEAD-box proteins expressed in mouse erythroleukaemia cells (MEL) (Gee and Conboy, 1994). The encoded protein is 95% identical at the aa level to PL10, although it is not clear whether the functions of PL10 and mDEAD3 are non-redundant.

1.13. 4 Xenopus *An3*

The mRNA encoding An3 protein was identified in a search for such RNAs that localise to specific parts of unfertilised *X. laevis* oocytes (Rebagliati *et al.*, 1985). An3 is expressed throughout oogenesis and embryogenesis (Rebagliati *et al.*, 1985; Gururajan *et al.*, 1994), and is also present in most adult tissues (Gururajan *et al.*, 1991). Recently, the protein has been shown to be exported from the nucleus by the soluble nuclear export factor CRM1 (Askjaer *et al.*, 1999). The protein also apparently shuttles back to the nucleus via an unidentified nuclear import pathway, or possibly via the same system which may be reversible under certain conditions (Askjaer *et al.*, 1999). *In vitro* ATPase and RNA helicase activity has been demonstrated for the protein. The ATPase activity is stimulated ~6-fold by RNA from *X. laevis* oocytes, while synthetic RNAs have no effect, suggesting a specific activator of An3 enzymatic activity could exist in the cellular context (Askjaer *et al.*,

2000). Not surprisingly, mutations in the DEAD-box of An3, a motif that is essential for ATP hydrolysis (section 1.10.6), reduces the rate of ATP hydrolysis by approximately 6-fold and abolishes RNA helicase activity (Askjaer *et al.*, 2000). Interestingly, however, the same mutation appeared to affect its rate of export from the nucleus, suggesting that this process is coupled to the enzymatic activity of An3 (Askjaer *et al.*, 2000).

1.13. 5 Drosophila *Vasa*

The *D. melanogaster* gene *vasa* encodes a DEAD-box protein with *in vitro* ATP-dependent helicase activity (Liang *et al.*, 1994). The vasa protein seems to regulate the translation of multiple downstream genes. Consistent with this hypothesis, vasa interacts with a *Drosophila* homologue of eIF2 (Carrera *et al.*, 2000). It is an essential component of germ plasm, a poorly characterised nucleoprotein complex that is required for germ cell differentiation (Saffman and Lasko, 1999), and analysis of a null mutant that removes the entire *vasa* coding region leads to female sterility with severe defects in oogenesis (Styhler *et al.*, 1998). Further functional studies suggested the protein was not only essential during this process of gametogenesis in the adult, but also for specification of the germ cell lineage during embryogenesis (Castrillon *et al.*, 2000). Vasa localises during *D. melanogaster* oogenesis to the posterior of the oocytes, the site of germ cell formation, and strong cytoplasmic staining is seen exclusively in germ cells during embryogenesis in both the male and female of the species (Lasko and Ashburner, 1990). A human orthologue of the *Drosophila vasa* gene has recently been identified (Castrillon *et al.*, 2000). The protein is specifically expressed in germs cells as in *D. melanogaster*.

1.13. 6 Yeast Ded1p

The *S. cerevisiae DED1* gene was isolated as a suppressor of a yeast pre-mRNA splicing mutant (*prp8-1*) (Jamieson *et al.*, 1991). However, Ded1p is predominantly cytoplasmic, conflicting with a role in pre-mRNA splicing (Chuang *et al.*, 1997). Indeed, analyses of its suppressor activity and of synthetic lethal interactions with

translation initiation mutants indicated that the Ded1p protein was involved in translation initiation, and not pre-mRNA splicing (Chuang *et al.*, 1997; de la Cruz *et al.*, 1997). Furthermore, immunodepletion of the protein from an *in vitro* translation system abolished translation activity (Chuang *et al.*, 1997). As noted previously (section 1.12.5), genetic analyses suggest that Ded1p and yeast eIF4A play independent roles in this process, while preliminary assays indicate the two proteins interact (Uetz *et al.*, 2000). An interaction with the yeast form of the cap-binding protein eIF4E was also reported (Uetz *et al.*, 2000), consistent with genetic analyses (de la Cruz *et al.*, 1997), further implicating Ded1p in translation initiation. In agreement with the presence of conserved motifs associated with RNA helicases in Ded1p (Jamieson *et al.*, 1991), the protein has RNA-dependent ATPase and ATP-dependent RNA helicase activities (Iost *et al.*, 1999). This property is reliant on the integrity of the DEAD-box, with an E → A mutation in this motif being lethal *in vivo* and inactive in enzymatic assays *in vitro*. As noted previously (1.9.6.9), mouse PL10 can functionally substitute for Ded1p *in vivo* (Chuang *et al.*, 1997; Mamiya and Worman, 1999). DDX3 appears to rescue the same lethal mutation (Mamiya and Worman, 1999), suggesting that the function of Ded1p has been evolutionarily conserved from yeast to mice and humans (Chuang *et al.*, 1997). Intriguingly, Ded1p has also been implicated in selective translation of an mRNA from a virus possessing a segmented genome that replicates in *S. cerevisiae* (Noueiry *et al.*, 2000). Using the previously reported ability of brome mosaic virus (BMV), a positive-strand RNA virus with a segmented genome, to replicate in yeast (Janda and Ahlquist, 1993), it was found that a mutation in the *DED1* gene that did not affect yeast growth specifically inhibited translation of one such RNA segment (Noiery *et al.*, 2000).

1. 14 Aims of the Study

Since little is known about DDX3, the major aim of this project was to characterise the protein, in terms of its fundamental properties and function in a normal cellular context, and determine any modification of these aspects in the presence of HCV core protein. Endogenous DDX3 from various cell lines, and that expressed by plasmid vectors or recombinant virus, were studied using a panel of previously

generated MAbs and PAbs or anti-tag antibodies (see Appendix I) as appropriate. Since preliminary studies on DDX3 and its cellular homologues from other organisms suggested functions in translation (section 1.13), this role for DDX3 was studied in greatest detail. Due to the lack of an efficient cell culture system for HCV, core protein was supplied by recombinant vaccinia or baculovirus, generally along with the HCV glycoproteins to ensure proper processing of core.

CHAPTER TWO:

Materials and Methods

2. 1 Bacterial Strains

Strain	*Phenotype*
TG1	*E. coli* F′ *traD36 lac*^{q}*Δ(lacZ)M15 proA*$^+$*B*$^+$*/supE Δ(hsdM-mcrB)5* ($r_k^- m_k^+$ *McrB*$^-$) *thiu Δ(lac-proAB)*
BL21 (Amersham)	*E. coli* B F$^-$ *omp*T *hsd*S (r_B^-, m_B^-) *gal*

2. 2 Vectors

pGEX-6P-3	Amersham
pGEX-2T	Amersham
pcDNA 3.1/Zeo(+)	Invitrogen
pZeoSV2 (+)	Invitrogen
pET-21a	Novagen
pBluescript SK (+)	Stratagene

2. 3 Chemicals

All chemicals were purchased from Sigma (Poole, UK) or BDH (Poole, UK), unless otherwise stated.

2. 4 Radiochemicals

[α^{32}P]-CTP, -dCTP, -ATP, dATP, and [γ^{32}P]-dATP were purchased from NEN (Boston, MA, USA), with specific activities of 10 μCi/μl each. [^{14}C]-chloramphenicol and [^{35}S]-L-methionine were obtained from Amersham with specific activities of 0.05 and 10 μCi/μl, respectively.

2. 5 Antibodies

A comprehensive list of monoclonal antibodies (MAbs) and polyclonal antisera (PAbs) is presented in Appendix I. Anti-DDX3 MAbs and PAbs, the anti-HCV core PAb, and the MAb raised against the HCV E2 glycoprotein were generously

provided by Dr A. Owsianka, MRC Virology Unit, Glasgow. The PAb directed against the HCV NS3 protease domain was a kind gift from Dr M. Harris, University of Leeds. The MAb directed against SC-35, and the PAb raised against U1A were supplied by Dr A. Lamond, University of Dundee. Commercial antibodies were employed to detect cellular tubulin (Sigma) and ATF-2 (Santa Cruz Biotechnology). The anti-histidine-tag MAb RGS-His (QIAGEN) was used to detect histidine-tagged fusion proteins containing the epitope MRGS(H)[6].

2. 6 cDNA Clones

A complete list of constructs used in this study is presented in Appendix II. A full-length DDX3 cDNA was cloned using RT-PCR by Dr A. Owsianka (Owsianka and Patel, 1999). Plasmids expressing DDX3 C-terminal truncations fused to glutathione S-transferase (GST) (Owsianka and Patel, 1999), and the core-E1-E2 mammalian expression plasmid were generated by Dr A. Patel. The full-length cDNA clone of HCV strain H77c was generously supplied by Dr J. Bukh (Yanagi *et al.*, 1997). Plasmids pcDNA3.1/Zeo(+)-5CC and -5CC3 were provided by Dr J. Wood (Wood *et al.*, 2001). The DDX3 DEAD-box mutant mammalian expression construct was made available by Drs P. Askjaer and J. Kjems (University of Aarhus, Denmark). The bacterial expression vector containing *Xenopus laevis* An3 cDNA (pET-21a-An3) was provided by Dr D. Weeks (National Institute of Child Health and Human Development, Bethesda, MD, USA). pAcCL29.1 was supplied by Dr I. Jones (Livingstone and Jones, 1994). All other constructs were generated by standard cloning techniques (Maniatis *et al.*, 1989), and are described where appropriate.

2. 7 Cells

Laboratory stocks of human hepatoma cell lines Huh-7 and HepG2, a human epitheloid carcinoma cell line (HeLa), an African Green Monkey cell line (COS-7), a Baby Hamster Kidney cell line (BHK-21), and a *Spodoptera frugiperda* insect cell line (Sf21) were used. H9-13 cells, containing selectable self-replicating HCV sub-genomic RNAs, and its parental (naïve) cell line Huh-7 (N), were a kind gift from Dr R. Bartenschlager (Lohmann *et al.*, 1999a).

2. 8 Cell Culture Growth Media

All cell culture media and reagents were purchased from Invitrogen (Paisley, UK) unless otherwise stated. For propagation of Huh-7, Huh-7 (N), HepG2, COS-7 and HeLa cell lines, Dulbecco's Modified Eagle's Medium (DMEM) supplemented with 10% foetal calf serum (FCS), 1% non-essential amino acids, 10 mM glutamine, and 100 units/ml penicillin-streptomycin was used. This medium was further supplemented with 500 μg/ml G-418 disulphate (Duchefa, Haalem, The Netherlands) for propagation of the H9-13 cell line. BHK-21 cells were grown in Glasgow Modified Eagle's Medium (GMEM) supplemented with 10% new-born calf serum (NCS), 5% tryptose-phosphate, 1.5% non-essential amino acids, 0.3% sodium bicarbonate, 20 mM glutamine, and 100 units/ml penicillin/streptomycin. The Sf21 cell line was grown in TC-100 medium supplemented with 10% FCS and 100 units/ml penicillin/streptomycin.

2. 9 Storage of Cell Lines

Confluent monolayers of cell lines grown in 175 cm^2 tissue culture flasks were harvested, resuspended in 10 ml cell storage medium (normal growth media supplemented with 25% FCS and 10% DMSO), and aliquoted into 1.5 ml screw-capped tubes. The tubes were stored overnight in a protective box at –70°C and subsequently transferred to –180°C for long-term storage.

2. 10 Propagation of Hybridoma Cell lines

Hybidoma cell lines were cultured in DMEM supplemented with 10% FCS, 4% hypoxanthine aminopterin (HAT), 0.1% Gentamycin, and 10 mM glutamine (HAT medium).

2. 11 Bacterial Culture Media

Bacterial strains carrying the pZeoSV2 (+) plasmid were cultured in Low Salt Luria broth (LB) (0.5% NaCl, 1% Tryptone, 0.5% yeast extract) containing 25 μg/ml Zeocin (Invitrogen). All other plasmids were propagated in bacterial strains grown in normal LB (1% NaCl, 1% tryptone, 0.5% yeast extract) or 2YT (0.5% NaCl,

1.6% tryptone, 1% yeast extract) containing the appropriate antibiotic for selection (typically ampicillin, 100 μg/ml). Colonies carrying the pZeoSV2 (+) plasmid were grown on Low Salt LB containing 1.5% agar and 25 μg/ml Zeocin in 90 mm diameter dishes. All other bacterial colonies were grown on LB containing 1.5% agar containing the appropriate antibiotic in 90 mm diameter dishes.

2. 12 Standard Solutions

PBS	170 mM NaCl, 3.4 mM KCl, 10 mM Na_2HPO_4, 1.8 mM KH_2PO_4 (pH 7.2).
PBSG	PBS containing 10% glycerol
PBST	PBS containing 0.05% Tween-20
10 × TBE	1.25 M Tris, 0.4 M Boric acid, 27 mM EDTA
SDS-PAGE Running Buffer	25 mM Tris, 192 mM glycine, 0.1% SDS
Towbin's Blotting Buffer	25 mM Tris, 192 mM glycine, 20% methanol (pH 8.3)

2. 13 Manipulation of DNA

2.13. 1 Small Scale Purification of DNA

A modified alkaline lysis method was used for routine isolation of plasmid DNA. Briefly, 1 ml of LB or 2YT medium containing the appropriate antibiotic was inoculated with a single fresh bacterial colony (2-3 mm) and incubated at 37°C for 5-16 hours with shaking (200 rpm). 200 μl of culture was transferred to a 1.5 ml microfuge tube and mixed by gentle inversion with 200 μl alkaline lysis buffer (200 mM NaOH, 1% SDS). To this, 200 μl neutralisation buffer (3 M potassium acetate, pH 5.5) was added prior to centrifugation at high speed (12,000 × *g*) to pellet cellular debris. The supernatants were transferred to a fresh 1.5 ml microfuge tube containing 0.5 ml isopropanol, mixed, and centrifuged at high speed to recover the precipitated DNA. The DNA pellet was washed briefly in 75% ethanol, air-dried and resuspended in 30 μl dH_2O containing 10 μg/μl RNase A (Sigma).

2.13. 2 Medium Scale Purification of DNA

The Quick Flow Midi Kit (Hybaid) was used for routine production of large amounts (250-750 μg) of high quality plasmid DNA from 100 ml cultures.

2.13. 3 Large Scale Purification of DNA

The QIAprep Mega Kit (QIAGEN) was used for production of milligram quantities of plasmid DNA from 1 L cultures.

2. 14 Quantitation of Nucleic Acid Concentration

DNA or RNA samples were diluted 1:50, 1:250, and 1:500 in 100 μl dH_2O and optical density (OD) readings taken at 260 nm and 280 nm. The concentration of nucleic acid in a sample is proportional to the absorbency at 260 nm - an OD of 1 corresponds to approximately 50 μg/ml for double-stranded DNA and 40 μg/ml for RNA (Maniatis *et al.*, 1989). Contamination by protein and other substances was assessed by calculating the ratio OD_{260}/OD_{280}. Pure preparations of DNA and RNA have OD_{260}/OD_{280} ratios of 1.8 and 2.0, respectively (Maniatis *et al.*, 1989). If necessary, significant contamination was eradicated by further precipitation.

2. 15 PEG-Precipitation of Miniprep DNA

DNA produced by the modified alkaline lysis method (section 2.13.1) was purified further as required by precipitation with polyethylene glycol (PEG). The DNA in solution was mixed with PEG-NaCl to a final concentration of 7.5% PEG and 0.4 M NaCl and chilled on ice for 1 hour. The precipitated DNA was recovered by centrifugation at high speed (12,000 × *g*, 15 minutes). The resulting pellet was washed with 75% ethanol and resuspended in 20 μl dH_2O. This purified DNA was of sufficient quality for sequencing and transfection into mammalian cells.

2. 16 Sequencing

DNA sequences were obtained by cycle sequencing using the ABI Prism BigDye Terminator Cycle Sequencing Ready Reaction Kit (Applied Biosystems, Perkin-

Elmer Corporation) and running the reactions on an ABI Prism automated sequencer. Sequencing was carried out by Ms L. Taylor (Institute of Virology, University of Glasgow) and Dr G. Riboldi-Tunicliffe (Molecular Biology Support Unit, University of Glasgow).

2. 17 Oligonucleotides

High purity salt-free (HPSF) purified oligonucleotides were purchased from MWG Biotech (Ebersberg, Germany).

2. 18 Polymerase Chain Reaction (PCR)-Mediated Amplification of cDNAs

PCR (Mullis *et al.*, 1986) was performed using a PTC-200 Peltier Thermal Cycler (MJ Research). Depending on the application, Taq (Invitrogen), Pwo (Roche), or High Fidelity (Roche) polymerases were used according to the manufacturer's instructions in conjunction with specific primers to amplify cDNAs of interest. A standard PCR programme is presented below.

Denaturation	95 °C	5 mins	
Annealing	95 °C	1 min	30 cycles
Elongation	55 °C	1 min	
Termination	72 °C	1 min	
Termination	72 °C	10 mins	

2. 19 Digestion of DNA with Restriction Endonucleases

Restriction endonucleases were purchased from Roche or New England Biolabs (NEB) and used according to the manufacturer's instructions.

2. 20 Nucleotide/Enzyme Removal from Digests and PCR Fragments

The QIAquick Nucleotide Removal Kit (QIAGEN) was used to remove nucleotides/enzymes prior to subsequent experimental procedures.

2. 21 Modification of Restriction Fragments

DNA polymerase 1 (Klenow fragement), T4 DNA polymerase, and Mung Bean nuclease were purchased from NEB and used according to the manufacturer's instructions.

2. 22 Electrophoretic Separation and Isolation of Restriction Fragments

DNA was resolved by horizontal electrophoresis in gels containing 0.7-1.5% agarose and run in 0.5 × TBE containing 1 μg/ml ethidium bromide. DNA samples were mixed with 0.1 volumes of 10 × DNA loading buffer (0.5 × TBE, 5% glycerol, coloured with bromophenol blue), loaded onto a gel and run at 100 V until the dye front had migrated close to the edge of the gel. Restriction analysis was performed using a BioRad Gel Doc 2000 imager with Quantity One software (BioRad). Alternatively, restriction fragments to be used in further applications were visualised using a long-wave UV light box (to minimise UV exposure), manually cut from the gel using a clean scalpel, and recovered using the QIAquick Gel Extraction Kit (QIAGEN).

2. 23 Production of DNA Size Markers

10 μg of purified bacteriophage λ DNA (NEB) was digested for 16 hours at 60°C with *Bst*EII in a 50 μl reaction volume. The reaction was mixed with 40 μl dH_2O and 10 μl 10 × DNA loading buffer. 10 μl of the digested DNA (1 μg) was run on each agarose gel as DNA size markers. The resulting fragments of the λ/*Bst*EII digest were, in bp, 8454, 7242, 6369, 5689, 4822, 4324, 3675, 2323, 1929, 1391, 1264, 702, 224 and 117.

2. 24 Ligation of Isolated DNA fragments to Expression Vectors

Standard ligation reactions were carried out using T4 DNA ligase (Invitrogen) according to the maunfacturer's instructions. Overhanging and blunt-ended DNA fragments were ligated for 16 hours at 25°C and 16°C, respectively. The ligated DNA was precipitated by addition of 0.1 volumes 3 M sodium acetate (pH 5.1) and

2.5 volumes of ethanol and chilling at –20°C for 5 hours. Precipitated DNA was recovered by centrifugation, washed with 75% ethanol, resuspended in 5 μl dH_2O, and used to transform electrocompetent *E. coli* strains (see section 2.26).

2. 25 Production of Electrocompetent Bacteria

10 ml 2YT inoculated with a single fresh *E. coli* TG1 or BL21 bacterial colony (1-2 mm) was grown for 16 hours at 37°C with shaking (200 rpm). The culture was transferred to 800 ml of 2YT media pre-heated to 37°C, and grown for approximately 3 hours until the OD_{600} reached 0.6-0.8. The culture was chilled on ice for 15-30 minutes and pelleted (5,000 × *g*, 5 minutes, 4°C) in pre-chilled 250 ml centrifuge tubes. The pellet was sequentially resuspended in 1 L and 500 ml of ice-cold dH_2O following recovery as before. The pellet was then resuspended in 20 ml ice-cold 10% glycerol, recovered as before, and finally resuspended in 1 ml ice-cold 10% glycerol. 60 μl aliquots of this were either kept on ice and used directly in transformations, or snap-frozen in liquid nitrogen and stored at –70°C. The frozen aliquots were stable for at least two months.

2. 26 Transformation of Electrocompetent *E. coli* with Plasmid DNA

2 μl of plasmid DNA precipitated as described in section 2.24 was electroporated (1.6 kV, 25 μF) using a BioRad Gene-Pulser II into one 60 μl aliquot of an electrocompetent *E. coli* strain. The bacteria were immediately resuspended in 1 ml 2YT or Low Salt LB and incubated for 1 hour at 37°C with shaking (200 rpm). The bacterial suspension was plated out on LB/agar or Low Salt LB/agar plates containing the appropriate antibiotic and incubated at 37°C for 16 hours.

2. 27 Northern Blot Analysis

Northern blotting (Alwine *et al.*, 1977; Alwine *et al.*, 1979) is the transfer of electrophoretically separated RNAs from a gel to positively charged membranes for subsequent fixation and hybridisation with a specific probe. Following extraction and purification of the RNA under investigation, Northern blot analysis typically

constitutes electrophoresis of the RNA, transfer of the RNA to a membrane, immobilisation of the RNA on the membrane, and subsequent hybridisation of a labelled probe and analysis of the hybridisation events.

2.27. 1 Extraction of Cellular and Viral RNA from Cell Lines

Total RNA from cell lines (or cells infected with recombinant virus) in cell culture dishes (diameter 35 mm) was prepared using Trizol LS Reagent (Invitrogen), employing basic precautions throughout to prevent contamination by exogenous RNases. Briefly, following removal of cell culture medium, 375 μl of Trizol was pipetted onto the cell monolayer and incubated at room temperature (RT, 18-25°C) for 5 minutes. The cell lysate was passed through a pipette several times to produce a homogenous suspension, and transferred to a 1.5 ml microfuge tube. 100 μl chloroform was added and the tubes were vigourously shaken by hand for 15 seconds. Following incubation at RT for 15 minutes, the samples were centrifuged (12,000 × *g*, 15 minutes, 4 °C). The upper aqueous layer was transferred to a fresh microfuge tube, mixed with 250 μl isopropanol, and incubated at RT for 10 minutes. The precipitated RNA was collected by centrifugation as above. RNA pellets were washed with 70% ethanol, collected by centrifugation (7,500 × *g*, 5 minutes, 4°C) and briefly air-dried. The extracted RNA was resuspended in 30 μl dH_2O and stored at –70°C prior to experimental procedures.

2.27. 2 Electrophoretic Separation of RNA

A method for fractionation of RNA by size adapted from those described previously (Goldberg, 1980; Lehrach *et al.*, 1977) was used. For electrophoresis in a 12 × 8 × 1 cm gel, 0.7-1.2g agarose was dissolved in 20 ml 5 × MOPS buffer (200 mM MOPS-HCl, pH 7.0, 2.5 mM EDTA, 25 mM sodium acetate) and 62 ml dH_2O by heating in a microwave. After cooling to 60°C, 18 ml 37% deionised formaldehyde was added to the molten agarose mixture. The gel was poured and allowed to set for 1 hour. RNA samples (10-40 μg total RNA) in dH_2O were denaturated by mixing with 3 volumes of formaldehyde load dye (Ambion) and heating at 55°C for 15 minutes. While the samples were cooling on ice, the gel was pre-run at 100 V for 10 minutes

in 1 × MOPS buffer. Samples were loaded onto the gel and electrophoresis was allowed to proceed at 100 V until the dye front had migrated at least half-way through the gel. The running buffer was changed once during this time to prevent over-heating of the gel.

2.27. 3 Capillary Blotting

Fractionated RNA was transferred to positively-charged nylon membranes (Hybond-N, Amersham) in a standard capillary transfer set-up (Maniatis *et al.*, 1989). Briefly, a stack of absorbent material, such as paper towelling, was used to draw the transfer buffer (20 × SSC; 3 M NaCl, 0.3 M sodium citrate) from a reservoir, up through the gel and finally into the stack of paper towels. As the buffer continued to move upward, the RNA was transferred out of the gel and trapped on positively-charged filter membranes. Prior to transfer, the membrane was submerged in dH_2O and then 20 × SSC before being gently overlaid onto the gel.

2.27. 4 UV Cross-Linking of RNA to Membranes

Fractionated RNA was immobilised on Hybond-N membranes using a UV Stratalinker 1800 (Stratagene) set to autocrosslink (120 mJ/cm^2).

2.27. 5 Hybridisation of Probes to RNA Immobilised on Membranes

10 ml hybridisation buffer (Rapid-Hyb Buffer, Stratagene, or ExpressHyb, Clontech) was warmed to 65°C. 0.1 mg of Herring Sperm DNA (Sigma) which had previously been boiled for 5 minutes and then chilled on ice was added to the hybridisation buffer and mixed. 5 ml of this solution was transferred to a hybridisation tube. Hybond-N membrane containing immobilised fractionated RNA to be probed was added to the hybridisation tube. The membrane was pre-hybridised at 65°C with constant rotation for 1 hour. During this time the probe solution was prepared: 5×10^6 cpm of ^{32}P-labelled probe (prepared as will be described in section 2.28) was mixed with 30 μg COT1-DNA (Roche), 150 μg Herring Sperm DNA, 50 μl 20 × SSC and dH_2O to a final volume of 200 μl. The probe solution was boiled

for 5 minutes and then heated at 68°C for 30 minutes. This solution was mixed with the remaining 5 ml of hybridisation buffer. The pre-hybridisation buffer was discarded before the probe solution in hybridisation buffer was added directly into the hybridisation tube. Hybridisation was allowed to proceed for 2-16 hours at 65°C. The hybridisation solution was discarded and replaced with 200 ml of wash solution 1 (2 × SSC, 1% SDS). The blot was washed in this solution 4 × 20 minutes with continuous rotation at 65°C. The blot was washed a further two times in wash solution 2 (0.1 × SSC, 0.5% SDS) at 55°C. The stringency of the wash steps was altered as required.

2.27. 6 Analysis of Hybridisation Events

The membrane was wrapped in cling-film prior to subsequent procedures. The approximate intensity of emitted radiation from hybridised ^{32}P-labelled probe was determined using a Geiger-Mueller tube. Depending on this rough value, membranes were exposed to a phosphorimager screen for 1 hour to 3 days. Hybridisation events were visualised using a Bio-Rad Molecular Imager FX with Quantity One software (Bio-Rad).

2. 28 Random Primer Labelling

Specific radiolabelled probes were produced using the Prime It II Random Primer Labelling kit (Stratgene). The system relies on the ability of random oligonucleotides to anneal at multiple sites along the length of a DNA template, forming a substrate for the Klenow fragment of DNA polymerase I. 25 ng of DNA template (PCR product or restriction fragment representing the region to be targeted by the probe) in 24 μl dH_2O was mixed with 10 μl random oligonucleotide primers (27 OD units/ml). The mixture was boiled for 5 minutes, before mixing with 10 μl 5 × dCTP buffer (containing 0.1 mM dATP, dGTP and dTTP), 5 μl [$\alpha^{32}P$]-dCTP (10 μCi/μl), and 5 units Exo(-) Klenow (3′-exonuclease-deficient mutant). The reaction was incubated at 37°C for 10-30 minutes. 2 μl stop mix (0.5 M EDTA, pH 8.0) was then added before removal of unincorporated nucleotides using a QIAquick Nucleotide Removal column (QIAGEN).

2. 29 Production of GST-fusion Proteins

GST-fusion proteins were produced according to the Amersham protocol following cloning of the relevant cDNA in frame with the GST-coding sequence in the pGEX-6P-3 vector. Briefly, an overnight culture inoculated with a fresh BL21 bacterial colony (transformed with the relevant plasmid) and supplemented with ampicillin (100 μg/ml) was diluted 1:10 in fresh medium containing the antibiotic and grown at 37°C to mid-log phase (A_{600} = 0.6-1.0). Expression of the GST-fusion protein was induced by addition of isopropyl-β-D-thiolgalactoside (IPTG) to a final concentration of 0.5-1.0 mM. Cells were allowed to grow for an additional 5 hours and then pelleted by centrifugation (6,000 × *g*, 5 minutes, 4°C). Bacterial pellets were resuspended in 10 mls PBSG (section 2.12). Cells were lysed by sonication using a Branson 450 Sonifier on continuous low power (setting 3) for 2 minutes. Triton X-100 (Sigma) was added to a final concentration of 1% to aid solubilisation of proteins and samples were incubated at 4°C for 30 minutes with rotation. Extracts were centrifuged (10,000 × *g*, 10 minutes, 4°C) to remove cellular debris. 400 μl slurry containing 50% glutathione linked to agarose beads in PBSG was added to the supernatant following transfer to a 15 ml polypropylene tube, and mixed for 1 hour at 4°C. GST-fusion protein bound to glutathione-agarose was collected by centrifugation (500 × *g*, 5 minutes, 4°C). The supernatant was decanted and sedimented agarose beads were washed with PBSG three times. For elution of protein from the beads, 100-200 μl glutathione elution buffer (50 mM Tris-HCl, 10 mM reduced glutathione, pH 8.0) in PBSG was added and mixed for 20 minutes at 4°C. The elution process was repeated a further 3 times. Eluted GST-fusion protein was stored at –70°C.

2. 30 Determination of Protein Concentration

Samples and standards were mixed with the Coomassie Plus Protein Assay Reagent (Pierce) according to the manufacturer's instructions. Protein concentration was determined using a Heλios α (Unicam) spectrophotometer.

2. 31 Fractionation of Proteins by SDS-PAGE

Proteins were separated according to the method of Laemmli *et al.* (1970) using Mini-Protean II apparatus (Bio-Rad). Samples (typically 10-20 μg total protein) were mixed with 0.33 volumes of 3 × SDS-PAGE denaturing buffer (200 mM Tris-HCl, pH 6.7, 0.5% SDS, 0.7% β-mercaptoethanol, 10% glycerol) and boiled for 2 minutes prior to loading. Gels containing 8-12.5% polyacrylamide depending on the molecular weight of the protein under investigation were run at 120 V until the dye front reached the bottom of the gel. Protein size markers (Rainbow Markers, Amersham) were run alongside protein samples in SDS-PAGE denaturing buffer. Fractionated proteins were analysed by Western blotting (see below) or fluorography (see section 2.46), or by staining directly with 0.1% Coomassie brilliant blue (Bio-Rad) in fix (50% methanol, 7% acetic acid) for 30 minutes followed by repeated destaining (10% methanol, 7% acetic acid).

2. 32 Western Blotting

Proteins separated by SDS-PAGE were electrophoretically transferred (90 V, 1 hour, 4°C) to nitrocellulose membranes (Hybond ECL, Amersham) essentially as described by Towbin *et al.* (1979) using Bio-Rad Gel Blotting apparatus. Following transfer, membranes were immersed in PBST containing 5% non-fat milk powder (Marvel) for 30 minutes to block non-specific binding of antibody. Membranes were then washed 3 × 15 minutes in PBST and incubated with the relevant primary antibody or antisera appropriately diluted in PBST containing 1% bovine serum albumin (BSA) for 1-2 hours. Membranes were washed as before to remove any unbound primary antibody/antisera and incubated with appropriately diluted secondary antibody conjugated to horse radish peroxidase (HRP). Membranes were washed as before and developed by addition of enhanced chemiluminescence (ECL) reagents (Amersham). Binding of antibody to fractionated proteins was visualised by autoradiography using Kodak X-OMAT film and a Konica SRX-101-A film processor.

2. 33 Enzyme-linked Immunosorbent Assay (ELISA)

An ELISA-based method was used to determine direct binding of MAbs to GST-fusion proteins. Wells in a 96-well plate (Immulon II, Dynex Technologies) were coated with 0.1 mg protein and a series of 3-fold dilutions thereof in PBS, and incubated at 4°C for 16 hours. Non-specific antibody binding sites were blocked by addition of 100 µl 2% Marvel in PBST. MAb supernatants were diluted in PBS 5-fold, added directly to the plates, and incubated at RT for 2 hours. The plates were washed four times with PBST. An anti-mouse IgG-HRP conjugate (Sigma) diluted 1:1000 in PBST was added to each well and incubated for a further 2 hours at RT. 100 µl TMB (3,3′,5,5′-tetra methylbenzidine) complete developing solution (Sigma) was added and reactions were allowed to proceed for up to 30 minutes. Reactions were stopped by addition of 100 µl 0.5 M H_2SO_4, and OD_{600} determined using an Opsys MR plate reader (Dynex Technologies).

2. 34 Production of Lipofection Reagent

A lipofection reagent for transfection of cell lines with DNA was produced essentially as described by Rose *et al.* (1991). 10 mg of phospatidyl ethanolamine dioleoyl in 1 ml $CHCl_3$ (Sigma) was added to 4 mg of dimethyl dioctadecyl ammonium bromide (Sigma) and vortexed briefly. The chloroform was evaporated from the mixture under a light stream of liquid nitrogen leaving a white precipitate. The precipitate was resuspended by adding 10 ml dH_2O and vortexing continuously for 5 minutes. The milky solution was clarified by sonication using a Branson 450 Sonifier on continuous low power (setting 3) for 15 minutes or until the solution had sufficiently cleared. The lipofection reagent was transferred to 1.5 ml screw-capped tubes in 1 ml aliquots and stored at 4°C.

2. 35 Transfection of Mammalian Cell Lines

Mammalian cell lines grown to a confluency of approximately 50% were transfected in 24-well dishes (diameter of wells 16 mm) employing standard lipofection protocols. Briefly, 1 µg plasmid DNA was mixed with 50 µl of Optimem-1 (Invitrogen), and subsequently mixed with 50 µl Optimem-1 containing 6 µl

lipofection reagent (see above). After incubation at RT for 15 minutes, 150 μl Optimem-1 was added and the mixture was immediately pipetted onto monolayers pre-washed with Optimem-1. Cells were incubated for 5 hours at 37°C, following which 250 μl of normal medium containing 20% FCS was added and returned to the incubator for 16 hours. Cells were replenished with fresh medium and grown for a further 24-48 hours before analysis for protein expression by Western blotting (as described in section 2.32) or other methods (see section 2.42). The volumes indicated above were scaled-up relative to the diameter of the cell culture dishes employed.

2. 36 Generation of Constitutively Expressing Cell Lines

Approximately 70-80% confluent monolayers of Huh-7 cells in 60 mm dishes were transfected as described above with appropriate plasmid containing the gene of interest and a selectable marker applicable to mammalian cell lines. Fresh medium was added to the cells 24 hours post-transfection. After a further 24 hours, the cells were washed with versene, trypsinised, and resuspended in 50 ml fresh media. 5 ml of this was plated out on ten 60 mm dishes and incubated at 37°C for 16 hours. The existing media was then replaced with medium containing the appropriate antibiotic. Fresh medium containing antibiotic was added to the transfected cells every 4-5 days until clearly separated colonies appeared. Suitably sized colonies (2-3 mm) were picked and transferred using a pipette to 24-well dishes containing fresh medium. The colonies were grown to confluency and transferred to small (25 cm^2) and then to medium (80 cm^2) tissue culture flasks. Cell lines were subsequently stored as described in section 2.9. Expression of the appropriate mRNA or protein product was evaluated by Northern or Western blotting, respectively.

2. 37 Generation of Recombinant Baculoviruses

2.37. 1 Background

Recombinant baculoviruses (rbacs) have become widely used as vectors to express heterologous genes of interest in Sf21 or other insect cell lines. The heterologous gene is placed under control of the strong polyhedrin promoter of the *Autographa*

california nuclear polyhedrosis virus (AcNPV) and is often abundantly expressed during the late stages of infection. For the most part, the recombinant proteins are processed, modified, and targeted to their appropriate cellular locations where they are functionally analogous to their authentic counterparts (King and Possee, 1992).

2.37. 2 General Overview of the Protocol

Since AcNPV has a large (130 kb) genome with multiple recognition sites for restriction endonucleases, rbacs were constructed in two steps. First, the heterologous gene of interest was cloned in frame with the polyhedrin promoter in the pAcCL29.1 transfer vector (Livingstone and Jones, 1989) flanked by baculovirus DNA derived from a non-essential locus. Second, the plasmid was introduced into Sf21 cells along with wild-type viral genomic DNA. Wild type baculovirus DNA was linearised with *Bsu*36I at a unique site located near the target site for insertion of the foreign gene and treated with calf intestinal phosphatase (CIP) to improve the fraction of recombinant progeny virus. The restriction endonuclease was subsequently inactivated by heating the reaction to 80°C for 20 minutes. 1 μg of this DNA plus 2-5 μg plasmid DNA consisting of the gene of interest in transfer vector pAcCL29.1 was transfected into Sf21 cells (as will be described in section 2.39) grown in 35 mm dishes to a confluency of approximately 50%. Following incubation of transfected cells at 28°C for 72 hours, the medium was collected and plaque purified as below.

2.37. 3 Plaque Purification of Rbacs

35 mm dishes seeded with 1×10^6 Sf21 cells were infected with 10-fold serial dilutions (10^{-1} to 10^{-4}) of the virus to be purified in 100 μl normal medium (TC-100). Infections were allowed to proceed for 1 hour with occasional gentle agitation. The inoculum was removed and the cell monolayer was covered with molten agarose as follows. 0.75 mls 3% low melting point agarose (Invitrogen), previously melted and cooled to 30°C, was mixed with 0.75 mls normal medium warmed to 30°C and gently overlayed onto the monolayer. The agarose mixture was allowed to set, and 1.5 mls normal medium was subsequently added to prevent drying of the

agarose layer. Following incubation at 28°C for 72 hours, plaques formed by virus infection were visualised by addition of 0.5 ml normal medium containing 0.02% neutral-red stain and incubation at 28°C for 6-24 hours. The medium was decanted and several agarose plugs at the site of well-separated plaques were picked using a sterile Pasteur pipette and transferred to individual 300 μl aliquots of normal medium. Cells in each agarose plug were lysed by repeated freezing and thawing, before briefly sonicating (Sonibath, Kerry Ultrasonics). 100 μl of this preparation and 4-fold dilutions thereof were used to infect Sf21 cells in 35 mm dishes as above, and each virus plaque purified once more.

2.37. 4 Production of High Titre Rbacs

10 μl plaque-purified virus preparation was used to infect 1×10^6 Sf21 cells in a 35 mm dish and incubated at 28°C for 72 hours. Expression of the recombinant protein was confirmed by Western blotting (section 2.32) of the infected cell extracts with relevant MAbs or PAbs. A further 10 μl plaque-purified virus preparation was then used to infect a separate 35 mm dish containing 1×10^6 Sf21 cells. The infection was allowed to proceed at 28°C until most of the cells had detached from the culture dish. 100 μl of the medium was used to inoculate 2×10^6 Sf21 cells in a small tissue culture flask (25 cm^2). Again, the infection was allowed to proceed until most of the cells had detached. 1 ml of the medium containing virus was stored at −70°C as a seed stock. The remainder was used to inoculate roller bottles (2 L) containing Sf21 cells to prepare a high titre stock. Following incubation at 28°C for 72 hours, the medium containing large amounts of recombinant virus was decanted and clarified by centrifugation (3,000 × *g*, 10 minutes, 4°C). Virus was subsequently pelleted by centrifugation (12,000 × *g*, 2 hours, 4°C) and resuspended in 2 ml normal medium. Rbacs generated using the above protocols were titrated as follows. 35 mm dishes seeded with 1×10^6 Sf21 cells were infected with 10-fold serial dilutions (10^{-4} to 10^{-12}) of the virus to be purified in a 100 μl inoculum. The monolayer was overlaid with agarose, and stained as before after incubation for 72 hours at 28°C. The number of plaques on two separate plates was counted and used to calculate the virus titre.

2. 38 Infection of Sf21 Cells with High Titre Rbacs

Sf21 cells were seeded in 35 mm dishes to reach 70-80% confluency following overnight incubation at 28°C. Appropriate dilutions of virus were prepared in 100 µl TC-100 medium to give an m.o.i. of 0.5 to 5 and then gently overlaid onto the cell monolayer. The infected cells on 35 mm dishes were incubated at 28°C with frequent shaking. After 1 hour, 3 ml TC-100 medium was added to the monolayers. Infections were allowed to proceed for 48-72 hours following which the cells were washed with PBS, harvested, and resuspended in appropriate buffer for Western blotting (section 2.32) or other applications (see section 2.42).

2. 39 Transfection of Sf21 Cells

Sf21 cells were transfected essentially as described in section 2.35 for mammalian cells using the lipofection reagent except that Optimem-1 was adjusted to pH 5.8-6.0 with concentrated HCl (10 ml Optimem-1 plus 26.5 µl HCl).

To look for transient expression of heterologous genes from the pAcCL29.1 transfer vector directly, Sf21 cells were infected with the wild-type baculovirus PAK6 at an m.o.i. of 5 for 1 hour at 28°C to supply the necessary factors for transcription from the baculovirus polyhedrin promoter and expression of protein. The infected cells were then transfected as above with the pAcCL29.1 vector containing the heterologous gene and incubated at 28°C for 48-72 hours.

2. 40 Production of High Titre Recombinant Vaccinia Virus

Recombinant vaccinia viruses (rVVs) used in these studies were previously generated by Dr A. Patel (Owsianka and Patel 1999; Owsianka *et al.*, 2001) (see Appendix III). To generate a high titre stock of these viruses, BHK-21 or Huh-7 cells grown in ten roller bottles to a confluency of approximately 80-90% were infected at a multiplicity of infection (m.o.i.) of 0.01 in 40 ml low serum medium (140 ml Eagle's A medium plus 20 ml Eagle's B, 20 ml tryptose/phosphate, and 5 ml new-born calf serum). Roller bottles infused with 5% CO_2 were incubated at 37°C with constant gentle agitation until complete cytopathic effect (c.p.e.) was

achieved (usually 3 to 5 days). The infected cells were recovered by centrifugation (3,000 × *g*, 15 minutes) and resuspended in 8 ml Tris buffer (10 mM Tris-HCl, pH 9.0). The cells were lysed on ice using a Dounce homogeniser (50 strokes) and cell debris pelleted (2,000 × *g*, 10 minutes, 4°C). Trypsin was added to the supernatant to a final concentration of 250 ug/ml and incubated at 37°C for 30 minutes with frequent shaking. Tris buffer was added to 36 ml final volume and 18 ml of this preparation was overlayed on an equal volume of 36% sucrose in Tris buffer in each of two centrifuge tubes. Virus particles were pelleted by centrifugation at 12,000 × *g* (80 minutes, 4°C) using an AH629 rotor (Sorvall). The pellet was resuspended in 2 ml 1 mM Tris-HCl (pH 9.0) and stored at –70°C.

2. 41 Titration of rVVs

10-fold dilutions (10^{-1} to 10^{-12}) of virus preparation in a 100 µl inoculum were plated onto sub-confluent monolayers of Huh-7 or BHK-21 cells in 35 mm dishes. Following incubation at 37°C for 1 hour, cell culture medium containing 1.5% carboxymethyl cellulose was added. The cells were incubated for 3 days at 37°C, the medium decanted, stained with Giemsa stain for 2 hours at RT, gently washed with tap water and allowed to dry. The plaques were counted and used to calculate the virus titre.

2. 42 CAT Assay

Following transfection, cells were washed with PBS and harvested by scraping. The total cell extract was resuspended in 100 µl 250 mM Tris-HCl (pH 7.8) and lysed by repeated freezing and thawing, before briefly sonicating to produce a homogenous solution. Cell debris was pelleted by centrifugation and the supernatant was assayed for CAT activity essentially as described by Seed and Sheen (1988). Briefly, equal total protein concentrations of cell extract were transferred to a 1.5 ml microfuge tube and the required amount of 250 mM Tris-HCl (pH 7.8) to give 25 µl final volume was added. The cell extract was mixed with 14 µl dH_2O, 1 µg acetyl-coenzyme A (Sigma), and 0.5 µl 0.05 µCi/µl [^{14}C]-chloramphenicol. A modified form (1-deoxy[dichloroacetyl-1-^{14}C]-chloramphenicol) of the standard radiolabelled

substrate (dichloroacetyl-1,2-[^{14}C]-chloramphenicol) was often used, particularly for quantitation of CAT activity, since this form only gave one product in the presence of CAT protein. After incubation for 30 minutes in a 37°C water-bath, the organic phase was extracted with 200 µl ethyl acetate (Sigma) by vigorous shaking and centrifugation. The sample was subsequently vacuum-dried, resuspended in 20 µl ethyl acetate, spotted onto thin-layer chromatography (TLC) plates (Merck) and separated by TLC in 100 ml solvent consisting of 95% $CHCl_3$ and 5% methanol. The dried plates were covered with ScreenGuard film (Bio-Rad), and exposed to a phosphorimager screen for 16 hours. CAT activity was quantitated as before (section 2.27.6).

2. 43 *In vitro* Transcription and Translation

The bacteriophage T7 or T3 RNA polymerase-driven Riboprobe Kit (Promega) was used according to the manufacturer's instructions to produce RNA run-off transcripts from linearised DNA constructs containing the appropriate promoter. The Rabbit Reticulocyte Lysate System (Promega) was used to translate *in vitro* transcribed RNA. Briefly, 1-2 µg RNA produced by *in vitro* transcription was denatured by heating at 65°C for 3 minutes in a total volume of 10.8 µl dH_2O and then cooled on ice. The RNA was mixed with 33 µl reticulocyte lysate, 1 µl of 1 mM amino acid mixture lacking methionine, 2 µl [^{35}S]-L-methionine (10 µCi/µl), 40 units RNasin, and 2.2 µl of 2.5 mM KCl. Reactions were incubated at 30°C for 90 minutes and then stored at –20°C prior to subsequent experimental procedures. To visualise *in vitro* translated products, 5 µl of the reaction was mixed with SDS-PAGE denaturing buffer, boiled for 2 minutes, loaded onto a gel containing an appropriate concentration of polyacrylamide, and analysed by fluorgraphy (see section 2.46).

2. 44 Indirect Confocal Immunofluorescence Microscopy

Cells on 13 mm glass coverslips in 24-well dishes were washed with PBS and fixed in ice-cold methanol for 10 minutes. The cells on coverslips were washed briefly with PBST (× 4). The cells were then permeabilised in 1 ml ice-cold acetone for 2

minutes, and washed with PBST a further 4 times. Coverslips were overlaid (cell-side down) onto 20 μl of the appropriate primary antibody diluted in PBST and incubated at RT for 45 minutes. The coverslips were washed (4 × PBST) and subsequently overlaid onto 20 μl of the appropriate conjugated secondary antibody prepared in PBST for 45 minutes. The coverslips were washed as above, then briefly dipped in dH_2O and overlaid onto 20 μl Citifluor fluorescence enhancing reagent (UKC Chemical Laboratories, Cantebury, UK) before sealing with clear nail varnish. Confocal analysis was performed using a Zeiss Laser Scanning Microscope with LSM510 software (Zeiss).

2. 45 Subcellular Fractionation

The method of Lee and Green (1990) was essentially followed for separation of nuclear and cytoplasmic fractions of cell lysates. Cells were seeded in 35 mm dishes to reach a confluency of 70-80% after 16 hours, washed with PBS, harvested by scraping, and pelleted by centrifugation (2,000 × *g*, 5 minutes, 4°C). The pellet was resuspended in 0.5 ml PBS and recovered as before. The cells were subsequently resuspended in 0.5 ml buffer A (10 mM Hepes pH 7.9, 1.5 mM $MgCl_2$, 10 mM KCl, 1 mM DTT, 1 × Protease inhibitor cocktail solution (Roche), 0.2 mM EDTA) and allowed to swell on ice for 15 minutes. Cells were lysed by 8 strokes in a 1 ml Dounce homogeniser. 0.25 ml of the total cellular lysate was stored at −70°C. The remaining lysate was pelleted (12,000 × *g*, 20 seconds). The supernatant containing the soluble cytoplasmic fraction was stored at −70°C. The pellet containing the nuclear fraction was resuspended in 0.25 ml buffer B (20 mM Hepes pH 7.9, 1.5 mM $MgCl_2$, 0.6 M KCl, 1 mM DTT, 1 × Protease inhibitor cocktail solution, 0.2 mM EDTA, 25% glycerol) and incubated at 4°C with continuous agitation to break open the intact nuclei. The nuclear debris was pelleted by centrifugation at high speed (5 minutes, 4°C). The supernatant containing the nuclear fraction was stored at −70°C.

2. 46 *In vitro* Protein-protein Interactions (GST-pulldowns)

A small aliquot of GST-fusion protein (previously captured on glutathione-agarose beads - section 2.29) was analysed by SDS-PAGE to evaluate the purity, quality and level of protein expression. The remaining captured protein was washed with binding buffer (40 mM Hepes pH 7.5, 100 mM KCl, 0.1% Nonidet P-40, 20 mM β-mercaptoethanol, 1 × Protease inhibitor cocktail solution). Approximately 5 μg of GST-fusion protein bound to glutathione-agarose beads was then resuspended in 1 ml binding buffer. 20 μl of [^{35}S]-L-methionine-labelled core protein produced as described in section 2.43 was added and binding was allowed to proceed for 2 hours at 4°C with continuous rotation. The beads were washed in binding buffer (3 ×) to remove unbound radiolabelled core protein. The remaining binding buffer was removed and replaced with 0.33 volumes 3 × SDS-PAGE denaturing buffer. The presence of bound core protein was determined by SDS-PAGE followed by fluorography. Briefly, the polyacylamide gel was soaked in fix solution (50% methanol, 7% acetic acid) and incubated at RT for 1 hour with gentle agitation. The solution was removed and replaced with a small volume of EN^{3}HANCE (NEN) and incubated as before. The enhancer solution was disposed of carefully before addition of dH_2O and incubation at RT for 30 minutes. The gel was dried and subjected to autoradiography as before (section 2.32).

2. 47 dATPase Assay

Hydrolysis of nucelotides was detected using a classical method based on visualisation of its breakdown products by TLC. Radiolabelled [α-^{32}P]-NTP or -dNTP is incubated with the protein under investigation in appropriate buffer. Radiolabelled breakdown products are subsequently separated by TLC and detected by exposure to a phosphorimager screen. The assay conditions described by You *et al.*, (1999b) were essentially followed. Briefly, 2μl ATPase buffer (250 mM Tris-HCl, pH 7.4, 5 mM NaCl, 12.5 mM $MgCl_2$) was mixed with 0.1 μl [α-^{32}P]-dATP (1 μCi), the purified protein under investigation in a range of concentrations (typically 10^{-7} to 1 μg) and dH_2O to a final volume of 10 μl. The reactions were incubated at 37°C for 30 minutes. 1 μl of 20 mM EDTA was then added to stop the reaction, and

2 μl of the reaction was spotted onto a TLC plate (Polygram Cel 300 PEI/UV_{254}, Merck). The reaction products were separated by TLC in phosphate buffer (0.5 M potassium phosphate pH 3.5), and the plate was air-dried then exposed to a phosphorimager screen.

2. 48 Helicase Assay

An overview of the helicase assay has been described previously (Fig. 18, section 1.10.7). Preparation of the duplex RNA used as a substrate in helicase assays is described in section 4.2.14. Helicase activity was assayed essentially as described by Gururajan and Weeks (1997) using a dsRNA substrate of specific activity 2×10^7 cpm/μg mixed with 2 μl helicase buffer (4% glycerol, 75 mM KCl, 40 units RNasin, 1 mM ATP), the protein under investigation in a range of concentrations (typically 0.01-10 μg), and dH_2O to a final volume of 20 μl. Following incubation at 37°C for 20 minutes, 3 μl loading buffer (50% glycerol, 2% SDS, 20 mM EDTA, 0.5% bromophenol blue) was added to stop the reaction. The reactions were run directly on 15% urea gels (Sequagel, National Diagnostics). Duplex RNA substrate incubated without protein at 37°C for 20 minutes, and single stranded RNA denatured by heating duplex RNA for 5 minutes at 90°C were run in parallel as controls. The gel was run until the dye front migrated two-thirds down the gel, dried on 1 mm Whatman filter paper and exposed to a phosphorimager screen.

CHAPTER THREE:

Investigation into Expression of DDX3 mRNA and Protein, and Preliminary Studies on the Interaction of DDX3 with Hepatitis C Virus Core Protein

3. 1 Introduction

Three independent reports have suggested DDX3 interacts with HCV core protein (section 1.9.6.9; Mamiya and Worman, 1999; Owsianka and Patel 1999; You *et al.*, 1999b). DDX3 is a human cellular protein that bears all of the conserved motifs associated with the DEAD-box RNA helicase family (sections 1.9.6.9 and 1.10.6). However, before any attempt can be made to understand the importance of the interaction between core and this putative RNA helicase, it is necessary to investigate the role of DDX3 in a normal, uninfected cell. To this end, this chapter initially focuses on the fundamental properties of cellular DDX3, namely expression of its mRNA and protein, to form a basis for further investigation of the protein and its interaction with core. The presence or absence of DDX3 mRNA in a variety of cell lines was established by Northern blotting using extracted total RNA. The expression of DDX3 mRNA was also determined using a commercially available dot-blot kit, produced using poly(A)$^+$ RNA extracted from a wide range of adult human and foetal tissues. Since the DDX3 sequence contains a central conserved region similar to all DEAD-box RNA helicases (Fig. 17, section 1.10.6; see Appendix IV), a radiolabelled probe directed against the coding seqeunce for the variable N-terminus of the protein was employed in both cases. In order to study endogenous cellular DDX3, two separate polyclonal antisera (PAbs) and a panel of monoclonal antibodies (MAbs) raised against the protein, generated by Dr A. Owsianka (see Appendix I), were used. One such anti-DDX3 MAb, previously shown to detect DDX3 in HeLa total cell extracts (Owsianka and Patel, unpublished), was used to initially characterise i) expression of DDX3 protein by Western blotting and ii) its subcellular localisation by indirect confocal immunofluorescence microscopy in a range of mammalian cell lines. A full study of the subcellular localisation of DDX3 using the entire panel of anti-DDX3 MAbs is presented in Chapter Four. The anti-DDX3 antibodies are fully characterised here in terms of their reactivities in Western blots and ELISAs to epitope-tagged DDX3 proteins produced in *E. coli* and endogenous DDX3 in human hepatocytes. Glutathione S-transferase (GST)-DDX3 fusion proteins previously used to delineate the domain of DDX3 interacting with core (Owsianka and Patel, 1999) were used to roughly map binding of anti-DDX3 MAbs to the C-terminal portion of DDX3 (aa

409-662 of the 662 aa full-length protein). A series of deletion mutants were generated to map antibodies which bound the full-length protein but not this C-terminal fragment of DDX3. Epitope-mapped anti-DDX3 antibodies were subsequently tested for their reactivity with human hepatocyte cell extracts.

Finally, the interaction between DDX3 and core was investigated by *in vitro* binding assays, and attempts were made to further delineate the domain of DDX3 that interacted with core protein. Co-localisation of the two proteins was studied by indirect immunofluorescence in hepatocytes expressing core protein and the HCV glycoproteins (E1 and E2) as supplied by recombinant vaccinia virus (rVV). This allowed expression of core in in a similar manner as it would be found during natural HCV infection of permissive cells, albeit without the nonstructural proteins. Co-localisation of DDX3 with core protein (again expressed by rVV carrying the entire HCV structural region) was further investigated in hepatocytes containing self-replicating HCV sub-genomic RNA, generously donated by Dr R. Bartensclager (Lohmann *et al.*, 1999a).

3. 2 Results

3.2. 1 Detection of DDX3 mRNA Transcripts in a Range of Cell Lines

The existence of DDX3 mRNA transcripts in a range of mammalian and non-mammalian cell lines was established by Northern blotting with total RNA extracted from such cell lines. Two different hepatocyte cell lines derived from human hepatomas (Huh-7 (N) and HepG2) were used in these studies since HCV is a hepatotropic virus. A further cell line derived from a different human tissue (HeLa) was used to determine any anomalies between expression in hepatocytes and in cell lines derived from other human tissues. Two further non-human mammalian cell lines (COS-7 and BHK-21) and one non-mammalian cell line (Sf21) were used to determine mRNA expression of DDX3 homologues in other organisms. Use of this range of cell lines extends the study of You *et al.* (1999b), suggesting that DDX3 mRNA is present in Huh-7, HepG2 and HeLa cells. DDX3 mRNA (or mRNA transcripts for its homologues) was detected using a specific ^{32}P-labelled probe,

generated as described in section 2.28 using nt 1-624 of the DDX3-coding sequence as a template (see Appendix IV). This region was chosen primarily because DDX3, like other known and putative RNA helicases, possesses a conserved central region containing domains critical for enzyme activity and divergent N- and C-termini believed to determine cellular localisation and substrate specificity (Fig. 17, section 1.10.6; Schmid and Linder, 1992; Wang and Guthrie, 1998). Total cellular RNA was extracted from the cell lines under investigation and equal quantities of total RNA were electrophoretically fractionated by size in a denaturing gel. The RNA was capillary blotted onto positively-charged membranes and immobilised by UV-cross-linking. To confirm the integrity of the extracted RNA, the same RNA samples were fractionated on a separate gel and stained with ethidium bromide. Visualisation of this gel under UV light showed the abundant 28s and 18s rRNAs in all samples (Fig. 22a), confirming that the extracted RNA was of sufficient quality for Northern blotting. Consistent with a previous report (Wang *et al.*, 1997), 18s rRNA in Sf21 total cellular RNA extracts was significantly more abundant than 28s rRNA (lane 6). Northern blot analysis allowed detection of a DDX3 mRNA transcript (~5 kb in size as judged by aligning the blot with rRNA bands as shown in Fig. 22a) in Huh-7 (N), HepG2 and HeLa cells (Fig. 22b, lanes 1-3), in agreement with previous studies (Chung *et al.*, 1995; You *et al.*, 1999b). The size of the mRNA transcript as compared with a DDX3 cDNA of around 2 kb (see Appendix IV) suggests the mRNA transcript has long 5′- and/or 3′-untranslated regions. Although abundance of DDX3 transcripts was low, DDX3 mRNA was detected in all mammalian cell lines tested (Fig. 22b, lanes 1-5), but not in Sf21 cells (lane 6), the only non-mammalian cell line tested. The presence of DDX3 transcripts was particularly low in total RNA extracted from COS-7 cells (lane 4), although the RNA extracted from this cell line appeared to be of poorer quality than the RNA extracted from the other cell lines (Fig. 22a, lane 4). Nevertheless, these data indicate that a DDX3 mRNA transcript is present in a wide range of mammalian cells.

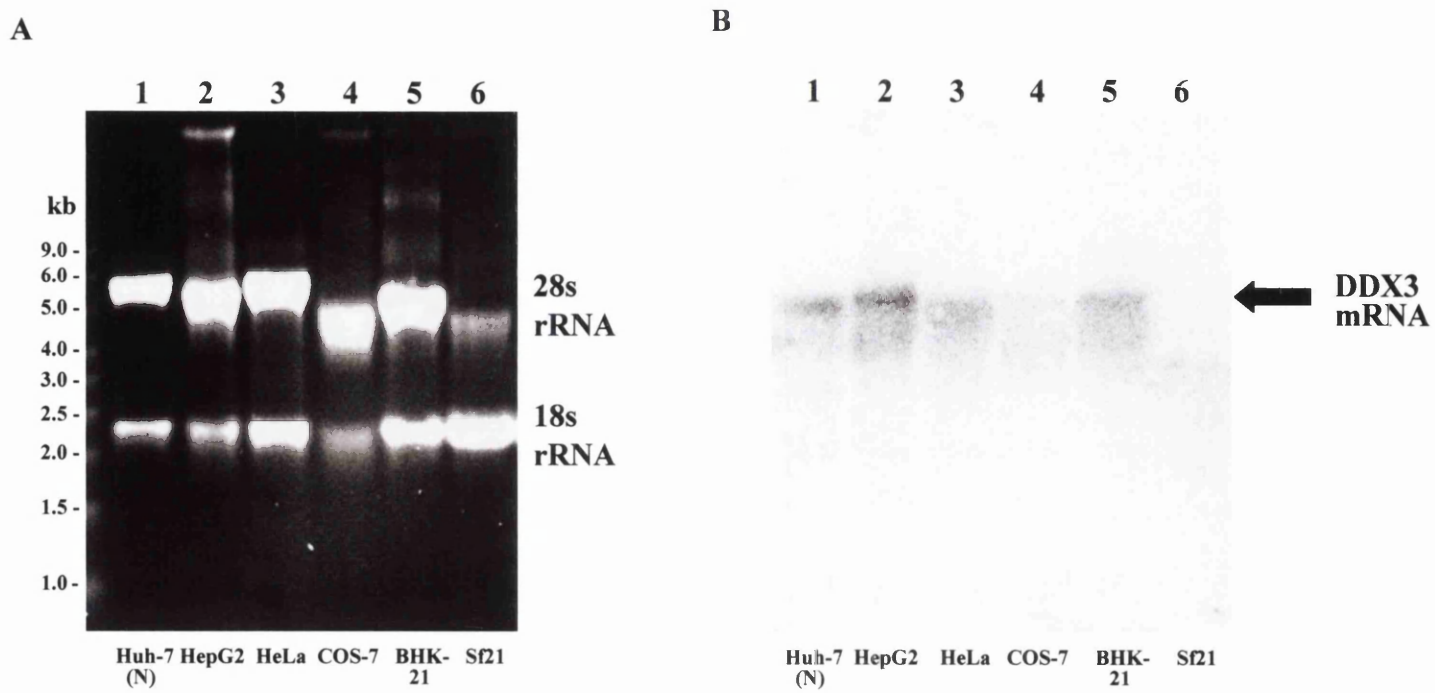

Figure 22: Northern blot analysis investigating DDX3 mRNA expression in total RNA from a range of mammalian and one insect cell line. (A) 20 μg total RNA extracted from cell lines as shown was fractionated on a denaturing agarose gel (1.0%), stained with ethidium bromide and visualised under UV light. (B) 20 μg total RNA fractionated as before was subjected to Northern blot analysis (as described in section 2.27) using a ^{32}P-labelled probe corresponding to DDX3 nt 1-624 (see Appendix IV).

3.2. 2 Detection of DDX3 mRNA in a Range of Human Tissues

A commercially available poly(A)$^+$ RNA dot-blot kit (Human RNA Master Blot, Clontech) was used to determine the relative abundance and tissue-specificity of DDX3 mRNA. The Master Blot consists of poly(A)$^+$ RNA immobilised as an array of spots on a positively-charged membrane, the mRNA having been isolated from different human tissues. The same probe which specifically detected DDX3 transcripts in fractionated total RNA from a range of mammalian cell lines (Fig. 22b, lanes 1-5) was used. Analysis of hybridisation events with this probe (under the same conditions of stringency) to the Master Blot indicated that DDX3 transcripts are expressed in all adult and foetal tissues tested (Fig. 23a). For reference, the position of all RNA samples on the Human RNA Master Blot is presented diagramatically in Fig. 25. The DDX3 probe did not hybridise to any of the control DNA or RNA samples (Fig. 23a, positions H1-H8). Although DDX3 mRNA was found in all tissues, distinct differences in its expression in different tissues was qualitatively evident. A ^{32}P-labelled ubiquitin probe (produced as described in section 2.28 using a cDNA provided in the Human RNA Master Blot kit as a template) was used as a control to determine the expression of a ubiquitously-expressed cellular mRNA. The blot was submerged in boiling 0.5% SDS in dH_2O to strip DDX3 probe, exposed to a phosphorimager screen overnight to check stripping was effective (data not shown), and re-probed for ubiquitin mRNA. Hybridisation of this control probe indicates that the level of ubiquitin mRNA is largely the same across the range of tissues (Fig. 23b), suggesting the amounts of RNA in each dot had been successfully normalised. This level of ubiquitin mRNA is expected to be approximately 2% of the total mRNA extracted from each tissue (Clontech). Quantitative analysis of this data (Fig. 24a) confirmed that the level of ubiquitin mRNA was consistent between tissues. The level of DDX3 expression was quantitated as before and correlated with ubiquitin levels. While DDX3 expression in tissues originating from the central nervous system (Fig. 24b, A1-B6) was proportional to the levels of ubiquitin mRNA expression in the same tissues (Fig. 24a, A1-B6), it is clear that DDX3 mRNA was expressed at much lower levels in the spinal cord than ubiquitin (Figs 24a and 24b, B7). However, most striking is the abundance of DDX3 mRNA in placental tissue - while ubiquitin levels were high in

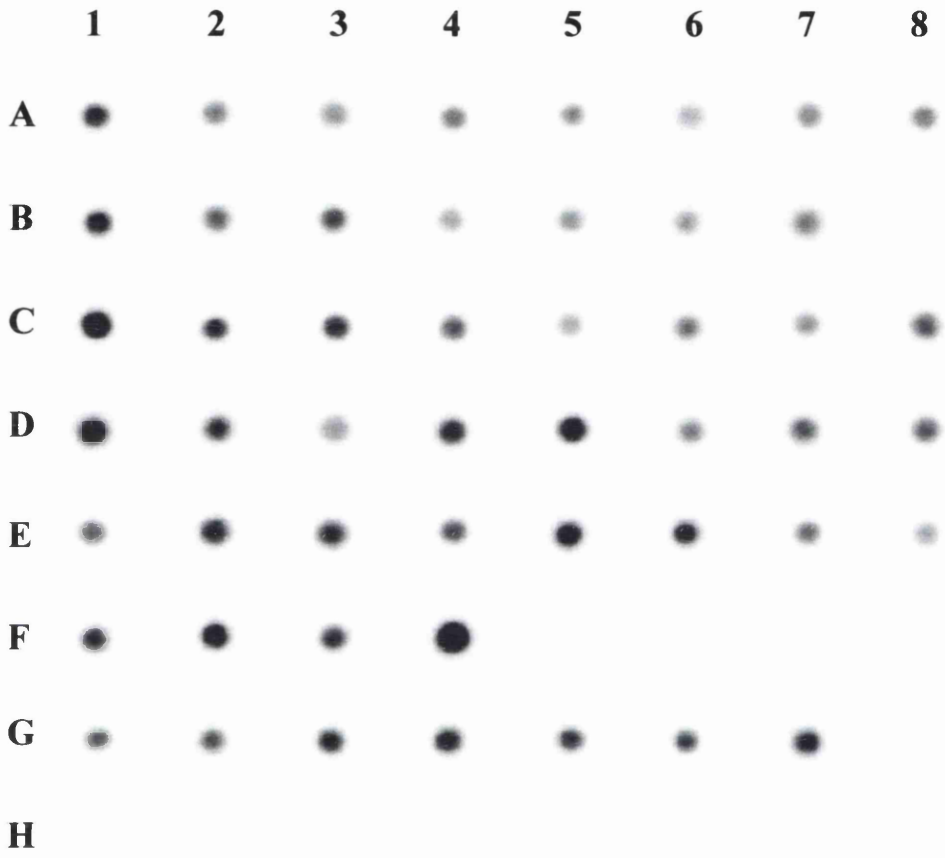

Figure 23a: Expression of DDX3 mRNA in a range of adult human and foetal tissues. A ^{32}P-labelled probe derived from DDX3 nt 1-624 (see Appendix IV) was hybridised to Human RNA Master Blot (Clontech), a poly(A)$^{+}$ RNA dot-blot for simultaneous quantitation of mRNA expression in different adult human and foetal tissues.

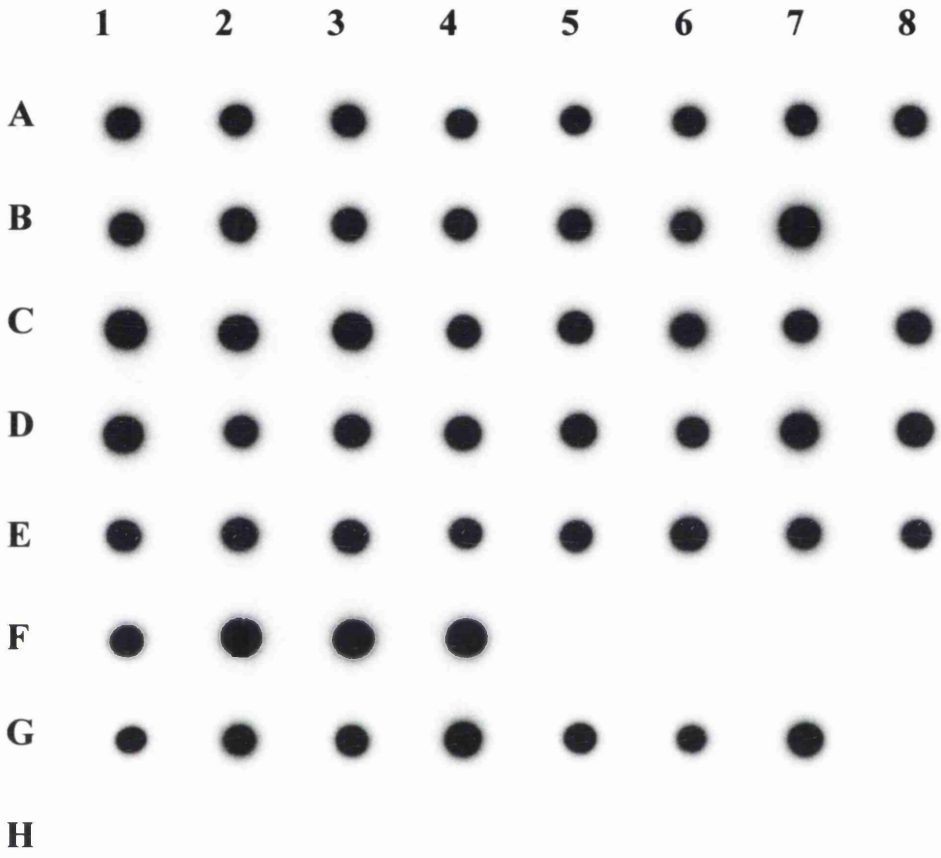

Figure 23b: Expression of ubiquitin mRNA in a range of human and foetal tissues. Human RNA Master Blot analysed for the presence of DDX3 mRNA as in Fig. 23a was stripped and re-probed with a ^{32}P-labelled probe derived from human ubiquitin cDNA (Clontech).

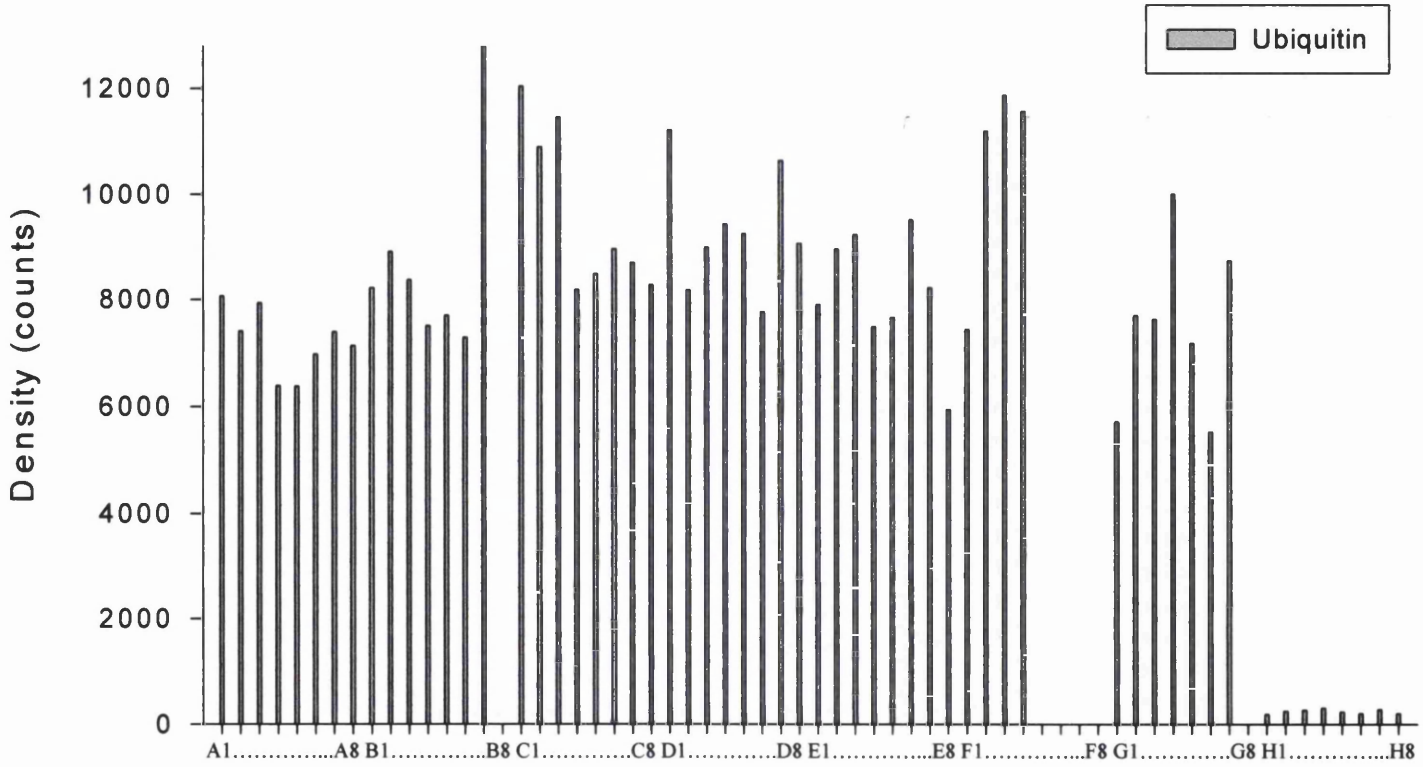

Figure 24a: Quantitation of ubiquitin mRNA in adult human and foetal tissues. Analysis was performed using a Molecular Imager FX (Bio-Rad) with Quantity One software.

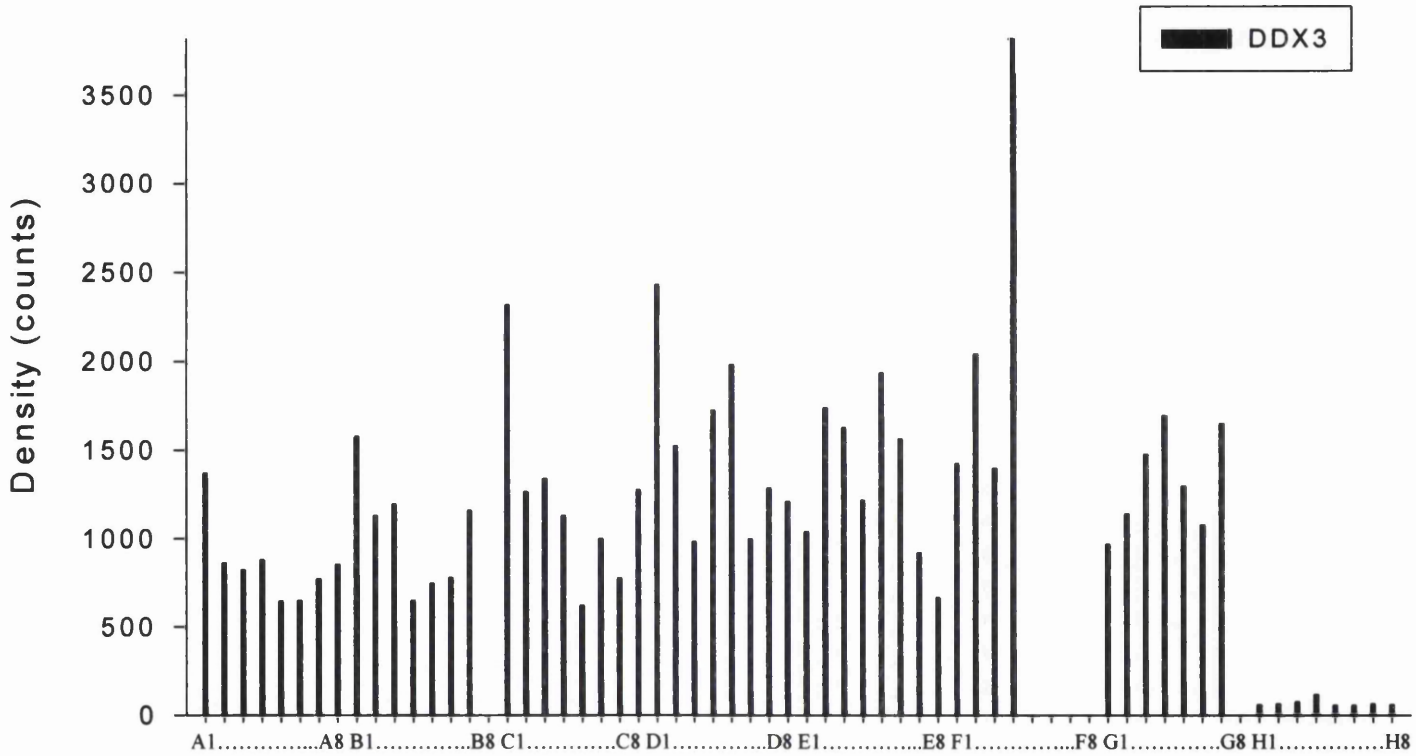

Figure 24b: Quantitation of DDX3 mRNA in adult human and foetal tissues. Analysis was performed using a Molecular Imager FX (Bio-Rad) with Quantity One software.

	1	2	3	4	5	6	7	8
A	Whole brain	Amygdala	Cudate nucleus	Cere-bellum	Cerebral cortex	Frontal lobe	Hippo-campus	Medulla oblongata
B	Occipital lobe	Putamen	Substantia nigra	Temporal lobe	Thalamus	Sub-thalamic nucleus	Spinal cord	
C	Heart	Aorta	Skeletal muscle	Colon	Bladder	Uterus	Prostate	Stomach
D	Testis	Ovary	Pancreas	Pituitary gland	Adrenal gland	Thyroid gland	Salivary gland	Mammary gland
E	Kidney	Liver	Small intestine	Spleen	Thymus	Peripheral leukocyte	Lymph node	Bone marrow
F	Appendix	Lung	Trachea	Placenta				
G	Foetal brain	Foetal heart	Foetal kidney	Foetal liver	Foetal spleen	Foetal thymus	Foetal lung	
H	Yeast total RNA 100ng	Yeast tRNA 100ng	*E. coli* rRNA 100ng	*E. coli* DNA 100ng	Poly r(A) 100ng	Human Cot-1 DNA 100ng	Human DNA 100ng	Human DNA 500ng

Figure 25: Key for the Human RNA Master Blot (taken from Clontech Technique protocol).

this sample (Fig. 24a, F4), levels of DDX3 mRNA (Fig. 24b, F4) were far higher than in all of the other samples. In fact, expression in placenta was two or three-fold higher than most other tissues. This may be consistent with the possibility that DDX3, like its homologues in other organisms (section 1.13), is a developmentally-regulated protein. Levels of DDX3 mRNA appeared to be significantly lower in other tissues relative to the ubiquitin control - ubiquitin mRNA expression in the lung and tranchea (Fig. 24b, F2 and F3) are among the highest seen, whereas DDX3 mRNA expression in these tissues is lower than on average (Fig. 24a, F2 and F3). On the other hand, expression of DDX3 mRNA in foetal tissues (Fig. 24b, G1-G7) is directly proportional to expression of ubiquitin mRNA (Fig. 24a, G1-G7). This does not necessarily provide contradictory evidence for the hypothesis that DDX3 is a developmentally-regulated, since the RNA that was probed was not extracted from different developmental stages.

3.2. 3 Detection of Endogenous DDX3 Protein in a Range of Cell Lines by Western Blotting

To establish the presence of DDX3 protein in cell lines derived from human tissues, and to assess the existence and expression of its homologues in other organisms, total cell extracts from a range of mammalian and non-mammalian cell lines were probed with an anti-DDX3 MAb by Western blotting. The MAb, AO196, had previously been shown to specifically detect DDX3 in HeLa total protein extracts (Owsianka and Patel, unpublished). The relevant cell lines were seeded in 35 mm dishes with the aim that they reached a confluency of approximately 80% following incubation at 37°C for 16 hours. Total cell extracts were prepared, fractionated by SDS-PAGE and electrophoretically transferred to ECL membranes (section 2.32), and probed with MAb AO196. Similarly, Huh-7 (N) cells infected with a recombinant vaccinia virus, rVV-DDX3 (which expresses the full-length DDX3 protein), were analysed in parallel. Consistent with Northern blot analysis of total cellular RNA extracted from the same range of mammalian and non-mammalian cell types (Fig. 22), DDX3 protein was detected in Huh-7 (N), HepG2, HeLa, COS-7 and BHK-21 cell extracts (Fig. 26, lanes 1-5) but not in Sf21 cell extracts (lane 6). As expected, the endogenously-expressed DDX3 co-migrated with that expressed by

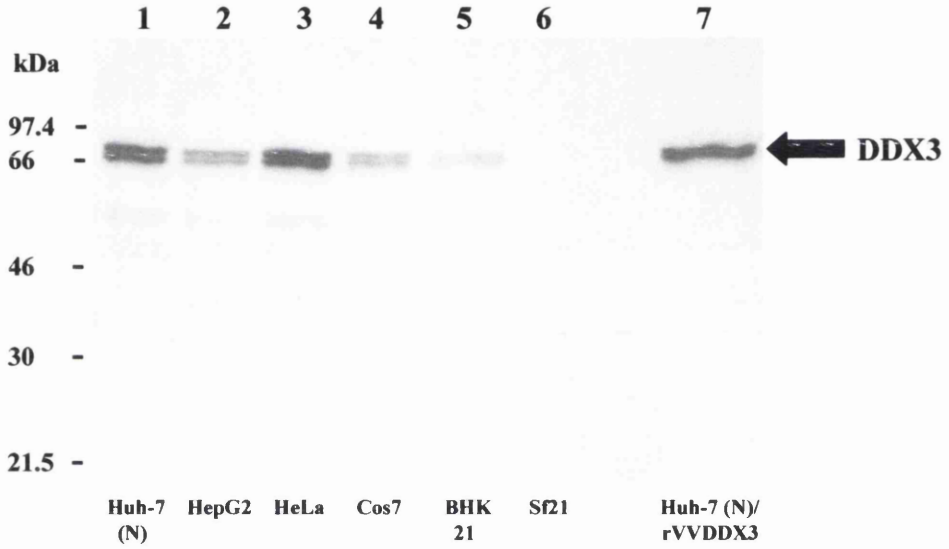

Figure 26: Detection of endogenous DDX3 protein in a range of mammalian cell lines and one non-mammalian cell line as shown. Total cell extracts (20 μg) were fractionated by SDS-PAGE (8%) and immunoblotted with anti-DDX3 MAb AO196 (lanes 1-6). Total cell extract (10 μg) from Huh-7 (N) cells infected with rVV-DDX3 was run in parallel as a positive control (lane 7).

rVV-DDX3 (lane 7), and had an apparent molecular weight similar to the previously reported molecular weight of 73 kDa (Owsianka and Patel, 1999; You *et al.*, 1999b). These data also provide strong evidence that there are two separate but closely related forms of DDX3 - the anti-DDX3 MAb AO196 detected two distinct bands resolved by SDS-PAGE (Fig. 26). This implies either that DDX3 is differentially modified by translational and/or post-translational mechanisms, or the DDX3 mRNA is differentially spliced, or closely related sequences encoding different isoforms of DDX3 exist. The latter hypothesis is consistent with the existence of DDX3 on the X chromosome in addition to a Y chromosome counterpart (section 1.13.1; Chung *et al.*, 1995; Lahn and Page, 1997), although Northern blot analysis of total RNA from a range of mammalian cell lines did not reveal multiple RNA species (Fig. 22b; section 3.2.1). The apparent differences in the level of expression of the protein in different cell types does not necessarily indicate that DDX3 expression is highest in Huh-7 (N) and HeLa cells. However, the low abundance of DDX3 in HepG2 cells (lane 2) is in agreement with a previous study (You *et al.*, 1999b), possibly suggesting variation in expression or stability of the protein in different hepatocyte cell lineages. In contrast to the earlier report (You *et al.*, 1999b), however, low amounts of DDX3 mRNA in total RNA extracted from HepG2 cells were not observed (Fig. 22b, lane 2; section 3.2.1). A full investigation into recognition of DDX3, and various truncated forms of the protein, expressed as GST-fusion proteins, and cellular DDX3 expressed in the Huh-7 (N) hepatocyte cell line by Western blotting with the full panel of anti-DDX3 antibodies will be presented later in this chapter (sections 3.2.11 to 3.2.18).

3.2. 4 Detection of Endogenous DDX3 Protein in a Range of Mammalian Cell Lines by Indirect Confocal Immunofluorescence Microscopy

Following confirmation by Western blotting that DDX3 protein is expressed in a range of mammalian cell lines, its subcellular localisation in the same cells was investigated by indirect immunofluorescence. Again, the anti-DDX3 MAb AO196 was used. Binding of the antibody to endogenous DDX3 was ascertained using an anti-mouse IgG-fluorescein isothiocyanate (FITC) secondary antibody conjugate. Consistent with the Northern blot analyses (Figs 22b and 23a; sections 3.2.1 and

3.2.2) and the Western blotting data (see above), staining for DDX3 was detected in all mammalian cell lines tested (Fig. 27). DDX3 did not appear to be expressed at high levels, but in all cell types DDX3 localised primarily in the cytoplasm. In general, a diffuse staining of the cytoplasm was detected, with some punctate staining also seen (Fig. 27). Within the cytoplasm there was some evidence that DDX3 accumulates in distinct areas, possibly in areas of cell-cell contact (Figs 27c and 27e). However, there was some staining of the nucleus, particularly evident in HeLa cells (Fig. 27c). This may represent a cross-reaction with another protein, although previous reports have suggested DDX3 is present in the nucleus (Owsianka and Patel, 1999; You *et al.*, 1999b). While these data only portray binding by one anti-DDX3 MAb, a full study of the endogenous protein as well as DDX3 expressed by a plasmid-based vector using the full panel of MAbs by indirect confocal inmmunofluorescence microscopy will be presented in Chapter Four.

3.2. 5 Generation of DDX3 Anti-sense Cell Lines

In order to investigate the role of DDX3 in cellular processes, a useful reagent would be a cell line, preferably of human origin, lacking DDX3. Such a cell line would allow us to perform proper genetic and biochemical analyses to delineate the function of DDX3 in normal cells. These analyses would include establishing any effects of removing DDX3 from the cell, and examining how its absence might affect core protein expression supplied via plasmid or rVV. However, as shown in Figs 22 to 27, DDX3 is a ubiquitously expressed and highly conserved protein, and as such it may be difficult to generate such a cell line lacking DDX3. Nevertheless, an attempt was made to generate hepatocyte cell lines constitutively expressing anti-sense DDX3 constructs to effectively prevent expression of cellular DDX3 by direct annealing to its mRNA transcript. The pGEX-6P-3-DDX3 construct (Owsianka and Patel, 1999) was digested with *Bam*HI and *Bst*YI (DDX3 nt 1-220; see Appendix IV) and blunt-ended. This restriction fragment was sub-cloned into pZeoSV2 (+). The resulting constructs, pDDX3-AS and pDDX3-S (Fig. 28a), containing DDX3 nt 1-220 in the anti-sense (3′ → 5′) or sense (5′ → 3′) orientation, respectively, were used to transfect Huh-7 cells and ultimately generate antibiotic-resistant cell lines (as described in section 2.36). The pZeoSV2 (+) plasmid confers resistance to the

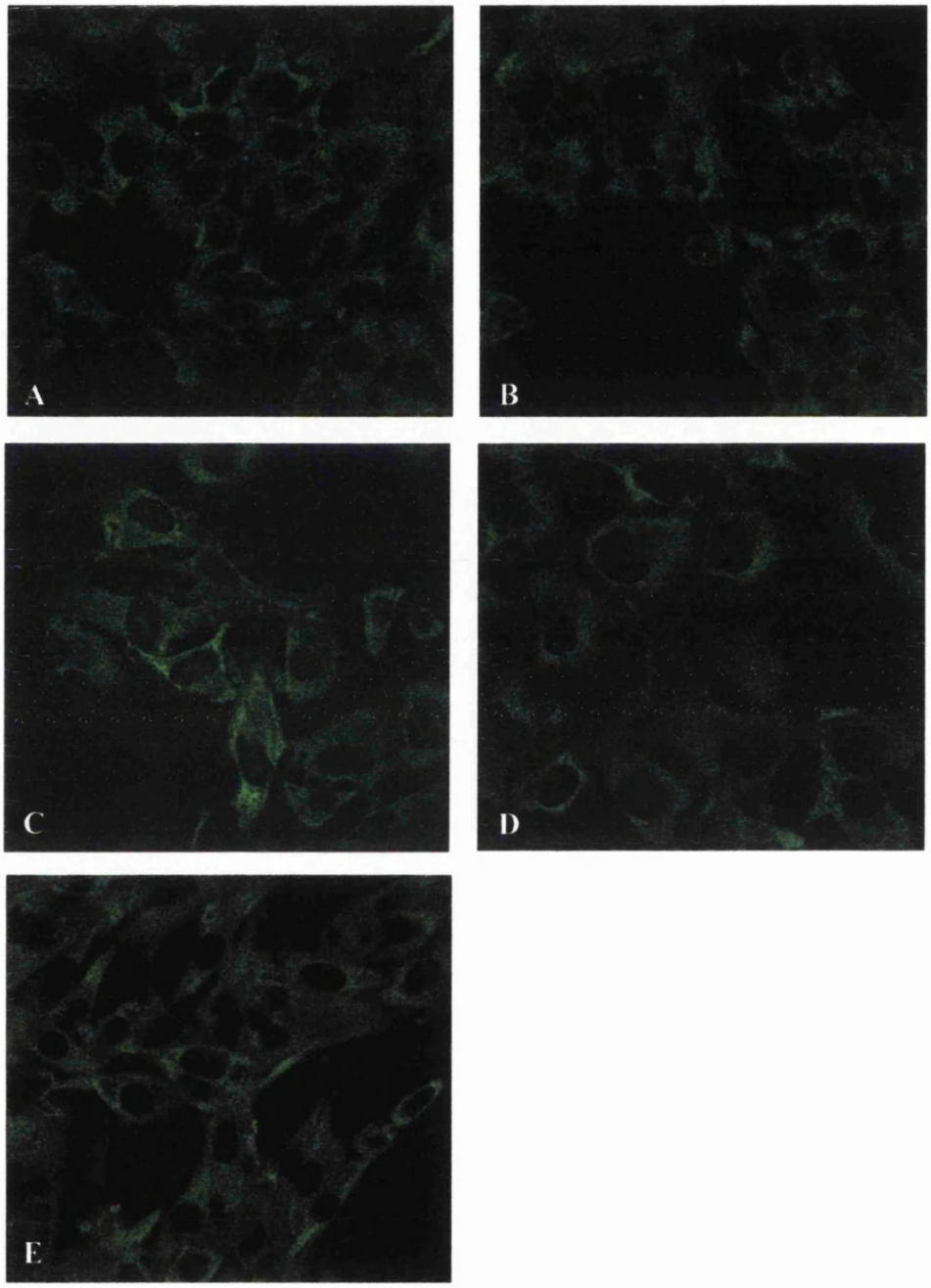

Figure 27: Detection of endogenous DDX3 protein in human cell lines, and DDX3 homologues in non-human mammalian cell lines. Cells were grown to a confluency of 70-80%, fixed, and probed with anti-DDX3 MAb AO196. Binding of antibody was visualised using anti-mouse IgG-FITC conjugate and confocal microscopy. (A) Huh-7 (N) cells; (B) HepG2; (C) HeLa; (D) COS-7; (E) BHK-21.

antibiotic Zeocin, and antibiotic-resistant colonies were isolated and tested for DDX3 expression by Western blotting, immunofluorescence and Northern blot analysis. Over 60 independent Zeocin-resistant colonies were screened for the presence of DDX3. For Western blotting, cells were harvested from 24-well dishes, fractionated by SDS-PAGE and immunoblotted with anti-DDX3 MAb AO196 - a selection of cell lines tested as such is shown in Fig. 28b. However, detection of a protein of the same molecular weight as DDX3 that co-migrated with that produced by the rVV-DDX3-infected cells run in parallel as a control implied that DDX3 was still present within the antibiotic-resistant hepatocytes. Large amounts of DDX3 protein presumably masked the existence of DDX3 as a doublet that was observed previously (Fig. 26). Consistent with these results, the anti-sense construct was apparently not detected by Northern blot analysis using an *in vitro*-transcribed DDX3 sense ^{32}P-labelled probe (data not shown). The likely explanation for this could be that hepatocytes in which the Zeocin resistance gene has integrated into the host chromosome are viable, whilst cells containing this gene in addition to the DDX3 anti-sense region are not. This is consistent with a role for DDX3 in essential cellular processes, as suggested by the ubiquitous presence of its mRNA in human tissue and the high degree of conservation of DDX3 mRNA and protein in a range of distantly related mammalian cell types (Figs 22-25; sections 3.2.1-3.2.4). However, it is also possible that too few colonies were screened to isolate a cellular clone that lacked DDX3.

3.2. 6 Co-localisation of Endogenous DDX3 with Core Protein in Hepatocytes

Studies by Owsianka and Patel (1999) using anti-DDX3 PAbs to detect DDX3 demonstrated co-localisation of the protein and core in HeLa cells. Here, the previous work was expanded to include hepatocytes, primarily because HCV is a hepatotropic virus. Huh-7 (N) cells were used to investigate the putative interaction of core and DDX3 since: i) these cells have previously been shown to support albeit inefficient replication of HCV itself (Yoo *et al.*, 1995), and ii) it is as yet the only cell line shown to permit replication of HCV sub-genomic replicon RNA (Lohmann *et al.*, 1999a; Rosenberg, 2001). Cells were seeded in 24-well tissue culture dishes containing coverslips such that confluency reached approximately 70% prior to

A

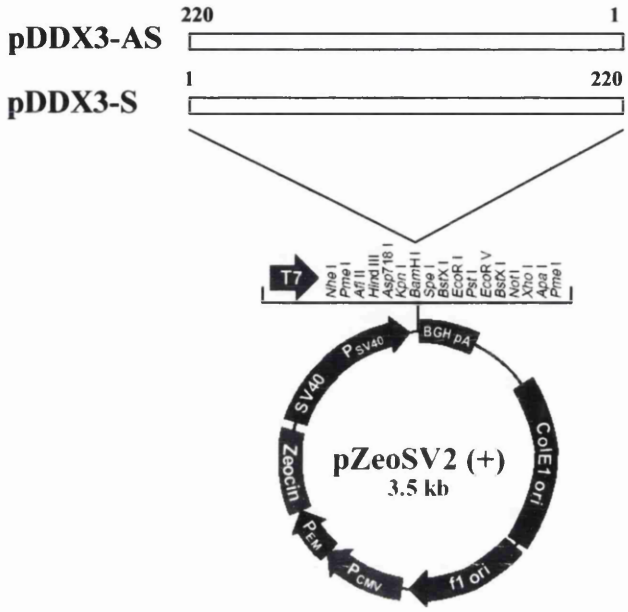

B

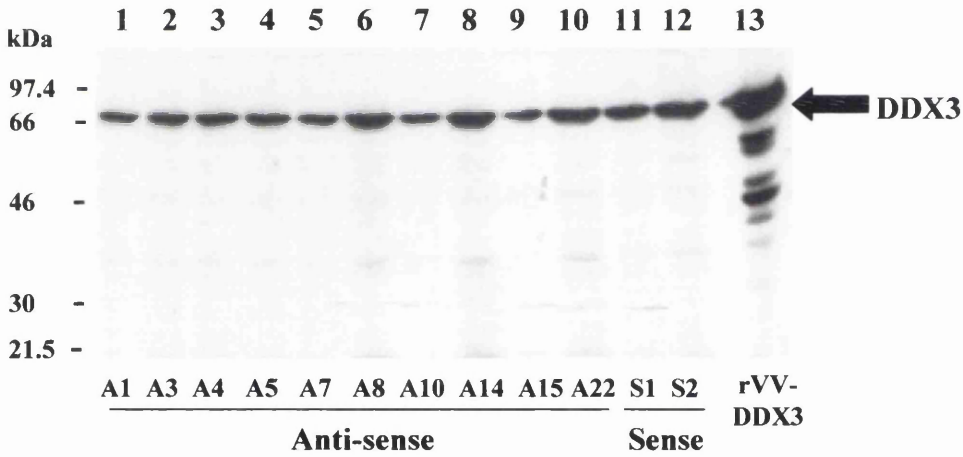

Figure 28: Generation of DDX3 anti-sense cell lines. (A) Constructs used to produce DDX3 anti-sense and sense (control) cell lines. DDX3 nt numbers for the antisense (pDDX3-AS) and sense (pDDX3-S) constructs in the pZeoSV2 (+) vector (Invitrogen) are shown. (B) Total cell extracts from each Zeocin resistant cell line previously transfected with pDDX3-AS (lanes 1-10) or pDDX3-S (lanes 11-12) were fractionated by SDS-PAGE (9%) and immunoblotted with anti-DDX3 MAb AO196. Total cell extract from Huh-7 cells infected with rVV-DDX3 was run in parallel as a positive control (lane 13).

infection with rVV-C-E1-E2 (expressing HCV core-E1-E2; see Appendix III). Following overnight incubation in normal medium the cells on coverslips were washed, fixed, permeabilised, and investigated by double immunofluorescent labelling and confocal microscopy. Endogenous DDX3 was detected using anti-DDX3 MAb AO196 and an anti-mouse FITC-conjugated secondary antibody, while core protein was detected using an anti-core rabbit PAb (R525; see Appendix I) and an anti-rabbit Cy5-conjugated secondary antibody. In uninfected cells, consistent with the immunofluorescence data presented earlier in this chapter (Fig. 27), DDX3 was located mainly in the cytoplasm with some punctuate staining (Fig. 29). Core protein expressed by rVV in the context of the HCV glycoproteins E1 and E2 appeared to localise in globular structures in the perinuclear cytoplasm (Fig. 29), a pattern of staining that is entirely consistent with the reported association of core protein with lipid droplets (section 1.7.3; Barba *et al.*, 1997; Hope and McLauchlan, 2000; Moradpour *et al.*, 1996). The normal localisation of DDX3 as described above was manifestly disrupted in cells expressing core protein, and anti-DDX3 MAb AO196 now gave strong staining of globular structures that mimicked the localisation of core protein (Fig. 29). Merging of the two images indicated strong co-localisation between DDX3 and core protein (Fig. 29). Huh-7 (N) cells infected with rVV-E1-E2 (expressing E1-E2 alone; see Appendix III) were used as a further control - consistent with Owsianka and Patel (1999), DDX3 did not re-localise in the presence of the HCV glycoproteins alone (data not shown).

3.2. 7 Characterisation of HCV Sub-genomic Replicon-expressing Cell Lines

To further substantiate the hypothesis that core protein binds to DDX3 during natural infection with HCV, the localisation of the two proteins was investigated in the H9-13 HCV sub-genomic replicon-expressing cell line. Although the H9-13 cell line has previously been characterised (Lohmann *et al.*, 1999a), the presence of HCV NS3 protein in these cells was used to verify indirectly that they were indeed expressing HCV sub-genomic RNA prior to further experimental procedures. Huh-7 (N) cell extracts, representing the parental cell line from which the H9-13 cell line was produced, were also tested in parallel as an appropriate control. As shown in Fig. 30, an anti-HCV NS3 protease PAb (see Appendix I) detected a single band in

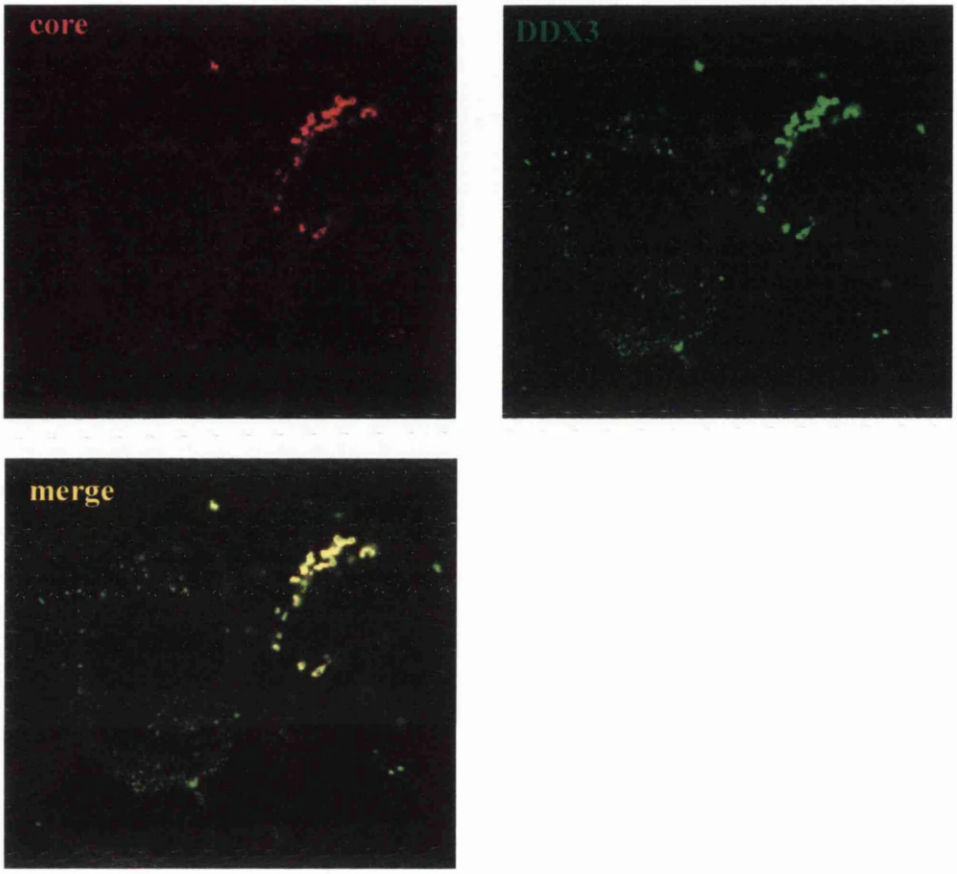

Figure 29: Co-localisation of DDX3 with core protein in hepatocytes. Huh-7 (N) cells were infected at an m.o.i. of 0.5 with rVV-C-E1-E2. Following incubation at 37°C for 16 hours, cells were fixed and then probed with anti-DDX3 MAb AO196 and anti-core PAb R525. Bound antibodies were detected by anti-mouse IgG-FITC and anti-rabbit IgG-Cy5 conjugates.

H9-13 cell extracts at the expected molecular weight for the full-length NS3 protein (72 kDa), in addition to a further non-specific band seen in both cell lines. While a previous report suggested that internal processing of the NS3 protein occurs in insect and mammalian cells (Shoji *et al.*, 1998), many other groups have not detected this (DeFranscesco and Steinkühler, 1999). Accordingly, lower molecular weight bands were not seen (Fig. 30). Detection of the 72 kDa band corresponding to full-length NS3 protein by PAbs raised against the protein in H9-13 but not Huh-7 (N) cell extracts suggested that the HCV sub-genomic replicon was likely present in the H9-13 cell line. The blot was stripped and re-probed with anti-DDX3 MAb AO196 to confirm equal amounts of Huh-7 (N) and H9-13 cell extracts had been fractionated (data not shown).

To unequivocally demonstrate the presence of the HCV sub-genomic replicon RNA in the H9-13 cell line, total RNA from these cells was extracted and subjected to Northern blot analysis as described in section 2.27. Total RNA from the Huh-7 (N) cell line was extracted in parallel as a control. Following transfer of the RNA to positively-charged Hybond-N membranes (Amersham), the RNA was probed for the presence of replicon RNA using a ^{32}P-labelled probe derived from an *Age*I/*Apa*L1 restriction fragment of pCV-5CC (see Appendix II) corresponding to HCV nt 155-336 within the 5′NCR (see Appendix IV). The probe was generated as described in section 2.28. Although an HCV genotype 1b strain was used to generate the sub-genomic replicon cDNA (Lohmann *et al.*, 1999a) and the radiolabelled probe described above originated from a genotype 1a strain, the high degree of conservation of the HCV 5′NCR was expected to allow detection of replicon RNA with this probe. Indeed, a clear band was seen in fractionated total RNA from the H9-13 cell line (Fig. 31a). In addition, extensive break-down products were visualised in H9-13 RNA-containing tracks. However, no hybridisation to fractionated RNA from the Huh-7 (N) cell line was seen (Fig. 31a). The possibility that the presence of the HCV sub-genomic replicon RNA in the H9-13 cell line represents integration of the replicon into the host chromosome has been ruled out previously (Lohmann *et al.*, 1999a). To verify that RNA from the Huh-7 (N) cell line was present, the blot was stripped and re-probed with a ^{32}P-labelled probe

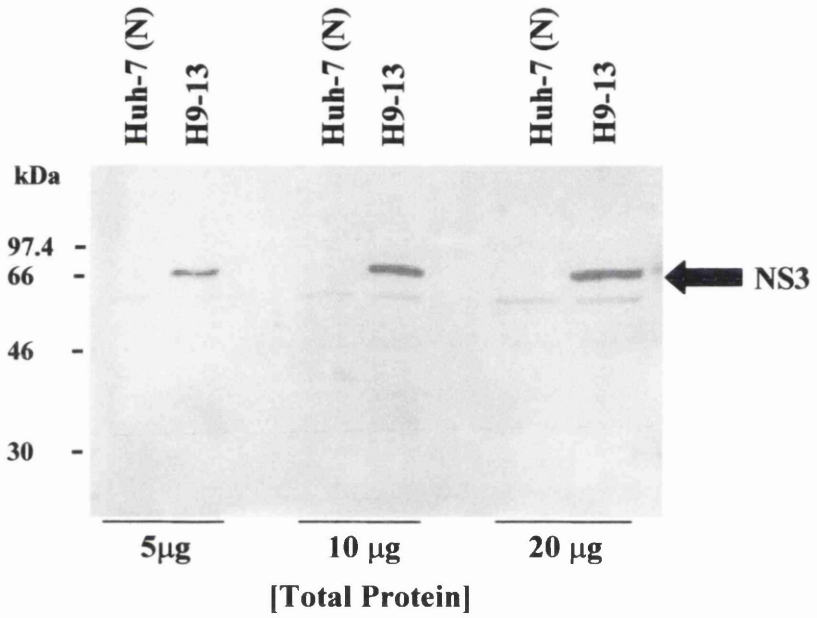

Figure 30: Expression of HCV NS3 protein in the H9-13 cell line. 5, 10 and 20 μg total cell extracts from Huh-7 (N) and H9-13 cell lines were separated by SDS-PAGE (10%) and immunoblotted with an anti-HCV NS3 protease PAb.

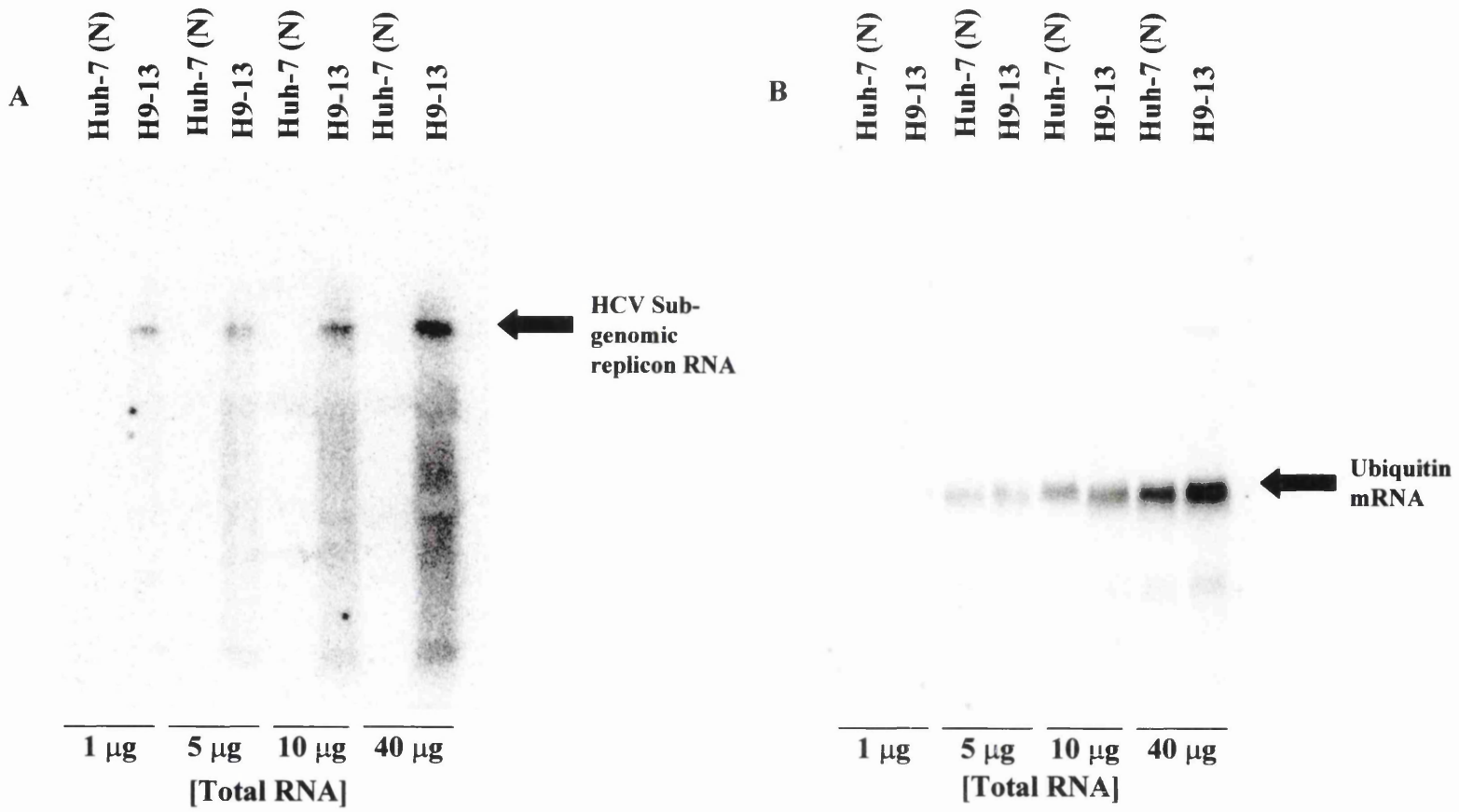

Figure 31: Detection of HCV sub-genomic replicon RNA in the H9-13 cell line. (A) 1, 5, 10 and 40 μg total cellular RNA was extracted from Huh-7 (N) and H9-13 cell lines, and subjected to Northern blot analysis with a ^{32}P-labelled probe originating from a ~180 nt fragment of the 5′NCR. (B) Expression of ubiquitin mRNA. The blot as shown in panel A was stripped and re-probed with a ^{32}P-labelled probe originating from a ubiquitin cDNA (Clontech) to verify the presence of RNA in each track.

originating from ubiquitin cDNA used previously (Fig. 23b; section 3.2.2). A clear band was seen in all lanes confirming the integrity of RNA from both H9-13 and Huh-7 (N) cell lines (Fig. 31b). This also suggested that hybridisation of the 5'NCR probe to many breakdown products in Fig. 31a was not due to poor quality RNA samples, as the ubiquitin probe bound exclusively to a single transcript on the same blot (Fig. 31b).

3.2. 8 Co-localisation of Endogenous DDX3 with Core Protein in HCV Sub-genomic Replicon-expressing Cell Lines

Due to the lack of an efficient cell culture system for HCV, it is not clear whether core protein interacts with DDX3 in HCV-infected cells. Therefore, the DDX3/core interaction was further investigated by infecting the H9-13 cell line, which closely mimics replication of HCV genomic RNA and expresses all HCV nonstructural proteins, with rVV-C-E1-E2 expressing the HCV structural proteins. Since DDX3 is an RNA binding protein (P. Askjaer and J. Kjems, personal communication), it may have an altered localisation in cells expressing the HCV sub-genomic replicon at high levels, thereby affecting its interaction with core. Similarly, in the presence of HCV RNA containing the 5'NCR, which may or may not be a specific target for encapsidation by core protein (section 1.9.1), core may also show a distinct subcellular localisation that has implications for its interaction with DDX3. As before for Huh-7 (N) cells (section 3.2.6), the H9-13 cell line was seeded in 24-well tissue culture dishes containing coverslips such that confluency reached approximately 70% prior to infection with rVV expressing core-E1-E2. Following overnight incubation in normal medium containing 500 μg/ml G-418, the coverslips were washed, fixed, and permeabilised. Endogenous DDX3 was subsequently detected using anti-DDX3 MAb AO196 and an anti-mouse FITC-conjugated secondary antibody, while core protein was detected by anti-core rabbit PAb R525 and an anti-rabbit Cy5-conjugated secondary antibody. In contrast to the above hypotheses for relocalisation of DDX3 and core in the presence of HCV sub-genomic RNA, extensive investigation of DDX3 and core protein in the H9-13 cell line suggested that the proteins did not re-localise in these cells when compared with their expression in the Huh-7 (N) cell line (Figs 32 and 29, respectively).

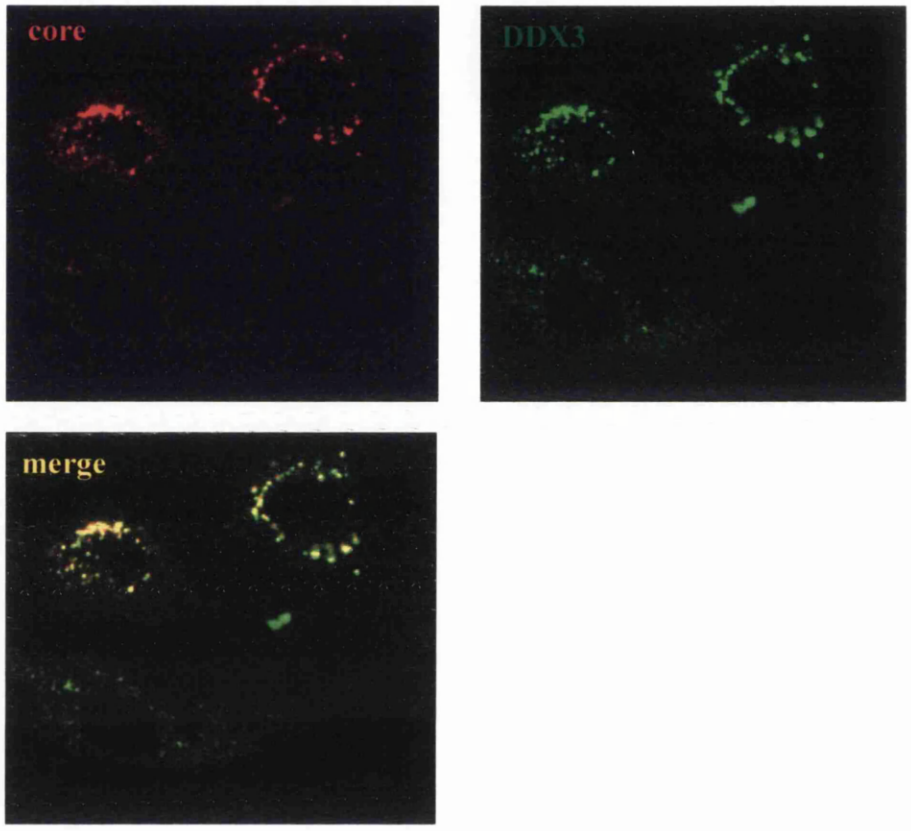

Figure 32: Co-localisation of DDX3 with core protein in the H9-13 cell line. H9-13 cells were infected at an m.o.i. of 0.5 with rVV-C-E1-E2. Following incubation at 37°C for 16 hours, cells were fixed and then probed with anti-DDX3 MAb AO196 and anti-core PAb R525. Bound antibodies were detected by anti-mouse IgG-FITC and anti-rabbit IgG-Cy5 conjugates.

Furthermore, in H9-13 cells infected with rVV-C-E1-E2, DDX3 re-localised to what appeared to be similar globular structures in the perinuclear cytoplasm, with normal DDX3 staining disappearing (Fig. 32). Merging of the two images confirmed that DDX3 co-localises with core protein in the context of the HCV glycoproteins in hepatocytes expressing HCV sub-genomic replicon RNA and all HCV nonstructural proteins (Fig. 32).

3.2. 9 Delineation of the DDX3-core Interacting Domain

It is known that the N-terminal 1-59 aa of core protein interact with the C-terminal 409-662 aa of DDX3 (section 1.9.6.9; Owsianka and Patel, 1999), and it has been postulated that a short 'RS'-like domain in DDX3 is responsible for this interaction (Owsianka and Patel, 1999; You *et al.*, 1999b). These domains are believed to be responsible for a number of protein-protein interactions primarily in splicing factors (section 1.9.6.9; Kohtz *et al.* 1994; Wu and Maniatis, 1993). To ascertain whether this region was involved in binding of DDX3 to core protein, GST-fusion proteins consisting of DDX3 lacking the RS domain (GST-ΔRS), or the DDX3 RS domain alone (GST-RS), were cloned. DDX3 cDNA in the pGEX-6P-3 vector (see Appendix II) was used as a template to generate the appropriate PCR products. Specific primers (see Appendix V) were used to amplify the 150 nt region encoding the RS domain (aa 582-632; see Appendix IV), and delete this domain (by blunt-end cloning of two separate PCR products flanking the RS domain) to produce the ΔRS clone, prior to cloning into pGEX-6P-3. As controls, GST-fusion proteins previously used in a similar GST-pulldown assay (Owsianka and Patel, 1999) consisting of regions of DDX3 which were i) able to bind core protein (full-length DDX3 aa 1-662 and DDX3 aa 409-622) or ii) unable to bind core protein (DDX3 aa 409-473) were used in parallel as controls. Schematic diagrams of all constructs involved in this study, and expression of all the resulting GST-fusion proteins, are shown in Figs 33a and b, respectively. To test whether these proteins could interact with core protein, a similar GST-pulldown assay to that previously described (section 2.46; Owsianka and Patel, 1999) was employed. HCV core protein was translated *in vitro* and radiolabelled with [^{35}S]-Methionine as described in section 2.43 using the Rabbit Reticulocyte Lysate System (Promega). The relevant construct

for *in vitro* transcription of core prior to translation is shown in Fig. 33c. *In vitro* translated core protein, in addition to luciferase protein (produced in the same manner as a control), are shown in Fig. 33d. Both proteins migrated as bands at their expected molecular weights (21 and 69 kDa, respectively). In addition to the 21 kDa *in vitro* translated core protein, several higher molecular weight species were seen (Fig. 33d). The identities of these proteins are unknown, although they are unlikely to be oligomers of full-length core protein due to their apparent molecular weights. The GST-fusion proteins bound to glutathione-agarose beads were mixed with [^{35}S]-Met-labelled core protein for 2 hours at 4°C, washed, and fractionated by SDS-PAGE. Core protein that had bound to DDX3-derived proteins was detected by fluorography (section 2.46). As can be seen in Fig. 33e, the positive (full-length DDX3 aa 1-662 and DDX3 aa 409-622) and negative (DDX3 aa 409-473) controls both behaved as expected. Unexpectedly, however, both the DDX3-RS and DDX3-ΔRS GST-fusion proteins appeared to bind radiolabelled core protein. This result was consistently seen in subsequent binding assays. Therefore, since the constructs used to produce the RS and ΔRS GST-fusion proteins were fully sequenced, it could be concluded that core protein does indeed bind the RS domain, but in the context of the full-length protein the RS domain is not essential for binding to core protein. Alternatively, there may be two or more distinct core-binding regions on DDX3.

3.2. 10 Isotype of All DDX3 Antibodies

Prior to full characterisation of anti-DDX3 MAbs, the isotype of all DDX3 MAbs was determined using Mouse Monoclonal Antibody Isotyping Reagents (Sigma) in an ELISA-based assay. The results are shown in Table 1. Isotyping was carried out by Dr R. Clayton.

Antibody	*Isotype*	*Antibody*	*Isotype*
AO2	IgM	AO88	IgG1
AO10	IgG1	AO158	IgG1
AO22	IgG1	AO166	IgM
AO34	IgM	AO171	IgG1
AO35	IgM	AO190	IgG1
AO43	IgG1	AO194	IgM
AO49	IgG1	AO196	IgG1
AO73	IgM	AO199	IgG1
AO86	IgM	AO215	IgM

Table 1: Isotype of all anti-DDX3 MAbs.

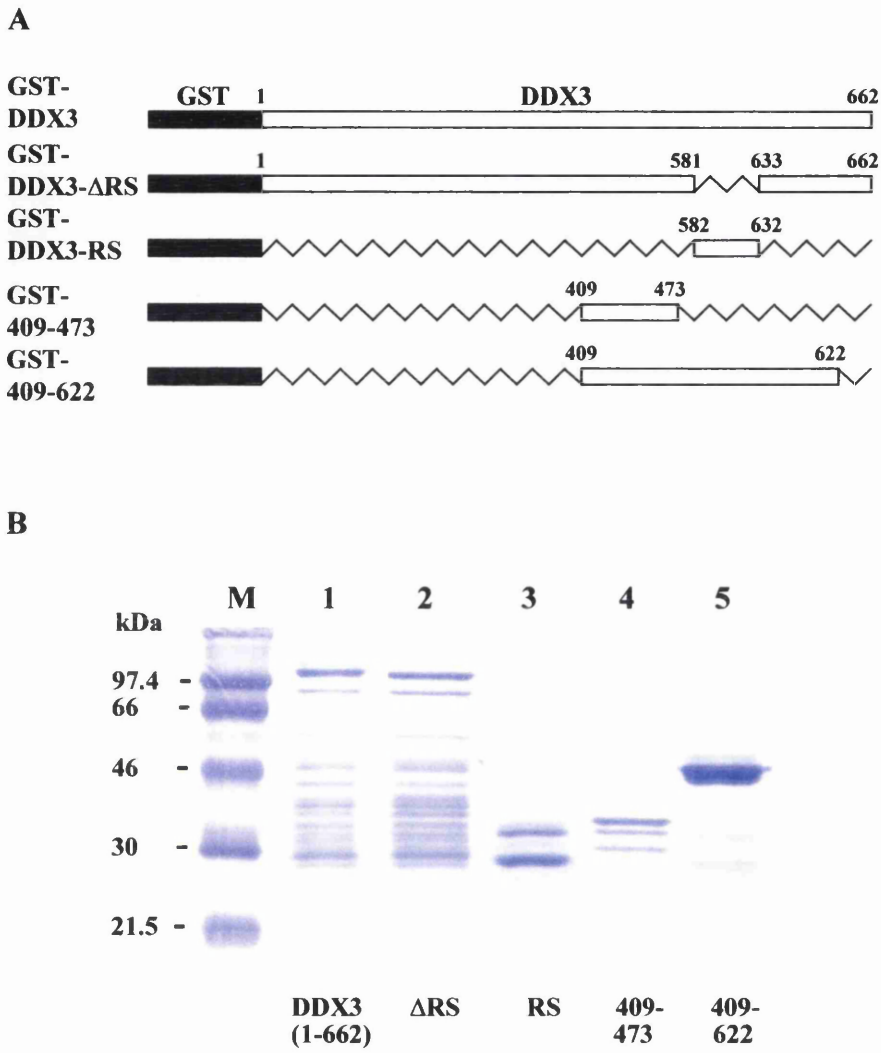

Figure 33: Delineation of the DDX3/core interacting domain. (A) Constructs in the pGEX-6P-3 vector used to produce GST-fusion proteins for pull-down assay. DDX3 aa numbers are shown. The GST-coding sequence is not drawn to scale. (B) SDS-PAGE (10%) of the resulting GST-fusion proteins (5 μg) purified from *E. coli*, together with size markers (M - Rainbow Markers, Amersham) stained with Coomassie brilliant blue.

C

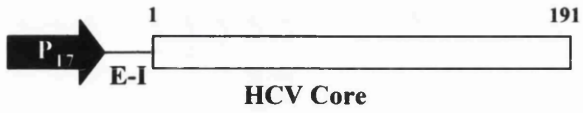

D

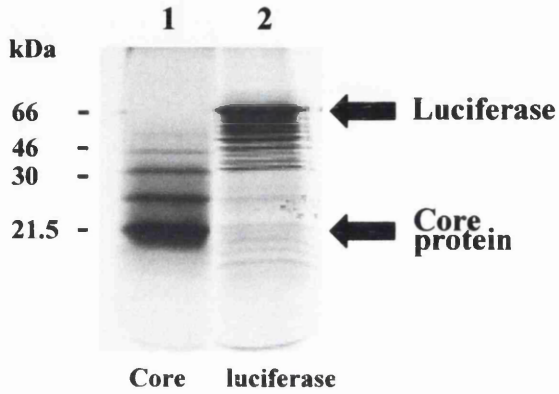

E

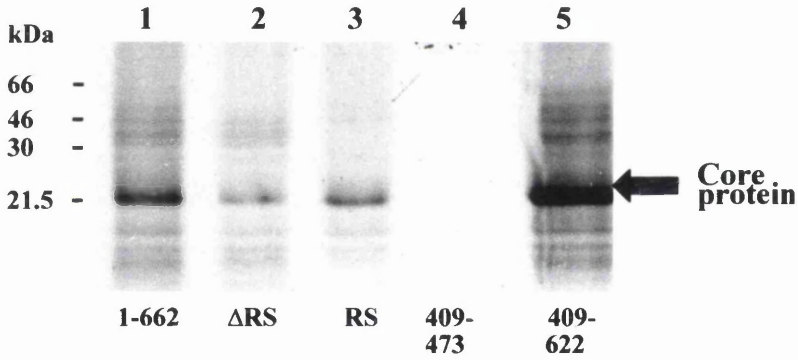

Figure 33 (cont.): Delineation of the DDX3/core interacting domain. (C) The full-length core-coding sequence preceded by the EMCV IRES (E-I) in the pTM1 vector (pTM1-core; Owsianka and Patel, 1999) was used to *in vitro* transcribe HCV core RNA. The RNA was subseqeuntly used to *in vitro* translate core protein (aa 1-191) using the Rabbit Reticulocyte Lysate System (Promega). (D) SDS-PAGE (12.5%) followed by fluorgraphy (section 2.46) of *in vitro* translated [^{35}S]-Met-labelled core protein and luciferase control. (E) Binding of [^{35}S]-Met-labelled core protein to truncated GST-DDX3 and GST-DDX3 deletion mutants as shown in Fig. 33b.

3.2. 11 Binding of MAbs to Free GST Protein

In characterising the anti-DDX3 MAbs and PAbs, it was initially necessary to establish whether any of the antibodies were binding to GST protein alone since the panel of anti-DDX3 MAbs, as well as PAb R648, had been raised against full-length DDX3 expressed in *E. coli* as a GST-fusion protein, while PAb R438 was raised against a GST-fusion protein consisting of the C-terminal 253 aa of DDX3, to which core protein was previously found to interact with in a yeast two-hybrid assay (Owsianka and Patel, 1999). Empty pGEX-6P-3 vector was transformed into *E. coli* and used to produce GST protein. The protein was purified and eluted from glutathione-agarose beads as described previously. Fig. 34a shows sequentially eluted purified GST protein after fractionation by SDS-PAGE and staining with Coomassie brilliant blue. 50 μg of purified GST protein was fractionated on two preparative SDS-PAGE gels and electrophoretically transferred to ECL membranes. The membranes were cut into strips and each probed with a separate anti-DDX3 MAb or PAb. In addition, a separate strip from each gel was probed with an anti-GST PAb as a positive control. A major band was detected by the anti-GST PAb at the expected molecular weight of 26 kDa, in addition to less pronounced but distinct bands at approximately 19, 55 and 60 kDa (Fig. 34b, lanes 11 and 22) which correlated with bands seen by direct staining with Coomassie brilliant blue. Both anti-DDX3 PAbs bound free GST protein (lanes 10 and 21), perhaps unsurprisingly since PAb epitopes would be expected across all exposed areas of the entire fusion protein. PAb R648 detected identical bands to the anti-GST PAb, while R438 appeared to specifically bind GST alone. However, on longer exposures weak binding by R438 to the minor bands detected by the anti-GST PAb and R648 was revealed (data not shown). MAb AO199 also strongly bound GST alone. This MAb therefore represents a reagent that could be useful in the specific detection of GST and GST-fusion proteins. There appeared to be weak binding by most of the other antibodies, likely due to non-specific protein-protein binding since large amounts of purified GST had been loaded on the gel. Of these antibodies, MAbs AO2 and AO35 appeared to have stronger affinity for free GST than the other antibodies. MAb AO34 also weakly bound GST, and gave a characteristic but unexplained

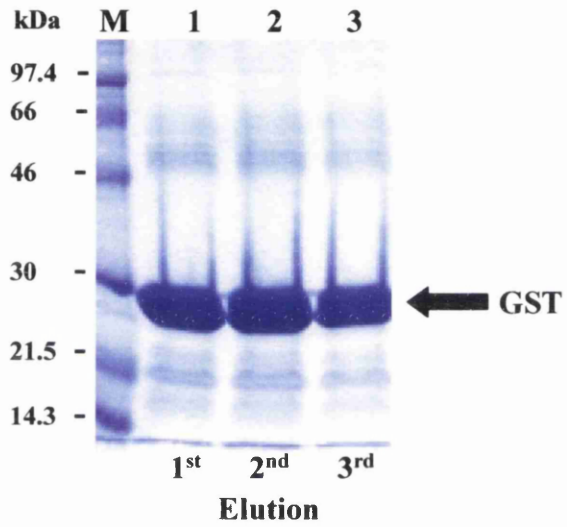

Figure 34a: Expression of GST protein. SDS-PAGE (10%) of bacterially-expressed GST purified by affinity chromatography on glutathione-agarose beads, and sequentially eluted using glutathione (section 2.29). 200 μl glutathione elution buffer was added to the beads, mixed for 20 minutes at 4°C, and protein recovered by centrifugation. 5 μl of each elution was loaded onto the gel.

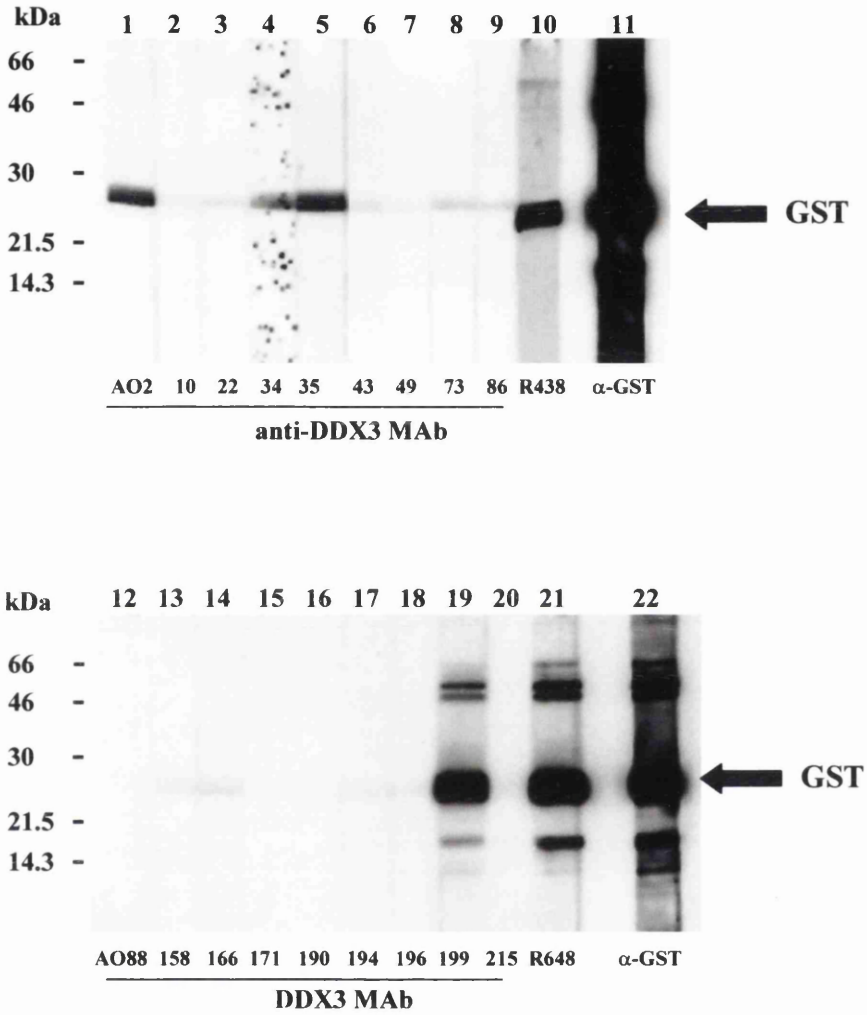

Figure 34b: Reactivity of anti-DDX3 MAbs and PAbs to free GST protein by Western blotting. 50 μg protein was fractionated on each SDS-PAGE preparative gel (12.5%) and transferred to ECL membranes. The membranes were cut into strips and each one probed with a separate anti-DDX3 MAb (lanes 1-9 and 12-20) or PAb (lanes 10 and 21). An anti-GST PAb was used as a positive control (lanes 11 and 22).

speckled pattern which was consistently seen with this antibody in Western blots of purified GST-fusion proteins and cell extracts.

3.2. 12 Expression and Purification of GST-DDX3 and GST-DDX3C Fusion Proteins

Both full-length and truncated DDX3 (coding for the C-terminal 253 aa of the protein) sequences cloned in frame with the GST-coding sequence were available (Appendix II; Owsianka and Patel, 1999). These constructs were used to express and purify the full-length (aa 1-662; GST-DDX3) and C-terminal portion (aa 409-662; GST-DDX3C) of DDX3 as GST-fusion proteins from *E. coli* in order to i) show binding of the panel of MAbs and PAbs to full-length DDX3 and ii) divide those recognising the full-length protein into those with epitopes in the N- or C-terminal regions of the protein. The constructs used are shown schematically in Fig. 35. The resulting proteins expressed in *E. coli* were eluted from glutathione-agarose beads, fractionated by SDS-PAGE, and stained with Coomassie blue. A single band corresponding to full-length DDX3 (expected molecular weight 73 kDa) fused to the 26 kDa GST moiety at approximately 99 kDa was seen in tracks containing purified GST-DDX3 (Fig. 35b, lanes 1-3). This single band contrasts with the doublet detected when mammalian cell extracts were immunoblotted with anti-DDX3 MAb AO196 (Fig. 26; section 3.2.3). This could be due to the lack of a second cellular isoform of the protein (as described in section 3.2.3), but could also suggest a lack of post-translational processing of the GST-DDX3 protein in the bacterial system. A distinct pattern of what are apparently breakdown products of GST-DDX3 were consistently seen even in the presence of a high concentration of protease inhibitors (Fig. 35b, lanes 1-3). The GST-DDX3C fusion protein was expressed as a triplet (Fig. 35b, lanes 4-6) , with a major product running at the expected molecular weight of 53 kDa, in addition to two further slightly smaller products. A single breakdown product of approximately 32 kDa was seen, which is too large to be free GST protein. This may suggest that sequences within the N-terminus of DDX3 are responsible for the large number of breakdown products detected with GST-DDX3 expressed in a bacterial system. Nevertheless, both proteins appear to have been purified to a satisfactory extent for subsequent experimental procedures.

A

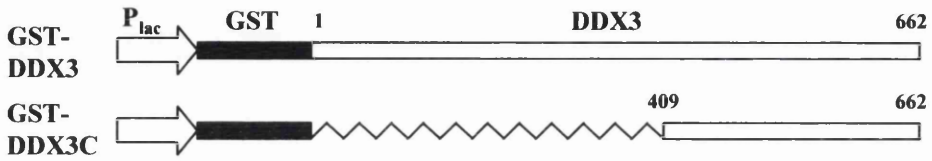

B

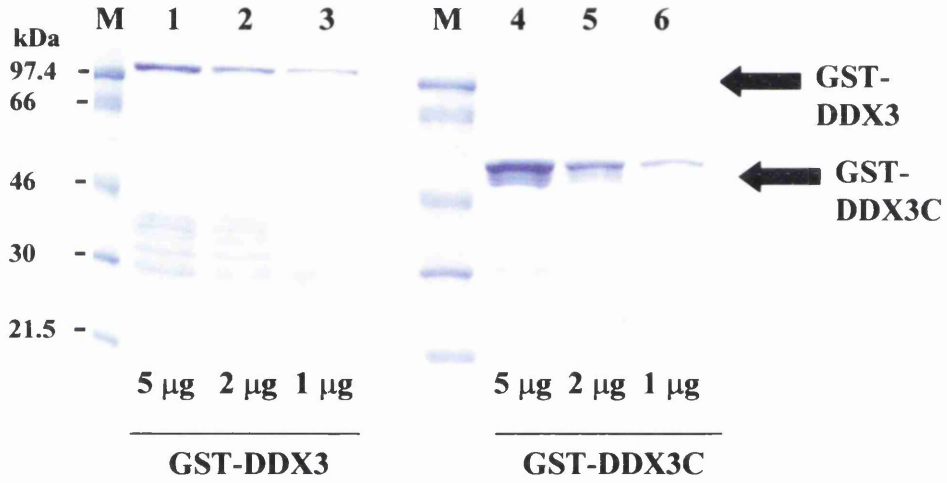

Figure 35: GST-DDX3 and -DDX3C proteins. (A) Schematic representation of the constructs in the pGEX-6P-3 (DDX3) or pGEX-2T (DDX3C) vector. Expression of the fusion proteins was under the under control of an inducible promoter (P_{lac}). (B) Bacterially-expressed GST-DDX3 (lanes 1-3) and GST-DDX3C (lanes 4-6) were purified by affinity chromatography on glutathione-agarose beads, and the bound protein eluted using glutathione (section 2.29). 1, 5 and 10 μg of purified protein was fractionated by SDS-PAGE (9%) and stained with Coomassie brilliant blue.

3.2. 13 Binding of MAbs to GST-DDX3

The same method employed to detect binding of the panel of antibodies to free GST protein was used to verify that the anti-DDX3 MAbs and PAbs could detect full-length DDX3 expressed as a GST-fusion protein (GST-DDX3). As before, 50 μg purified protein was fractionated on two preparative SDS-PAGE gels and electrophoretically transferred to ECL membranes. The membranes were cut into strips and each probed with a separate anti-DDX3 MAb or PAb. As shown in Fig. 36a, the majority of the antibodies recognised GST-DDX3 at the expected molecular weight of 99 kDa. Interestingly, while most of the antibodies appeared to have distinct patterns of affinities for different breakdown products of DDX3, only MAb AO190 recognised the 99 kDa full-length product alone. Antibodies AO88 and AO194 did not detect DDX3 expressed as a GST-fusion protein by Western blotting. Instead, AO88 appeared to exclusively bind a protein at a molecular weight of approximately 32 kDa, while AO194 did not appear to react with any fractionated proteins in the purified preparation of GST-DDX3. The identity of the 32 kDa protein is unknown.

3.2. 14 Binding of MAbs to GST-DDX3C

As a preliminary test prior to more exact epitope mapping of the panel of MAbs, the antibodies were tested for their ability to bind the C-terminal 253 aa of DDX3 expressed as a GST-fusion protein (GST-DDX3C). This fragment of DDX3 was initially identified as an interacting partner to HCV core protein in a yeast two-hybrid screening of a human (liver-derived) cDNA library (Owsianka and Patel, 1999). 50 μg purified GST-DDX3C as shown previously (Fig. 35b) was fractionated on a preparative gel and blotted to ECL membranes as before. The membranes were cut into strips and each one probed with a separate anti-DDX3 MAb or PAb. MAb AO194 that was unable to detect GST-DDX3 (Fig. 36a; section 3.2.13) and anti-GST MAb AO199 (Fig. 34b; section 3.2.11) were used as negative and positive controls, respectively. These antibodies reacted as expected (Fig. 36b, lanes 16 and 18). In addition to the PAbs which would likely bind GST-DDX3C, not least because they also bind GST alone (Fig. 34b; section 3.2.11), the majority of the MAbs bound to this fusion protein (Fig. 36b). Only MAbs AO2, 35, 166 and 196

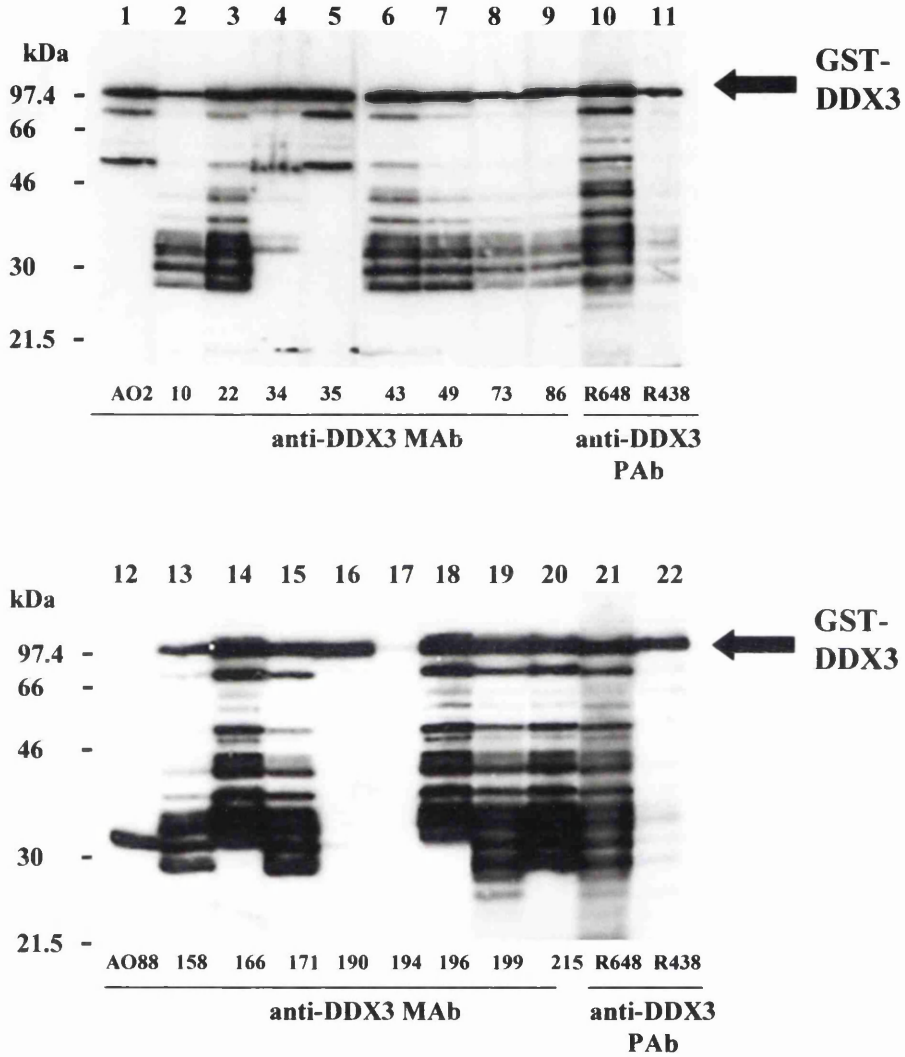

Figure 36a: Reactivity of anti-DDX3 MAbs and PAbs to GST-DDX3 by Western blotting. 50 μg protein was fractionated on each SDS-PAGE preparative gel (8%) and transferred to ECL membranes. The membranes were cut into strips and each one probed with a separate anti-DDX3 MAb (lanes 1-9 and 12-20) or PAb (lanes 10-11 and 21-22).

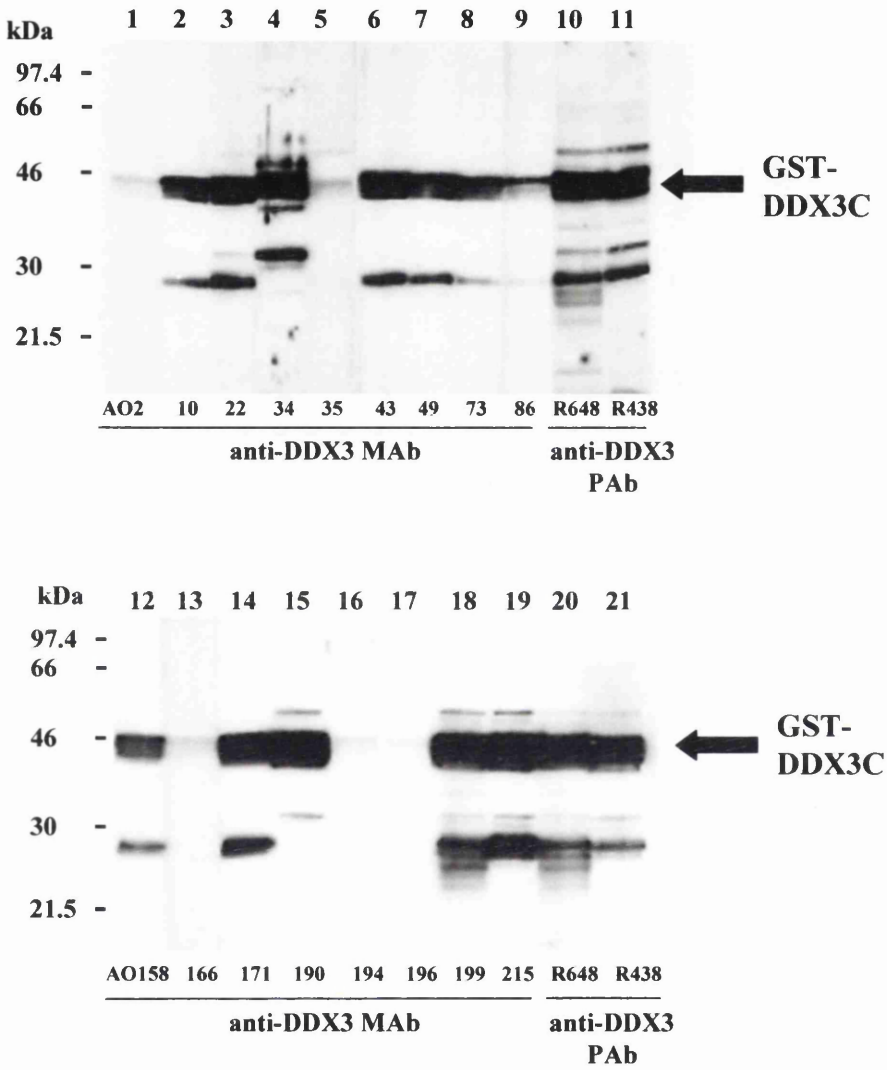

Figure 36b: Reactivity of anti-DDX3 MAbs and PAbs to GST-DDX3C by Western blotting. 50 μg protein was fractionated on each SDS-PAGE preparative gel (10%) and transferred to ECL membranes. The membranes were cut into strips and each one probed with a separate anti-DDX3 MAb (lanes 1-9 and 12-20) or PAb (lanes 10-11 and 21-22).

did not bind the truncated DDX3 GST-fusion protein (lanes 1, 5, 13, and 17, respectively), suggesting their epitopes lie within the N-terminal aa 1-408 of DDX3.

3.2. 15 Epitope Mapping of MAbs Using Deletion Mutants within DDX3C

An ELISA-based method was employed to roughly determine the epitopes of the MAbs binding the C-terminal 253 aa of DDX3. PAbs R438 and R648 were not tested by this method as both were shown to recognise GST alone (Fig. 34b; section 3.2.11). Various deletions had been made within this C-terminal region and cloned in frame with the GST-coding seqeunce in pGEX-2T (Owsianka and Patel, 1999). The constructs are shown schematically in Fig. 37, and the resulting GST-fusion proteins expressed in *E. coli* are shown in Fig. 38. As described in detail previously (section 2.33), diluted purified protein was bound to a 96-well plate (Immulon II, Dynex Technologies) by incubation at 4°C for 16 hours. Antibody supernatants were diluted in PBST and incubated with the protein for 2 hours. Unbound antibody was washed away, while that which had bound the protein was detected by anti-mouse IgG-HRP conjugated secondary antibody followed by visualisation with TMB developing solution. OD_{450} was determined using an Opsys MR plate reader (Dynex Technologies). AO199 which was shown previously to specifically bind free GST protein was used as a positive control - binding data for this antibody indicated strong affinity for all of the GST-fusion proteins as expected, although only weak binding was seen to the DDX3 409-622 GST-fusion protein (data not shown) indicating this protein was possibly too dilute even though expression levels of this protein were reasonable (Fig. 38a, lanes 1-2). Binding of the antibodies to the various deletion mutants was used to deduce the epitope of the anti-DDX3 MAbs. The majority of the antibodies previously shown to bind GST-DDX3C (Fig. 36b; section 3.2.14) recognised an epitope within aa 409-473 (Fig. 39). One exception to this was AO190 - this antibody possessed an epitope within aa 474-552 (Fig. 39). The epitope of AO34, however, was unclear since this antibody recognised epitopes in both 409-473 and 474-662 regions of the protein (Fig. 39). These results were confirmed by Western blotting with the same GST-fusion proteins used in the ELISA (data not shown).

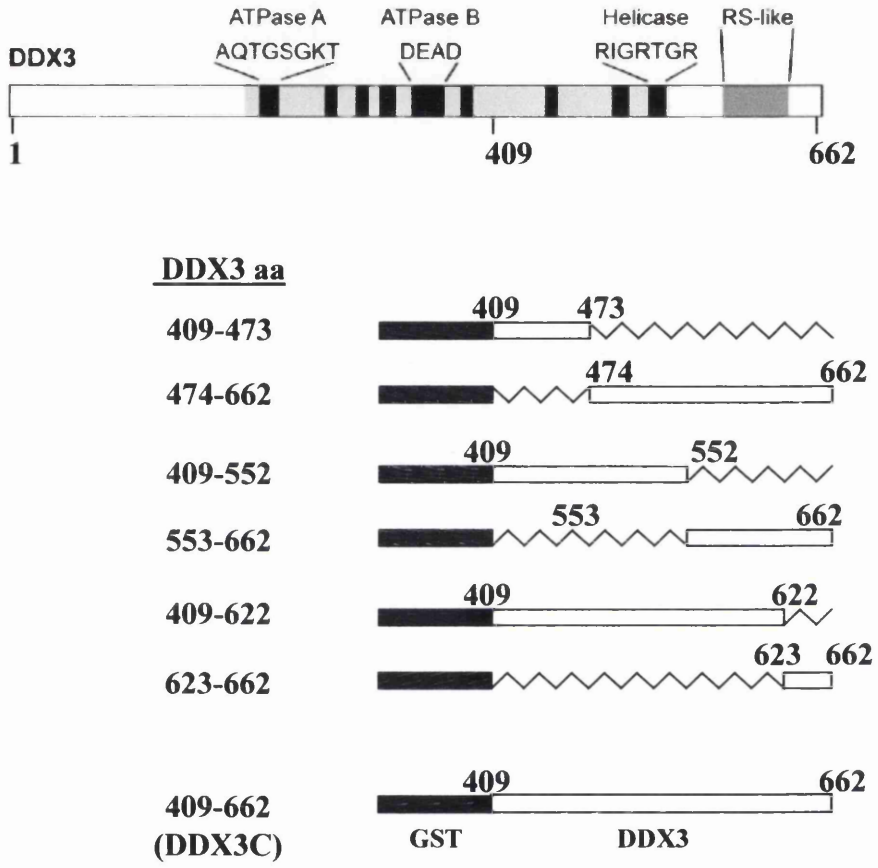

Figure 37: Schematic diagram of the DDX3C deletion mutants used to map epitopes of anti-DDX3 MAbs binding GST-DDX3C. The full-length protein is also included above for reference. The shaded area represents the central core of the protein, containing the conserved motifs (highlighted by dark boxes) present in all other DEAD-box RNA helicases (adapted from Owsianka and Patel, 1999).

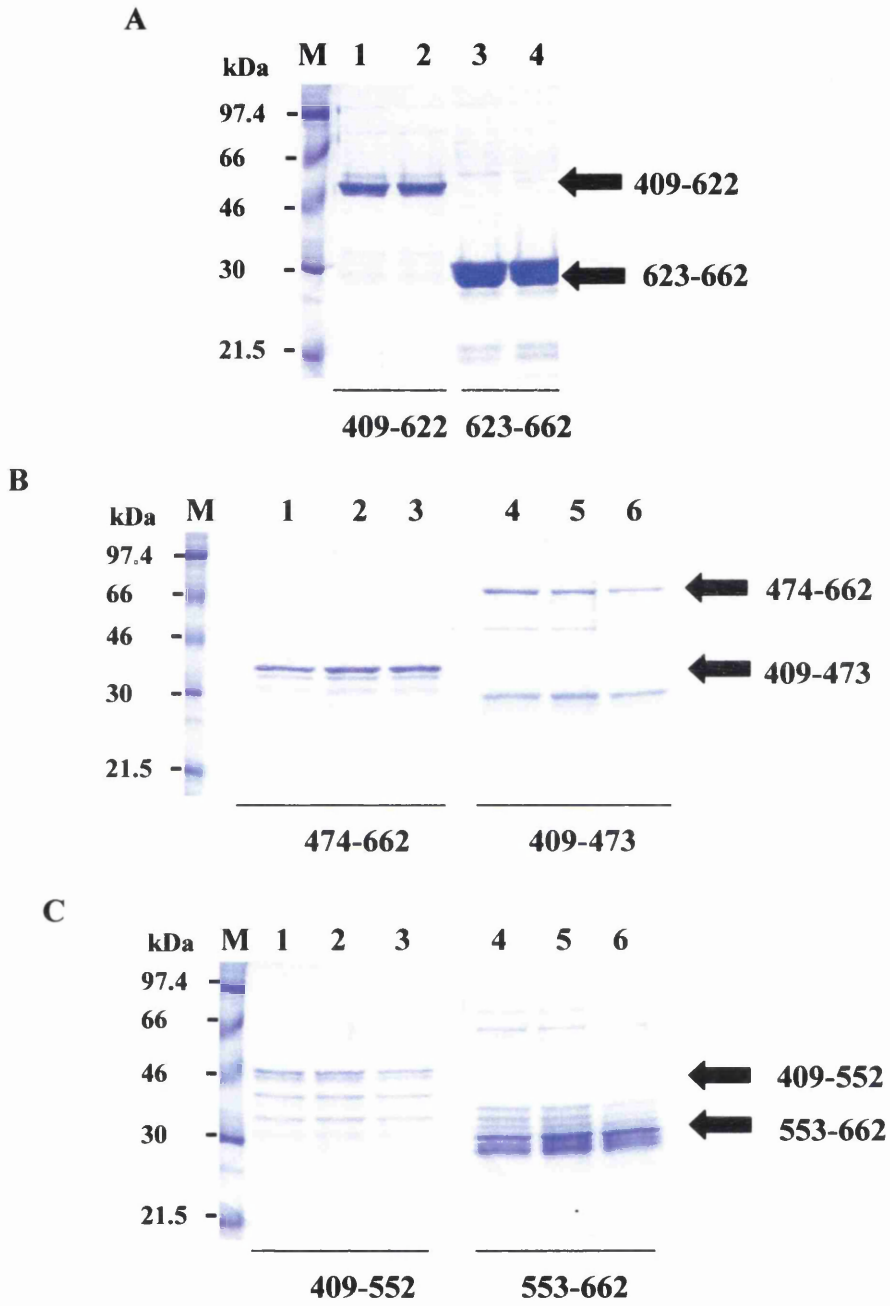

Figure 38: Expression of DDX3C deletion mutants from constructs shown in Fig. 37 as GST-fusion proteins. The bacterially-expressed fusion proteins were purified by affinity chromatography on glutathione-agarose beads, and the bound protein eluted using glutathione (section 2.29). 10 µl of purified protein as indicated from the first two or three elutions was fractionated by SDS-PAGE (10%) and stained with Coomassie brilliant blue.

Figure 39 - see following pages: Binding of anti-DDX3 MAbs to GST-DDX3C deletion mutants. The following pages present the binding data generated by ELISA for each of the anti-DDX3 MAbs shown previously to bind GST-DDX3C. Three-fold serial dilutions of the proteins shown in Fig. 38 were bound to 96-well Immulon II ELISA dishes and probed with MAb supernatants diluted 1:5 in PBST. Unbound antibody was washed away, while that which had bound protein was detected by anti-mouse IgG-HRP conjugated secondary antibody followed by visualisation with TMB developing solution. OD_{450} was determined using an Opsys MR plate reader (Dynex Technologies).

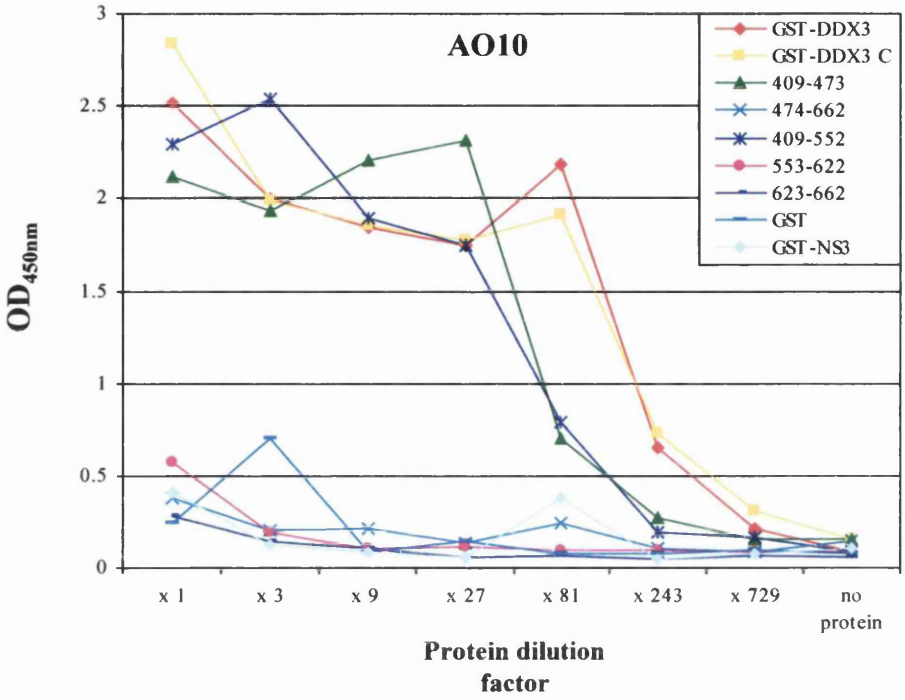
AO10
GST-DDX3
GST-DDX3 C
409-473
474-662
409-552
553-622
623-662
GST
GST-NS3
OD450nm
3
2.5
2
1.5
1
0.5
0
x 1
x 3
x 9
x 27
x 81
x 243
x 729
no protein
Protein dilution factor

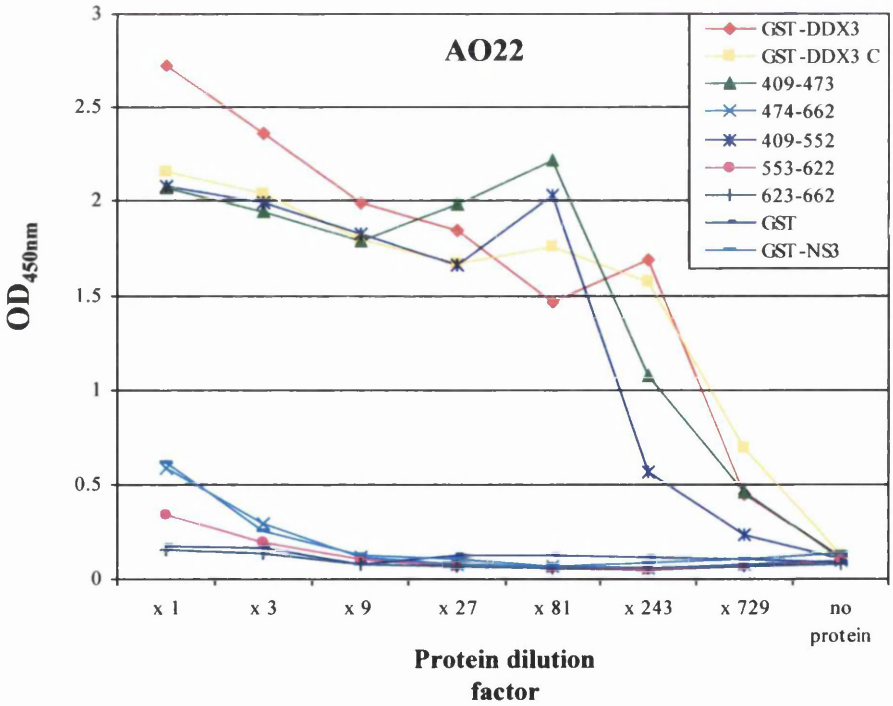
AO22
GST-DDX3
GST-DDX3 C
409-473
474-662
409-552
553-622
623-662
GST
GST-NS3
OD450nm
3
2.5
2
1.5
1
0.5
0
x 1
x 3
x 9
x 27
x 81
x 243
x 729
no protein
Protein dilution factor

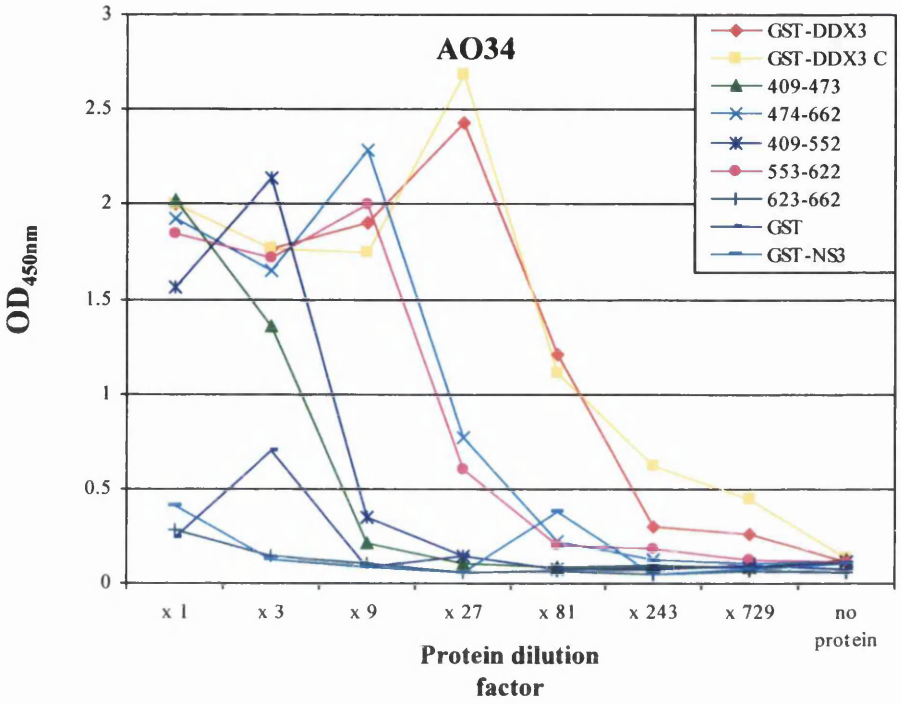
AO34
GST-DDX3
GST-DDX3 C
409-473
474-662
409-552
553-622
623-662
GST
GST-NS3
OD450nm
3
2.5
2
1.5
1
0.5
0
x 1
x 3
x 9
x 27
x 81
x 243
x 729
no protein
Protein dilution factor

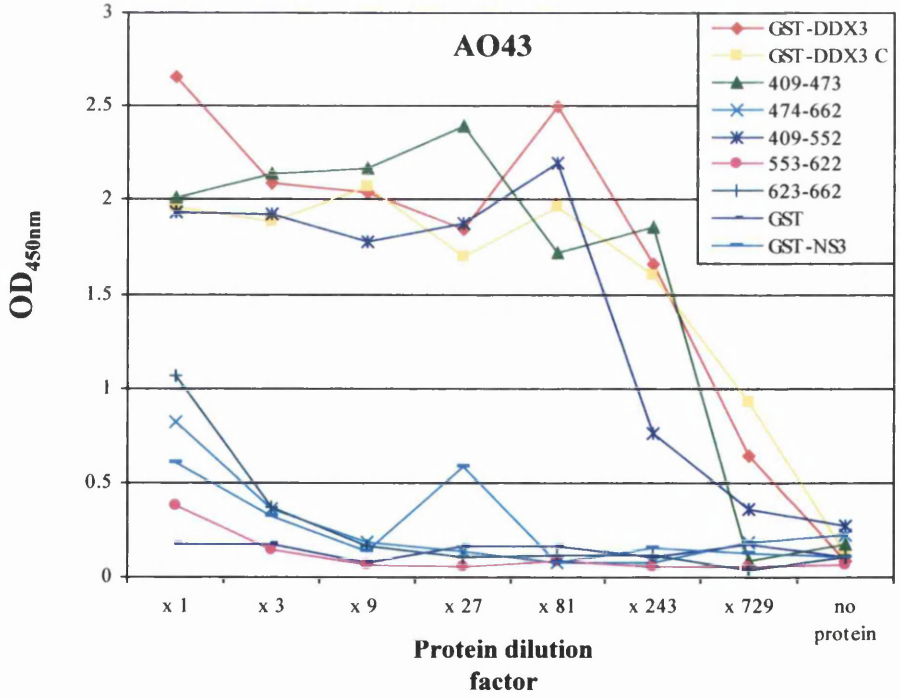
AO43
GST-DDX3
GST-DDX3 C
409-473
474-662
409-552
553-622
623-662
GST
GST-NS3
OD450nm
3
2.5
2
1.5
1
0.5
0
x 1
x 3
x 9
x 27
x 81
x 243
x 729
no protein
Protein dilution factor

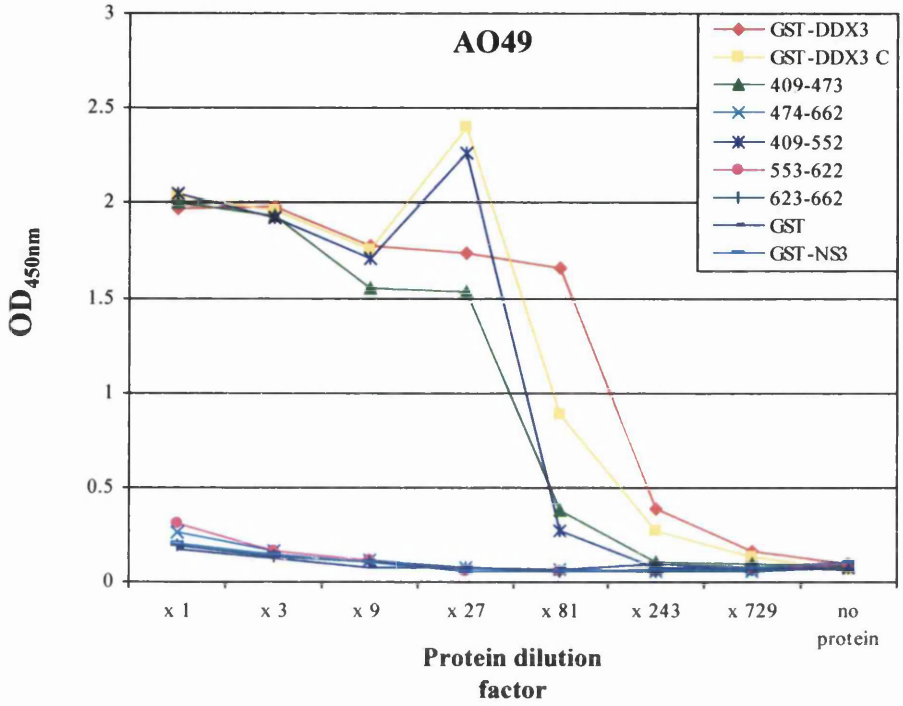
AO49
GST-DDX3
GST-DDX3 C
409-473
474-662
409-552
553-622
623-662
GST
GST-NS3
OD450nm
3
2.5
2
1.5
1
0.5
0
x 1
x 3
x 9
x 27
x 81
x 243
x 729
no protein
Protein dilution factor

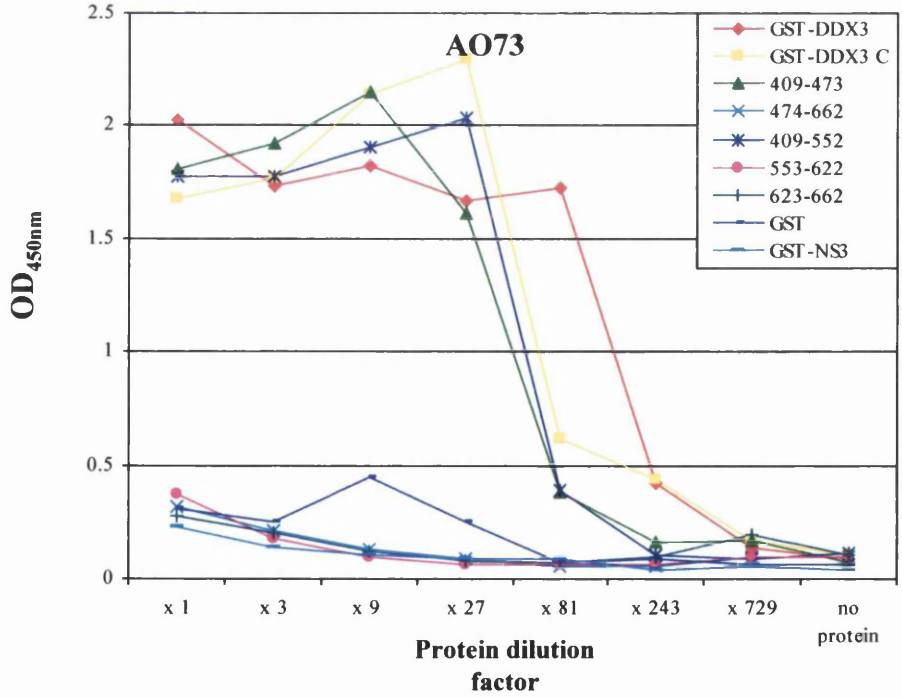
AO73
GST-DDX3
GST-DDX3 C
409-473
474-662
409-552
553-622
623-662
GST
GST-NS3
OD450nm
2.5
2
1.5
1
0.5
0
x 1
x 3
x 9
x 27
x 81
x 243
x 729
no protein
Protein dilution factor

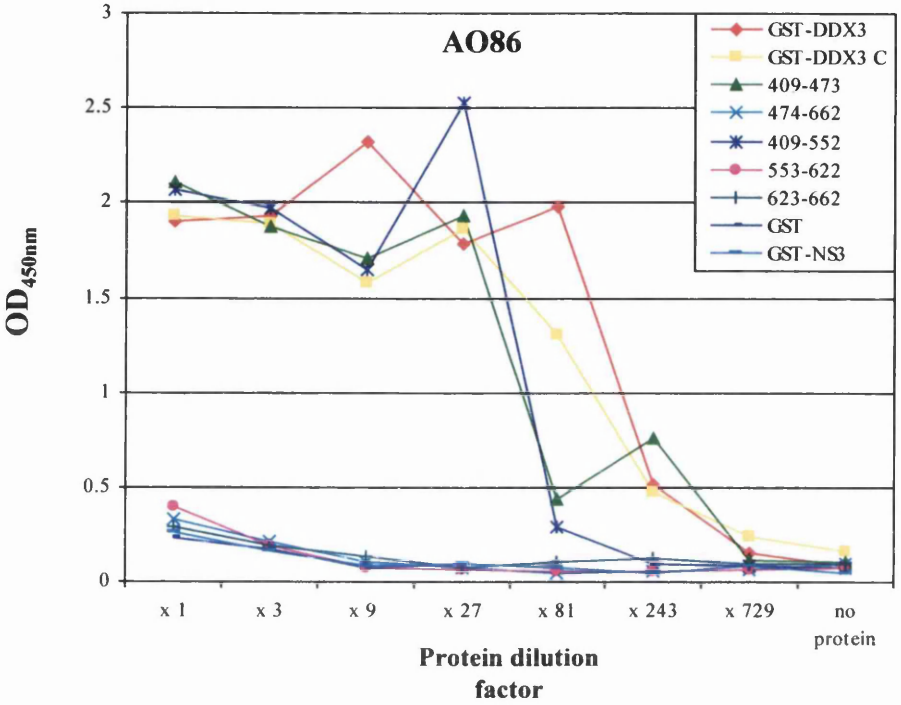
AO86
GST-DDX3
GST-DDX3 C
409-473
474-662
409-552
553-622
623-662
GST
GST-NS3
OD450nm
3
2.5
2
1.5
1
0.5
0
x 1
x 3
x 9
x 27
x 81
x 243
x 729
no protein
Protein dilution factor

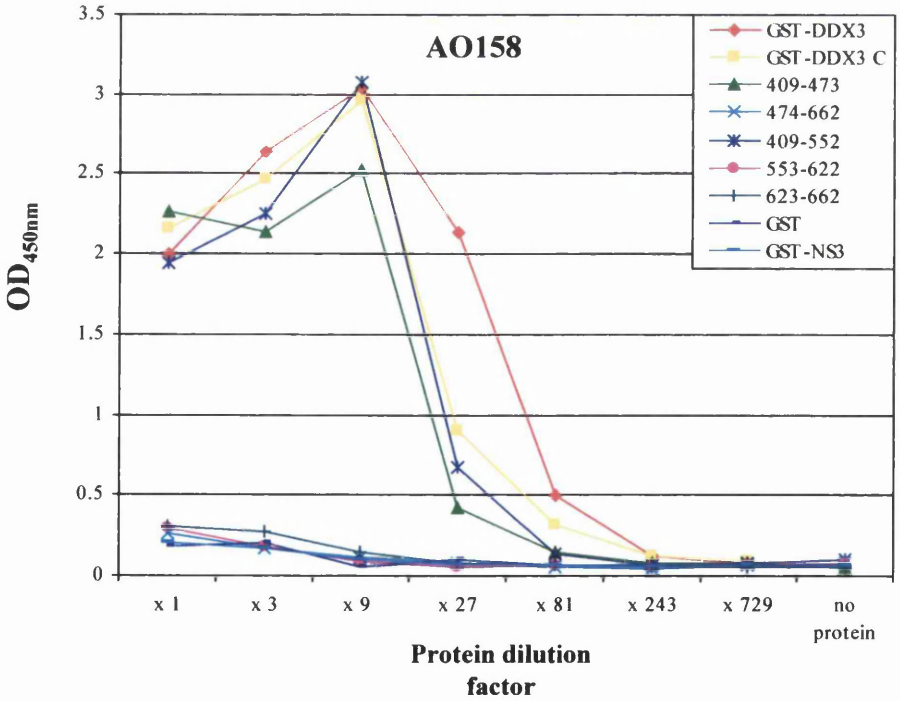
AO158
GST-DDX3
GST-DDX3 C
409-473
474-662
409-552
553-622
623-662
GST
GST-NS3
OD450nm
3.5
3
2.5
2
1.5
1
0.5
0
x 1
x 3
x 9
x 27
x 81
x 243
x 729
no protein
Protein dilution factor

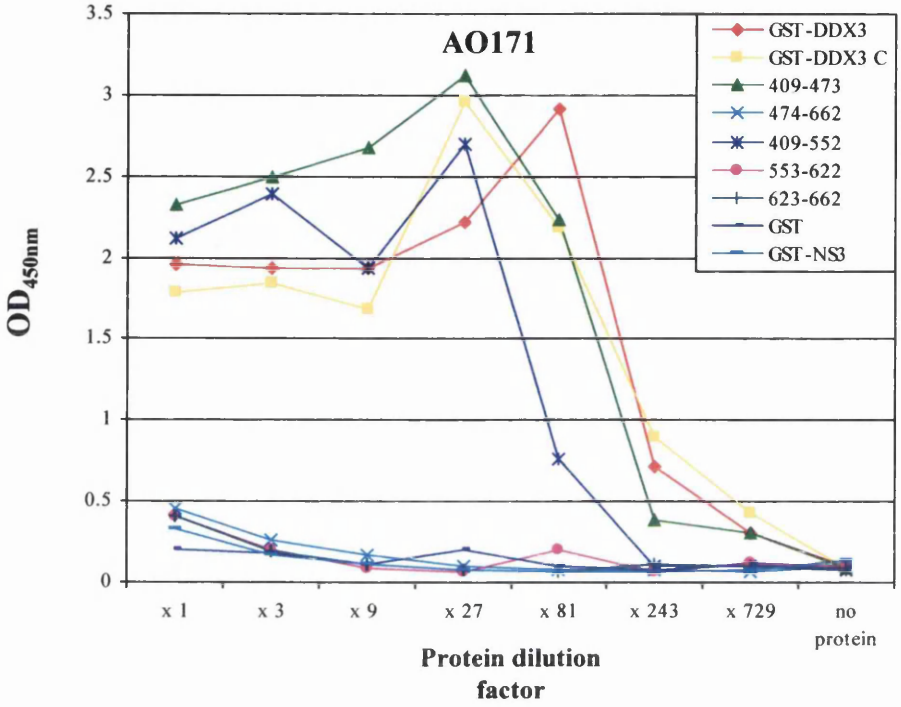
AO171
GST-DDX3
GST-DDX3 C
409-473
474-662
409-552
553-622
623-662
GST
GST-NS3
OD450nm
3.5
3
2.5
2
1.5
1
0.5
0
x 1
x 3
x 9
x 27
x 81
x 243
x 729
no protein
Protein dilution factor

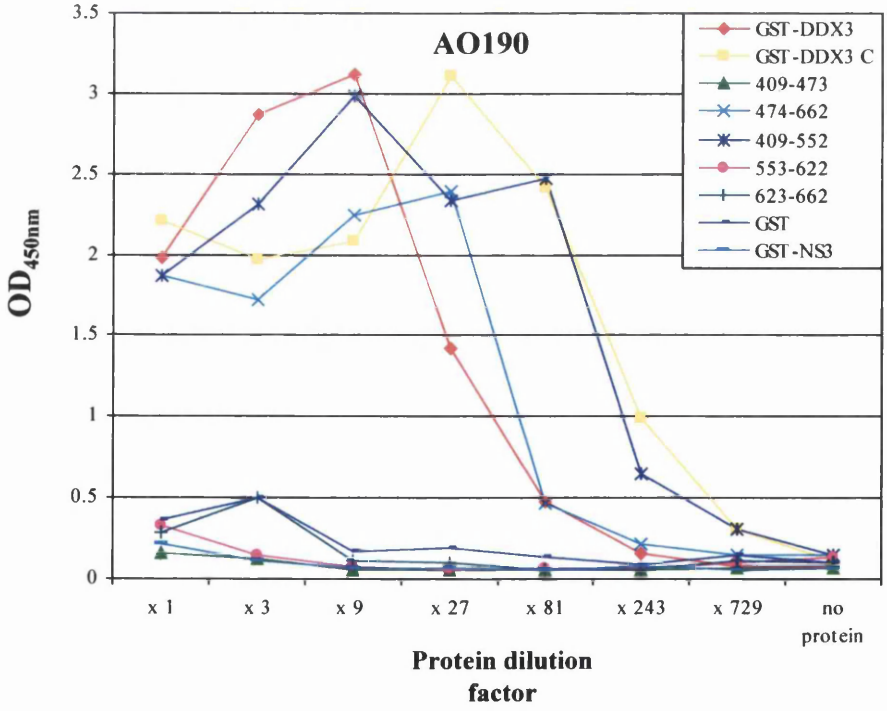
AO190
GST-DDX3
GST-DDX3 C
409-473
474-662
409-552
553-622
623-662
GST
GST-NS3
OD450nm
3.5
3
2.5
2
1.5
1
0.5
0
x 1
x 3
x 9
x 27
x 81
x 243
x 729
no protein
Protein dilution factor

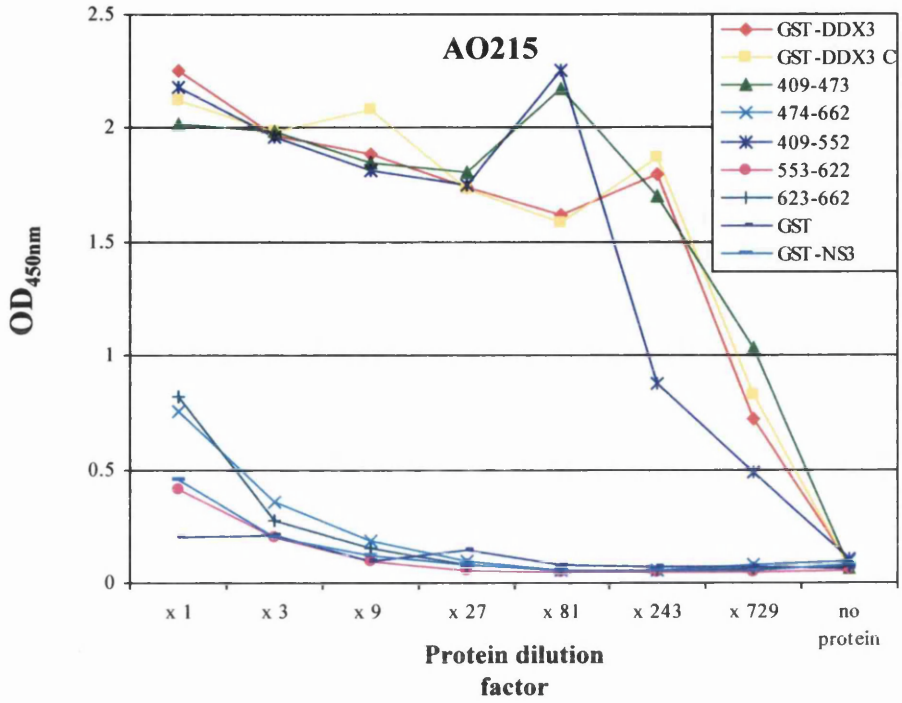
AO215
GST-DDX3
GST-DDX3 C
409-473
474-662
409-552
553-622
623-662
GST
GST-NS3
2.5
2
1.5
1
0.5
0
OD450nm
x 1
x 3
x 9
x 27
x 81
x 243
x 729
no protein
Protein dilution factor

3.2. 16 Production of DDX3 Mutants to Map MAbs with N-terminal Epitopes

To roughly map the epitopes of the remaining anti-DDX3 MAbs which did not interact with the C-terminal 253 aa of DDX3, a series of deletions were made from the C-terminus of the protein. pGEX-6P-3-DDX3 (see Appendix II) was cut with the relevant restriction enzyme as shown in Fig. 40a in a double digest with *Eco*RI, a unique restriction site in the pGEX-6P-3 multi-cloning site downstream of the DDX3-coding sequence. The resulting vector plus DDX3 sequence containing deletions from the 3′-end of the coding seqeunce was blunt ended with T4 DNA polymerase and/or DNA polymerase I (Klenow fragment) depending on the overhangs produced by the restriction enzymes, and re-ligated. The resulting N-terminal DDX3 mutants were expressed in *E. coli*, purified on glutathione-agarose beads, and eluted (section 2.29). The purified proteins were fractionated by SDS-PAGE along with GST-DDX3 (aa 1-662) and visualised by direct staining with Coomassie brilliant blue (Fig. 40b).

3.2. 17 Reactivity of Anti-DDX3 MAbs to the N-terminus of DDX3 by Western Blotting

Each of the MAbs which bound GST-DDX3 but did not bind GST-DDX3C or GST alone were tested by Western blotting with the GST-DDX3 N-terminal fusion proteins described above. It was previously shown that none of these antibodies bound free GST protein with high affinity (Fig. 34b; section 3.2.11). Full-length DDX3 expressed as a GST-fusion protein (GST-DDX3) was used as a positive control; all of the antibodies used in this study interacted with the full-length protein as expected (Fig. 41a-41d, lane 5). By detecting binding to N-terminal DDX3 mutants expressed as GST-fusion proteins it was possible to deduce the epitope of the MAbs. Antibodies AO2 and AO35 possessed epitopes within DDX3 aa 143-208, whereas antibodies AO166 and AO196 had epitopes within the extreme N-terminal aa 1-142 of DDX3. None of the antibodies bound to epitopes within aa 209-472, possibly suggesting epitopes in this region are not exposed, at least when DDX3 is bacterially-expressed as a GST-fusion protein. The epitopes of all anti-DDX3 MAbs are summarised in Appendix I. A detailed analysis of the precise regions recognised will be performed in future.

A

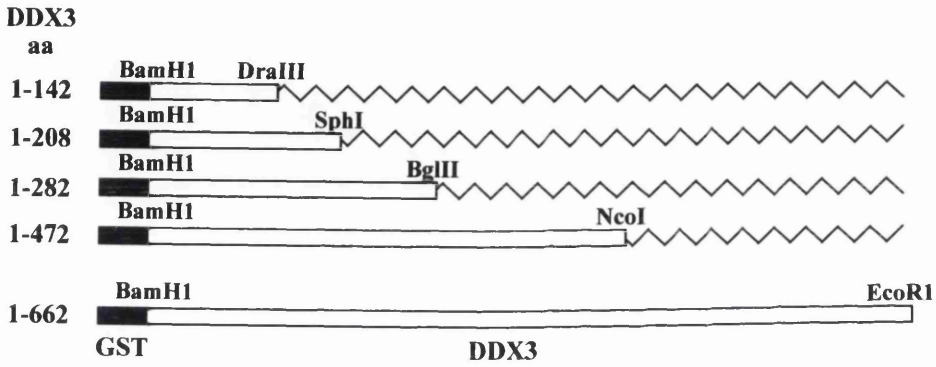

B

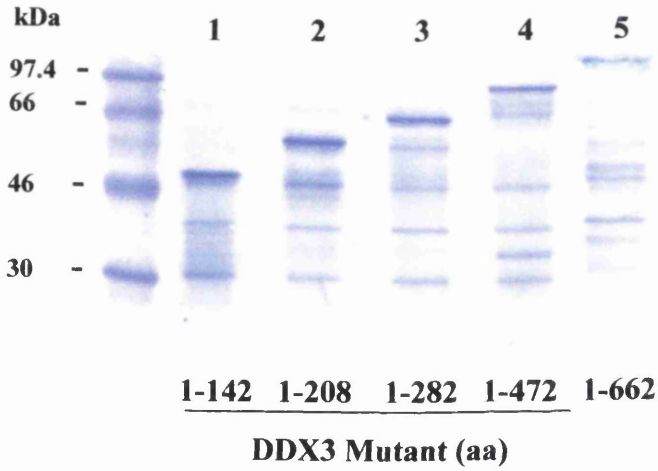

Figure 40: Cloning and expression of DDX3 deletion mutants used to map epitopes of anti-DDX3 MAbs binding the N-terminus. (A) Constructs used: restriction sites within the DDX3-coding sequence (see Appendix IV) employed, the resulting DDX3 aa numbers, and the position of the GST-coding sequence are shown. B) SDS-PAGE (10%) of 5 μg GST-DDX3 deletion mutants (lanes 1-4) and full-length (aa 1-662) GST-DDX3 (lane 5) expressed in and purified from *E. coli*. Proteins were visualised by staining with Coomassie brilliant blue.

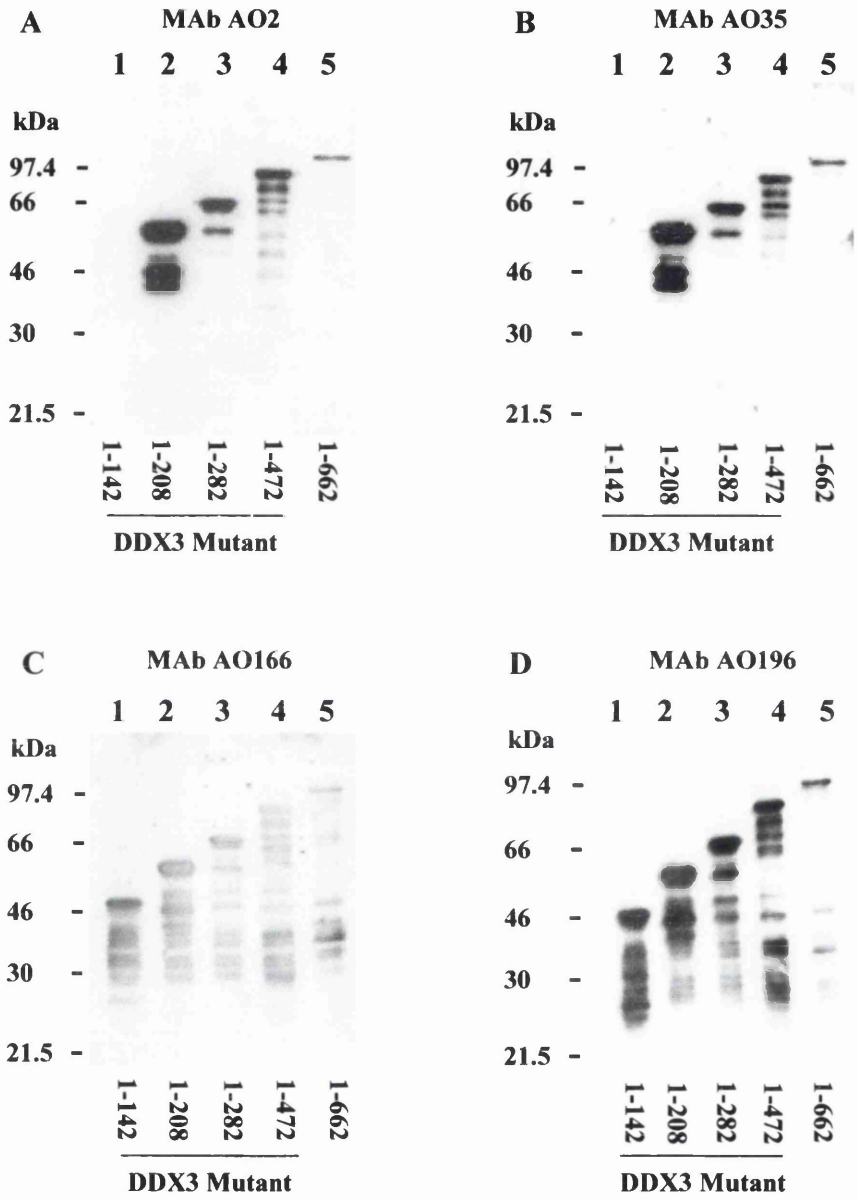

Figure 41: Reactivity of anti-DDX3 MAbs with GST-DDX3 N-terminal mutants and full-length (1-662) GST-DDX3 as a control. 5 μg purified protein was fractionated by SDS-PAGE (8%) and immunoblotted with anti-DDX3 MAbs AO2 (A), AO35 (B), AO166 (C), or AO196 (D).

3.2. 18 Reactivity of Anti-DDX3 MAbs and PAbs to Endogenous DDX3 in Hepatocyte Cell Extracts

Although all of the anti-DDX3 MAbs excluding AO194 and AO199 specifically bound bacterially-produced full-length DDX3 expressed as a GST-fusion protein, it was important for future studies of DDX3 to verify that these antibodies could recognise the endogenous DDX3 expressed within mammalian cells. To this end, 50 μg Huh-7 (N) total cell extract was fractionated on a preparative SDS-PAGE gel, blotted to ECL membranes, and probed with each anti-DDX3 MAb or PAb in parallel by Western blotting. Both R438 and R648 PAbs recognised endogenous DDX3 expressed in Huh-7 (N) cell extracts (Fig. 42; lanes 9 and 19, respectively). Binding of AO34 to hepatocyte cell extracts was not shown due to the very strong binding to numerous protein bands with a range of molecular weights, suggesting that the protein was non-specifically reacting with several proteins. Surprisingly, only two of the remaining MAbs (AO166 and AO196) recognised a distinct band corresponding to full-length DDX3 in cell extracts from this cell line (Fig. 42, lanes 12 and 16). As shown previously (Fig. 26; section 3.2.3), anti-DDX3 MAb AO196 detected a doublet in Huh-7 (N) cell extracts at the expected molecular weight of approximately 73 kDa (Fig. 42, lane 16) - the larger of the two isoforms of DDX3 is in greater abundance in this Western blot. AO166 also recognised the doublet at approximately 73 kDa (lane 12). In addition, this antibody detected a further protein of molecular weight 46 kDa. MAbs AO2 and AO35 exclusively bound what is apparently the same 46 kDa protein (lanes 1 and 4, respectively). Binding to proteins in the range of 70-80 kDa was not seen with these antibodies. It is possible this protein represents a truncated form of DDX3. Interestingly, AO166 has a different epitope to both AO2 and AO35, but still apparently recognises the 46 kDa protein. Nevertheless, it appears that while the majority of the panel of MAbs recognise DDX3 expressed as a GST-fusion protein (the antigen used to generate the antibodies) and not GST alone, all but two of the antibodies do not recognise endogenous full-length DDX3 expressed in a hepatocyte cell line. In summary, these data show that only two anti-DDX3 MAbs, in addition to the PAbs, are able to specifically detect the endogenously-expressed DDX3 protein, in addition to DDX3 as a bacterially-expressed fusion protein in both Western blotting and

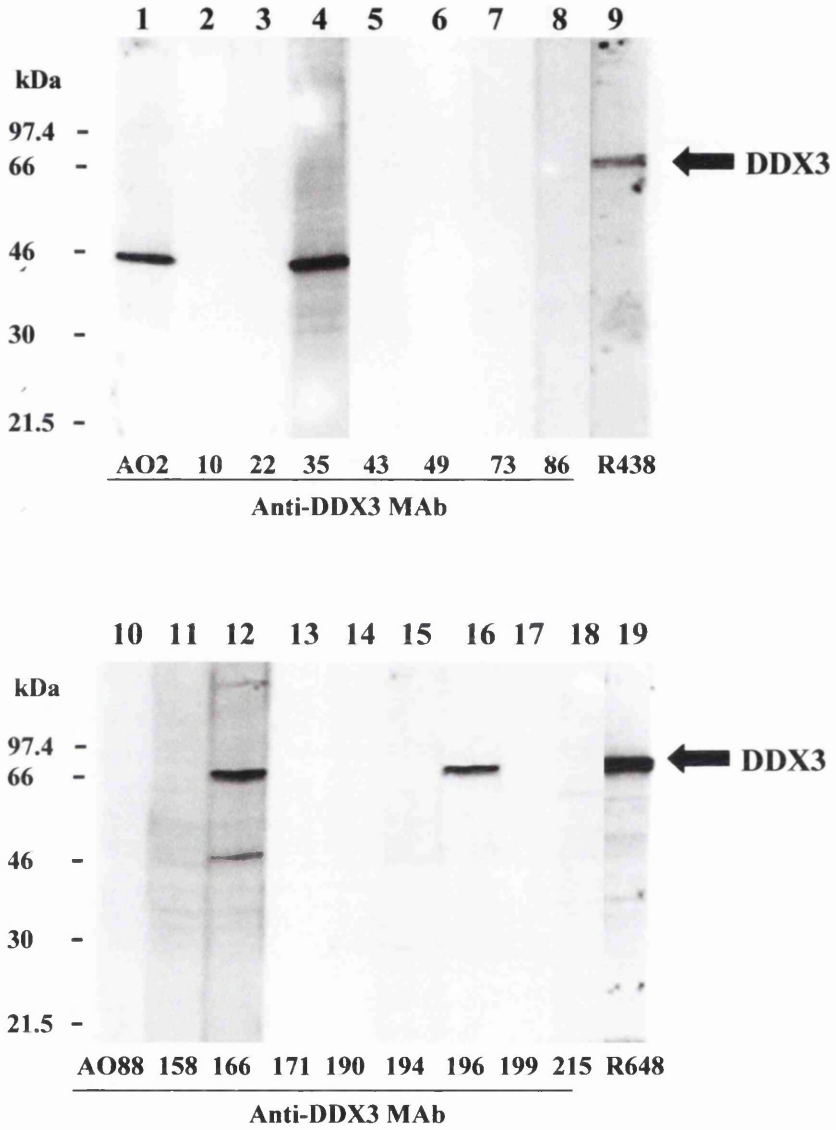

Figure 42: Reactivity of anti-DDX3 MAbs and PAbs to endogenous DDX3 in Huh-7 (N) cell extracts by Western blotting. 50 μg total cell protein extract was fractionated on each preparative SDS-PAGE gel (8%) and transferred to ECL membranes. The membranes were cut into strips and each one probed with a separate anti-DDX3 MAb (lanes 1-8 and 10-18) or PAb (lanes 9 and 19).

immunofluorescence. These antibodies are also capable of immunoprecipitating DDX3 from hepatocytes (Owsianka and Patel, unpublished).

3. 3 Discussion

An investigation presented here into the expression of DDX3 mRNA and protein suggests it is a highly conserved and ubiquitous cellular factor, possibly indicating its involvement in essential processes within the cell. A DDX3-specific probe (derived from a region of DDX3 that codes for the variable N-terminus of the protein in order to detect the mRNA transcript encoding DDX3 only, rather than every mRNA coding for the central conserved domain), was used in Northern blot analyses. DDX3 mRNA was detected in total extracted RNA from a range of mammalian cell lines and in poly(A)$^+$ RNA from many diverse human tissues. Similarly, an anti-DDX3 MAb directed against the extreme N-terminal 1-142 aa of the protein was able to specifically detect a protein at the expected molecular weight in all mammalian cell lines tested by Western blotting. The same antibody detected a diffuse staining of the cytoplasm in the same range of mammalian cell lines by indirect immunofluorescence. If the above data are taken as suggestive of a protein that is indispensable for normal cellular function, this could explain why generation of DDX3 anti-sense cell lines was not possible. The apparently lethal effect of removing DDX3 from the cellular context is consistent with the requirement of the yeast homologue of DDX3 (Ded1p) in an essential cellular process, as determined by genetic knockout assays (section 1.13.6; Chuang *et al.*, 1997).

Endogenous DDX3 was shown to co-localise with core protein expressed in the context of the other HCV structural proteins in hepatocytes, consistent with previous studies in this cell type or other mammalian cell lines with over-expressed DDX3 (Mamiya and Worman, 1999; You *et al.*, 1999b), or endogenous DDX3 detected by specific PAbs in HeLa cells (Owsianka and Patel, 1999). The same co-localisation was seen in the HCV sub-genomic replicon expressing cell line H9-13, providing the first evidence that the interaction between the two proteins occurs in an experimental situation that is as close to natural infection as possible in the absence of an efficient cell culture system for HCV. However, the exact domain of DDX3

which interacts with core protein remains elusive. While an 'RS-like' region at the C-terminus of the protein could specifically pull-down *in vitro*-translated core protein, the full-length protein lacking this domain also bound core protein. This suggests that although core protein can bind the RS domain of DDX3 (or *vice versa*), it is not the only domain essential for such binding. It is possible that the DDX3 'RS'-like domain may be involved in protein-protein interactions within the cell, but with regard to its interaction with core protein the RS domain is not absolutely required; other region(s) of DDX3 may also be involved.

MAbs and PAbs raised against full-length or truncated DDX3 expressed as a GST-fusion proteins were characterised here in terms of their epitopes on DDX3. The majority of antibodies bound the bacterially-expressed full-length protein, and their epitopes were mapped further using truncated forms of DDX3, again expressed as GST-fusion proteins. However, only two anti-DDX3 MAbs (AO166 and AO196), in addition to both PAbs (R438 and R648), were capable of recognising cellular DDX3 in hepatocyte cell extracts (Fig. 42; section 3.2.18). It is unlikely that the reason for this is due to the presence of DDX3 as part of a cellular complex or due to conformational anomalies that would conceal potential epitopes, since these complexes and any folding should be disrupted by the denaturing conditions of SDS-PAGE. It is therefore possible that DDX3 undergoes extensive post-translational modifications in mammalian cells, which may obscure potential epitopes that are available in bacterially-expressed DDX3. Indeed, analysis of the protein sequence indicates DDX3 possesses two N-linked glycosylation sites within the 409-473 region of DDX3 (see Appendix IV), an epitope on bacterially-expressed DDX3 bound by many of the MAbs (see Appendix I, Fig. 88). Numerous casein kinase II and protein kinase C phosphorylation sites are also predicted in this region (data not shown). The importance of a putative truncated form of DDX3 detected by three anti-DDX3 MAbs in hepatocyte cell extracts is unclear at this stage, although since neither of the anti-DDX3 PAbs are able to detect this form it may well be that this is a distinct cellular factor. Indeed, the archetypal and most-studied DEAD-box RNA helicase eIF4A (Linder *et al.*, 1989; Rogers *et al.*, 2001), which shares homology with a small portion of the epitope of both AO2 and AO35 (see Appendix

IV, Fig. 88), also has a molecular weight of approximately 46 kDa (Lorsch and Herschlag, 1998).

Having established that i) DDX3 is a highly conserved and ubiquitous cellular protein and ii) it interacts with core protein in a currently available assay mimicking an HCV cell culture system, further investigation of DDX3 is now required to determine its normal cellular function, and any modulation of this function by core protein.

CHAPTER FOUR:

Subcellular Localisation and Biochemical Properties of DDX3

4. 1 Introduction

An detailed understanding of the localisation of DDX3 within human hepatocytes is critical in establishing the normal cellular function of DDX3, and in determining the significance of its interaction with HCV core protein. To achieve this, the full panel of MAbs raised against DDX3, characterised previously by Western blotting, were tested for their ability to recognise the endogenous protein in a hepatocyte cell line by indirect confocal immunofluorescence microscopy. These studies were also performed in the presence of the HCV structural proteins (supplied by rVV-C-E1-E2) to assess the effect of core protein on the localisation of cellular DDX3 as detected by these antibodies. The subcellular localisation of a putative truncated form of DDX3, detected in hepatocyte total cell extracts by Western blotting with anti-DDX3 MAbs AO2 and AO35 (Fig. 42; section 3.2.18), was also investigated. To gain further insight into DDX3 and its normal cellular function, the full-length protein and a homologous protein from a different organism (*Xenopus laevis* An3; section 1.13.4) as a control were expressed from a plasmid construct transfected into the Huh-7 (N) cell line. As valuable tools to determine the role of specific domains in localisation of DDX3, mutated or truncated forms of this protein were similarly expressed (by generation of the appropriate plasmid constructs followed by transfection into hepatocytes) and investigated in detail. One such mutant lacking a leucine-rich putative nuclear export signal (NES), identified in DDX3 following reports of a functional NES in *X. laevis* An3 (Askjaer *et al.*, 1999), was investigated. Subcellular fractionation of mammalian cell lines into cytoplasmic and nuclear extracts was also carried out to investigate this potentially important aspect of DDX3 by Western blotting with anti-DDX3 MAbs. The localisation in cells of DDX3 carrying a mutation within the DEAD-box (section 1.10.6), a protein which shows a markedly diminished ability to hydrolyse ATP relative to the wild-type DDX3 (P. Askjaer and J. Kjems, personal communication), is also studied here. The ability of all the plasmid-expressed DDX3 proteins to interact with core protein expressed by rVV-C-E1-E2 in hepatocytes was tested to gain further insight into the DDX3/core interaction.

The biochemical properties of bacterially-expressed DDX3 are also investigated here. RNA helicases, and indeed all helicases, are believed to utilise the energy derived from the hydrolysis of ATP or other nucleotides to drive mechanical movement of bound nucleic acid (section 1.10.1). To investigate hydrolysis of nucleotides by purified GST-DDX3, the protein was incubated with radiolabelled dATP and breakdown products separated by thin-layer chromatography. To investigate helicase activity, GST-DDX3 was incubated with a radiolabelled non-specific double-stranded (ds) RNA substrate produced by *in vitro* transcription. The dsRNA and any unwound single-stranded (ss) RNA species were separated by PAGE. As an appropriate positive control in the dATPase and helicase enzymatic assays described above, the helicase domain of the HCV NS3 protein (section 1.2.5.2) was cloned and expressed as a GST-fusion protein.

4. 2 Results

4.2. 1 Further Investigation into Subcellular Localisation of Endogenous DDX3 by Indirect Confocal Immunofluorescence Microscopy

While initial studies indicated that all the anti-DDX3 MAbs and PAbs recognised DDX3 expressed as a GST-fusion protein (Fig. 36a; section 3.2.13), apparently only two MAbs (AO166 and AO196) from a panel of 18 such antibodies, in addition to both PAbs, detected full-length cellular DDX3 in human hepatocyte cell extracts by Western blotting (Fig. 42; section 3.2.18). Indeed, AO196 appeared to be the only anti-DDX3 MAb that detected a single band at the expected molecular weight of full-length DDX3 in hepatocytes cell extracts. Immunofluorescence studies of DDX3 detected by anti-DDX3 MAb AO196 in mammalian cells suggested a diffuse localisation within the cytoplasm, with some punctate staining (Figs 27 and 29; sections 3.2.4 and 3.2.6). This immunofluorescence assay allowed detection of DDX3 in its native conformation, as opposed to a denatured form by Western immunoblotting, and is expanded here to include the entire panel of anti-DDX3 antibodies. The antibodies were tested in parallel with MAb AO196 for their ability to recognise endogenous DDX3 in the Huh-7 (N) cell line. As controls, antibodies raised against the cytoplasmically localised β-subunit of tubulin and the nuclear-

targeted splicing factor SC-35 were used (see Appendix I). Huh-7 (N) cells were seeded on coverslips with the aim to reach 70-80% confluency following 16 hours at 37°C. Cells were then fixed, permeabilised and probed with the appropriate antibody as described previously (section 2.44). As expected, tubulin localised exclusively in the cytoplasm, either in intricate networks or in the vicinity of the cell membrane (Fig. 43a) representing part of the cellular cytoskeletal system (Alberts *et al.*, 1994). On the other hand, SC-35 was abundant in nuclear speckles (Fig. 43b), consistent with previous reports (Spector, 1996). Detection of SC-35 with this specific MAb confirms that the method of fixation and permeabilisation allows access of antibody to the nuclear compartment. In addition, appropriate binding by both anti-β-tubulin and anti-SC-35 antibodies verified that the methods used for sample preparation and detection were suitable for this study. However, consistent with the Western blotting data, where the full panel of anti-DDX3 antibodies was tested against the cellular form of the protein in the same hepatocyte cell line (Fig. 42; section 3.2.18), only 2 of the MAbs (AO166, in addition to the positive control AO196) detected a cellular protein in the Huh-7 (N) cell line which was likely to be DDX3. Both antibodies exhibited a diffuse cytoplasmic staining (Fig. 44). Although AO166 detected a protein with weak affinity at 46 kDa in Western blots of hepatocyte cell extracts (Fig. 42; section 3.2.18), this antibody did not appear to have a different pattern of staining of hepatocytes relative to that seen with AO196 (Fig. 44). Potentially, detection of the 46 kDa putative truncated form of DDX3 by AO166 could be masked by the diffuse staining of the cytoplasm corresponding to the full-length DDX3 protein. Indeed, MAbs AO2 and AO35, both of which specifically detected the 46 kDa band with stronger affinity than AO166 in hepatocyte cell extracts (Fig. 42; section 3.2.18), showed a distinct punctate pattern of staining in the cytoplasm of a small proportion of cells (Fig. 45). The fact that so few cells in the population contained this putative truncated form of DDX3 suggests its expression may be cell-cycle related. Interestingly, both AO2 and AO35 MAbs detect the same epitope containing a small portion of the central conserved domain of DDX3 (aa 143-208; Fig. 41a and b), and are the only antibodies within the panel generated that recognise this region. This could indicate that the protein is a related cellular factor, although neither of the two anti-DDX3 PAbs detect this protein in

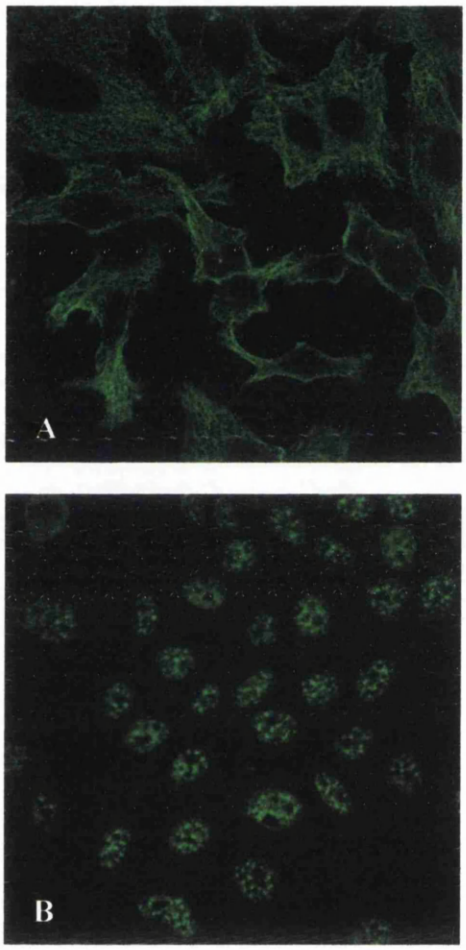

Figure 43: Detection of β-tubulin and SC-35 in hepatocytes by specific MAbs. Huh-7 (N) cells grown on coverslips were fixed and then probed with appropriately diluted primary antibody (panel A: anti-β-tubulin, panel B: anti-SC-35) followed by anti-mouse IgG-FITC conjugated antibody.

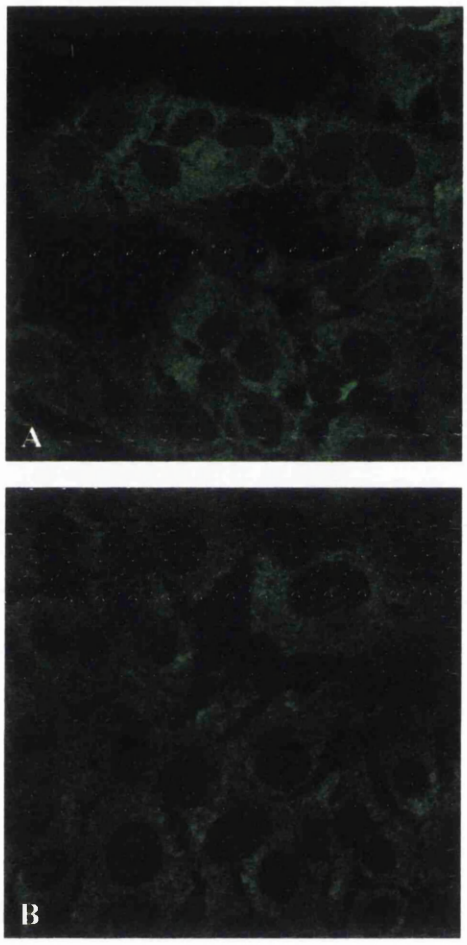

Figure 44: Detection of DDX3 in hepatocytes by MAbs AO166 and AO196. Huh-7 (N) cells grown on coverslips were fixed and then probed with appropriately diluted primary antibody (panel A: AO166, panel B: AO196) followed by anti-mouse IgG-FITC conjugated antibody.

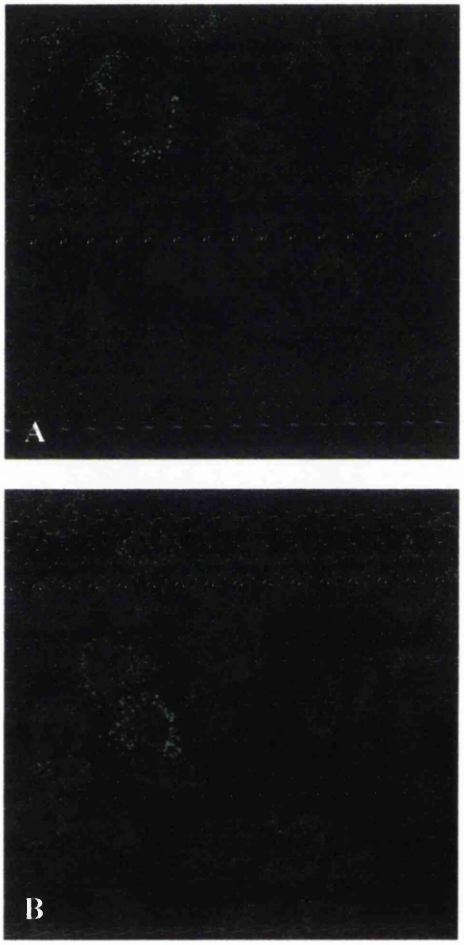

Figure 45: Detection of a putative truncated form of DDX3 in hepatocytes by MAbs AO2 and AO35. Huh-7 (N) cells grown on coverslips were fixed and then probed with appropriately diluted primary antibody (panel A: AO2, panel B: AO35) followed by anti-mouse IgG-FITC conjugated antibody.

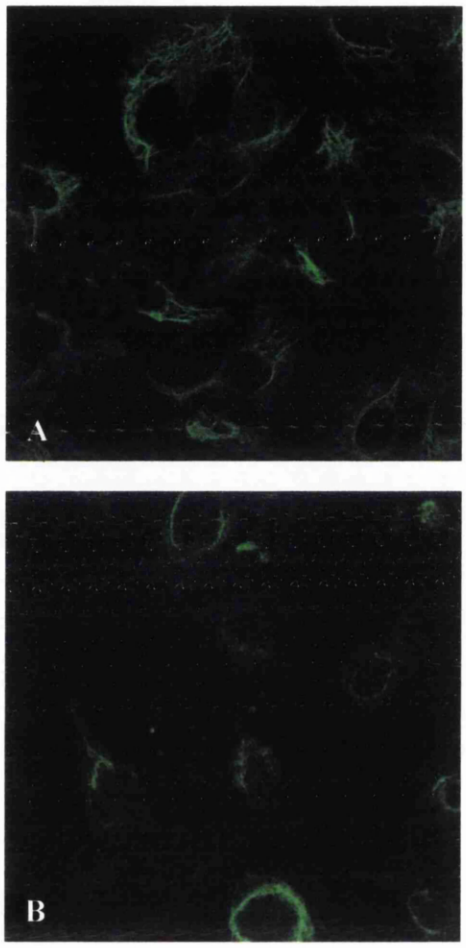

Figure 46: Detection of unknown cellular factors by MAbs AO34 and AO190 in hepatocytes. Huh-7 (N) cells grown on coverslips were fixed and then probed with appropriately diluted primary antibody (panel A: AO34, panel B: AO190) followed by anti-mouse IgG-FITC conjugated antibody.

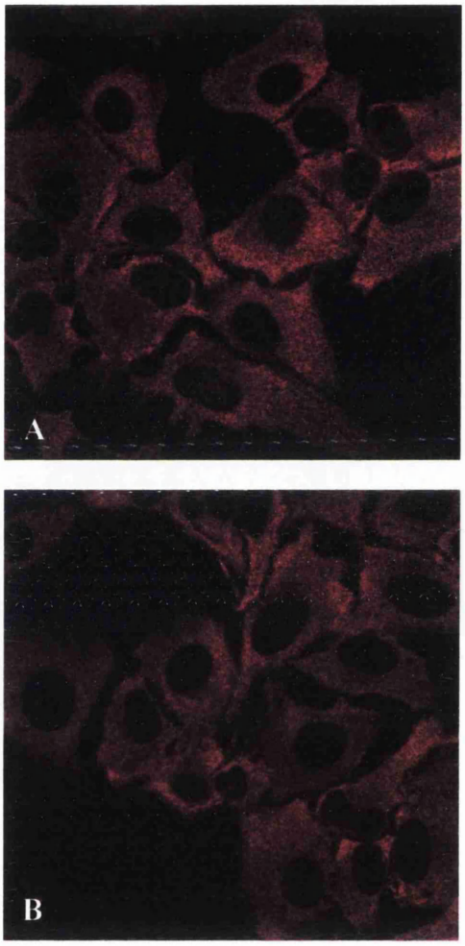

Figure 47: Detection of DDX3 in hepatocytes by specific PAbs R438 and R648. Huh-7 (N) cells grown on coverslips were fixed and then probed with appropriately diluted primary antibodies (panel A: R438, panel B: R648) followed by anti-rabbit IgG-Cy5 conjugated antibody.

hepatocyte cell extracts (Fig. 42; section 3.2.18). As shown in Fig. 46a, AO34 showed staining for protein(s) that were unlikely to be DDX3, due to the pattern of staining which suggested an association of the cellular factor detected with the cytoskeletal network. Moreover, this antibody previously showed strong affinity for many proteins with a wide range of molecular weights in Huh-7 (N) extracts (section 3.2.18). AO190 appeared to recognise a protein which may or may not be DDX3 that was located in varying amounts within the perinuclear cytoplasm, tightly associated with the nucleus (Fig 46b). This antibody bound full-length DDX3 expressed as a GST-fusion protein, but was the only MAb not to bind any of fusion protein breakdown products (Fig. 36a; section 3.2.13). AO190 was also unique in its ability to bind to the DDX3 epitope aa 474-552 (Fig. 39; section 3.2.15). However, this MAb did not detect DDX3 in hepatocyte cell extracts by Western blotting (Fig. 42; section 3.2.18). The pattern of staining of the Huh-7 (N) cell line by anti-DDX3 PAbs R438 and R648 (Fig. 47) is similar to that of anti-DDX3 MAbs AO166 and AO196 (Fig. 44). Since only these four antibodies/antisera detect a protein corresponding to full-length DDX3 in Huh-7 (N) cell extracts (Fig. 42; section 3.2.18), these data add weight to the theory that only these antibodies are able to detect cellular DDX3 in its full-length form.

4.2. 2 Further Investigation of DDX3 Co-localising with Core Protein

Previously, it was shown that the anti-DDX3 MAb AO196 could detect DDX3 co-localising with core protein in cells infected with rVV-C-E1-E2 (Fig. 29; section 3.2.6). The ability of the remaining MAbs to detect cellular DDX3 co-localising with core protein detected by anti-core PAb R525 (see Appendix I) in hepatocytes by indirect confocal immunofluorescence microscopy was investigated in parallel with MAb AO196. Anti-DDX3 PAbs R438 and R648 have previously been shown to detect DDX3 co-localising with core protein (Owsianka and Patel, 1999; unpublished). MAbs specific for cellular β-tubulin and SC-35 (see above) were used in conjunction with the anti-core PAb to probe Huh-7 (N) cells to confirm the specificity of anti-DDX3 MAbs for DDX3 bound to core protein, and determine any gross cellular changes induced by infection with vaccinia virus. Both proteins retained their original locations in the presence of core protein and the HCV

glycoproteins (Figs 48a and b), although changes in localisation of β-tubulin, possibly attributable to infection with vaccinia virus, were seen. In contrast, MAbs AO166 and the positive control AO196 were able to detect DDX3 co-localising with core protein (Figs 48c and d, respectively). The cellular factor bound by MAbs AO2 and AO35 (Figs 48e and 48f, respectively), likely to be the same 46 kDa protein as determined by Western blotting using Huh-7 (N) total cell extracts, did not appear to re-localise in the presence of core protein and/or vaccinia virus. This is perhaps unsurprising, given that this protein could potentially be a truncated form of DDX3 that lacks the core protein-interacting domain. However, it is possible that staining for core protein masked detection of this protein by MAbs AO2 and AO35. Proteins detected by AO34 and AO190 did not alter localisation in the presence of core protein (Figs 48g and 48h, respectively), even although AO190 detected a protein in a similar subcellular domain as core protein (Fig. 46b; section 4.2.1).

4.2. 3 Comparative Analysis of Protein Expression in Huh-7 (N) and H9-13 Cell Lines

Relative to its localisation in the Huh-7 (N) cell line, DDX3 detected by MAb AO196 does not appear to re-localise in the HCV sub-genomic replicon-expressing cell line H9-13 (Fig. 32; section 3.2.8). The remaining MAbs were tested in parallel with AO196 for their reactivities in H9-13 cells to verify this original result, since DDX3 is an RNA-binding protein (P. Askjaer, personal communication), and may alter localisation in the presence of large amounts of HCV RNA. Consistent with the AO196 binding data, DDX3 detected by AO166 did not re-localise in H9-13 cells (data not shown). However, whereas AO2 and AO35 detect a very distinct punctate staining in a small proportion of the population of Huh-7 (N) cells (Fig. 45; section 4.2.1), both antibodies detected the same pattern of staining in the majority of H9-13 cells. The data for AO2 only is presented in Fig. 49. This suggests expression of this protein is upregulated or switched-on in the presence of the HCV replicon RNA and/or HCV nonstructural proteins. The apparent ubiquitous expression of the 46 kDa protein in H9-13 but not Huh-7 (N) cells could also be attributable to a clonal effect. In other words, a cell expressing the protein that allowed replication of the HCV sub-genomic replicon RNA gave rise to the H9-13

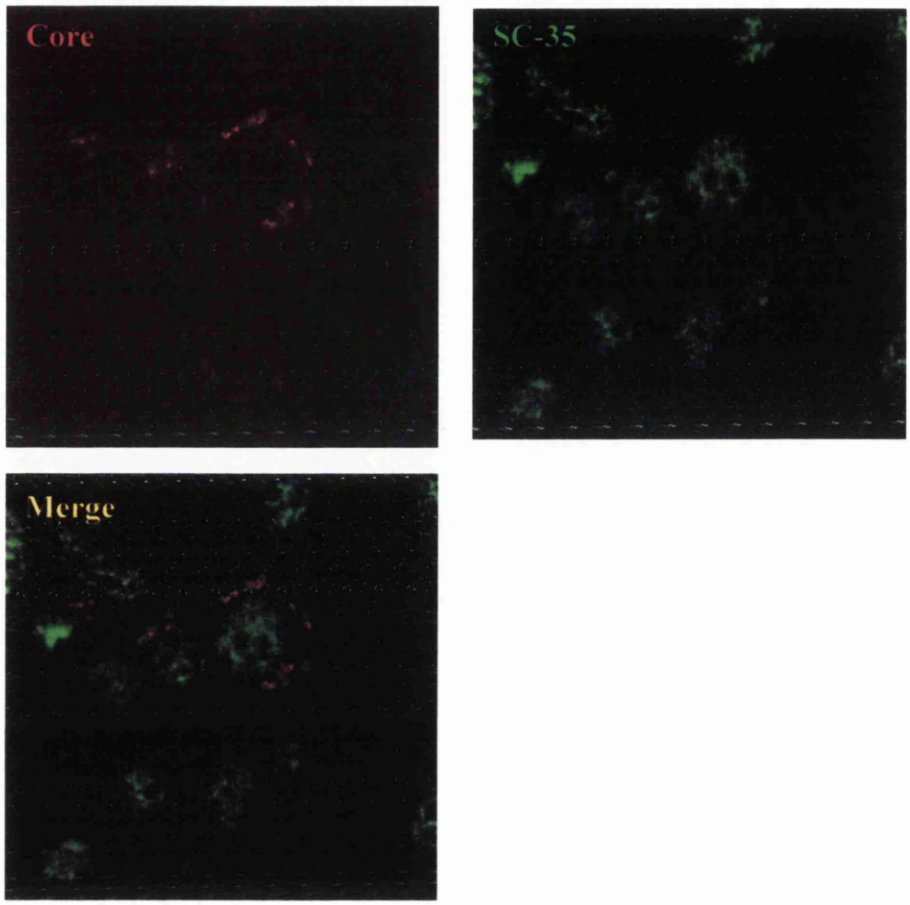

Figure 48a: Localisation of SC-35 in the presence of HCV structural proteins in hepatocytes. Huh-7 (N) cells grown on coverslips were infected at m.o.i. of 0.5 with rVV-C-E1-E2, fixed, and then probed with anti-SC-35 MAb/anti-core PAb R525 in combination followed by anti-mouse IgG-FITC/anti-rabbit IgG-Cy5 conjugated antibodies.

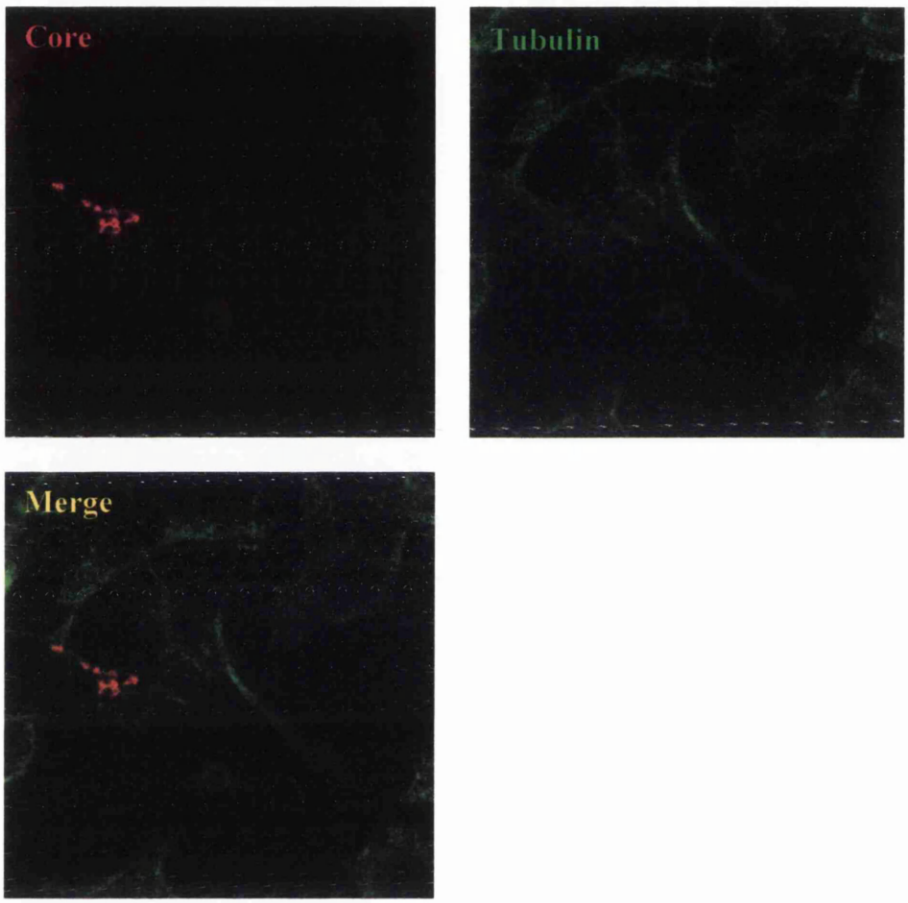

Figure 48b: Localisation of β-tubulin in the presence of HCV structural proteins in hepatocytes. Huh-7 (N) cells grown on coverslips were infected at m.o.i. of 0.5 with rVV-C-E1-E2, fixed, and then probed with anti-β-tubulin/anti-core PAb R525 followed by anti-mouse IgG-FITC and anti-rabbit IgG-Cy5 conjugated antibodies.

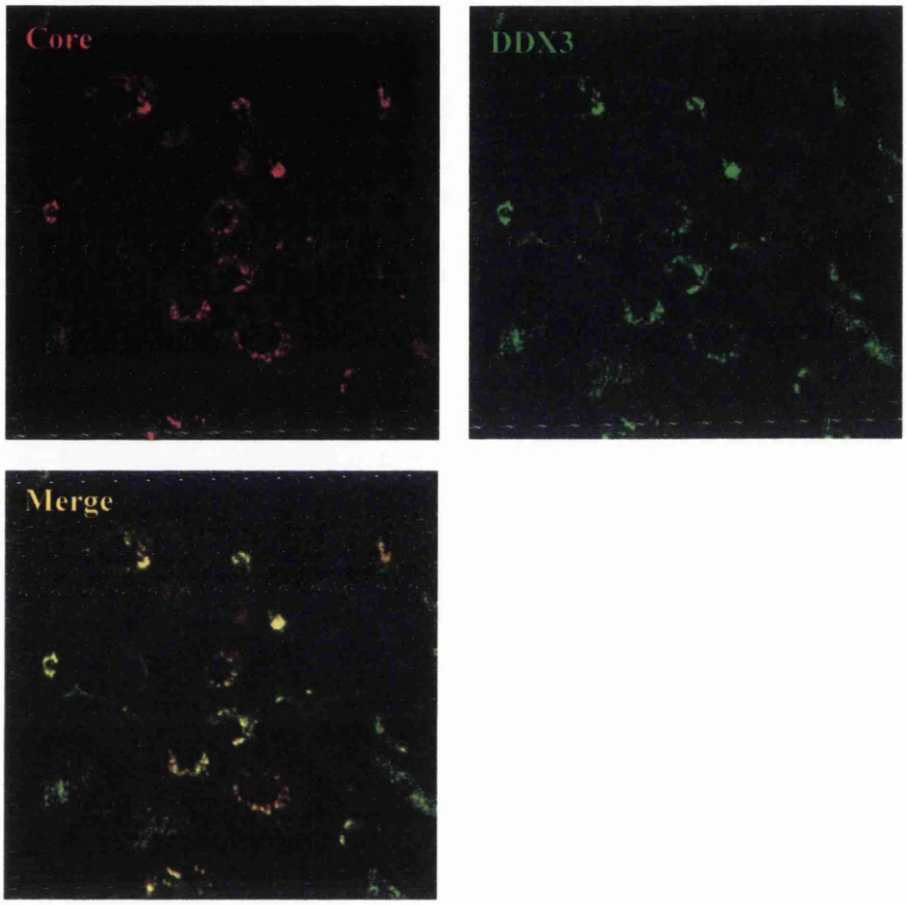

Figure 48c: Localisation of DDX3 in the presence of HCV structural proteins by MAb AO166 in hepatocytes. Huh-7 (N) cells were infected at m.o.i. of 0.5 with rVV-C-E1-E2, fixed, and then probed with appropriately diluted AO166/anti-core PAb R525 in combination, followed by anti-mouse IgG-FITC and anti-rabbit IgG-Cy5 conjugated antibodies.

.

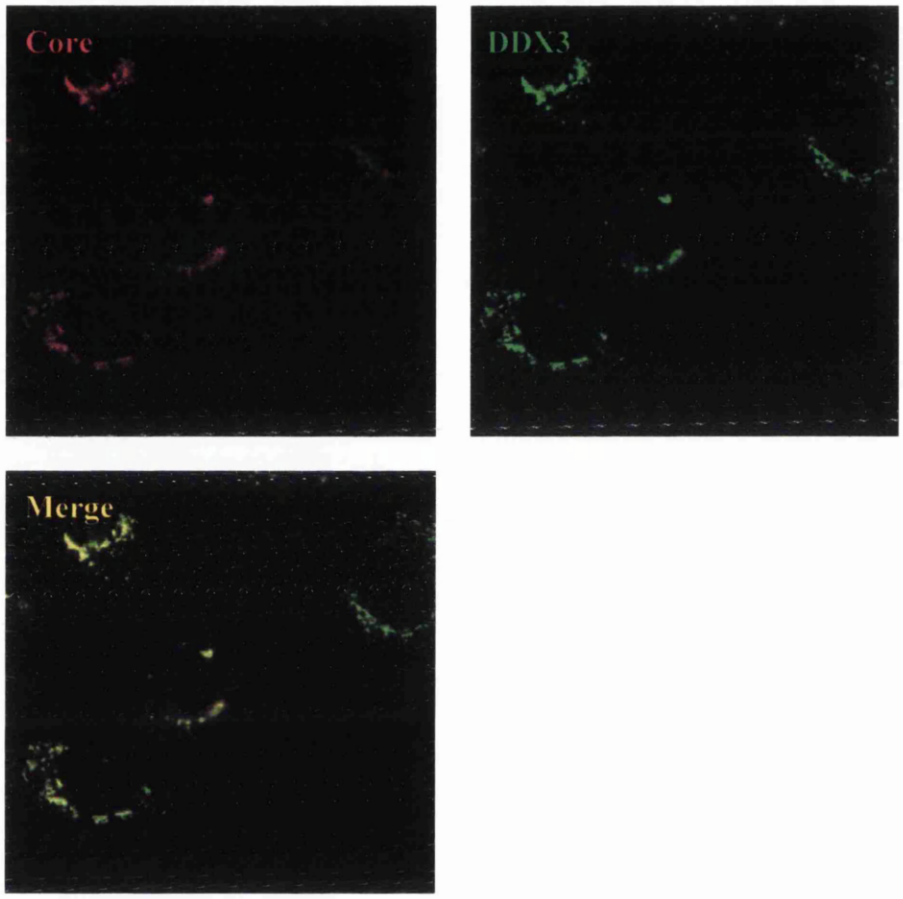

Figure 48d: Localisation of DDX3 in the presence of HCV structural proteins by MAb AO196 in hepatocytes. Huh-7 (N) cells were infected at m.o.i. of 0.5 with rVV-C-E1-E2, fixed, and then probed with appropriately diluted AO196/anti-core PAb R525 in combination, followed by anti-mouse IgG-FITC and anti-rabbit IgG-Cy5 conjugated antibodies.

.

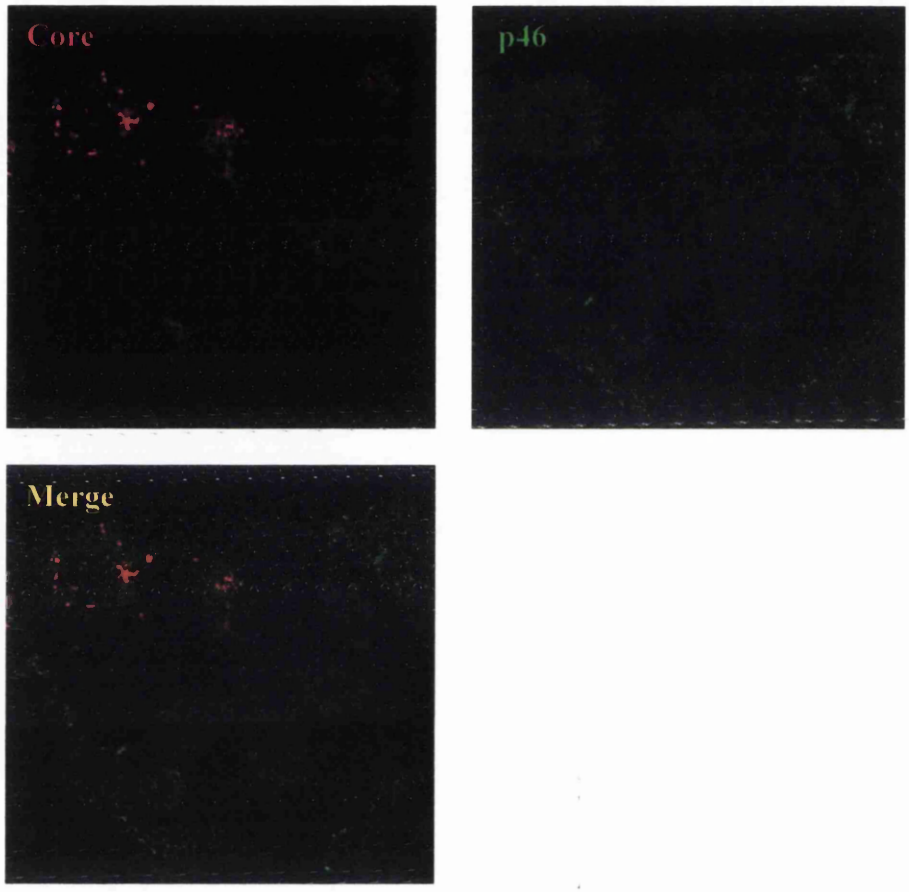

Figure 48e: Localisation of putative truncated form of DDX3 in the presence of HCV structural proteins by MAb AO2. Huh-7 (N) cells were infected at m.o.i. of 0.5 with rVV-C-E1-E2, fixed, and then probed with appropriately diluted AO2/anti-core PAb R525 in combination, followed by anti-mouse IgG-FITC and anti-rabbit IgG-Cy5 conjugated antibodies.

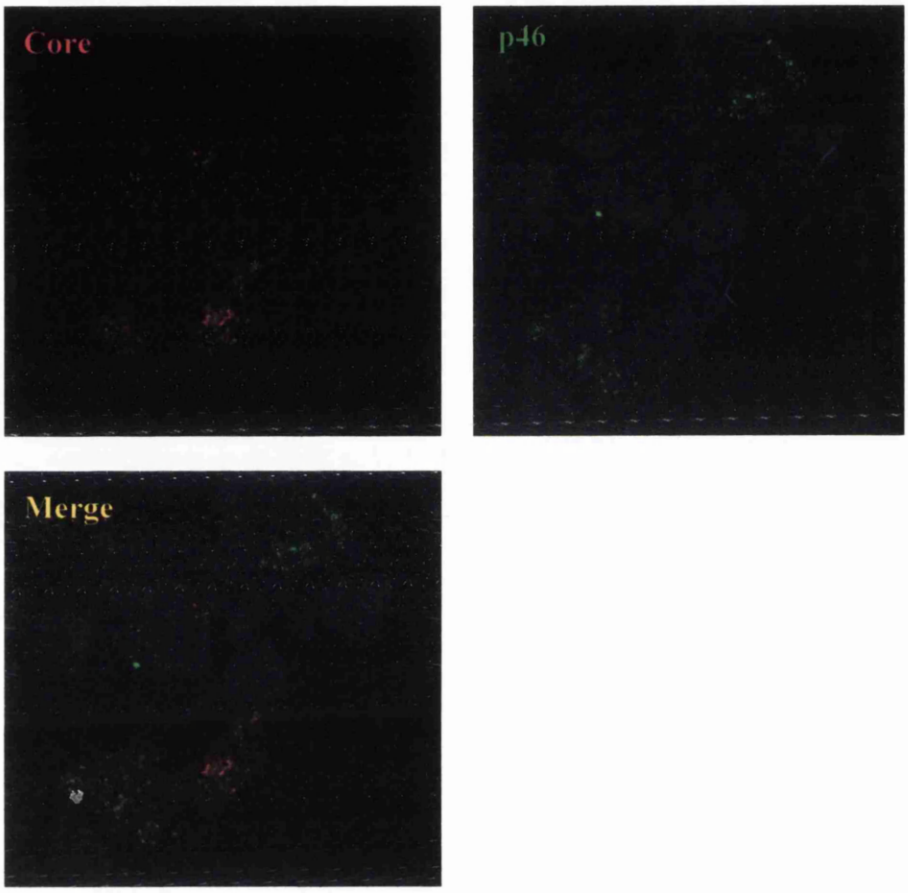

Figure 48f: Localisation of a putative truncated form of DDX3 in the presence of HCV structural proteins by MAb AO35 in hepatocytes. Huh-7 (N) cells were infected at m.o.i. of 0.5 with rVV-C-E1-E2, fixed, and then probed with appropriately diluted AO35/anti-core PAb R525 in combination, followed by anti-mouse IgG-FITC and anti-rabbit IgG-Cy5 conjugated antibodies.

.

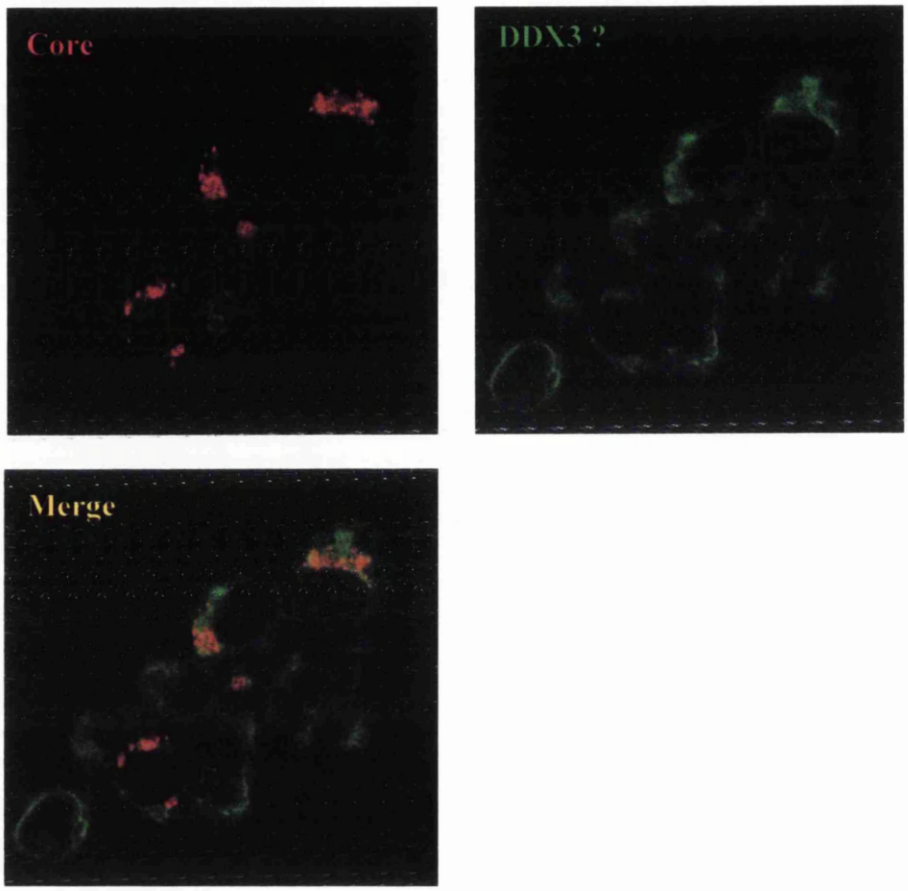

Figure 48g: Localisation of unknown cellular factor(s) in the presence of HCV structural proteins by MAb AO34 in hepatocytes. Huh-7 (N) cells were infected at m.o.i. of 0.5 with rVV-C-E1-E2, fixed, and then probed with appropriately diluted MAb AO34/anti-core PAb R525 in combination, followed by anti-mouse IgG-FITC and anti-rabbit IgG-Cy5 conjugated antibodies.

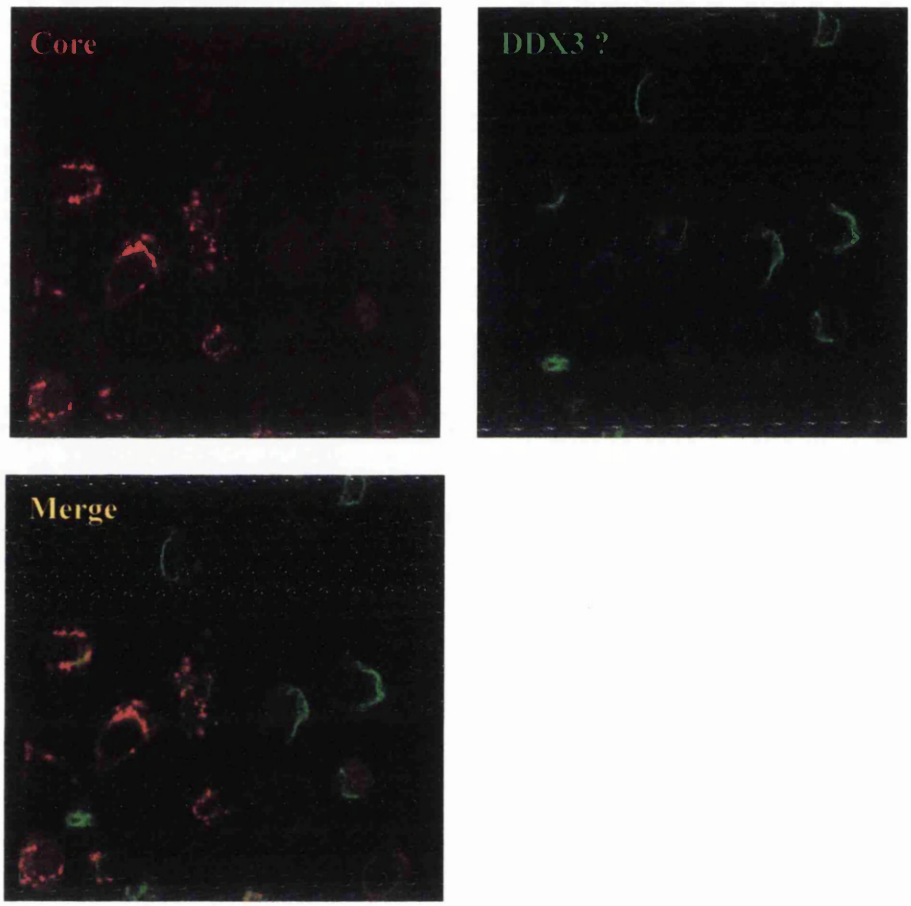

Figure 48h: Localisation of unknown cellular factor(s) in the presence of HCV structural proteins by MAb AO190 in hepatocytes. Huh-7 (N) cells were infected at m.o.i. of 0.5 with rVV-C-E1-E2, fixed, and then probed with appropriately diluted A190/anti-core PAb R525 in combination, followed by anti-mouse IgG-FITC and anti-rabbit IgG-Cy5 conjugated antibodies.

cell line. Expression of this protein may therefore have implications for HCV replication, although its presence may simply be coincidental. Regardless, any upregulation of expression of this protein was not qualitatively detectable by Western blotting - total cell extracts from Huh-7 (N) and H9-13 cells were probed in parallel using AO2 and appeared to show the same level of expression of this 46 kDa protein (Fig. 49c). Consistent with previous immunofluorescence studies in the Huh-7 (N) cell line (section 4.2.1), none of the remaining MAbs recognised proteins in the H9-13 cell line (data not shown).

4.2. 4 Expression of DDX3 and X. laevis *An3 from a Mammalian Expression Construct*

In order to study DDX3 in more detail, particularly with a view to subsequent rational mutagenesis/deletion analysis of DDX3, constructs were generated to allow expression of the protein in mammalian cells (see Appendix II for a full list of DDX3 constructs generated here and in following sections). The pZeoSV2 (+) mammalian expression vector (Fig. 28a; section 3.2.5) was used for expression of DDX3. This vector contains SV40 and bacteriophage T7 RNA polymerase promoter sites allowing high level expression in mammalian cells, particularly when T7 RNA polymerase is supplied *in trans*. Transfections with pZeoSV2 (+) constructs were preceded by mock-infection or infection with rVV expressing T7 RNA polymerase (vTF7.3, see Appendix III; Fuerst *et al.*, 1986) to increase transfection efficiency and expression levels. DDX3 cDNA was sub-cloned from the pGEX-6P-3-DDX3 construct and transferred to the *Bam*HI site downstream from SV40 and T7 promoters in the pZeoSV2 (+) vector (Fig. 28a; section 3.2.5) to produce pDDX3. An oligonucleotide linker was used to insert the seqeunce encoding MRGS(H)^6 immediately preceeding and in frame with the full-length DDX3 cDNA. This histidine-tagged version of DDX3 (p6h-DDX3) was cloned as an appropriate control to differentiate between endogenous DDX3 and DDX3 expressed from the plasmid, and to verify results obtained with anti-DDX3 MAbs or PAbs. As a control in the investigation of the localisation of DDX3 expressed by a plasmid-based vector in the presence of vTF7.3, cDNA encoding the *X. laevis* An3 protein (section 1.13.4), a protein which shares 86% similarity with DDX3, was amplified from

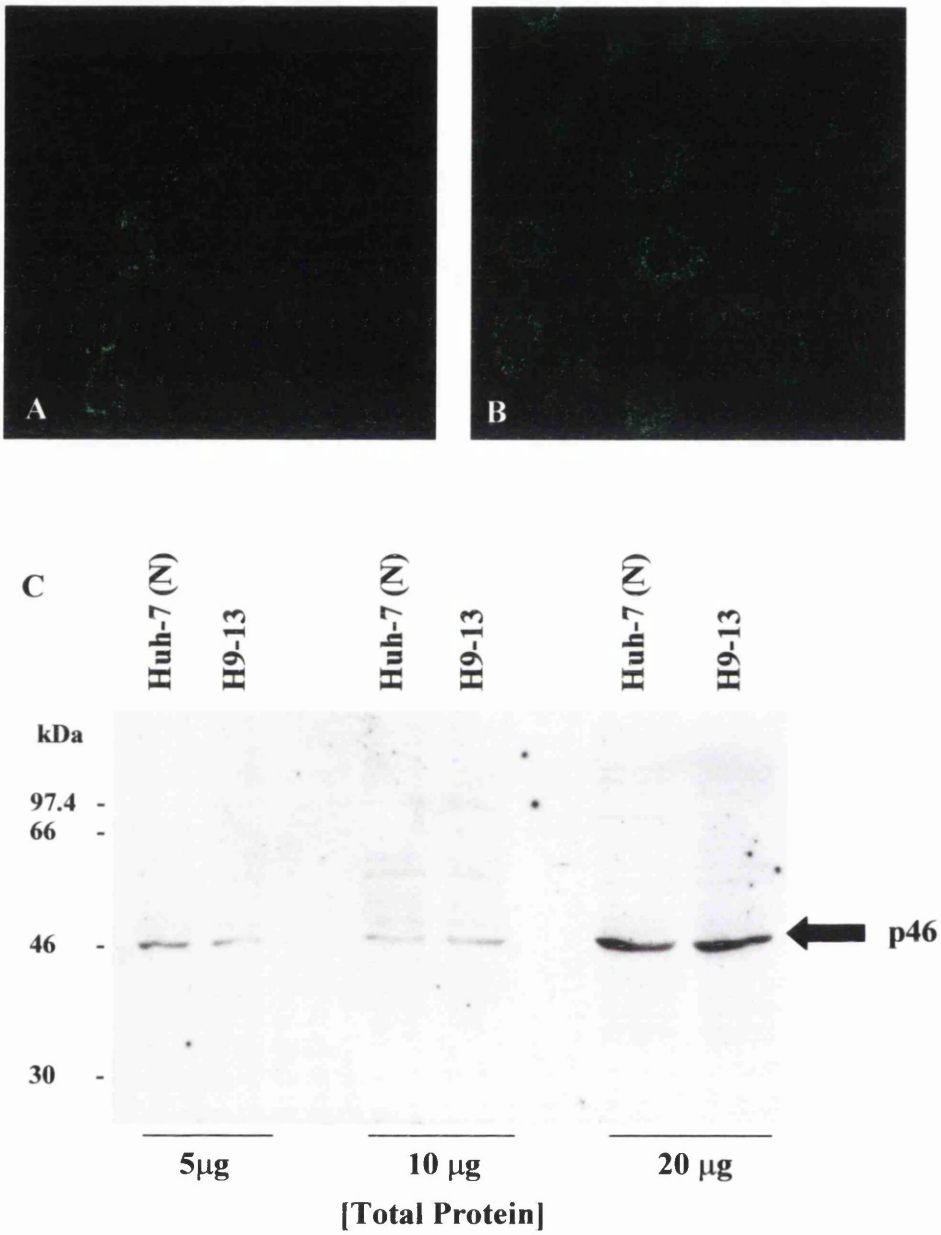

Figure 49: Detection of a putative truncated form of DDX3 or a related cellular factor by MAb AO2 in Huh-7 (N) and H9-13 cells. Confocal images of AO2 reactivity in (A) Huh-7 (N) and (B) H9-13 cell lines. (C) Total cell extracts from Huh-7 (N) and H913 cell lines at the protein concentration shown were fractionated by SDS-PAGE (10%) and immunoblotted with AO2.

pET-21a-An3 (see Appendix II) with and without histidine-tag by PCR using specific primers and transferred to pZeoSV2 (+) to make pAn3 and p6h-An3 constructs. Following sequencing of the new constructs with appropriate primers, recombinant protein expression in transfected cell extracts was confirmed by Western blotting the extracts with anti-DDX3 MAb AO196 (Fig. 50a). DDX3 expressed from construct pDDX3 or p6h-DDX3 had the same molecular weight and was apparently processed in a similar manner to endogenous DDX3 in Huh-7 (N) cells detected by AO196 (Fig. 50a, lanes 1 and 3). In addition, infection of cells with vTF7.3 had no discernible effect on expression of DDX3, and cross-reaction of anti-DDX3 MAb AO196 with vaccinia virus proteins did not occur (lanes 1-3 and 5). Previous results indicated that recombinant An3 expressed in *E. coli* via the pET-21a-An3 construct was sufficiently similar to DDX3 to be detected by both anti-DDX3 MAbs AO166 and AO196 (data not shown). Expression from either pAn3 or p6h-An3 construct gave rise to a product detected by AO196 of the expected molecular weight of 77 kDa (lane 4 and 6), although protein expressed from pAn3 gave an slightly altered banding pattern. Expression from constructs p6h-DDX3 and p6h-An3, each containing a histidine-tag, was confirmed using the RGS-His MAb (QIAGEN) (Fig. 50b, lanes 5 and 6). This antibody recognises the epitope MRGS(H)^6 (section 2.5). Expression from these constructs detected by the RGS-His MAb was similar to expression of endogenous DDX3 and expression of DDX3 or An3 by plasmid lacking the histidine-tag (Fig. 50b).

4.2. 5 Investigation into the Subcellular Localisation of DDX3 and An3 Expressed Via Mammalian Expression Construct by Indirect Confocal Immunofluorescence Microscopy.

Following confirmation that introduction of either DDX3 or An3 (with or without histidine-tag) expression constructs into Huh-7 (N) cells led to production of the appropriate protein, their localisation was studied by indirect confocal immunofluorescence microscopy. Huh-7 (N) cells grown to a confluency of 80-90% on coverslips were infected with vTF7.3 at an m.o.i. of 5 for 1 hour prior to transfection (as described in section 2.35) with the relevant construct (1 μg). The cells were washed, fixed and permeabilised as described in section 2.44. The

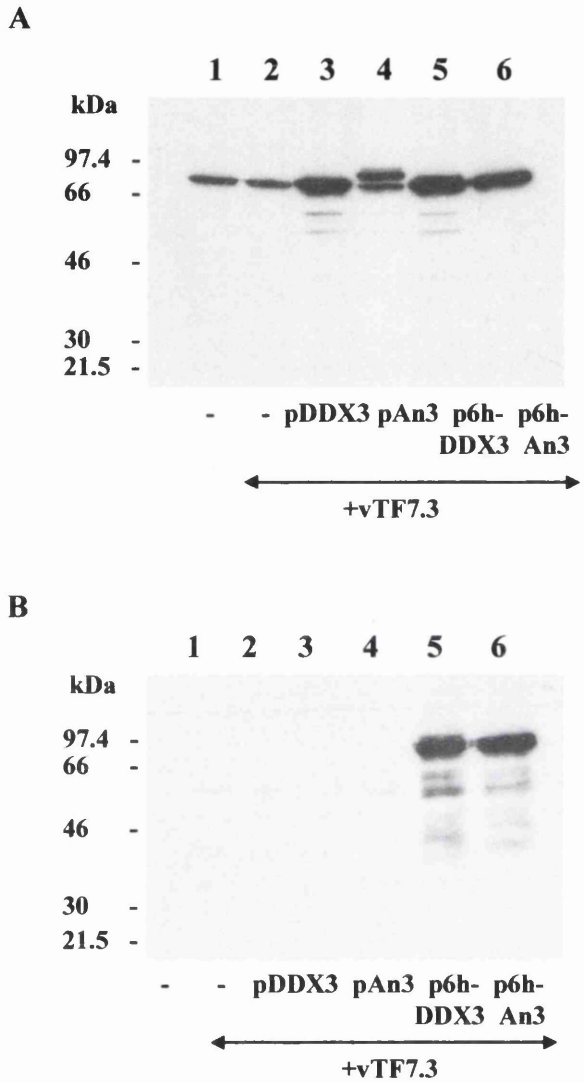

Figure 50: Detection of DDX3, An3 and their histidine-tagged counterparts expressed by plasmid in hepatocytes. Huh-7 (N) cells were either mock-transfected (lanes 1 and 2), or transfected with the constructs as indicated, following mock-infection (lane 1) or infection with vTF7.3 at m.o.i of 5 (lanes 2-6). At 16 hours post-transfection, cells were washed, harvested and 20 μg total protein subjected to SDS-PAGE (8%) followed by Western immunoblotting with (A) anti-DDX3 MAb AO196 or (B) anti-histidine tag MAb RGS-His.

localisation of DDX3 or An3 was determined using either anti-DDX3 MAb AO196, which would be expected to detect recombinant DDX3 or An3 in addition to cellular DDX3, or the RGS-His antibody, which should allow detection of the recombinant 6h-DDX3 or 6h-An3 alone. Consistent with a previous report of punctate cytoplasmic staining for over-expressed DDX3 in Huh-7 cells (You *et al.*, 1999b), DDX3 expressed via mammalian expression construct either with or without histidine-tag detected by MAbs AO196 or RGS-His was consistently found in distinct ring-like structures distributed throughout the cytoplasm together with some diffuse staining of the cytoplasm (Figs 51a and 51c). In contrast, An3 was located in the perinuclear cytoplasm, although ring-like structures similar to those seen with the DDX3 expression construct were present (Figs 50b and 50d). This localisation of An3 is consistent with a role in intracellular shuttling (Askjaer *et al.*, 1999). In both cases, the RGS-His antibody did not detect anything above background levels of cellular auto-fluorescence when the histidine-tag was not present (data not shown). The fact that An3 has a different localisation to its homologue DDX3 expressed from the pZeoSV2 (+) vector suggests it is unlikely that the localisation of DDX3 is an artifact of the expression system used. Furthermore, neither AO196 nor RGS-His antibodies detected extra bands, relative to the expression of endogenous protein detected by AO196, in Western blots when cell extracts from cells infected with vTF7.3 were examined (Fig. 50; section 4.2.4). Most importantly, the localisation of DDX3 expressed by plasmid described here occurred without vTF7.3 infection (Fig. 51e), although expression levels were consistently low.

To test whether plasmid-expressed (exogenous) DDX3 (and An3) interact with HCV core, cells were co-infected with vTF7.3 and rVV-C-E1-E2 (m.o.i = 0.5 each), and transfected with the relevant construct. As expected, 6h-DDX3 detected by the RGS-His antibody co-localised with core protein expressed by rVV-C-E1-E2 (Fig. 52a). Furthermore, 6h-An3 expressed and detected in the same manner also co-localised with core protein (Fig. 52b), presumably due to the high degree of similarity between the proteins. Co-localisation of recombinant An3 with core protein had no discernible effects on the localisation of core.

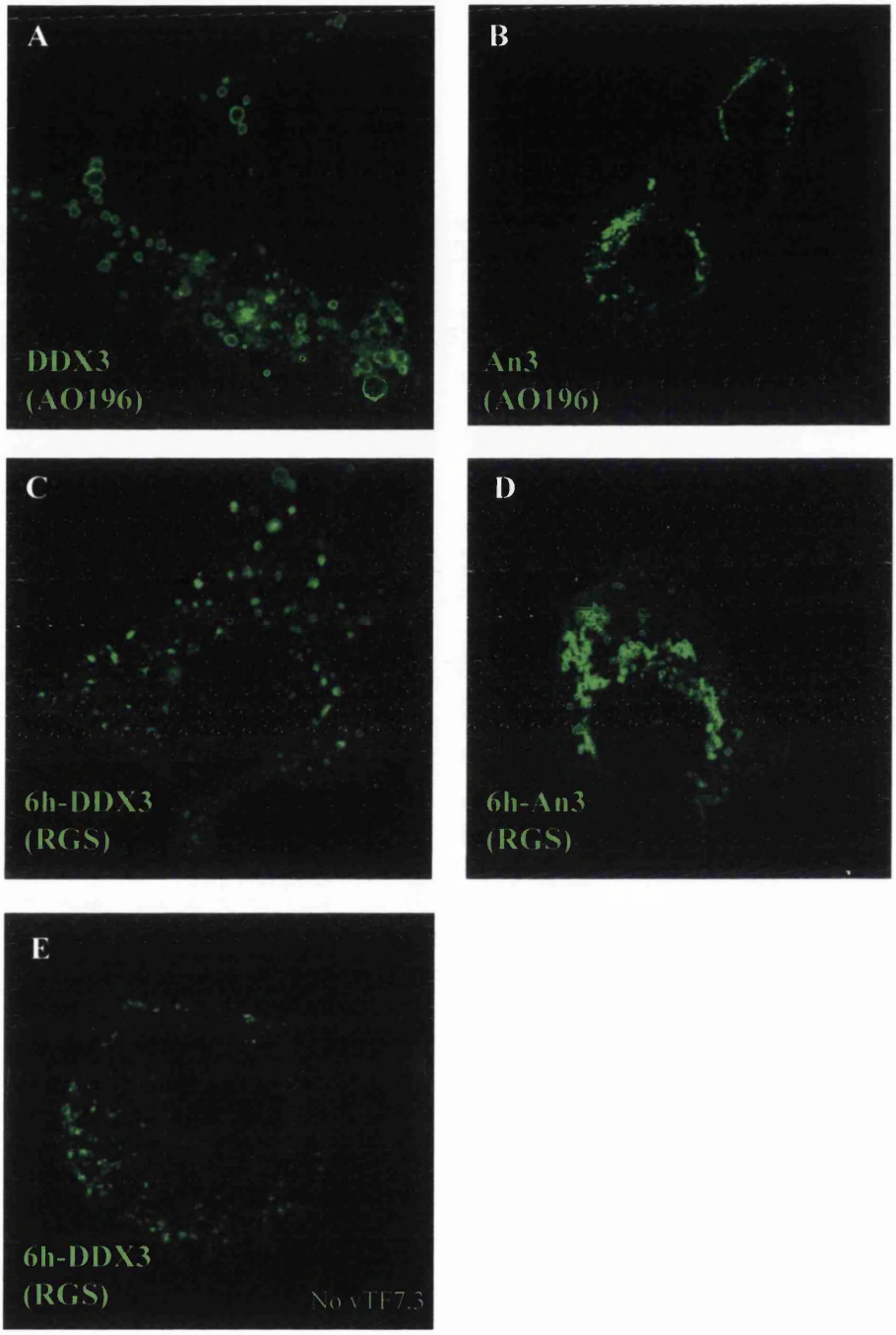

Figure 51: Localisation of DDX3, An3, and their histidine-tagged counterparts expressed by plasmid in hepatocytes. Huh-7 (N) cells on coverslips were mock-infected (E) or infected with vTF7.3 (m.o.i. = 5) (A to D) prior to transfection with the plasmids (1 μg) as shown. The cells were fixed at 16 hours post-transfection and probed with either MAb AO196 or RGS-His as indicated. Bound antibodies were visualised with anti-mouse IgG-FITC conjugated antibody.

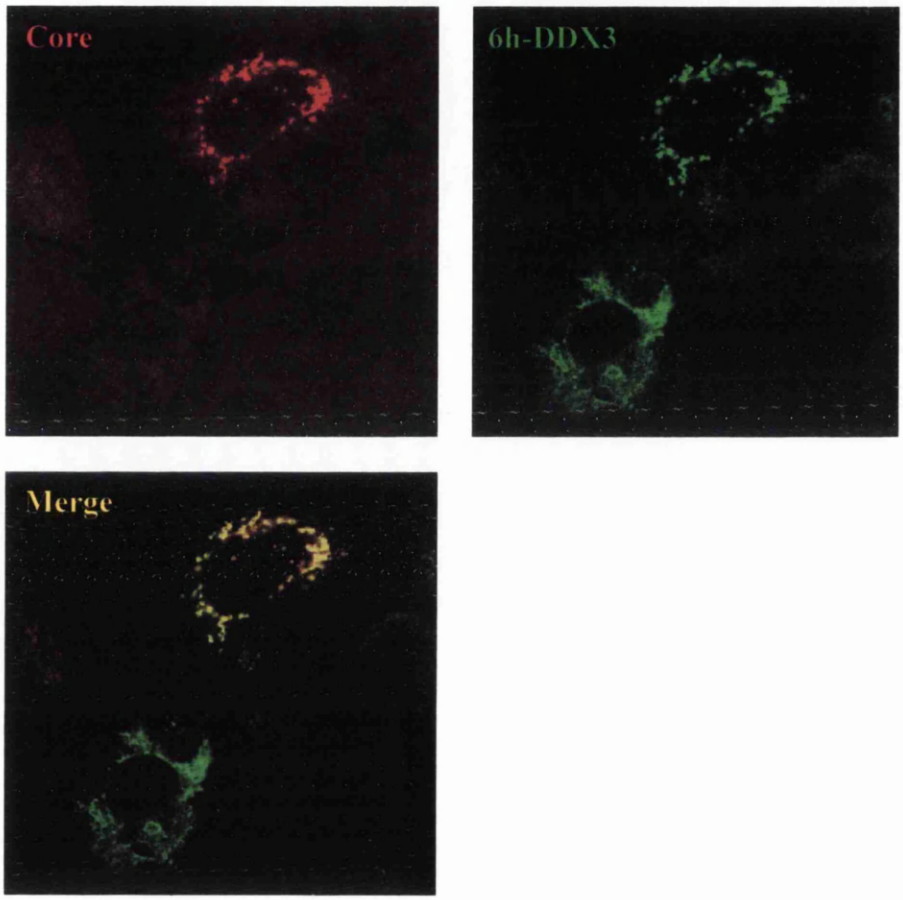

Figure 52a: Co-localisation of histidine-tagged DDX3 expressed by plasmid with core protein. Huh-7 (N) cells were infected with rVV-C-E1-E2 and vTF7.3 (m.o.i. = 0.5 each) for 1 hour and subsequently transfected with p6h-DDX3 construct (1 μg). 16 hours post-transfection, cells were fixed and then probed with appropriately diluted MAb RGS-His/anti-core PAb R525 in combination, followed by anti-mouse IgG-FITC/anti-rabbit IgG-Cy5 conjugated antibodies.

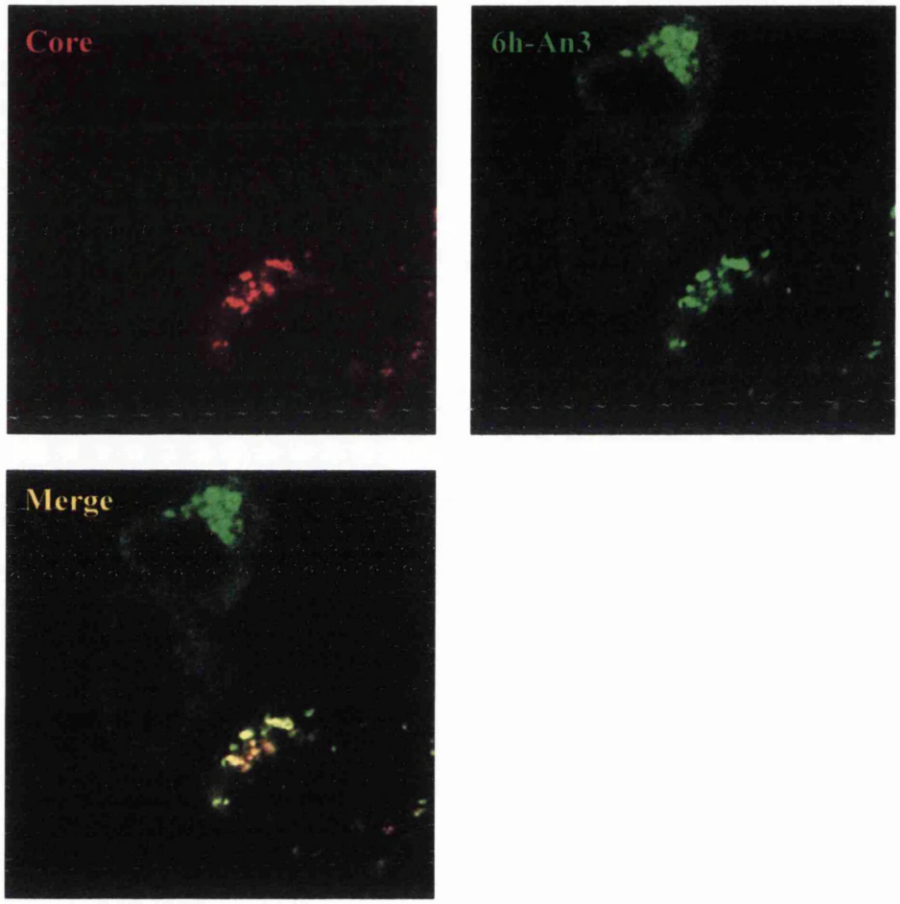

Figure 52b: Co-localisation of histidine-tagged An3 expressed by plasmid with core protein. Huh-7 (N) cells were infected with rVV-C-E1-E2 and vTF7.3 (m.o.i. = 0.5 each) for 1 hour and subsequently transfected with p6h-An3 construct (1 μg). 16 hours post-transfection, cells were fixed and then probed with appropriately diluted MAb RGS-His/anti-core PAb R525 in combination, followed by anti-mouse IgG-FITC/anti-rabbit IgG-Cy5 conjugated antibodies.

4.2. 6 Identification of a Nuclear Export Signal at the N-terminus of DDX3

Analysis of the protein sequence of DDX3 suggested the protein contains all of the conserved motifs of a member of the DEAD-box family of RNA helicases, and a putative RS domain (section 1.9.6.9; Owsianka and Patel, 1999; You *et al.*, 1999b). Following reports of a nuclear export signal (NES) at the extreme N-terminus of *X. laevis* An3 that participates in its nucleocytoplasmic shuttling (Askjaer *et al.*, 1999), a similar sequence was searched for in DDX3. Consistent with the idea that DDX3 and its homologues are highly related, a putative NES was detected. This NES is itself highly related to other proteins that are known to be recognised by CRM1 (Fig. 53a) - a soluble, saturable factor that mediates export of such proteins from the nucleus (Fornerod *et al.*, 1997; Fukada *et al.*, 1997; Stade *et al.*, 1997). CRM1 binding of its cargo via the leucine-rich NES is stabilised by cooperative binding of the small GTPase Ran in its GTP-bound form (Fig. 53b; Askjaer *et al.*, 1998; Fornerod *et al.*, 1997; Weis, 1998). The associated GTPase-activating protein RanGAP (termed RanGAP1 in vertebrates and Rna1p in yeast) promotes GTP hydrolysis, while the nucleotide exchange factor RanGEF (termed RCC1 in vertebrates) promotes RanGDP to RanGTP exchange. A steep RanGTP-RanGDP gradient is predicted across the nuclear envelope, since RanGAP1 is found in the cytoplasm whereas RCC1 is chromatin bound and present only in the nucleus (Görlich *et al.*, 1996). Based on the RanGTP dependent NES-CRM1 interaction, this implies that NES binding to CRM1 is stable in the nucleus and unstable in the cytoplasm, suggesting a mechanism for the unidirectional transport of NES-containing proteins, possibly together with bound RNAs (Fig. 53b; Fornerod *et al.*, 1997). The putative NES in the DDX3 protein sequence (Fig. 53a) may indicate it is one such protein that uses the above pathway to be actively transported from the nucleus. This mechanism is exemplified by HIV-1 Rev protein that uses its NES to export genomic and subgenomic HIV-1 mRNAs from the nucleus (Pollard and Malim, 1998).

Following the identification of such an NES in DDX3, binding of CRM1 to the protein was determined *in vitro* by collaboration with P. Askjaer and J. Kjems (University of Aarhus, Denmark) using the pGEX-6P-3-DDX3 construct described

	1							21
DDX3	MSHVAVENALG	L	DQQ	F	AG	L	D	L
PL10	MSHVAEEDELG	L	DQQ	L	AG	L	D	L
An3	MSHVAVENVLN	L	DQQ	F	AG	L	D	L
Ded1p	MAE	L	S EQ	V	QN	L	S	I
HIV-1 Rev		L	- PP	L	ER	L	T	L
Consensus		L		Φ		L		Φ

Figure 53a: DDX3 contains a putative NES that is conserved amongst proteins from varied organisms and exploited by viral proteins, such as HIV-1 Rev. The symbol Φ denotes L, F, V or I neutral non-polar aa residues (adapted from Askjaer *et al.*, 1999)

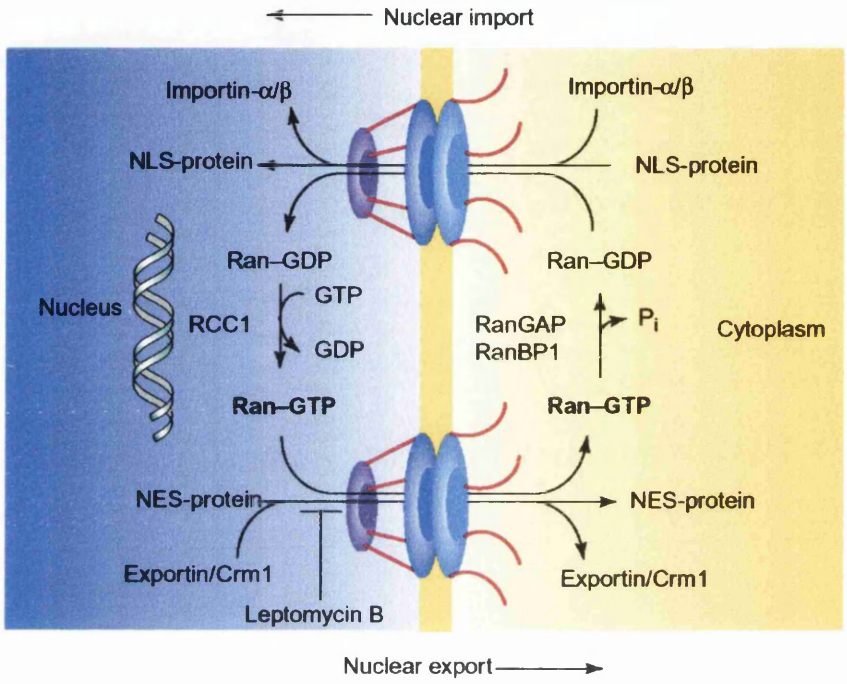

Figure 53b: Modulation of CRM1-dependent nuclear-cytoplasmic transport by the small GTPase, Ran. CRM1 binding of its cargo via the leucine-rich NES is stabilised by cooperative binding of Ran-GTP. A steep RanGTP-RanGDP gradient is predicted across the nuclear envelop; based on the RanGTP dependent NES-CRM1 interaction, this implies that NES binding to CRM1 is stable in the nucleus and unstable in the cytoplasm, suggesting a mechanism for the unidirectional transport of NES-containing proteins, possibly together with bound RNAs (taken from Clarke and Zhang, 2001)

previously (Fig. 35a; section 3.2.12) to supply the protein in the same assay originally described for An3 (Askjaer *et al.*, 1999). Accordingly, DDX3 bound CRM1 in a RanGTP dependent manner (P. Askjaer and J. Kjems, personal communication). DDX3 did not bind CRM1 in the presence of RanGDP, consistent with the model described above. The following sections describe an investigation into the functionality of the putative NES of DDX3 by using i) an immunofluorsecence assay similar to that described in section 4.2.5, and ii) subcellular fractionaction of cell lines and Western blotting for DDX3 to delineate the cellular compartment(s) in which the protein is found.

4.2. 7 Cloning and Expression of DDX3 Lacking a Leucine-rich Putative Nuclear Export Signal in Hepatocytes

It was postulated that removing the putative NES of DDX3 would lead to accumulation of DDX3 in the nucleus. To investigate this, appropriate primers were designed (see Appendix V) to amplify DDX3 cDNA without the putative NES-coding sequence (nt 1-63 of the full-length DDX3 sequence - see Appendix IV). The PCR products were transferred to the pZeoSV2 (+) mammalian expression construct (Fig. 28a, section 3.2.5), with and without a histidine-tag, to produce pΔNES-DDX3 and p6h-ΔNES-DDX3. The resulting constructs contained the DDX3-coding sequence from nt 64 to the stop codon. Following sequencing of the constructs with suitable primers, expression from the new constructs was confirmed by Western blotting transfected cell extracts as described in section 4.2.4. ΔNES-DDX3 with or without the histidine-tag migrated slighlty below the wild-type protein, as would be expected for such a deletion mutant lacking the N-terminal 21 aa, and was processed in a similar manner to endogenous DDX3 in Huh-7 (N) cells and over-expressed DDX3 containing the NES expressed from the same vector when detected by anti-DDX3 MAb AO196 (Fig. 54a, lanes 3-6). Expression from all constructs containing the histidine-tag was confirmed using the RGS-His MAb (Fig. 54b). Expression from the p6h-ΔNES-DDX3 construct detected by MAb RGS-His was similar to expression of endogenous DDX3 detected by AO196, and was indistinguishable from DDX3 or ΔNES lacking the histidine-tag.

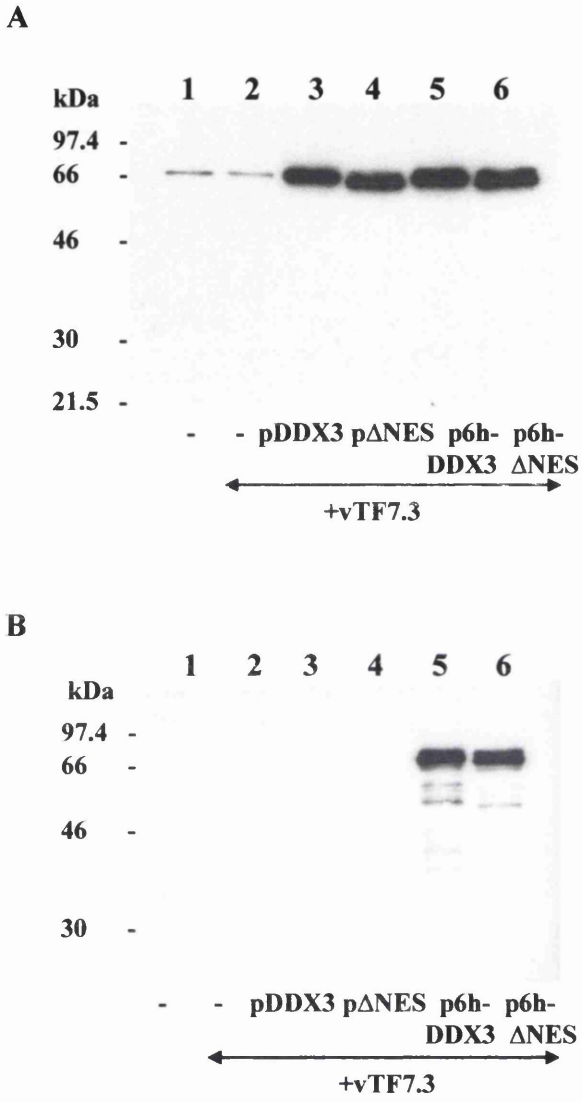

Figure 54: Detection of ΔNES-DDX3 protein expressed by plasmid in hepatocytes. Huh-7 (N) cells were either mock-transfected (lanes 1 and 2), or transfected with the constructs as shown following mock-infection (lane 1) or infection with vTF7.3 at m.o.i of 5 (lanes 2-6). At 16 hours post-transfection, cells were washed, harvested and 20 μg total protein subjected to SDS-PAGE (8%) followed by Western immunoblotting with (A) MAb AO196 or (B) MAb RGS-His.

4.2. 8 Intracellular Distribution of DDX3 Lacking the Putative NES

To investigate the subcellular localisation of DDX3 lacking the putative NES, the relevant constructs were transfected into Huh-7 (N) cells grown on coverslips in 24-well dishes. All four constructs carrying the wild-type DDX3 or ΔNES-DDX3, with and without the histidine-tag, were tested in parallel. As before, infection with vTF7.3 (m.o.i. = 5) preceded introduction of these constructs into cells to increase transfection efficiency and expression levels. The localisation of the expressed proteins was determined using either anti-DDX3 MAb AO196 or MAb RGS-His. Although AO196 possesses an epitope in the N-terminal 1-142 aa of DDX3, it was able to detect ΔNES-DDX3 in cell extracts previously transfected by Western blotting (Fig. 54a; section 4.2.7), suggesting its epitope does not lie within the N-terminal 1-21 aa. This antibody was therefore considered suitable to detect transfected DDX3 lacking the putative NES and the wild-type protein in this study. As before, the RGS-His antibody was employed to detect expressed proteins containing histidine-tags in order to distinguish the proteins expressed via plasmid from endogenous DDX3 within the hepatocytes. Nevertheless, it was found that the localisation of ΔNES protein either with or without histidine-tag was not markedly different from that of the wild-type protein (Fig. 55) when both were expressed in parallel by plasmid. The same distinct ring-like structures were seen, with no apparent accumulation of ΔNES-DDX3 in the nucleus. However, it appeared that while the ring-like structures formed by DDX3 were randomly distributed throughout the cytoplasm, such structures formed by ΔNES-DDX3 were in greater concentration in the perinuclear cytoplasm (Fig. 55). This suggests that this N-terminal sequence is required for the specific localisation of wild-type DDX3. Interestingly, although an NES sequence is present at the extreme N-terminus of An3 (Fig. 53a), it showed a similar localisation to ΔNES-DDX3. Nonetheless, these data suggest that although DDX3 can bind CRM1 *in vitro* (P. Askjaer and J. Kjems, personal communication), the putative NES of DDX3 is seemingly not functional as an NES in cultured hepatocytes. Use of the RGS-His antibody in parallel with anti-DDX3 MAb AO196 confirmed this localisation of ΔNES-DDX3 (Fig. 55). Further investigation of ΔNES-DDX3 is required in other cell types and with other anti-DDX3 MAbs and PAbs to verify these results. Indeed, these data might imply that

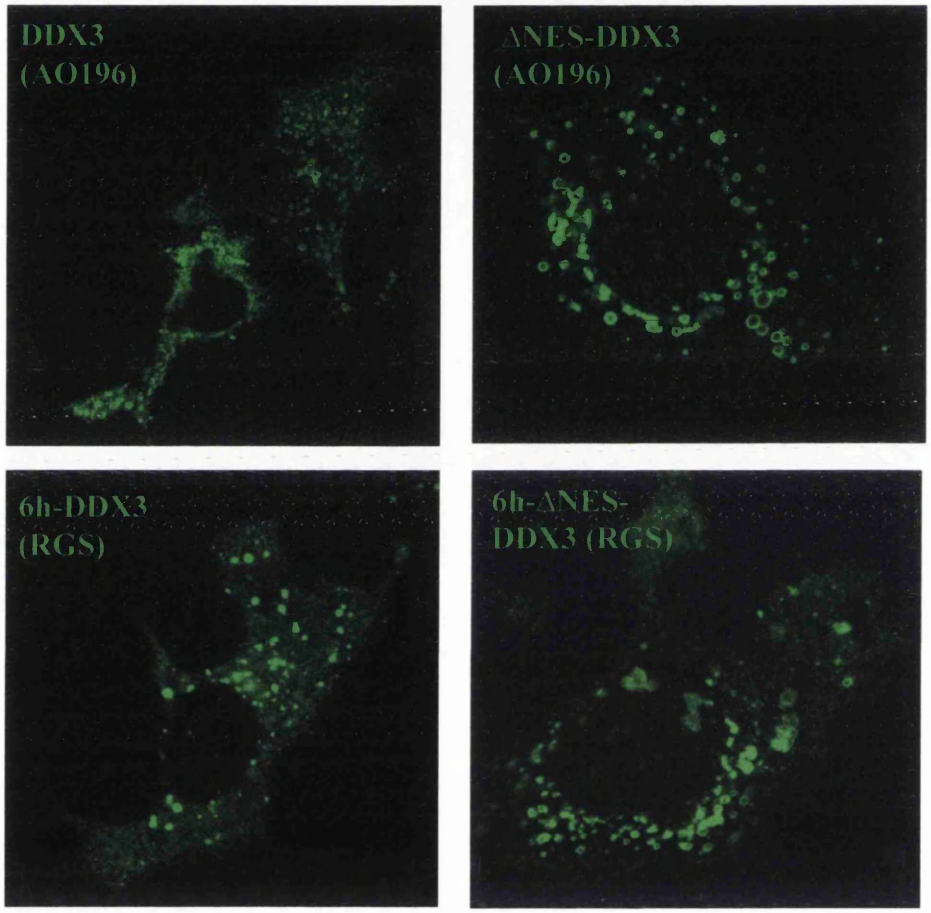

Figure 55: Localisation of DDX3, ΔNES-DDX3 and their histidine-tagged counterparts expressed by plasmid in hepatocytes. Huh-7 (N) cells on coverslips were infected with vTF7.3 prior to transfection with the plasmids (1 μg) as shown, then fixed and probed with either anti-DDX3 MAb AO196 or anti-histidine tag MAb RGS-His as indicated. Bound antibodies were visualised with anti-mouse IgG-FITC conjugated antibody.

MAb AO196 does not detect a conformationally distinct nuclear form of DDX3. It is also entirely possible that DDX3 simply does not localise to the nucleus at all.

It has been previously shown that a potent antifungal antibiotic, leptomycin B (LMB), can inhibit CRM1-mediated export of proteins such as HIV-1 Rev by directly binding CRM1 (Fornerod *et al.*, 1997; Fukada *et al.*, 1997) and covalently modifiying cysteine residues in its conserved region (Kudo *et al.*, 1999). To confirm the above results, LMB (Sigma) was tested for possible effects on the localisation of DDX3 due to inhibition of CRM1. Huh-7 (N) cells were seeded on coverslips, infected with vTF7.3 (m.o.i. = 5), and transfected as before (section 4.2.5). 16 hours post-transfection, the cell culture medium was removed, and fresh medium, or medium containing LMB at a concentration of 200 nM, a concentration which has been shown to inhibit CRM1-mediated nucleocytoplasmic transport (Koffa *et al.*, 2001), was added. The cells were incubated at 37°C for a further 4 hours. Consistent with the localisation of ΔNES-DDX3, LMB appeared to have no effect on the distribution of endogenous or over-expressed DDX3 in Huh-7 (N), HeLa, or COS-7 cell lines (data not shown). However, it is essential to confirm the results of the LMB assay using an appropriate positive control such as the HIV-1 Rev protein (section 4.2.6; Pollard and Malim, 1998) expressed in the same manner.

To test whether the putative NES of DDX3 was of any importance for the interaction with core protein, the same experiment as described in section 4.2.5, detailing an investigation of the co-localisation of DDX3 and An3 with core, was performed. As before, ΔNES-DDX3 was found in uninfected cells throughout the cytoplasm, with a greater concentration around the nucleus (Fig. 56). Core protein expressed via rVV-C-E1-E2 was also localised as before to structures likely to be lipid droplets. ΔNES-DDX3 strongly co-localised with core protein (Fig. 56), suggesting the putative NES is not involved in the interaction of DDX3 with core protein.

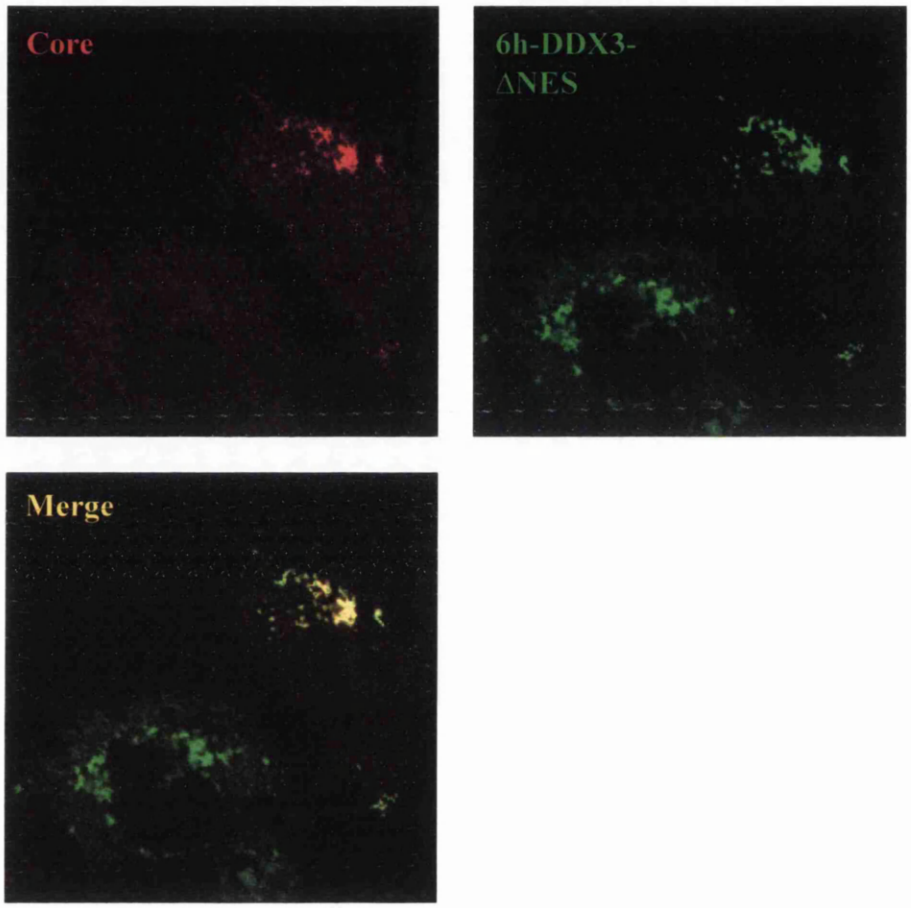

Figure 56: Co-localisation of histidine-tagged ΔNES-DDX3 expressed by plasmid with core protein. Huh-7 (N) cells were infected with rVV-C-E1-E2 and vTF7.3 (m.o.i. = 0.5 each) for 1 hour and subsequently transfected with p6h-ΔNES-DDX3 construct (1 μg). 16 hours post-transfection, cells were fixed and then probed with appropriately diluted MAb RGS-His/anti-core PAb R525 in combination, followed by anti-mouse IgG-FITC/anti-rabbit IgG-Cy5 conjugated antibodies.

4.2. 9 Subcellular Fractionation of Hepatocyte and Non-hepatocyte Cell Lines

The localisation of DDX3 and ΔNES-DDX3 within cells was further investigated by subcellular fractionation of two separate cell lines followed by Western blotting to detect DDX3. A human hepatoma cell line (Huh-7) and a further mammalian cell line (COS-7) were tested in parallel. Each cell line was transfected with either pDDX3 or pΔNES-DDX3 mammalian expression plasmid. Following 16 hours post-transfection, cells were lysed and total, cytoplasmic and nuclear fractions prepared as described in Materials and Methods (section 2.45). Equal amounts of protein from such fractions were analysed by Western blotting for DDX3 with MAb AO196. As expected, this antibody detected DDX3 abundantly in total and cytoplasmic extracts of both Huh-7 (Fig. 57a, lanes 1 and 3) and COS-7 (lanes 7 and 9) cells. Interestingly, a small quantity of DDX3 protein was detected in Huh-7 nuclear extracts (lane 2), suggesting that DDX3 is present in the nucleus of hepatocytes. Furthermore, a slightly larger amount of DDX3 protein was found in COS-7 nuclear extracts (lane 8), although some cytoplasmic fraction may have contaminated the COS-7 nuclear extract (see below). The MAb used here would detect both the plasmid-expressed ΔNES-DDX3 as well as the endogenous full-length DDX3. However, the fact that there was no discernible increase of ΔNES-DDX3 (or endogenous DDX3) in the nucleus of cells transfected with pΔNES-DDX3 indicates that ΔNES protein is not localised to the nucleus (Fig. 57a, lanes 5 and 11). This is in keeping with the confocal microscopy data shown above (Fig. 55). As controls to confirm fractionation had occurred such that cytoplasmic proteins had not leached into the nuclear fraction or *vice versa*, anti-ATF-2 and anti-β-tubulin antibodies were used to probe the same samples. These antibodies were chosen since the transcription factor ATF-2 is exclusively nuclear (Alonso *et al.*, 1996; Beier *et al.*, 1999), while the β-subunit of tubulin is a purely cytoplasmic protein (Fig. 43a; Alberts *et al.*, 1994). Appropriate compartmentalisation of Huh-7 nuclear extracts was confirmed by the exclusive presence of ATF-2 in total and nuclear cell extracts (Fig. 57b, lanes 1, 2, 4 and 5). A small quantity of ATF-2 was found in COS-7 cytoplasmic extracts (lanes 9 and 12), although the vast majority of this cellular factor was to be found in total and nuclear extracts (lanes 7, 8, 10 and 11). Potential leakage of cytoplasmic cellular factors into nuclear extracts was not

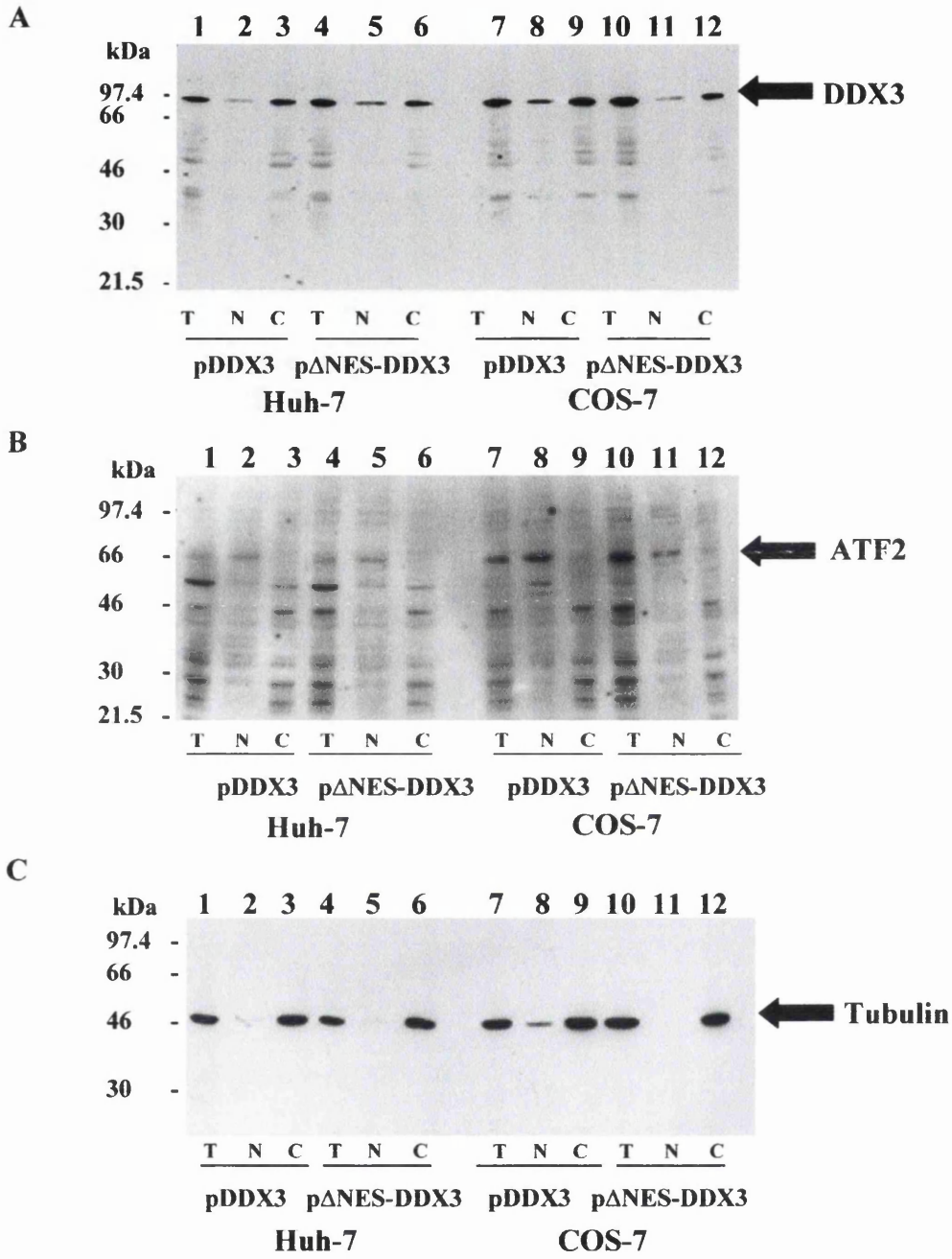

Figure 57: Subcellular fractionation of mammalian cell lines. Huh-7 or COS-7 cells in 6-well dishes were transfected with pZeoSV2 (+) vector carrying either full-length DDX3 (pDDX3) or ΔNES-DDX3 (pΔNES-DDX3) coding seqeunces as shown. Total (T), nuclear (N), and cytoplasmic (C) extracts were prepared, fractionated by SDS-PAGE (10%), and Western immunoblotted with (A) MAb AO196 for DDX3, as well as (B) anti-ATF2 or (C) anti-β-tubulin to confirm appropriate fractionation had occured.

found with fractionated Huh-7 cells, since β-tubulin was not detected in nuclear extracts (Fig. 57c, lanes 2 and 5) but was abundant in total and cytoplasmic extracts (lanes 1, 3-4 and 6). However, a small amount of cytoplasmic extract had apparently leaked into the COS-7 nuclear extract transfected with the pDDX3 expression construct (lane 8), which could explain the increased level of DDX3 in the nucleus of this cell line (Fig. 57a, lane 8). In contrast, β-tubulin was not detected in nuclear extracts previously transfected with pΔNES-DDX3 expression construct. These data show that DDX3 is present in the nucleus of Huh-7 cells, and confirm previously published reports of such a nuclear form of DDX3 in mammalian cells (Owsianka and Patel, 1999; You *et al.*, 1999b).

4.2. 10 Analysis of DEAD-box (E → Q) Mutant of DDX3

A mutation within the DEAD-box (ATPase B domain; Fig. 17, section 1.10.6) of the *X. laevis* DDX3 homologue An3 protein (changing Glutamic acid → Glutamine, E → Q) was previously reported to exhibit a 6-fold decrease in dATPase activity (Askjaer *et al.*, 2000). In collaboration with P. Askjaer and J. Kjems (University of Aarhus, Denmark), using the pGEX-6P-3-DDX3 construct as a template (Fig. 35a; section 3.2.12), the same mutation was introduced into the DDX3-coding sequence by site-directed mutagenesis (see Appendix II). As for An3 protein, a marked decrease in dATPase activity relative to the wild-type protein was observed (P. Askjaer and J. Kjems, personal communication). This provides further evidence that the DDX3 protein expressed in this manner does indeed possess dATPase enzymatic activity. Interestingly, the An3 DEAD-box (E → Q) mutant also exhibited an altered nuclear export rate compared with the wild-type protein (Askaer *et al.*, 1999). By analogy with this DDX3 homologue, the expression and localisation of the DDX3 DEAD-box (E → Q) mutant in hepatocytes was investigated. The DDX3-EQ clone was generated by P. Askjaer (see Appendix II) using the pZeoSV2 (+)-DDX3 construct described in section 4.2.4. A histidine-tagged version of the original DDX3-EQ clone was generated to allow differentiation from the endogenous protein. This construct was made by restriction digestion with *Nco*I (in DDX3) and *Eco*RI (in the MCS of the vector) of the pZeoSV2 (+)-DDX3-EQ clone, to produce a ~600 bp fragment containing the

A

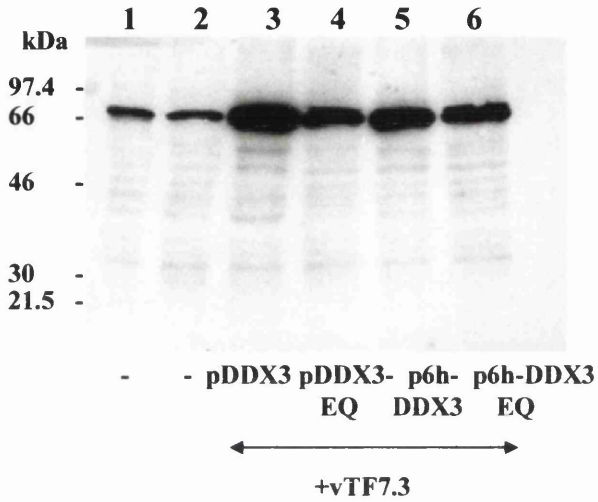

B

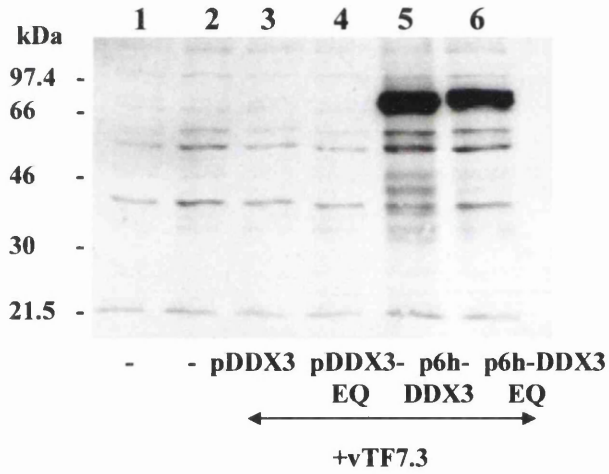

Figure 58: Detection of a DDX3 DEAD-box mutant (DDX3-EQ) expressed by plasmid in hepatocytes. Huh-7 (N) cells were either mock-transfected (lanes 1 and 2), or transfected with the constructs as shown following mock-infection (lane 1) or infection with vTF7.3 at m.o.i of 5 (lanes 2 to 6). At 16 hours post-transfection, cells were washed, harvested and 20 μg total protein subjected to SDS-PAGE (8%) followed by Western immunoblotting with A) MAb AO196 or B) MAb RGS-His.

sequence coding for the E → Q mutation, and inserting this into *NcoI/EcoRI* cut 6h-DDX3 mammalian expression construct (described in section 4.2.4). To confirm expression, the relevant constructs were transfected into the Huh-7 (N) cell line following infection with vTF7.3, and total cell extracts prepared. Total cell extracts were prepared from mock-transfected Huh-7 (N) cells following mock-infection or infection with vTF7.3 (m.o.i. = 5) to act as controls. As before, the cell extracts were probed either with anti-DDX3 MAb AO196 or with the anti-histidine-tag MAb RGS-His. There was no indication of any gross effects on expression or processing of DDX3 containing the DEAD-box mutation (Fig. 58).

4.2. 11 Localisation of DDX3-EQ Mutant Compared with Wild-type DDX3 by Indirect Confocal Immunofluorescence Microscopy in Hepatocytes

Following confirmation of expression from the DDX3-EQ constructs, their localisation in hepatocytes was investigated in parallel with constructs containing wild-type DDX3 cDNA. The plasmids were transfected into Huh-7 (N) cells grown on coverslips, and subsequently probed with either anti-DDX3 MAb AO196 or anti-histidine tag MAb RGS-His as before. Intriguingly, the DDX3-EQ mutant had a quite different distribution to the wild-type protein as detected by AO196 (Fig. 59). While wild-type DDX3 formed or localised to distinct ring-like structures and gave a small amount of diffuse staining as before, DDX3-EQ was located in greater amounts diffusely throughout the cytoplasm in addition to forming or coating globular structures randomly distributed in the cytoplasm (Fig. 59). This altered localisation was confirmed by detection of histidine-tagged DDX3 and DDX3-EQ with MAb RGS-His (Fig. 59). This antibody did not exhibit any staining of Huh-7 (N) cells transfected with constructs lacking the histidine-tag (data not shown).

Interestingly, the DDX3 DEAD-box mutant detected by this antibody was still able to co-localise with core protein expressed by rVV-C-E1-E2. While the same diffuse distribution of 6h-DDX3-EQ described above was detected with RGS-His antibody in Huh-7 (N) cells, in infected cells expressing core protein at lipid droplets in the perinuclear cytoplasm, 6h-DDX3-EQ was seen to strongly co-localise with core (Fig. 60). These data reveal two important details about DDX3, and its interaction

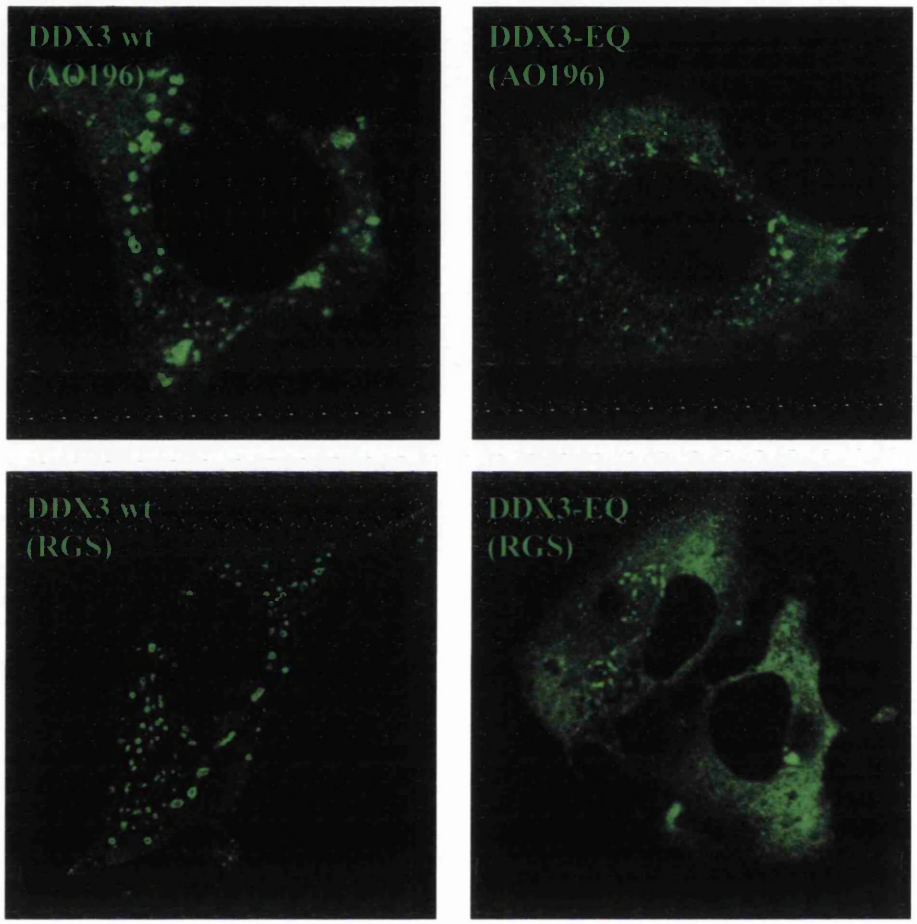

Figure 59: Localisation of DDX3, DDX3-EQ, or their respective histidine-tagged counterparts expressed by plasmid in hepatocytes. Huh-7 (N) cells on coverslips were infected with vTF7.3 (m.o.i. = 5)prior to transfection with the plasmids as shown, then fixed following expression for 16 hours, and probed using either anti-DDX3 MAb AO196 or anti-histidine tag MAb RGS-His as indicated. Bound antibodies were visualised with anti-mouse IgG-FITC conjugated antibody.

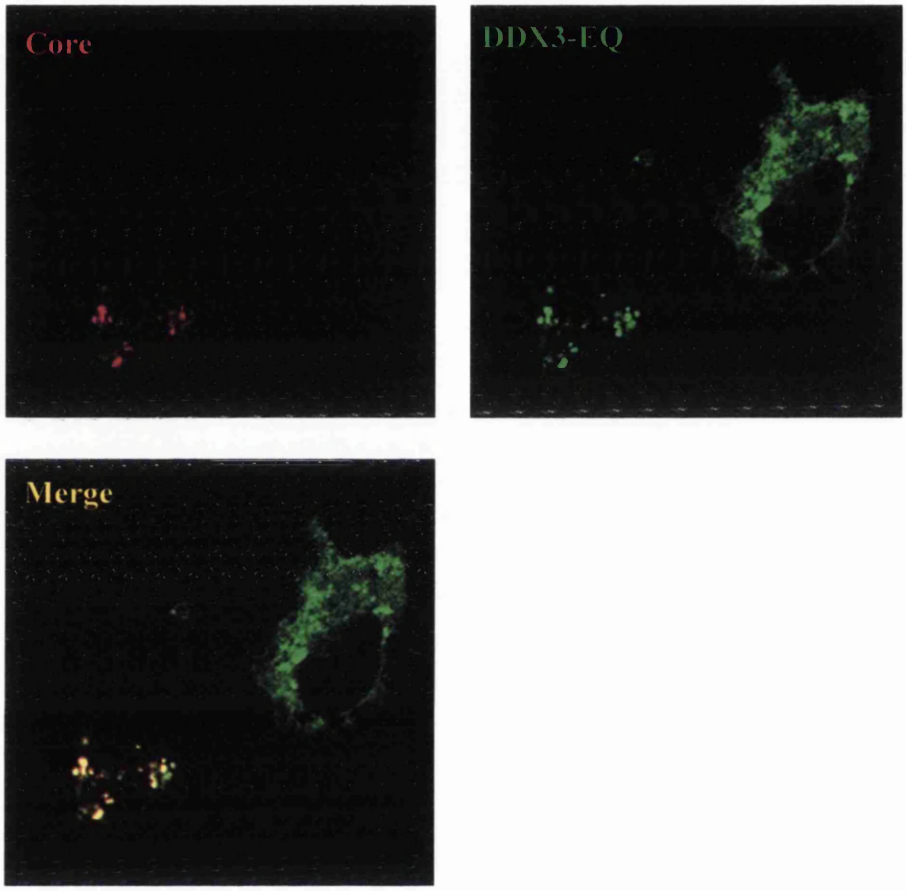

Figure 60: Co-localisation of histidine-tagged DDX3-EQ fusion protein expressed via plasmid with core protein. Huh-7 (N) cells on coverslips were infected at m.o.i. of 0.5 with rVV-C-E1-E2, transfected with p6h-DDX3-EQ, fixed and then probed with appropriately diluted anti-histidine tag MAb RGS-His and anti-HCV core PAb R525 in combination. Bound antibodies were visualised with anti-mouse IgG-FITC and anti-rabbit IgG-Cy5 conjugated antibodies.

with core protein. First of all, the altered localisation of DDX3-EQ relative to the wild-type protein suggests that the enzymatic activity of DDX3 is linked to its subcellular localisation. The DDX3-EQ protein contained a single amino acid change relative to the wild-type protein - this not only greatly diminished dATPase activity (P. Askjaer and J. Kjems, personal communication) and hence would also be expected to be non-functional in terms of RNA helicase activity as a consequence, but also had a discernible effect on the subcellular location of DDX3. Secondly, in view of the fact that the DDX3-EQ protein apparently co-localises with core protein, it seems that neither the original subcellular location of DDX3 nor its functional competence are essential for its interaction with core protein. This implies that the interaction between DDX3 and core occurs co- or post-translationally, and not following targeting of DDX3 to its normal cellular location. Indeed, the reported localisation of core protein at the ER (Selby *et al.*, 1993), albeit in small quantities, may allow core protein to hijack DDX3 immediately following or during post-translational processing.

The following sections describe an investigation into the enzymatic properties of DDX3, which may reveal information regarding the function of DDX3 and any modulation of this by core protein.

4.2. 12 Cloning and Expression of the HCV NS3 Helicase Domain as GST-fusion Protein for use in Enzymatic Assays

HCV encodes a well-characterised ATP-dependent RNA helicase, located in the C-terminal two-thirds of the NS3 protein (section 1.2.5.2; Gwack *et al.* 1996; Kim *et al.*, 1995, 1997; Yao *et al.*, 1997). To use as a positive control in the biochemical assays described below, the RNA helicase domain of NS3 from a genotype 1a infectious clone of HCV (H77c; Yanagi *et al.*, 1997) was amplified by PCR with specific primers (see Appendix V) and cloned into pGEX-6P-3. The resulting construct contained an initiating ATG codon followed by nt 3915 to 5312 of H77c (see Appendix IV), and encodes a protein consisting of the entire HCV NS3 helicase domain. The construct was used to express the NS3 helicase domain as a GST-fusion protein in *E. coli.* As before, GST-NS3 helicase was purified by affinity

chromatography on glutathione-agarose beads, and the bound protein eluted using glutathione (section 2.29). 5 μg of the purified protein eluted from beads, together with 5 μg purified GST-DDX3 expressed in parallel, was fractionated by SDS-PAGE and visualised by staining with Coomassie brilliant blue (Fig. 61). GST-NS3 helicase was expressed as doublet at approximately the expected molecular weight of 78 kDa, taking the 26 kDa GST moiety into account (Fig. 61, lane 1). As before (Fig. 35b; section 3.2.12), GST-DDX3 was detected at approximately 99 kDa (lane 2).

4.2. 13 dATPase Activity of GST-NS3 Helicase Domain and GST-DDX3 Fusion Proteins

The classical method of detecting hydrolysis of dATP and other nucleotides was used to determine dATPase activity of the NS3 helicase domain expressed as a GST-fusion protein, prior to investigating this property of DDX3 expressed in the same manner. A description of the assay and the method itself is found in section 2.47. A series of 10-fold dilutions of purified GST-NS3 helicase domain protein were mixed with reaction buffer and [α^{32}P]-labelled dATP. As a control, free GST protein was tested in parallel. Reactions were allowed to proceed for 30 minutes, and subsequently fractionated by thin-layer chromatography (TLC). dATP breakdown products, namely dADP and dAMP, were visualised by exposure to a phosphorimager screen. While GST alone at a concentration of 1 μg, or no protein at all, did not hydrolyse dATP above background levels (Fig. 62a, lanes 1 and 2, respectively), GST-NS3 helicase domain at a concentration of 0.01 μg or above was able to fully hydrolyse all of the available radiolabelled dATP (lanes 8-10). In fact, dATPase activity for GST-NS3 helicase domain was detectable at a concentration of 10^{-3} μg (lane 7). However, apparently only dADP was resolved with no other dATP breakdown products visible.

The same assay was used to determine dATPase activity of full-length DDX3 protein expressed as a GST-fusion protein. 1.5 μg of free GST protein and GST-NS3 helicase were assayed separately for dATPase activity in parallel with a series of 2-fold dilutions of GST-DDX3. As before, free GST protein or no protein did not

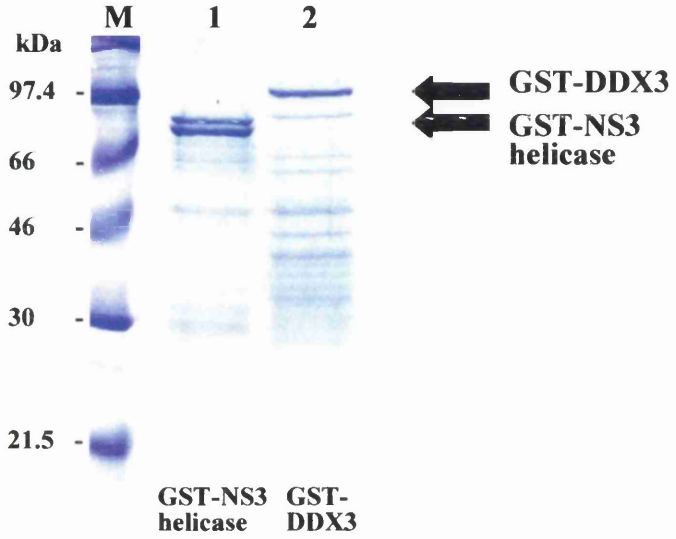

Figure 61: Expression of the HCV NS3 helicase domain as a GST-fusion protein. The bacterially-expressed fusion protein was purified by affinity chromatography on glutathione-agarose beads, and the bound protein eluted using glutathione (section 2.29). 5 μg of eluted protein (lane 1, GST-NS3 helicase; lane 2, GST-DDX3 as control) was fractionated by SDS-PAGE (9%) and stained with Coomassie brilliant blue.

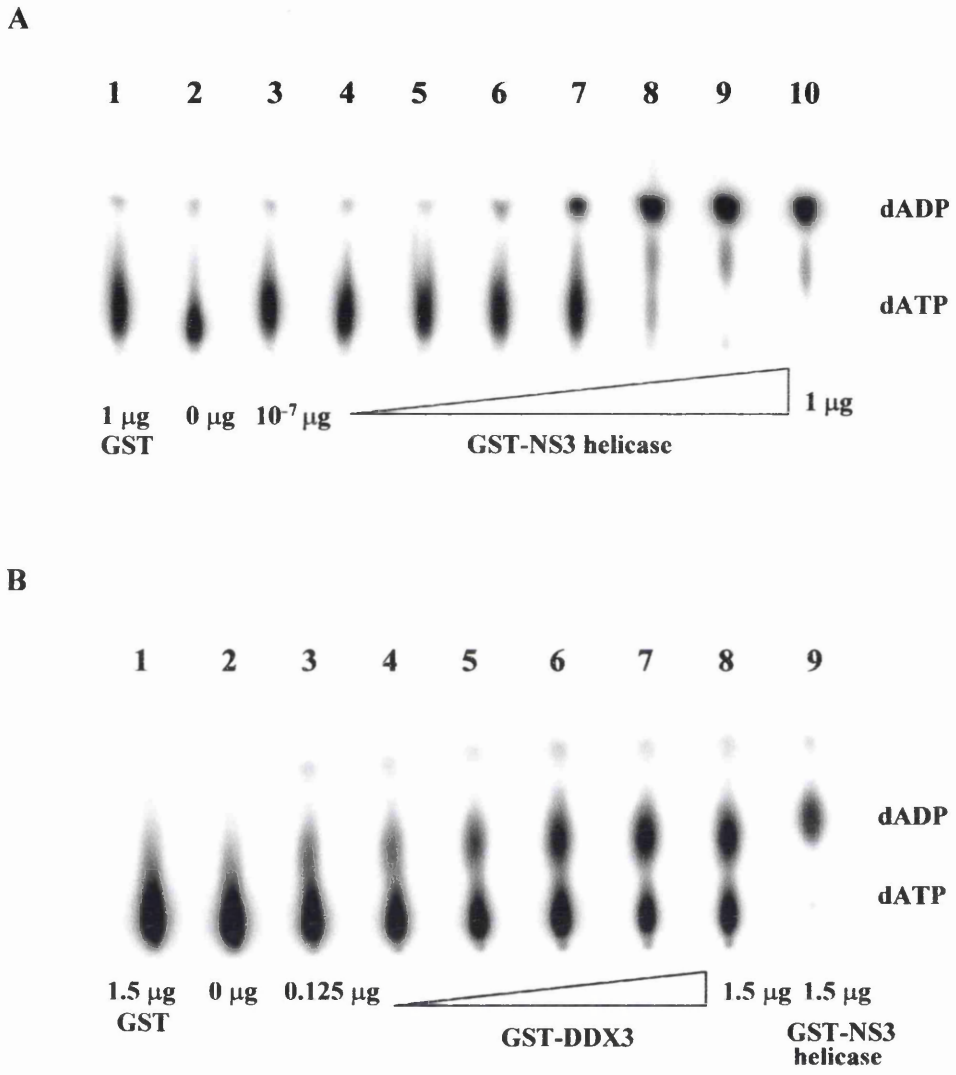

Figure 62: dATPase activity of the HCV NS3 helicase and DDX3 expressed as GST-fusion proteins. A series of 10-fold dilutions of GST-NS3 helicase (A) and 2-fold dilutions of purified GST-DDX3 (B) were made and incubated with [α^{32}P]-dATP in appropriate buffer. The dATP breakdown products were fractionated by TLC and visualised using a phosphorimager.

hydrolyse the substrate (Fig. 62b, lanes 1 and 2, respectively), while the positive control (GST-NS3 helicase) was able to hydrolyse all of the substrate at the same concentration (lane 9). Analogous to the positive control protein, GST-DDX3 was able to hydrolyse dATP in a 'dose-dependent' manner. However, consistent with previous reports (You *et al.*, 1999b), GST-DDX3 was only capable of hydrolysing approximately 50% of the substrate even when 1.5 μg of purified protein was added to the reaction (lane 8). This suggests that DDX3 is a less active protein than the NS3 helicase protein in terms of enzymatic properties when both are expressed as GST-fusion proteins. As discussed previously (section 4.2.10), it has been shown that GST-DDX3 containing a single amino acid change from Glu to Gln in the DEAD-box (DEAD → DQAD) significantly decreases dATPase activity (P. Askjaer and J. Kjems, personal communication), thus confirming the functionality of dATP hydrolysis by the DDX3 GST-fusion protein *in vitro*. In direct contrast to a previous report suggesting a marked stimulation of DDX3 ATPase and dATPase activity by bacterially-expressed truncated core protein (aa 1-101, and 1-122) (section 1.9.6.9; You *et al.*, 1999b), full-length core (aa 1-191) expressed in the same manner had no effect on the dATPase activity of DDX3 (data not shown).

4.2. 14 Development of an RNA Helicase Assay: Production of a Double-stranded RNA Substrate

Unwinding of RNA substrates is typically assayed by constructing duplex RNAs with single-stranded overhangs, required to allow binding of protein onto the nucleic acid, and visualising the duplex and monomeric products by electrophoretic separation (Fig. 18; section 1.10.7). The protein under analysis is mixed with the dsRNA substrate in appropriate buffer and incubated at 37°C. The reaction is stopped with EDTA and run on 15% urea gels. The shorter of the two RNA species is usually radiolabelled, in order to increase electrophoretic separation between the displaced ssRNA and the unwound duplex. The above method was used to investigate the ability of GST-DDX3 to unwind a dsRNA substrate, following confirmation of its ability to hydrolyse dATP (Fig. 62b; section 4.2.13). To this end, a non-specific dsRNA substrate was generated by *in vitro* transcription of linearised pBluescript SK (+) (Stratagene) DNA templates followed by annealing of the two

transcripts. The vector map for pBluescript SK (+), including location of the promoters and key restriction endonuclease sites, is shown (Fig. 63a). As described previously (section 1.10.7), RNA helicases may have a preference for 5′ and 3′ overhangs, thus conferring directionality of the enzyme. The duplex RNA substrate (Fig. 63b) was designed to possess both 5′ and 3′ overhangs, since it was not known whether DDX3 had a preference for either formation of duplex RNA. To generate the 233 nt top strand, pBluescript SK (+) was linearised with *PvuII* and the RNA transcribed from a bacteriophage T3 RNA polymerase promoter site. The 93 nt bottom strand was synthesised from a bacteriophage T7 RNA polymerase promoter site following linearisation of the vector with *SacI*. This RNA was radiolabelled during *in vitro* transcription with [α^{32}P]-CTP to allow discrimination between ds and ssRNA. The 93 nt bottom strand is complimentary to a section near the 5′ end of the 233 nt top strand, thus generating a duplex RNA substrate that possesses 5′ and 3′ single-stranded overhangs. Each RNA transcript was gel purified as follows. The *in vitro* transcibed RNA was run on a 15% urea gel (Sequagel, National Diagnostics) and excised from the gel under UV light. The gel pieces were finely cut and transferred to a 1.5 ml microfuge tube. One gel volume of TE buffer (10 mM Tris-HCl pH 8.0, 1 mM EDTA) containing 0.5% SDS was added and the tubes incubated at 37°C for 16 hours. Gel pieces were pelleted by centrifugation (12, 000 × *g*, 5 minutes) and the supernatant consisting of the RNA transcript in buffer was transferred to a fresh tube. The RNA was phenol-chloroform extracted and precipitated with 0.5 volumes 7.5 M ammonium acetate and 2.5 volumes ethanol. The RNA recovered by centrifugation (12,000 × *g*, 15 minutes) was washed with 75% ethanol, centrifuged as before, and resuspended in 100 μl dH_2O. Complimentary RNA transcripts were annealed by mixing equal volumes of gel purified RNA in annealing buffer (10 mM Hepes-KOH, pH7.6, 1 M NaCl, 2 mM EDTA, 1% SDS), and then boiling for 5 minutes and cooling to 65°C for 30 minutes. The mixture was stored at room temperature (18-25°C) prior to subsequent experimental procedures.

A

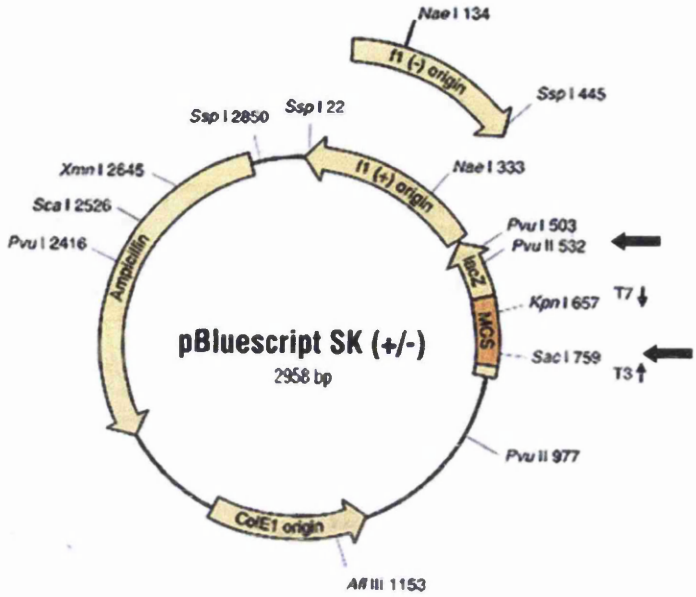

B

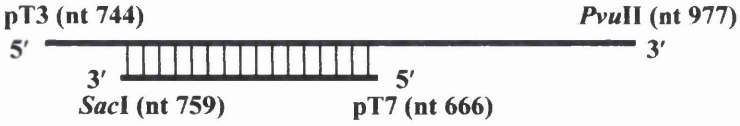

Figure 63: Production of dsRNA substrate for use in helicase assays. (A) Schematic diagram of pBluescript SK (+) showing T3 and T7 promoter sites, and the relevant restriction endonuclease sites (marked with arrow) (taken from Stratagene website). (B) Schematic diagram of the resulting dsRNA substrate with nt numbers of the promoter (pT3 and pT7) and restriction sites used.

4.2. 15 Helicase Activity of GST-NS3 Helicase Domain and GST-DDX3 Fusion Protein

The HCV NS3 helicase domain expressed as a GST-fusion protein, previously shown to possess dATPase activity (Fig. 62a; section 4.2.12), was tested for its ability to unwind the dsRNA substrate described above. The helicase assay methodology is found in section 2.48. As with ATPase assays, two negative control reactions were used in assays for helicase activity - one reaction lacking any protein and the other containing free GST protein. As a control, dsRNA was denatured by heating the duplex RNA for 5 minutes at 90°C to produce single-stranded (ss) RNA. As can be seen in Fig. 64, this produced a band visibly lower relative to the negative control reactions (lanes 1 and 2-3, respectively). A range of concentrations of GST-NS3 helicase from 0.01 to 10 μg were tested for the ability to produce ssRNA of similar size to that produced by heat denaturation of duplex RNA. GST-NS3 helicase was able to unwind a small proportion of the dsRNA substrate at a concentration of 2 μg (Fig. 64a, lane 7). Increasing the amount to 5 μg yielded approximately 50% ssRNA (lane 8), while doubling this almost completely converted the dsRNA to its monomeric form (lane 9). This 'dose-dependent' ability of GST-NS3 helicase protein to unwind the non-specific duplex RNA substrate confirmed that appropriate methodology had been employed. Furthermore, as has been shown for proteins such the *X. laevis* An3 protein (Gururajan and Weeks, 1997), RNA helicase activity was apparently not affected by fusion of the HCV NS3 helicase domain to GST.

DDX3 expressed as a GST-fusion protein was tested in parallel with the GST-NS3 helicase protein in the same manner as described above. While GST-NS3 helicase could unwind the non-specific dsRNA substrate with 5′ and 3′ overhangs (see above), GST-DDX3 was consistently unable to unwind the same substrate (Fig. 64b, lanes 4-9) even at a concentration of 10 μg (lane 9). It is unlikely that the GST-moiety is inhibiting helicase activity of DDX3, since the HCV NS3 helicase (see above) and the *X. laevis* An3 protein (Gururajan and Weeks, 1997), have been shown to possess helicase activity when expressed as GST-fusion proteins. Thus, the reason for this lack of activity for DDX3 is currently unclear. This observation

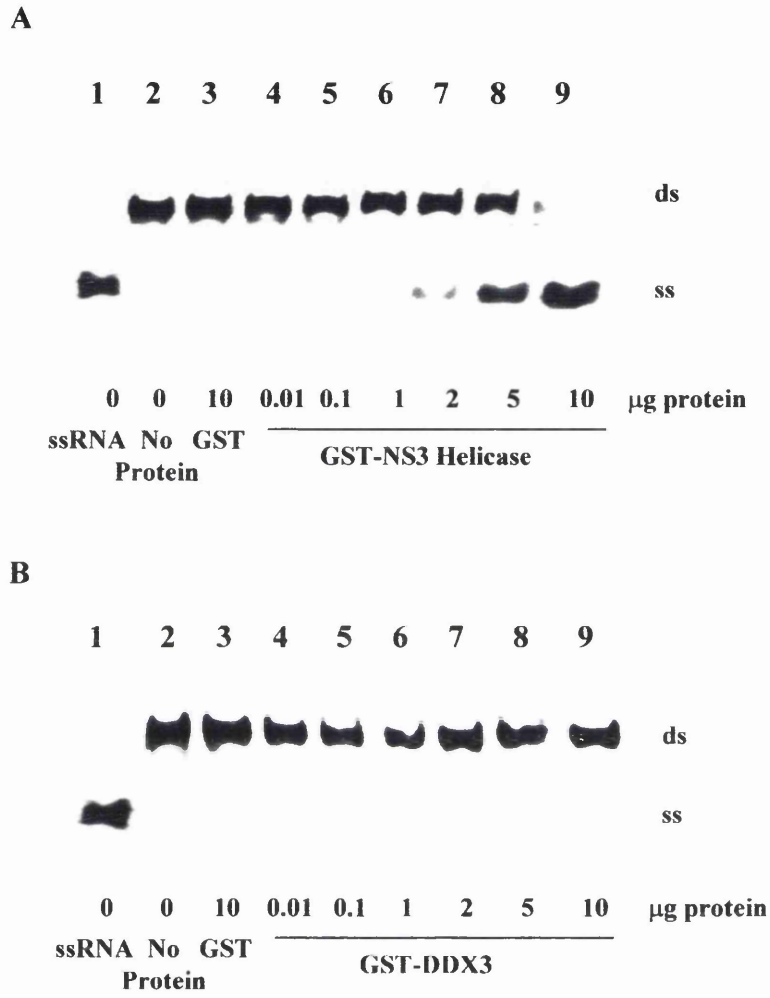

Figure 64: RNA helicase activity of HCV NS3 helicase (A) and DDX3 (B) expressed as GST-fusion proteins. Duplex RNA substrate was either heated at 90°C for 5 minutes (lane 1), or incubated at 37°C for 20 minutes in the absence of any protein (lane 2), or in the presence of 10 µg purified free GST protein (lane 3), or purified protein at the concentrations indicated (lanes 4-9). The reactions were separated on a 15% urea gel (SequaGel, National Diagnostics) and visualised using a phosphorimager.

has been independently reported by You *et al.*, (1999b), who used bacterially-expressed histidine-tagged DDX3 and a different non-specific RNA substrate that had previously been used to show activity of other RNA helicases. One possibility that DDX3 requres a cellular co-factor or a specific RNA substrate for helicase activity. Interestingly, although RNA helicases such as the HCV NS3 protein have been well characterised in their ability to unwind a variety of RNA substrates (section 1.2.5.2), the majority of mammalian putative helicases have not been shown to possess helicase activity when assayed *in vitro* (section 1.10.7). A common reason cited for this lack of activity is that the protein under investigation may require a specific cellular co-factor or a specific RNA ligand, as demonstrated for a number of helicases (section 1.10.7). It is not clear at this stage whether this is the case for DDX3. Indeed, the lack of helicase activity for DDX3 may be consistent with the lower dATPase activity of this protein relative to the NS3 helicase, suggesting that the amount of enzymatically active DDX3 protein used was not sufficient to give detectable activity.

4. 3 Discussion

The subcellular localisation of DDX3, an important factor in determining the function of the protein, has been studied in detail in the preceding chapter using the full range of anti-DDX3 MAbs. However, their reactivity in an immunofluorescence assay was largely consistent with detection of cellular DDX3 by Western blotting with the same panel of antibodies in Huh-7 (N) total cell extracts (Fig. 42; section 3.2.18), and co-localisation studies of DDX3 detected by MAb AO196 with core protein (Fig. 29; section 3.2.6). AO166 was the only MAb, in addition to AO196, to detect what is presumably the endogenous full-length protein. Although MAb AO166 was previously shown to detect a putative truncated form of DDX3 in hepatocyte cell extracts (Fig. 42; section 3.2.18), it showed a similar pattern of immunofluorescent staining to MAb AO196. This antibody was also able to detect DDX3 strongly co-localising with core protein. Interestingly, the putative truncated form of DDX3 detected by anti-DDX3 MAbs AO2 and AO35 showed a different subcellular localisation, suggesting it has a different role in the cell. However, if a hypothesis that this form represents the N-terminal half of DDX3 is correct, it is

perhaps not surprising that it did not detect DDX3 co-localising with with core protein, since the domain interacting with core resides in the C-terminus of DDX3. Re-localisation of other proteins in H9-13 cells was also studied - specific MAbs raised against ribosomal protein L22, the interferon-inducible protein kinase PKR, and poly-pyrimidine tract binding protein (PTB) were used to probe Huh-7 (N) and H9-13 cells in parallel. Localisation of these proteins in H9-13 cells was investigated following their implication in HCV pathogenesis or replication (Ali and Siddiqui, 1995; Ito and Lai, 1997; Taylor *et al.*, 1999, 2001; Wood *et al.*, 2001) but no consistent differences in localisation were detected (data not shown). Furthermore, cellular factors bound by AO34 and AO190 did not re-localise in H9-13 cells (data not shown). These data suggest that the localisation of the studied cellular factors is apparently unaffected by the presence of HCV sub-genomic replicon RNA and HCV nonstructural proteins.

To gain further insight into DDX3 and its normal cellular function, the full-length protein, in addition to a homologous protein from a different organism as a control (*X. laevis* An3), was expressed from a plasmid construct in the Huh-7 (N) cell line. As a valuable tool to determine the role of specific domains in localisation of DDX3, mutated or truncated forms of this protein were similarly expressed and investigated in detail. Full-length DDX3 protein expressed in this manner localised to or formed distinct ring-like structures which varied in size, in addition to showing some diffuse staining of the cytoplasm. However, while these data are consistent with an independent report of an exclusively cytoplasmic localisation for DDX3 by immunofluorescence (Mamiya and Worman, 1999; You *et al.*, 1999b), they contradict a previous report detailing a nuclear localisation for the same protein (Owsianka and Patel, 1999). This may be due to the use of different anti-DDX3 antibodies used by the authors. As a control, cDNA coding for the *X. laevis* (African clawed frog) An3 protein, which is approximately 86% identical in protein sequence to DDX3 (Owsianka and Patel, 1999), was cloned into the same expression vector and used to transfect Huh-7 (N) cells. Over-expressed *X. laevis* An3 protein had a somewhat different localisation to DDX3 and was predominantly found in the perinuclear cytoplasm, concurrent with its role in intracellular shuttling (Askjaer *et al.*, 2000). However, like DDX3 expressed from a plasmid, An3 was not found in

the nucleus, but was able to co-localise with core protein. This is presumably due to the high degree of identity between the two proteins at the aa level (Owsianka and Patel, 1999).

DDX3 was shown to possess a nuclear export signal (NES), and was subsequently shown to bind CRM1 in a RanGTP-dependent manner *in vitro* (P. Askjaer and J. Kjems, personal communication). Further studies investigated the possibility that removing the putative NES of DDX3 would lead to accumulation of DDX3 in the nucleus. This would suggest that DDX3 is not only partially localised in the nucleus, suggestive of protein involved in intracellular shuttling or a protein with a dual cellular role, but that export from the nucleus is rapid (or entry into the nucleus is rare) if previous immunofluorescence studies were correct. However, deletion of this region in the extreme N-terminus of the protein did not lead to accumulation of DDX3 in the nucleus of hepatocytes when expressed by plasmid. This truncated protein (ΔNES-DDX3) appeared to have a subcellular localisation analogous to the wild-type protein containing the putative NES, although ΔNES-DDX3 protein was more inclined to accumulate in the perinuclear cytoplasm than wild-type DDX3. In agreement with these data, treatment of cells with an antibiotic known to block leucine-rich NES-mediated export of endogenous cellular and exogenous viral proteins (LMB) had no effect on the apparent exclusively cytoplasmic localisation of DDX3 (data not shown). However, consistent with previous reports (Owsianka and Patel, 1999; You *et al.*, 1999b), subcellular fractionation experiments indicated a small quantity of DDX3 protein in the nucleus. This could suggest that DDX3 has a dual role in the cell. For example, DDX3 may be involved in cellular translation in the cytoplasm and pre-mRNA splicing in the nucleus. Alternatively, it may indicate the protein is involved in nucleocytoplasmic transport of cellular factors and/or RNAs. These possibilities regarding the function of DDX3 will be investigated in the following chapter. The nuclear form of DDX3 may also have implications for its interaction with core protein - core may exploit its interaction with this cellular protein to enter the nucleus, where it has been detected by several investigators (section 1.7.3). The localisation in hepatocytes of DDX3 carrying a mutation within the DEAD-box, a protein which shows a markedly diminished ability to hydrolyse dATP relative to the wild-type DDX3 (P. Askjaer and J. Kjems, personal

communication), was also studied. This protein did not localise to or form ring-like structures, but was distributed diffusely throughout the cytoplasm with some staining of globular structures. Western blotting of cell extracts previously transfected with the appropriate constructs indicated that the altered localisation of the DEAD-box mutant was not due to targeting of this functionally crippled protein for degradation. It therefore appears that this single amino acid change which greatly diminishes dATPase activity, and in all probability RNA helicase activity as a consequence, has a discernible effect on subcellular localisation as well. This implies that the enzymatic activity of DDX3 is linked to its subcellular targeting. Nevertheless, the DDX3 DEAD-box mutant maintained its ability to co-localise with core protein. Thus, neither the original subcellular location of DDX3 nor its enzymatic activity are apparently critical for its interaction with core protein. It is possible that since the DEAD-box motif of DDX3 is presumably in the active site of the protein (section 1.10.6), mutations in this area could potentially cause gross changes in conformation of the protein, which may have effects on cellular targeting of DDX3.

The biochemical properties of DDX3 were also investigated in this chapter. RNA helicases, and indeed all helicases, are believed to utilise the energy derived from the hydrolysis of ATP or other nucleotides to drive mechanical movement of bound RNA or DNA (section 1.10.1). To confirm that bacterially-expressed GST-DDX3 fusion protein was enzymatically active, it was assayed for its ability to hydrolyse an [α-^{32}P]-labelled dATP substrate. Free GST protein purified in parallel was employed as a negative control. The helicase domain of HCV NS3 (section 1.2.5.2) was cloned and expressed in the same manner as DDX3 to be used as an appropriate positive control in all enzymatic assays. GST-DDX3 hydrolysed ATP in a 'dose-dependent' manner, while free GST protein was not able to hydrolyse ATP. The NS3 helicase domain exhibited the same 'dose-dependent' hydrolysis of dTP, but appeared to be a more active protein in this hydrolysis. Thus it appears that (in the absence of cellular co-factors), per μg of protein, the HCV NS3 helicase domain purified as a GST-fusion protein is more efficient at hydrolysing dATP than DDX3 expressed by the same approach. Enzymatic breakdown of other nucleotide substrates by DDX3 have been investigated (You *et al.*, 1999b). DDX3 was able to

hydrolyse all NTPs, albeit at around half the activity of dNTPs. Of these, dATP appeared to be hydrolysed at a higher rate (You *et al.*, 1999b). Interestingly, it has also been reported that both DDX3 ATPase and dATPase activity is stimulated by HCV core protein (section 1.9.6.9; You *et al.*, 1999b). However, repeated attempts to emulate these results did not reveal the same effect (data not shown). It therefore appears that the two truncated core GST-fusion proteins (lacking aa 102-191 or 123-191) used by You *et al.* (1999b) are able to exert this effect, although the full-length core protein (aa 1-191) used here are unable to do so. While the aa 1-191 protein is not the mature form of core, it is detectable in mammalian cells (section 1.7.1), whereas the truncated forms have no relevance with regard to core protein expressed *in vivo*. Both DDX3 and NS3 helicase domain GST-fusion proteins were subsequently tested for their ability to unwind a non-specific double-stranded (ds) RNA substrate. While 10 μg GST-NS3 helicase domain protein was capable of unwinding approximately all of the dsRNA substrate, GST-DDX3 was consistently unable to unwind the substrate with the methodology used. Consistent with the lack of effect of core protein on dATPase activity of DDX3, helicase activity was not detected on addition of core protein to the reaction (data not shown). The reason for this lack of activity is unclear, although it is possible DDX3 may require a specific RNA sequence or a cellular co-factor to stimulate its helicase activity (section 1.10.7). On the other hand, the apparently inefficient hydrolysis of dATP by DDX3, relative to the NS3 helicase, may be consistent with its inability to unwind the duplex RNA substrate. This could be due to a poor yield of enzymatically active, properly folded and processed DDX3 from the bacterial system. Attempts were made to purify histidine-tagged DDX3 expressed by p6h-DDX3 (section 4.2.4) from mammalian cells, but sufficiently purified protein was not readily obtainable.

Valuable insights into DDX3 and its interaction with core protein have been given by the studies presented here. In the following chapter, functional assays for DDX3 in cell culture systems are described, while modulation of any effects of DDX3 in such assays by core protein is investigated to build on current knowledge of DDX3 and its interaction with core.

CHAPTER FIVE:

Functional Characterisation of DDX3 and its Interaction with Core Protein

5. 1 Introduction

Previously, DDX3 has been shown to bind HCV core protein *in vitro* (Fig. 33e; section 3.2.9) and to co-localise with this viral protein in a hepatocyte cell line also expressing HCV sub-genomic replicon RNA and HCV nonstructural proteins (Fig. 32; section 3.2.8). This co-localisation, which may be a result of redistribution of DDX3 in the presence of core protein, or may occur during post-translational modification of DDX3 in the ER, is not dependent on the presence of a putative NES (Fig. 56; section 4.2.8), or on the subcellular targeting or enzymatic function of DDX3 (Fig. 60; section 4.2.11). However, these studies have not ascertained whether the DDX3/core interaction is having discernible effects on expression or processing of DDX3, or indeed on core protein, in cell culture systems. To this end, the possibility that the HCV protein in some way modifies DDX3, or *vice versa*, was investigated. The full-length coding sequence for each protein were used to generate recombinant baculoviruses (rbacs), and expression of both proteins in the Sf21 insect cell line, either singly or in combination, was examined by Western blotting using specific MAbs and PAbs. The effect of expressing core protein on endogenous DDX3 was also investigated in a human hepatocyte cell line. Huh-7 (N) cells were infected with rVV-C-E1-E2, and their expression analysed as before by Western blotting.

However, these assays still do not delineate a possible role of DDX3 in replication or pathogenesis of HCV. Previous reports point to a role of DDX3 in translation in systems unrelated to HCV, or with non-specific substrates (Mamiya and Worman, 1999; You *et al.*, 1999b). These assays are described in some detail in section 1.9.6.9. Briefly, DDX3 was shown to i) rescue yeast cells containing an otherwise lethal mutation in its homologue Ded1p (Mamiya and Worman, 1999), a protein that is implicated in translation initiation (section 1.13.6), and ii) upregulate translation from a transfected reporter plasmid in Huh-7 cells (You *et al.*, 1999b). In both cases core protein modulated the observed effects - it was able to reverse the rescue of Ded1p mutant yeast expressing DDX3 (Mamiya and Worman, 1999), and, seemingly in contrast, markedly increased the level of reporter activity in hepatocytes (You *et al.*, 1999b). Here, DDX3 was investigated for its ability to

specifically alter translation of the HCV genome by alleviating a previously reported translational block of rbacs carrying the HCV 5'NCR in insect cells (section 1.3.4; Wang *et al.*, 1997). The possible effect of DDX3 on HCV 5'NCR-mediated translation was also examined in a transient-transfection assay in human hepatocytes. The effect of DDX3 expressed by plasmid, and co-expressed with core protein, on transiently-expressed CAT reporter gene in hepatocytes was also investigated, in view of the results of You *et al.* (1999b) (see above).

RNA helicases may be grouped into categories based on their function (section 1.12; de la Cruz *et al.*, 1999). These categories include translation, pre-mRNA splicing and RNA nucleocytoplasmic export. Although previous reports (Mamiya and Worman, 1999; You *et al.*, 1999b) necessitated that the role of DDX3 in translation was studied in greatest detail, attempts were also made to allocate DDX3 to other functional categories in which putative and known RNA helicases may be placed. Following identification of an 'RS'-like domain in the protein seqeunce of DDX3 (Owsianka and Patel, 1999; You *et al.*, 1999b) that is potentially invovled in protei-protein interactions with splicing factors (section 1.9.6.9), and subcellular fractionation experiments that suggested a small amount of DDX3 is present in the nucleus (Fig. 57a; section 4.2.9), the presence of the protein in purified spliceosome complexes was investigated. Such complexes were generously provided by Dr A. Lamond (University of Dundee). By analogy with the *X. laevis* DDX3 homologue An3 (Askjaer *et al.*, 2000), the effect of Huh-7 total RNA (and synthetic poly(A) RNA as a control) on dATPase activity of DDX3 was also examined. The presence of a specific RNA activator could have implications for the substrate specificity and therefore function of DDX3. For example, a specific upregulation of DDX3 dATPase activity by a subset of cellular RNA such as tRNA may implicate the protein in processing and/or export of these RNAs.

5. 2 Results

5.2. 1 Generation and Expression of DDX3 and Core Protein-expressing Rbacs

To further investigate expression of DDX3 and the functional significance of its interaction with core protein, coding sequences for both proteins were transferred to the pAcCL29.1 transfer vector (Fig. 65a; Livingstone and Jones, 1994) and used to generate appropriate rbacs (see Appendix III for a comprehensive list). The pAcCL29.1-DDX3 construct, generated by Dr A. Patel by transfer of DDX3 cDNA from pGEX-6P-3-DDX3 to the transfer vector, was used to create rbac-DDX3. This rbac is expected to produce full-length (aa 1-662) DDX3 protein and is shown schematically in Fig. 65b. HCV strain H77c in the pGEM 9zf(-) vector (pCV-H77c; Yanagi *et al.*, 1997) was used as a template to amplify the full-length HCV core-coding sequence (Appendix IV) using specific primers (see Appendix V). Since there is no stop codon following the core-coding sequence in the HCV ORF, a stop codon was engineered to immediately follow the coding sequence ensuring only full-length 191 aa core protein and its processed form were expressed. The rbac expressing full-length core protein was named rbac-C (Fig. 65b). Expression of DDX3 and core protein by rbacs-DDX3 and -C, respectively, in Sf21 cells is shown in Fig. 66. Consistent with previous data (Fig. 26; section 3.2.3), anti-DDX3 MAb AO196 did not detect any proteins in Sf21 total cell extracts by Western blotting (Fig. 66a, lane 1). Similarly, Sf21 cells infected with wild-type baculovirus were negative for DDX3 when tested with MAb AO196 (lane 2). However, in Sf21 cells infected with rbac-DDX3, protein of approximate molecular weight 73 kDa was detected using anti-DDX3 MAb AO196 (lane 3). Two closely migrating proteins were observed on shorter exposures (data not shown) similar to the two closely running proteins detected by the same antibody in human hepatocytes and other mammalian cell lines (Fig. 26; section 3.2.3). This pattern of expression by rbac suggests that the doublet band expressed in hepatocytes is more likely due to a property inherent in the protein rather than the presence of cellular isoforms produced from separate chromosomes as discussed previously (section 3.2.3). Nevertheless, this implies that processing of DDX3 expressed by rbac in insect cells is similar to that of endogenous DDX3 in human hepatocytes.

A

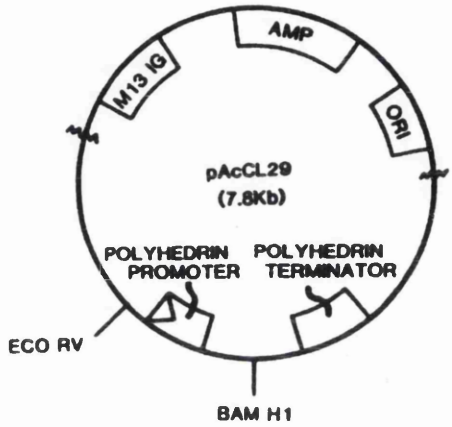

B

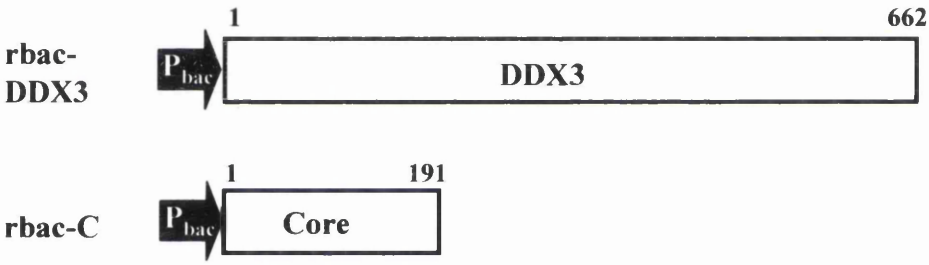

Figure 65: The baculovirus transfer vector used to generate rbacs. (A) Vector map of the pAcCL29 plasmid - pAcCL29.1, identical to pAcCL29 apart from the addition of further unique restriction sites at the *Bam*HI site, was used in generation of all rbacs in these studies. The location of the β-lactamase gene (AMP), the origin of replication (ORI), and baculovirus expression signals are indicated (taken from Livingstone and Jones, 1994). (B) Schematic diagram of rbacs-DDX3 and -C, carrying the full-length (aa 1-662 and 1-191, respectively) DDX3 and HCV core coding sequences, with expression driven by the baculovirus polyhedrin promoter (P_{bac}).

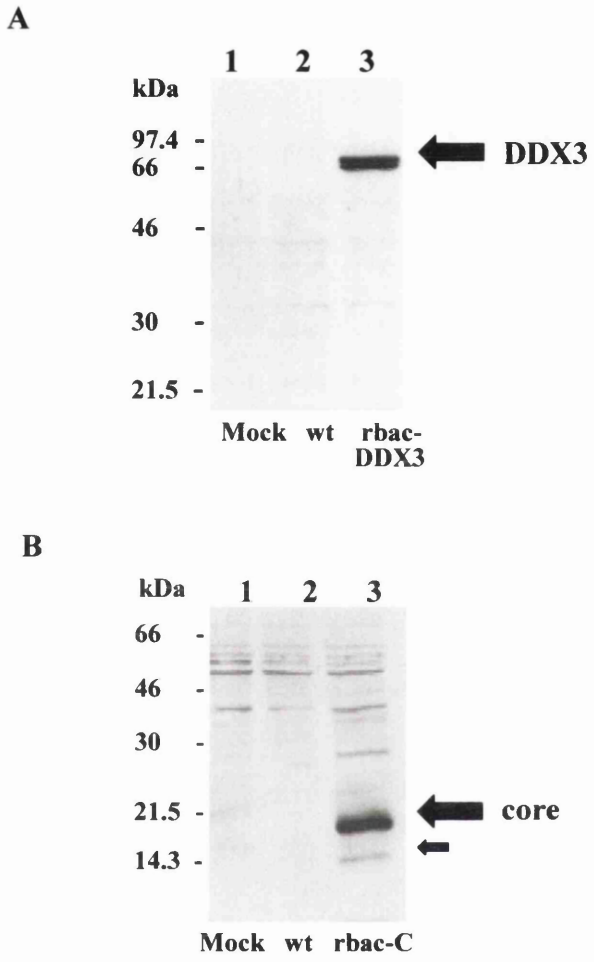

Figure 66: Detection of DDX3 and core protein expressed by rbac in an insect cell line. Sf21 cells were mock-infected (lane 1), or infected at m.o.i. of 0.5 with wild-type baculovirus (wt, lane 2), or infected at the same m.o.i. with (A) rbac-DDX3 (lane 3) or (B) rbac-C (lane 3). Following incubation at 28°C for 72 hours, cell extracts were prepared, fractionated by SDS-PAGE (9 and 12.5%, respectively), and immunoblotted with (A) anti-DDX3 MAb AO196 or (B) anti-core PAb R525.

Expression of core protein was investigated using anti-core PAb R525. This antisera was raised against HCV strain H77c full-length core (see Appendix I). PAb R525 showed weak affinity for proteins in mock-infected and wt-infected cell extracts (Fig. 66b, lanes 1-2). However, core protein similar to that described in other reports regarding its expression in insect cells (Wang *et al.*, 1997), with a major protein product detectable at 21 kDa, in addition to a smaller product at approximately 17 kDa, was detected in Sf21 cell extracts previously infected with rbac-C (Fig. 66b, lane 3). Both these products have previously been reported in mammalian cells (sections 1.7.1 and 1.7.4), suggesting core protein produced by rbac-C is appropriately processed in Sf21 cells. Thus, detection of DDX3 and core protein expressed by their respective rbacs in insect cells by Western blotting with specific antibodies, indicate that both proteins are processed in a similar manner to that seen in mammalian cells.

5.2. 2 Co-expression of DDX3 and Core Protein in Sf21 Cells

As detailed previously, core protein has been shown to interact with a multitude of cellular factors, and the resultant effects on the functions of some of these host cell proteins have been described (section 1.9.6). Given the multiple effects that these interactions could have on host cellular processes, it is plausible that core directly or indirectly modifies cellular proteins. However, there are currently no published reports of physical modification of cellular factors with which core has been shown to interact. To look for possible effects of core protein on targeting of DDX3 for degradation or modification of its post-translational processing, or indeed *vice versa*, both proteins were expressed by rbac in Sf21 cells either singly or in combination and their expression analysed by Western blotting. Here, DDX3 protein was detected by the previously characterised R438 PAb (sections 3.2.13, 3.2.14, and 3.2.18; Owsianka and Patel, 1999) raised against GST-DDX3C protein (section 3.2.12; aa 409-662). This PAb detects DDX3 expressed as a GST-fusion protein (Fig. 36a; section 3.2.13), and more importantly, detects endogenous DDX3 in hepatocyte and non-hepatocyte cell lines (Fig. 42; section 3.2.18). Consistent with previous data using anti-DDX3 MAb AO196 (Fig. 66a; section 5.2.1), PAb R438 did not react with any cellular factors in mock-infected or wild-type infected Sf21

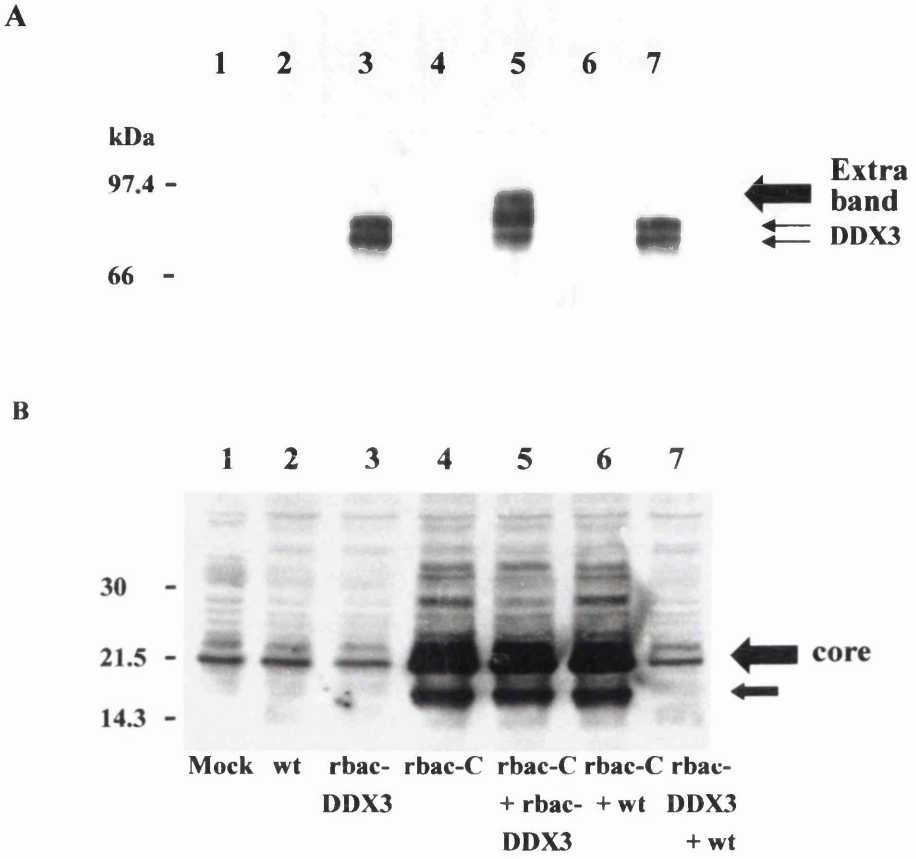

Figure 67: Effect of core protein on expression of DDX3 by rbac in insect cells. Sf21 cells were mock-infected (lane 1), or infected at m.o.i. of 0.5 with wild-type (wt) baculovirus (lane 2), or infected at the same m.o.i. with rbacs either singly or in combination with wt or other rbacs (lanes 3-7). Following incubation at 28°C for 72 hours, cell extracts were prepared, fractionated by SDS-PAGE, and immunoblotted with (A) anti-DDX3 MAb AO196 or (B) anti-core PAb R525.

cell extracts (Fig. 67a, lanes 1 and 2). However, R438 was able to detect a protein corresponding to the molecular weight for DDX3 in Sf21 cell extracts previously infected with rbac-DDX3 (lane 3). The closely migrating DDX3 species are better resolved here since the gel was run further than normal. Intriguingly, co-expression of core protein with DDX3 led to the appearance of a further band above the doublet of DDX3 (Fig. 67a, lane 5). This band is unlikely to be DDX3 bound to core protein as this protein-protein interaction would be disrupted by the denaturing conditions of SDS-PAGE. The same effect was seen when core protein was expressed in the context of HCV glycoproteins E1 and E2, as it would be during natural infection (A. Patel, unpublished). To rule out the possibility that this extra band is produced as a result of co-expression of rbac-DDX3 with another baculovirus, rbac-DDX3 was co-infected with the wild-type baculovirus. There was apparently no effect of co-expressing wt baculovirus proteins on DDX3 expression (Fig. 67a, lane 7). Similarly, co-infection of Sf21 cells with rbac-DDX3 and other rbacs did not generate the extra higher molecular weight DDX3 band (data not shown). Potentially, this altered expression of DDX3 represents modified processing of DDX3 in the presence of core protein. Expression of the core protein in Sf21 cells infected with rbac-C or co-infected with rbacs-C and -DDX3 was confirmed with anti-core PAb R525 (Fig 67b). There were apparently no effects of DDX3 on the expression of core protein as detected by this antisera. The above data implicate HCV core in modification of a human cellular protein.

5.2. 3 Effect of Core Protein Expression on DDX3 in Hepatocytes

To determine whether the higher molecular weight isoform of DDX3 is produced in the presence of HCV core in human hepatocytes, Huh-7 cells were infected with the previously described rVV-C-E1-E2 (section 3.2.6; see Appendix III). As controls, Huh-7 cells were either mock-infected, or infected with rVV expressing E1 and E2 alone (rVV-E1-E2). Following infection, cell extracts were prepared and analysed by Western blotting. As above, endogenous DDX3 was detected by anti-DDX3 PAb R438. In mock-infected cells, DDX3 was again detected as a doublet (Fig. 68a, lane 1). While infection of cells with rVV-E1-E2 did not alter the banding pattern of DDX3 as detected by R438 (lane 2), infection of cells with rVV-C-E1-E2 gave rise

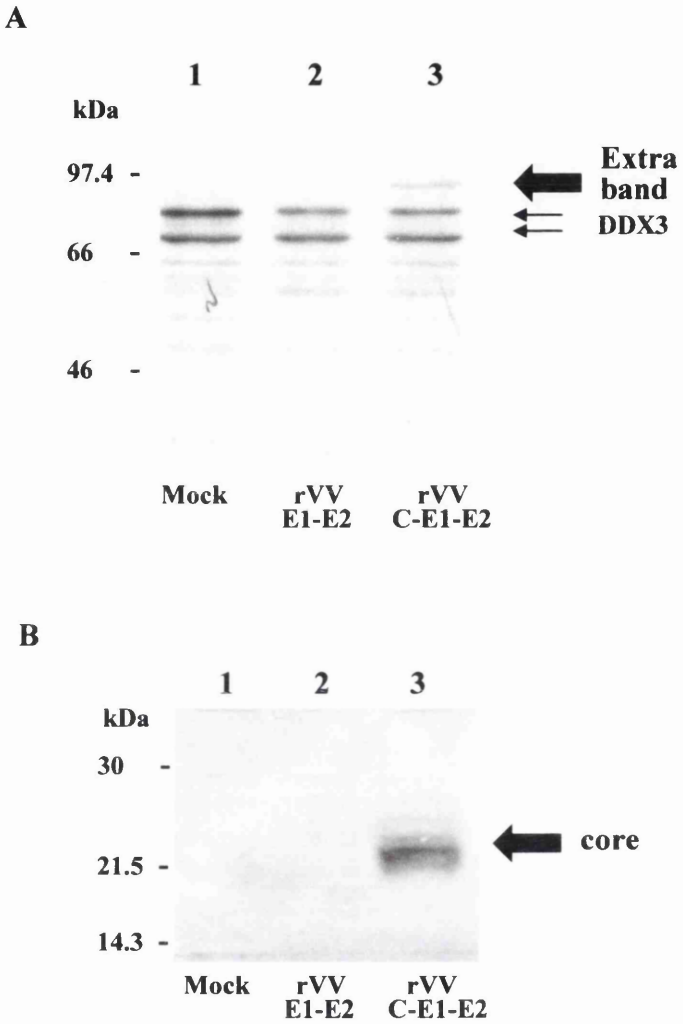

Figure 68: Effect of core protein on expression of endogenous DDX3 in hepatocytes. Huh-7 cells were mock-infected (lane 1), or infected at m.o.i. of 5 with rVV-E1-E2 (lane 2), or infected at the same m.o.i. with rVV-C-E1-E2 (lane 3). Following incubation at 37°C for 16 hours, cell extracts were prepared, fractionated by SDS-PAGE, and immunoblotted with (A) anti-DDX3 MAb AO196 or (B) anti-core PAb R525 (lanes 4-6).

to a third band above the doublet (lane 3), consistent with the results seen in insect cells following co-infection of DDX3 and core-expressing rbacs. Expression of core protein was confirmed by probing the same cell extracts with anti-core PAb R525 (Fig. 68b). Further investigation into the mechanism by which core protein exerts this effect on DDX3 is required to fully understand the significance of the observed result, but it is a further indication that the DDX3/core interaction is genuine.

5.2. 4 Effect of Core Protein Expression on DDX3 mRNA

As part of a comprehensive investigation of the effect of core protein on DDX3, possible modification of DDX3 mRNA in the presence of core protein or its coding sequence was investigated by Northern blot analysis. Huh-7 (N) or H9-13 cells were mock-infected, or infected with rVV-E1-E2 or with rVV-C-E1-E2. Following incubation at 37°C for 16 hours, cells were washed, total RNA prepared, and analysed by Northern blotting using a ^{32}P-labelled probe directed against nt 1-624 of the DDX3 coding sequence (previously described in section 3.2.1). As shown in Fig. 69a, expression of core in the context of HCV glycoproteins E1 and E2 had no effect on expression of DDX3 mRNA in either Huh-7 (N) cells (lane 3), or in H9-13 cells (lane 7) previously shown to contain self-replicating HCV sub-genomic RNA and nonstructural proteins (Figs 30 and 31; section 3.2.7). This indicated that the effect of core on the banding pattern of DDX3 detected in Western blots with anti-DDX3 PAb R438 (Figs 67 and 68; see above) was not occurring at the RNA level. However, it appeared that, for unknown reasons, infection of cells with rVV-E1-E2 reduced amount of DDX3 mRNA (Fig. 69a; lanes 4 and 8). The significance of this effect is unclear at this time. To confirm the integrity of the extracted RNA and verify that equal amounts of RNA were loaded, a ^{32}P-labelled probe originating from cellular ubiquitin cDNA (section 3.2.2) was hybridised to the same membrane following stripping. Accordingly, concurrent levels of ubiquitin mRNA expression in each extract previously infected with a wild-type VV (Western Reserve, WR) or rVV were detected by this probe (Fig. 69b, lanes 2-4 and 6-8). The apparent decrease in DDX3 and ubiquitin mRNA levels in these samples relative to the mock-infected samples (lanes 1 and 5) may be due to down-regulation of cellular transcription in the presence of vaccinia virus, or alternatively reflects the lower

A

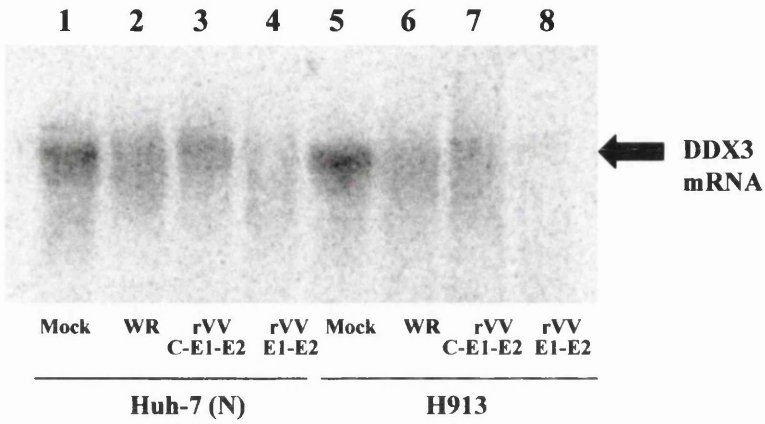

B

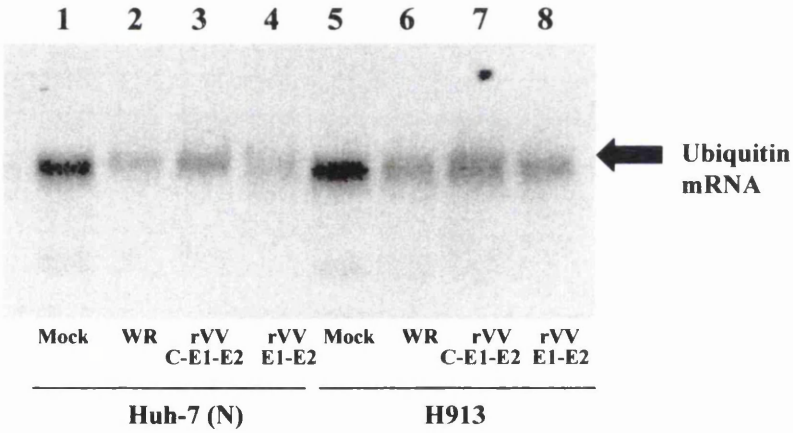

Figure 69: Effect of core protein or its coding sequence on expression of DDX3 mRNA in Huh-7 (N) and H913 cells. Cells were mock-infected (lane 1), infected at m.o.i. of 5 with a wild-type VV (Western Reserve, WR, lanes 2 and 6), or infected at the same m.o.i. with rVV-C-E1-E2 (lanes 3 and 7) or rVV-E1-E2 (lanes 4 and 8) as shown. Following incubation at 37°C for 24 hours, total RNA was extracted from cells and subjected to Northern blot analysis with a ^{32}P-labelled probe specific for (A) nt 1-624 of DDX3 or (B) ubiquitin (Clontech).

fraction of mRNA coding for cellular proteins in total RNA extracted from cells expressing high levels of rVV-derived mRNA.

5.2. 5 Generation of Rbacs for Investigation of HCV 5'NCR-mediated Translation in Insect Cells

A previous report suggested that the HCV 5'NCR is not functional in Sf21 cells (section 1.3.4; Wang *et al.*, 1997). While rbacs carrying the core-coding sequence alone produced core protein of the expected molecular weight, rbacs containing the HCV 5'NCR fused to core protein did not. The reason for this phenomenon was not a lack of transcription from the 5'NCR-core rbac, as the appropriate transcript was produced in large amounts and could be translated *in vitro* (Wang *et al.*, 1997). A speculative reason for the block in translation is that viral or cellular protein(s) are lacking in insect cells which allow translation of 5'NCR-containing rVVs or transfected plasmid constructs or RNAs in mammalian cells. If true, this could be exploited as a novel system to investigate the effect of supplying recombinant proteins *in trans* on HCV 5'NCR-mediated translation. DDX3 could be one of the factors lacking in insect cells that leads to the HCV 5'NCR-mediated block in translation. Preliminary data suggested a closely related homologue of DDX3 was not present in insect cells (Figs 22b and 26; sections 3.2.1 and 3.2.3), and the protein has already been implicated in translation using yeast and mammalian cell assays (section 1.9.6.9; Mamiya and Worman, 1999; You *et al.*, 1999b).

To investigate this system, primarily with a view to exploiting it as a functional assay for DDX3, a number of rbacs were generated. Core protein produced from a 5'NCR-core containing rbac was used as a reporter to determine whether DDX3 could relieve the translational block. If DDX3 expressed by rbac has an effect on translation from the HCV 5'NCR, core protein will be produced and may be detected by Western blotting using specific antibodies. Further rbacs containing the bacterial chloramphenicol acetyl-transferase (CAT)-coding seqeunce as a reporter gene were generated to investigate the effect of core protein supplied *in trans* on translation from the 5'NCR, in the presence and absence of DDX3. CAT protein

levels were determined by qualitative or quantitative measurements of CAT activtiy using [^{14}C]-labelled chloramphenicol (section 2.42). Rbac-DDX3 and rbac-C, previously described in section 5.2.1, were used to supply the proteins under investigation. Schematic diagrams of the rbacs containing HCV sequences used in this study are shown in Fig. 70. HCV strain H77c, a genotype 1a infectious clone (Yanagi *et al.*, 1997), was used to construct these rbacs in pAcCL29.1. The HCV nt numbers (corresponding to the sequence presented in Appendix IV) and the expected transcript of each rbac are shown in Table 2. In all cases the full-length H77c 5′NCR and coding sequences were used. Similarly, rbacs as indicated in Table 2 carried the the full-length H77c 3′NCR, fused immediately downstream of the CAT-coding sequence.

Rbac	*HCV Strain H77c Nucleotide Number*	*Expected Transcript/ Product*
C	342-915	core
CC	342-915	core-CAT
5C	1-915	5′NCR-core
5C3	1-915, 9375-9599	5′NCR-core-3′NCR
5CC	1-915	5′NCR-core-CAT
5CC3	1-915, 9375-9599	5′NCR-core-CAT-3′NCR

Table 2: HCV nucleotide numbers and expected transcripts produced by rbacs used to determine role of DDX3 and core protein in HCV 5′NCR-mediated translation.

Rbac-C contains full-length (aa 1-191) core protein followed by a stop codon at aa 192, as described in section 5.2.1. Rbac-5C contains the 5′NCR followed by full-length core-coding sequence placed downstream of the baculovirus promoter. Rbac-5C3 is identical to rbac-5C, except for the addition of the 3′NCR placed downstream from the core-coding sequence. Rbacs-CC, -5CC and -5CC3 were produced by fusing the CAT gene in frame with the relevant HCV sequences. All

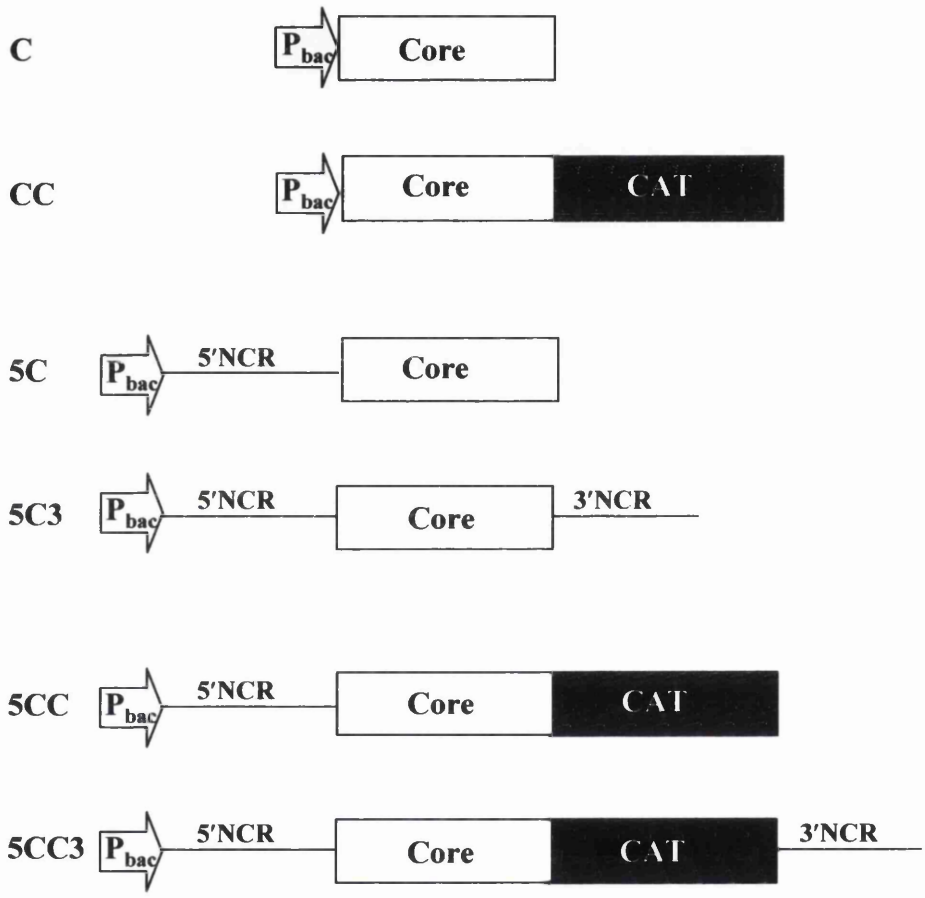

Figure 70: Schematic diagram of rbacs containing HCV sequences used to determine effect of expressing recombinant proteins *in trans* on HCV 5'NCR-mediated translation. Relevant sequences as shown were fused downstream of the baculovirus polyhedrin promoter (P_{bac}). The co-ordinates of HCV sequences in these constructs is shown in Table 2.

rbacs were amplified and purified by standard protocols (section 2.37) to produce high titre stocks (~10^{10} pfu ml^{-1}). These stocks were used to infect ~$2x10^6$ Sf21 cells at m.o.i of 0.5 per virus. Increasing m.o.i. was found to give only slight experimental variations (data not shown). Following incubation at 28°C for 72 hours, cells were harvested and tested for expression of appropriate proteins by Western blotting using anti-core PAb R525. Sf21 cells were either mock-infected or infected with the wild type baculovirus (wt) or with rbacs. As expected, rbac-C produced the core protein of approximately 21 kDa in infected cells (Fig. 71a, lane 7). Furthermore, rbac-CC expressed a core-CAT fusion product most of which was cleaved into the individual core and CAT products (lane 8). The molecular weight of the cleaved core was identical to that produced by rbac-C (lane 8) indicating that the cleavage takes place at the authentic signal peptidase cleavage site within core. The presence of the cleaved CAT product in rbac-CC infected cells was confirmed using an anti-CAT PAb (Fig. 71b, lane 8). In contrast, rbacs-5C, -5C3, -5CC, and -5CC3, all of which carry the HCV IRES, failed to synthesise detectable levels of core or core-CAT fusion product in infected cells (Figs 71a and b, lanes 3-6), consistent with the previous report suggesting that the HCV IRES is non-functional in Sf21 cells (Wang *et al.*, 1997). However, rbac-5CC produced a small amount of what appeared to be CAT protein as detected by the anti-CAT PAb (Fig. 71b, lanes 5) suggesting the translational block, at least regarding this rbac, is leaky. PAb R525 may require a larger amount of its target protein to allow detection by Western blotting.

5.2. 6 Further Investigation of an Apparent Block in HCV 5'NCR-mediated Translation in Insect Cells

Although the HCV 5'NCR is functionally inoperative in Sf21 cells, it is known to be active in mammalian cell lines (for example, Honda *et al.*, 2000). To further confirm the results of Wang *et al.* (1997) (section 5.2.5), production of core protein from mammalian expression constructs with and without the 5'NCR fused upstream of the core-coding sequence (generated by J. Wood; see Appendix II) in two separate cell lines was compared with expression of rbacs-5C and -C in Sf21 cells. Huh-7 and COS-7 cell lines were either mock-transfected, or transfected with a DNA

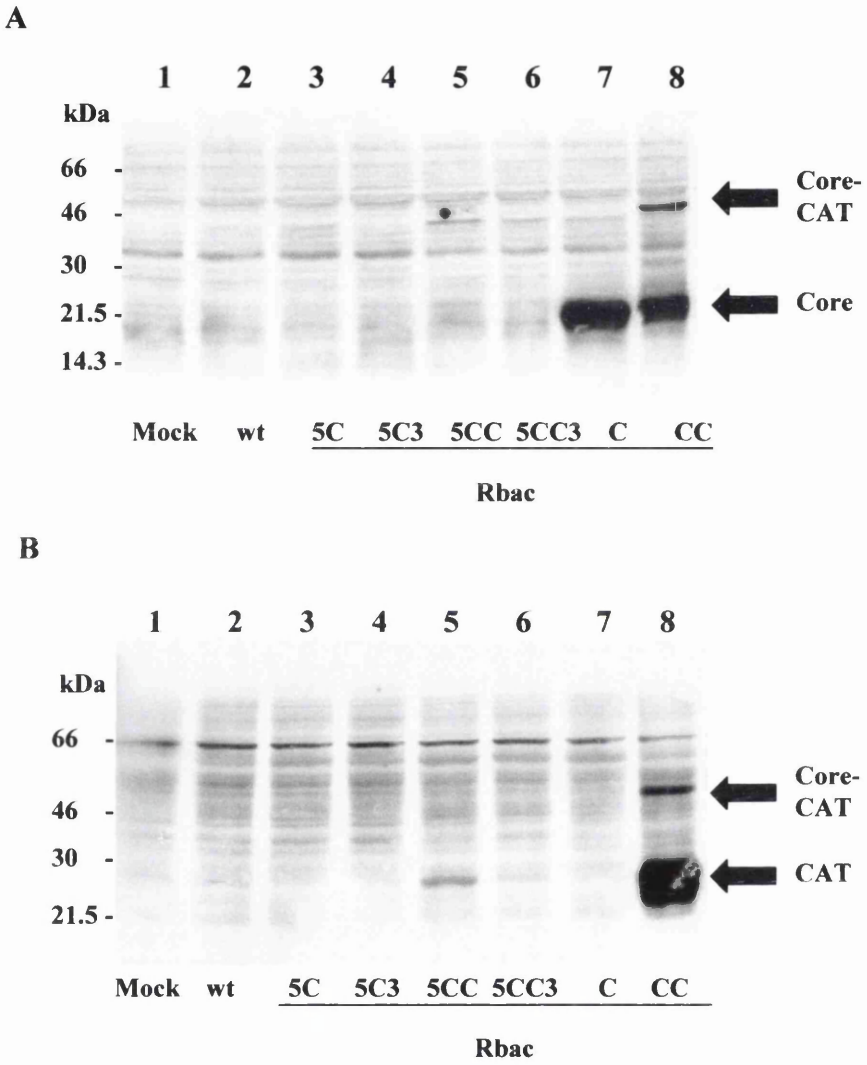

Figure 71: Detection of core or core-CAT fusion protein expressed by rbacs shown in Fig. 70. Sf21 cells were mock-infected (lane 1), infected with wild-type baculovirus (wt; lane 2), or with rbacs as shown (lanes 3-8). Following incubation at 28°C for 72 hours, cell extracts were prepared, fractionated by SDS-PAGE, immunoblotted with (A) anti-core PAb R525 or (B) an anti-CAT PAb.

construct in pcDNA 3.1/Zeo(+) containing the core-coding sequence (pcDNA-C), or transfected with a similar construct carrying the 5′NCR upstream of core (pcDNA-5C) (Fig. 72a). While mock-transfected Huh-7 or COS-7 cells were negative when probed with anti-core PAb R525 by Western blotting (Fig. 72b and c, lane 1), core protein of the expected molecular weight (~21 kDa) was detected in cells transfected with plasmid pcDNA-C (lane 2). Similarly, transfection of Huh-7 or COS-7 cells with pcDNA-5C also led to the production of core protein (lane 3). Interestingly, the level of translation in Huh-7 cells from the 5′NCR-containing construct was far greater than that without the 5′NCR (Fig. 72b, lanes 2 and 3, respectively), whereas this trend was reversed in COS-7 cells (Fig. 72c). This suggests there is a hepatocyte-specific upregulation of translation in the presence of the 5′NCR. It is also possible that this phenomenon is cell-cycle related (Honda *et al.*, 2000). Nevertheless, as described previously (section 5.2.5), infection of Sf21 cells with rbacs carrying the HCV 5′NCR fused to the core-coding sequence did not produce detectable levels of core protein, while infection of Sf21 cells with rbac lacking the 5′NCR but containing the core coding sequence produced core (Figs 72b and c, lanes 5 and 6).

To confirm the reported finding that this lack of core protein was not due to lack of transcription from the 5′NCR-core virus (Wang *et al.*, 1997), RNA was extracted from Sf21 cells infected with the same rbacs, and the presence of 5′NCR-containing transcripts was verified. As shown in Fig. 73, a ^{32}P-labelled probe derived from an *Age*I/*Apa*L1 restriction fragment of pCV-5CC (see Appendix II) corresponding to HCV nt 155-336 within the 5′NCR (see Appendix IV) detected a transcript from Sf21 cells infected with the 5′NCR-core virus, but not from Sf21 cells infected with the wild-type baculovirus. Thus, although appropriate transcripts are generated, the HCV IRES is not able to drive translation of downstream sequences in insect cells.

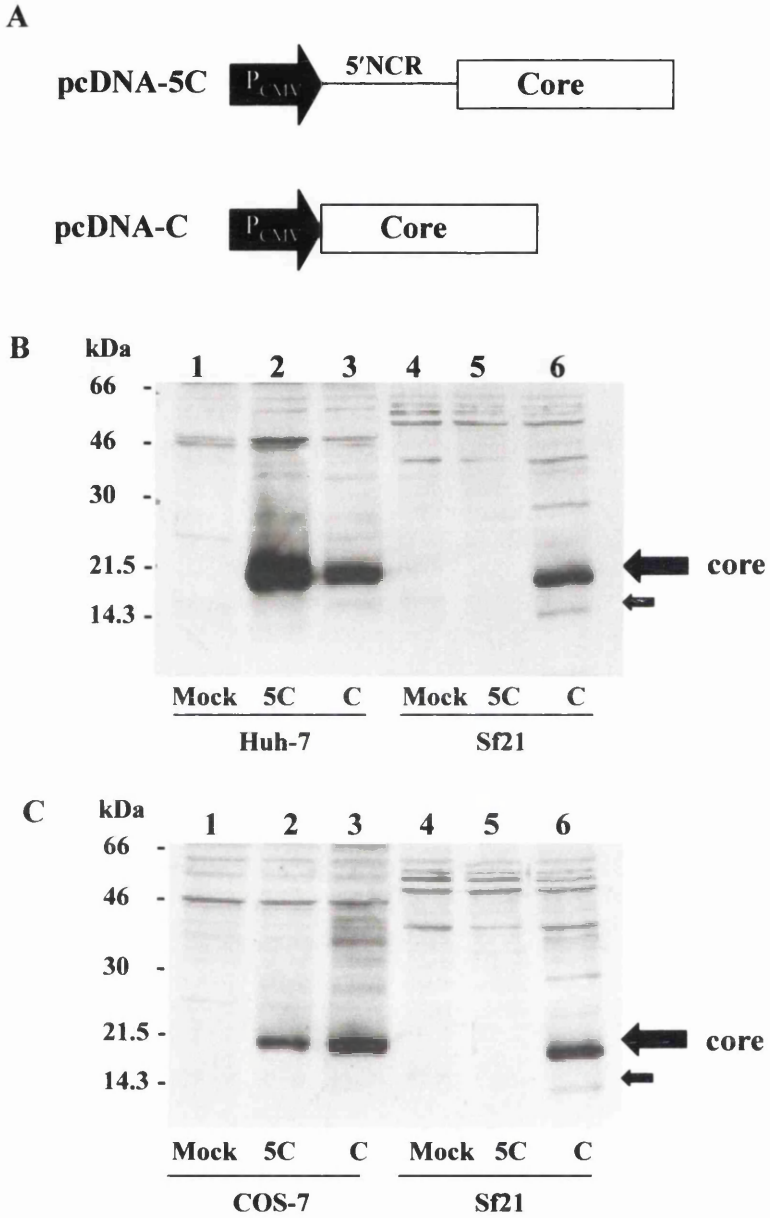

Figure 72: Further confirmation of an apparent block in HCV 5'NCR-mediated translation in insect cells but not in mammalian cells. (A) Schematic representation of mammalian expression constructs used. (B) Huh-7 or (C) COS-7 cells were mock-transfected, or transfected with mammalian expression vectors containing 5'NCR-core (HCV nt 1-915), or the core coding-sequence alone (HCV nt 342-915), as shown in panel (A) (lanes 1-3). Lanes 4-6 in each panel: Sf21 cells were mock-infected, or infected with rbacs as shown. Transfected or infected total cell extracts (15 μg) were fractionated by SDS-PAGE (12.5%) and immunoblotted with anti-core PAb R525.

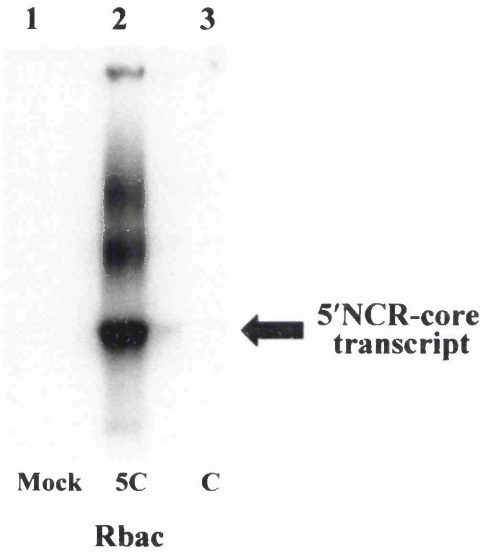

Figure 73: Confirmation of 5′NCR-core transcript expression by rbac-5C. Sf21 cells were mock-infected (lane 1), or infected at m.o.i. of 0.5 with rbac-5C (lane 2) or rbac-C (lane 3). Following incubation at 28°C for 72 hours, total RNA was extracted from cells and subjected to Northern blot analysis using a ^{32}P-labelled probe derived from a 5′NCR *Age*I/*Apa*LI restriction fragment (nt 155-336 of HCV strain H77c; see Appendix IV).

5.2. 7 Western Blotting of Mock-infected and Rbac-DDX3 Infected Sf21 Cell Extracts Probed with a Panel of DDX3 MAbs

It was hypothesised that since a closely related DDX3 homologue may not be present in insect cells (Figs 22b and 26; sections 3.2.1 and 3.2.3), a lack of this cellular factor may be responsible for the block in HCV 5'NCR-mediated translation in insect cells. To verify that Sf21 cells lack a closely related homologue of DDX3, the full panel of anti-DDX3 MAbs and PAbs were used to probe mock-infected Sf21 cell extracts. Sf21 cell extracts previously infected with rbac-DDX3 were probed with the same panel of antibodies as a positive control to determine whether any of the MAbs or PAbs could detect DDX3 expressed by rbac-DDX3. As shown in Fig. 74a, none of the MAbs tested detect a DDX3 homologue in Sf21 cell extracts. Interestingly, however, both AO2 and AO35 detected a 46 kDa protein in Sf21 total cell extracts (lanes 1 and 5), the same size as the putative truncated form of DDX3 detected by the same MAbs in Huh-7 (N) total cell extracts (Fig. 42; section 3.2.18). Anti-DDX3 PAb R648 detected a band at approximately the correct molecular weight for DDX3, but it had high backgorund (Fig. 74a, lane 9). In agreement with previous data (Fig. 67a; section 5.2.2), PAb R438 did not detect a DDX3 homologue in Sf21 cell extracts (lane 19). These data indicate that a closely related homologue of DDX3 does not exist in Sf21 cells. As would be expected given previous results (Figs 42 and 66a; sections 3.2.18 and 5.2.1), anti-DDX3 MAbs AO166 and AO196, and both PAbs (R438 and R648), detected DDX3 expressed in Sf21 cells by rbac-DDX3 (Fig. 74b, lanes 9, 12, 18 and 19, respectively). In addition, MAbs AO2 and AO35 were also able to detect DDX3 expressed by rbac (lanes 1 and 5), although they did not interact with endogenously-expressed full-length DDX3 in hepatocyte cell extracts (Fig. 42; section 3.2.18). AO190, which did not detect DDX3 by Western blotting with hepatocyte cell extracts (Fig. 42; section 3.2.18), showed affinity for a protein of the same molecular weight as DDX3 produced by rbac-DDX3 (Fig. 74b, lane 15). In fact, on closer inspection of lower exposure blots, this antibody seemingly only detected a protein as a single band of molecular weight intermediate between the doublet detected by MAbs AO166 or AO196 (data not shown). AO34 appeared to detect a protein of slightly lower molecular weight than DDX3 in both mock-infected Sf21

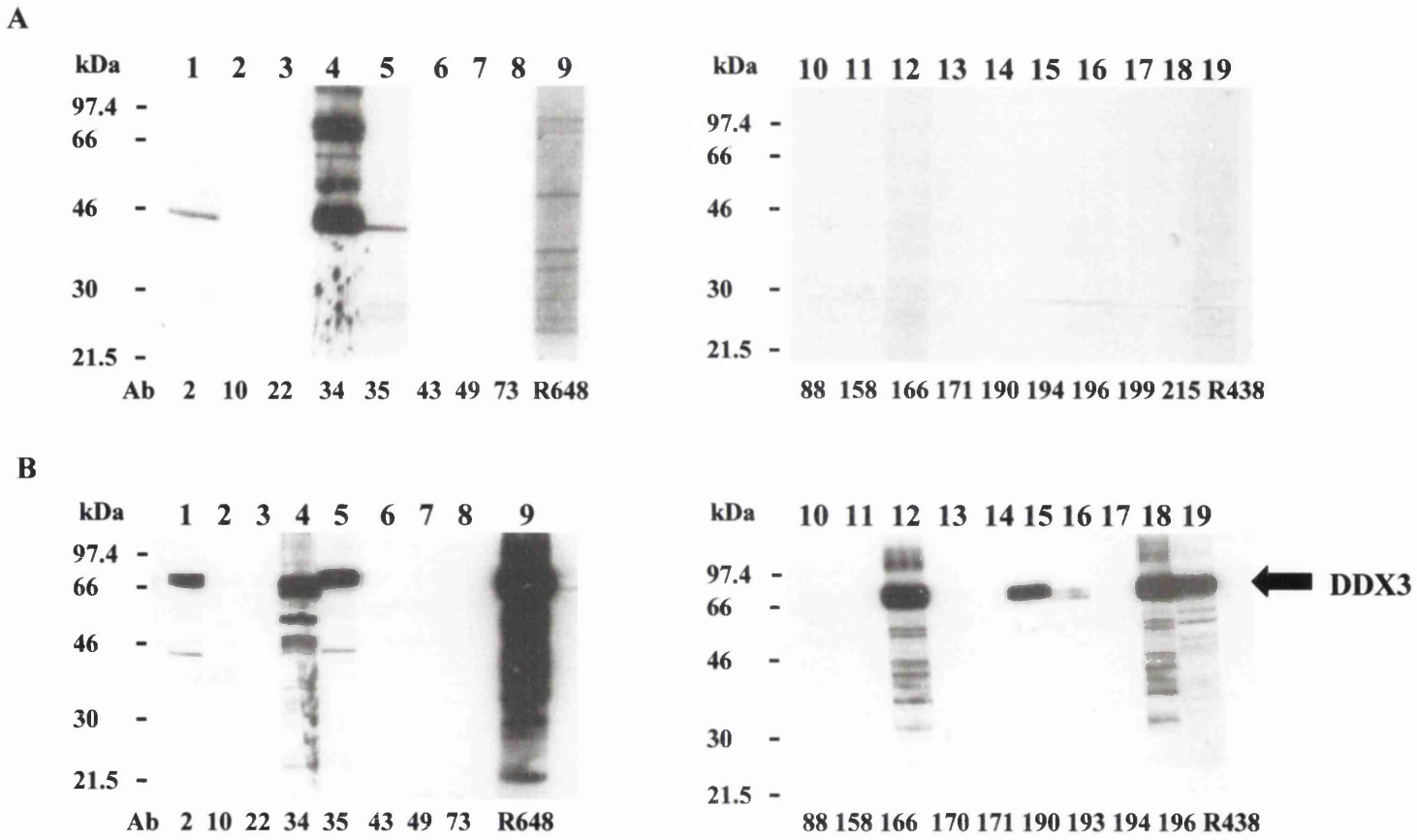

Figure 74: Detection of expression from rbac-DDX3 in an insect cell line. Sf21 cells were either mock-infected (A) or infected with rbac-DDX3 (B). At 72 hours post-infection, cell extracts were prepared and 50 μg total protein of each fractionated by SDS-PAGE (8%) and immunoblotted with different anti-DDX3 Mabs.

cells and Sf21 cells infected with rbac-DDX3 (Figs 74a and b, lane 4). MAb AO193 also very weakly interacted with two closely migrating bands in rbac-DDX3-infected Sf21 cell extracts, although this was of slightly lower molecular weight to that detected by the other MAbs described above.

5.2. 8 Effect of DDX3 on HCV 5'NCR-mediated Translation in Insect Cells

Following confirmation that Sf21 cells lack a closely related homologue of DDX3 as determined by Western blotting, the possible effect of DDX3 on IRES-mediated translation of HCV core was investigated. Sf21 cells were either mock-infected, infected with wild-type baculovirus, or with rbac-C, -5C, or -5C3 either alone or together with rbac-DDX3. Following incubation at 28°C for 72 hours, cell extracts were prepared and analysed for DDX3 or HCV core protein synthesis by Western blotting using anti-DDX3 MAb AO196 and anti-core PAb R525, respectively. As before, the antibodies failed to recognise DDX3 or core in mock- and wild-type-infected Sf21 cells (Figs 75a and b, lanes 1 and 2). In rbac-DDX3 or rbac-C infected cells, DDX3 and core protein were detected by AO196 (Fig. 75a, lane 4) and R525 (Fig. 75b, lane 3), respectively, as shown previously (Figs 66a and 66b; section 5.2.1). Furthermore, no detectable levels of core protein were seen in Sf21 cells infected with rbac-5C and -5C3 (Fig. 75b, lanes 5 and 6) as before (Fig. 71a; section 5.2.5). Interestingly, however, both of these rbacs synthesised a small quantity of core in cells co-infected with rbac-DDX3 (Fig. 75b, lanes 9 and 10). Seemingly less core protein was produced in the presence of the 3'NCR (lane 11). These results indicate that DDX3 expressed by rbac is able to slightly relieve the block in IRES-mediated translation of core in insect cells. A role for DDX3 in HCV IRES-mediated translation would be consistent with the findings of others that it can rescue yeast cells with a lethal mutation in its homologue *ded1* gene (section 1.9.6.9; Mamiya and Worman, 1999) which is known to be involved in translational initiation (1.13.6; Chuang *et al.*, 1997).

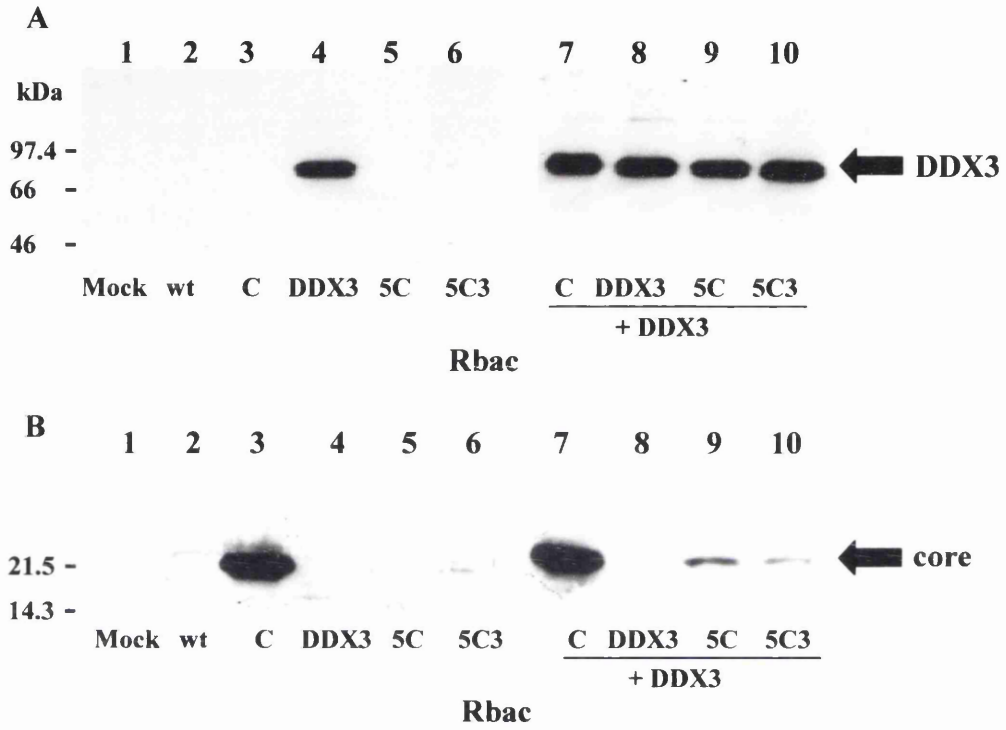

Figure 75: Effect of DDX3 on translation from HCV 5′NCR-carrying rbacs. Sf21 cells were mock-infected (lane 1), infected with wild-type baculovirus (wt; lane 2), or with rbacs either singly (lanes 3-6) or in combination with rbac-DDX3 (lanes 7-10) as shown. Following incubation at 28°C for 72 hours, cell extracts were prepared, fractionated by SDS-PAGE, and immunoblotted with MAb (A) anti-DDX3 MAb AO196 or (B) anti-core PAb R525.

5.2. 9 Effect of DDX3 on Transcription of HCV 5'NCR-containing Rbacs

To determine whether the effect of DDX3 on translation of the 5'NCR-containing rbacs was due to increased transcription, total RNA from mock-infected Sf21 cells or cells previously infected with wild-type baculovirus or with rbac-DDX3, -5C, or -5C together with rbac-DDX3, was extracted and investigated by Northern blot analysis. Each sample containing 10 μg total RNA was fractionated and subjected to Northern blotting as before using a ^{32}P-labelled probe derived from an *AgeI/ApaL1* restriction fragment within the 5'NCR (section 3.2.7). This probe was able to detect 5'NCR-core transcripts in total RNA from rbac-5C singly-infected cells (Fig. 76a, lane 4), but not in total RNA from mock-infected (lane 1), wt-infected (lane 2) or rbac-DDX3-infected (lane 3) Sf21 cells. Crucially, there was no apparent increase in 5'NCR-core transcripts in total RNA extracted from Sf21 cells co-infected with rbac-5C and rbac-DDX3 (lane 5). In fact, qualitative analysis of 5'NCR-containing RNA transcripts produced from rbac-5C infected cells suggested an slight decrease in the presence of DDX3 transcripts, although this could be consistent with competition of co-infecting rbacs for cellular machinery needed for viral processes. The same total RNA samples were subjected to Northern blot analysis with a ^{32}P-labelled probe originating from nt 1-624 of the DDX3 coding sequence described previously (section 3.2.1) to confirm expression of DDX3 mRNA from rbac-DDX3. This probe was able to detect DDX3 mRNA at similar levels in total RNA samples expected to express this transcript (Fig. 76b, lanes 3 and 5), but did not detect transcripts in any of the other samples (lanes 1, 2 and 4). These data confirm that the effect of DDX3 on translation of HCV 5'NCR-containing rbacs does not occur at the transcriptional level.

5.2. 10 Effect of Core Protein on HCV 5'NCR-mediated Translation in Insect Cells

To test the possible effect of core protein on IRES-dependent translation, rbacs described previously (Fig. 70; section 5.2.5) carrying HCV 5'NCR linked core-CAT fusion protein-encoding sequences both in the presence and absence of 3'NCR were used. Sf21 cells were either infected singly with rbac-5C, -5C3, -5CC, -5CC3 or -C, or co-infected with these viruses and rbac-C. Following incubation at 28°C for 72

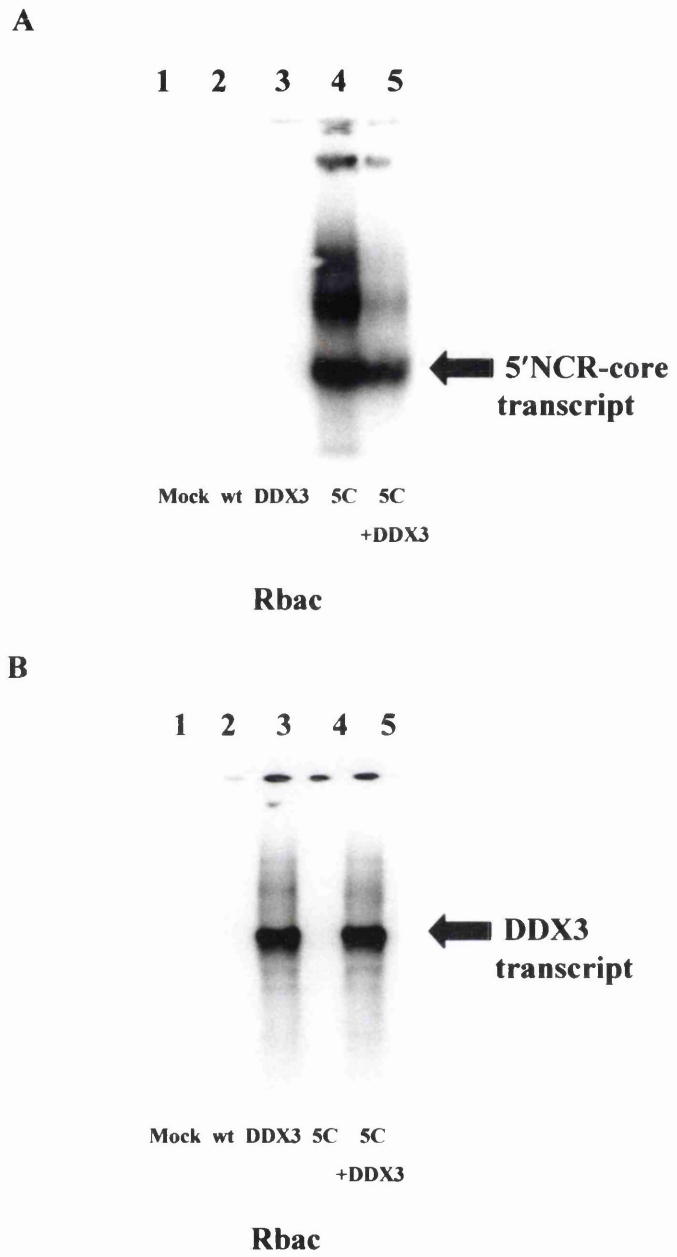

Figure 76: Effect of DDX3 expression on transcription from HCV 5′NCR-carrying rbacs in insect cells. Sf21 cells were mock-infected (lane 1), or infected with wild-type baculovirus (wt, lane 2), or with rbacs either singly (lanes 3-4) or in combination with rbac-DDX3 (lane 5) as shown. Total RNA was extracted following incubation at 28°C for 72 hours, fractionated, and analysed by Northern blotting using ^{32}P-labelled probes derived from (A) a ~180 nt HCV 5′NCR *Age*I/*Apa*LI restriction fragement or (B) DDX3 nt 1-624.

hours, cell extracts were prepared and their total protein concentration determined. Each extract containing 25 μg total protein was assayed for CAT activity using [^{14}C]-labelled chloramphenicol as described (section 2.42). Acetylated products were visualised and quantitated as described in section 2.27.6. No significant CAT activity was seen in Sf21 cells infected, either singly with rbac-5C, -5C3, or -C, or in combination with these rbacs and rbac-C (Fig. 77), not surprisingly as these viruses lack the CAT-coding sequence. However, both rbac-5CC and rbac-5CC3 also failed to produce CAT activity that was above background levels (Fig. 77), which is consistent with the non-functionality of HCV 5′NCR-mediated translation in the insect cell system. In contrast, upon co-infection of Sf21 cells with rbac-C and rbac-5CC, there was a 3.2-fold increase in the levels of CAT activity (Fig. 77) indicating that HCV core (or its coding sequence) alone can activate IRES-mediated translation in Sf21 cells. Interestingly, only a small increase in the levels of CAT was seen in cells co-infected with rbac-C and rbac-5CC3 (Fig. 77), indicating that the 3′NCR may downregulate this effect of core protein (or its RNA) on HCV IRES-mediated translation. To confirm these data, the CAT assay samples as above were subjected to Western immunoblotting using anti-core PAb R525 or an anti-CAT PAb. As before, rbac-C produced the core protein of approximately 21 kDa in infected cells (Fig. 78a, lane 7) and rbac-CC expressed a core-CAT fusion product most of which was cleaved into the individual core and CAT products (lane 8). In contrast, rbacs-5C, -5C3, -5CC, and -5CC3, all of which carry the HCV IRES, failed to synthesise detectable levels of core or core-CAT fusion product in infected cells (Fig. 78a, lanes 3-6), although rbac-5CC produced a small amount of what appears to be CAT protein as detected by PAb anti-CAT (Fig. 78b, lane 5). These data (Figs 78a and 78b, lanes 1-8) have been presented elsewhere (Fig. 71; section 5.2.5), but are presented here for reference. Co-infection of the rbacs as above with rbac-C produced core protein of the expected molecular weight at similar levels in all samples (Fig. 78a, lanes 9-13). Consistent with the CAT assay (Fig. 77; section 5.2.9), cleaved CAT protein was detected by the anti-CAT PAb at increased levels in rbac-5CC and rbac-C co-infected cells compared to rbac-5CC infected cells (Fig. 78b, lane 11). A small amount of CAT protein was also detected in Sf cells co-infected with rbac-5CC3 and rbac-C (lane 12).

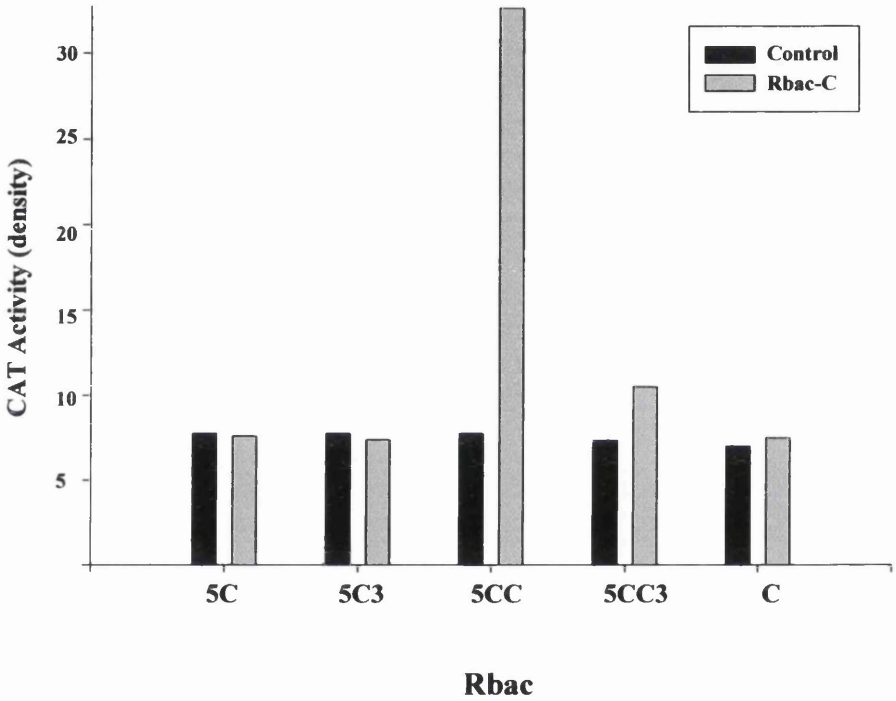

Figure 77: Effect of core protein on HCV 5′NCR-mediated translation in insect cells. Sf21 cells were infected either singly (black bars) with the rbacs as shown, or co-infected with rbac-C (grey bars). Following incubation at 28°C for 72 hours, cell extracts were prepared and 25 μg of each extract was assayed for CAT activity. CAT activity was quantitated using a Bio-Rad Molecular Imager FX with Quantity One software (Bio-Rad).

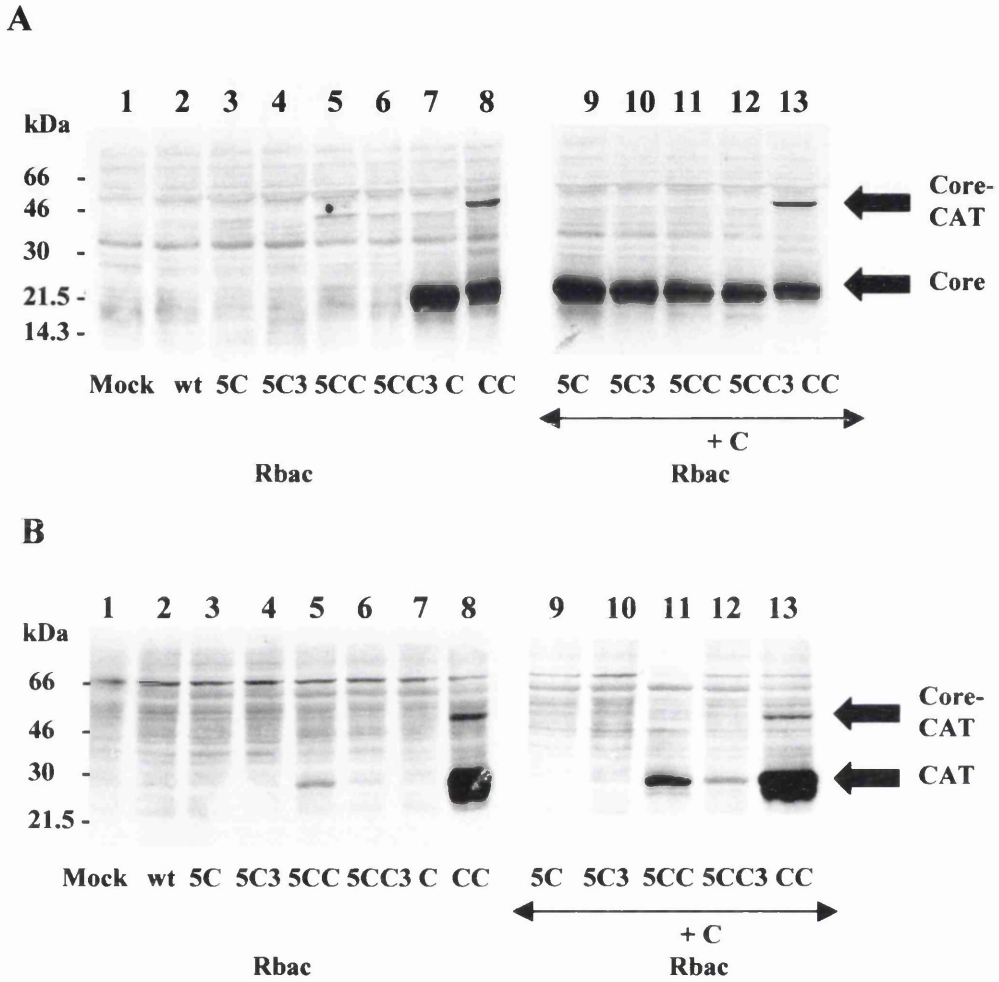

Figure 78: Detection of core and CAT products expressed by rbacs. Extracts from infected Sf21 cells used in Fig. 77 were fractionated by SDS-PAGE (12.5%) and Western immunoblotted using (A) anti-core PAb R525 or (B) anti-CAT PAb.

The effect of core protein or its coding sequence on translation from rbac-5CC was titrated by increasing the m.o.i. (from 0.05 to 5) of rbac-C while keeping that of the rbac-5CC reporter baculovirus constant (at m.o.i. = 0.5). The core expressing rbac had a 'dose-dependent' effect on translation from rbac-5CC (Fig. 79a and b, lanes 5-8). Since core protein is expressed as a part of a polyprotein that is cleaved into discrete products during HCV infection, its effect in the context of HCV glycoproteins E1 and E2 on HCV 5'NCR-mediated translation in Sf21 cells was investigated. As before (Fig. 77), core protein expressed in this manner had a similar ability to drive production of the reporter as when expressed in isolation (Fig. 80, lanes 7-10).

To determine whether DDX3 and core protein could act synergistically to increase IRES activity, rbac-DDX3 was co-infected with rbac-C, and rbac-5CC or -5CC3 with the relevant controls. However, DDX3 was consistently unable to alter CAT activity relative to that of rbac-5CC or -5CC3 co-infected with rbac-C alone (data not shown).

5.2. 11 Effect of Core Protein on Transcription of HCV 5'NCR-containing Sequences

Core protein has been reported to have effects on cellular and viral promoters (section 1.8.4). To rule the possibility that core protein was simply upregulating transcription from the baculovirus polyhedrin promoter to increase translation, RNA was extracted from Sf21 cells infected with appropriate rbacs and investigated by Northern blot analysis. Total RNA from Sf21 cells co-infected with rbac-C and rbac-5C or -5C3, together with the relevant controls as described in section 5.2.9, was extracted. Each sample containing 10 μg total RNA was fractionated and probed in the same manner as before (section 5.2.9), with expression of mRNA from 5'NCR-containing rbacs determined using a radiolabelled probe derived from an *Age*I/*Apa*LI fragment of the HCV 5'NCR. This probe was able to detect 5'NCR-core transcripts in total RNA from rbac-5C singly-infected cells (Fig. 81a, lane 4), but not in total RNA from mock-infected (lane 1), wt-infected (lane 2) or rbac-C infected (lane 3) Sf21 cells. Importantly, there was no apparent increase in 5'NCR-

A

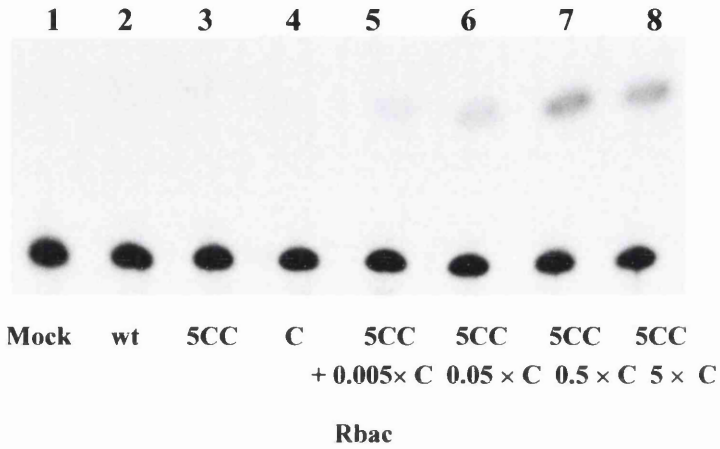

B

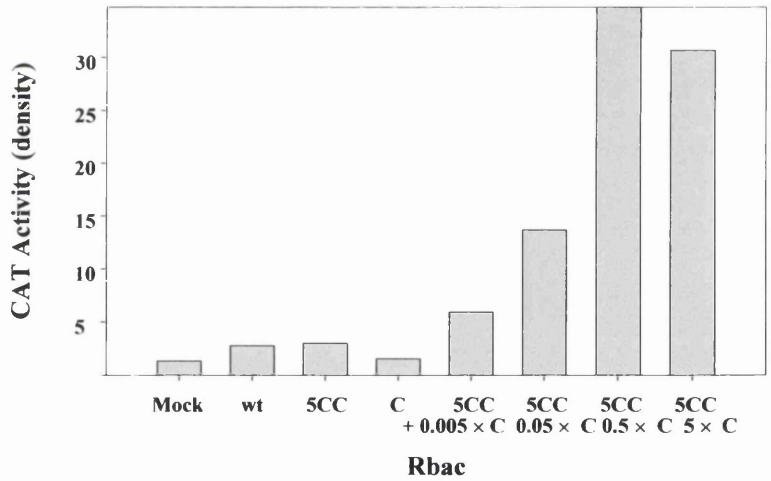

Figure 79: Titration of effect of core protein on HCV 5'NCR-mediated translation in insect cells. (A) Sf21 cells were mock-infected (lane 1), infected at m.o.i. of 0.5 with wild-type baculovirus (wt, lane 2), or with rbacs at the same m.o.i. either singly (lanes 3-4) or in combination (lanes 5-8, increasing m.o.i. of rbac-C from 0.005 to 5) as shown. Cell extracts were prepared following incubation at 28°C for 72 hours, quantitated in terms of protein concentration and assayed for CAT activity. (B) Quantitation of CAT activity of samples shown in (A).

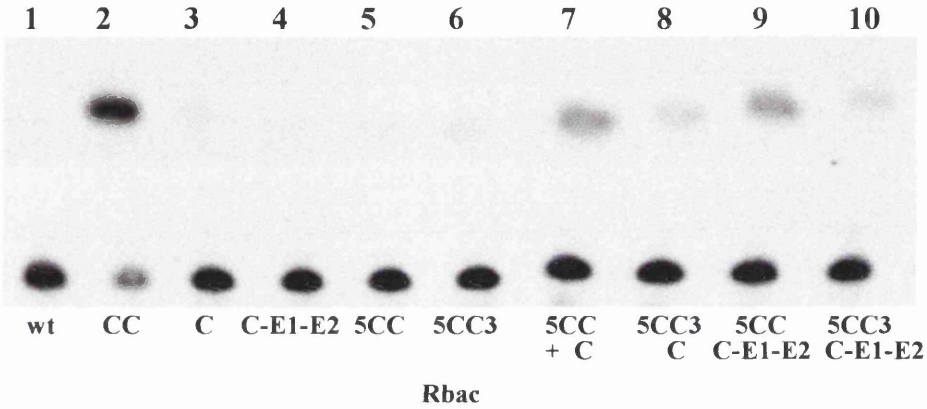

Figure 80: Effect of core protein expressed in the context of E1 and E2 on HCV 5′NCR-mediated translation. Sf21 cells were infected at m.o.i. of 0.5 with wild-type baculovirus (wt, lane 1), or infected with rbacs either singly (lanes 2-6) or in combination (lanes 7-10) as shown. Cell extracts were prepared following incubation at 28°C for 72 hours, quantitated in terms of protein concentration, and assayed for CAT activity.

core transcripts in total RNA extracted from Sf21 cells co-infected with rbac-5C and rbac-C (lane 5). In fact, the quantity of transcripts from rbac-5C infected cells markedly decreased in the presence of core protein. The same total RNA samples were used to confirm expression of core mRNA from rbac-C. A radiolabelled probe originating from a ~200 bp *XhoI/ClaI* restriction fragement of pcDNA-C-E1-E2 (see Appendix II) was employed to detect core mRNA produced by this rbac. This probe was able to detect core mRNA at similar levels in total RNA extracted from Sf21 cells singly infected with rbac-C (Fig. 81b, lane 3), or co-infected with rbac-5C (lane 5). This probe was also able to detect the 5′NCR-core transcript (lane 4). However, the transcript produced by rbac-5C was only detected at low levels when cells were co-infected with rbac-C (lane 5). Therefore, for unknown reasons, it appears that the high levels of core protein indicated by the level of transcription from this rbac is inhibiting the normally high level transcription from the 5′NCR-containing rbac. A possible reason for this is dual infection of Sf cells (section 5.2.9), although the level of transcription from rbac-C did not decrease in the presence of rbac-5C (lane 5). Nevertheless, these data do not suggest that the effect of core protein on HCV 5′NCR-mediated translation is due to upregulation of transcription from 5′NCR-containing rbacs.

5.2. 12 Effect of Other HCV Proteins on HCV 5′NCR-mediated Translation in Insect Cells

To rule out the possibility that mere expression of recombinant proteins, particularly RNA binding proteins like DDX3 and core protein, are having effects on translation from 5′NCR-containing rbacs, other proteins were tested for their ability to relieve the HCV 5′NCR-mediated translational block observed in insect cells. To this end, the HCV NS3 RNA helicase (section 1.2.5.2), was tested in the same assay. Although its function in HCV pathogenesis is unclear (section 1.2.5.2), it would not be unreasonable to suggest that this protein could influence translation by unwinding RNA secondary structures in the HCV genome. The recently reported interaction of NS3 with the 3′NCR (section 1.4.3; Banerjee and Dasgupta, 2001), could also alter translation, due to cross-talk between the NCRs (section 1.4.2). The coding sequence for the NS3 helicase domain which had been cloned and expressed

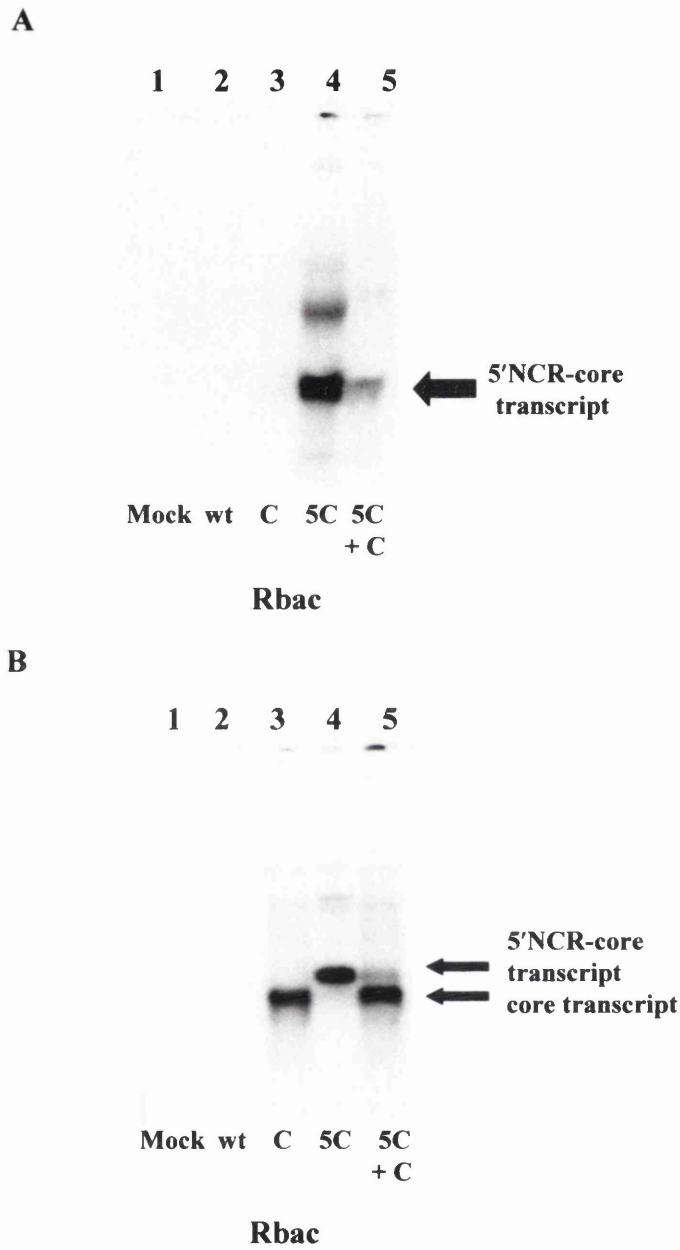

Figure 81: Effect of core protein on transcription from HCV 5′NCR-containing sequences. Sf21 cells were mock-infected (lane 1), infected with wild-type baculovirus (wt, lane 2), or infected with rbacs either singly (lanes 3 and 4) or in combination with rbac-C (lane 5) as shown. Following incubation at 28°C for 72 hours, total RNA was extracted, fractionated, and analysed by Northern blotting using ^{32}P-labelled probes derived from (A) a ~180 bp HCV 5′NCR *Age*I/*Apa*LI restriction fragement or (B) a ~200 bp HCV core *Xho*I/*Cla*I restriction fragement.

previously (Fig. 61; section 4.2.12), and shown to possess ATPase and RNA helicase activity (Figs 62a and 64a; sections 4.2.13 and 4.2.15), was transferred from the pGEX-6P-3-NS3 helicase plasmid to pAcCL29.1 (Fig. 65a) immediately downstream of the baculovirus polyhedrin promoter. The resulting construct (pAcNS3) was used directly to transfect Sf21 cells in order to determine its effect on 5′NCR-mediated translation. As a positive control, pAcCL29.1 transfer vector containing full-length core cDNA that was used to generate rbac-C (pAcC) was transfected in parallel. A further positive control plasmid containing core-CAT coding sequences alone that was used to generate rbac-CC (pAcCC) was used. To express proteins from these constructs, Sf21 cells were infected with baculovirus (wt or recombinant) prior to mock-transfection, or transfection with pAcNS3, pAcC, or pAcCC plasmid as described (section 2.39). Infection with wild-type or recombinant baculovirus supplied the required transcription factors and other baculovirus proteins necessary for efficient expression from the polyhedrin promoter in the plasmid DNA constructs. To determine the role of these proteins in HCV 5′NCR-mediated translation, Sf21 cells were infected with either rbac-5CC or -5CC3, and then mock-transfected or transfected with the appropriate construct. As shown in Fig. 82a, wt-infected cells that were subsequently mock-transfected did not have any CAT activity (lane 1). In contrast, cells infected with wt baculovirus and then transfected with pAcCL29.1 vector containing the core-CAT fusion (pAcCC) gave high level CAT activity (lane 2). As expected, cells infected with wt baculovirus and then transfected with pAcNS3 (lane 3) or pAcC (lane 4), or cells infected with rbac-5CC or -5CC3 did not give detectable levels of CAT activity. However, infection of Sf21 cells with wt baculovirus followed by transfection with pAcNS3 also did not give detectable CAT activity (lanes 7 and 8), thus confirming that the effect of DDX3 and core protein is specific in this system. To verify that proteins expressed by plasmid in insect cells could relieve the HCV 5′NCR-mediated translational block, cells were infected with rbac-5CC or -5CC3 and then transfected with pAcC. Consistent with the previous data (Fig. 77; section 5.2.10), core protein expressed in this manner gave a detectable level of CAT activity from rbac-5CC3 (lanes 9 and 10). Co-transfection of pNS3 and pC following infection with rbac-5CC or -5CC3 did not alter CAT activity relative to that without pAcNS3

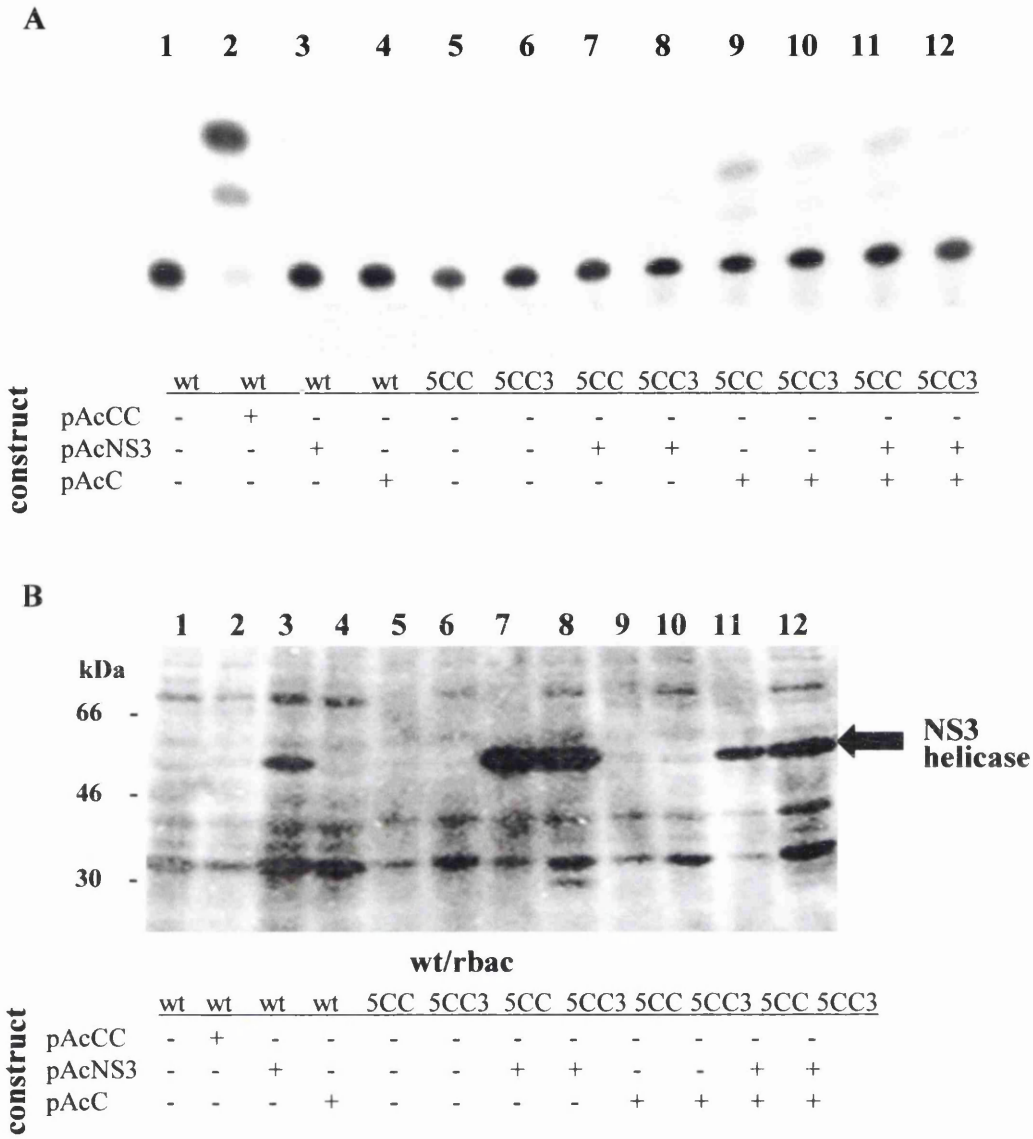

Figure 82: Effect of HCV NS3 helicase on 5′NCR-mediated translation in insect cells. (A) Lanes 1-4: Sf21 cells were infected with wild-type baculovirus (wt) and then mock-transfected (lane 1) or transfected with pAcCL29.1-CC (pAcCC, lane 2), -NS3 (pAcNS3, lane 3), or -C (pAcC, lane 4). Lanes 5-12: Cells were infected with rbac-5CC or -5CC3, and mock-transfected (lanes 5 and 6), or transfected with constructs as shown (lanes 7-12). (B) CAT assay samples as in (A) were fractionated by SDS-PAGE (10%) and immunoblotted with an anti-NS3 PAb.

(lanes 11 and 12), suggesting that the NS3 helicase has no effect on the ability of core protein to alter HCV 5′NCR-mediated translation. The presence of NS3 helicase protein in the appropriate samples was determined by fractionating the same samples used for CAT assay as above by SDS-PAGE and immunoblotting with an anti-NS3 PAb (raised against the full-length NS3 protein) (see Appendix I). Protein of the expected molecular weight of 51 kDa for the NS3 helicase domain was detected in all samples expected to contain the protein (Fig. 82b, lanes 3, 7, 8, 11, and 12). A further construct containing the HCV E1 and E2 coding sequence was tested in the same manner described above as an additional control. Expression of these HCV glycoproteins apparently did not have any effects on translation from the HCV 5′NCR in this system (data not shown).

5.2. 13 Effect of DDX3 and Core Protein on HCV 5′NCR-mediated Translation in Mammalian Cells

While the results described in the preceding sections suggest that DDX3 and core protein, but not the HCV NS3 helicase or E1-E2, can relieve a translational block in 5′NCR-containing rbacs, the actual significance of these effects have not been validated in mammalian cells. To investigate this, two previously reported constructs, pCV-5CC and pCV-5CC3 (Wood *et al.*, 2001; see Appendix II) driven by a T7 promoter alone, carrying the HCV 5′NCR linked to full-length core fused in-frame to CAT, or these sequences followed by the 3′NCR, were used as reporter plasmids (Fig. 83a). Use of these plasmids allowed generation of 5′NCR-containing transcripts without extra nucleotides at the 5′-end. Two further constructs generated by Dr A. Patel in the mammalian expression vector pcDNA3.1^{+}/Zeo (Invitrogen), each carrying HCV or DDX3 sequences downstream from a composite CMV/bacteriophage T7 promoter ($P_{CMV/T7}$) (Fig. 83b) were used (see Appendix II). These plasmids, expressing core-E1-E2, or E1-E2 alone, or DDX3 (pcDNA-C-E1-E2, pcDNA-E1-E2 or pcDNA-DDX3, respectively), were used to supply appropriate proteins in transfected cells. Prior to transfection with these DNA constructs, Huh-7 cells were infected with vTF7.3 expressing the bacteriophage T7 RNA polymerase (Fuerst *et al.*, 1986; see Appendix III) for 1 hour at m.o.i = 5. The infected cells were then transfected with 3 μg pCV-5CC or pCV-5CC3 and 1.5 μg

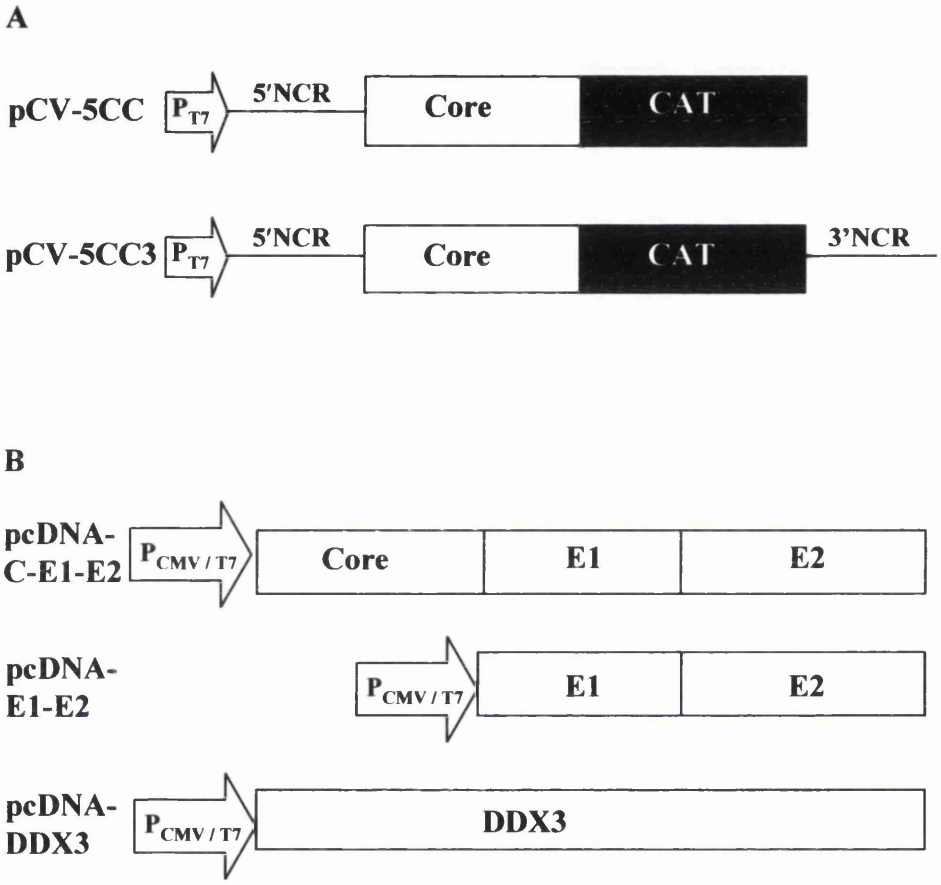

Figure 83: Schematic diagram of mammalian expression constructs used to study effect of core protein on HCV 5'NCR-mediated translation. (A) Reporter constructs (Wood *et al.*, 2001; see Appendix II) analogous to rbacs-5CC and -5CC3. (B) Constructs used to supply appropriate recombinant proteins *in trans* (see Appendix II). Expression of constructs as shown in (A) and (B) was driven by a T7 promoter (P_{T7}) or composite CMV/T7 promoters ($P_{CMV/T7}$), respectively.

control pcDNA 3.1/Zeo(+) vector to gauge the normal level of IRES activity from each construct in hepatocytes, or co-transfected with 3 μg of either reporter plasmid and 1.5 μg of mammalian expression plasmid in the pcDNA 3.1/Zeo(+) background. All transfections were carried out in triplicate. Following incubation at 37°C for 24 hours, cell extracts were prepared and each sample containing 25 μg total protein was assayed for CAT activity as described (section 2.42). CAT activity was produced in Huh-7 cells transfected with pCV-5CC or 5CC3 and empty pcDNA vector alone, since the HCV IRES is functional in hepatocytes when introduced into cells in this manner as shown previously (Fig. 72b; section 5.2.6). This level of CAT activity was arbitrarily set at 100% IRES activity. However, while DDX3 appeared to be able to relieve the block in IRES-mediated translation of core in insect cells (Fig. 75; section 5.2.8), it did not upregulate CAT activity of either 5CC or 5CC3 constructs (Fig. 84a), indicating that it might not increase IRES activity as originally expected. In fact, IRES activity was consistently inhibited by the presence of DDX3. The reason for the anomaly between results in Sf21 and Huh-7 cells is unclear. However, the mammalian cell assay relies on expression of DDX3 over and above that of normal levels of the endogenous protein, whereas insect cells do not express a closely-related DDX3 homologue. It is therefore possible that the normal balance of DDX3 and its cellular partners is disrupted in transfected hepatocytes which may account for the observed effect. As shown in Fig. 84b, core protein was able to markedly increase IRES activity in the mammalian cell assay described above, in addition to its effects in the insect cell-based system (Fig. 77; section 5.2.10). As before, the CAT activity of Huh-7 cells transfected with pCV-5CC or 5CC3 and empty pcDNA vector was arbitrarily set at 100% IRES activity. Co-transfection of pCV-5CC or -5CC3 with E1-E2 mammalian expression construct served as an appropriate control to elucidate any modulation of CAT activity by core protein. Cells co-transfected with pCV-5CC and pcDNA-E1-E2 produced a similar amount of CAT activity indicating that E1-E2 has no effect on IRES-mediated translation, although for unknown reasons with the 3′NCR present there was a down-regulation of IRES activity. In contrast, there was a 5-fold increase in CAT activity in cells co-transfected with pcDNA-5CC and pcDNA-C-E1-E2 (Fig. 84b). Interestingly, little effect on CAT activity was seen in cells co-transfected with pcDNA-5CC3 and

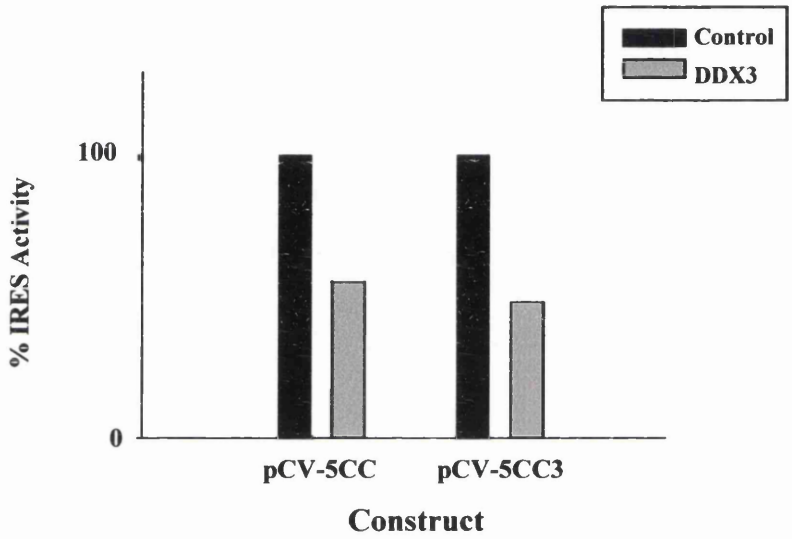

Figure 84a: Effect of DDX3 on HCV IRES activity of 5'NCR-containing constructs in hepatocytes. Huh-7 (N) cells were infected with vTF7.3 and then transfected with either pCV-5CC or -5CC3 in combination with empty pcDNA vector (control) or DDX3 expression construct as shown. Following incubation at 37°C for 24 hours, cell extracts were prepared and CAT activity quantitated. The value of the control transfection was arbitrarily set at 100% IRES activity. Values represent means obtained in triplicate.

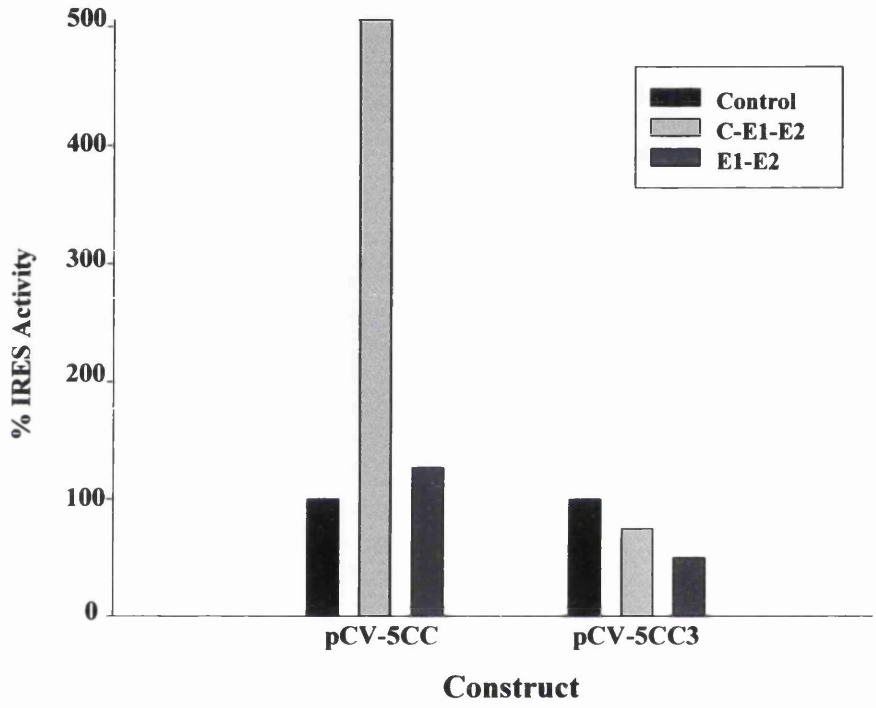

Figure 84b: Effect of core protein on IRES activity of 5NCR-containing constructs in hepatocytes. Huh-7 (N) cells were infected with vTF7.3 and then transfected with either pCV-5CC or -5CC3 in combination with empty pcDNA vector (control), or expression constructs as shown. Following incubation at 37°C for 24 hours, cell extracts were prepared for CAT assay, and CAT activity quantitated. The CAT activity of the control transfection was arbitrarily set at 100% IRES activity. Values represent means obtained in triplicate.

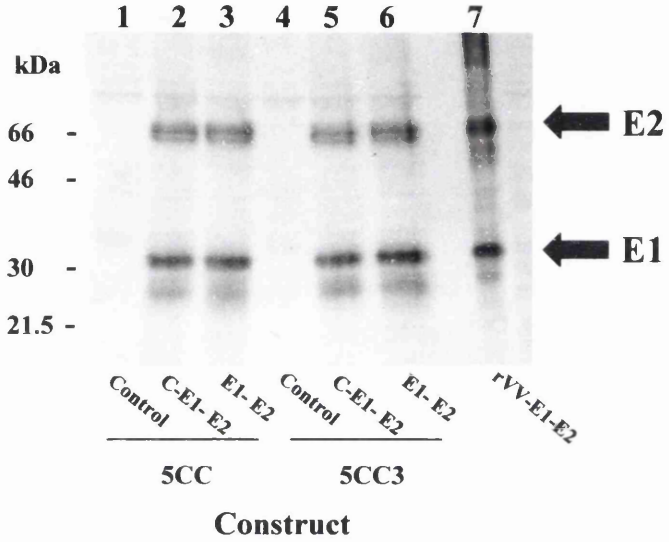

Figure 84c: Expression of proteins supplied *in trans* to determine role in HCV 5′NCR-mediated translation. Samples in Fig. 84b were fractionated by SDS-PAGE (10%) and immunoblotted using a mixed antibody preparation of anti-E2 MAb AP33 and anti-E1 PAb R528.

pcDNA-C-E1-E2 or pcDNA-E1-E2, consistent with previous data (Fig. 77; section 5.2.10) suggesting the 3′NCR modulates the effect of core protein on HCV 5′NCR-mediated translation in the insect cell system. To confirm the presence of proteins expressed by pcDNA-C-E1-E2 or -E1-E2, CAT assay samples used as above were fractionated by SDS-PAGE and immunoblotted with a mixed antibody preparation of anti-E2 MAb AP33 and anti-E1 PAb R528 (see Appendix I). As a positive control, rVV-E1-E2-infected Huh-7 total cell extracts were fractionated and probed in parallel. As shown in Fig. 84c, E1 and E2 expressed from pcDNA-C-E1-E2 (lanes 2 and 5) or -E1-E2 (lanes 3 and 6) were found at similar levels and processed appropriately as E1-E2 expressed via rVV (lane 7), but not detected in samples previously transfected with empty pcDNA vector (lanes 1 and 4).

5.2. 14 Effect of DDX3 and Core Protein on Translation of CAT Gene from a Standard Expression Plasmid

A previous report suggested that core protein could markedly upregulate translation of a reporter gene from a CMV promoter in the presence of DDX3 in Huh-7 cells (section 1.9.6.9; You *et al.*, 1999b). To investigate this phenomenon, particularly with a view to using truncated or mutated DDX3 expression constructs, the mammalian expression plasmid pcDNA 3.1/Zeo(+) carrying the CAT gene (pcDNA-CAT; Appendix II) was transfected into Huh-7 cells either alone, or with plasmids (described previously, section 5.2.13) expressing either DDX3, HCV core-E1-E2, or both. Core-E1-E2 sequences from two different HCV strains - Glasgow (gla), kindly provided by Dr M. McElwee and Professor R. Elliot (University of Glasgow), and H77c, kindly provided by Dr J. Bukh (Yanagi *et al.*, 1997), were tested to determine any strain-specific differences. As controls, cells were either mock-transfected, or transfected with all mammalian expression plasmids under investigation except the CAT reporter plasmid. As expected, these samples were all negative when assayed for CAT activity (Fig. 85, lanes 1-6). Consistent with the previous data (Fig. 84a; section 5.2.13), over-expression of DDX3 qualitatively down-regulated translation from the CAT plasmid (lane 8) compared to that from the CAT plasmid alone (lane 7). This indicates that the effect of this protein on 5′NCR mediated constructs in Huh-7 cells (Fig. 84a; section 5.2.13) was not

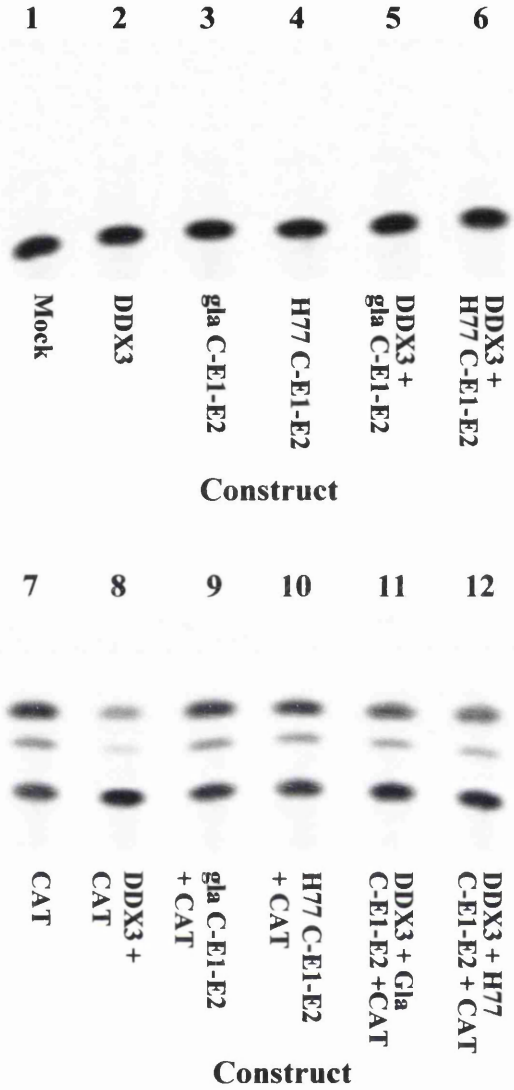

Figure 85: Effect of DDX3 and core protein on translation of transiently expressed CAT reporter gene. Huh-7 cells were either mock-transfected (lane 1), or transfected with expression plasmids alone (lanes 2-6) as controls. To test the effect of these expression plasmids on translation of CAT protein, cells were transfected with CAT plasmid either alone (lane 7) or with DNA construct as shown (lanes 8-12). Following incubation at 37°C for 48 hours, cell extracts were prepared and assaye for CAT activity. Core-E1-E2 seqeunces from two different HCV strains were used - gla, Glasgow strain; H77, H77c infectious clone (Yanagi *et al.*, 1997).

specific. Core-E1-E2 from either strain of HCV used did not have any effect on translation from the reporter plasmid (Fig. 85, lanes 7, 9 and 10). In contrast to previous data (section 1.9.6.9; You *et al.*, 1999b), co-expression of DDX3 and core protein did not upregulate translation from the CAT plasmid (lanes 11 and 12). In fact, the level of CAT activity was slightly lower than that of CAT plasmid alone. The reason for this inconsistency is not clear, although the study presented here used full-length core protein together with the HCV glycoproteins, whereas the other report (You *et al.*, 1999b) used only truncated core which may have a distinct localisation (section 1.7.3) and hence could have unusual properties in a cellular context.

5.2. 15 Effect of RNA on dATPase Activity of GST-DDX3 Fusion Protein

It has previously been shown that the dATPase activity of the *X. laevis* An3 protein, a homologue of DDX3, is specifically stimulated by RNA from *X. laevis* oocytes (Askjaer *et al.*, 2000). Synthetic poly(U) RNA did not have any effect on dATPase activity, suggesting the existence of a specific RNA activator which is recognised by the protein. By analogy with this protein and other RNA helicases, such as DbpA which is specifically stimulated by 23s rRNA (section 1.10.7), it was postulated that a specific sequence in total RNA extracted from Huh-7 cells could stimulate dATPase activity of DDX3. As a control, synthetic poly(A) RNA (Sigma) was tested in parallel. As in previous dATPase assays (Fig. 62; section 4.2.13), GST-NS3 helicase protein was tested as a positive control for the dATPase assay. 2 μg of purified GST-NS3 helicase protein was able to convert all dATP to dADP (Fig. 86a, lane 8). Consistent with previous reports (You *et al.*, 1999b), relative to the dATPase activity of 2 μg GST-DDX3 without RNA (lane 1), the same amount of protein plus poly(A) RNA at a concentration of 0.02 and 0.2 μg (Fig. 86a, lanes 2 and 3; Fig. 86b) exhibited a lower percentage conversion of dATP to dADP. This suggests that poly(A) RNA can inhibit dATPase activity of DDX3, although other synthetic polynucleotides have also been shown to inhibit NTP- or dNTPase of DDX3 expressed in *E. coli* (You *et al.*, 1999b). At higher concentrations of poly(A) RNA (2 μg), however, this inhibition was not evident (Fig. 86a, lane 4; Fig. 86b). Consistent with the previous reports of *X. laevis* An3 (see above), total RNA

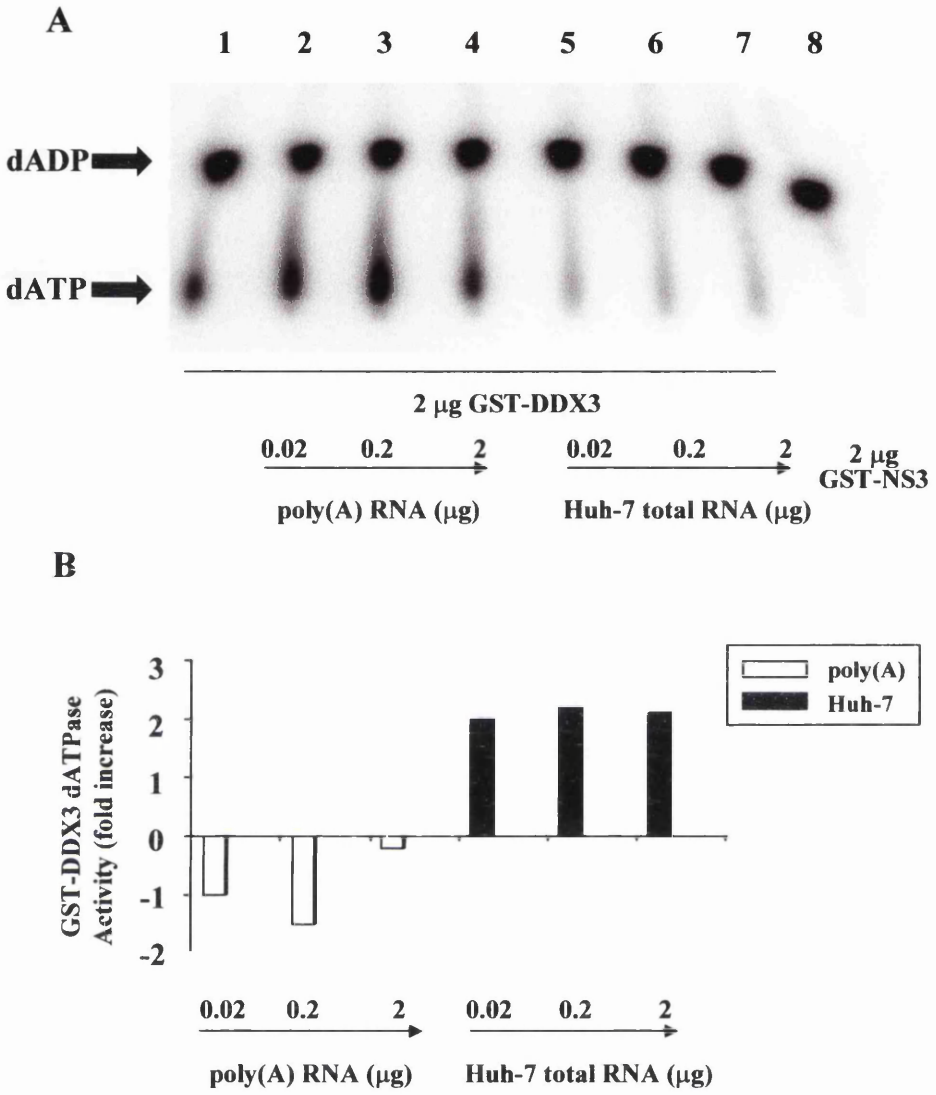

Figure 86: Effect of synthetic poly(A) RNA and Huh-7 total cellular RNA on dATPase activity of GST-DDX3. (A) The dATPase activity of GST-DDX3 was investigated using [α-^{32}P]-dATP as a substrate and analysed by TLC. 2 µg purified GST-DDX3 protein alone (lane 1), or protein incubated with 10-fold serial dilutions of poly(A) (lanes 2-4) or Huh-7 total cellular RNA (lanes 5-7) was assayed as described (section 2.47). As a positive control, the dATPase activity of 2 µg purified GST-NS3 helicase protein was assayed in the same manner (lane 8). (B) The level of unconverted dATP was quantitated by phosphorimager. dATPase activity is represented as values relative to sample without RNA.

extracted from Huh-7 cells at a concentration of 0.02, 0.2 or 2 μg stimulated dATPase activity of DDX3 (Fig. 86a, lanes 5-7; Fig. 86b). This stimulation allowed hydrolysis of the dATP substrate by DDX3 to a level similar to that of the NS3 helicase control (lanes 5-7 and 8, respectively). dATPase activity was not stimulated or inhibited by poly(A) RNA or total RNA extracted from Huh-7 cells without GST-DDX3 protein (data not shown). It would be interesting to test whether this RNA could stimulate helicase activity of DDX3, since it is possible that the low level of dATPase activity of the protein, relative to the NS3 helicase, is responsible for its apparent inability to unwind a non-specific RNA duplex (Fig. 62b; section 4.2.15). The ability of certain RNAs to bind DDX3 and stimulate dATPase activity has been investigated (P. Askjaer and J. Kjems, personal communication). However, as yet, no particular RNA sequence or secondary structure that bound DDX3 has been shown to stimulate dATPase activity.

5.2. 16 Investigation into the Presence of DDX3 in Purified Spliceosome Complexes

Previous data suggested that DDX3 was mainly located in the cytoplasm of hepatocytes (Figs 27, 44 and 51; sections 3.2.4, 4.2.1 and 4.2.5), with a small amount detected in the nucleus by subcellular fractionation (Fig. 57a; section 4.2.9) consistent with other reports of a nuclear form of DDX3 (Owsianka and Patel, 1999; You *et al.*, 1999b). These data, together with the presence of an 'RS-like' domain that may be involved in protein-protein interactions between splicing factors (Owsianka and Patel, 1999; You *et al.*, 1999b), could suggest DDX3 has a role in pre-mRNA splicing. To determine directly whether DDX3 was part of the spliceosome, a large nucleoprotein complex believed to contain many DEAD-box RNA helicases that participate in pre-mRNA splicing (Hamm and Lamond, 1998), purified spliceosome (kindly provided by Dr A. Lamond, University of Dundee) was probed for DDX3 protein. As with anti-DDX3 MAb AO196 (Fig. 57a; section 4.2.9), anti-DDX3 PAb R648 detected DDX3 abundantly in total cell extracts and at low levels in nuclear extracts (Fig. 87a, lanes 2 and 3, respectively). However, a corresponding band in fractionated purified spliceosome complex was not seen (lane 1). To confirm that spliceosome complex was indeed present, a PAb directed against

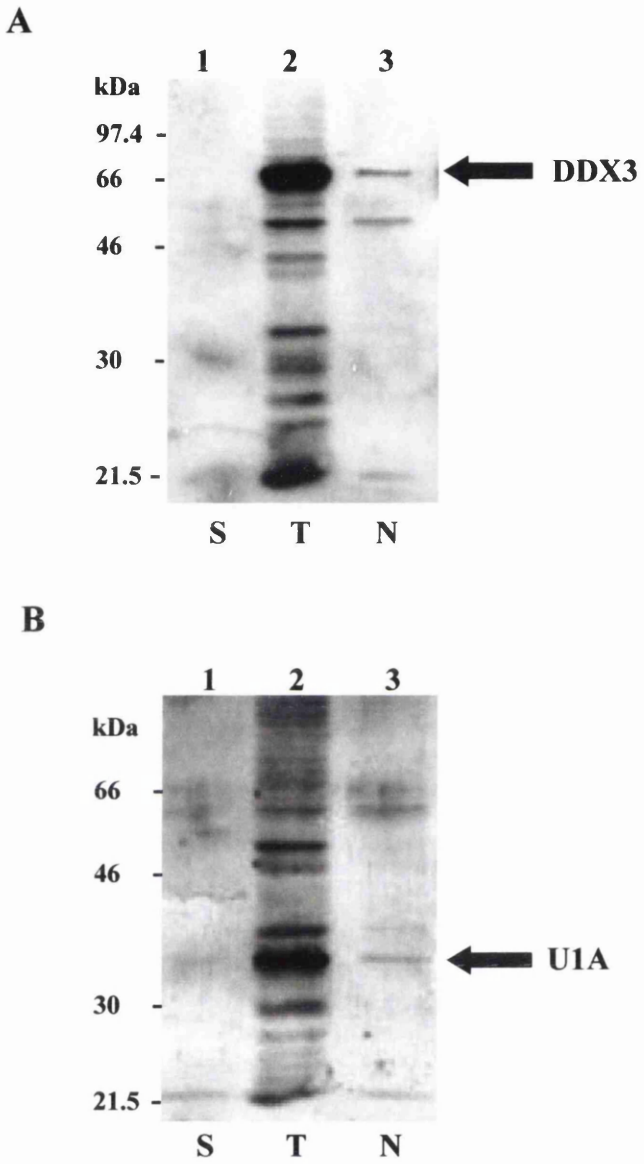

Figure 87: Investigation into the possible presence of DDX3 in purified spliceosome complexes. Spliceosome complex (S) purified from HeLa cells, total HeLa cell extracts (T), or HeLa nuclear extracts (N) were fractionated by SDS-PAGE (9%) and immunoblotted using (A) anti-DDX3 PAb R648 or (B) an anti-U1A PAb.

U1A, a protein that should be present in this purified complex (Hamm and Lamond, 1998) was used in parallel with R648. Accordingly, U1A was detected at high levels in total cell extracts (Fig. 87b, lane 2), and at low levels in nuclear extracts and at barely detectable levels in purified spliceosome complex (lanes 3 and 1, respectively). Although the protein concentration of the purified spliceosome complex appeared to be low, these data suggest that DDX3 is not part of the spliceosome, but do not directly rule out the possibility that this protein is indirectly involved in this process.

5. 3 Discussion

Functional aspects of DDX3 and its interaction with core protein were investigated in the preceding chapter. Initially, the possibility that core in some way modifies DDX3, or *vice versa*, as detected in Western blots using specific MAbs and PAbs, was investigated. The full-length coding sequences for each protein were used to generate rbacs, and their expression in an insect cell line, either singly or in combination, was analysed. This was further examined in a human hepatocyte cell line by infection with rVV-C-E1-E2. Core protein expressed by this rVV was found in a subcellular localisation that fitted with previous reports (section 1.7.3) by indirect confocal immunofluorescence microscopy (for example: Fig. 29; section 3.2.6). The results suggested core protein physically modifies the processing of DDX3 *in vivo*, and would be consistent with a prevention of normal transit through the ER following an interaction with core protein (discussed in section 4.3). If accurate, these data suggest a novel mechanism by which this viral protein can subvert host cellular processes by modifying a highly conserved and ubiquitous house-keeping protein (Figs 22-28; sections 3.2.1-3.2.5). Further investigation into the mechanism by which core protein exerts this effect on DDX3 is required. Studies with anti-DDX3 MAbs that possibly detect the higher molecular weight isoform may allow delineation of the region of DDX3 that is modified by core. If this isoform of DDX3 is generated by direct or indirect phosphorylation in the presence of core protein, it may be possible to immunoprecipitate this modified species and detect phophorylated residues with commerically available antibodies. Northern blotting of core-E1-E2 expressing hepatocytes with DDX3-specific probes

suggested it is unlikely that core alters expression/splicing of DDX3 mRNA to modify this protein, although the technique may not allow detection of subtle differences in mRNA transcripts.

The actual function of DDX3 in relation to replication or pathogenesis of HCV is unclear. Previous reports pointed to a role of DDX3 in translation in systems unrelated to HCV, or with non-specific substrates (section 1.9.6.9; Mamiya and Worman, 1999; You *et al.*, 1999b). Here, DDX3 was implicated in specifically altering translation of the HCV genome since it appears to alleviate a previously reported translational block of rbacs carrying the HCV 5'NCR in Sf21 cells (section 1.3.4; Wang *et al.*, 1997). The effect of DDX3 in upregulating HCV IRES-mediated translation would be in agreement with the findings of others that it can rescue yeast cells with a lethal mutation in its homologue *ded1* gene (section 1.9.6.9; Mamiya and Worman, 1999), which is required for translational initiation in yeast (section 1.13.6; Chuang *et al.*, 1997). Nevertheless, the effect of DDX3 on HCV 5'NCR-mediated translation was not consistent with a similar hepatocyte-based transfection assay, making the role of this protein in translation of the HCV genome unclear. It is possible, however, that the over-expression of DDX3 in this system may disrupt the normal balance of DDX3 and could aberrantly sequester its cellular partners, thus crippling cellular DDX3.

In direct contrast to an earlier study (section 1.9.6.9; You *et al.*, 1999b), DDX3 was unable to upregulate transiently-expressed CAT reporter gene when expressed by plasmid. Neither was there any significant modulation of CAT activity when CAT plasmid was co-transfected with DDX3- and core-E1-E2-expressing plasmids. A possible reason for this anomaly could be that core protein in this study was expressed along with E1 and E2, as it would be during natural infection of target cells with HCV, while the previous study used core protein on its own (You *et al.* 1999b). Furthermore, the previous study did not use full-length core protein - in fact, the most complete core-expressing construct used lacks an entire 69 aa stretch of the 191 aa full-length protein. Taken together, these data suggest that core protein on its own, or more likely truncated forms of core, can potentially exert this effect in

conjunction with DDX3, but there is no actual *in vivo* significance in terms of HCV infection.

Although previous reports (section 1.9.6.9; Mamiya and Worman, 1999; You *et al.*, 1999b) and preliminary data dictated that the role of DDX3 in translation was studied in greatest detail, attempts were also made to allocate DDX3 to other functional categories in which putative and known RNA helicases may be placed (Fig. 20; section 1.12; de la Cruz *et al.*, 1999), including pre-mRNA splicing and RNA export. Following subcellular fractionation experiments that suggested the localisation of a small amount of DDX3 in the nucleus (Fig. 57a; section 4.2.9), and previously reported analysis suggesting the presence of a short 'RS-like' domain that could be involved in protein-protein interactions between splicing factors, the presence of the protein in purified spliceosome complexes was investigated. However, the protein was apparently not present in such complexes, suggesting it is not directly involved in this process. By analogy with the *X. laevis* DDX3 homologue An3 that is specifically stimulated by total RNA from *X. laevis* oocytes (Askjaer *et al.*, 2000), the effect of Huh-7 total RNA and synthetic poly(A) RNA on dATPase activity of DDX3 was examined. Consistent with the An3 data, dATPase activity of DDX3 was stimulated by total RNA from Huh-7 cells. Furthermore, dATPase activity of DDX3 was inhibited by synthetic poly(A) RNA, consistent with the results of You *et al.* (1999b) suggesting that synthetic RNAs can inhibit NTPase and dNTPase activity of DDX3. The effect of Huh-7 RNA on dATPase activity of DDX3 may suggest that a specific activator of this protein exists in hepatocytes. However, an *in vitro* assay involving binding of random RNAs to GST-DDX3 captured on glutathione-agarose beads and subsequent removal and sequencing of the bound RNAs, suggested that RNAs bound to DDX3 had no similarites in terms of sequence or secondary structure and were not able to stimulate dATPase activity (P. Askjaer and J. Kjems, personal communication).

The same assay used to determine a role for DDX3 in translation of the HCV genome unexpectedly suggested core protein could affect the HCV 5'NCR-mediated translational inhibition. In contrast to DDX3, core protein also upregulated IRES

activity in hepatocytes. While there have been conflicting reports about the possible role of core protein or core protein-coding sequence in HCV translational regulation (section 1.3.5; Shimoike *et al.*, 1999; Wang *et al.*, 2000), the evidence presented here strongly suggests that core protein can elevate IRES activity, thus enhancing translation of the HCV genome. There is also an indication that the 3′NCR modulates translation from the 5′NCR in this assay, in agreement with previously reported 'cross-talk' between the NCRs, thought to be mediated by cellular proteins (section 1.4.2). DDX3 apparently has no effect on the ability of core protein to increase IRES activity in the Huh-7 cell assay, although this requires further investigation.

CHAPTER SIX:

Conclusions

6. 1 Properties of DDX3

The following sections draw together and discuss the data presented here, as well as published information, regarding the properties of DDX3 at both the RNA and protein level.

6.1. 1 DDX3 Gene Structure and mRNA

DDX3 is encoded on the human X chromosome at position p11.3-11.23 (Fig. 21; Park *et al.*, 1998), and its gene structure contains 17 exons spanning around 16 kb (section 1.13.1; Kim *et al.*, 2001). These exons are presumably spliced to produce the mature DDX3 mRNA of around 5.3 kb (Fig. 22b; section 3.2.1; Chung *et al.*, 1995). Since DDX3 cDNA is approximately 2 kb (see Appendix IV), this suggests the existence of a long poly(A) tail and/or extensive untranslated regions at the 5′- and 3′-ends of the mRNA. Extending the studies of Chung *et al.*, (1995), Northern blotting analysis with DDX3-specific probes indicated the presence of a single mRNA transcript in a range of cell types, representing human hepatocyte and non-hepatocyte human cell types, as well as other mammalian cells (Fig. 22b; section 3.2.1). Interestingly, a Y chromosomal counterpart of DDX3 (termed DDXY) has been found (Lahn and Page, 1997). The presence of a Y chromosomal counterpart could indicate DDX3 has a highly related functionally interchangeable cellular homologue, as shown for related proteins on the X and Y chromosomes (Lahn and Page, 1997). However, since only one transcript was detected by Northern blotting either i) mRNA transcripts for DDX3 and DDXY are of very similar or identical size which prevents their resolution by gel electrophoresis or ii) their nucleotide sequence is sufficiently diverse to prevent detection with a DDX3-specific probe. DDX3 mRNA was subsequently detected in a diverse array of adult human and foetal tissues (Fig. 23a; section 3.2.2). Although expression was low relative to the ubiquitin control (Fig. 23b, section 3.2.2), and expression fluctuated moderately between different tissues, the ubiquitous presence of DDX3 strongly implies it is an essential cellular protein. This could very well be the main factor that prevented isolation of cell lines lacking DDX3 (Fig. 28; section 3.2.5), although this is difficult to confirm. HCV core protein expressed along with glycoproteins E1 and E2 had no effect on expression of DDX3 mRNA in Huh-7 cells, or the H9-13 HCV

sub-genomic replicon-expressing cell line (Fig. 69; section 5.2.4), suggesting that the previously reported effect of core on the function of DDX3 (Mamiya and Worman, 1999; You *et al.*, 1999b) is not occuring at the RNA level.

6.1. 2 DDX3 Protein

Endogenous DDX3 protein and that over-expressed in a variety of systems was generally found as a doublet (particularly evident in Figs 26 and 68; sections 3.2.3 and 5.2.3), possibly reflecting the presence of a similar but not identical Y-chromosomal counterpart that may be functionally interchangeable with DDX3 (see above; Lahn and Page, 1997). Its Y-chromosomal counterpart, DDXY, is just two aa shorter than DDX3 (Lahn and Page, 1997), making it unlikely that this difference alone is responsible for the difference in size. However, the pattern of expression by rbac-DDX3 in insect cells (Fig. 67; section 5.2.2) suggested that the doublet detected in hepatocyte cell extracts was more likely due to a property inherent in the protein rather than the presence of cellular isoforms produced from separate chromosomes. Interestingly, a third species is detected by an anti-DDX3 PAb in cell extracts expressing core protein. However, it is not clear how this isoform is generated. Specifically, is not obvious whether it represents an inhibition of complete proteolytic processing or increased phosphorylation and/or other modifications. The presence of the third isoform of DDX3 does not affect expression of the two closely migrating bands seen in uninfected cells (Figs 67 and 68; sections 5.2.2 and 5.2.3). Further assays, for example those allowing visualisation of phosphorylation states of DDX3 (section 5.3), could provide the key to this intriguing effect that may have important implications for the DDX3/core interaction and its significance regarding cellular and viral processes.

Analysis of the protein sequence of DDX3 suggested it contains several highly conserved motifs, notably those characteristic of known RNA helicases (section 1.9.6.9; Owsianka and Patel, 1999), and a putative nuclear export signal (NES) (Fig. 53a; section 4.2.6; see below) that binds CRM1 *in vitro* in a RanGTP dependent manner (P. Askjaer and J. Kjems, communication). A short 'RS-like' domain, believed to mediate protein-protein interactions in splicing factors (section 1.9.6.9),

was previously identified in the domain involved in core binding (Owsianka and Patel, 1999; You *et al.*, 1999b). *In vitro* GST-pulldown assays suggested core protein does indeed bind the 'RS-like' domain of DDX3 (or *vice versa*), but in the context of the full-length protein, this domain was not essential for binding to core protein (Fig. 33e; section 3.2.9). Nevertheless, specific binding of the 'RS-like' domain alone by core protein could imply that other cellular factors possessing similar domains can bind, or more likely are targeted by, core protein. Whether these interactions occur *in vivo* remains to be determined. This could, however, represent another mechanism for disruption of cellular processes by core protein (section 1.8).

6.1. 3 Insight into DDX3 Structure from Antibody Binding Data

For unknown reasons, only antibodies directed against the N-terminal ~200 aa of DDX3, as judged by reactivities with bacterially-expressed GST-DDX3 deletion mutants (Figs 35-41; sections 3.2.13-3.2.17), are able to detect discrete proteins in hepatocyte cell extracts by Western blotting (Fig. 42; section 3.2.18) and by indirect immunofluorescence (Figs 44 and 45; section 4.2.1). All antibodies directed against the remainder of the protein do not appear to recognise distinct protein factors in hepatocytes (Fig. 42; section 3.2.18). In theory, extensive post-translational modification occuring at the C-terminus may provide a rational explanation for antibody binding in mammalian *versus* bacterial systems. Indeed, analysis of the DDX3 protein seqeunce predicted two N-linked glycosylation sites in close proximity within the 409-473 region (see Appendix IV), an epitope bound by many of the antibodies recognising bacterially expressed DDX3 (see Appendix I, Fig. 88). A high proportion of putative casein kinase-II and protein kinase C phosphorylation sites are also found in this region (data not shown). Interestingly, two of the anti-DDX3 MAbs (AO2 and AO35) detect a 46 kDa protein by Western blotting (Fig. 42; section 3.2.18). This protein shows a quite distinct localisation to that of the full-length protein (Fig. 45; section 4.2.1). DBY, a protein that shows 93% homology to DDX3 (section 1.13.2), apparently shares a similar property. Full-length mRNA encoding DBY is ubiquitously expressed in human tissues, while a truncated form is solely produced in the testis (Foresta *et al.*, 2000). Due to the

inferred importance of DBY in spermatogenesis - DBY is frequently deleted in male infertile patients leading to severe spermatogenic damage that significantly reduces or abolishes production of germ cells (section 1.13.2; Foresta *et al.*, 2000) - a truncated form of the protein may be crucial in this process. However, Northern blotting analyses did not suggest the presence of a second shorter DDX3 mRNA transcript in any of the mammalian cell lines tested (Fig. 22b; section 3.2.1), indicating the putative truncated form might arise due to proteolytic processing of full-length DDX3. Interestingly, the localisation of the endogenous 46 kDa protein was similar to that of DDX3 expressed by plasmid constructs (Figs 51, 55 and 59; sections 4.2.5, 4.2.8 and 4.2.11). Conflicting with the above hypothesis, a 46 kDa band was also detected by MAbs AO2 and AO35 in mock-infected Sf21 cells (Fig. 74; section 5.2.7), which do not appear to possess a closely-related DDX3 homologue (Figs 22b and 26; sections 3.2.1 and 3.2.3). It is therefore possible that this represents a related cellular factor.

6.1. 4 Enzymatic Properties

Even though the motifs critical in ATP-dependent RNA helicase activity are perfectly conserved from *S. cerevisiae* Ded1p to DDX3 (section 1.13), and this human cellular protein possesses dATPase activity (Fig. 62b; section 4.2.13; You *et al.*, 1999b), DDX3 is apparently unable to unwind random RNA duplexes (Fig. 64b; section 4.2.15; You *et al.*, 1999b). This could simply be due to the low dATPase activity of DDX3, relative to the HCV NS3 helicase used here a positive control (Fig. 62a; section 4.2.13). In fact, while 0.01 μg NS3 helicase completely hydrolysed the radiolabelled dATP substrate (Fig. 62a; section 4.2.13), DDX3 was unable to do so even at a concentration of 1.5 or 2.0 μg (Fig. 62b; section 4.2.13). Although the dATPase activity of DDX3 was moderately stimulated by total RNA from Huh-7 cells (Fig. 86a and b; 5.2.15), the functional importance of this observation for helicase activity, and its interaction with core protein, has not yet been determined. Interestingly, this property is similar to that seen with DDX3 homologues Ded1p (Iost *et al.*, 1999) and An3 (Askjaer *et al.*, 1999), but is in stark contrast to most other known RNA helicases, such as eIF4A that is more efficiently stimulated by synthetic homopolymeric RNA than cellular substrates such as human

globin mRNA (Abramson *et al.*, 1987). Another possible reason for the lack of helicase activity is that DDX3 may require a cellular co-factor for enzymatic activity, which could confer specificity of the protein on a particular substrate (section 1.10.7). A search for cellular co-factors of DDX3 by a library screening approach may well reveal a protein that is essential for DDX3 RNA helicase activity *in vivo*. This search could also provide clues to the specific subcellular localisation and function of DDX3. If the protein is part of a cellular complex, for example the translation initiation complex, these factors could be isolated using this approach.

6. 2 Significance of the DDX3/core Interaction in Cellular and Viral Processes

The aberrant sequestration of DDX3 at lipid droplets by HCV core protein in human hepatocytes or other mammalian cells (Fig. 29; section 3.2.6; Mamiya and Worman, 1999; Owsianka and Patel, 1999; You *et al.*, 1999b), and in HCV sub-genomic replicon-expressing hepatocyte cell lines (Fig. 32; section 3.2.8), could suggest DDX3 is being 'hijacked' by core to perform a function relevant to the replication cycle of HCV. Indeed, DDX3 apparently removes the previously reported HCV 5′NCR-mediated translational block in insect cells (Wang *et al.*, 1997) (Fig. 75; section 5.2.8) consistent with the observed effect of DDX3 on translation in yeast (Mamiya and Worman, 1999), and on non-HCV related substrates in mammalian cells (You *et al.*, 1999b) (section 1.9.6.9). Since core protein is not present at detectable levels in insect cells infected with rbacs carrying the HCV 5′NCR followed by the core-coding sequence (Fig. 71a; section 5.2.5), it is possible that high levels of 5′NCR-core transcripts negate the need for redirection of DDX3 by core protein in this system. Alternatively, translation in this system may be 'leaky' allowing low, but undetectable, levels of core to be produced. Indeed, a low level of CAT protein was detected in rbac-5CC-infected insect cell extracts (Fig. 71b; section 5.2.5). Since the effect of DDX3 on 5′NCR-mediated translation in insect cells is subtle, this could suggest that other mammalian cell factors are required for full IRES activity in this insect cell system. The implication of DDX3 in cellular translation, and possible diversion of this role to meet the needs of HCV, is also in agreement with the essential role of Ded1p, the yeast homologue of DDX3, in translation initiation (section 1.13.6; Chuang *et al.*, 1997) and the apparent

specificity of Ded1p for certain viral mRNAs (section 1.13.6; Noueiry *et al.*, 2000). Although the HCV IRES does not require many of the canonical eIFs (section 1.3.4), DDX3 may be involved in or be required for full IRES activity. A non-specific effect on RNA stability due to the RNA-binding properties of DDX3 (P. Askjaer and J. Kjems, personal communication) seemed unlikely to be responsible for such activity, since the HCV NS3 helicase does not have any effect in this system (Fig. 82; section 5.2.12).

However, a similar effect to that seen in insect cells of exogenously-expressed DDX3 on HCV IRES activity was not seen in mammalian cells (Fig. 84a; section 5.2.13), making the actual relevance of the effect in terms of natural infection with HCV unclear. Indeed, DDX3 over-expressed by plasmid appeared to actually suppress translation from the HCV IRES in the hepatocyte-based system. This was consistent with a moderate downregulation of translation in a reporter gene assay (Fig. 85; section 5.2.14), although this did not involve HCV-derived sequences. The reason for the disparity between the insect and mammalian cell-based systems is unclear. However, one difference between the insect and mammalian systems is that endogenous DDX3 is already present in hepatocytes. Expression by plasmid over and above that of the normal levels of DDX3 may disrupt a fine balance, for example with possible co-factors, of this protein in hepatocytes leading to the observed effect. This issue cannot be resolved until a human heptocyte cell line lacking DDX3 becomes available. Nevertheless, the strong co-localisation of core protein, expressed as part of the entire structural region of the HCV polyprotein, with DDX3 in hepatocyte-based cell lines containing self-replicating HCV sub-genomic RNA (Fig. 32; section 3.2.8) implied that the DDX3/core interaction is indeed of actual *in vivo* significance during natural HCV infection. In this co-localisation study, most viral components involved in virion morphogenesis and the replicative cycle of HCV were present. Moreover, owing to the ubiquitous nature of DDX3 (Figs 22-27; sections 3.2.1-3.2.4; Chung *et al.*, 1995), and its conservation from yeast to man (section 1.13), the abnormal localisation of the protein in the presence of core most likely removes it from an essential cellular function, representing an additional mechanism of HCV core-mediated subversion of the host cell (section 1.8).

These studies, although currently unclear, and previous reports detailing a role for DDX3 in translation (section 1.9.6.9; Mamiya and Worman, 1999; You *et al.*, 1999b), do not exclude a role for the protein in other cellular processes involving RNA helicases (section 1.12), such as pre-mRNA splicing, ribosome biogenesis (including processing of rRNAs and recruitment/rearrangement of ribosomal proteins in formation of the ribosome), processing of tRNAs, and RNA nucleocytoplasmic export. However, if DDX3 is indeed targeted by core protein to perform a function relevant to HCV, it is improbable that it is involved in pre-mRNA splicing, since HCV genomic RNA is not spliced. Consistent with this presumption, DDX3 did not appear to be present in purified spliceosome complexes (Fig. 87; section 5.2.16), although the positive control antibody (anti-U1A) detected only very small amounts of its target antigen, suggesting the concentration of the purified complexes was low. While the HCV replicase complex is situated in the cytoplasm (Fig. 9; section 1.5.3), a role for DDX3 in RNA/protein nucleocytoplasmic transport is possibly advantageous for HCV due to the reputed presence of core protein in the nucleus (section 1.7.3), which may mediate the effects of core on cellular transcription (section 1.8.4). It is possible that core protein uses DDX3 as a means to shuttle between the nucleus and the cytoplasm. The importance of such transport in the normal cellular function of DDX3, whether relevant for HCV or not, seemed plausible due to identification of a putative nuclear export signal (NES) (Fig. 53a; section 4.2.6). However, although the putative NES of DDX3 binds the soluble nuclear export factor CRM1 in a RanGTP-dependent manner *in vitro* (P. Askjaer and J. Kjems, personal communication), removal of this sequence did not cause accumulation in the nucleus of hepatocytes transfected with a DDX3 construct lacking the NES (Fig. 56; 4.2.8), possibly suggesting it is not functional *in vivo*. A good control that was not available to be tested by P. Askjaer and J. Kjems in the *in vitro* protein-protein binding assays was ΔNES-DDX3 expressed as a GST-fusion protein. This would rule out the possibility that DDX3 non-specifically interacts with CRM1. Nevertheless, the apparent lack of activity of the DDX3 NES in a cellular context could be similar to that of Epstein-Barr virus (EBV) nuclear antigen 1 (EBNA1). Although this protein contains a putative NES, it does not interact with CRM1 in yeast two-hybrid assays, nor does it shuttle to the

cytoplasm in heterokaryon analyses (Fischer *et al.*, 1999). Thus, the presence of a putative NES recognised by CRM1 appears to be redundant in this viral protein and the present data suggests this could well be the case for DDX3. Interestingly, however, ΔNES-DDX3 protein showed a slightly altered cellular distribution compared with the wild-type protein when expressed by plasmid in hepatocytes (Fig. 55; section 4.2.8), and appeared to subtly modify the distribution of core protein (Fig. 56; section 4.2.8), although these aspects also require further investigation.

Although indirect immunofluorescence studies suggested DDX3 was an almost exclusively cytoplasmic protein (Fig. 27; section 3.2.4; Mamiya and Worman, 1999), subcellular fractionation of mammalian cell extracts did indeed indicate a nuclear form of DDX3 exists (Fig. 57; section 4.2.9). Such a nuclear form was previously detected using the same approach (You *et al.*, 1999b), although it was not detected here in the same abundance as indicated in this report. Nevertheless, this result could imply DDX3 has a dual role in the cell, owing to two very distinct subcellular localisations, or that nucleocytoplasmic transport (by a pathway other than via CRM1) is important for its normal cellular function. Detailed studies of the endogenous DDX3 protein are required to confirm this result, since only transfected DDX3 cell extracts were probed (containing endogenous DDX3 as well as that expressed by plasmid).

6.2. 1 Insight into the Nature of the DDX3/core Interaction Using DDX3 Mutants and Co-expression Studies

It was interesting to note that a DDX3 mutant (DDX3-EQ) that was found to be enzymatically incapacitated (P. Askjaer and J. Kjems, personal communication) also showed a distinct localisation in relation to the wild-type protein (Fig. 59; section 4.2.11). The altered localisation is not due to targeting of DDX3-EQ for degradation (Fig. 58; section 4.2.10). This strongly implies that the functional capabilities of DDX3 are linked to its subcellular localisation. Since the altered distribution of the DDX3-EQ mutant was found to be irrelevant for its interaction with core protein (Fig. 60; section 4.2.11), it is likely that the DDX3/core interaction occurs prior to

targeting of DDX3 to its normal subcellular localisation. This could be related to the reported presence of core protein, albeit in low amounts, at the ER (section 1.7.3). It is also feasible that the interaction occurs as DDX3 is being translated, since the domain responsible for interaction with core is found near the C-terminus of the protein (Fig. 33e; section 3.2.9; Owsianka and Patel, 1999; You *et al.*, 1999b). However, the question remains as to why core protein maintains its ability to interact with an energetically-redundant DDX3 mutant protein. It will be interesting to test whether this DDX3 mutant interferes with viral processes when an HCV-permissive cell culture system becomes available.

The identification of possible modified processing of DDX3 attributable to core protein, indicated by the presence of a higher molecular weight isoform of DDX3, in both insect and mammalian cell-based co-expression studies (Figs 67-68; sections 5.2.2-5.2.3), is in agreement with the above hypothesis. This indicates that the interaction with core protein occurs before DDX3 can be properly processed. Alternatively, it could indicate the interaction with core causes DDX3 to undergo further post-translational modifications. Nevertheless, the DDX3 isoform that is induced by core protein is in fact the first indication that core is able to modify a cellular protein with which it interacts. Other studies describing the interaction of core protein with host cell factors (section 1.9) have failed to reveal any modification of the individual proteins, although aberrant sequestration of the targeted proteins and alteration of their functions is commonly reported. Further studies are needed to determine the actual mechanism of this modification in the presence of core protein. It is unlikely that the higher molecular weight isoform represents core bound to DDX3, since this heterodimer would be denatured by SDS-PAGE. Furthermore, the effect is not due to copious quantities of the HCV glycoproteins at the ER, since the higher molecular weight DDX3 species is not seen when E1 and E2 alone are expressed in hepatocytes (Fig. 68; section 5.2.3). It also appears that the effect is not due to modification of DDX3 mRNA by core protein or its coding sequence (Fig. 69; section 5.2.4), as mentioned briefly above. Whatever the mechanism, the alteration of endogenous DDX3 by core in hepatocytes attaches additional credence to the actual biological significance of their interaction, particularly in view of three independent reports isolating DDX3 as an

interacting partner of core protein (section 1.9.6.9; Mamiya and Worman, 1999; Owsianka and Patel, 1999; You *et al.*, 1999b).

6. 3 Effect of Core Protein on IRES Activity

Intriguingly, core protein was able to remove the HCV 5′NCR-mediated translational block in insect cells (Fig. 77 and 80; section 5.2.10), and also markedly upregulated IRES activity of a transfected reporter constructs driven by the HCV 5′NCR in human hepatocytes (Fig. 84b; section 5.2.13). In both cases, full-length core protein in the context of the HCV glycoproteins was able to mediate the effect, while E1 and E2 had little or no influence on translation (Figs 80 and 84b; sections 5.2.10 and 5.2.13). The observed differences between the experimental findings presented here and the previous reports of an apparent suppression by core protein (Shimoike *et al.*, 1999) or its coding sequence (Wang *et al.*, 2000) (section 1.3.5) could be due to a number of experimental disparities. Genotype sequence variations might give rise to differences in phosphorylation or proteolytic processing of core protein that could affect its function - the study by Wang *et al.*, (2000) used a HCV genotype 1b infectious clone (Beard *et al.*, 1999), in contrast to the genotoype 1a infectious clone used here (H77c; Yanagi *et al.*, 1997; see Appendix IV) and by Shimoike *et al.*, (1999). In addition, unlike those used in previous studies (Shimoike *et al.*, 1999; Wang *et al.*, 2000), all constructs carrying HCV 5′NCR used here are expected to express transcripts initiating from the first nucleotide of the viral genome, thus negating possible effect of heterologous sequences on IRES structure and/or its activity. Furthermore, the published studies have neglected to use core protein in its entirety to ensure proper processing and/or core protein in the context of the HCV glycoproteins, as it would be expressed during natural infection. The use of core protein together with E1 and E2 counteracts any possible effects of core protein in isolation. Finally, although frameshifting the core-coding sequence suggested that core protein itself is not responsible for an observed suppression of translation (Wang *et al.*, 2000), the situation is unclear following two independent reports of an actual frameshift site within the core-coding sequence used by HCV (section 1.7.4; Walewski *et al.*, 2001; Xu *et al.*, 2001), giving rise to a product (the F protein) with an as yet undetermined function. It is entirely possible that the F

protein has some effect on translation of the HCV ORF, which could be responsible for the observations of Wang *et al.* (2000) that a frameshifted core-coding seqeunce suppresses translation from the HCV IRES. Although the effect observed here was not due to effects at the transcriptional level in the insect cell system (Fig. 81; section 5.2.11), this possibility needs to be investigated in the hepatocyte-based system. However, if anything, core protein expressed by rbac in Sf21 cells appears to downregulate transcription or stability of the 5′NCR-core RNA generated by rbac-5C, while showing a discernible upregulation of translation (Figs 77 and 79-81; sections 5.2.10 and 5.2.11).

Interestingly, addition of the authentic 3′NCR at the 3′-end of the reporter constructs led to only a moderate effect of core on HCV 5′NCR-mediated translation. This effect was consistent in both insect and mammalian cell-based assays (Figs 77 and 84b; sections 5.2.10 and 5.2.13). However, the reason for this is currently unclear. It is possible, given recent insight into the HCV ORF (section 1.7.4; Walewski *et al.*, 2001; Xu *et al.*, 2001), that HCV generates two separate genomic RNAs, one of which is a shortened form that lacks the 3′NCR. Indeed, many positive-strand RNA viruses synthesise subgenomic RNAs (Miller and Koev, 2000) and RNA analysis performed by Walewski *et al.*, (2001) suggests unusual features at the 3′-end of the E2-coding sequence (Fig. 12; section 1.7.4). This may represent a ribosomal frameshift site, or a stable stem loop, marking the end of a shortened HCV ORF that lacks the nonstructural region and the 3′NCR. Such a shortened form could allow cellular resources to be directed towards high level production of HCV structural proteins in a late stage of infection to generate large amounts of virions prior to egress from the cell. In this case, in the absence of the 3′NCR, core protein may be involved in a feedback loop to generate more viral particles by upregulating IRES activity. Nevertheless, the effect of core protein on HCV 5′NCR-mediated translation is clearly not fully elucidated. Indeed, until an efficient cell culture system for HCV is available, these results, or indeed previous studies, and various hypotheses put forward here and by others, cannot be validated *in vivo*.

REFERENCES

Abramson RD, Dever TE, Lawson TG, Ray BK, Thach RE and Merrick WC (1987). The ATP-Dependent Interaction of Eukaryotic Initiation Factors with Messenger RNA. *Journal of Biological Chemistry* **262**, 3826-3832

Agnello V, Ábel G, Elfahal M, Knight GB and Zhang Q-X (1999). Hepatitis C Virus and Other *Flaviviridae* Viruses Enter Cells Via Low Density Lipoprotein Receptor. *Proceedings of the National Academy of Sciences USA* **96**, 12766-12771

Aitken A (1996). 14-3-3 Proteins on the MAP. *Trends in Cell Biology* **6**, 341-347

Alberts B, Bray D, Lewis J, Raff M, Roberts K and Watson JD (1994). *Molecular Biology of the Cell* (3rd edition). New York: Garland

Ali N and Siddiqui A (1995). Interaction of Polypyrimidine Tract-binding Protein with the 5′-Noncoding Region of the Hepatitis C Virus RNA Genome and its Functional Requirement in Internal Initiation of Translation. *Journal of Virology* **69**, 6367-6375

Ali N and Siddiqui A (1997). The La Antigen Binds 5′-Noncoding Region of the Hepatitis C Virus RNA in the Context of the Initiator AUG Codon and Stimulates Internal Ribosome Entry Site-mediated Translation. *Proceedings of the National Academy of Sciences USA* **94**, 2249-2254

Ali JA and Lohman TM (1997). Kinetic Measurement of the Step Size of DNA Unwinding by *Escherichia coli* UvrD Helicase. *Science* **275**, 377-380

Alonso CR, Pesce CG and Kornblihtt AR (1996). The CCAAT-binding Proteins CP1 and NF-I Co-operate with ATF-2 in the Transcription of the Fibronectin Gene. *Journal of Biological Chemistry* **271**, 22271-22279

Alter HJ, Holland PV, Morrow AG, Purcell RH, Feinstone SM and Moritsugu Y (1975). Clinical and Serological Analysis of Transfusion-transmitted Hepatitis. *Lancet* **2**, 838-841

Alter MJ, Margolis HS, Krawczynski K, Judson FN, Mares A, Alexander WJ, Hu PY, Miller JK, Gerber MA, Sampliner RE, Meeks EL and Beach MJ (1992). The Natural History of Community-acquired Hepatitis C in the United States. *New England Journal of Medicine* **327**, 1899-1905

Alwine JC, Kemp DJ and Stark GR (1977). Method for Detection of Specific RNAs in Agarose Gels by Transfer to Diazobenzyloxymethyl-paper and Hybridisation with DNA Probes. *Proceedings of the National Academy of Sciences USA* **74**, 5350

Alwine JC, Kemp DJ, Parker BA, Reiser J, Renart J, Stark GR and Wahl GM (1979). Detection of Specific RNAs or Specific Fragments of DNA by Fractionation in Gels and Transfer to Diazobenzyloxymethyl-paper. *Methods in Enzymology* **68**, 220

Anderson JSJ and Parker R (1996). RNA Turnover: The Helicase Story Unwinds. *Current Biology* **6**, 780-782

Anderson JSJ and Parker R (1998). The 3′ to 5′ Degradation of Yeast mRNAs is a General Mechanism for mRNA Turnover that Requires the SKI2 DEVH Box Protein and 3′ to 5′ exonucleases of the Exosome Complex. *EMBO Journal* **17**, 1497-1506

Aoki H, Hayashi J, Moriyama M, Arakawa Y and Hino O (2000). Hepatitis C Virus Core Protein Interacts with 14-3-3 Protein and Activates the Kinase Raf-1. *Journal of Virology* **74**, 1736-1741

Aoubala M, Holt J, Clegg RA, Rowlands DJ and Harris M (2001). The Inhibition of cAMP-Dependent Protein Kinase by Full-length Hepatitis C Virus NS3/4A Complex is Due to ATP Hydrolysis. *Journal of General Virology* **82**, 1637-1646

Asabe SI, Tanji Y, Satoh S, Kaneko T and Shimotohno K (1997). The N-terminal Region of Hepatitis C Virus-encoded NS5A is Important for NS4A-dependent Phosphorylation. *Journal of Virology* **71**, 790-796

Askjaer P, Jensen TH, Nilsson J, Englmeier L and Kjems J (1998). The Specificity of the CRM1-Rev Nuclear Export Signal Interaction is Mediated by Ran-GTP. *Journal of Biological Chemistry* **273**, 33414-33422

Askjaer P, Bachi A, Wilm M, Bischoff FR, Weeks DL, Ogniewski V, Ohno M, Niehrs C, Kjems J, Mattaj IW and Fornerod M (1999). RanGTP-Regulated Interactions of CRM1 with Nucleoporins and a Shuttling DEAD-Box Helicase. *Molecular and Cellular Biology* **19**, 6276-6285

Askjaer P, Rosendahl R and Kjems J (2000). Nuclear Export of the DEAD Box An3 Protein by CRM1 is Coupled to An3 Helicase Activity. *Journal of Biological Chemistry* **275**, 11561-11568

Baker SJ and Reddy EP (1996). Transducers of Life and Death: TNF Receptor Superfamily and Associated Proteins. *Oncogene* **12**, 1-9

Banerjee R and Dasgupta A (2001). Specific Interaction of Hepatitis C Virus Protease/Helicase NS3 with the 3′-Terminal Sequences of Viral Positive- and Negative-Strand RNA. *Journal of Virology* **75**, 1708-1721

Barba G, Harper F, Harada T, Kohara M, Goulinet S, Matsuura Y, Eder G, Schaff Z, Chapman MJ, Miyamura T and Bréchot C (1997). Hepatitis C Virus Core Protein shows a Cytoplasmic Localisation and Associates to Cellular Lipid Storage Droplets. *Proceedings of the National Academy of Sciences USA* **94**, 1200-1205

Bartenschlager R (1999). The NS3/4A Proteinase of the Hepatitis C Virus: Unravelling Structure and Function of an Unusual Enzyme and a Prime Target for Antiviral Therapy. *Journal of Viral Hepatitis* **6**, 165-181

Bartenschlager R and Lohmann V (2000). Replication of Hepatitis C Virus. *Journal of General Virology* **81**, 1631-1648

Bartenshclager R, Ahlborn LL, Mous J and Jacobsen H (1994). Kinetic and Structural Analyses of Hepatitis C Virus Polyprotein Processing. *Journal of Virology* **68**, 5045-5055

Battegay M, Fikes J, Di Bisceglie AM, Wentworth PA, Sette A, Celis E, Ching W-M, Grakoui A, Rice CM, Kurokohchi K, Berzofsky JA, Hoofnagle JH, Feinstone SM and Akatsuka T (1995). Patients with Chronic Hepatitis C have Circulating Cytotoxic T Cells which Recognise Hepatitis C Virus-Encoded Peptides Binding to HLA-A2.1 Molecules. *Journal of Virology 69*, 2462-2470

Baumert TF, Ito S, Wong DT and Liang TJ (1998). Hepatitis C Virus Structural Proteins Assemble into Virus-like Particles in Insect Cells. *Journal of Virology* **72**, 3827-3836

Baumert TF, Vergalla J, Satoi J, Thomson M, Lechmann M, Herion D, Greenberg HB, Ito S and Liang TJ (1999). Hepatitis C Virus-like Particles Synthesized in Insect Cells as a Potential Vaccine Candidate. *Gastroenterology* **117**, 1397-1407

Baumert TF, Wellnitz S, Aono S, Satoi J, Herion D, Gerlach JT, Pape GR, Lau JYN, Hoofnagle JH, Blum HE and Liang TJ (2000). Antibodies Against Hepatitis C Virus-like Particles and Viral Clearance in Acute and Chronic Hepatitis C. *Hepatology* **32**, 610-617

Beales LP, Rowlands DJ and Holzenburg A (2001). The Internal Ribosome Entry Site (IRES) of Hepatitis C Virus Visualized by Electron Microscopy. *RNA* **7**, 661-670

Beard MR, Abell G, Honda M, Carroll A, Gartland M, Clarke B, Suzuki K, Lanford R, Sangar DV and Lemon SM (1999). An Infectious Molecular Clone of a Japanese Genotype 1b Hepatitis C Virus. *Hepatology* **30**, 316-324

Behrens S-E, Tomei L and De Francesco R (1996). Identification and Properties of the RNA-dependent RNA Polymerase of Hepatitis C Virus. *EMBO Journal* **15**, 12-22

Behrens S-E, Grassmann CW, Thiel HJ, Meyers G and Tautz N (1998). Characterization of an Autonomous Subgenomic Pestivirus RNA Replicon. *Journal of Virology* **72**, 2364-2372

Beidler DR, Tewari M, Friesen PD, Poirier G and Dixit DM (1995). The Baculovirus p35 Protein Inhibits *Fas*- and Tumour Necrosis Factor-induceed Apoptosis. *Journal of Biological Chemistry* **270**, 16526-16528

Beier F, Lee RJ, Taylor AC, Pestell RG and LuValle P (1999). Identification of the Cyclin D1 Gene as a Target of Activating Transcription Factor 2 in Chondrocytes. *Proceedings of the National Academy of Sciences USA* **96**, 1433-1438

Bell LR, Horabin JI, Schedl P and Cline TW (1991). Positive Autoregulation of Sex-lethal by Alternative Splicing Maintains the Female Determined State in *Drosophila. Cell* **65**, 229-239

Benvegnu L, Pontisso P, Cavalletto D, Noventa F, Chemello L and Alberti A (1997). Lack of Correlation between Hepatitis C Virus Genotypes and Clinical Course of Hepatitis C Virus-Related Cirrhosis. *Hepatology* **25**, 211-215

Beutler B and van Huffel C (1994). An Evolutionary and Functional Approach to the TNF Receptor/Ligand Family Microbial Pathogenesis and Immune Response. *Annals of the New York Academy of Sciences* **730**, 118-133

Blight KJ, Kolykhalov AA and Rice CM (2000). Efficient Initiation of HCV RNA Replication in Cell Culture. *Science* **290**, 1972-1974

Blight and Gowans (1995). *In situ* Hybridisation and Immunohistochemical Staining of Hepatitis C Virus Products. *Viral Hepatitis Reviews* **1**, 143-155

Blight KJ and Rice CM (1997). Secondary Structure Determination of the Conserved 98-base Sequence at the 3′ Terminus of Hepatitis C Virus Genome RNA. *Journal of Virology* **71**, 7345-7352

Blum S, Schmid SR, Pause A, Buser P, Linder P, Sonenberg and Trachhsel H (1992). ATP Hydrolysis by Initiation Factor 4A is Required for Translation Initiation in *Saccharomyces cerevisiae. Proceedings of the National Academy of Sciences USA* **89**, 7664-7668

Bolten R, Egger D, Gosert R, Schaub G, Landmann L and Bienz K (1998). Intracellular Localization of Poliovirus Plus- and Minus-strand RNA Visualized by Strand-specific Fluorescent *In situ* Hybridization. *Journal of Virology* **72** , 8578-8585

Bomsztyk K, VanSeuningen I, Suzuki H, Denisenko O and Ostrowski J (1997). Diverse Molecular Interactions of the hnRNP K Protein. *FEBS Letters* **403**, 113-115

Boyer JC and Haenni AL (1994). Infectious Transcripts and cDNA Clones of RNA Viruses. *Virology* **198**, 415-426

Borowski P, Heiland M, Oehlmann, Becker B, Kornetzky L, Feucht H and Laufs R (1996). Non-structural Protein 3 of Hepatitis C Virus Inhibits Phosphorylation Mediated by cAMP-dependent Protein Kinase. *European Journal of Biochemistry* **237**, 611-618

Borowski P, Oehlman K, Heiland M and Laufs R (1997). Non-structural Protein 3 of Hepatitis C Virus Blocks the Distribution of the Free Catalytic Subunit of Cyclic AMP-dependent Protein Kinase. *Journal of Virology* **71**, 2838-2843

Bradley DW (1999). Studies of Non-A, Non-B Hepatitis and Characterization of the Hepatitis C Virus in Chimpanzees. In *"The Hepatitis C Viruses"*, pp 1-24. Edited by CH Hagedorn and CM Rice. Germany: Springer.

Bradley DW, Maynard JE, McCaustland KA, Murphy BL, Cook EH and Ebert JW (1983). Non-A, Non-B Hepatitis in Chimpanzees: Interference with Acute Hepatitis A Virus and Chronic Hepatitis B Virus Infections. *Journal of Medical Virology* **11**, 207-213

Brennan CA, Dombrowski AJ and Platt T (1987). Transcription Termination Factor Rho is an RNA-DNA Helicase. *Cell* **48**, 945-952

Brown EA, Zhang H, Ping L-H, and Lemon SM (1992). Secondary Structure of the 5′ Non-translated Regions of the Hepatitis C Virus and Pestivirus Genomic RNAs. *Nucleic Acids Research* **20**, 5041-5045

Buchenau P, Saumweber H and Arndt-Jovin DJ (1997). The Dynamic Nuclear Redistribution of an hnRNP K-homologous Protein during Drosophila Embryo Development. *Journal of Cell Biology* **137**, 291-303

Bukh J, Purcell RH and Miller RH (1992). Sequence Analysis of the 5′ Noncoding Region of Hepatitis C Virus. *Proceedings of the National Academy of Sciences USA* **89**, 4942-4946

Bukh J, Purcell RH and Miller RH (1994). Sequence Analysis of the Core Gene of 14 Hepatitis C Virus Genotypes. *Proceedings of the National Academy of Sciences USA* **91**, 8239-8243

Bukh J, Miller RH and Purcell RH (1995). Genetic Heterogeneity of Hepatitis C Virus Quasispecies and Genotypes. *Seminars in Liver Disease* **15**, 41-63

Bukh J, Apgar CL and Yanagi M (1999). Toward a Surrogate Model for Hepatitis C Virus: An Infectious Molecular Clone of the GB Virus B Hepatitis Agent. *Virology* **262**, 470-478

Caprara MG and Nilsen TW (2000). RNA: Versatility in Form and Function. *Nature Structural Biology* **7**, 831-833

Carrera P, Johnstone O, Nakamura A, Casanova J, Jackle H and Lasko P (2000). VASA Mediates Translation through Interaction with a *Drosophila* yIF2 Homolog. *Molecular Cell* **5**, 181-187

Castrillon DH, Quade BJ, Wang TY, Quigley C and Crum CP (2000). The Human *VASA* Gene is Specifically Expressed in the Germ Cell Lineage. *Proceedings of the National Academy of Sciences USA* **97**, 9585-9590

Cha T-A, Beall E, Irvine B, Kolberg J, Chien D, Kuo G and Urdea MS (1992). At Least Five Related, But Distinct, Hepatitis C Virus Genotypes Exist. *Proceedings of the National Academy of Sciences USA* **89**, 7144-7148

Chan-Fook C, Jiang WR, Clarke BE, Zitzmann N, Maidens C, McKeating JA and Jones IM (2000). Hepatitis C Virus Glycoprotein E2 Binding to CD81: The Role of E1-E2 Cleavage and Protein Glycosylation in Bioactivity. *Virology* **273**, 60-66

Chang SC, Yen JH, Kang HY, Jang MH and Chang MF (1994). Nuclear-localization Signals in the Core Protein of Hepatitis C Virus. *Biochemical and Biophysical Research Communications* **205**, 1284-1290

Chang J, Yang S-H, Cho Y-G, Hwang SB, Hahn YS and Sung YC (1998). Hepatitis C Virus Core from Two Different Genotypes Has an Oncogenic Potential but Is Not Sufficient for Transforming Primary Rat Embryo Fibroblasts in Cooperation with the H-*ras* Oncogene. *Journal of Virology* **72**, 3060-3065

Chang JC, Seidel C, Ofenloch B, Jue DL, Fields HA, Khudyakov YE (1999). Antigenic Heterogeneity of the Hepatitis C Virus NS4 Protein as Modeled with Synthetic Peptides. *Virology* **257**, 177-190

Chazouilleres O and Wright TL (1995). Hepatitis C and Liver Transplantation. *Journal of Gastroenterology and Hepatology* **10**, 471-480

Chen C-M, You L-R, Hwang L-H and Lee WY-H (1997). Direct Interaction of Hepatitis C Virus Core Protein with the Cellular Lymphotoxin-β Receptor Modulates the Signal Pathway of the Lymphotoxin-β Receptor. *Journal of Virology* **71**, 9417-9426

Chen JY-F, Stands L, Staley JP, Jackups Jr. RR, Latus LJ and Chang T-H (2001). Specific Alterations of U1-C Protein or U1 Small Nuclear RNA Can Elimiate the Requirement of Prp28p, an Essential DEAD Box Splicing Factor. *Molecular Cell* **7**, 227-232

Cheng J-C, Chang M-F and Chang SC (1999). Specific Interaction between the Hepatitis C Virus NS5B RNA Polymerase and the 3′ End of the Viral RNA. *Journal of Virology* **73**, 7044-7049

Chien CT, Bartel PL, Sternglanz R and Fields S (1991). The Two-Hybrid System - A Method to Identify and Clone Genes for Proteins that Interact with a Protein of Interest. *Proceedings of the National Academy of Sciences USA* **88**, 9578-9582

Chien DY, Choo Q-L, Ralston R, Spaete R, Tong M, Houghton M and Kuo G (1993). Persistence of HCV Despite Antibodies to both Putative Envelope Glycoproteins. *Lancet* **342**, 933

Chinnaiyan AM, O'Rourke K, Tewari M and Dixit VM (1995). FADD, A Novel Death Domain-containing Protein, Interacts with the Death Domain of *Fas* and Initiates Apoptosis. *Cell* **81**, 505-512

Cho H-S, Ha N-C, Kang L-W, Chung KM, Back SH, Jang SK and Oh B-H (1998). Crystal Structure of RNA Helicase from Genotype 1b Hepatitis C Virus. *Journal of Biological Chemistry* **273**, 15045-15052

Choo Q-L, Kuo G, Weiner AJ, Overby LR, Bradley DW and Houghton M (1989). Isolation of a cDNA Clone derived from a Blood-borne Non-A, Non-B Viral Hepatitis Genome. *Science* **244**, 359-362

Choo Q-L, Richman KH, Han H, Berger K, Lee C, Dong C, Gallegos C, Coit D, Medina-Selby A, Barr PJ, Weiner AJ, Bradley DW, Kuo G and Houghton M (1991). Genetic Organisation and Diversity of the Hepatitis C Virus. *Proceedings of the National Academy of Sciences USA* **88**, 2451-2455

Choo Q-L, Kuo G, Ralston R, Weiner A, Chien D, Vannest G, Han J, Berger K, Thudium K, Kuo C, Kansopon J, McFarland J, Yabrizi A, Ching K, Moss B, Cummins LB and Houghton M (1994). Vaccination of Chimpanzees Against Infection by the Hepatitis C Virus. *Proceedings of the National Academy of Sciences USA* **91**, 1294-1298

Chuang R-Y, Weaver PL, Liu Z and Chang T-H (1997). Requirement of the DEAD-Box Protein Ded1p for Messenger RNA Translation. *Science* **275**, 1468-1471

Chung J, Lee S-G and Song K (1995). Identification of a Human Homolog of a Putative RNA Helicase Gene (mDEAD3) Expressed in Mouse Erythroid Cells. *Korean Journal of Biochemistry* **27**, 193-197

Clarke B (1997). Molecular Virology of Hepatitis C Virus. *Journal of General Virology* **78**, 2397-2410

Clarke PR and Zhang C (2001). RanGTPase: A Master Regulator of Nuclear Structure and Function During the Eukaryotic Cell Cycle. *Trends in Cell Biology* **11**, 366-371

Cocquerel L, Meunier J-C, Pillez A, Wychowski C and Dubuisson J (1998). A Retention Signal Necessary and Sufficient for Endoplasmic Reticulum Localization Maps to the Transmembrane Domain of Hepatitis C Virus Glycoprotein E2. *Journal of Virology* **72**, 2183-2191

Cocquerel L, Duvet S, Meunier J-C, Pillez A, Cacan R, Wychowski C and Dubuisson J (1999). The Transmembrane Domain of Hepatitis C Virus Glycoprotein E1 is a Signal for Static Retention in the Endoplasmic Reticulum. *Journal of Virology* **73**, 2641-2649

Crowe PD, VanArsdale TL, Walter BN, Ware CF, Hession C, Ehrenfels B, Browning WS, Din WS, Goodwin RG and Smith CA (1994). A Lymphotoxin-β-specific Receptor. *Science* **264**, 707-710

Czaplinski K, Ruiz-Echevarria MJ, Paushkin SV, Han X, Weng YM, Perlick HA, Dietz HC, Ter-Avanesyan MD and Peltz SW (1998). The Surveillance Complex Interacts with the Translation Release Factors to Enhance Termination and Degrade Aberrant mRNAs. *Genes and Development* **12**, 1665-1677

D'Souza EDA, Grace K, Sangar DV, Rowlands DJ and Clarke BE (1995). *In vitro* Cleavage of Hepatitis C Virus Polyprotein Substrates by Purified Recombinant NS3 Protease. *Journal of General Virology* **76**, 1729-1736

Daugeron MC, Kressler D and Linder P (2001). Dbp9p, a Putative ATP-Dependent RNA Helicase Involved in 60S-Ribosomal-Subunit Biogeneis, Functionally Interacts with DBp6p. *RNA* **7**, 1317-1334

Dash S, Halim A-B, Tsuji H, Hiramatsu N and Gerber MA (1997). Transfection of HepG2 Cells with Infectious Hepatitis C Virus Genome. *American Journal of Pathology* **151**, 363-373

de la Cruz J, Iost I, Kressler D and Linder P (1997). The p20 and Ded1 Proteins have Antagonistic Roles in eIF4E-dependent Translation in *Saccharomyces cerevisiae*. *Proceedings of the National Academy of Sciences USA* **94**, 5201-5206

de la Cruz J, Kressler D, Rojo M, Tollervey D and Linder P (1998). Spb4p, an essential putative RNA helicase, is required for a late step in the assembly of 60S ribosomal subunits in *Saccharomyces cerevisiae*. *RNA* **4**, 1268-1281

de la Cruz J, Kressler D and Linder P (1999). Unwinding RNA in *Sacchraomyces cerevisiae*: DEAD-box Proteins and Related Families. *Trends in Biochemical Sciences* **24**, 192-198

DeFranscesco R and Steinkühler C (1999). Structure and Function of the Hepatitis C Virus NS3-NS4A Serine Protease. In: "*The Hepatitis C Viruses*", pp 149-169. Edited by CH Hagedorn and CM Rice. Germany: Springer.

Deleersnyder V, Pillez A, Wychowski C, Blight K, Xu J, Hahn YS, Rice CM and Dubuisson (1997). Formation of Native Hepatitis C Virus Glycoprotein Complexes. *Journal of Virology* **71**, 697-704

Denisenko ON, ONeill B, Ostrowski J, VanSeuningen I and Bomsztyk K (1996). Zik1, a Transcriptional Repressor that Interacts with the Heterogeneous Nuclear Ribonucleoprotein Particle K Protein. *Journal of Biological Chemistry* **271**, 27701-27706

Di Bisceglie AM (1998). Hepatitis C. *Lancet* **351**, 351-355

Diges CM and Uhlenbeck OC (2001). *Escherichia coli* DbpA is an RNA Helicase that Requires Hairpin 92 of 23S rRNA. *EMBO Journal* **20**, 5503-5512

Dodson MS and Lehman IR (1991). Association of DNA Helicase and Primase Activities with a Sub-assembly of the Herpes Simplex Virus-1 Helicase Primase Composed of the UL5 and UL52 Gene-products. *Proceedings of the National Academy of Sciences USA* **88**, 1105-1109

Dreyfuss G, Matunis M-J, Pinol-Roma S and Burd CG (1993). hnRNP Proteins and the Biogenesis of mRNA. *Annual Reviews in Biochemistry* **62**, 289-321

Dubuisson J and Rice CM (1996). Hepatitis C Virus Glycoprotein Folding: Disulphide Bond Formation and Association with Calnexin. *Journal of Virology* **70**, 778-786

Dubuisson J, Hsu HH, Cheung RC, Greeberg HB, Russell DG and Rice CM (1994). Formation and Intracellular Localization of Hepatitis C Virus Envelope Glycoprotein Complexes Expressed by Recombinant Vaccinia and Sinbis Viruses. *Journal of Virology* **68**, 6147-6160

Duvet S, Cocquerel L, Pillez A, Cacan R, Verbert A, Moradpour D, Wychowski C and Dubuisson J (1998). Hepatitis C Virus Glycoprotein Complex Localization in the Endoplasmic Reticulum Involves a Determinant for Retention and Not Retrieval. *Journal of Biological Chemistry* **273**, 32088-32095

Elbers K, Tautz N, Becher P, Stoll D, Rümennapf T, and Thiel H-J (1996). Processing in the Pestivirus E2-NS2 Region: Identification of Proteins p7 and E2-p7. *Journal of Virology* **70**, 4131-4135

Enomoto N, Sakuma I, Asahina Y, Kurosaki M, Murakami T, Yamamoto C, Izumi N, Marumo F and Sato C (1995). Comparison of Full-length Sequences of Interferon-sensitive and Resistant Hepatitis C Virus 1b - Sensitivity is Conferred by Amino Acid Substitutions in the NS5A Region. *Journal of Clinical Investigation* **96**, 224-230

Enomoto N, Sakuma I, Asahina Y, Kurosaki M, Murakami T, Yamamoto C, Ogura Y, Izumi N, Marumo F and Sato C (1996). Mutations in the Nonstructural Protein 5A Gene and Response to Interferon in Patients with Chronic Hepatitis C Virus 1b Infection. *New England Journal of Medicine* **334**, 77-81

Esteban R (1993). Epidemiology of Hepatitis C Virus Infection. *Journal of Hepatology* **17 (Suppl. 3)**, 67-71, 1993

Failla C, Tomei L and DeFrancesco R (1994). Both NS3 and NS4A are Required for Proteolytic Processing of Hepatitis C Virus Nonstructural Proteins. *Journal of Virology* **68**, 3753-3760

Fan Z, Yang QR, Twu J-S and Sherker AH (1999). Specific *In Vitro* Association Between the Hepatitis C Viral Genome and Core Protein. *Journal of Medical Virology* **59**, 131-134

Farci P, Shimoda A, Wong D, Cabezon T, DeGioannis D, Strazzera A, Shimizu Y, Shapiro M, Alter HJ and Purcell RH (1996). Prevention of Hepatitis C Virus Infection in Chimpanzees by Hyperimmune Serum Against the Hypervariable Region 1 of the Envelope 2 Protein. *Proceedings of the National Academy of Sciences USA* **93**, 15394-15399

Feinstone SM, Mihalik KB, Kamimura T, Alter HJ, London WT and Purcell RH (1983). Inactivation of Hepatitis B Virus and Non-A, Non-B Hepatitis by Chloroform. *Infection and Immunity* **41**, 816-821

Fischer N, Voss MD, Muller-Lantzsch N and Grasser FA (1999). A Potential NES of Epstein-Barr Virus Nuclear Antigen 1 (EBNA1) Does Not Confer Shuttling. *FEBS Letters* **447**, 311-314

Flint M, Thomas JM, Maidens CM, Shotton C, Levy S, Barclay WS and McKeating JA (1999). Functional Analysis of Cell Surface-expressed Hepatitis C Virus E2 Glycoprotein. *Journal of Virology* 73, 6782-6790

Fong T-L, Di Bisceglie AM, Waggoner JG, Banks SM and Hoofnagle JH (1991). The Significance of Antibody to Hepatitis C Virus in Patients with Chronic Hepatitis B. *Hepatology* **14**, 64-67

Foresta C, Ferlin A and Moro E (2000). Deletion and Expression Analysis of AZFa genes on the Human Y Chromosome Revealed a Major Role for DBY in Male Fertility. *Human Molecular Genetics* **9**, 1161-1169

Fornerod M, Ohno M, Yoshida M and Mattaj IW (1997). CRM1 is an Export Receptor for Leucine-Rich Nuclear Export Signals. *Cell* **90**, 1051-1060

Forns X, Thimme R, Govindarajan S, Emerson SU, Purcell RH, Chisari FV and Bukh J (2000). Hepatitis C Virus Lacking the Hypervariable Region 1 of the Second Envelope Protein is Infectious and Causes Acute Resolving or Persistent Infection in Chimpanzees. *Proceedings of the National Academy of Sciences USA* **97**, 13318-13323

Fortes P, Lamond AI and Ortin J (1995). Influenza Virus NS1 Protein Alters the Subnuclear Localization of Cellular Splicing Components. *Journal of General Virology* **76**, 1001-1007

Francis SH and Corbin JD (1994). Structure and Function of Cyclic Nucleotide-dependent Protein Kinases. *Annual Review of Physiology* **56**, 237-272

Frank C, Mohamed MK, Strickland GT, Lavanchy D, Arthur RR, Magder LS, El Khoby T, Abdel-Wahab Y, Ohn EA, Anwar W and Sallam I (2000). The Role of Parenteral Antischistosomal Therapy in the Spread of Hepatitis C Virus in Egypt. *Lancet* **355**, 887-891

Friebe P, Lohmann V, Krieger N and Bartenschlager R (2001). Sequences in the 5′ Nontranslated Region of Hepatitis C Virus Required for RNA Replication. *Journal of Virology* **75**, 12047-12057

Frolov I, McBride MS and Rice CM (1998). Cis-acting RNA Elements Required for Replication of Bovine Viral Diarrhea Virus Hepatitis C Virus 5′ Nontranslated Region Chimeras. *RNA* **4**, 1418-1435

Fu X-D (1995). The Superfamily of Arginine/Serine-rich Splicing Factors. *RNA* **1**, 663-680

Fu X-D and Maniatis T (1992). The 35 kDa Mammalian Splicing Factor SC35 Mediates Specific Interactions Between U1 and U2 Small Nuclear Ribonucleoprotein-particles at the 3′ Splice Site. *Proceedings of the National Academy of Sciences USA* **89**, 1725-1729

Fuerst TR, Niles EG, Studier FW and Moss B (1986). Eukaryotic Transient-expression System Based on Recombinant Vaccinia Virus that Synthesizes Bacteriophage T7 RNA-Polymerase. *Proceedings of the National Academy of Sciences USA* **83**, 8122-8126

Fukada M, Asano S, Nakamura T, Adachi M, Yoshida M, Yanagida M and Nishida E (1997). CRM1 is Responsible for Intracellular Transport Mediated by the Nuclear Export Signal. *Nature* **390**, 308-311

Fukushi S, Kurihara C, Ishiyama N, Hoshino FB, Oya A and Katayama K (1997). The Sequence Element of the Internal Ribosome Entry Site and a 25-kilodalton Cellular Protein Contribute to Efficient Internal Initiation of Translation of Hepatitis C Virus RNA. *Journal of Virology* **71**, 1662-1666

Fukushi S, Okada M, Stahl J, Kageyama T, Hoshino FB and Katayama K (2001). Ribosomal Protein S5 Interacts with the Internal Ribosomal Entry Site of Hepatitis C Virus. *Journal of Biological Chemistry* **276**, 20824-20826

Fuller-Pace FV, Nicol SM, Reid AD and Lane DP (1993). DbpA: A DEAD Box Protein Specifically Activated by 23C rRNA. *EMBO Journal* **12**, 3619-3626

Gale M, Korth MJ, Tang NM, Tan SL, Hopkins DA, Dever TE, Polyak SJ, Gretch DR and Katze MG (1997). Evidence that Hepatitis C Virus Resistance to Interferon is Mediated Through Repression of the PKR Protein Kinase by the Nonstructural 5A Protein. *Virology* **230**, 217-227

Gale M, Blakely CM, Kwieciszewski B, Tan SL, Dossett M, Tang NM, Korth MJ, Polyak SJ, Gretch DR and Katze MG (1998). Control of PKR Protein Kinase by Hepatitis C Virus Nonstructural 5A Protein: Molecular Mechanisms of Kinase Regulation. *Molecular and Cellular Biology* **18**, 5208-5218

Ge H, Zuo P and Manley JL (1991). Primary Structure of the Human Splicing Factor ASF Reveals Similarities with Drosophila Regulators. *Cell* **66**, 373-382

Gee SL and Conboy JG (1994). Mouse Erythroid Cells Express Multiple Putative RNA Helicase Genes Exhibiting High Sequence Conservation from Yeast to Mammals. *Gene* **140**, 171-177

Ghosh S, May MJ and Kopp EB (1998). NF-κB and Rel Proteins: Evolutionary Conserved Mediators of Immune Responses. *Annual Review of Immunology* **16**, 225-260

Giovannini M, Tagger A, Ribero ML, Zuccoti G, Pogliani L, Grossi A, Ferroni P and Fiocchi A (1990). Maternal-Infant Transmission of Hepatitis C Virus and HIV Infections: A Possible Interaction. *Lancet* **336**, 1166

Glue P, Rouzier-Panis R, Raffanel C, Sabo R, Gupta SK, Salfi M, Jacobs S and Clement RP (2000). A Dose-ranging Study of Pegylated Interferon Alfa-2b and Ribavirin in Chronic Hepatitis C. *Hepatology* **32**, 647-653

Goldberg (1980). Isolation and Partial Characterization of the *Drosophila* Alcohol Dehydrogenase Gene. *Proceedings of the National Academy of Sciences USA* **77**, 5794

Goodburn S, Didcock L and Randall RE (2000). Interferons: Cell Signalling, Immune Modulation, Antiviral Responses and Virus Countermeasures. *Journal of General Virology* **81**, 2341-2364

Gómez J, Martell M, Cabot B and Esteban JI (1999). Hepatitis C Virus Quasispecies. *Journal of Viral Hepatitis* **6**, 3-16

Gonzalez-Amaro R, Garcia-Monzon C, Garcia-Buey L, Moreno-Otero R, Alonso JL, Yague E, Pivel JP, Lopez-Cabrera M, Fernandez-Ruiz E and Sanchez-Madrid F (1994). Induction of Tumour Necrosis Factor α by Human Hepatocytes in Chronic Viral Hepatitis. *Journal of Experimental Medicine* **179**, 841-848

Gonzalez-Peralta RP, Fang JWS, Davis GL, Gish R, Tsukiyama-Kohara K, Kohara M, Mondelli MU, Lesniewski R, Phillips MI, Mizokami M and Lau JYN (1994). Optimization for the Detection of Hepatitis C Virus Antigens in the Liver. *Journal of Hepatology* **20**, 143-147

Goodling LR (1992). Virus Proteins that Counteract Host Immune Defences. *Cell* **71**, 5-7

Gorbalenya AE and Koonin EV (1993). Helicases: Amino Acid Sequence Comparisons and Structure-Function Relationships. *Current Opinion in Structural Biology* **3**, 419-429

Gorbalenya AE, Koonin EV, Donchenko AP and Blinov VM (1988a). A Conserved NTP-Motif in Putative Helicases. *Nature* **333**, 22-22

Gorbalenya AE, Koonin EV, Donchenko AP and Blinov VM (1988b). A Novel Superfamily of Nucleoside Triphosphate-binding Motif Containing Proteins which are Probably Involved in Duplex Unwinding in DNA and RNA Replication and Recombination. *FEBS Letters* **235**, 16-24

Gorbalenya AE, Koonin EV, Donchenko AP and Blinov VM (1989). Two Related Superfamilies of Putative Helicases Involved in Replication, Recombination, Repair and Expression of DNA and RNA Genomes. *Nucleic Acids Research* **17**, 4713-4729

Gorbalenya AE, Koonin EV and Wolf YI (1990). A New Superfamily of Putative NTP-binding Domains Encoded by Genomes of Small DNA and RNA Viruses. *FEBS Letters* **262**, 145-148

Grakoui A, Wychowski C, Lin C, Feinstone SM and Rice CM (1993a). Expression and Identification of Hepatitis C Virus Polyprotein Cleavage Products. *Journal of Virology* **67**, 1385-1395

Grakoui A, McCourt DW, Wychowski C, Feinstone SM and Rice CM (1993b). A Second Hepatitis C Virus-Encoded Proteinase. *Proceedings of the National Academy of Sciences USA* **90**, 10583-10587

Grakoui A, McCourt DW, Wychowski C, Feinstone SM and Rice CM (1993c). Characterization of the Hepatitis C Virus-Encoded Serine Protease: Determination of Protease-Dependent Polyprotein Cleavage Sites. *Journal of Virology* **67**, 2832-2343

Gross CH and Shuman S (1995). Mutational Analysis of Vaccinia Virus Nucleoside Triphosphate Phosphohydrolase-II, a DExH Box RNA Helicase. *Journal of Virology* **69**, 4727-4736

Guzder SN, Sung P, Bailly V, Prakash L and Prakash S (1994). RAD25 is a DNA Helicase Required for RNA Repair and RNA-Polymerase II Transcription. *Nature* 369, 578-581

Gururajan R and Weeks DL (1997). An3 Protein Encoded by a Localized Maternal mRNA in *Xenopus Laevis* is an ATPase with Substrate-specific RNA Helicase Activity. *Biochimica et Biophysica Acta* **1350**, 169-182

Gururajan R, Perry OH, Melto DA and Weeks DL (1991). The *Xenopus* Localised Messenger RNA An3 may encode an ATP-dependent RNA Helicase. *Nature* **349**, 717-719

Gururajan R, Mathews L, Longo FJ and Weeks DL (1994). An3 mRNA Encodes an RNA Helicase that Colocalises with Nucleoli in *Xenpopus* Oocytes in a Stage-specific Manner. *Proceedings of the National Academy of Sciences USA* **91**, 2056-2060

Gwack Y, Kim DW, Han JH and Choe J (1996). Characterization of RNA Binding Activity and RNA Helicase Activity of the Hepatitis C Virus NS3 Protein. *Biochemical and Biophysical Research Communications* **225**, 654-659

Gwack Y, Kim DW, Han JH and Choe J (1997). DNA Helicase Activity of Hepatitis C Virus Nonstructural Protein 3. *European Journal of Biochemistry* **250**, 47-54

Hall MC and Matson SW (1999). Helicase Motifs: The Engine that Powers DNA Unwinding. *Molecular Microbiology* **34**, 867-877

Han JH, Shyamala V, Richman KH, Brauer MJ, Irvine B, Urdea MS, Tekampolson P, Kuo G, Choo Q-L and Houghton M (1991). Characterization of the Terminal Regions of Hepatitis C Virus RNA - Identification of Conserved Sequences in the 5′ Untranslated Region and Poly(A) Tails at the 3′ End. *Proceedings of the National Academy of Sciences USA* **88**, 1711-1715

Hahm B, Kim YK, Kim JH, Kim TY and Jang SK (1998). Heterogenous Nuclear Ribonucleoprotein L Interacts with the 3′ Border of the Internal Ribosomal Entry Site of Hepatitis C Virus. *Journal of Virology* **72**, 8782-8788

Hahn CS, Cho YG, Kang B-S, Lester IM and Hahn YS (2000). The HCV Core Protein Acts as a Positive Regulator of *Fas*-Mediated Apoptosis in a Human Lymphoblastoid T Cell Line. *Virology* **276**, 127-137

Han JH and Houghton M (1992). Group-specific Sequences and Conserved Secondary Structures at the 3' End of the HCV Genome and Its Implication for Viral Replication. *Nucleic Acids Research* **20**, 3520-3520

Hamm J and Lamond AI (1998). Spliceosome Assembly: The Unwinding Role of DEAD-box Proteins. *Current Biology* **8**, R532-R534

Harada S, Watanabe Y, Takeuchi K, Suzuki T, Katayama T, Takebe Y, Saito I and Miyamura T (1991). Expression of Processed Core Protein of Hepatitis C Virus in Mammalian Cells. *Journal of Virology* **65**, 3015-3021

Hata H, Mitsui H, Liu H, Bai YL, Denis CL, Shimizu Y and Sakai A (1998). Dhh1p, a putative RNA Helicase, Associates with the General Transcription Factors Pop2p and Ccr4p from *Saccharomyces cerevisiae. Genetics* **148**, 571-579

He LF, Alling D, Popkin T, Shapiro M, Alter HJ and Purcell RH (1987). Determining the Size of Non-A, Non-B Hepatitis Virus by Filtration. *Journal of Infectious Diseases* **156**, 636-640

He F and Jacobson A (1995). Identification of a Novel Component of the Nonsense-mediated Messenger-RNA Decay Pathway by Use of an Interacting Protein Screen. *Genes and Development* **9**, 437-454

He F, Brown AH and Jacobson A (1997). Upf1p, Nmd2p, and Upf3p are Interacting Components of the Yeast Nonsense-mediated mRNA Decay Pathway. *Molecular and Cellular Biology* **17**, 1580-1594

Hellen CUT and Pestova TV (1999). Translation of Hepatitis C Virus RNA. *Journal of Viral Hepatitis* **6**, 79-87

Henn A, Medalia O, Shi S-P, Steinberg M, Franceschi F and Sagi I (2001). Visualization of Unwinding Activity by DbpA, a DEAD Box RNA Helicase, at Single-molecule Resolution by Atomic Force Microscopy. *Proceedings of the National Academy of Sciences USA* **98**, 5007-5012

Hiasa Y, Horiike N, Akbar SMF, Saito I, Miyamura T, Matsuura Y and Onji M (1998). Low Stimulatory Capacity of Lymphoid Dendritic Cells Expressing Hepatitis C Virus Genes. *Biochemical and Biophysical Research Communications* **249**, 90-95

Higginbottom A, Quinn ER, Kuo CC, Flint M, Wilson LH, Bianchi E, Nicosia A, Monk PN, McKeating JA and Levy S (2000). Identification of Amino Acid Residues in CD81 Critical for Interaction with Hepatitis C Virus Envelope Glycoprotein E2. *Journal of Virology* **74**, 3642-3649

Hijikata M, Kato N, Ootsuyama Y, Nakagawa M, Ohkoshi S and Shimotohno K (1991a). Hypervariable Regions in the Putative Glycoprotein of Hepatitis C Virus. *Biochemical and Biophysical Research Communications* **175**, 220-228

Hijikata M, Kato N, Ootsuyama Y, Nakagawa M and Shimotohno K (1991b). Gene Mapping of the Putative Structural Region of the Hepatitis C Genome by *In Vitro* Processing Analysis. *Proceedings of the National Academy of Sciences USA* **88**, 5547-5551

Hijikata M, Mizushima H, Akagi T, Mori S, Kakiuci N, Kato N, Tanaka T, Kimura K and Shimotohno K (1993). Two Distinct Proteinase Activities Required for the Processing of a Putative Non-Structural Precursor Protein of Hepatitis C Virus. *Proceedings of the National Academy of Sciences USA* **90**, 10773-10777

Hirling H, Scheffner M, Restle T and Stahl H (1989). RNA Helicase Activity Associated with the Human p68 Protein. *Nature* **339**, 562-564

Hodgeman TC (1988). A New Superfamily of Replicative Proteins. *Nature* **333**, 22-23

Holland JJ, De La Torre JC and Steinhauer DA (1992). RNA Virus Populations as Quasispecies. *Current Topics in Microbiology and Immunology* **176**, 1-20

Honda M, Brown EA and Lemon SM (1996a). Stability of Stem-loop Involving the Initiator AUG Controls the Efficiency of Internal Translation on Hepatitis C Virus RNA. *RNA* **2**, 955-968

Honda M, Ping LH, Rijnbrand RC, Amplett E, Clarke B, Rowlands D, Lemon SM (1996b). Structural Requirements for Initiation of Translation by Internal Ribosome Entry Within Genome-length Hepatitis C Virus RNA. *Virology* **222**, 31-42

Honda M, Rijnbrand R, Abell G, Kim D and Lemon SM (1999). Natural Variation in Translational Activities of the 5′ Nontranslated RNAs of Hepatitis C Virus Genotypes 1a and 1b: Evidence for a Long-Range RNA-RNA Interaction outside of the Internal Ribosome Entry Site. *Journal of Virology* **73**, 4941-4951

Honda M, Kaneko S, Matsushita E, Kobayashi K, Abell GA and Lemon SM (2000). Cell Cycle Regulation of Hepatitis C Virus Internal Ribosomal Entry Site-Directed Translation. *Gastroenterology* **11**, 152-162

Hong Z, Beaudet-Miller M, Lanford RE, Guerra B, Wright-Minogue J, Skelton A, Baroudy BM, Reyes GR and Lau JYN (1999). Generation of Transmissible Hepatitis C Virions from a Molecular Clone in Chimpanzees. *Virology* **256**, 36-44

Hope RG and McLauchlan J (2000). Sequence Motifs Required for Lipid Droplet Association and Protein Stability are Unique to the Hepatitis C Virus Core Protein. *Journal of General Virology* **81**, 1913-1925

Hosein B, Fang CT, Popovsky MA, Ye J, Zhang ML and Wang CY (1991). Improved Serodiagnosis of Hepatitis C Virus Infection with Synthetic Peptide Antigen from Capsid Protein. *Proceedings of the National Academy of Sciences USA* **88**, 3647-3651

Houghton M (1996). Hepatitis C Viruses. In *"Fields Virology"* (3rd edn), pp 1035-1058. Edited by: BN Fields, DM Knipe and PM Howley. Philadelphia: Lippincott-Raven

Howe LR, Leevers SJ, Gomez N, Nakielny S, Cohen P and Marshall CJ (1992). Activation of the MAP Kinase by the Protein Kinase Raf-1. *Cell* **71**, 335-342

Hseih T-Y, Matsumoto M, Chou H-C, Schneider R, Hwang SB, Lee AS and Lai MMC (1998). Hepatitis C Virus Core Protein Interacts with Heterogenous Nuclear Ribonucleoprotein K. *Journal of Biological Chemistry* **273**, 17651-17659

Hu KQ, Vierling JM and Redeker AG (2001). Viral, Host and Interferon-related Factors Modulating the Effect of Interferon Therapy for Hepatitis C Virus Infection. *Journal of Viral Hepatitis* **8**, 1-18

Huber KR, Sebesta C, Bauer K (1996). Detection of Common Hepatitis C Virus Subtypes with a Third-generation Enzyme Immunoassay. *Hepatology* **24**, 471-473

Hugle T, Fehrmann F, Bieck E, Kohara M, Krausslich HG, Rice CM, Blum HE and Moradpour D (2001). Hepatitis C virus Nonstructural Protein 4B is an Integral Endoplasmic Reticulum Membrane Protein. *Virology* **284**, 70-81

Hunter T and Karin M (1992). The Regulation of Transcription by Phosphorylation. *Cell* **70**, 375-387

Hussain MJ, Lau JYN, Williams R and Vergani D (1994). Hepatic Expression of Tumour Necrosis Factor α in Chronic Hepatitis B Virus Infection. *Journal of Clinical Pathology* **47**, 1112-1115

Hüssy P, Langen H, Mous I and Jacobsen H (1996). Hepatitis C Virus Core Protein: Carboxy-Terminal Boundaries of Two Processed Species Suggest Cleavage by a Signal Peptide Peptidase. *Virology* **224**, 93-104

Hirling H, Scheffner M, Restle T and Stahl H (1989). RNA Helicase Activity Associated with the Human p68 Protein. *Nature* **339**, 562-564

Hwang SB, Park K-J, Kim Y-S, Sung YC and Lai MC (1997). Hepatitis C Virus NS5B Protein is a Membrane-Associated Phosphoprotein with a Predominately Perinuclear Localisation. *Virology* **227**, 439-446

Ide Y, Tanimoto A, SasaGuri Y and Padmanabhan R (1997). Hepatitis C Virus NS5A Protein is Phosphorylated *In Vitro* by a Stably Bound Protein Kinase from HeLa Cells by cAMP-Dependent Protein Kinase A-α Catalytic Subunit. *Gene* **201**, 151-158

Idilman R, De Maria N, Colantoni A and Van Thiel DH (1998). Pathogenesis of Hepatitis B and C-Induced Hepatocellular Carcinoma. *Journal of Viral Hepatitis* **5**, 285-299

Ilyina TV, Gorbalenya AE and Koonin EV (1992). Organization and Evolution of Bacterial and Bacteriophage Primase Helicase Systems. *Journal of Molecular Evolution* **34**, 351-357

Ina Y, Mizokami M, Ohba K and Gojobori T (1994). Reduction in Synonymous Substitutions in the Core Protein Gene of Hepatitis C Virus. *Journal of Molecular Evolution* **38**, 50-56

Iost I, Dreyfus M and Linder P (1999). Ded1p, a DEAD-box Protein Required for Translation Initiation in *Saccharomyces cerevisiae*, is an RNA Helicase. *Journal of Biological Chemistry* **274**, 17677-17683

Inoue K, Hoshijima K, Sakamoto H and Shimura Y (1990). Binding of the Drosophila Sex-Lethal Gene-Product to the Alternative Splice Site of Transformer Primary Transcript. *Nature* **344**, 461-463

Ishido S, Fujita T and Hotta H (1998). Complex formation of NS5B with NS3 and NS4A proteins of Hepatitis C Virus. *Biochemical and Biophysical Research Communications* **244**, 35-40

Ito T and Lai MMC (1997). Determination of the Secondary Structure of and Cellular Protein Binding to the 3′-untranslated Region of the Hepatitis C Virus RNA Genome. *Journal of Virology* **71**, 8698-8706

Ito T and Lai MMC (1999). An Internal Polypyrimidine-Tract-Binding Protein-Binding Site in the Hepatitis C Virus RNA Attenuates Translation, which is Relieved by the 3′-Untranslated Sequence. *Virology* **254**, 288-296

Ito T, Tahara SM and Lai MMC (1998a). The 3′-Untranslated Region of Hepatitis C Virus RNA Enhances Translation from an Internal Ribosomal Entry Site. *Journal of Virology* **72**, 8789-8796

Ito Y, Sasaki Y, Horimoto M, Wada S, Tanaka Y, Kasahara A, Ueki T, Hirano T, Yamamoto H, Fujimoto J, Okamoto E, Hayashi N and Hori M (1998b). Activation of Mitogen-activated Protein Kinases Extracellular Signal-regulated Kinases in Human Hepatocellular Carcinoma. *Hepatology* **27**, 951-958

Jackson RJ, Howell MT and Kaminski A (1990). The Novel Mechanism of Initiation of Picornavirus RNA Translation. *Trends in Biochemical Sciences* **15**, 477-483

Jamieson DJ and Beggs JD (1991). A Suppressor of Yeast SPP81/DED1 Mutations Encodes a Very Similar Putative ATP-dependent RNA Helicase. *Molecular Microbiology* **5**, 805-812

Jamieson DJ, Rahe B, Pringle J and Beggs JD (1991). A Suppressor of a Yeast Splicing Mutation (PRP8-1) Encodes a Putative ATP-dependent RNA Helicase. *Nature* **349**, 715-717

Janda M and Ahlquist P (1993). RNA-dependent Replication, Transcription, and Persistence of Brome Mosaic Virus RNA Replicons in *Saccharomyces cerevisiae. Cell* **72**, 961-970

Jankowsky E, Gross CH, Shuman S and Pyle AM (2000). The DExH Protein NPH-II is a Processive and Directional Motor for Unwinding RNA. *Nature* **403**, 447-451

Jänicke RU, Sprengart ML, Wati MR, Porter AG (1998). Caspase-3 is Required for DNA Fragmentation and Morphological Changes Associated with Apoptosis. *Journal of Biological Chemistry* **273**, 9357-9360

Jaramillo M, Dever TE, Merrick WC and Sonenberg N (1991). RNA Unwinding in Translation: Assembly of Helicase Complex Intermediates Comprising Eukaryotic Elongation Factors eIF-4A and eIF-4B. *Molecular and Cellular Biology* **11**, 5992-5997

Jin L and Peterson DL (1995). Expression, Isolation, and Characterization of the Hepatitis C Virus ATPase/Helicase. *Archives of Biochemistry and Biophysics* **323**, 47-53

Jin D-Y, Wang H-L, Zhou Y, Chun ACS, Kibler KV, Hou Y-D, Kung H-f and Jeang K-T (2000). Hepatitis C Virus Core Protein-induced Loss of LZIP Function Correlates with Cellular Transformation. *EMBO Journal* **19**, 729-740

Kadaré G and Haenni A-L (1997). Virus-Encoded RNA Helicases. *Journal of Virology* **71**, 2583-2590

Kai N, Mishina M and Yagi T (1997). Molecular Cloning of Fyn-associated Molecules in the Mouse Central Nervous System. *Journal of Neuroscience Research* **48**, 407-424

Kaito M, Watanabe S, Tsukiyama-Kohara K, Yamaguchi K, Kobayashi Y, Konishi M, Yokoi M, Ishida S, Suzuki S and Kohara M (1994). Hepatitis C Virus Particle Detected by Immunoelectron Microscopic Study. *Journal of General Virology* **75**, 1755-1760

Kanto T, Hayashi N, Takehara T, Tatsumi T, Kuzushita N, Ito A, Sasaki Y, Kasahara A and Hori M (1999). Impaired Allostimulatory Capacity of Peripheral Blood Dendritic Cells Recovered from Hepatitis C Virus-infected Individuals. *Journal of Immunology* **162**, 5584-5591

Kapoor M, Zhang LW, Ramachandra M, Kusukawa J, Ebner KE and Padmanabhan R (1995). Association Between NS3 and NS5 Proteins of Dengue Virus Type 2 in the Putative RNA Helicase is Linked to Differential Phosphorylation of NS5. *Journal of Biological Chemistry* **270**, 19100-19106

Kato N, Hijikata M, Ootsuyama Y, Nakagawa M, Ohkoshi S, Sugimura T and Shimotohno K (1990). Molecular Cloning of the Human Hepatitis C Virus Genome from Japanese Patients with Non-A, Non-B Hepatitis. *Proceedings of the National Academy of Sciences USA* **87**, 9524-9528

Kato N, Sekiya H Ootsuyama Y, Nakazawa T, Hijikata M, Ohkoshi S and Shimotohno (1993). Humoral Immune Response to Hypervariable Region 1 of the Putative Envelope Glycoprotein (gp70) of Hepatitis C Virus. *Journal of Virology* **67**, 3923-3930

Kawamura T, Furusaka A, Koziel MJ, Chung RT, Wang TC, Schmidt EV and Liang TJ (1997). Transgenic Expression of Hepatitis C Virus Structural Proteins in the Mouse. *Hepatology* **25**, 1014-1021

Kemp BE and Pearson RB (1990). Protein Kinase Recognition Sequence Motifs. *Trends in Biological Sciences* **15**, 342-346

Khromykh AA and Westaway EG (1997). Subgenomic Replicons of the Flavivirus Kunjin: Construction and Applications. *Journal of Virology* **71**, 1497-1505

Khromykh AA, Meka H, Guyatt KJ, and Westaway EG (2001). Essential Role of Cyclization Sequences in Flavivirus RNA Replication. *Journal of Virology* **75**, 6719-6728

Kieft JS, Zhou KH, Jubin R, Murray MG, Lau JYN and Doudna JA (1999). The Hepatitis C Virus Internal Ribosome Entry Site Adopts an Ion-dependent Tertiary Fold. *Journal of Molecular Biology* **292**, 513-529

Kieft JS, Zhou KH, Jubin R, Doudna JA (2001). Mechanism of Ribosome Recruitment by Hepatitis C IRES RNA. *RNA* **7**, 194-206

Kim DW, Suzuki R, Harada T, Saito I and Miyamura (1994). Transcriptional Suppression of Gene Expression by Hepatitis C Virus Core Protein. *Japanese Journal of Medical Science and Biology* **47**, 211-220

Kim DW, Gwack Y, Han JH and Choe J (1995). C-terminal Domain of the Hepatitis C Virus NS3 Protein Contains an RNA Helicase Activity. *Biochemical and Biophysical Research Communications* **215**, 160-166

Kim JL, Morgenstern KA, Lin C, Fox T, Dwyer MD, Landro JA, Chambers SP, Markland W, Lepre CA, O'Malley ET, Harbeson SL, Rice CM, Murcko MA, Caron PR and Thomson JA (1996). Crystal Structure of the Hepatitis C Virus NS3 Protease Domain Complexed with a Synthetic NS4A Cofactor Peptide. *Cell* **87**, 343-355

Kim DW, Kim J, Gwack Y, Han JH and Choe J (1997). Mutational Analysis of the Hepatitis C Virus RNA Helicase. *Journal of Virology* **71**, 9400-9409

Kim YS, Lee SG, Park SH and Song K (2001). Gene Structure of the Human DDX3 and Chromosome Mapping of its Related Sequences. *Molecules and Cells* **12**, 209-214

King LA and Possee RD (1992). *The Baculovirus Expression System: A Laboratory Guide.* Chapman & Hall: London.

Kita H, Moriyama T, Kaneko T, Harase I, Nomura M, Miura H, Nakamura I, Yazaki Y and Imawari M (1993). HLA B44-Restricted Cytotoxic T-Lymphocytes Recognizing an Epitope on Hepatitis C Virus Nucelocapsid Protein. *Hepatology* **18**, 1039-1044

Kitadokoro K, Bordo D, Galli G, Petracca R, Falugi F, Abrignani S, Grandi G and Bolognesi M (2001). CD81 Extracellular Domain 3D Structure: Insight into the Tetraspanin Superfamily Structural Motifs. *EMBO Journal* **20**, 12-18

Koffa MD, Clements JB, Izaurralde E, Wadd S, Wilson SA, Mattaj IW and Kuersten S (2001). Herpes Simplex Virus ICP27 Protein Provides Viral mRNAs with Access to the Cellular mRNA Export Pathway. *EMBO Journal* **20**, 5769-5778

Kolykhalov AA, Feinstone SM and Rice CM (1996). Identification of a Highly Conserved Sequence Element at the 3′ Terminus of Hepatitis C Virus Genome RNA. *Journal of Virology* **70**, 3363-3371

Kolykhalov AA, Agapov EV, Blight KJ, Mihalik, Feinstone SM and Rice CM (1997). Transmission of Hepatitis C by Intrahepatic Inoculation with Transcribed RNA. *Science* **277**, 570-574

Kolykhalov AA, Mihalik K, Feinstone SM and Rice CM (2000). Hepatitis C Virus-encoded Enzymatic Activities and Conserved RNA Elements in the 3′ Nontranslated Region are Essential for Virus Replication *In Vivo. Journal of Virology* **74**, 2046-2051

Kohtz JD, Jamison SF, Will CL, Zuo P, Lührmann R, Garcia-Blanco MA and Manley JL (1994). Protein-protein Interactions and 5′-splice-site Recognition in Mammalian mRNA Precursors. *Nature* **368**, 119-124

Kozak M (1999). Initiation of Translation in Prokaryotes and Eukaryotes. *Gene* **234**, 187-208

Koziel MJD, Dudley N, Afdhal N, Choo Q-L, Houghton M, Ralston and Walker BD (1993). Hepatitis C Virus-Specific Cytotoxic T lymphocytes Recognise Epitopes in the Core and Envelope Proteins of HCV. *Journal of Virology* **67**, 7522-7532

Krainer AR, Mayeda A, Kozak D and Binns G (1991). Functional Expression of Cloned Human Splicing Factor SF2 - Homology to RNA-binding Proteins, U1 70K, and *Drosophila* Splicing Regulators. *Cell* **66**, 383-394

Kressler D, De la Cruz J, Rojo M and Linder P (1998). Dbp6p is an Essential Putative ATP-dependent RNA Helicase Required for SOS-ribosomal-subunit Assembly in *Saccharomyces cerevisiae. Molecular and Cellular Biology* **18**, 1855-1865

Krieger N, Lohmann V and Bartenschlager R (2001). Enhancement of Hepatitis C Virus RNA Replication by Cell Culture-adaptive Mutations. *Journal of Virology* **75**, 4614-4624

Kruger M, Beger C, Li QX, Welch PJ, Tritz R, Leavitt M, Barber JR and Wong-Staal F (2000). Identification of eIF2B gamma and eIF2 gamma as Cofactors of Hepatitis C Virus Internal Ribosome Entry Site-mediated Translation Using a Functional Genomics Approach. *Proceedings of the National Academy of Sciences USA* **97**, 8566-8571

Kudo N, Matsumori N, Taoka H, Fujiwara D, Schriner EP, Wolff B, Yoshida M and Horinouchi S (1999). Leptomycin B Inactivates CRM1/Exportin 1 by Covalent Modification at a Cyteine Residue in the Central Conserved Region. *Proceedings of the National Academy of Sciences USA* **96**, 9112-9117

Kunkel M, Lorinczi M, Rijnbrand R, Lemon SM and Watowich SJ (2001). Self-Assembly of Nucleocapsid-Like Particles from Recombinant Hepatitis C Virus Core Protein. *Journal of Virology* **75**, 2119-2129

Kuo G, Choo Q-L, Alter HJ, Gitnick GL, Redeker AG, Purcell RH, Miyamura T, Dienstag JL, Alter MJ, Stevens CE, Tegtmeier GE, Bonino F, Colombo M, Lee WS, Kuo C, Shuster JR, Overby LR, Bradley DW and Houghton M (1989). An Assay for Circulating Antibodies to a Major Etiologic Virus of Human Non-A, Non-B Hepatitis. *Science* **244**, 362-364

Kwong (1999). Structure and Function of the Hepatitis C Virus NS3 Helicase. In "*The Hepatitis C Viruses*", pp 117-134. Edited by CH Hagedorn and CM Rice. Germany: Springer.

Kyriakis JM, App H, Zhang XF, Banerjee P, Brautigan P, Brautigan DL, Rapp UR and Avruch J (1992). RAF-1 Activates MAP Kinase-Kinase. *Nature* 358, 417-421

Laemmli UK (1970). Cleavage of Structural Proteins During the Assembly of the Head of Bacteriophage T4. *Nature* **227**, 570-574

Lahn BT and Page DC (1997) Functional Coherence of the Human Y Chromosome. *Science* **278**, 675-680

Lai and Ware (1999). Hepatitis C Virus Core Protein: Possible Roles in Viral Pathogenesis. In *"The Hepatitis C Viruses"*, pp 117-134. Edited by CH Hagedorn and CM Rice. Germany: Springer.

Lain S, Riechmann JL, Martin MT and Garcia JA (1989). Homologous Potyvirus and Flavivirus Proteins Belonging to a Superfamily of Helicase-like Proteins. *Gene 82*, 357-362

Lanford RE, Chavez D, Chisari FV and Sureau C (1994). Demonstration of *In vitro* Infection of Chimpanzee Hepatocytes with Hepatitis C Virus Using Strand-Specific RT/PCR. *Virology* **202**, 606-614

Large MK, Kittlesen DJ and Hahn YS (1999). Suppression of Host Immune Response by Core Protein of Hepatitis C Virus: Possible Implications for Hepatitis C Virus Persistence. *Journal of Immunology* **162**, 931-938

Lasko PF and Ashburner M (1990). Posterior Localization of Vasa Protein Correlates with, but is Not Sufficient for, Pole Cell Development. *Genes and Development* **4**, 905-921

Lavanchy D, Purcell R, Hollinger FB, Howard C, Alberti A, Kew M, Dusheiko G, Alter M, Ayoola E, Beutels P, Bloomer R, Ferret B, Decker R, Esteban R, Fay O, Fields H, Fuller EC, Grob P, Houghton M, Leung N, Locarnini SA, Margolis H, Meheus A, Miyamura T, Mohamed MK, Tandon B, Thomas D, Head HT, Toukan AU, Van Damme P, Zanetti A, Arthur R, Couper M, D'Amelio R, Emmanuel JC, Esteves K, Gavinio P, Griffiths E, Hallaj Z, Heuck CC, Heymann DL, Holck SE, Kane M, Martinez LJ, Meslin F, Mochny IS, Ndikuyeze A, Padilla AM, Rodier GRM, Roure C, Savage F and Vercauteren G (1999). Global Surveillance and Control of Hepatitis C. *Journal of Viral Hepatitis* **6**, 35-47

Leary TP, Muerhoff AS, Simons JN, Pilot-Matias TJ, Erker JC, Chalmers ML, Schlauder GG, Dawson GJ, Desai SM and Mushahwar IK (1996). Sequence and Genomic Organization of GBV-C: A Novel Member of the *Flaviviridae* Associated with Human Non-A-E Hepatitis. *Journal of Medical Virology*, **48**, 60-67

Lee KAW and Green MR (1990). Small-scale Preparation of Extracts from Radiolabeled Cells Efficient in Pre-messenger RNA Splicing. *Methods in Enzymology* **181**, 20-30

Lee C-G and Hurwitz J (1992). A New RNA Helicase Isolated from HeLa Cells That Catalytically Translocates in the 3′ to 5′ Direction. *Journal of Biological Chemistry* **267**, 4398- 4407

Lee C-G, da Costa Soares V, Newberger C, Manova K, Lacy E and Hurwitz J (1998). RNA Helicase A is Essential for Normal Gastrulation. *Proceedings of the National Academy of Sciences USA* **95**, 13709–13713

Lefkowitch JH, Schiff ER, Davis GL, Perrillo RP, Lindsay K, Bodenheimer HC, Balart LA, Ortego TJ, Payne J, Dienstag JL, Gibas A, Jacobson IM, Tamburro CH, Carey W, O'Brien C, Sampliner R, Vanthiel DH, Feit D, Albrecht J, Meschievitz C, Sanghvi B and Vaughan RD (1993). Pathological Diagnosis of Chronic Hepatitis C – A Multicenter Comparative Study with Chronic Hepatitis B. *Gastroenterology* **104**, 595-603

Lehrach H, Diamond D, Wozney JM and Boedtker H (1977). RNA Molecular Weight Determinations by Gel Electrophoresis Under Denaturing Conditions, a Critical Re-examination. *Biochemistry* **16**, 4743

Leroy P, Alzari P, Sassoon D, Wolgemuth D and Fellous M (1989). The Protein Encoded by a Murine Male Germ Cell-Specific Transcript is a Putative ATP-dependent RNA Helicase. *Cell* **57**, 549-559

Li F, Srinivasan A, Wang Y, Armstrong RC, Tomaselli KJ and Fritz LC (1997). Cell-specific Induction of Apoptosis by Microinjection of Cytochrome *c*. *Journal of Biological Chemistry* **272**, 30299-30305

Li H and Bingham PM (1991). Arginine Serine-rich Domains of the SU(WA) and Tra RNA Processing Regulators Target Proteins to a Subnuclear Compartment in Splicing. *Cell* **67**, 335-342

Liang L, Diehljones W and Lasko P (1994). Localization of Vasa Protein to the Drosophila Pole Plasm is Independent of its RNA-binding and Helicase Activities. *Development* **120**, 1201-1211

Liang WQ, Clark JA and Fournier MJ (1997). The rRNA-processing Function of the Yeast U14 Small Nucleolar RNA can be Rescued by a Conserved RNA Helicase-like Protein. *Molecular and Cellular Biology* **17**, 4124-4132

Liaw Y-F, Lin SM, Sheen IS and Chu CM (1991). Acute Hepatitis C Virus Superinfection Followed by Spontaneous HBeAg Seroconversion and HBsAg Elimination. *Infection* **250**, 54-55

Lin C, Lindenbach BD, Prágai BM, McCourt DW and Rice CM (1994a). Processing in the Hepatitis C Virus E2-NS2 Region: Identification of p7 and Two Distinct E2-Specific Products with Different C Termini. *Journal of Virology* **68**, 5063-5073

Lin C, Pragai BM, Grakoui A, Xu J and Rice CM (1994b). Hepatitis C Virus NS3 Serine Protease – Trans-cleavage Requirements and Processing Kinetics. *Journal of Virology* **68**, 8147-8157

Lin C, Wu JW, Hsiao K and Su MSS (1997). The Hepatitis C Virus NS4A Protein: Interactions with the NS4B and NS5A Proteins. *Journal of Virology* **71**, 6465-6471

Lin BH, Williams-Skipp C, Tao YX, Schleicher MS, Cano LL, Duke RC and Scheinman RI (1999). NF-κB Functions as Both a Proapoptotic and Antiapoptotic Regulatory Factor within a Single Cell Type. *Cell Death and Differentiation* **6**, 570-582

Linder P and Daugeron M-C (2000). Are DEAD-box Proteins Becoming Respectable Helicases? *Nature Structural Biology* **7**, 97-99

Linder P, Lasko PF, Leroy P, Nielsen PJ, Nishi K, Schnier J and Slonimski PP (1989). Birth of the D-E-A-D Box. *Nature* **337**, 121-122

Linnen J, Wages J, Zhang-Keck ZY, Fry KE, Krawczynski KZ, Alter H, Koonin E, Gallagher M, Alter M, Hadziyannis S, Karayiannis P, Fung K, Nakatsuji Y, Shih JWK, Young L, Piatak M, Hoover C, Fernandez J, Chen S, Zou JC, Morris T, Hyams KC, Ismay S, Lifson JD, Hess G, Foung SKH, Thomas H, Bradley D, Margolis H and Kim JP (1996). Molecular Cloning and Disease Association of Hepatitis G Virus: A Transfusion-transmissible Agent. *Science* **271**, 505-508

Liu ZG, Hsu HL, Goeddel DV and Karin M (1996). Dissection of TNF Receptor 1 Effector Functions: JNK Activation is not Linked to Apoptosis While NF-κB Activation Prevents Cell Death. *Cell* **87**, 565-576

Liu Q, Tackney C, Bhat RA, Prince AM and Zhang P (1997). Regulated Processing of Hepatitis C Virus Core Protein is Linked to Subcellular Localization. *Journal of Virology* **71**, 657-662

Livingstone C and Jones I (1989). Baculovirus Expression Vectors with Single Strand Capability. *Nucleic Acids Research* **17**, 2366

Lo S-Y, Selby M, Tong M and Ou JH (1994). Comparitive Studies of the Core Gene Products of Two Different Hepatitis C Virus Isolates: Two Alternative Forms Determined by a Single Amino Acid Substitution. *Virology* **19**, 124-131

Lo S-Y, Masiarz F, Hwang SB, Lai MC and Ou J-H (1995). Differential Subcellular Localization of Hepatitis C Core Gene Products. *Virology* **213**, 455-461

Lo S-Y, Selby MJ and Ou J-H (1996). Interaction between Hepatitis C Virus Core Protein and E1 Envelope Protein. *Journal of Virology* **70**, 5177-5182

Lohman TM and Bjornson KP (1996). Mechanisms of Helicase-catalyzed DNA Unwinding. *Annual Review of Biochemistry* **65**, 169-214

Lohmann V, Körner F, Koch J-O, Herian U, Theilmann L and Bartenschlager R (1999a). Replication of Subgenomic Hepatitis C Virus RNAs in a Hepatoma Cell Line. *Science* **285**, 110-113

Lohmann V, Overton H and Bartenschlager R (1999b). Selective Stimulation of Hepatitis C Virus and Pestivirus NS5B RNA Polymerase Activity by GTP. *Journal of Biological Chemistry* **274**, 10807-10815

Lohmann V, Korner F, Dobierzewska A and Bartenschlager R (2001). Mutations in Hepatitis C Virus RNAs Conferring Cell Culture Adaptation. *Journal of Virology* **75**, 1437-1449

Londos C, Brasaemle DL, Schultz CJ, Segrest JP and Kimmel AR (1999). Perilipins, ADRP, and Other Proteins that Associate with Intracellular Neutral Lipid Droplets in Animal Cells. *Seminars in Cell and Developmental Biology* **10**, 51-58

Lorsch JR and Herschlag D (1998). The DEAD Box Protein eIF4A. 2. A Cycle of Nucleotide and RNA-dependent Conformational Changes. *Biochemistry* **37**, 2194-2206

Lu H-H and Wimmer E (1996). Poliovirus Chimeras Replicating Under the Translational Control of Genetic Elements of Hepatitis C Virus Reveal Unusual Properties of the Internal Ribosomal Entry Site of Hepatitis C Virus. *Proceedings of the National Academy of Sciences USA* **93**, 1412-1417

Lu W, Lo S-Y, Chen M, Wu K-J, Fung YKT and Ou J-H (1999). Activation of p53 Tumour Suppressor by Hepatitis C Virus Core Protein. *Virology* **264**, 134-141

Lukavsky PJ, Otto GA, Lancaster AM, Sarnow P and Puglisi JD (2000). Structures of Two RNA Domains Essential for Hepatitis C Virus Internal Ribosome Entry Site Function. *Nature Structural Biology* **7**, 1105-1110

Luo GX (1999). Cellular Proteins Bind to the Poly(U) Tract of the 3′ Untranslated Region of Hepatitis C Virus RNA Genome. *Virology* **256**, 105-118

Maillard P, Krawczynski K, Nitkiewicz J, Bronnert C, Sidorkiewicz M, Gounon P, Dubuisson J, Faure G, Crainic R and Budkowska A (2001). Nonenveloped Nucleocapsids of Hepatitis C Virus in the Serum of Infected Patients. *Journal of Virology* **75**, 8240-8250

Major M and Feinstone S (1997). The Molecular Virology of Hepatitis C. *Hepatology* **25**, 1527-1538

Maki Y, Bos TJ, Davis C, Starbuck M and Vogt PK (1987). Avian Sarcoma Virus 17 Carries the *Jun* Oncogene. *Proceedings of the National Academy of Sciences USA* **84**, 2848-2852

Mamiya N and Worman HJ (1999). Hepatitis C Virus Core Protein Binds to a DEAD Box RNA Helicase. *Journal of Biological Chemistry* **274**, 15751-15756

Maniatis T, Fritsch, and Sambrook J (1989). *Molecular Cloning - A Laboratory Manual* (2nd edn). New York: Cold Spring Harbour Laboratory Press

Martoglio B and Dobberstein B (1998). Signal Sequences: More than just greasy peptides. *Trends in Cell Biology* **8**, 410-415

Marusawa H, Hijikata M, Chiba T and Shimotohno K (1999). Hepatitis C Virus Core Protein Inhbits *Fas*- and Tumour Necrosis Factor α-Mediated Apoptosis via NF-κB Activation. *Journal of Virology* **73**, 4713-4720

Matson SW, Tabor S and Richardson CC (1983). The Gene 4 Protein of Bacteriophage T7 - Characterization of Helicase Activity. *Journal of Biological Chemistry* **258**, 4017-4024

Matsumoto M, Hwang SB, Jeng K-S, Zhu N and Lai MMC (1996a). Homotypic Interaction and Multimerization of Hepatitis C Virus Core Protein. *Virology* **218**, 43-51

Matsumoto M, Mariathasan S, Nahm MH, Baranyay F, Peschon JJ, Chaplin DD (1996b). Role of Lymphotoxin and the Type 1 TNF Receptor in the Formation of Germinal Cancers. *Science* **271**, 1289-1291

Matsumoto M, Hseih T-Y, Zhu N, VanArsdaleT, Hwang SB, Jeng K-S, Gorbalenya AE, Lo S-Y, Ou J-H, Ware CF and Lai MMC (1997). Hepatitis C Virus Core Protein Interacts with the Cytoplasmic Tail of Lymphotoxin-β Receptor. *Journal of Virology* **71**, 1301-1309

Matsuura Y, Suzuki T, Suzuki R, Sato M, Aizaki H, Saito I and Miyamura T (1994). Processing of E1 and E2 Glycoproteins of Hepatitis C Virus Expressed in Mammalian and Insect Cells. *Virology* **205**, 141-150

McLauchlan J (2000). Properties of the Hepatitis C Virus Core Protein: A Structural Protein that Modulates Cellular Processes. *Journal of Viral Hepatitis* **7**, 2-14

Meola A, Sbardellati A, Ercole BB, Cerretani M, Pezzanera M, Ceccacci A, Vitelli A, Levy S, Nicosia A, Traboni C, McKeating J and Scarselli E (2000). Binding of Hepatitis C Virus E2 Glycoprotein to CD81 does not Correlate with Species Permissiveness to Infection. *Journal of Virology* **74**, 5933-5938

Mercer DF, Schiller DE, Elliot JF, Douglas DN, Hao C, Rinfret A, Addison WR, Fischer KP, Churchill TA, Lakey RT, Tyrrell DLJ and Kneteman NM (2001). Hepatitis C Virus Replication in Mice with Chimeric Human Livers. *Nature Medicine* **7**, 927-933

Merrick WC (1992). Mechanism and Regulation of Eukaryotic Protein Synthesis. *Microbiological Reviews* **56**, 291-315

Michelak J-P, Wychowski C Choukhi A, Meunier J-C, Ung S, Rice CM and Dubuisson J (1997). Characterisation of Truncated Forms of Hepatitis C Virus Glycoproteins. *Journal of General Virology* **78**, 2299-2306

Michelotti EF, Michelotti GA, Aronsohn AI and Levens D (1996). Heterogeneous Nuclear Ribonucleoprotein K is a Transcription Factor. *Molceular and Cellular Biology* **16**, 2350-2360

Miller WA and Koev G (2000). Synthesis of Subgenomic RNAs by Positive-strand RNA Viruses. *Virology* **273**, 1-8

Miller RH and Purcell RH (1990). Hepatitis C Virus Shares Amino Acid Sequence Similarity with Pestiviruses and Flaviviruses as well as Members of Two Plant Virus Supergroups. *Proceedings of the National Academy of Sciences USA* **87**, 2057-2061

Miyamura T and Matsuura Y (1993). Structural Proteins of Hepatitis C Virus. *Trends in Microbiology* **1**, 229-231

Mizushima H, Hijikata M, Asabe S-I, Hirota M, Kimura K and Shimotohno K (1994). Two Hepatitis C Virus Glycoprotein E2 Products with Different C Termini. *Journal of Virology* **68**, 6215-6222

Monazahian M, Bohme I, Bonk S, Koch A, Scholz C, Grethe S and Thomssen R (1999). Low Density Lipoprotein Receptor as a Candidate Receptor for Hepatitis C Virus. *Journal of Medical Virology* **57**, 223-229

Moradpour D, Englert C, Wakita T and Wands JR (1996). Characterization of Cell Lines Allowing Tightly Regulated Expression of Hepatitis C Virus Core Protein. *Virology* **222**, 51-63

Moradpour D, Wakita T, Wands JR and Blum HE (1998). Tightly Regulated Expression of the Entire Hepatitis C Virus Structural Region in Continuous Human Cell Lines. *Biochemical and Biophysical Research Communications* **246**, 920-924

Moriya K, Yotsuyangi H, Shintani Y, Fujie H, Ishibashi K, Matsuura Y, Miyamura T and Koike K (1997). Hepatitis C Virus Core Protein Induces Hepatic Steatosis in Transgenic Mice. *Journal of General Virology* **78**, 1527-1531

Moriya K, Fujie H, Shintani Y, Yotsuyangi H, Tsutsumi T, Ishibashi K, Matsuura Y, Kimura S, Miyamura T and Koike K (1998). The Core Protein of Hepatitis C Virus Induces Hepatocellular Carcinoma in Transgenic Mice. *Nature Medicine* **4**, 1065-1067

Morrison D (1994). 14-3-3: Modulators of Signalling Proteins? *Science* **266**, 56-57

Morrison DK and Cutler RE (1997). The Complexity of Raf-1 Regulation. *Current Opinion in Cell Biology* **9**, 174-179

Motohashi H, Shavit JA, Igarashi K, Yamamoto M and Engel JD (1997). The World According to Maf. *Nucleic Acids Research* **25**, 2953-2959

Muerhoff AS, Leary TP, Simons JN, Pilot-Matias TJ, Dawson GJ, Erker JC, Chalmers ML, Schlauder GG, Desai SM and Mushahwar IK (1995). Genomic Organization of GB Viruses A and B: Two New Members of the *Flaviviridae* Associated with GB Agent Hepatitis. *Journal of Virology* **69**, 5621-5630

Mullis K, Faloona F, Scharf S, Saiki R, Horn G and Erlich H (1986). Specific Enzymatic Amplification of DNA *In vitro* - The Polymerase Chain Reaction. *Cold Spring Harbor Symposia on Quantitiative Biology* **51**, 263-273

Murphy DJ and Vance J (1999). Mechanisms of Lipid Body Formation. *Trends in Biochemical Sciences* **24**, 109-115

Neumann AU, Lam NP, Dahari H, Gretch DR, Wiley TE, Layden TJ and Perelson AS (1998). Hepatitis C Viral Dynamics *In Vivo* and the Antiviral Efficacy of Interferon-α Therapy. *Science* **282**, 103-107

Nishizawa M, Goto N and Kawai S (1987). An Avian Transforming Retrovirus Isolated from a Nephroblastoma that Carries the *Fos* Gene as the Oncogene. *Journal of Virology* **61**, 3733-3740

Noueiry AO, Chen J and Ahlquist P (2000). A Mutant Allele of Essential, General Translation Initiation Factor *DED1* Selectively Inhibits Translation of a Viral mRNA. *Proceedings of the National Academy of Sciences USA* **97**, 12985-12990

Nolandt O, Kern V, Müller H, Pfaff E, Theilmann L, Welker R and Kräusslich (1997). Analysis of Hepatitis C Virus Core Protein Interacting Domains. *Journal of General Virology* **78**, 1331-1340

O'Brien V (1998). Viruses and Apoptosis. *Journal of General Virology* **79**, 1833-1845

Oh EY and Grossman L (1987). Helicase Properties of the *Escherchia coli* UvrAB Protein Complex. *Proceedings of the National Academy of Sciences USA* **84**, 3638-3642

Oh JW, Ito T and Lai MMC (1999). A Recombinant Hepatitis C Virus RNA-dependent RNA Polymerase Capable of Copying the Full-length Viral RNA. *Journal of Virology* **73**, 7694-7702

Ohto H, Terazawa S, Sasaki N, Hino K, Ishiwata C, Kako M, Ujiie N, Endo C, Matsui A, Okamoto H, Mishiro S, Kojima M, Aikawa T, Shimoda K, Sakamoto M, Akahane Y, Yoshizawa H, Tanaka T, Tokita H and Tsuda F (1994). Transmission of Hepatitis C Virus from Mothers to Infants. *New England Journal of Medicine* **330**, 744-750

Okamoto H, Okada S, Sugiyama Y, Kurai K, Ilzuka H, Machida A, Miyakawa Y and Mayumi M (1991). Nulceotide Sequence of the Genomic RNA of Hepatitis C Virus Isolated from a Human Carrier - Comparison with Reported Isolates for Conserved and Divergent Regions. *Journal of General Virology* **72**, 2697-2704

Okamoto H, Mishiro S, Tokita H, Tsuda F, Miyakawa Y and Mayumi M (1994). Superinfection of Chimpanzees Carrying Hepatitis C Virus of Genotype II/1B with that of Genotype III/2A or I/1A. *Hepatology* **20**, 1131-1136

Otsuka M, Kato N, Lan K-H, Yoshida H, Kato J, Goto T, Shiratori Y and Omata M (2000). Hepatitis C Virus Core Protein Enhances p53 Function through Augmentation of DNA Binding Affinity and Transcriptional Ability. *Journal of Biological Chemistry* **275**, 34122-34130

Owsianka AM and Patel AH (1999). Hepatitis C Virus Core Protein Interacts with a Human DEAD Box Protein DDX3. *Virology* **257**, 330-340.

Owsianka A, Clayton RF, Loomis-Price LD, McKeating JA and Patel AH (2001). Functional Analysis of Hepatitis C Virus E2 Glycoproteins and Virus-like Particles Reveals Structural Dissimilarities between Different Forms of E2. *Journal of General Virology* **82**, 1877-1883

Pain VM (1996). Initiation of Protein Synthesis in Eukaryotic Cells. *European Journal of Biochemsitry* **236**, 747-771

Park SH, Lee SG, Kim Y and Song K (1998). Assignment of a Human Putative RNA Helicase Gene, DDX3, to Human X Chromosome Bands p11.3 →p11.23. *Cytogenetics and Cell Genetics* **81**, 178-179

Pasquinelli C, Shoenberger JM, Chung J, Chang KM, Guidotti LG, Selby M, Berger K, Lesniewski R, Houghton M and Chisari FV (1997). Hepatitis C Virus Core and E2 Protein Expression in Transgenic Mice. *Hepatology* **25**, 719-727

Patel AH, Wood J, Penin F, Dubuisson J and McKeating JA (2000). Construction and Characterisation of Chimeric Hepatitis C Virus E2 Glycoproteins: Analysis of Regions Critical for Glycoprotein Aggregation and CD81 Binding. *Journal of General Virology* **81**, 2873-2883

Pause A and Sonenberg N (1992). Mutational Analysis of a DEAD Box RNA Helicase: the Mammalian Translation Initiation Factor eIF4A. *EMBO Journal* **11**, 2643-2654

Pause A and Sonenberg N (1993). Helicases and RNA Unwinding in Translation. *Current Opinion in Structural Biology* **3**, 953-959

Pawlotsky JM, Germanidis G, Neumann AU, Pellerin M, Frainais PO and Dhumeaux D (1998). Interferon Resistance of Hepatitis C Virus Genotype 1b: Relationship to Nonstructural 5A Gene Quasispecies Mutations. *Journal of Virology* **72**, 2795-2805

Pazin MJ and Kadonaga JT (1997). SW12/SNF2 and Related Proteins: ATP-Driven Motors that Disrupt Protein-DNA Interactions? *Cell* **88**, 737-740

Pestova TV, Shatsky IN, Fletcher SP, Jackson RT, Hellen CUT (1998). A Prokaryotic-like Mode of Cytoplasmic Eukaryotic Ribosome Binding to the Initiation Codon during Internal Translation Initiation of Hepatitis C and Classical Swine Fever Virus RNAs. *Genes and Development* **12**, 67-83

Petracca R, Falugi F, Galli G, Norais N, Rosa D, Campagnoli S, Burgio V, Di Stasio E, Giardina B, Houghton M, Abrignani S and Grandi G (2000). Structure-function Analysis of Hepatitis C Virus Envelope-CD81 Binding. *Journal of Virology* **74**, 4824-4830

Petrik J, Parker H and Alexander GJM (1999). Human Hepatic Glyceraldehyde-3-phosphate Dehydrogenase Binds to the Poly(U) Tract of the 3′ Non-coding Region of Hepatitis C Virus Genomic RNA. *Journal of General Virology* **80**, 3109-3113

Pietschmann T, Lohmann V, Rutter G, Kurpanek K and Bartenschlager R (2001). Characterization of Cell Lines Carrying Self-replicating Hepatitis C Virus RNAs. *Journal of Virology* **75**, 1252-1264

Pietschmann T, Lohmann V, Kaul A, Krieger N, Rinck G, Rutter G, Strand D and Bartenschlager R (2002). Persistent and Transient Replication of Full-length Hepatitis C Virus Genomes in Cell Culture. *Journal of Virology* **76**, 4008-4021

Pileri P, Uematsu Y, Campagnoli S, Galli G, F Falugi, Petracca R, Weiner AJ, Houghton M, Rosa D, Grandi G and Abrignani S (1998). Binding of Hepatitis C Virus to CD81. *Science* **282**, 938-941

Pollard VW and Malim MH (1998). The HIV-1 Rev Protein. *Annual Review of Microbiology* **52**, 491-532

Poole TL, Wang CY, Popp RA, Potgieter LND, Siddiqui A and Collett MS (1995). Pestivirus Translation Initiation Occurs by Internal Ribosome Entry. *Virology* **206**, 750-754

Prince AM, Brotman B, Grady GF, Kuhns, WJ, Hazzi C, Levine RW, Millian SJ (1974). Long-incubation Post-transfusion Hepatitis Without Serological Evidence of Exposure to Hepatitis B Virus. *Lancet* **2**, 241-246

Prince AM, Huima-Byron T, Parker TS and Levine DM (1996). Visualization of Hepatitis C Virions and Putative Defective Infectious Particles Isolated from Low-Density Lipoproteins. *Journal of Viral Hepatitis* **3**, 11-17

Radkowski M, Wilkinson J, Nowicki M, Adair D, Vargas H, Ingui C, Rakela J and Laskus T (2002). Search for Hepatitis C Virus Negative-Strand RNA Sequences and Analysis of Viral Sequences in the Central Nervous System: Evidence of Replication. *Journal of Virology* **76**, 600-608

Raghunathan PL and Guthrie C (1998). RNA Unwinding in U4/U6 snRNPs Requires ATP Hydrolysis and the DEIH-box Splicing Factor Brr2. *Current Biology* **8**, 847-855

Ralston R, Thudium K, Berger K, Kuo C, Gervase B, Hall J, Selby M, Kuo G, Houghton M and Choo Q-L (1993). Characterisation of Hepatitis C Virus Envelope Glycoprotein Complexes Expressed by Recombinant Vaccinia Viruses. *Journal of Virology* **67**, 6753-6761

Ramratnam B, Bonhoeffer S, Binley J, Hurley A, Zhang LQ, Mittler JE, Markowitz M, Moore JP, Perelson AS and Ho DD (1999). Rapid Production and Clearance of HIV-1 and Hepatitis C Virus Assessed by Large Volume Plasma Apheresis. *Lancet* **354**, 1782-1785

Ravaggi A, Natoli G, Primi D, Albertini A, Levrero M and Cariani E (1994). Intracellular Localization of Full-length and Tuncated Hepatitis C Virus Core Protein Expressed in Mammalian Cells. *Journal of Hepatology* **20**, 833-836

Ray RB, Lagging LM, Meyer K, Steele R and Ray R (1995). Transciprional Regulation of Cellular and Viral Promoters by Hepatitis C Virus Core Protein. *Virus Research* **37**, 209-220

Ray RB, Lagging LM, Meyer K, and Ray R (1996). Hepatitis C Virus Core Protein Co-operates with *ras* and Transforms Primary Rat Embryo Fibroblasts to Tumourigenic Phenotype. *Journal of Virology* **70**, 4438-4443

Ray RB, Steele R, Meyer K and Ray R (1997). Transcriptional Repression of p53 Promoter by Hepatitis C Virus Core Protein. *Journal of Biological Chemistry* **272**, 10983-10986

Ray RB, Meyer K, Steele R, Shrivastava A, Aggarwal BB and Ray R (1998). Inhibition of Tumor necrosis factor (TNF-α)-mediated Apoptosis by Hepatitis C Virus Core Protein. *Journal of Biological Chemistry* **273**, 2256-2259

Ray RB, Meyer K and Ray R (2000). Hepatitis C Virus Core Protein Promotes Immortalization of Primary Human Hepatocytes. *Virology* **271**, 197-204

Rebagliati MR, Weeks DL, Harvey RP and Melton DA (1985). Identification and Cloning of Localized Maternal RNAs from *Xenopus* Eggs. *Cell* **42**, 769-777

Reddy KR, Wright TL, Pockros PJ, Shiffman M, Everson G, Reindollar R, Fried MW, Purdum PP, Jensen D, Smith C, Lee WM, Boyer TD, Lin A, Pedder S and DePamphilis J (2001). Efficacy and Safety of Pegylated (40-kd) Interferon α-2a Compared with Interferon α-2a in Noncirrhotic Patients with Chronic Hepatitis C. *Hepatology* **33**, 433-438

Reed KE and Rice CM (1999). Overview of Hepatitis C Virus Genome Structure, Polyprotein Processing, and Protein Properties. In *"The Hepatitis C Viruses"*, pp 55-84. Edited by CH Hagedorn and CM Rice. Germany: Springer.

Reed KE, Xu J and Rice CM (1997). Phosphorylation of the Hepatitis C Virus NS5A Protein *In vitro* and *In vivo*: Properties of the NS5A-associated Kinase. *Journal of Virology* **71**, 7187-7197

Reed KE, Gorbalenya AE and Rice CM (1998). The NS5A/NS5 Proteins of Viruses from Three Genera of the Family *Flaviviridae* are Phosphorylated by Associated Serine/threonine Kinases. *Journal of Virology* **72**, 6199-6206

Reynolds JE, Kaminski A, Kettinen HJ, Grace K, Clarke BE, Carroll AR, Rowlands DJ and Jackson RJ (1995). Unique Features of the Internal Initiation of Hepatitis C Virus-RNA Translation. *EMBO Journal* **14**, 6010-6020

Reynolds JE, Kaminski A, Carroll AR, Clarke BE, Rowlands DJ and Jackson RJ (1996). Internal Initiation of Translation of Hepatitis C Virus RNA: The Ribosome Entry Site is at the Authentic Initiation Codon. *RNA* **2**, 867-878

Rice (1996). *Flaviviridae*: The Viruses and Their Replication. In *"Fields Virology"* (3rd edn), pp931-959. Edited by BN Fields, DM Knipe and PM Howley. Philadelphia: Lippincott-Raven

Rijnbrand R, Bredenbeek P, Vanderstraaten T, Whetter L, Inchauspe G, Lemon S and Spaan W (1995). Almost the Entire 5′ Non-translated Region of Hepatitis C Virus is Required for Cap Independent Translation. *FEBS Letters* **365**, 115-119

Rijnbrand RCA, Abbink TEM, Haasnoot J, Spaan WJM and Bredenbeek PJ (1996). The Influence of AUG Codons in the Hepatitis C Virus 5′ Nontranslated Region on Translation and Mapping of the Translation Initiation Window. *Virology* **226**, 47-56

Rijnbrand RCA, Bredenbeek PJ, Haasnoot, Kieft JS, Spaan WJM and Lemon SM (2001). The Influence of Downstream Protein-coding Sequence on Internal Ribosome Entry on Hepatitis C Virus and Other Flavivirus RNAs. *RNA* **7**, 585-597

Robertson B, Myers G, Howard C, Brettin T, Bukh J, Gaschen B, Gojobori T, Maertens G, Mizokami M, Nainan O, Netesov S, Nishioka K, Shin-i T, Simmonds P, Smith D, Stuyver L and Weiner A (1998). Classification, Nomenclature, and Database Development for Hepatitis C Virus (HCV) and Related Viruses: Proposals for Standardization. *Archives of Virology* **143**, 2493-2503

Rogers GW, Richter NJ and Merrick WC (1999). Biochemical and Kinetic Characterization of the RNA Helicase Activity of Eukaryotic Initiation Factor 4A. *Journal of Biological Chemistry* **274**, 12236-12244

Rogers GW, Richter NJ, Lima WF and Merrick WC (2001). Modulation of Helicase Activity of eIF4A by eIF4B, eIF4H, and eIF4F. *Journal of Biological Chemistry* **276**, 30914-30922

Rogler CE and Chisari FV (1992). Cellular and Molecular Mechanisms of Hepatocarcinogenesis. *Seminars in Liver Disease* **12**, 265-278

Rosa D, Campagnoli S, Moretto C, Guenzi E, Cousens L, Chin M, Dong C, Weiner AJ, Lau JYN, Choo QL, Chien D, Pileri P, Houghton M and Abrignani S (1996). A Quantitative Test to Estimate Neutralizing Antibodies to the Hepatitis C Virus: Cytofluorimetric Assessment of Envelope Glycoprotein 2 Binding to Target Cells. *Proceedings of the National Academy of Sciences USA* **93**, 1759-1763

Rose JK, Buonocore L and Whitt MA (1991). A New Cationic Liposome Reagent Mediating Nearly Quantitative Transfection of Animal Cells. *Biotechniques* **10**, 520-525

Rozen F, Edery I, Meerovitch K, Dever TE, Merrick WC and Sonenberg N (1990). Bidirectional RNA Helicase Activity of Eukaryotic Translation Initiation Factors 4A and 4F. *Molecular and Cellular Biology* **10**, 1134-1144

Rosenberg S (2001). Recent Advances in the Molecular Biology of Hepatitis C Virus. *Journal of Molecular Biology* **313**, 451-464

Ruggieri A, Harada T, Matsuura Y and Miyamura T (1997). Sensitization to *Fas*-Mediated Apoptosis by Hepatitis C Virus Core Protein. *Virology* **229**, 68-76

Ruiz-Echevarria MJ, Czaplinski K and Peltz SW (1996). Making Sense of Nonsense in Yeast. *Trends in Biochemical Sciences* **21**, 433-438

Sabile A, Perlemuter G, Bono F, Kohara K, Demaugre F, Kohara M, Matsuura, Miyamura T, Bréchot C and Barba G (1999). Hepatitis C Virus Core Protein Binds to Apolipoprotein AII and Its Secretion is Modulated by Fibrates. *Hepatology* **30**, 1064-1076

Saffman EE and Lasko P (1999). Germline Development in Vertebrates and Invertebrates. *Cellular and Molecular Life Sciences* **55**, 1141-1163

Saito I, Miyamura T, Ohbayashi A, Harada H, Katayama T, Kikuchi S, Watanbe TY, Koi S, Onji M, Ohta Y, Choo Q-L, Houghton M and Kuo G (1990). Hepatitis C Virus Infection is Associated with the Development of Hepatocellular Carcinoma. *Proceedings of the National Academy of Sciences USA* **87**, 6547-6549

Sakamuro D, Furukawa T, and Takegami T (1995). Hepatitis C Virus Non-Structural Protein NS3 Transforms NIH3T3 Cells. *Journal of Virology* **69**, 3893-3896

Santolini E, Migliaccio G and la Monica N (1994). Biosynthesis and Biochemical Properties of the Hepatitis C Virus Core Protein. *Journal of Virology* **68**, 3631-3641

Sato K, Okamoto H, Aihara S, Hoshi Y, Tanaka T and Mishiro S (1993). Demonstration of Sugar Moiety on the Surface of Hepatitis C Virions Recovered from the Circulation of Infected Humans. *Virology* **196**, 354-357

Scheffner M, Knippers R and Stahl H (1989). RNA Unwinding Activity of SV40 Large T Antigen. *Cell* **57**, 955-963

Scheuer PJ, Ashrafzadeh P, Sherlock S, Brown D and Dusheiko GM (1992). The Pathology of Hepatitis C. *Hepatology* **15**, 567-571

Schmid SR and Linder P (1991). Translation Initiation Factor 4A from *Sacchraromyces cerevisiae* - Analysis of Residues Conserved in the D-E-A-D Family of RNA Helicases. *Molecular and Cellular Biology* **11**, 3463-3471

Schmid SR and Linder P (1992). D-E-A-D Protein Family of Putative RNA Helicases. *Molecular Microbiology* **6**, 283-292

Schroder HC, Ugarkonic D, Langen P, Bachman M, Dorn A, Kuchino Y and Muller WEG (1990). Evidence for the Involvement of a Nuclear Envelope-Associated RNA Helicase Activity in Nucleocytoplasmic RNA Transport. *Journal of Cellular Physiology* **145**, 136-146

Schulz GE (1992). Binding of Nucleotides by Proteins. *Current Opinion in Structural Biology* **2**, 61-67

Schwer B (2001). A New Twist on RNA Helicases: DExH/D Box Proteins as RNPases. *Nature Structural Biology* **8**, 113-116

Schwikowski B, Uetz P, Fields S (2000). A Network of Protein-protein Interactions in Yeast. *Nature Biotechnology* **18**, 1257-1261

Seed B and Sheen JY (1988). A Simple Phase-extraciton Assay for Chloramphenicol Acetyltransferase Activity. *Gene* **67**, 271-277

Selby MJ, Choo Q-L, Berger K, Kuo G, Glazer E, Eckart M, Lee C, Chien D, Kuo C, Houghton M (1993). Expression, Identification and Subcellular Localization of the Proteins Encoded by the Hepatitis C Viral Genome. *Journal of General Virology* **74**, 1103-1113

Selby MJ, Glazer E, Masiarz F and Houghton M (1994). Complex Processing and Protein-protein Interactions in the E2-NS2 Region of HCV. *Virology* **204**, 114-122

Sheen IS, Liaw YF, Chu CM and Pao CC (1992). Role of Hepatitis C Virus Infection in Spontaneous Antigen Clearance During Chronic Hepatitis B Virus Infection. *Journal of Infectious Diseases* **165**, 831-834

Sherlock S (1999). The Hepatic *Flaviviridae*: Summary. *Journal of Viral Hepatitis* **6 (Suppl. 1)**, 1-5

Shi ST, Polyak SJ, Tu H, Taylor DR, Gretch DR and Lai MMC (2002). Hepatitis C Virus NS5A Colocalizes with the Core Protein on Lipid Droplets and Interacts with Apolipoproteins. *Virology* **292**, 198-210

Shih CM, Lo SJ, Miyamura T, Chen SY and Lee YW (1993). Suppression of Hepatitis B Virus Expression and Replication by Hepatitis C Virus Core Protein in Huh-7 cells. *Journal of Virology* **67**, 5823-5832

Shih CM, Chen CM, Chen SY and Lee YHW (1995). Modulation of the Trans-Suppression Activity of Hepatitis C Virus Core Protein by Phosphorylation. *Journal of Virology* **69**, 1160-1171

Shimoike T, Mimori S, Tani H, Matsuura Y and Miyamura T (1999). Interaction of Hepatitis C Virus Core Protein with Viral Sense RNA and Suppression of its Translation. *Journal of Virology.* **73**, 9718-9725

Shimotohno K (2000). Hepatitis C Virus and its Pathogenesis. *Seminars in Cancer Biology* **10**, 233-240

Shimizu YK, Feinstone SM, Kohara M, Purcell RH and Yoshikura H (1996). Hepatitis C Virus: Detection of Intracellular Virus Particles by Electron Microscopy. *Hepatology* **23**, 205-209

Shrivastava A, Manna SK, Ray R and Aggarwal BB (1998). Ectopic Expression of Hepatitis C Virus Core Protein Differentially Regulates Nuclear Transcription Factors. *Journal of Virology* **72**, 9722-9728

Shoji I, Suzuki T, Sato M, Aizaki H, Chiba T, Matsuura Y and Miyamura T (1998). Internal Processing of Hepatitis C Virus NS3 Protein. *Virology* **254**, 315-323

Shuman S (1992). Vaccinia Virus RNA Helicase: An Essential Enzyme Related to the D-E-X-H Family of RNA-Dependent NTPases. *Proceedings of the National Academy of Sciences USA* **89**, 10935-10939

Simmonds P (1995). Variability of Hepatitis C Virus. *Hepatology* **21**, 570-583

Simmonds P (2001). The Origin and Evolution of Hepatitis Viruses in Humans. *Journal of General Virology* **82**, 693-712

Simons JN, Pilotmatias TJ, Leary TP, Dawson GJ, Desai SM, Schlauder GG, Muerhoff AS, Erker JC, Buijk SL and Mushahwar IK (1995a). Identification of Two Flavivirus-like Genomes in the GB Hepatitis Agent. *Proceedings of the National Academy of Sciences USA* **92**, 3401-3405

Simons JN, Leary TP, Dawson GJ, Pilotmatias TJ, Muerhoff AS, Schlauder GG, Desai SM and Mushahwar IK (1995b). Isolation of Novel Virs-like Sequences Associated with Human Hepatitis. *Nature Medicine* **1**, 564-569

Sizova DV, Kolupaeva VG, Pestova TV, Shatsky IN, Hellen CUT (1998). Specific Interaction of Eukaryotic Translation Initiation Factor 3 with the 5′ Nontranslated Regions of Hepatitis C Virus and Classical Swine Fever Virus RNAs. *Journal of Virology* **72**, 4775-4782

Smith DB and Simmonds P (1997). Characteristics of Nucleotide Substitution in the Hepatitis C Virus Genome: Constraints on Sequence Change in Coding Regions at Both Ends of the Genome. *Journal of Molecular Evolution* **45**, 238-246

Snay-Hodge CA, Colot HV, Goldstein AL, Cole CN (1998). Dbp5p/Rat8p is a Yeast Nuclear Pore-associated DEAD-box Protein Essential for RNA Export. *EMBO Journal* **17**, 2663-2676

Spahn CMT, Kieft JS, Grassucci RA, Penczek PA, Zhou KH, Doudna JA, Frank J (2001). Hepatitis C Virus IRES RNA-induced Changes in the Conformation of the 40S Ribosomal Subunit. *Science* **291**, 1959-1962

Spangberg K, Goobar-Larsson L, Wahren-Herlenius M, Schwartz S (1999). The La Protein from Human Liver Cells Interacts Specifically with the U-rich Region in the Hepatitis C Virus 3′ Untranslated Region. *Journal of Human Virology* **2**, 296-307

Spector DL (1996). Nuclear Organization and Gene Expression. *Experimental Cell Research* **229**, 189-197

Srinvas RV, Ray RB, Meyer K and Ray R (1996). Hepatitis C Virus Core Protein Inhibits Human Immunodeficiency Virus Type 1 Replication. *Virus Research* **45**, 87-92

Stade K, Ford CS, Guthrie C and Weis K (1997). Exportin 1 (Crm1p) Is an Essential Nuclear Export Factor. *Cell* **90**, 1041-1050

Staley JP and Guthrie C (1998). Mechanical Devices of the Spliceosome: Motors, Clocks, Springs, and Things. *Cell* **92**, 315-326

Styhler S, Nakamura A, Swan A, Suter B and Lasko P (1998). Vasa is Required for GURKEN Accumulation in the Oocyte, and is Involved in Oocyte Differentiation and Germline Cyst Development. *Development* **125**, 1569-1578

Sugiyama K, Kato N, Mizutani T, Ikeda M, Tanaka T and Shimotohno K (1997). Genetic Analysis of the Hepatitis C Virus (HCV) Genome from HCV-infected Human T Cells. *Journal of General Virology* **78**, 329-336

Sun J, Bodola F, Fan X, Irshad H, Soong L, Lemon SM and Chan T-S (2001). Hepatitis C Virus Core and Envelope Proteins Do Not Suppress the Host's Ability to Clear a Hepatic Viral Infection. *Journal of Virology* **75**, 11992-11998

Suzuki R, Matsuura Y, Suzuki T, Ando A, Chiba J, Harada S, Saito I and Miyamura T (1995). Nuclear Localization of the Truncated Hepatitis C Virus Core Protein with its Hydrophobic C-terminus Deleted. *Journal of General Virology* **76**, 53-61

Tai C-L, Chi W-K, Chen D-S and Hwang L-H (1996). The Helicase Activity Associated with Hepatitis C Virus Non-Structural Protein 3. *Journal of Virology* **70**, 8477-8484

Takahashi K, Kishimoto S, Yoshizawa H Okamoto H, Yoshikawa A and Mishiro S (1992). p26 Protein and 33 nm Particle Associated with Nucleocapsid of Hepatitis C Virus Recovered from the Circulation of Infected Hosts. *Virology* **191**, 431-434

Takamizawa A, Mori C, Fuke I, Manabe S, Murakami S, Fujita J, Onishi E, Andoh T, Yoshida I and Okayama H (1991). Strucuture and Organization of the Hepatitis C Virus Genome Isolated from Human Carriers. *Journal of Virology* **65**, 1105-1113

Takimoto M, Tomonaga T, Matunis M, Avigan M, Krutzsch H, Dreyfuss G and Levens D (1993). Specific Binding of Heterogeneous Ribonucleoprotein Particle Protein K to the Human c-*myc* Promoter *In Vitro*. *Journal of Biological Chemistry* **268**, 18249-18258

Tanaka T, Kato N, Cho M-J and Shimotohno K (1995). A Novel Sequence found at the 3′ Terminus of the Hepatitis C Virus Genome. *Biochemical and Biophysical Research Communications* **215**, 744-749

Tanji Y, Hijikata M, Hirowatari Y and Shimotohno K (1994). Hepatitis C Virus Polyprotein Processing - Kinetics and Mutagenic Analysis of Serine Protease-depedent Cleavage. *Journal of Virology* **68**, 8418-8422

Tanji Y, Kaneko T, Satoh S and Shimotohno K (1995). Phosphorylation of Hepatitis C Virus Encoded Nonstructural Protein NS5A. *Journal of Virology* **69**, 3980-3986

Tartaglia LA, Ayres TM, Wong GHW and Goeddel DV (1993). A Novel Domain within the 55 kD TNF Receptor Signals Cell Death. *Cell* **74**, 845-853

Taylor SJ and Shalloway D (1994). An RNA-binding Protein Associated with Src through its SH2 and SH3 Domains in Mitosis. *Nature* **368**, 867-871

Taylor DR, Shi ST, Romano PR, Barber GN and Lai MMC (1999). Inhibition of the Interferon-Inducible Protein Kinase PKR HCV E2 Protein. *Science* **285**, 107-109

Taylor DR, Tian B, Romano PR, Hinnebusch AG, Lai MMC and Mathews MB (2001). Hepatitis C Virus Envelope Protein E2 Does Not Inhibit PKR by Simple Competition with Autophosphorylation Sites in the RNA-binding Domain. *Journal of Virology* **75**, 1265-1273

Theodore D and Fried M (1999). Natural History and Disease Manifestations of Hepatitis C Infection. In *"The Hepatitis C Viruses"*, pp 43-54. Edited by CH Hagedorn and CM Rice. Germany: Springer.

Thomas (1999). Hepatitis C Epidemiology. In *"The Hepatitis C Viruses"*, pp 25-42. Edited by CH Hagedorn and CM Rice. Germany: Springer.

Thomson BJ, Efstathiou S and Honess RW (1991). Acquisition of the Human Adeno-associated Virus Type 2 Rep Gene by Human Herpesvirus 6. *Nature* **351**, 78-80

Thomssen R, Bonk S, Proppe C, Heermann KH, Kochel HG and Uy A (1992). Association of Hepatitis C Virus in Human Sera with β-Lipoproteins. *Medical Microbiology and Immunology* **181**, 293-300

Trowbridge R and Gowans EJ (1998). Identification of Novel Sequences at the 5′ Terminus of the Hepatitis C Virus Genome. *Journal of Viral Hepatitis* **5**, 95-98

Tseng SSL, Weaver PL, Liu Y, Hitomi M, Tartakoff AM and Chang TH (1998). Dbp5p, a Cytosolic RNA helicase, is Required for poly(A)$^+$ RNA Export. *EMBO Journal* **17**, 2651-2662

Tsu CA and Uhlenbeck OC (1998). Kinetic Analysis of the RNA-dependent Adenosinetriphosphatase Activity of DbpA, an Escherichia coli DEAD protein Specific for 23S Ribosomal RNA. *Biochemistry* **37**, 16989-16996

Tsuchihara K, Tanaka T, Hijikata M, Kuge S, Toyoda H, Nomoto A, Yamamoto N, and Shimotohno K (1997). Specific Interaction of Polypyrimidine Tract-binding Protein with the Extreme 3′-terminal Structure of the Hepatitis C Virus Genome, the 3′X. *Journal of Virology* **71**, 6720-6726

Tsukiyama-Kohara K, Iizuka N, Kohara M and Nomoto A (1992). Internal Ribosome Entry Site Within Hepatitis C Virus RNA. *Journal of Virology* **66**, 1476-1483

Uetz P, Glot L, Cagney G, Mansfiled TA, Judson RS, Knight JR, Lockshon D, Narayan V, Srinivasan M, Pochart, Qureshi-Emili A, Li Y, Godwin B, Conover D, Kalbfeisch T, Vijayadamodar G, Yang M, Johnston M, Fields S and Rothberg JM (2000). A Comprehensive Analysis of Protein-protein Interactions in *Saccharomyces cerevisiae*. *Nature* **403**, 623-631

Vaux DL and Strasser A (1996). The Molecular Biology of Apoptosis. *Proceedings of the National Academy of Sciences USA* **93**, 2239-2244

Venema J and Tollervey D (1995). Processing of Pre-ribosomal RNA in *Saccharomyces cerevisiae*. *Yeast* **11**, 1629-1650

Venema J, Bousquet-Antonelli C, Gelugne JP, Caizergues-Ferrer M and Tollervey D (1997). Rok1p is a Putative RNA Helicase Required for rRNA Processing. *Molecular and Cellular Biology* 17, 3398-3407

Venkatesan M, Silver LL and Nossal NG (1982). Bacteriophage T4 Gene 41 Protein, required for the Synthesis of RNA Primers is also a DNA helicase. *Journal of Biological Chemistry* **257**, 2426-2434

Wack A, Soldaini E, Tseng CTK, Nuti S, Kimpel GR, Abrignani S (2001). Binding of the Hepatitis C Virus Envelope Protein E2 to CD81 Provides a Co-stimulatory Signal for Human T cells. *European Journal of Immunology* **31**, 166-175

Wagner JDO, Jankowsky E, Company M, Pyle AM and Abelson JN (1998). The DEAH-box Protein PRP22 is an ATPase that Mediates ATP-dependent mRNA Release from the Spliceosome and Unwinds RNA Duplexes. *EMBO Journal* **17**, 2926-2937

Wakita T, Taya C, Katsume A, Kato J, Yonekawa H, Kanegae Y, Saito I, Hayashi Y, Koike M and Kohara M (1998). Efficient Conditional Transgene Expression in Hepatitis C Virus cDNA Transgenic Mice Mediated by the Cre/loxP System. *Journal of Biological Chemistry* **273**, 9001-9006

Walewski JL, Keller TR, Stump DD and Branch AD (2001). Evidence for a New Hepatitis C Virus Antigen Encoded in an Overplapping Reading Frame. *RNA* **7**, 710-721

Walker JE, Saraste M, Runswick MJ, Gay NJ (1982). Distantly Related Sequences in the α-subunits and β-subunits of ATP Synthase, Myosin, Kinases and Other ATP-requiring Enzymes and a Common Nucleotide Binding Fold. *EMBO Journal* **1**, 945-951

Wang CY, Sarnow P and Siddiqui A (1993). Translation of Hepatitis C Virus RNA in Cultured Cells is Mediated by an Internal Ribosome-Binding Mechanism. *Journal of Virology* **67**, 3338-3344

Wang T-H, Rijnbrand RCA and Lemon SM (2000). Core Protein-Coding Sequence, but Not Core Protein, Modulates the Efficiency of Cap-Independent Translation Directed by the Internal Ribosome Entry Site of Hepatitis C Virus. *Journal of Virology*. **74**, 11347-11358

Wang Y-H, Trowbridge R and Gowans EJ (1997). Expression and Interaction of the Hepatitis C Virus Structural Proteins and the 5′ Untranslated Region in Baculovirus Infected Cells. *Archives of Virology* **142**, 2211-2223

Wang Y and Guthrie C (1998). PRP16, a DEAH-box RNA Helicase, is Recruited to the Spliceosome Primarily Via its Nonconserved N-terminal Domain. *RNA* **4**, 1216-1229

Wardell AD, Errington W, Ciarmella G, Merson J and McGarvey MJ (1999). Characterization and Mutational Analysis of Hepatitis C Virus Full-length NS3 Protein. *Journal of General Virology* **80**, 701-709

Ware CF, VanArsdale TL, Crowe PD and Browning JL (1995). The Ligands and Receptors of the Lymphotoxin System. *Current Topics in Microbiology and Immunology* 198, 175-218

Warrener P and Collet MC (1995). Pestivirus NS3 (p80) Protein Possesses RNA Helicase Activity. *Journal of Virolgy* **69**, 1720-1726

Warrener P, Tamura JK and Collett MS (1993). RNA-Stimulated NTPase Activity Associated with Yellow Fever Virus NS3 Protein Expressed in Bacteria. *Journal of Virology* **67**, 989-996

Wasserman DA and Steitz JA (1991). Alive with DEAD Proteins. *Nature* **349**, 463-464

Watanabe M, Zinn AR, Page DC, Nisimoto T (1993). Functional Equivalence of Human X and Y Encoded Isoforms of Ribosomal Protein S4 Consistent with a Role in Turner Syndrome. *Nature Genetics* **4**, 268-271

Weaver PL, Sun C and Chang TH (1997). Dbp3p, a Putative RNA Helicase in *Saccharomyces cerevisiae*, is Required for Efficient Pre-rRNA Processing Predominantly at site A(3). *Molecular and Cellular Biology* **17**, 1354-1365

Weiner AJ, Brauer MJ, Rosenblatt J, Richman KH, Tung J, Crawford K, Bonino F, Saracco G, Choo Q-L, Houghton M and Han JH (1991). Variable and Hypervariable Domains are Found in the Regions of HCV Corresponding to the Flavivirus Envelope and NS1 Proteins and the Pestivirus Envelope Glycoproteins. *Virology* **180**, 842-848

Weiner AJ, Geysen HM, Christopherson C, Hall JE, Mason TJ, Saracco G, Bonino F, Crawford K, Marion CD, Crawford KA, Brunetto M, Barr PJ, Miyamura T, McHutchinson J and Houghton M (1992). Evidence for Immune Selection of Hepatitis C Virus (HCV) Putative Envelope Glycoprotein Variants - Potential Role in Chronic HCV Infections. *Proceedings of the National Academy of Sciences USA* **89**, 3468-3472

Weiner AJ, Thaler MM, Crawford K, Ching K, Kansopon J, Chien DY, Hall JE, Hu F and Houghton M (1993). A Unique, Predominant Hepatitis C Virus Variant Found in an Infant Born to a Mother with Multiple Variants. *Journal of Virology* **67**, 4365-4368

Weis K (1998). Importins and Exporting: How to Get In and Out of the Nucleus. *Trends in Biochemical Sciences* **23**, 185-189

Wellnitz S, Klumpp B, Barth H, Ito S, Depla E, Dubuisson, Blum HE and Baumert TF (2002). Binding of Hepatitis C Virus-Like Particles Derived from Infectious Clone H77C to Defined Human Cell Lines. *Journal of Virology* **76**, 1181-1193

Weng ZG, Thomas SM, Rickles RJ, Taylor JA, Brauer AW, Seidelugan C, Michael WM, Dreyfuss G and Brugge JS (1994). Identification of Src, Fyn, and Lyn-SH3 Binding-Proteins - Implications for a Function of SH3 Domains. *Molecular and Cellular Biology* **14**, 4509-4521

Wengler G and Wengler G (1991). The Carboxy-terminal Part of the NS3 Protein of the West Nile Flavivirus can be Isolated as a Soluble Protein After Proteolytic Cleavage and Represents an RNA-stimulated NTPase. *Virology* **184**, 707-715

Wengler G, Wukrner D and Wengler G (1992). Identification of a Sequence Element in the Alphavirus Core Protein which Mediates Interaction of Cores with Ribosomes and Disassembly of Cores. *Virology* **191**, 880-888

Westaway EG, MacKenzie JM, Kenney MT, Jones MK and Khromykh AA (1997). Ultrastructure of Kunjin Virus-infected Cells: Co-localization of NS1 and NS3 with Double-stranded RNA, and of NS2B with NS3, in Virus-induced Membrane Structures. *Journal of Virology* **71**, 6650-6661

White E (1996). Life, Death, and the Pursuit of Apoptosis. *Genes and Development* **10**, 1-15

Wood J, Frederickson RM, Fields S and Patel AH (2001). Hepatitis C Virus 3'X Region Interacts with Human Ribosomal Proteins. *Journal of Virology* **75**, 1348-1358

Wu JY and Maniatis T (1993). Specific Interactions between Proteins Implicated in Splce Site Selection and Regulated Alternative Splicing. *Cell* **75**, 1061-1070

Xu DM, Nouraini S, Field D, Tang SJ and Friesen JD (1996). An RNA-dependent ATPase Associated with U2/U6 snRNAs in pre-mRNA splicing. *Nature* **381**, 709-713

Xu Z, Choi J, Yen TSB, Lu W, Strohecker A, Govindarajan S, Chien D, Selby MJ and Ou J-H (2001). Synthesis of a Novel Hepatitis C Virus Protein by Ribosomal Frameshift. *EMBO Journal* **20**, 3840-3848

Yaffe MB, Rittinger K, Volinia S, Caron PR, Aitken A, Leffers H, Gamblin SJ, Smerdon SJ and Cantley LC (1997). The Structural Basis for 14-3-3:Phosphopeptide Binding Specificity. *Cell* **91**, 961-971

Yamada N, Tanihara K, Takada A, Yorihuzi T, Tsutsumi M, Shimomura H, Tsuji T and Date T (1996). Genetic Organization and Diversity of the 3' Noncoding Region of the Hepatitis C Virus Genome. *Virology* **223**, 255-261

Yan BS, Tam MH and Syu WJ (1998). Self-association of the C-terminal Domain of the Hepatitis-C Virus Core Protein. *European Journal ofBiochemistry* **258**, 100-106

Yanagi M, Purcell RH, Emerson SU and Bukh J (1997). Transcripts from a Single Full-length cDNA Clone of Hepatitis C Virus are Infectious when Directly Transfected into the Liver of a Chimpanzee. *Proceedings of the National Academy of Sciences USA* **94**, 8738-8743

Yanagi M, St. Claire M, Shapiro M, Emerson SU, Purcell RH and Bukh J (1998). Transcripts of a Chimeric cDNA Clone of Hepatitis C Virus Genotype 1b Are Infectious *In Vivo*. *Virology* **244**, 161-172

Yanagi M, Purcell RH, Emerson SU and Bukh J (1999). Hepatitis C Virus: An Infectious Molecular Clone of a Second Major Genotype (2a) and Lack of Viability of Intertypic 1a and 2a Chimeras. *Virology* **262**, 250-263

Yano M, Kumada H, Kage M, Ikeda K, Shimamatsu K, Inoue O, Hashimoto E, Lefkowitch JH, Ludwig J and Okuda K (1996). The Long-term Pathological Evolution of Chronic Hepatitis C. *Hepatology* **23**, 1334-1340

Yao N, Hesson T, Cable M, Hong Z, Kwong D, Le HV and Weber PC (1997). Structure of the Hepatitis C Virus RNA Helicase Domain. *Nature Structural Biology* **4**, 463-467

Yap SH, Willems M, Vanenoord J, Habets W, Middeldorp JM, Hellings JA, Nevens F, Moshage H, Desmet V and Fevery J (1994). Detection of Hepatitis C Virus by Immunohistochemical Staining - A Histological Marker of Hepatitis C Virus Infection. *Journal of Hepatology* **20**, 275-281

Yasui K, Wakita T, Tsukiyama-Kohara K, Funahashi S-I, Ichikawa M, Kajita T, Moradpour D, Wands JR and Kohara M (1998). The Native Form and Maturation Process of Hepatitis C Virus Core Protein. *Journal of Virology* **72**, 6048-6055

Yoo BJ, Selby MJ, Choe J, Suh BS, Choi SH, Joh JS, Nuovo GJ, Lee H-S, Houghton M and Han JH (1995). Transfection of a Differentiated Human Hepatoma Cell Line (Huh7) with *In Vitro*-Transcribed Hepatitis C Virus (HCV) RNA and Establishment of a Long-Term Culture Persistently Infected with HCV. *Journal of Virology* **69**, 32-38

Yoshiba M, Dehara K, Inoue K, Okamoto H and Mayumi M (1994). Contribution of Hepatitis C Virus to Non-A, Non-B Fulminant Hepatitis in Japan. *Hepatology* **19**, 829-835

Yoshida H, Kato N, Shiratori Y, Otsuka M, Maeda S, Kato J and Omata M (2001). Hepatitis C Virus Core Protein Activates Nuclear Factor κB-dependent Signaling through Tumour Necrosis Factor Receptor-associated Factor. *Journal of Biological Chemistry* **276**, 16399-16405

You LR, Chen CM and Lee YHW (1999a). Hepatitis C Virus Core Protein Enhances NF-κB Signal Pathway Triggering by Lymphotoxin-β Receptor Ligand and Tumor Necrosis Factor α. *Journal of Virology* **73**, 1672-1681

You L-R, Chen C-M, Yeh T-S, Tsai T-Y, Mai R-T, Lin C-H and Lee Y-H W (1999b). Hepatitis C Virus Core Protein Interacts with Cellular Putative RNA Helicase. *Journal of Virology* **73**, 2841-2853

Zeuzem S, Lee J-H and Roth WK (1997). Mutations in the Nonstructural 5A Gene of European Hepatitis C Virus Isolates and Response to Interferon Alpha. *Hepatology* **25**, 740-744

Zhu N, Khoshnan A, Schneider R, Matsumoto M, Dennert G, Ware C and Lai MC (1998). Hepatitis C Virus Core Protein Binds to the Cytoplasmic Domain of Tumour Necrosis Factor (TNF) Receptor 1 and Enhances TNF-Induced Apoptosis. *Journal of Virology* **72**, 3691-3697

Zibert A, Schreier E and Roggendorf M (1995). Antibodies in Human Sera Specific to Hypervariable Region-1 of Hepatitis C Virus can Block Viral Attachment. *Virology* **208**, 653-661

APPENDIX I:

Monoclonal and Polyclonal Antibodies

Antibodies used in the preceding studies are shown below. Although anti-DDX3 antibodies were generated by Dr A. Owsianka, detailed characterisation was undertaken as part of these studies. A summary of the epitopes bound by anti-DDX3 MAbs AO2 to AO215 is shown schematically in Fig. 88 on the following page.

Antibody	*Name*	*Type*	*Raised in*	*Source*
Anti-DDX3	AO2 to AO215	Monoclonal	Mouse	A. Owsianka
Anti-DDX3	R438 and R648	Polyclonal	Rabbit	A. Owsianka (Owsianka and Patel, 1999)
Anti-HCV core	R525	Polyclonal	Rabbit	A. Owsianka
Anti-HCV E1	R528	Polyclonal	Rabbit	A. Patel
Anti-HCV E2	AP33	Monoclonal	Mouse	A. Patel (Owsianka *et al.*, 2000)
Anti-HCV NS3	Anti-NS3	Polyclonal	Sheep	A. Patel
Anti-HCV NS3 Protease	Anti-NS3	Polyclonal	Sheep	M. Harris, Leeds (Aoubala *et al.*, 2001)
Anti-SC-35	Anti-SC-35	Monoclonal	Mouse	A. Lamond, Dundee (Fortes *et al.*, 1995)
Anti-U1A	Anti-U1A	Polyclonal	Rabbit	A. Lamond, Dundee
Anti-CAT	Anti-CAT	Polyclonal	Rabbit	J. McLauchlan, Glasgow
Anti-histidine-tag	RGS-His	Monoclonal	Mouse	QIAGEN
Anti-GST	Anti-GST	Polyclonal	Rabbit	A.Patel
Anti-β-tubulin	Anti-β-tubulin	Monoclonal	Mouse	Sigma
Anti-ATF-2	Anti-ATF-2	Polyclonal	Rabbit	Santa Cruz Biotech

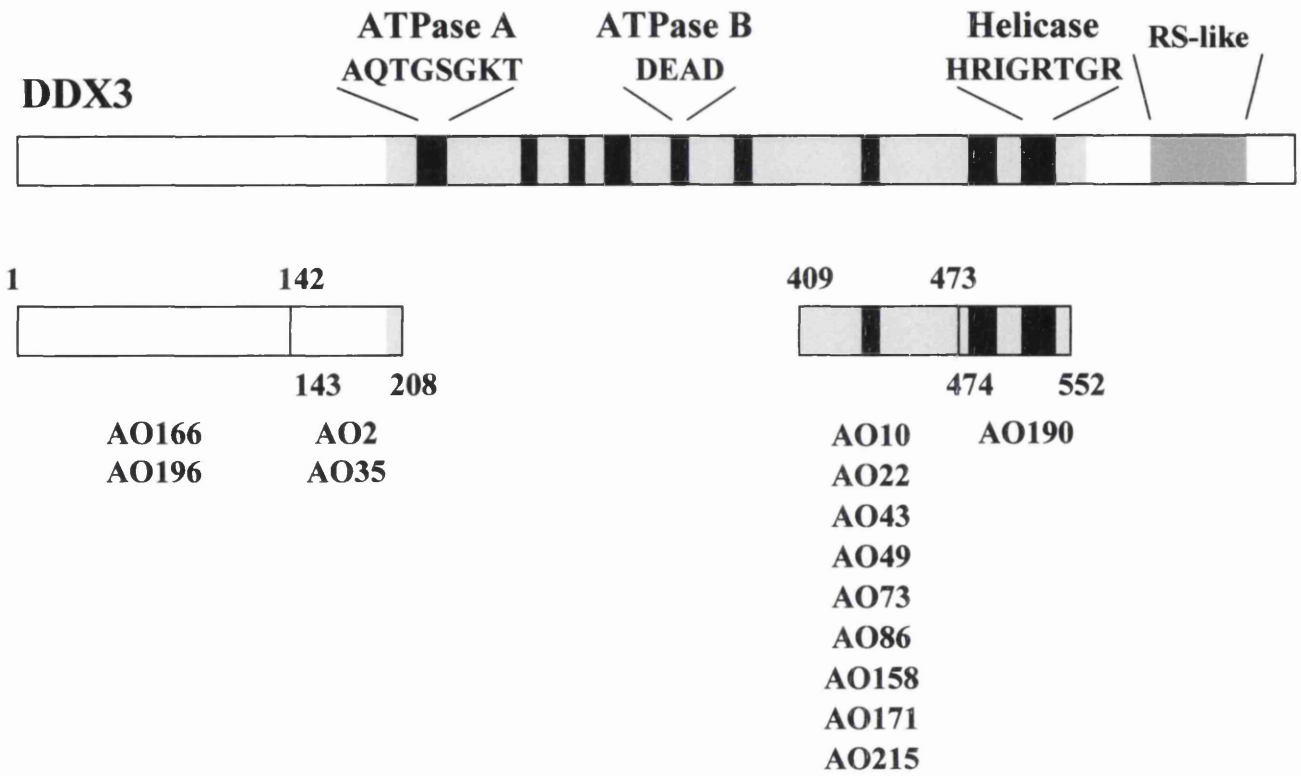

Figure 88: Epitopes of all anti-DDX3 MAbs. Binding sites were deduced by Western blotting or ELISA with DDX3 deletion mutants expressed as GST-fusion proteins (Figs 36-41; sections 3.2.14-3.2.17) and all epitopes mapped to the DDX3 protein sequence. The epitope of MAb AO34 was not clear from ELISA data (Fig. 39; section 3.2.15) and is not included. A central conserved region of high homology with eIF4A is shaded grey on the DDX3 protein sequence, while conserved motifs are indicated by black boxes (adapted from Owsianka and Patel, 1999).

APPENDIX II:

Plasmid Constructs

Constructs used in the preceding studies are shown below. DDX3 aa numbers relate to the sequence reported by Owsianka and Patel (1999) (see Appendix IV). The HCV infectious clone H77c (Yanagi *et al.*, 1997; see Appendix IV) was used in generation of HCV constructs unless otherwise stated. Constructs generated by the author are denoted 'MJS'.

Construct	*Vector*	*Source*	*Reference*
pDDX3-AS	pZeoSV2 (+)	A. Patel	-
pDDX3-S	pZeoSV2 (+)	A. Patel	-
GST-DDX3 (1-662)	pGEX-6P-3	A. Owsianka	Owsianka and Patel (1999)
GST-DDX3C (409-662)	pGEX-2T	A. Owsianka	"
GST-DDX3 409-622	pGEX-2T	A. Patel	"
GST-DDX3-623-662	pGEX-2T	A. Patel	"
GST-DDX3-409-473	pGEX-2T	A. Patel	"
GST-DDX3-474-662	pGEX-2T	A. Patel	"
GST-DDX3-409-552	pGEX-2T	A. Patel	"
GST-DDX3-553-662	pGEX-2T	A. Patel	"
GST-RS	pGEX-6P-3	MJS	-
GST-ΔRS	pGEX-6P-3	MJS	-
GST-DDX3-1-142	pGEX-6P-3	MJS	-
GST-DDX3-1-208	pGEX-6P-3	MJS	-
GST-DDX3-1-282	pGEX-6P-3	MJS	-
GST-DDX3 1-472	pGEX-6P-3	MJS	-
GST-NS3 Helicase	pGEX-6P-3	MJS	-
6h-An3	pET-21a	D. Weeks	-
pDDX3	pZeoSV2 (+)	MJS	-
p6h-DDX3	pZeoSV2 (+)	MJS	-
pDDX3-EQ	pZeoSV2 (+)	P. Askjaer	-
p6h-DDX3-EQ	pZeoSV2 (+)	MJS	-
pΔNES-DDX3	pZeoSV2 (+)	MJS	-
p6h-ΔNES-DDX3	pZeoSV2 (+)	MJS	-
pAn3	pZeoSV2 (+)	MJS	-
p6h-An3	pZeoSV2 (+)	MJS	-

Construct	*Vector*	*Source*	*Reference*
pTM1-core	pTM1	A. Patel	Owsianka and Patel (1999)
pcDNA-C-E1-E2	pcDNA 3.1/Zeo(+)	A. Patel	-
pcDNA-C-E1-E2 (Gla)	pcDNA 3.1/Zeo(+)	A. Patel	-
pcDNA-E1-E2	pcDNA 3.1/Zeo(+)	A. Patel	-
pcDNA-DDX3	pcDNA 3.1/Zeo(+)	A. Patel	-
pCV-H77c	pGEM 9zf(-)	J. Bukh	Yanagi *et al.* (1997)
pCV-5CC	pGEM 9zf(-)	J. Wood	Wood *et al.* (2001)
pCV-5CC3	pGEM 9zf(-)	J. Wood	"
pcDNA-CAT	pcDNA 3.1/Zeo(+)	A. Patel	-
pcDNA-C	pcDNA 3.1/Zeo(+)	J. Wood	-
pcDNA-5C	pcDNA 3.1/Zeo(+)	J. Wood	-
pAc-DDX3	pAcCL29.1	A. Patel	-
pAcC	pAcCL29.1	MJS	-
pAcCC	pAcCL29.1	MJS	-
pAcNS3	pAcCL29.1	MJS	-
pAcC-E1-E2	pAcCL29.1	MJS	Owsianka *et al.*, 2000
pAcE1-E2	pAcCL29.1	J. Wood	-
pAcDDX3	pAcCL29.1	A. Patel	-
pAc5C	pAcCL29.1	A. Patel	-
pAc5C3	pAcCL29.1	A. Patel	-
pAc5CC	pAcCL29.1	MJS	-
pAc5CC3	pAcCL29.1	MJS	-

APPENDIX III:

Recombinant Viruses

Recombinant baculoviruses (rbacs) used in the preceding studies are shown below. All cDNAs were transferred to the pAcCL29.1 vector (Fig. 65a; Livingstone and Jones, 1994) prior to generation of each virus. DDX3 nt numbers relate to the sequence reported by Owsianka and Patel (1999) (see Appendix IV). HCV nt numbers relate to the genotype 1a infectious clone, H77c (Yangi *et al.*, 1997; see Appendix IV). Rbacs produced by the author are denoted 'MJS'.

rbac	*Expected Transcript (nt)*	*Expected Product (aa)*	*Source*
DDX3	DDX3 1-1989	DDX3 1-662	MJS
C	HCV 342-915	Core 1-191	MJS
CC	HCV 342-915-CAT	Core 1-191-CAT	MJS
5C	HCV 1-915	Core 1-191	A. Patel
5C3	HCV 1-915, 9375-9599	Core 1-191	A. Patel
5CC	HCV 1-915-CAT	Core 1-191-CAT	MJS
5CC3	HCV 1-915-CAT-HCV 9375-9599	Core 1-191-CAT	MJS
C-E1-E2	HCV 342-2576	Core-E1-E2 (1-746)	A. Patel (Owsianka *et al.*, 2000)
E1-E2	HCV 916-2576	E1-E2 (192-746)	J. Wood

Recombinant vaccinia viruses (rVVs) used in the preceding studies are shown below.

rVV	*Expected Transcript (nt)*	*Expected Product*	*Source*
DDX3	DDX3 (1-1989)	DDX3 (1-662)	A. Patel
C-E1-E2	HCV (342-2579)	Core-E1-E2 (1-746)	A. Patel
E1-E2	HCV (916-2579)	E1-E2 (192-746)	A. Patel
vTF7.3	-	T7 RNA polymerase	B. Moss (Fuerst *et al.*, 1986)

APPENDIX IV:

Sequences

Full-length DDX3 (Owsianka and Patel, 1999; accession no. AF061337) and HCV sequences (5′NCR-core-E1-E2, NS3 helicase, and 3′NCR) from HCV strain H77c (Yanagi *et al.*, 1997; accession no. AF011751) used in the preceding studies are shown below. Features of the protein/nucleotide seqeunces and restriction sites used in cloning procedures are highlighted.

DDX3

```
                                Putative NES
 M   S   H   V   A   V   E   N   A   L   G   L   D   Q   Q   F     16
ATG AGT CAT GTG GCA GTG GAA AAT GCG CTC GGG CTG GAC CAG CAG TTT    48
                    Putative N-linked Glycosylation Sites
 A   G   L   D   L   N   S   S   D   N   Q   S   G   G   S   T     32
GCT GGC CTA GAC CTG AAC TCT TCA GAT AAT CAG AGT GGA GGA AGT ACA    96

 A   S   K   G   R   Y   I   P   P   H   L   R   N   R   E   A     48
GCC AGC AAA GGG CGC TAT ATT CCT CCT CAT TTA AGG AAC CGA GAA GCT   144

 T   K   G   F   Y   D   K   D   S   S   G   W   S   S   S   K     64
ACT AAA GGT TTC TAC GAT AAA GAC AGT TCA GGG TGG AGT TCT AGC AAA   192
                                    BstYI
 D   K   D   A   Y   S   S   F   G   S   R   S   D   S   R   G     80
GAT AAG GAT GCG TAT AGC AGT TTT GGA TCT CGT AGT GAT TCA AGA GGG   240

 K   S   S   F   F   S   D   R   G   S   G   S   R   G   R   F     96
AAG TCT AGC TTC TTC AGT GAT CGT GGA AGT GGA TCA AGG GGA AGG TTT   288

 D   D   R   G   R   S   D   Y   D   G   I   G   S   R   G   D    112
GAT GAT CGT GGA CGG AGT GAT TAC GAT GGC ATT GGC AGC CGT GGT GAC   336

 R   S   G   F   G   K   F   E   R   G   G   N   S   R   W   C    128
AGA AGT GGC TTT GGC AAA TTT GAA CGT GGT GGA AAC AGT CGC TGG TGT   384
                                                    DraIII
 D   K   S   D   E   D   D   W   S   K   P   L   P   P   S   E    144
GAC AAA TCA GAT GAA GAT GAT TGG TCA AAA CCA CTC CCA CCA AGT GAA   432

 R   L   E   Q   E   L   F   S   G   G   N   T   G   I   N   F    160
CGC TTG GAA CAG GAA CTC TTT TCT GGA GGC AAC ACT GGG ATT AAT TTT   480

 E   K   Y   D   D   I   P   V   E   A   T   G   N   N   C   P    176
GAG AAA TAC GAT GAC ATT CCA GTT GAG GCA ACA GGC AAC AAC TGT CCT   528

 P   H   I   E   S   F   S   D   V   E   M   G   E   I   I   M    192
CCA CAT ATT GAA AGT TTC AGT GAT GTT GAG ATG GGA GAA ATT ATC ATG   576
          → eIF4A-like
 G   N   I   E   L   T   R   Y   T   R   P   T   P   V   Q   K    208
GGA AAC ATT GAG CTT ACT CGT TAT ACT CGC CCA ACT CCA GTG CAA AAG   624
 SphI
 H   A   I   P   I   I   K   E   K   R   D   L   M   A   C   A    224
CAT GCT ATT CCT ATT ATC AAA GAG AAA AGA GAC TTG ATG GCT TGT GCC   672
```

```
   Motif I (ATPase A)
 Q   T   G   S   G   K   T   A   A   F   L   L   P   I   L   S   240
CAA ACA GGG TCT GGA AAA ACT GCA GCA TTT CTG TTG CCC ATC TTG AGT  720
                                            Putative Tyrosine Kinase
 Q   I   Y   S   D   G   P   G   E   A   L   R   A   M   K   E   256
CAG ATT TAT TCA GAT GGT CCA GGC GAG GCT TTG AGG GCC ATG AAG GAA  768
Phosphorylation Site
 N   G   R   Y   G   R   R   K   Q   Y   P   I   S   L   V   L   272
AAT GGA AGG TAT GGG CGC CGC AAA CAA TAC CCA ATC TCC TTG GTA TTA  816
                Motif Ia            BglII          Putative cAMP/cGMP
 A   P   T   R   E   L   A   V   Q   I   Y   E   E   A   R   K   288
GCA CCA ACG AGA GAG TTG GCA GTA CAG ATC TAC GAG GAA GCC AGA AAA  864
Phosphorylation Site
 F   S   Y   R   S   R   V   R   P   C   V   V   Y   G   G   A   304
TTT TCA TAC CGA TCT AGA GTT CGT CCT TGC GTG GTT TAT GGT GGT GCC  912

 D   I   G   Q   Q   I   R   D   L   E   R   G   C   H   L   L   320
GAT ATT GGT CAG CAG ATT CGA GAC TTG GAA CGT GGA TGC CAT TTG TTA  960
                                                Putative Tyrosine
 V   A   T   P   G   R   L   V   D   M   M   E   R   G   K   I   336
GTA GCC ACT CCA GGA CGT CTA GTG GAT ATG ATG GAA AGA GGA AAG ATT 1008
Kinase Phosphorylation Site         MotifII (ATPase B)
 G   L   D   F   C   K   Y   L   V   L   D   E   A   D   R   M   352
GGA TTA GAC TTT TGC AAA TAC TTG GTG TTA GAT GAA GCT GAT CGG ATG 1056

 L   D   M   G   F   E   P   Q   I   R   R   I   V   E   Q   D   368
TTG GAT ATG GGG TTT GAG CCT CAG ATT CGT AGA ATA GTC GAA CAA GAT 1104
                                                    Motif III
 T   M   P   P   K   G   V   R   H   T   M   M   F   S   A   T   384
ACT ATG CCT CCA AAG GGT GTC CGC CAC ACT ATG ATG TTT AGT GCT ACT 1152

 F   P   K   E   I   Q   M   L   A   R   D   F   L   D   E   Y   400
TTT CCT AAG GAA ATA CAG ATG CTG GCT CGT GAT TTC TTA GAT GAA TAT 1200
                                Putative N-linked Glycosylation Site
 I   F   L   A   V   G   R   V   G   S   T   S   E   N   I   T   416
ATC TTC TTG GCT GTA GGA AGA GTT GGC TCT ACC TCT GAA AAC ATC ACA 1248

 Q   K   V   V   W   V   E   E   S   D   K   R   S   F   L   L   432
CAG AAA GTA GTT TGG GTG GAA GAA TCA GAC AAA CGG TCA TTT CTG CTT 1296
   Putative N-linked Glycosylation Site          Motif IV
 D   L   L   N   A   T   G   K   D   S   L   T   L   V   F   V   448
GAC CTC CTA AAT GCA ACA GGC AAG GAT TCA CTG ACC TTA GTG TTT GTG 1344

 E   T   K   K   G   A   D   S   L   E   D   F   L   Y   H   E   464
GAG ACC AAA AAG GGT GCA GAT TCT CTG GAG GAT TTC TTA TAC CAT GAA 1392
                            NcoI
 G   Y   A   C   T   S   I   H   G   D   R   S   Q   R   D   R   480
GGA TAC GCA TGT ACC AGC ATC CAT GGA GAC CGT TCT CAG AGG GAT AGA 1440

 E   E   A   L   H   Q   F   R   S   G   K   S   P   I   L   V   496
GAA GAG GCC CTT CAC CAG TTC CGC TCA GGA AAA AGC CCA ATT TTA GTG 1488
                            Motif V
 A   T   A   V   A   A   R   G   L   D   I   S   N   V   K   H   512
GCT ACA GCA GTA GCA GCA AGA GGA CTG GAC ATT TCA AAT GTG AAA CAT 1536

 V   I   N   F   D   L   P   S   D   I   E   E   Y   V   H   R   528
GTT ATC AAT TTT GAC TTG CCA AGT GAT ATT GAA GAA TAT GTA CAT CGT 1584
            Motif VI
 I   G   R   T   G   R   V   G   N   L   G   L   A   T   S   F   544
ATT GGT CGT ACG GGA CGT GTA GGA AAC CTT GGC CTG GCA ACC TCA TTC 1632

Putative N-linked Glycosylation Site
 F   N   E   R   N   I   N   I   T   K   D   L   L   D   L   L   560
TTT AAC GAG AGG AAC ATA AAT ATT ACT AAG GAT TTG TTG GAT CTT CTT 1680
```

```
                        eIF4A-like ←
 V   E   A   K   Q   E   V   P   S   W   L   E   N   M   A   Y   576
GTT GAA GCT AAA CAA GAA GTG CCG TCT TGG TTA GAA AAC ATG GCT TAT 1728
                            'RS-like' Domain
 E   H   H   Y   K   G   S   S   R   G   R   S   K   S   S   R   592
GAA CAC CAC TAC AAG GGT AGC AGT CGT GGA CGT TCT AAG AGT AGC AGA 1776

 F   S   G   G   F   G   A   R   D   Y   R   Q   S   S   G   A   608
TTT AGT GGA GGG TTT GGT GCC AGA GAC TAC CGA CAA AGT AGC GGT GCC 1824

 S   S   S   S   F   S   S   S   R   A   S   S   S   R   S   G   624
AGC AGT TCC AGC TTC AGC AGC AGC CGC GCA AGC AGC AGC CGC AGT GGC 1872

 G   G   G   H   G   S   S   R   G   F   G   G   G   G   Y   G   640
GGA GGT GGC CAC GGT AGC AGC AGA GGA TTT GGT GGA GGT GGC TAT GGA 1920

 G   F   Y   N   S   D   G   Y   G   G   N   Y   N   S   Q   G   656
GGC TTT TAC AAC AGT GAT GGA TAT GGA GGA AAT TAT AAC TCC CAG GGG 1968

 V   D   W   W   G   N   -                                       662
GTT GAC TGG TGG GGT AAC TGA                                     1989
```

HCV 5'NCR-core-E1-E2

```
GCCAGCCCCCTGATGGGGGCGACACTCCACCATGAATCACTCCCCTGTGAGGAACTACTGTCTTC  65

ACGCAGAAAGCGTCTAGCCATGGCGTTAGTATGAGTGTCGTGCAGCCTCCAGGACCCCCCCTCCC  130
                          AgeI
GGGAGAGCCATAGTGGTCTGCGGAACCGGTGAGTACACCGGAATTGCCAGGACGACCGGGTCCTT  195

TCTTGGATAAACCCGCTCAATGCCTGGAGATTTGGGCGTGCCCCCGCAAGACTGCTAGCCGAGTA  260

GTGTTGGGTCGCGAAAGGCCTTGTGGTACTGCCTGATAGGGTGCTTGCGAGTGCCCCGGGAGGTC  325
                  → core
          ApaLI   M   S   T   N   P   K   P   Q   R   K   T   K   12
TCGTAGACCGTGCACC ATG AGC ACG AAT CCT AAA CCT CAA AGA AAA ACC AAA  377
                        DDX3-Interacting Domain
 R   N   T   N   R   R   P   Q   D   V   K   F   P   G   G   G   28
CGT AAC ACC AAC CGT CGC CCA CAG GAC GTC AAG TTC CCG GGT GGC GGT  425

 Q   I   V   G   G   V   Y   L   L   P   R   R   G   P   R   L   44
CAG ATC GTT GGT GGA GTT TAC TTG TTG CCG CGC AGG GGC CCT AGA TTG  473
                                                        XhoI
 G   V   R   A   T   R   K   T   S   E   R   S   Q   P   R   G   60
GGT GTG CGC GCG ACG AGG AAG ACT TCC GAG CGG TCG CAA CCT CGA GGT  521

 R   R   Q   P   I   P   K   A   R   R   P   E   G   R   T   W   76
AGA CGT CAG CCT ATC CCC AAG GCA CGT CGG CCC GAG GGC AGG ACC TGG  569

 A   Q   P   G   Y   P   W   P   L   Y   G   N   E   G   C   G   92
GCT CAG CCC GGG TAC CCT TGG CCC CTC TAT GGC AAT GAG GGT TGC GGG  617
                    Putative DNA Binding Domain
 W   A   G   W   L   L   S   P   R   G   S   R   P   S   W   G   108
TGG GCG GGA TGG CTC CTG TCT CCC CGT GGC TCT CGG CCT AGC TGG GGC  665
                                                        ClaI
 P   T   D   P   R   R   R   S   R   N   L   G   K   V   I   D   124
CCC ACA GAC CCC CGG CGT AGG TCG CGC AAT TTG GGT AAG GTC ATC GAT  713
```

```
 T   L   T   C   G   F   A   D   L   M   G   Y   I   P   L   V   140
ACC CTT ACG TGC GGC TTC GCC GAC CTC ATG GGG TAC ATA CCG CTC GTC  761

 G   A   P   L   G   G   A   A   R   A   L   A   H   G   V   R   156
GGC GCC CCT CTT GGA GGC GCT GCC AGG GCC CTG GCG CAT GGC GTC CGG  809

 V   L   E   D   G   V   N   Y   A   T   G   N   L   P   G   C   172
GTT CTG GAA GAC GGC GTG AAC TAT GCA ACA GGG AAC CTT CCT GGT TGC  857
                                E1 Signal Sequence
 S   F   S   I   F   L   L   A   L   L   S   C   L   T   V   P   188
TCT TTC TCT ATC TTC CTT CTG GCC CTG CTC TCT TGC CTG ACT GTG CCC  905
            → E1
 A   S   A   Y   Q   V   R   N   S   S   G   L   Y   H   V   T   204
GCT TCA GCC TAC CAA GTG CGC AAT TCC TCG GGG CTT TAC CAT GTC ACC  953

 N   D   C   P   N   S   S   I   V   Y   E   A   A   D   A   I   220
AAT GAT TGC CCT AAC TCG AGT ATT GTG TAC GAG GCG GCC GAT GCC ATC 1001

 L   H   T   P   G   C   V   P   C   V   R   E   G   N   A   S   236
CTG CAC ACT CCG GGG TGT GTC CCT TGC GTT CGC GAG GGT AAC GCC TCG 1049

 R   C   W   V   A   V   T   P   T   V   A   T   R   D   G   K   252
AGG TGT TGG GTG GCG GTG ACC CCC ACG GTG GCC ACC AGG GAC GGC AAA 1097

 L   P   T   T   Q   L   R   R   H   I   D   L   L   V   G   S   268
CTC CCC ACA ACG CAG CTT CGA CGT CAT ATC GAT CTG CTT GTC GGG AGC 1145
                    Predicted Transmembrane Region
 A   T   L   C   S   A   L   Y   V   G   D   L   C   G   S   V   284
GCC ACC CTC TGC TCG GCC CTC TAC GTG GGG GAC CTG TGC GGG TCT GTC 1193

 F   L   V   G   Q   L   F   T   F   S   P   R   R   H   W   T   300
TTT CTT GTT GGT CAA CTG TTT ACC TTC TCT CCC AGG CGC CAC TGG ACG 1241

 T   Q   D   C   N   C   S   I   Y   P   G   H   I   T   G   H   316
ACG CAA GAC TGC AAT TGT TCT ATC TAT CCC GGC CAT ATA ACG GGT CAT 1289

 R   M   A   W   D   M   M   M   N   W   S   P   T   A   A   L   332
CGC ATG GCA TGG GAT ATG ATG ATG AAC TGG TCC CCT ACG GCA GCG TTG 1337

 V   V   A   Q   L   L   R   I   P   Q   A   I   M   D   M   I   348
GTG GTA GCT CAG CTG CTC CGG ATC CCA CAA GCC ATC ATG GAC ATG ATC 1385
        Predicted Transmembrane Region
 A   G   A   H   W   G   V   L   A   G   I   A   Y   F   S   M   364
GCT GGT GCT CAC TGG GGA GTC CTG GCG GGC ATA GCG TAT TTC TCC ATG 1433

 V   G   N   W   A   K   V   L   V   V   L   L   L   F   A   G   380
GTG GGG AAC TGG GCG AAG GTC CTG GTA GTG CTG CTG CTA TTT GCC GGC 1481
            → E2                        HVR-1
 V   D   A   E   T   H   V   T   G   G   N   A   G   R   T   T   396
GTC GAC GCG GAA ACC CAC GTC ACC GGG GGA AAT GCC GGC CGC ACC ACG 1529

 A   G   L   V   G   L   L   T   P   G   A   K   Q   N   I   Q   412
GCT GGG CTT GTT GGT CTC CTT ACA CCA GGC GCC AAG CAG AAC ATC CAA 1577
 L   I   N   T   N   G   S   W   H   I   N   S   T   A   L   N   428
CTG ATC AAC ACC AAC GGC AGT TGG CAC ATC AAT AGC ACG GCC TTG AAT 1625

 C   N   E   S   L   N   T   G   W   L   A   G   L   F   Y   Q   444
TGC AAT GAA AGC CTT AAC ACC GGC TGG TTA GCA GGG CTC TTC TAT CAA 1673

 H   K   F   N   S   S   G   C   P   E   R   L   A   S   C   R   460
CAC AAA TTC AAC TCT TCA GGC TGT CCT GAG AGG TTG GCC AGC TGC CGA 1721

 R   L   T   D   F   A   Q   G   W   G   P   I   S   Y   A   N   476
CGC CTT ACC GAT TTT GCC CAG GGC TGG GGT CCT ATC AGT TAT GCC AAC 1769
```

```
 G   S   G   L   D   E   R   P   Y   C   W   H   Y   P   P   R    492
GGA AGC GGC CTC GAC GAA CGC CCC TAC TGC TGG CAC TAC CCT CCA AGA  1817

 P   C   G   I   V   P   A   K   S   V   C   G   P   V   Y   C    508
CCT TGT GGC ATT GTG CCC GCA AAG AGC GTG TGT GGC CCG GTA TAT TGC  1865

 F   T   P   S   P   V   V   V   G   T   T   D   R   S   G   A    524
TTC ACT CCC AGC CCC GTG GTG GTG GGA ACG ACC GAC AGG TCG GGC GCG  1913

 P   T   Y   S   W   G   A   N   D   T   D   V   F   V   L   N    540
CCT ACC TAC AGC TGG GGT GCA AAT GAT ACG GAT GTC TTC GTC CTT AAC  1961

 N   T   R   P   P   L   G   N   W   F   G   C   T   W   M   N    556
AAC ACC AGG CCA CCG CTG GGC AAT TGG TTC GGT TGT ACC TGG ATG AAC  2009

 S   T   G   F   T   K   V   C   G   A   P   P   C   V   I   G    572
TCA ACT GGA TTC ACC AAA GTG TGC GGA GCG CCC CCT TGT GTC ATC GGA  2057

 G   V   G   N   N   T   L   L   C   P   T   D   C   F   R   K    588
GGG GTG GGC AAC AAC ACC TTG CTC TGC CCC ACT GAT TGC TTC CGC AAA  2105

 H   P   E   A   T   Y   S   R   C   G   S   G   P   W   I   T    604
CAT CCG GAA GCC ACA TAC TCT CGG TGC GGC TCC GGT CCC TGG ATT ACA  2153

 P   R   C   M   V   D   Y   P   Y   R   L   W   H   Y   P   C    620
CCC AGG TGC ATG GTC GAC TAC CCG TAT AGG CTT TGG CAC TAT CCT TGT  2201

 T   I   N   Y   T   I   F   K   V   R   M   Y   V   G   G   V    636
ACC ATC AAT TAC ACC ATA TTC AAA GTC AGG ATG TAC GTG GGA GGG GTC  2249

 E   H   R   L   E   A   A   C   N   W   T   R   G   E   R   C    652
GAG CAC AGG CTG GAA GCG GCC TGC AAC TGG ACG CGG GGC GAA CGC TGT  2297

 D   L   E   D   R   D   R   S   E   L   S   P   L   L   L   S    668
GAT CTG GAA GAC AGG GAC AGG TCC GAG CTC AGC CCG TTG CTG CTG TCC  2345

 T   T   Q   W   Q   V   L   P   C   S   F   T   T   L   P   A    684
ACC ACA CAG TGG CAG GTC CTT CCG TGT TCT TTC ACG ACC CTG CCA GCC  2393

 L   S   T   G   L   I   H   L   H   Q   N   I   V   D   V   Q    700
TTG TCC ACC GGC CTC ATC CAC CTC CAC CAG AAC ATT GTG GAC GTG CAG  2441

 Y   L   Y   G   V   G   S   S   I   A   S   W   A   I   K   W    716
TAC TTG TAC GGG GTA GGG TCA AGC ATC GCG TCC TGG GCC ATT AAG TGG  2489
                Predicted Transmembrane Region
 E   Y   V   V   L   L   F   L   L   L   A   D   A   R   V   C    732
GAG TAC GTC GTT CTC CTG TTC CTT CTG CTT GCA GAC GCG CGC GTC TGC  2537

 S   C   L   W   M   M   L   L   I   S   Q   A   E   A            746
TCC TGC TTG TGG ATG ATG TTA CTC ATA TCC CAA GCG GAG GCG          2576
```

HCV NS3 Helicase

```
        NS3 Protease Domain
 P   A   A   V   C   T   R   G   V   A   K   A   V   D   F   I    1196
AGG GCC GCG GTG TGC ACC CGT GGA GTG GCT AAA GCG GTG GAC TTT ATC  3929

 P   V   E   N   L   G   T   T   M   R   S   P   V   F   T   D    1212
CCT GTG GAG AAC CTA GGG ACA ACC ATG AGA TCC CCG GTG TTC ACG GAC  3977

 N   S   S   P   P   A   V   P   Q   S   F   Q   V   A   H   L    1228
AAC TCC TCT CCA CCA GCA GTG CCC CAG AGC TTC CAG GTG GCC CAC CTG  4025
```

Motif I (ATPase A)

H A P T G S G K S T K V P A A Y 1244
CAT GCT CCC ACC GGC AGC GGT AAG AGC ACC AAG GTC CCG GCT GCG TAC 4073

A A Q G Y K V L V L N P S V A A 1260
GCA GCC CAG GGC TAC AAG GTG TTG GTG CTC AAC CCC TCT GTT GCT GCA 4121

T L G F G A Y M S K A H G V D P 1276
ACG CTG GGC TTT GGT GCT TAC ATG TCC AAG GCC CAT GGG GTT GAT CCT 4169

N I R T G V R T I T T G S P I T 1292
AAT ATC AGG ACC GGG GTG AGA ACA ATT ACC ACT GGC AGC CCC ATC ACG 4217

Y S T Y G K F L A D G G C S G G 1308
TAC TCC ACC TAC GGC AAG TTC CTT GCC GAC GGC GGG TGC TCA GGA GGT 4265

Motif II (ATPase B)

A Y D I I I C D E C H S T D A T 1324
GCT TAT GAC ATA ATA ATT TGT GAC GAG TGC CAC TCC ACG GAT GCC ACA 4313

S I L G I G T V L D Q A E T A G 1340
TCC ATC TTG GGC ATC GGC ACT GTC CTT GAC CAA GCA GAG ACT GCG GGG 4361

Motif III

A R L V V L A T A T P P G S V T 1356
GCG AGA CTG GTT GTG CTC GCC ACT GCT ACC CCT CCG GGC TCC GTC ACT 4409

V S H P N I E E V A L S T T G E 1372
GTG TCC CAT CCT AAC ATC GAG GAG GTT GCT CTG TCC ACC ACC GGA GAG 4457

I P F Y G K A I P L E V I K G G 1388
ATC CCC TTT TAC GGC AAG GCT ATC CCC CTC GAG GTG ATC AAG GGG GGA 4505

R H L I F C H S K K K C D E L A 1404
AGA CAT CTC ATC TTC TGC CAC TCA AAG AAG AAG TGC GAC GAG CTC GCC 4553

A K L V A L G I N A V A Y Y R G 1420
GCG AAG CTG GTC GCA TTG GGC ATC AAT GCC GTG GCC TAC TAC CGC GGT 4601

L D V S V I P T S G D V V V V S 1436
CTT GAC GTG TCT GTC ATC CCG ACC AGC GGC GAT GTT GTC GTC GTG TCG 4649

T D A L M T G F T G D F D S V I 1452
ACC GAT GCT CTC ATG ACT GGC TTT ACC GGC GAC TTC GAC TCT GTG ATA 4697

D C N T C V T Q T V D F S L D P 1468
GAC TGC AAC ACG TGT GTC ACT CAG ACA GTC GAT TTC AGC CTT GAC CCT 4745

T F T I E T T T L P Q D A V S R 1484
ACC TTT ACC ATT GAG ACA ACC ACG CTC CCC CAG GAT GCT GTC TCC AGG 4793

Motif IV

T Q R R G R T G R G K P G I Y R 1500
ACT CAA CGC CGG GGC AGG ACT GGC AGG GGG AAG CCA GGC ATC TAT AGA 4841

F V A P G E R P S G M F D S S V 1516
TTT GTG GCA CCG GGG GAG CGC CCC TCC GGC ATG TTC GAC TCG TCC GTC 4889

L C E C Y D A G C A W Y E L T P 1532
CTC TGT GAG TGC TAT GAC GCG GGC TGT GCT TGG TAT GAG CTC ACG CCC 4937

A E T T V R L R A Y M N T P G L 1548
GCC GAG ACT ACA GTT AGG CTA CGA GCG TAC ATG AAC ACC CCG GGG CTT 4985

P V C Q D H L E F W E G V F T G 1564
CCC GTG TGC CAG GAC CAT CTT GAA TTT TGG GAG GGC GTC TTT ACG GGC 5033

```
 L   T   H   I   D   A   H   F   L   S   Q   T   K   Q   S   G    1580
CTC ACT CAT ATA GAT GCC CAC TTT TTA TCC CAG ACA AAG CAG AGT GGG   5081

 E   N   F   P   Y   L   V   A   Y   Q   A   T   V   C   A   R    1596
GAG AAC TTT CCT TAC CTG GTA GCG TAC CAA GCC ACC GTG TGC GCT AGG   5129

 A   Q   A   P   P   P   S   W   D   Q   M   W   K   C   L   I    1612
GCT CAA GCC CCT CCC CCA TCG TGG GAC CAG ATG TGG AAG TGT TTG ATC   5177

 R   L   K   P   T   L   H   G   P   T   P   L   L   Y   R   L    1628
CGC CTT AAA CCC ACC CTC CAT GGG CCA ACA CCC CTG CTA TAC AGA CTG   5225

 G   A   V   Q   N   E   V   T   L   T   H   P   I   T   K   Y    1644
GGC GCT GTT CAG AAT GAA GTC ACC CTG ACG CAC CCA ATC ACC AAA TAC   5273

 I   M   T   C   M   S   A   D   L   E   V   V   T                1651
ATC ATG ACA TGC ATG TCG GCC GAC CTG GAG GTC GTC ACG               5312
```

HCV 3′NCR

```
                NS5B
 I   Y   L   L   P   N   R   -   → Variable Region                 3011
ATC TAC CTC CTC CCC AAC CGA TGA AGGTTGGGGTAAACACTCCGGCCTCTTAAGCCA  9410
→ Poly(U/C)Tract
TTTCCTGTTTTTTTTTTTTTTTTTTTTTTTTTTTTTCTTTTTTTTTTTCTTTCCTTTCCTTCTTTT  9475
                          → 3′X Region
TTTCCTTTCTTTTTCCCTTCTTTAATGGTGGCTCCATCTTAGCCCTAGTCACGGCTAGCTGTGAA  9540

AGGTCCGTGAGCCGCATGACTGCAGAGAGTGCTGATACTGGCCTCTCTGCAGATCATGT       9599
```

APPENDIX V:

Oligonucleotides

Oligonucleotides used to generate particular cDNAs for insertion into appropriate plasmid vectors are shown below. The HCV infectious clone H77c (Yanagi *et al.*, 1997; Appendix IV) was used in generation of constructs carrying HCV sequences. DDX3 nt numbers relate to the sequence reported by Owsianka and Patel (1999) (Appendix IV).

GST-NS3 helicase

*Sma*I *Sal*I *Bam*HI → HCV nt 3915

H77A 5′- CCC GGG TCG ACG ACG GAT CCA **TGG** CGG TGG ACT TTA TCC CTG TGG AGA ACC TAG GGA CAA CCA TGA GA -3′

*Pst*I *Kpn*I *Not*I *Hind*III

H77B 5′- CTG CAG GTA CCG CGG CCG CAA GCT TCG TGA CGA CCT CCA GGT CGG CCG ACA TGC ATG TCA TGA TGT ATT T -3′

Cloned into pGEX-6P-3 (in frame with the GST-coding sequence) using *Bam*HI and *Not*I sites.

pAcC

*Bam*HI Kozak → HCV nt 342

core A 5′- CAG GGA TCC GCC ACC **ATG** AGC ACG AAT CCT AAA -3′

core B 5′- CTG TCT AGA CTA GGC TGA AGC GGG CAC -3′
*Xba*I

Cloned into pAcCL29.1 (in frame with the baculovirus polyhedrin promoter) using *Bam*HI and *Xba*I sites.

GST-RS

*Bam*HI → DDX3 nt 1744

DDX1 5′- CTG GGA TCC GGT AGC AGT CGT GGA CGT -3′

*Xho*I

DDX2 5′- TCC GAA TTC TCA TCT GCT GCT ACC GTG GCC -3′

Cloned into pGEX-6P-3 using *Bam*HI and *Xho*I sites.

GST-ΔRS

*Nco*I (DDX3 nt 1413)

DDX3 5′- CAT CCA TGG AGA CCG TTC TCA GAG GGA T -3′

DDX4 5′- CTT GTA GTG GTG TTC ATA -3′

→ DDX3 nt 1997

DDX5 5′- GGA TTT GGT GGA GGT GGC -3′

*Eco*RI

DDX6 5′- TCC GAA TTC TCA GTT ACC CCA CCA GTC -3′

PCR product generated using DDX3/DDX4 cut with *Nco*I. PCR product generated using DDX5/DDX6 cut with *Eco*RI. Cloned into *Nco*I/*Eco*RI cut pGST-DDX3 carrying the full-length DDX3 sequence.

pΔNES-DDX3

*Hind*III Kozak → DDX3 nt 139

MJS 3 5'- CCC AAG CTT GCC ACC **ATG** AAC TCT TCA GAT AAT -3'

*Bgl*II

MJS 6 5'- CTC GTA GAT CTG TAC TGC CAA CTC TCT CGT -3'

PCR product cut with *Hind*III and *Bgl*II. pDDX3 cut with *Bgl*II and *Xho*I. Ligated to *Hind*III/*Xho*I cut pZeoSV2 (+).